Ecology of picophytoplankton from the waters surrounding India

A Thesis submitted to
Goa University
for the award of the Degree of
Doctor of Philosophy
in
Marine Sciences

By
Rajaneesh K. M.

CSIR-National Institute of Oceanography
Dona Paula, Goa – 403004, India

Under the Guidance of
Dr. Smita Mitbavkar
CSIR-National Institute of Oceanography
Dona Paula, Goa – 403004, India

2018

Dedicated to my mother.

Contents

Page

Statement of the Candidate

*As required under the University ordinance 0.19.8 (vi), I state that the present thesis entitled "**Ecology of picophytoplankton from the waters surrounding India**" is my original contribution and the same has not been submitted on any previous occasion. To the best of my knowledge, the present study is the first comprehensive work of its kind from the area mentioned.*

The literature related to the problem investigated has been cited. Due acknowledgements have been made wherever facilities and suggestions have been availed of.

Rajaneesh K. M.

Certificate

This is to certify that the thesis entitled " Ecology of picophytoplankton from the waters surrounding India", submitted by Mr. Rajaneesh K. M. for the award of the degree of Doctor of Philosophy in Marine Science is based on his original studies carried out by him under my supervision. The thesis or any part thereof has not been previously submitted for any other degree or diploma in any Universities or Institutions.

Dr. Smita Mitbavkar
Research Guide
Senior Scientist
Biofouling and Bioinvasion Division
CSIR- National Institute of Oceanography
Dona Paula-403 004, Goa

Acknowledgements

It gives me enormous pleasure to express my sincere gratitude towards several people who were associated with me directly or indirectly for the completion of this thesis.

I would like to express my sincere gratitude to my guide Dr. Smita Mitbavkar. I am deeply indebted for her aspiring guidance, invaluable constructive criticism, and friendly advice during my thesis work. However, “Thank you” is a too small word to show my gratitude towards her for the guidance and introducing me to the research topic.

I am very much grateful to Dr. A. C. Anil, Chief Scientist and Head, Biofouling and Bioinvasion Division, for giving me an opportunity to work in the lab, as well as for the support on the way. Also, providing all the facilities required for my work and funding for each page of research.

I would like to thank the Director, Council of Scientific and Industrial Research (CSIR)-National Institute of Oceanography (NIO), for giving me an opportunity to carry out this research in this institute.

My sincere thanks to Dr. Narasinh Thakur (my V.C.'s nominee) for his meticulous comments. I also acknowledge the insightful comments and advice given by the other members of the Ph.D. faculty committee, Prof. Janarthanam, Prof. C. U. Rivonker and Dr. G. N. Nayak.

I would like to express my gratitude towards Dr. V. V. Gopalakrishna for helping and encouraging me during the initial days of my research.

I acknowledge the NIO Ph.D. registration standing committee members Dr. Dileep Kumar, Dr. N. Ramaiah, Dr. Shyam Prasad, Dr. V. P. C. Rao, Dr. R. Mukhopadhyay, Dr. D. Shankar, Dr. P. Dewangan, and Mr. Krishna Kumar for their valuable suggestions and advice to improve my thesis work.

My special thanks to Mr. K. Venkat, for his support and assistance in different problems. His readiness to help will always be valued.

I sincerely thank Dr. Jagadish Patil for the useful comments, remarks, and engagement through the learning process of this thesis.

I would also like to thank Dr. S. S. Sawant and Dr. Temjensangba Imchen for constructive suggestions during scientific as well as personal difficulties.

I also thank Dr. Dattesh Desai and Dr. Lidita Kandeparker for their support and guidance during the period of my work, especially during port samplings.

I acknowledge CSIR for providing Senior Research fellowship. This work was also supported by the Indian-XBT programme (INCOIS, Ministry of Earth Science), Ballast Water Management Programme (Ministry of Shipping and DG Shipping, India) and CSIR funded Ocean Finder Program.

I would like to thank Dr. V. Banakar, Mr. Vijay Khedekar and Mr. Areef A. sardar for providing scanning electron microscopy (SEM) facility. I wish to acknowledge the library and administrative staff of NIO for their help during this work.

I wish to acknowledge Mr. Kaushal Mapari for the help and support rendered during the work. I would like to thank Dr. V.V.S.S. Sarma, Mr. Sundar, Mr. Michael, Mr. Prakash Mehra, and Mr. Subha Anand for providing physicochemical data for my thesis.

I am obliged to my seniors, Dr. Chetan, Dr. Ravi, Dr. Priya, Dr. Shamina, Dr. Sumit Mondal, Dr. Dhiraj Narale, Mr. Rajath Chitari, Mr. Amar Musale, Mrs. Kirti Kesarkar and Mr. Vinayak for the valuable information provided by them in their respective fields. Even though, I did not agree with some of their arguments and suggestions, it was found to be true at the end. I am grateful for their support and encouragements during the period of my work.

I take this opportunity to complement the bond of love shared for years with my friends Mr. Vijayraj A.S., Dr. Lalita Baragi, Mr. Deepak Naik, Ms. Devika, Dr. Sabhapathy, Dr. Chetan C. Gaonkar, Dr. Rajesh Paravathkar and Ms. Geetanjali D.

These acknowledgements would not be complete without thanking the wonderful labmates Mr. Roy Rodrigues, Mr. Ranjith E., Mr. Dipesh Kale, Mr. Aseem Rath, Mr. Suchandan Bemal, Mr. Gobardhan sahoo, Ms. Conchita Monteiro, Mrs. Dipti Verlekar, Mr. Pawan Dharmadhikari, Mr. Sathish K, Mr. Sathish P, Mr. Dayakaran, Mr. Nishanth Kuchi, Mr. Atchutan, Mr. Laxman Gardade, Mr. Noyel, Mr. Sumit, Mrs. Manjitha, Ms. Nikita, Mr. Deodatta Gajbiye, Ms. Sangeeta Naik, Mr. Sailesh Nair, Mr. Sidhesh Shirodkar, Ms. Samanta, Mr. Pronoy Paul, Mr. Wasim Ezaz, Mr. Manuel Esteves, Ms.

Saili Naik, Mr. Andrew, Mr. Sagar, Ms. Karishma Prabhu, Mr. Krishnasamy and Ms. Vivienne, for their enormous help and support, which made the journey enjoyable.

My immense thanks to Dr. Raghavendra Rao, Dr. Rama Bhat, Dr. Parthasarathy C, Dr. Mahesh Majik, Dr. Vinay, Dr. Dinesh and Dr. Vijith for their valuable suggestions and help.

I would like to thank my NIO family, Mr. Suresh, Mr. Santhosh, Mr. Vinod, Mr. Darwin, Mr. Sam Kamaleson, Mr. Thava Pandian, Dr. Manikandan, Dr. Sunil, Dr. Singam, Mr. Azeesh, and Mr. Akshay.

I would like to thank Mr. Vinith Jain, Ms. Remya, Mr. Srikanth Dora and Mr. Anil for helping me with ferret software.

I would thank all the crew members of boat/ ship for their invaluable help in these extensive samplings. I honestly thank all those who helped me directly or indirectly other in the successful completion of this thesis.

My Mother (Ms. Gangamma D.) always stood by me, motivated me throughout my career. My gratitude for her cannot be expressed in words, and without her generous care, this work would not have been completed. The moral backing, happiness, and enthusiasm offered to me by my bellowed brothers (Mr. Thirumalesh and Mr. Satyaprakash), cousins (Mr. Devraj Kolchar, Dr. Praveen A.S., Mr. Prasad A.S) and sisters in law (Mrs. Bhavya and Mrs. Keerthi) is deeply remembered. I also thank Mr. Vithal Baragi, Mrs. Shanti, Ms Laxmi, Mrs. Lalini, Mr. Manjunath and Mr. Banneshwar for their support. Their prayers and wishes have motivated me in the successful completion of my work.

Rajaneesh K. M.

Abbreviations

ANOVA- Analysis of variance

AS- Arabian Sea

BOD- Biological oxygen demand

CB- Cochin backwaters

Chl *a*- Chlorophyll *a*

CTD- Conductivity, temperature and depth

D- Days

DIN- Dissolved inorganic nitrogen

DIP- Dissolved inorganic phosphate

DO- Dissolved oxygen

F- Factor

FALS- Forward angle light scatter

FCM- Flow cytometer

GF/F- Glass fiber filter

HL- High light

IMD- Indian meteorological department

KOPT- Kidderpore

LL- Low light

MON- Monsoon

ML- Mixed layer

NBW- Near bottom waters

NEM- North east monsoon

NSD- Netaji Subhas Dock

NT- Neap tide

PC- Phycocyanin

PCA- Principle Component Analysis

PE- Phycoerythrin

PEUK- Picoeukaryotes

PEB- Phycoerythrobilin

PM- Post-monsoon

POL- Petroleum Oil Lubricants

PP- Picophytoplankton

PrM- Pre-monsoon

PRO- Prochlorococcus

PUB- Phycourobilin

RALS- Right angle light scatter

RDA- Redundancy analysis

SD- Secchi disk

SR- Solar radiation

S-Station

ST- Spring tide

SWM- South west monsoon

SYN- Synechococcus

TP- Transition period

TRIX- Trophic index

TSI- - Trophic status index

ΔS-Stratification parameter

Chapter 1

General Introduction

Phytoplankton, an integral part of the marine life, are microscopic unicellular, autotrophic organisms that inhabit a range of aquatic environments from freshwater to marine. Though they are small, they help to sustain almost all life in the ocean through photosynthesis. Phytoplankton obtains energy through the process of photosynthesis wherein they fix carbon dioxide (greenhouse gas) into organic compounds. Thereby also contributing significantly to climatic processes (Jeffrey and Vesk, 1997). Since, they account for half of all photosynthetic activity on Earth, they are responsible for much of the oxygen present in the Earth's atmosphere (Falkowski, 1994). Their cumulative energy fixation in carbon compounds known as primary production is the source for the larger part of oceanic and also many freshwater food webs. Therefore, they play an important role in determining ecosystem functioning and trophic dynamics.

Till late 1970's, it was believed that diatoms and dinoflagellates are the main primary producers (Pomeroy, 1974). Later it was observed that there was a mismatch between chlorophyll (chl) concentrations, primary productivity, and phytoplankton abundance wherein phytoplankton abundance was low, chl *a* concentration and primary productivity were high. When these samples were observed under epifluorescence microscope, large number of fluorescing tiny cells were observed, which led to the discovery of picophytoplankton (PP) (Waterbury et al., 1979; Li et al., 1983). Until the discovery of PP, it was thought that the classical food web only exists with the diatoms and dinoflagellates as the base of food web (Pomeroy, 1974; Azam et al., 1983). In this, phytoplankton are fed upon by microzooplankton which are in turn consumed by mesozooplankton, which forms the main diet for fishes. However, with the discovery of PP, studies showed the existence of a microbial loop, which also can sustain higher organisms (Azam et al., 1983; Ituriaga and Mitchell,

1986) (Fig. 1.1). In this loop, PP forms the base of the food web but because of their small size these organisms cannot be consumed by the mesozooplankton. These organisms are grazed by microzooplankton, heterotrophic nanoflagellates and ciliates; which are then fed upon by mesozooplankton (Richardson and Jackson, 2007), and subsequently enter in to the classical food chain. This food web is especially important in oligotrophic conditions when the larger phytoplankton are in lower numbers.

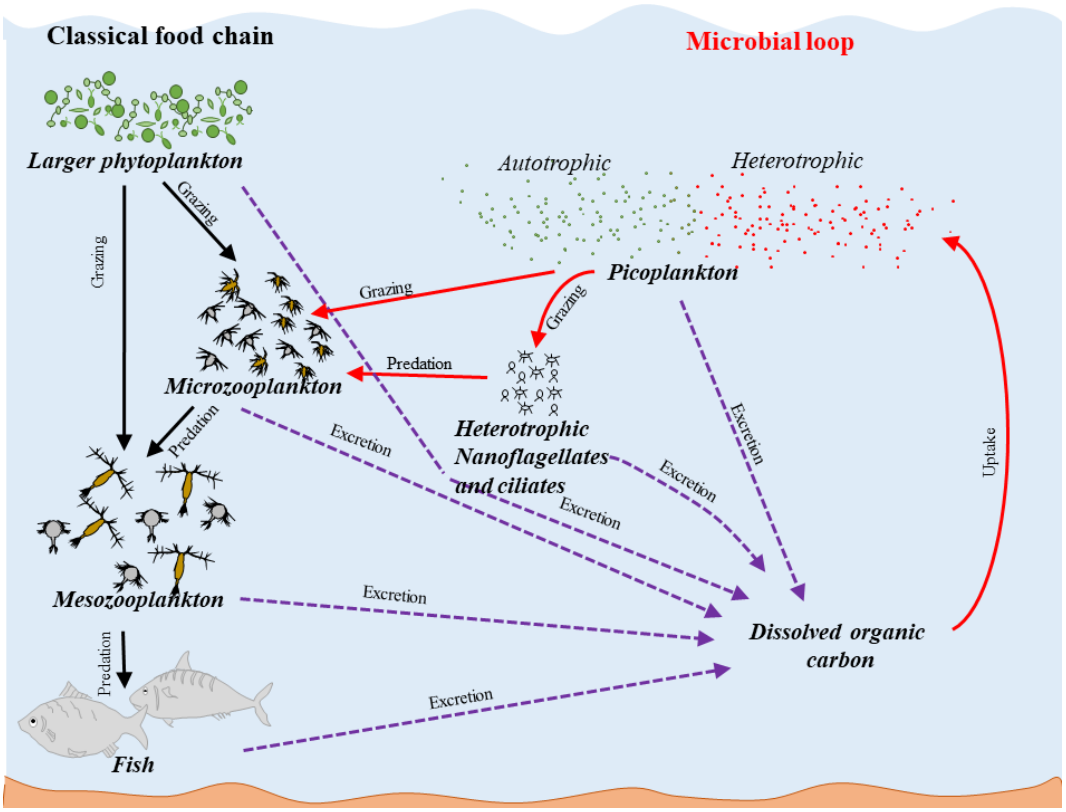

Fig. 1.1 The role of picophytoplankton in marine food web dynamics.

Based on their cell size, phytoplankton are divided into three major groups; microphytoplankton (20 to 200 µm), nanophytoplankton (3 to 20 µm) and PP (0.2 to 3 µm). PP, the smallest group of phytoplankton forms a major component of phytoplankton in both marine and freshwater including nutrient rich to poor

ecosystems (Shiomoto et al., 1997), contributing significantly to primary productivity and total phytoplankton biomass (Paerl, 1977; Azam et al., 1983). Based on pigment composition PP is further classified into two major groups of cyanobacteria, *Prochlorococcus* (*PRO*) and *Synechococcus* (*SYN*), and small eukaryotes known as picoeukaryotes (PEUK). Amongst these, *SYN* was the first group to be studied in detail (Waterbury et al., 1979). They are rod to coccoid shaped organisms, with size ranging from 0.8 to 1.5 µm and divide by binary fission into equal halves in one plane (Holt et al., 1994). They possess photosynthetic thylakoid membranes positioned peripherally with the absence of structured sheaths (Waterbury and Rippka, 1989). They are the dominant phycobilisome-containing cyanobacteria found in all types of aquatic ecosystems from freshwater to marine, generally being more abundant in nutrient-rich than oligotrophic regions. They contribute up to 20% of global marine carbon fixation (Li, 1994), thereby playing an important part in pelagic food-web structure via energy transfer within the microbial loop through heterotrophic nanoflagellate and ciliate grazing, especially in the oligotrophic regions (Azam et al., 1983; Chiang et al., 2013). Approximately 35 to 100% of the *SYN* standing stock can be grazed per day by these organisms (Campbell and Carpenter, 1987).

Based on phycobilisome composition, *SYN* is classified into two groups; one containing phycoerythrin (PE; *SYN*-PE) and the other phycocyanin (PC; *SYN*-PC) as major accessory pigment. Former group is present in all kinds of aquatic systems whereas latter is present only in freshwater and estuarine environments. Based on PE fluorescence intensity, different clades of *SYN*-PE have been observed in the Mississippi River plume (Liu et al., 2004) and Pearl River estuary (Lin et al., 2010; Partensky et al., 1999). These different clades of *SYN*-PE are a result of variation in the two chromophores, i.e., phycoerythrobilin (PEB) (λ_{AbsMax}= 540-570 nm) and

phycourobilin (PUB) (λ_{AbsMax}= 495-500 nm) that attach to the light-harvesting pigment phycoerythrin (Glazer, 1985). In general, PUB rich populations are present only in oceanic waters whereas PEB rich populations dominate the mesotrophic or coastal waters. PUB : PEB ratios show increasing trend with depth of water column (Lantoine and Neveux, 1997). Generally, *SYN*-PE group abundance is high in clear waters whereas *SYN*-PC is higher in turbid waters (Stomp et al., 2007). In the clear waters, short wavelength blue light tends to penetrate deepest, whereas in turbid waters blue and red light are considerably decreased and green light shows the maximum transmission (Li et al., 1983; Wood et al., 1985). This variation of light quality is one of the factors for altering the PP composition in oceanic, coastal and estuarine waters (Wood et al., 1985; Scanlan, 2003). It reflects the importance of the blue green light on the PP accessory pigments (Wood et al., 1985; Scanlan, 2003).

Discovery of *PRO* (Chisholm et al., 1988) was a breakthrough in biological oceanography research. It is the smallest (0.2 to 0.8 µm) known photoautotrophic organism that is capable of flourishing in the oligotrophic regions and are accountable for a high percentage of oxygen through photosynthetic production. They are coccoid shaped, non-motile and free-living cells, which are the most abundant photosynthetic organism on the planet, with approximate global population of ~10^{27} cells (Partensky et al., 1999; Schattenhofer et al., 2009; Flombaum et al., 2013). They account for 50% of the total chl in most of the surface oceans (Partensky et al., 1999). Thus, it has been estimated to produce 4 gigatons of fixed carbon each year (Flombaum et al., 2013). It has been found to be ubiquitous between 40°N and 40°S, mostly in a temperature range of 10 to 33ºC (Partensky et al., 1999). It has a unique light-harvesting complex, consisting predominantly of divinyl derivatives of chl *a* (chl *a*2) and *b* (chl *b*2) (Ting et al., 2002). It lacks monovinyl chl and phycobilisomes (Ting et

al., 2002). This unique pigment increases the absorption of blue light, which is the dominant wavelength in deep waters. It is the only phytoplankton known to absorb more light than it scatters (Morel et al., 1993). Therefore, some strains can grow at deeper depths in the water column (deep as 150 to 200 m; Partensky et al., 1999), where light penetration is < 1% and defines the lower limit of photosynthetic life in the ocean. *PRO* consist of two groups, the low light (LL) and high light (HL) adapted, which vary in pigment ratios (Partensky et al., 1999; Zinser et al., 2009). LL group has a high ratio of chl *b*2 : *a2* and occupies deeper depths whereas HL group has a low ratio of chl *b*2 : *a*2 and occupies shallower depths. The higher chl *b* to *a* ratio enables the LL group to absorb blue light (Chisholm et al., 1988; Goericke and Repeta, 1992), which penetrates deeper oceanic waters and can reach depths of > 200 m. Thus, enabling *PRO* to survive at depths of up to 200 m (Olson et al., 1990). Their smaller size and large surface-area-to-volume ratio, gives them an advantage in oligotrophic condition (Raven, 1998). They are believed to assimilate reduced nitrogen source (ammonium) rather than nitrate (Raven, 1998). However, it is assumed that *PRO* have a very small nutrient requirement (Biller et al., 2015).

The third group, PEUK are also ubiquitous in aquatic ecosystems. In general, PEUK abundance reach 10^3 cells ml^{-1} in oligotrophic waters, and in coastal waters 10^4 cells ml^{-1} or more (Massana, 2011). Although PEUK are less abundant compared to the above two genera, their relative importance in PP biomass in the coastal waters is higher (Shapiro and Guillard, 1986). In the open ocean, they are generally much less abundant than *PRO*, and similar in magnitude or lower than *SYN*. However, they can co-vary with *SYN*, while they do not with *PRO* (Worden et al., 2004). Due to their high cell-specific carbon uptake rates and high carbon content, their contribution to carbon fixation is substantial (Zubkov et al., 2000; Worden, 2006). In the oligotrophic

waters, PEUK forms a large portion of the primary producer biomass amongst the PP. However, based on abundance, they appear much less important than *PRO* and *SYN* (Li, 1994; Li et al., 1992).

PEUK size ranges from 1 to 3 µm and belong mainly to three divisions, Chlorophyta, Heterokonta, and Haptophyta. They possess chl as their major light harvesting system. They can be either autotrophic or heterotrophic, and generally contain lesser number of organelles. For example, species belonging to class Bicosoecida (heterotrophic) contain two mitochondria, one food vacuole and a nucleus. An autotrophic PEUK belonging to the class Prasinophyceae, *Ostreococcus tauri*, contains only the nucleus, one mitochondrion and one chloroplast (Moreira and Lopez-Garcia, 2002). Generally, higher PEUK abundance have been found in higher nitrate and phosphate concentration conditions (Worden et al., 2004; Jing et al., 2010). Therefore, in the open ocean, these groups show increasing trend with depth and higher concentration is observed in the subsurface waters, even in deep chl maximum (Massana, 2011). In the Arabian Sea, PEUK contributed 29 to 60% to the total PP biomass, and 18 to 33 % to the total phytoplankton biomass (Shalapyonok et al., 2001). Generally, PEUK are grazed at a rate between 0.71 to 1.29 day^{-1} (Brown et al., 1999). Due to the difficulty in the analysis of the small sized PP, it has been ignored in many phytoplankton studies. But with the use of flow cytometer, observations on PP has been made less laborious and more accurate with statistically significant results as compared to epifluorescence microscopy.

The response of these PP groups to the hydrographic conditions varies under different environmental conditions such as riverine, estuarine, coastal, and oceanic ecosystems (Partensky et al., 1999; Murrell and Lores, 2004; Mitbavkar and Anil, 2011). PP often dominate high-temperature conditions (Agawin et al., 1998; Chen et

al., 2014). They tend to grow better at high temperature than other phytoplankton in estuarine and freshwater environments (Ray et al., 1989; Qiu et al., 2010). In sub-tropical and temperate estuaries, PP contribution was restricted to < 10% when water temperature was < 20^{o}C and subsequently increased to > 50% at higher temperatures (> 20^{o}C, Ray et al., 1989, Caroppo, 2000, Buchanan et al., 2005, Qiu et al., 2010). Phytoplankton size structure, among other factors, also depends on the maximum growth rate of the different groups of phytoplankton (Irwin et al., 2006). A general trend of an increase in relative *SYN* and PEUK abundance with increasing water temperature due to the higher activation energy of their growth rates than that of larger phytoplankton has been reported (Chen et al., 2014). In estuarine environments, salinity plays a major role in the spatial and temporal variation in PP community structure and abundance (Ray et al., 1989). Previous studies have suggested that salinity plays an important role in the spatial distribution of *SYN* where PE rich *SYN* dominates high saline waters whereas, PC rich *SYN* are abundant in lower saline waters (Murrell and Lores, 2004).

Coastal and estuarine waters are the most productive regions in the world, especially estuarine ecosystems. These ecosystems are important for millions of interacting organisms, including fishes. The studies on phytoplankton community structure are well documented and mostly focused on larger phytoplankton (Madhu et al., 2009; Marshal, 2009; Patil and Anil, 2011; Patil and Anil, 2015). PP are now being highlighted as an important component of phytoplankton in coastal and estuarine regions of temperate, subtropical and tropical latitudes (Sin et al., 2000; Gaulke et al., 2010; Zhang et al., 2013) contributing substantially to the total biomass and primary production. However, the only couple of reports is from Indian coastal

and estuarine waters (Mitbavkar and Anil, 2011; Jyothibabu et al., 2013; Mitbavkar et al., 2015; Anas et al., 2015; Mohan et al., 2016).

Information on PP are well established in the Pacific and Atlantic Oceans (Kazuhiko et al., 2004; Yves and Awa, 2007) and least studied in the Indian Ocean (Campbell et al., 1998; Brown et al., 1999; Shalapyonok et al., 2001) especially in the eastern Arabian Sea (Roy et al., 2015; Ahmed et al., 2016). Since PP is known to occur in high numbers and contributes significantly to the total phytoplankton biomass in oceanic and coastal regions, it is worthwhile to understand their distribution in response to the prevailing environmental factors on temporal and spatial scales. Also, high frequency sampling will provide the knowledge of population behavior on shorter time scales with respect to environmental conditions. Since, not much information is available from Indian waters, it is essential to understand their distribution patterns and its contribution to the total phytoplankton biomass in coastal and oceanic waters of India. Such studies will improve the knowledge about their role in the food web of the waters surrounding India. Also, monsoon plays an important role in the environmental set up of Indian estuarine, coastal and oceanic regions. PP dynamics in such environments could be different from other tropical, subtropical and temperate regions. Therefore, understanding the ecology of PP under various environmental conditions is important. In view of this, the present study was undertaken to investigate the PP community structure and its response to hydrographic conditions on temporal (fortnightly, monthly and seasonal) and spatial basis around the Indian waters. Different environments such as oceanic, coastal, estuarine and riverine ecosystems encompassing varied trophic status of waters such as oligotrophic, mesotrophic, eutrophic and hypertrophic were included in the present study. Thus, the present study will give an overall information about the

distribution and importance of PP groups and their relation to environmental factors in estuarine, coastal and oceanic waters of India.

Objectives of the present study

1. Picophytoplankton community structure and its contribution to the total phytoplankton biomass in the Zuari estuary.
2. Picophytoplankton community structure under different environmental settings along the coast of India.
3. Picophytoplankton community structure from eastern Arabian Sea.
4. Influence of salinity on the picophytoplankton groups through laboratory experiments.

Chapter 2

Picophytoplankton community structure and its contribution to the total phytoplankton biomass in the Zuari estuary

2A Picophytoplankton community dynamics during fortnightly spring and neap tides in a monsoonal estuary

2A.1 Introduction

Estuaries, one of the most productive natural habitats in the world, are exposed to short term physical forcing from both marine influences such as tides, waves, and influx of saline water; and riverine influences such as fresh water and sediment discharges (Cloern and Nichols, 1985). Amongst these, tides are the major controller of the hydrographic variations (Shetye and Murty, 1987) affecting biological productivity, water quality, material transport and dispersion (Kasai et al., 2010; Long et al., 2012). Salt water intrusion, due to tidal activity, lead to a gradient of increasing salinity from the downstream to upstream, which has intense effect on the estuarine ecosystem (Stephens and Imberger, 1996), thus, reducing the species diversity (Telesh et al., 2011). The extent of salt water intrusion varies with tidal phases i.e. spring (ST) and neap (NT) tides, with higher intrusion during ST compared to NT. This brings fortnightly changes in hydrographic conditions in the estuarine ecosystem (Balch, 1981), consequently influencing the organisms inhabiting therein (Zhou et al., 2016). Since estuarine environments are recognised as potential fishery zones (Gillanders et al., 2003), the understanding of phytoplankton dynamics during different tidal phases is important.

Phytoplankton are important primary producers fuelling the food webs of estuarine ecosystems. Their growth, community structure and diversity in the estuarine ecosystem is known to be influenced by tide induced changes in physico-chemical factors such as water column stability (mixed and stratified water column) (Paerl et al., 2007), turbidity (Phlips et al., 2012; Chen et al., 2016), nutrient concentration (Madhu et al., 2009; Qiu et al., 2010), amount of river discharge (Sarma

et al., 2009; Patil and Anil, 2015) and water residence time (Lu and Gan, 2014). The above factors have variable influence on phytoplankton, depending on the size classes (Gaulke et al., 2010; Qiu et al., 2010). Smaller phytoplankton i.e., picophytoplankton (cell size < 3 µm; PP) are now being highlighted as an important component of phytoplankton in coastal and estuarine regions (Gaulke et al., 2010; Qiu et al., 2010; Contant and Pick, 2013; Mitbavkar et al., 2015). Amongst the PP groups, *Prochlorococcus (PRO)* is restricted to oligotrophic waters (Partensky et al., 1999). However, recently *PRO*-like cells were identified in the low salinity waters (Shang et al., 2007). *Synechococcus (SYN)* has received much attention in previous studies due to its higher abundance in the coastal and estuarine regions. Two types of *SYN* are recognised in the estuarine environment based on pigment composition i.e., *SYN* containing phycoerythrin (PE), which is a high saline species and the other containing phycocyanin (PC), which is a low saline species (Murrell and Lores, 2004). The third group, picoeukaryotes (PEUK) are generally less abundant compared to the above two genera. However, its relative importance increases in the coastal waters as compared to the open ocean (Johnson and Sieburth, 1982; Shapiro and Guillard, 1986).

The Indian tropical estuaries are influenced by the southwest monsoon (SWM) with higher freshwater discharge during monsoon (MON) compared to the non-MON seasons, which makes these tropical estuaries different compared to other estuaries (Vijith et al., 2009). Thus, the annual variation in hydrodynamics is mainly controlled by the freshwater discharge and tides during MON and tidal activity during non-MON periods. As a result, during MON, the estuary is stratified whereas during non-MON it is vertically homogenous (Qasim and Sen Gupta, 1981; Shetye and Murty, 1987). In these waters, phytoplankton show wide seasonal changes in species composition and abundance (Patil and Anil, 2011; Pednekar et al., 2011) with occasional

phytoplankton blooms (Patil and Anil, 2015). Some studies are also available on the PP community structure in such environments (Mitbavkar and Anil, 2011; Mitbavkar et al., 2015; Anas et al., 2015; Mohan et al., 2016), which shows that salinity variation, water column stability and freshwater discharge affect the PP growth, community structure and its distribution. However, these studies have mainly focused on their temporal and spatial variations, with inferences drawn from monthly samplings. There are reports on larger phytoplankton community structure and their regulation mechanisms during fortnightly tidal phases (ST and NT) in temperate and subtropical estuaries, with higher stratification during NT favouring relatively higher phytoplankton production than during disturbed ST (Holligan and Harbour, 1977; Domingues et al., 2010; Blauw et al., 2012; Zhou et al., 2016). Since the intensity of tidal activity during ST and NT is modulated by the influx of freshwater discharge which varies seasonally and spatially, the effect on PP will differ along the estuary and over the seasons. Our objective was to assess the seasonal and spatial response of PP distribution with respect to ST and NT on a fortnightly scale. Since PP is favoured by stratification, we hypothesised that the water column conditions during NT will favour the growth of PP as compared to ST.

2A.2 Materials and Methods

2A.2.1 Description of the study region

The Zuari River is one of the largest river in Goa, located along the central west coast of India (Fig. 2A.1; Table 2A.1). It originates at Hemad-Barshen in the Western Ghats and flows up to the Arabian Sea with a length of 65 km and several rivers drains in to the estuary upstream. The average depth of this estuary is ~ 5 m with a catchment area of 1152 km^2 and a width of 5 km at the mouth which decreases towards the head (0.05 km) (Shetye et al., 2007). The annual cycle is classified into 3

seasons, based on the physiochemical characteristics, i.e. June to September – MON season; October to January - post-monsoon (PM) season; and February to May - pre-monsoon (PrM) season. Strong influence of SWM leads to high river discharge, exceeding 400 $m^3 s^{-1}$ during MON whereas rest of the year it is < 10 $m^3 s^{-1}$ (Shetye and Murty, 1987). The huge quantity of freshwater discharge during MON results in drastic changes in physiochemical characteristics of the water column whereas in the remaining period tidal flow dominates (Qasim and Sen Gupta, 1981). This is a mesotidal estuary, which experiences semidiurnal tide with the highest tidal height of 2.5 m during ST and ~ 1 m during NT (Manoj and Unnikrishnan, 2009).

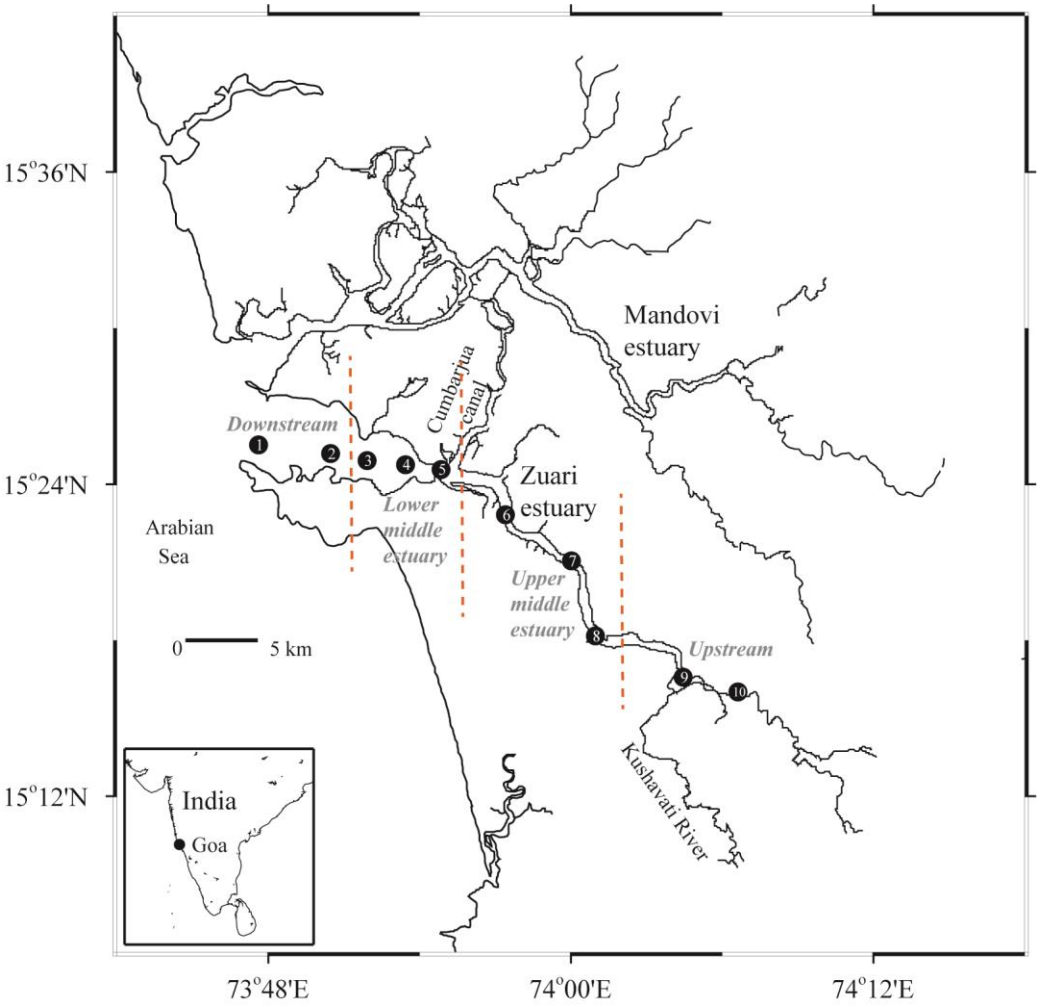

Fig. 2A.1 Sampling stations located in the Zuari estuary, west coast of India.

Table 2A.1 Details of sampling stations in the Zuari estuary

Station No.	Station name	Latitude (N)	Longitude (E)	Distance from mouth (km)	Approximate depth (m)
1	Marmugao	15° 25' 16.9"	73° 47' 36.9"	0	16
2	Chicalim	15° 25' 8.5"	73° 47' 22.4"	5.8	5
3	Island	15° 25' 57.4"	73° 47' 57.0"	8.6	5
4	Sancoale	15° 25' 45.1"	73° 47' 30.6"	11	7.1
5	Cortalim	15° 25' 32.0"	73° 47' 50.2"	13	9.6
6	Loutulim	15° 25' 54.0"	73° 47' 24.4"	19.7	10.5
7	Borim	15° 25' 03.6"	73° 47' 58.0"	23.9	12.9
8	Shiroda	15° 25' 12.3"	73° 47' 55.5"	31.4	9.1
9	Kushavati	15° 25' 31.7"	73° 47' 28.3"	38.4	9.9
10	Sanvordem	15° 25' 01.1"	73° 47' 36.0"	42.2	4.9

2A.2.2 Sampling

Fortnightly sampling was carried out in the Zuari estuary during NT and ST phases, from January 2010 to April 2012 (Table 2A.2). Surface and near-bottom water (NBW) samples were collected from 10 stations (S) with a Niskin sampler (Fig. 2A.1; Table 2A.1). Based on the distance from estuarine mouth, stations are demarcated as the downstream (S1 to S2), lower middle estuary (S3 to S5), upper middle estuary (S6 to S8) and upstream (S9-S10) (Table 2A.1). Generally, sampling was carried out during mid tide at S1 during both the tidal phases. As sampling continued, high tide was observed while sampling in the upper middle estuary during ST whereas during NT, low tide was observed in middle estuary, except on some occasions (Fig. 2A.3a and b). Vertical profiles of temperature and salinity were determined using portable seabird CTD (SBE 19 plus). Stratification parameter (ΔS) was calculated using salinity data of surface and NBW for the entire study period. Tidal height was estimated from the tidal range for the respective sampling time. Water transparency was measured with a secchi disk (SD). Rainfall data for the study period were acquired from the Indian Meteorological Department (IMD) (Table 2A.2). Solar radiation (SR) was obtained from CSIR-National Institute of Oceanography, Dona Paula, Goa.

Table 2A.2 Rainfall data for the sampling days (48 h) during neap and spring tides

	Neap tide		Spring tide	
Sr. No	Date (d-m-y)	Rainfall (mm)	Date (d-m-y)	Rainfall (mm)
1	22-Jan-10	0	3-Jan-10	0
2	8-Feb-10	0	29-Jan-10	0
3	10-Mar-10	0	3-Mar-10	0
4	9-Apr-10	0	1-Apr-10	0
5	7-May-10	0	29-Apr-10	0
6	8-Jun-10	69.8	27-Jun-10	292.4
7	19-Jul-10	157.7	13-Jul-10	0.9
8	18-Aug-10	132.8	11-Aug-10	51.7
9	17-Sep-10	78.5	10-Sep-10	46.3
10	16-Oct-10	0.4	23-Oct-10	55.4
11	12-Nov-10	7	6-Nov-10	13
12	13-Dec-10	0	6-Dec-10	0
13	10-Jan-11	0	20-Jan-11	0
14	11-Feb-11	0	18-Feb-11	0
15	29-Mar-11*	0	21-Mar-11	0
16	27-Apr-11	0	19-Apr-11	0
17	27-May-11	0	20-May-11*	0
18	27-Jun-11	61.2	16-Jun-11	99.5
19	25-Jul-11	4.2	15-Jul-11	92.2
20	24-Aug-11	11.8	1-Aug-11*	32
21	22-Sep-11	6.4	27-Sep-11	0
22	21-Oct-11*	0	29-Oct-11*	11.6
23	19-Nov-11	0	25-Nov-11	0
24	16-Dec-11	0	23-Dec-11	0
25	17-Jan-12	0	23-Jan-12	0
26	16-Feb-12	0	8-Feb-12	0
27	16-Mar-12	0	9-Mar-12	0
28	16-Apr-12	0	9-Apr-12	0

* Samples were collected from 4 stations (Station 1, Station 5, station 7 and station 10)

For chlorophyll *a* (chl *a*) estimation, known volume (500 mL) of seawater sample was filtered through a Whatman GF/F filter and immediately placed in a dark vial containing 90% acetone. After extraction in the dark at 4ºC for 24 h, chl *a* was determined on a Turner Design Triology fluorometer calibrated with commercial chl *a* (Parsons et al., 1984). Nutrients [nitrate (NO_3^-), phosphate (PO_4^{3-}), nitrite (NO_2^-) and silicate (SiO_4^{4-})] were analyzed by SKALAR SAN^{plus} ANALYSER. Seawater

samples for PP analysis were preserved with paraformaldehyde (0.2% final concentration), quick frozen in liquid nitrogen and stored at -80°C until analysis.

2A.2.3 Flow cytometric analysis of picophytoplankton

Samples stored for PP analysis were thawed and analysed using flow cytometer (FACS Aria II) equipped with blue (488 nm) and red (630 nm) lasers. Samples were run in log mode and 10000 events were acquired at a speed of 40-80 µl min^{-1}. Flow cytometeric data on forward angle light scatter (FALS), right angle light scatter (RALS), red fluorescence from chl (> 650 nm) and phycocyanin (630 nm) and orange fluorescence from phycoerythrin (564-606 nm) was recorded for individual particles as they pass through a laser. BD FacsDiva (Version 6.2) software was used to process the data obtained. The different PP groups present in the sample was discriminated based on their scattering and specific fluorescence properties. To calibrate the cell fluorescence emission and light scatter signals, yellow green latex beads of 2 µm (polysciences co., USA) were used as internal standards, which permitted us to compare fluorescence and cell size among different samples. Based on flow cytometric signatures, two groups of *SYN* were distinguished: one rich in phycoerythrin (*SYN*-PE) and the other in phycocyanin (*SYN*-PC) throughout the study period. RALS and FALS (proxy for cell size) signals revealed that the cell size of *SYN*-PC is bigger than *SYN*-PE whereas chlorophyll fluorescence is comparable with *SYN*-PE (Fig. 2A.2). The *SYN*-PE group was further differentiated into 2 subgroups based on the PE fluorescence intensity and was designated as *SYN*-PEI which had a lower fluorescence intensity and *SYN*-PEII with a comparatively higher fluorescence intensity. Another group of *SYN*-PE whose flow cytrometric signatures were similar to *SYN*-PEI but which was found only in freshwater was designated as *SYN*-PEIII. The PEUK group comprised of two subgroups based on the intensity of the chl

fluorescence wherein one possessed lower fluorescence (PEUK-I) than the other (PEUK-II). Compared to PEUK, cells with smaller size and lower chl fluorescence were designated as *PRO*-like cells.

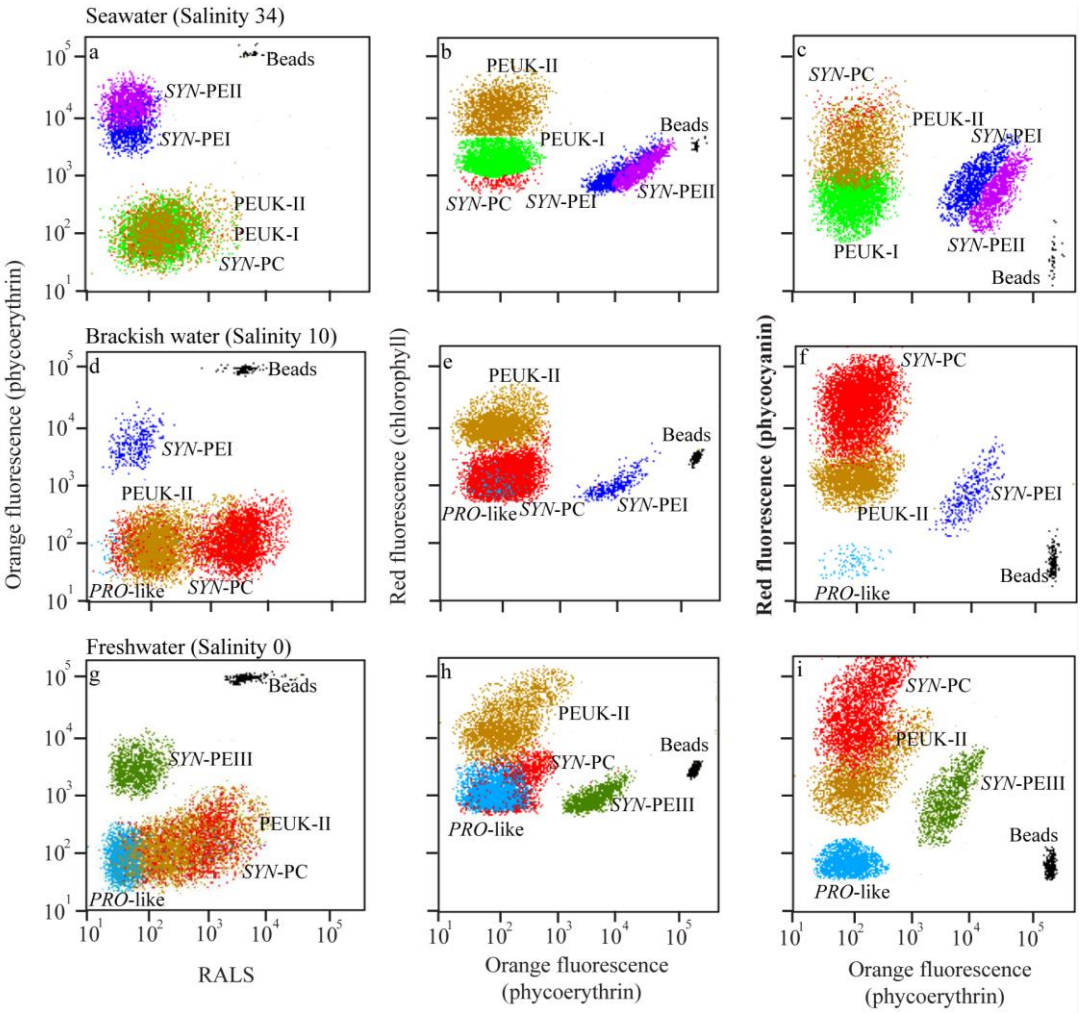

Fig. 2A.2 Flow cytometric analysis of picophytoplankton community from (a-c) seawater, (d-f) brackish water, and (g-i) freshwater of Zuari estuary.

2A.2.4 Data analyses

Three-way analysis of variance (ANOVA) was used to assess the significant variations in cell abundance (log (x+1)) of the PP groups with respect to tidal phases (ST and NT), stations and depth using SPSS statistics 16.0 with the significance level of $p < 0.05$. Redundancy analysis (RDA) was used to assess the relationship between PP groups, chl *a* and environmental factors. RDA biplot depicts how closely

environmental variables are associated with PP groups. The length of an environmental arrow indicates the importance of the variable with respect to PP group and chl *a*. Above analysis was performed using Canoco version 4.5 (Ter Braak and Smilauer, 2002). Regression analysis was performed to assess the relationship of PP groups and chl *a* with tidal height and of *SYN*-PC: *SYN*-PE ratio with salinity during stratified conditions.

2A.3 Results

2A.3.1 Environmental parameters

During PrM's, water column temperature gradually increased from February (27.45 ± 0.5°C) to May (31.87 ± 0.9°C), with higher temperature during NT ($p < 0.05$) (Fig. 2A.3c-f). After the onset of rainfall, temperature dropped (27.5 ± 0.7°C) and varied significantly ($p < 0.05$) between ST and NT. During PM's, water temperature increased in October and gradually decreased by January. Salinity was higher (34.9 ± 0.42) during PrM (Fig. 2A.3g-j). During ST, water column was mixed and the salt water intrusion covered ~ 10 km more distance than that in the NT, where water column was partially mixed in the lower and upper estuary. Therefore, ST showed significantly higher salinity compared to NT at any particular station ($p < 0.05$). During MON, higher precipitation and freshwater runoff led to lower salinity at the estuarine mouth resulting in stronger stratification downstream and lower middle estuary (Fig. 2A.3k and l). A break in MON (July-10, ST) increased the salinity in the downstream. During MON-II, water column was less stratified compared to MON-I which could be due to higher rainfall during MON-I (905.9 mm) compared to MON-II (318.2 mm) (Table 2A.2). Stratified condition in the downstream continued in October-10 due to rainfall. During PMs, the freshwater discharge reduced and the

seawater intrusion towards the upstream gradually increased from November to May, with higher ($p < 0.05$) salinity during ST. Water transparency was higher (1.65 ± 0.83 m) during non-MON seasons, with consistently higher values during NT compared to ST ($p < 0.05$) in the middle estuary (Fig. 2A.3m and n). During MON, water transparency dropped and increased during MON breaks. SR was high during PrM seasons followed by PM and MON (Fig. 2A.3o and p). Since sampling was carried out in the morning, lower SR was observed in the downstream. During PrMs, chl *a* increased from February to May, with higher values upstream (Fig. 2A.3q-t) and with higher concentration ($p < 0.05$) during NT except on some occasions. During MON, decreasing trend in chl *a* concentration was observed from downstream to upstream, with higher ($p < 0.05$) concentration during MON-I. Highest values were recorded at S3, lower middle estuary (12.60 µg L^{-1}) in August-10, ST. During PM, chl *a* was higher during PM-I compared to PM-II with increasing concentration from October to January.

Nutrient (NO_3^-, PO_4^{3-}, SiO_4^{4-}) concentrations were higher during MON except NO_2^-, which was higher during PrM (Fig. 2A.4a-p). Significant variation in NO_3^- concentration was observed between ST and NT, only during MONs ($p < 0.05$) due to the fluctuation in rainfall. Increased NO_3^- concentration (6.19 ± 2.97 µM) was observed in October, which gradually decreased in the following months. PO_4^{3-} decreased from downstream to upstream during MON, whereas during non-MON no trend was observed (Fig. 2A.4e-h). Its concentration (1.15 ± 0.36 µM) was higher during PrM-III, compared to other PrMs. PO_4^{3-} increased before MON shower (May) and further increased after the onset of MON. Insignificant variation ($p > 0.05$) in PO_4^{3-} concentration was observed in ST and NT. Generally, NO_2^- and SiO_4^{4-} increased from downstream to upstream, except during MON, where opposite trend was

observed (Fig. 2A.4i-p). Only during PrM, NO_2^- was higher ($p < 0.05$) during ST. SiO_4^{4-} was significantly higher ($p < 0.05$) during NT of MON and PM. Nutrients (NO_3^-, PO_4^{3-}, and SiO_4^{4-}) did not show significant variation between surface and NBW.

2A.3.2 Intra and inter-seasonal variation of picophytoplankton during spring and neap tides

SYN-PEI and PEII abundance exhibited a significant decreasing ($p < 0.05$) trend from downstream to upstream. During PrM, their abundance decreased from February to May, except *SYN*-PEI in NT (Fig. 2A.5a-h). Generally, *SYN*-PEI abundance was significantly ($p < 0.05$) higher during NT (except in February) and *SYN*-PEII during ST (except in May-11). Highest abundance of *SYN*-PEI ($5.8 \pm 2.3 \times 10^4$ cells mL^{-1}) and PEII ($11.92 \pm 0.11 \times 10^4$ cells mL^{-1}) were observed in May-11 (NT). *SYN*-PEI was also high in April-12 (at S6; $15.5 \pm 1.1 \times 10^4$ cells mL^{-1}). With the onset of rainfall, their abundance reduced drastically by an order of magnitude (*SYN*-PEI: $< 0.8 \times 10^4$ cells mL^{-1}; *SYN*-PEII: $< 0.2 \times 10^4$ cells mL^{-1}) throughout the estuary. Increased *SYN*-PEI abundance was observed up to S6 in July-10 which coincided with the MON break. Generally, in both MONs their abundance was low except *SYN*-PEI in September-10 (38.4×10^4 cells mL^{-1}) and August-11 (9×10^4 cells mL^{-1}). *SYN*-PEII abundance was significantly ($p < 0.05$) higher in NBW. In October-10 (PM-I) NT, a prominent rise in cell abundance was observed which declined in subsequent months during NT, except *SYN*-PEII in ST. Compared to PM-I, their cell abundance was low during PM-II. In January, their abundance was higher during ST compared to NT. *SYN*-PEIII was observed at the upstream during the study period (Fig. 2A.5i-l). The abundance was maximum during PrMs and significantly ($p < 0.05$) higher in NT.

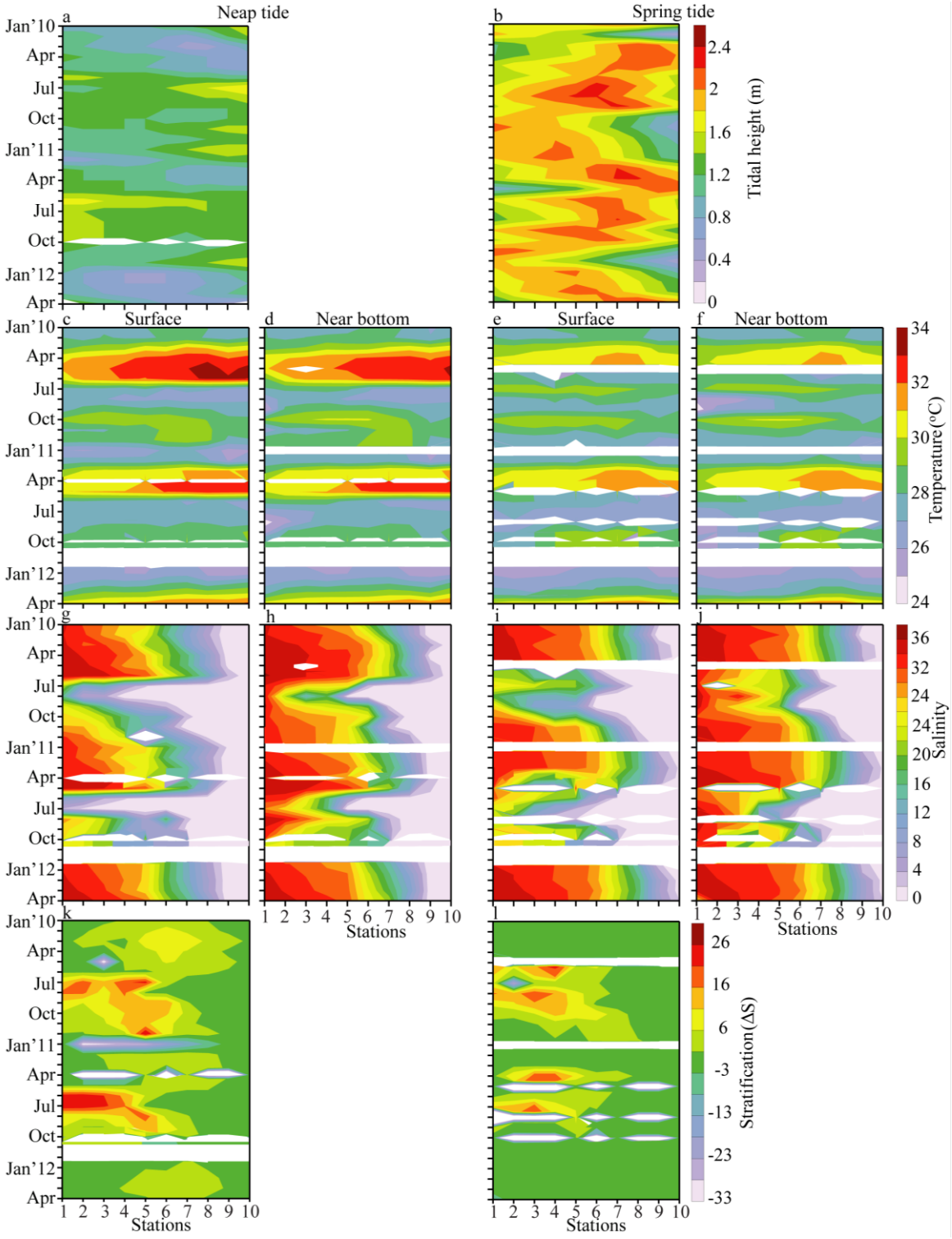

Fig. 2A.3 Temporal and spatial variations in (a, b) tidal height, (c-f) temperature, and (g-j) salinity, (k, l) stratification parameter, (m, n) secchi disk depth, (o, p) solar radiation, and (q-t) chl *a*, during neap and spring tides.

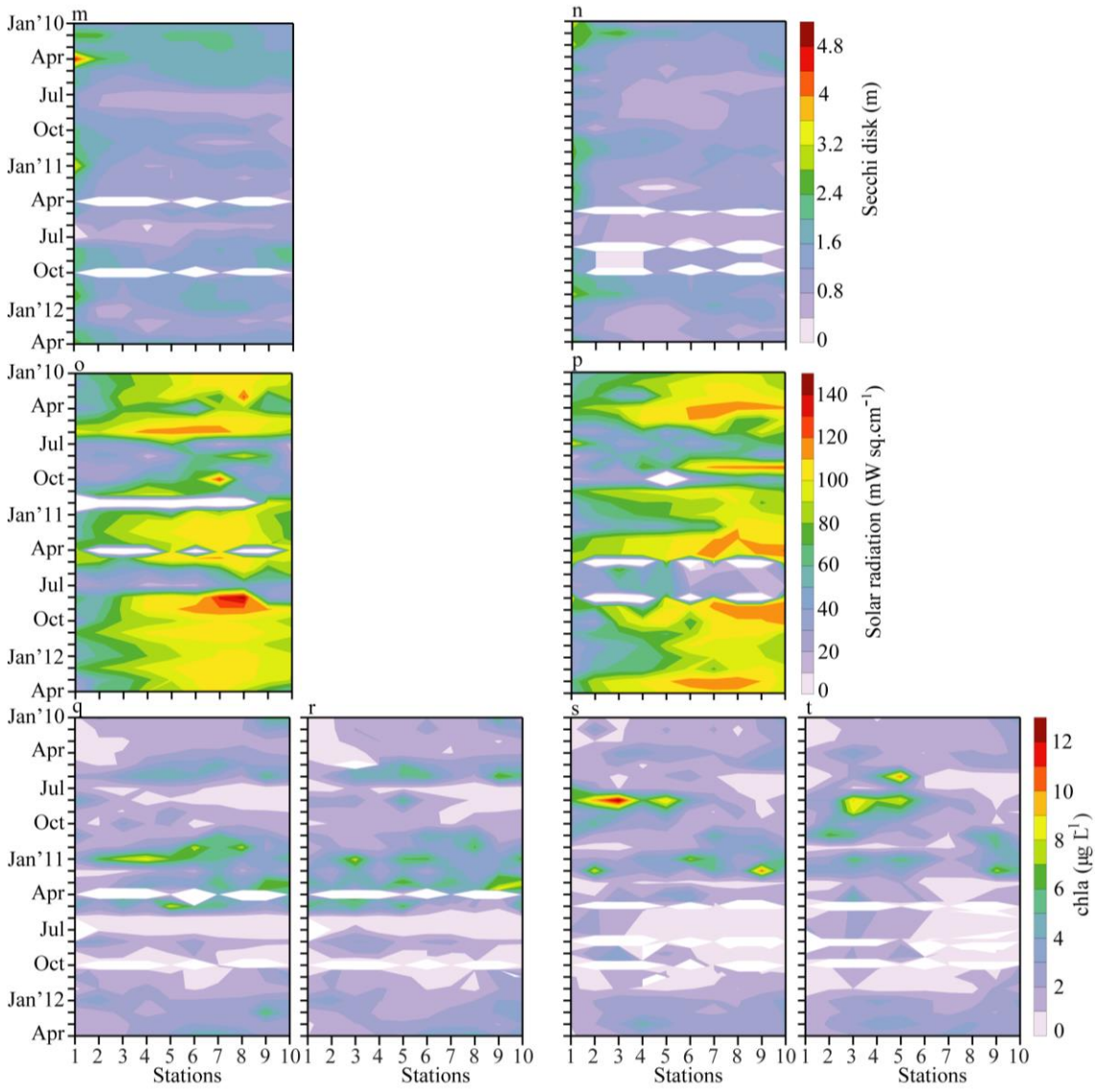

Fig. 2A.3 continued

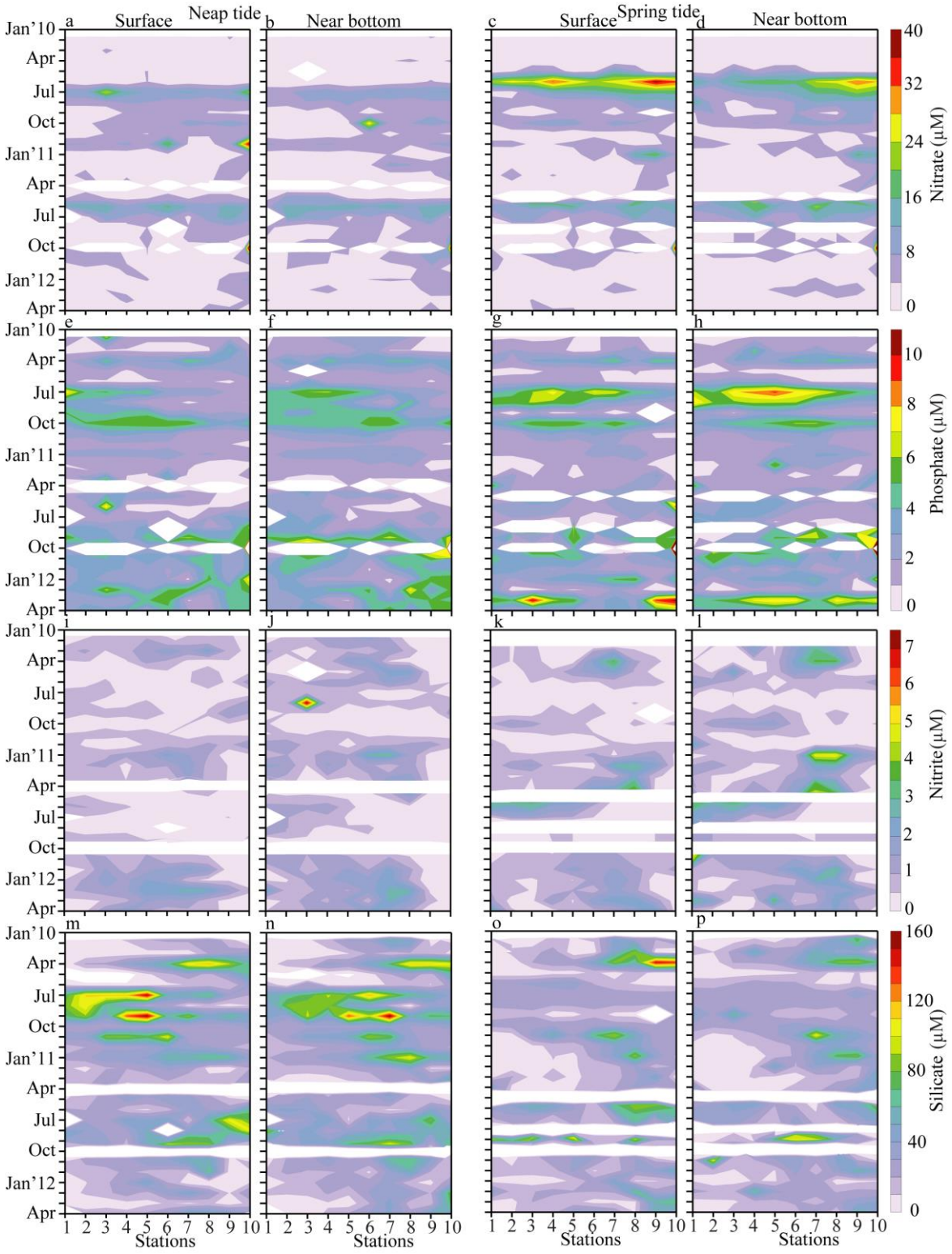

Fig. 2A.4 Temporal and spatial variations in the concentration of (a-d) nitrate, (e-h) phosphate, (i-l) nitrite and (m-p) silicate during neap and spring tides.

After the onset of MON, abundance declined; and it was observed from the middle estuary. Lower abundance continued into the PM's. From November-10, abundance started increasing (> 1.3×10^4 cells mL^{-1}) during PM-I whereas during PM-II it continued to be low.

SYN-PC abundance gradually increased from February to May with consistently ($p < 0.05$) higher abundance during NT, in surface waters (Fig. 2A.5m-p). Generally, during PrMs abundance progressively increased towards the upstream with the highest abundance at S10 during ST whereas, during NT cell abundance showed increasing trend up to upper middle estuary, which subsequently dropped. With the onset of MON, abundance declined (< 1.0×10^4 cells mL^{-1}), with higher abundance in downstream and lower middle estuary. In July-10 and August-10, the abundance increased in the downstream during ST. Generally during MON, *SYN*-PC abundance was significantly ($p < 0.05$) higher in the surface. The abundance was low (< $2.43 \pm 1.52 \times 10^4$ cells mL^{-1}) during MON-II in both the tidal phases. During PM, in October, higher abundance was observed in lower and upper middle estuary during NT, followed by decrease in following months; and increased in January. During this period, significantly ($p < 0.05$) higher abundance was observed in ST.

Among PEUK, PEUK-I was observed only in January-11 and May-11 (Fig. 2A.5q and r). During PrM, PEUK-II abundance increased from February to May with higher abundance in the upper middle estuary (Fig. 2A.5s-v). During PrM-I, cell abundance was lower compared to that in the PrM-II and PrM-III. The highest abundance of PEUK-I was in May-11 (NT) and PEUK-II in May-11 (NT) and April-12 (NT). The abundance was significantly ($p < 0.05$) higher during NT. After the onset of MON, PEUK-II abundance (< 1.5×10^4 cells mL^{-1}) drastically declined in both tidal phases. Since MON effect continued in October-10 (PM-I), the abundance

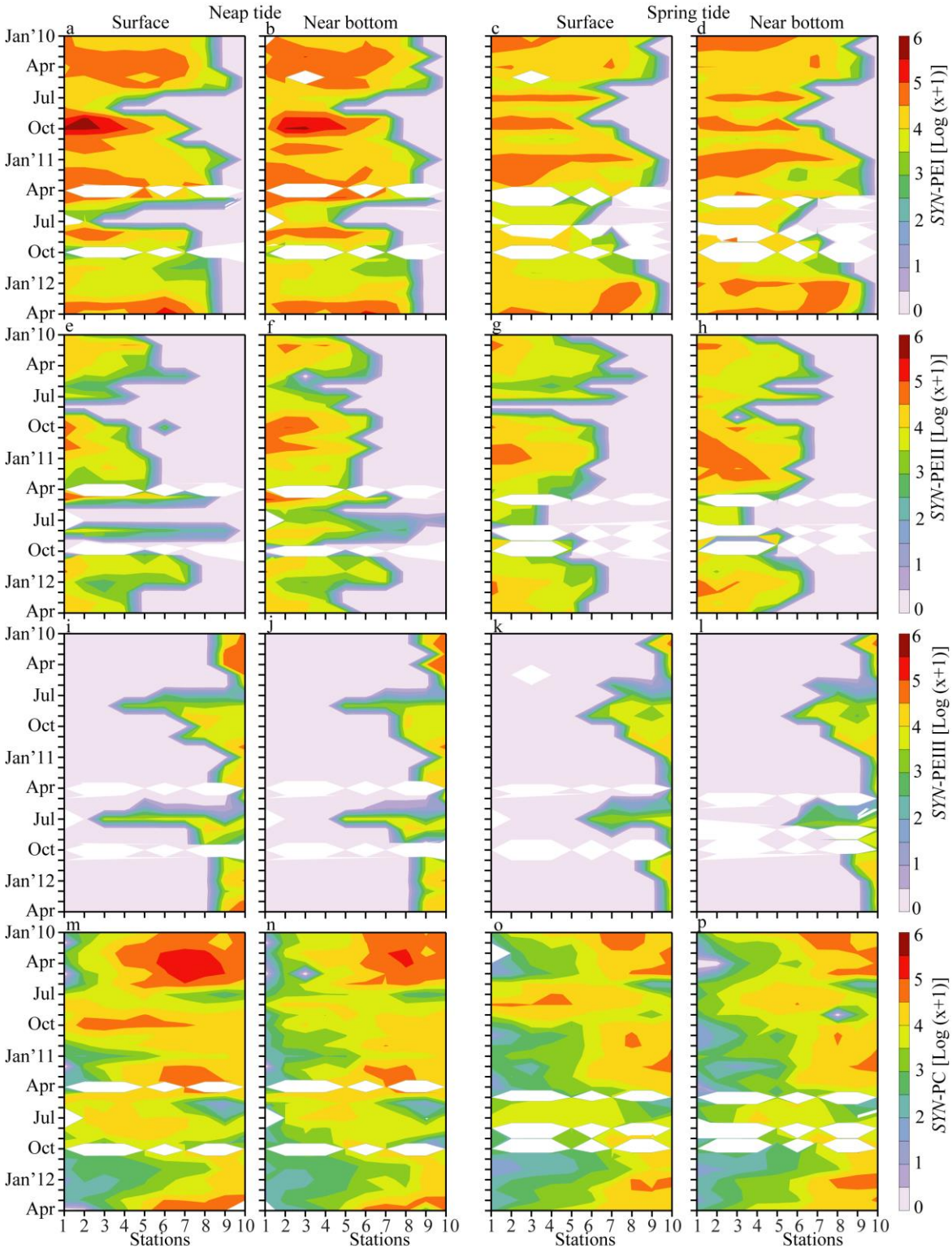

Fig. 2A.5 Temporal and spatial variations in the abundance (log(x+1)) of (a-d) *SYN*-PEI, (e-h) *SYN*-PEII, (i-l) *SYN*-PEIII, (m-p) *SYN*-PC, (q-r) PEUK-I, (s-v) PEUK-II and (w-z) *PRO*-like cells during neap and spring tides.

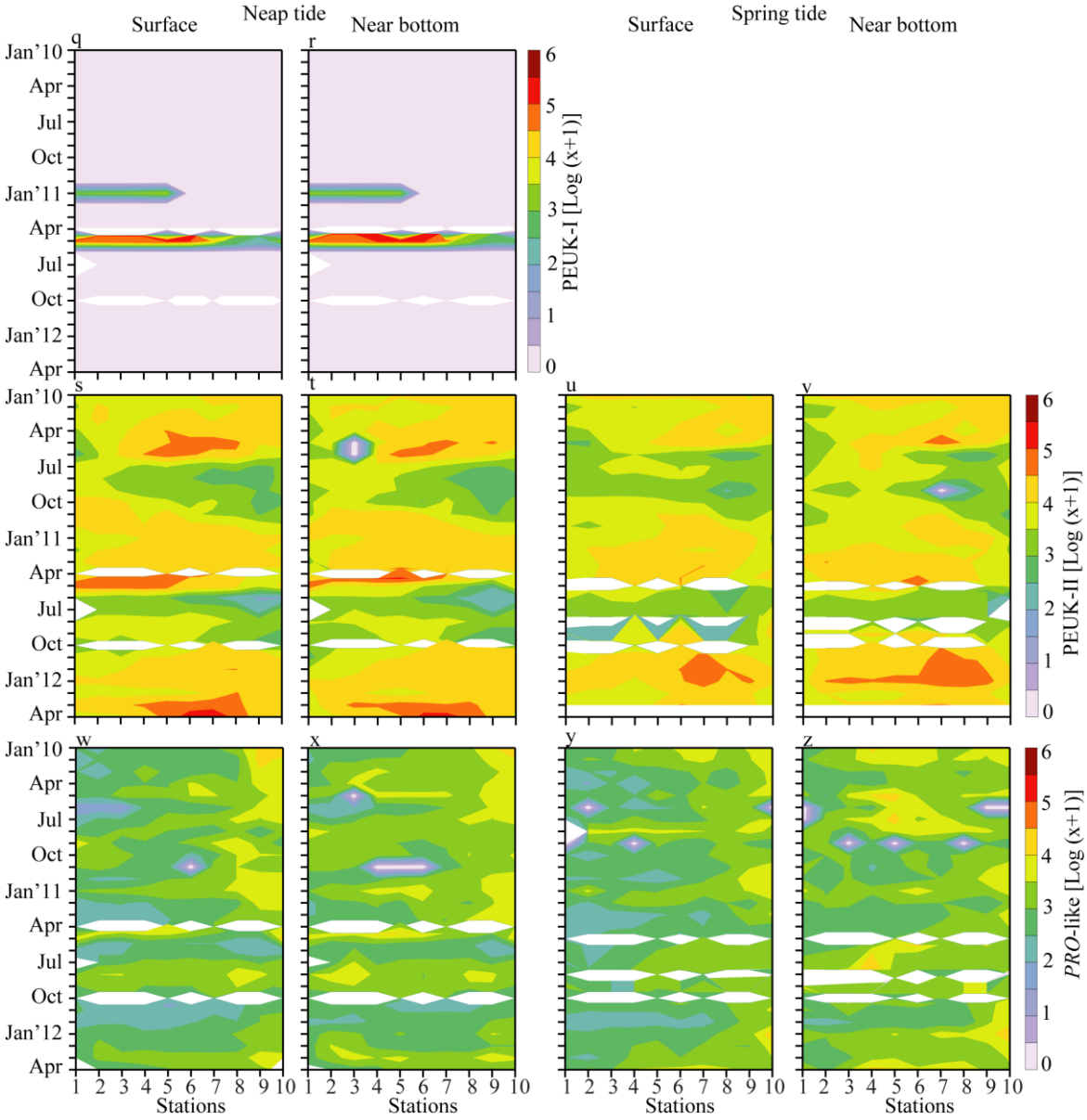

Fig. 2A.5 continued

was low (ST and NT). During PM, increasing trend in abundance was observed from October to January with highest ($1.82 \pm 0.61 \times 10^4$ cells mL^{-1}) in January-12, NBW during ST. *PRO*-like cells abundance ranged from 0.001 to 4×10^4 cells mL^{-1} during the study period, with increasing trend from downstream to upstream (Fig. 2A.5w-z). During PrM, the abundance was higher in May-10 (ST) and May-11 (NT). Generally, the abundance was significantly ($p < 0.05$) higher during NT compared to ST. During MON-I and II (June-July) ST, increased abundance was observed in NBW at S5 and S6. In August and September, increased abundance was observed in the upstream of

estuary. Low abundance (< 0.5 × 10^4 cells mL^{-1}) continued in PMs, except in January-10 (NT) and January-12 (ST) in the upstream.

2A.3.3 Relationship between environmental parameters and picophytoplankton groups during neap and spring tides

In stratified waters, *SYN*-PC: *SYN*-PE ratio was significantly higher in surface waters compared to NBW (Fig. 2A.6). For the entire data, regression analysis revealed that in both surface and NBW, *SYN*-PEIII, *SYN*-PC and PEUK showed significant negative relation with tidal height whereas *SYN*-PEII showed positive relation only in the surface waters (Table 2A.3).

Table 2A.3 Regression analysis of different PP groups and chl *a* with tidal height for the entire study period. *p*-values *< 0.05 and **< 0.01 are statistically significant and are highlighted in bold.

	Tidal height (m)	
	Surface	Near bottom
SYN-PEI	0.064	0.059
SYN-PEII	**0.085***	0.064
SYN-PEIII	**-0.131****	**-0.118****
SYN-PC	**-0.166****	**-0.133****
PEUK-II	**-0.221****	**-0.159****
PRO-like	-0.052	0.003
Chl *a*	-0.056	-0.065

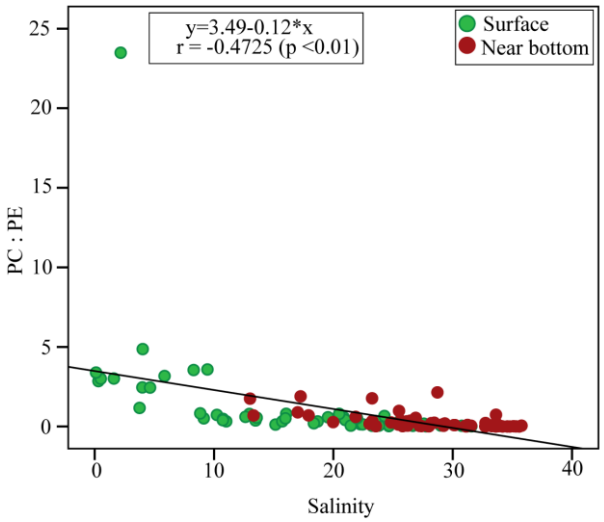

Fig. 2A.6 Regression analysis of *SYN*-PC: *SYN*-PE ratio with salinity during stratification in downstream and lower middle estaury.

Based on RDA and Monte Carlo permutation test, the significant environmental factors influencing PP groups and chl *a* during different tidal phases, depth and seasons are presented in table 2A.4. During NT and ST, the two axes explained > 75% of the cumulative variance of species-environmental relation in surface and NBW (Table 2A.5). During PrM, irrespective of tidal phase and depth, *SYN*-PEI, *SYN*-PEII and PEUK-I were strongly related with salinity and SD, also with tidal height only during NT (Fig. 2A.7a and b). *SYN*-PC, *PRO*-like cells, and chl *a* showed strong positive association with SR, NO_3^- (only in NT), PO_4^{3-} and SiO_4^{4-} and weak relation with temperature. PEUK-II was positively correlated with temperature, NO_3^- (only during ST), PO_4^{3-} and SR.

During MON, in NT (surface and NBW), *SYN*-PEI and *SYN*-PEII, were positively correlated with salinity, PO_4^{3-} and ΔS (Fig. 2A.7c). In surface waters, *SYN*-PC, chl *a*, and PEUK-II were positively correlated with temperature, SD and SR; and negatively with NO_3^-, tidal height and rainfall. In NBW, *SYN*-PC was positively associated with temperature, SR and negatively with tidal height. Chl *a* and PEUK-II were positively correlated with temperature, SD, SR and NO_2^-; and negatively with NO_3^- and rainfall. In ST (surface and NBW), *SYN*-PEI, *SYN*-PEII and chl *a* were positively correlated with salinity, ΔS and NO_2^- (Fig. 2A.7d). *SYN*-PC, *PRO*-like cells, and PEUK-II were positively correlated with SR, PO_4^{3-}, SiO_4^{4-}, temperature, NO_3^- and tidal height.

During PM, *SYN*-PEI and *SYN*-PEII were positively correlated with salinity (Fig. 2A.7e). *SYN*-PC, *PRO*-like cells, and chl *a* were positively associated with temperature. *SYN*-PEIII showed positive association with tidal height, and NO_3^-. PEUK-I and PEUK-II were positively associated with SD, SiO_4^{4-}, and NO_2^-; and negatively associated with SR and ΔS. In NBW, *SYN*-PEI, *SYN*-PEII, and PEUK-I

were positively associated with salinity, SD, and NO_2^-. *SYN*-PEIII showed positive association with PO_4^{3-}, NO_3^- and ΔS. *SYN*-PC, *PRO*-like cells, PEUK-II and chl *a* were positively associated with tidal height, SR, temperature, and SiO_4^{4-}. In ST (surface and NBW), *SYN*-PEI and *SYN*-PEII were positively associated with salinity and ΔS (Fig. 2A.7f). *SYN*-PEIII showed positive association with SR and negative with tidal height. *SYN*-PC, *PRO*-like cells, PEUK-II and chl *a* were positively related to NO_3^-, PO_4^{3-}, SiO_4^{4-}, and temperature.

Table 2A.4 Eigenvalues for RDA axes and results related to species-environment correlations, variation and cumulative % of species data and species-environment relation (denoted in bold).

	Surface (Neap)		Near bottom (Neap)		Surface (Spring)		Near bottom (Spring)	
	Axis 1	Axis 2	Axis 1	Axis 2	Axis 1	Axis 2	Axis 1	Axis 2
Pre-monsoon								
Eigenvalues :	0.436	0.278	0.483	0.262	0.477	0.227	0.504	0.204
Species-environment correlations :	0.954	0.943	0.964	0.952	0.935	0.898	0.942	0.887
Cumulative percentage variance								
of species data :	43.60	71.40	48.30	74.50	47.70	70.40	50.40	70.70
of species-environment relation:	55.40	**90.70**	59.20	**91.20**	63.90	**94.20**	67.20	**94.40**
Monsoon								
Eigenvalues :	0.476	0.073	0.438	0.094	0.425	0.235	0.471	0.240
Species-environment correlations :	0.915	0.614	0.909	0.732	0.914	0.906	0.937	0.897
Cumulative percentage variance								
of species data :	47.60	54.90	43.80	53.20	42.50	66.00	47.10	71.10
of species-environment relation:	76.40	**88.20**	70.80	**86.10**	59.20	**92.00**	62.70	**94.50**
Post-monsoon								
Eigenvalues :	0.261	0.213	0.434	0.164	0.350	0.183	0.352	0.160
Species-environment correlations :	0.843	0.823	0.945	0.844	0.901	0.703	0.895	0.664
Cumulative percentage variance								
of species data :	26.10	47.40	43.40	59.80	35.00	53.20	35.20	51.20
of species-environment relation:	41.80	**76.10**	58.60	**80.70**	59.50	**90.60**	63.70	**92.70**

Table 2A.5 Results of RDA showing significant environmental variables influencing the PP community and chl *a* during neap and spring tide in different seasons. Lambda (λ) is the eigenvalue explained by the environment variable. λI and λA represents marginal effect and conditional effect, respectively. *p*-vlaues < 0.05 are statistically significant and are highlighted in bold.

	Neap surface				Neap near bottom				Spring surface				Spring near bottom		
Variable	λI	λA	*P*	Variable	λ1	λA	*P*	Variable	λ1	λA	*P*	Variable	λ1	λA	*P*
Pre-monsoon															
Salinity	0.27	0.27	**0.00**	Temperature	0.46	0.46	**0.00**	Salinity	0.17	0.15	**0.00**	Salinity	0.17	0.14	**0.00**
SR	0.30	0.03	**0.00**	Salinity	0.29	0.25	**0.00**	Temperature	0.17	0.07	**0.00**	Temperature	0.16	0.06	**0.00**
NO_2^-	0.04	0.02	**0.00**	SR	0.30	0.04	**0.00**	NO_2^-	0.06	0.03	**0.00**	SR	0.35	0.03	**0.00**
ΔS	0.03	0.01	**0.00**	ΔS	0.12	0.02	**0.00**	SR	0.35	0.02	**0.00**	NO_2^-	0.05	0.01	**0.00**
PO_4^{3-}	0.04	0.01	**0.00**	SD	0.10	0.01	**0.00**	ΔS	0.00	0.01	**0.00**	SD	0.07	0.01	**0.00**
TideH	0.04	0.01	**0.01**	NO_2^-	0.07	0.01	**0.00**	SD	0.06	0.02	**0.00**	NO_3^-	0.06	0.01	**0.01**
Temperature	0.41	0.01	**0.00**	TideH	0.20	0.01	**0.01**	NO_3^-	0.03	0.00	0.27	ΔS	0.01	0.01	**0.07**
SD	0.09	0.01	**0.01**	SiO_4^{4-}	0.10	0.00	**0.07**	TideH	0.03	0.00	0.32	PO_4^{3-}	0.06	0.00	**0.05**
SiO_4^{4-}	0.06	0.00	**0.02**	NO_3^-	0.06	0.01	**0.02**	PO_4^{3-}	0.03	0.00	0.38	TideH	0.04	0.01	0.38
NO_3^-	0.08	0.01	0.35	PO_4^{3-}	0.07	0.00	0.51	SiO_4^{4-}	0.07	0.01	0.22	SiO_4^{4-}	0.08	0.00	0.52
Monsoon															
Salinity	0.36	0.36	**0.00**	Salinity	0.40	0.40	**0.00**	Salinity	0.30	0.30	**0.00**	Temperature	0.37	0.37	**0.00**
ΔS	0.10	0.09	**0.00**	Temperature	0.10	0.08	**0.00**	Temperature	0.30	0.26	**0.00**	Salinity	0.35	0.29	**0.00**
Temperature	0.17	0.06	**0.00**	SiO_4^{4-}	0.03	0.05	**0.00**	ΔS	0.10	0.06	**0.00**	PO_4^{3-}	0.21	0.03	**0.00**
SiO_4^{4-}	0.01	0.02	**0.00**	ΔS	0.21	0.01	**0.05**	SD	0.19	0.03	**0.00**	ΔS	0.12	0.02	**0.00**
SR	0.07	0.01	**0.03**	SD	0.04	0.02	0.10	PO_4^{3-}	0.12	0.02	**0.00**	TideH	0.04	0.01	**0.01**
PO_4^{3-}	0.05	0.01	0.18	NO_2^-	0.05	0.01	0.10	SiO_4^{4-}	0.07	0.01	**0.00**	Rainfall	0.00	0.01	0.13
Rainfall	0.02	0.01	0.25	Rainfall	0.01	0.01	0.15	NO_2^-	0.04	0.01	**0.02**	NO_2^-	0.08	0.00	0.15
SD	0.12	0.01	0.09	SR	0.04	0.00	0.23	TideH	0.02	0.01	**0.04**	SR	0.04	0.01	0.18
TideH	0.02	0.01	0.23	TideH	0.03	0.01	0.34	NO_3^-	0.02	0.01	0.12	NO_3^-	0.05	0.00	0.23
NO_3^-	0.10	0.01	0.24	PO_4^{3-}	0.09	0.01	0.33	Rainfall	0.00	0.01	0.48	SiO_4^{4-}	0.09	0.01	0.25
NO_2^-	0.02	0.00	0.31	NO_3^-	0.07	0.00	0.69	SR	0.09	0.00	0.81	SD	0.10	0.00	0.58
Post-monsoon															
SD	0.16	0.16	**0.00**	TideH	0.33	0.33	**0.00**	TideH	0.26	0.26	**0.00**	TideH	0.26	0.26	**0.00**
Temperature	0.13	0.10	**0.00**	ΔS	0.10	0.10	**0.00**	SD	0.11	0.10	**0.00**	SD	0.09	0.08	**0.00**
Salinity	0.14	0.16	**0.00**	Salinity	0.08	0.10	**0.00**	NO_2^-	0.04	0.04	**0.00**	Temperature	0.04	0.05	**0.00**
ΔS	0.10	0.11	**0.00**	Temperature	0.09	0.07	**0.00**	Temperature	0.05	0.06	**0.00**	Salinity	0.14	0.05	**0.00**
NO_2^-	0.05	0.03	**0.00**	SR	0.13	0.05	**0.00**	Salinity	0.14	0.03	**0.00**	NO_2^-	0.03	0.03	**0.01**
SiO_4^{4-}	0.04	0.02	**0.01**	Rainfall	0.01	0.03	**0.00**	Rainfall	0.01	0.04	**0.00**	Rainfall	0.01	0.03	**0.00**
SR	0.02	0.01	**0.02**	NO_2^-	0.05	0.03	**0.00**	ΔS	0.03	0.02	**0.01**	ΔS	0.03	0.02	**0.04**
Rainfall	0.01	0.01	**0.05**	SiO_4^{4-}	0.06	0.01	**0.00**	SR	0.07	0.01	0.13	NO_3^-	0.04	0.01	0.15
TideH	0.07	0.01	0.11	SD	0.14	0.01	**0.01**	NO_3^-	0.02	0.01	0.17	SR	0.07	0.01	0.13
NO_3^-	0.04	0.01	0.25	PO_4^{3-}	0.01	0.01	0.11	PO_4^{3-}	0.01	0.01	0.05	SiO_4^{4-}	0.04	0.01	0.21
PO_4^{3-}	0.01	0.00	0.26	NO_3^-	0.03	0.00	0.51	SiO_4^{4-}	0.05	0.01	0.33	PO_4^{3-}	0.02	0.00	0.60

SR - Solar radiation, TideH - Tidal height, ΔS – Stratification parameter, SD – Secchi disk (water transparency), NO_2^- – Nitrite, NO_3^- – Nitrate, PO_4^{3-}- Phosphate, SiO_4^{4-} - Silicate

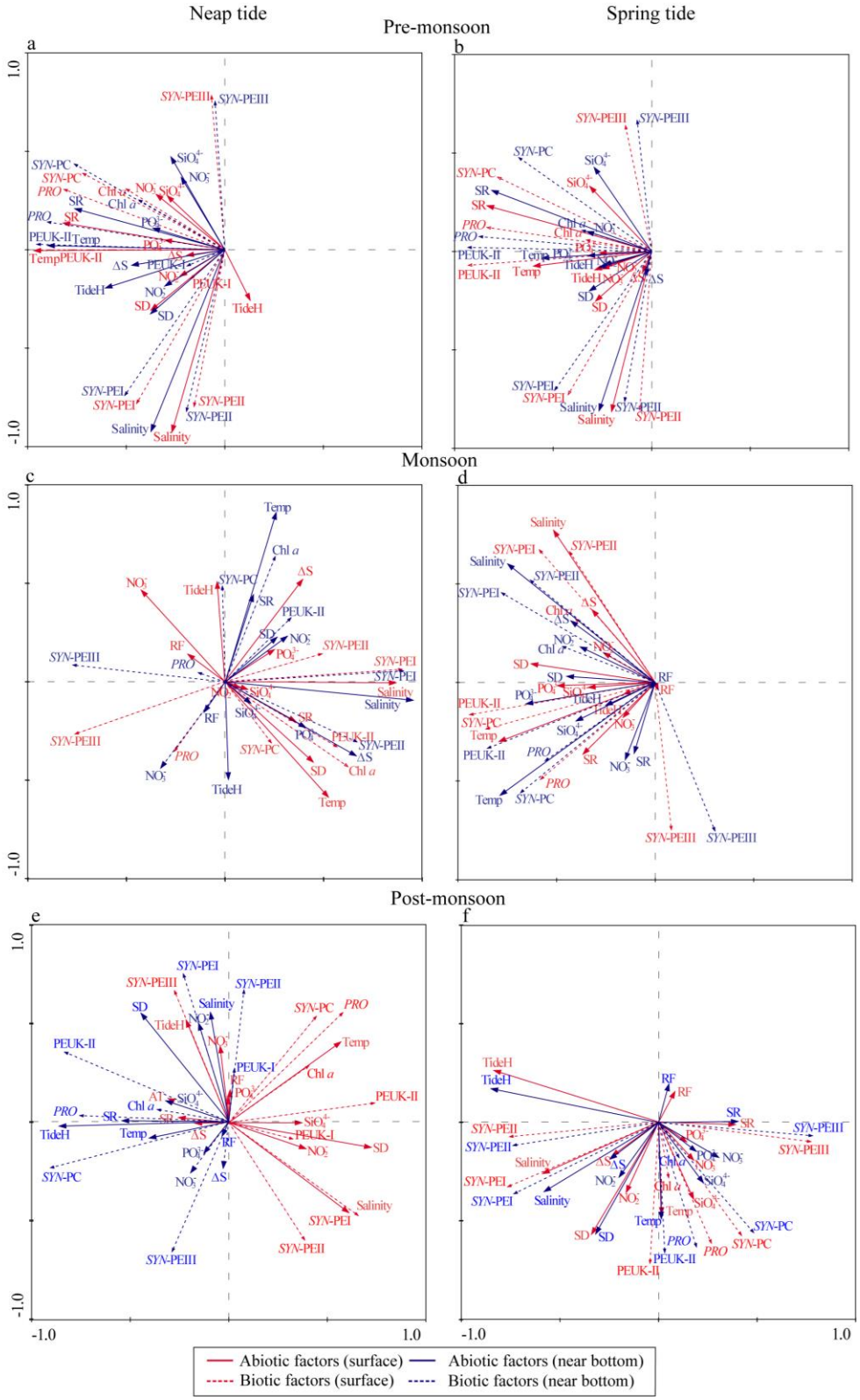

Fig. 2A.7 Redundancy analysis (RDA) of PP groups, chl *a* and environmental parameters during (a, b) PrM, (c, d) MON, and (e, f) PM of spring and neap tide. The environmental parameters [tidal height (TideH), rainfall (RF), temperature (Temp), salinity, stratification parameter (ΔS), secchi disk depth (SD), solar radiation (SR), nitrate (NO_3^-), phosphate (PO_4^{3-}), nitrite (NO_2^-) and silicate (SiO_4^{4-})] are indicated by straight arrows. The PP groups and chl *a* are indicated by dotted arrows.

2A.4 Discussion

Tides and freshwater discharge are recognized as the major controlling factors for variations in the estuarine physico-chemical variables, such as nutrient loading, light availability due to turbidity and water column stratification. In monsoonal estuary, river runoff during MON and tidal activity during non-MON seasons control the annual variation in hydrodynamics (Shetye and Murty, 1987). Biological processes are strongly coupled with these physical processes (Harrison et al., 2008). During PrM, Zuari estuary experiences calm weather and a mixed water column with long water residence time due to very low freshwater discharge (Shetye and Murty, 1987; Shetye et al., 2007; Manoj, 2012). Under these conditions, tide plays a major role in the variation of hydrological parameters (Shetye and Murty, 1987; Sundar et al., 2015), especially on salinity. Stratification parameter indicated a well-mixed water column during ST, along the transect and a stratified middle estuary during NT. In the downstream, along with tidal action, wind and wave actions help in the mixing of water column irrespective of tidal phase thus increasing the suspended particulate matter (Shynu et al., 2013; Suja et al., 2016), whereas in the middle estuary narrow width, longitudinal and weaker tidal flow along with low saline water from upstream makes the water column stratified during NT as opposed to ST (Sundar et al., 2015). In the upstream, weaker tidal flow and dominance of freshwater makes the water column mixed during both the tidal phases (Sundar et al., 2015). Intensity of tidal activity during the two tidal phases was evident from the distance of salt water intrusion. During ST, saltwater intruded up to upstream, whereas during NT it was restricted up to the upper middle estuary (S8). This was more prominent in the surface compared to NBW. The difference in saltwater intrusion during two tidal phases was well reflected in the PP distribution along the transect. The abundance of high saline

species, *SYN*-PEI was low in downstream and high in upper middle estuary during ST, whereas during NT its abundance was high in downstream and lower middle estuary. In contrast, low saline species, *SYN*-PC showed consistently exponential increase in abundance from downstream to upstream during ST whereas during NT it was restricted from upstream to upper middle estuary (relatively higher abundance than ST), wherein peak in abundance was observed. Such a trend could be ascribed to the tidal phase amplitude along with the species specific optimum salinity range (*SYN*-PE: 20 to 30 and *SYN*-PC: 5 to 20). *SYN*-PEII is known as offshore species (Campbell et al., 1998). So, observed high abundance in the downstream during ST suggests that these cells could be brought to the estuarine mouth from intruding high saline offshore waters (Campbell et al., 1998; Mitbavkar et al., 2015). PEUK-II and *PRO*-like cells showed high abundance in the upper middle estuary and upstream, respectively with highest during NT. The intensity of salt water intrusion was not reflected in the distribution trend of these groups. The higher abundance of these PP groups in their native salinity during NT can be linked to many factors, which are controlled by tide (Balch, 1981; Montani et al., 1998; Lallu et al., 2014;). One such factor is turbidity (Hynes, 1970; Phlips et al., 2012; Chen et al., 2016). Compared to NT, the relatively higher tidal force during ST makes water column mixed with high turbidity/ lower transparency as observed in the SD data. Gianesella et al. (2000) also reported lower transparency during ST over NT which can hamper the phytoplankton growth in the estuarine waters with decreased light penetration (Peters, 1997; Blauw et al., 2012; Zhou et al., 2016). These conditions were favourable for heterotrophic bacterial growth due to increased suspended particulate matter in this estuary (Khandeparker et al., 2017). Another reason for lower PP abundance during ST could be the dilution of water column by incoming high saline low nutrient waters during

high tide (Vinita et al., 2015; Zhou et al., 2016). This was also reflected in RDA analysis, where NO_3^- and PO_4^{3-} were less influential factors during ST compared to NT. As low saline phytoplankton requires abundant nutrients than high saline species (Kasai et al., 2010), *SYN*-PC and PEUK-II showed high growth during NT because of the influx of nutrient rich freshwater. This was corroborated by the positive correlation of *SYN*-PC and PEUK-II with PO_4^{3-} and NO_3^- (only *SYN*-PC) concentrations during NT. Johnson (2000) and Becker et al. (2016) observed higher number of smaller zooplankton and fishes during NT. This suggests that higher PP abundance during NT may have positive cascading effect on higher trophic levels, including fishes thus, NT can be a potential fishing period. In February, high saline species *SYN*-PEI and *SYN*-PEII showed lower abundance during NT, which could be attributed to higher grazing activity due to high zooplankton abundance, compared to ST (Fatema et al., 2016; Johnson, 2000). Generally, in the monsoonal estuary, grazing pressure is reported to increase during this transition period (Padmavati and Goswami, 1996). *PRO*-like cells were detected in the upstream and was the least contributor to total PP abundance, which is also reported earlier in the Changjiang Estuary (Shang et al., 2007). In the present study, the relation between this group and environmental factors were similar to the observation for *SYN*-PC and PEUK, based on RDA. Recently, *PRO*-like cells were identified as a group of *SYN*-PC based on laboratory experiment (Liu et al., 2013). However, further studies are needed to confirm the strain using recent molecular approach.

Gradual increase in *SYN*-PC and PEUK-II abundance were observed from February to May in all the three PrM seasons, which was prominent in the NT compared to ST. Increase in temperature (from 27 to 32°C) could be the reason for increasing abundance, as it is known to increase the activation energy of PP growth

rates (Chen et al., 2014), which exceeds its grazing mortality rates (Xia et al., 2015). In temperate and subtropical regions, abundance peaks are observed only during summer mainly due to increase in temperature wherein annual variation in temperature is 14°C (Agawin et al., 1998; Chiang et al., 2002; Murrell and Lores, 2004). Along with higher temperature, higher PO_4^{3-} and SiO_4^{4-} concentrations could be another reason for their higher abundance, which is also evident in the RDA. In the present study, intraseasonal variation in the dominance of PP groups was observed. In PrM-I, *SYN*-PC was dominant whereas in PrM-II and III probably PEUK-II was dominant, with highest abundance during May-11 with dominance of PEUK-I. Such variation in the dominance pattern could be linked to the variation in temperature and PO_4^{3-} concentration, wherein higher temperature and PO_4^{3-} concentration during PrM-II and III favoured PEUK growth (Katano et al., 2005; Chen et al., 2014). During this period, high PO_4^{3-} concentrations resulted from sediment resuspension (Anand et al., 2014).

During MON, heavy precipitation and resulting freshwater discharge at the upstream causes low salinity induced stratification from the lower middle estuary to downstream. During this period, freshwater discharge outplayed the tidal effect on the variation of hydrological parameters. Intraseasonal variation in the biotic and abiotic parameters during both tidal phases were largely dependent on the amount of freshwater discharge regulated by MON intensity. In general, *SYN*-PEI was observed from downstream to lower middle estuary, whereas *SYN*-PC was present along the transect with high abundance in the lower middle estuary and downstream. Thus, suggesting that lowered salinity range (0 to 19) due to freshwater discharge restricts their growth in the upper middle estuary and upstream. In June, cloud coverage and heavy precipitation brings sudden changes in the hydrography resulting in a sharp

decrease in PP abundance, even though nutrient concentrations were high. Studies have also reported such response in PP (Qiu et al., 2010; Mitbavkar et al., 2015; Mohan et al., 2016;) and larger phytoplankton (Sarma et al., 2009; Qiu et al., 2010; Pednekar et al., 2011; Patil and Anil, 2015) by affecting their growth and osmosis processes (Copeland, 1966). However, higher bacterial abundance was observed during this period mainly driven by freshwater runoff from land (Khandeparker et al., 2015).

During MON break (July-10, ST), lowering of freshwater runoff and consequent increase in tidal activity led to increase in salinity in the downstream and lower middle estuary. This along with increased solar radiation, temperature, and accumulated nutrients corresponded with a higher abundance of *SYN*-PEI in downstream to lower middle estuary and *SYN*-PC in middle estuary. This period is considered conducive for phytoplankton growth with the occurrence of phytoplankton blooms (Pednekar et al., 2011; Patil and Anil, 2015;). This supports the observation on the incidence of higher chl *a* concentration in the downstream. Highest chl *a* was observed during August-10 ST, which coincided with higher PO_4^{3-} and lower precipitation. During this month, overall PP abundance was low, signifying the dominance of larger phytoplankton especially larger diatoms as observed by Patil and Anil (2015). Since, *SYN*-PC is a low saline species (Murrell and Lores, 2004) it dominated the PP community during this month. As rainfall intensity reduced in September-10, stratification reduced whereas tidal activity started dominating in the downstream during both the tidal phases. During this period, *SYN*-PEI started increasing in the downstream due to increased water transparency, water residence time, and PO_4^{3-} concentration, with highest abundance during NT.

Compared to MON-I, MON-II showed different trend possibly due to relatively lower precipitation. During, MON-II in July-11 NT, even though the rainfall was low on the sampling day, the higher rainfall on the previous days of sampling might have led to lower surface salinity (highest stratification) and PP abundance. Earlier study in the same estuary has reported that the lag period of rainfall influence on salinity is 5 days (Mitbavkar et al., 2015). In August-11, as was observed in September-10 in MON-I, the PP abundance, especially *SYN*-PEI, started increasing due to reduction in precipitation, which resulted in higher tidal activity thus leading to lower stratification downstream. Due to stronger tidal activity and lower freshwater discharge the *SYN*-PEI distribution extended up to upper middle estuary whereas *SYN*-PC showed normal distribution trend with increasing abundance from downstream to upstream. Such trend indicates the recovery of estuarine conditions much earlier than MON-I. Thus, variations in the PP abundance indicates the impact of rainfall intensity. These observations suggest that among the PP groups, *SYN*-PEI is the first to respond to the varying estuarine hydrographic conditions. On the other hand, PEUK-II showed consistently lower abundance during MON seasons, as they are known to prefer stable and less turbid water column with higher light intensity (Jing et al., 2010). This is also found to be true in the RDA where PEUK-II showed positive relation with SD. Stratification of water column influenced the PP community structure with the dominance of high saline species *SYN*-PEI and *SYN*-PEII during less stratified condition and low saline species *SYN*-PC during strong stratification. Under stratified condition, the high PE: PC ratio in NBW and low in surface waters suggest the niche segregation of *SYN* groups, which is clearly observed in August-10.

During PM, tide and freshwater discharge equally play major role in the variation of hydrological parameters (Shetye et al., 2007). During this period, estuary

experiences partially mixed water column, increased water residence time, light availability, and enormous amount of accumulated nutrients favouring phytoplankton (Devassy and Goes, 1988; Mann, 2009) and bacterial growth (Khandeparker et al., 2017). This period is also known as a recovery period because the environmental conditions are on the verge of returning to normal as in PrM (Devassy and Goes, 1988). This is also reflected in the spatial variation of PP groups, wherein the distribution trend was similar as observed in PrM. Due to continuation of rainfall with low intensity, stratification was observed downstream during both the tidal phases in October-10 to December-10 up to middle estuary. The peak in abundance of *SYN*-PEI, *SYN*-PEII and *SYN*-PC was observed in the downstream and lower middle estuary during NT due to the conducive environmental condition along with the increased temperature (Devassy and Goes, 1988). RDA also indicated significant positive relation between these groups and temperature. The decreasing influence of freshwater led to dominance of PEUK-II in January during NT. The lower abundance during ST could be due to high rainfall and lower temperature as the sampling was carried out in the second half of the month where temperature starts decreasing due to the beginning of winter season. However, this was not observed in October-11(PM-II) possibly due to relatively lower rainfall that led to the dominance of tidal influence, which made the water column well mixed. These conditions did not support the growth of PP downstream. This influence was not effective in the upper middle estuary and upstream where *SYN*-PC was abundant. In following months, even though tidal influence increases and freshwater discharge decreases, there was no particular trend in PP distribution between the two tidal phases. In these conditions, *SYN*-PEI was restricted to lower middle estuary and *SYN*-PC in the upper middle and upstream. Even though, high nutrient was available, low PP abundance was observed due to the

lower temperature which acts as limiting factor for the PP growth. In lower temperature, low PP growth resulted in lower abundance due to high grazing rates (Xia et al., 2015). The PP abundance was higher during January ST possibly due to higher nutrients (NO_3^- - January 2011 and PO_4^{3-} - January 2012) and lower grazing pressure or growth rates exceeding grazing rates as observed in February. PEUK abundance started increasing from November to January suggesting the onset of favorable condition for its growth (Jing et al., 2010). In RDA, PEUK-I and PEUK-II showed significant positive correlation with SiO_4^{4-} (prominent during ST) suggesting that these groups could be representing the pico-sized diatoms (Vaulot et al., 2008), which responded to SiO_4^{4-}, that was resuspended in water column due to turbulence during mixing.

2A.5 Conclusions

The present study highlights the strong coupling of spatio-temporal variation in PP abundance and community structure with hydrographic variation induced by physical processes such as tide and freshwater discharge during two tidal phases (ST and NT). *SYN* was the dominant species observed over the sampling period with occasional dominance of PEUK. During PrM, due to low freshwater discharge, tidal activity played major role in the variations of the hydrography thus consequently influencing the spatial variation of PP groups during the two tidal phases. During ST, saltwater intruded up to upstream, whereas during NT it was restricted up to the upper middle estuary. This was well reflected in the spatial variation of PP during ST and NT with relatively higher abundance during NT. This suggests that during ST, high salt water intrusion and high tidal activity led to well mixed water column, which negatively influenced the PP growth. On the other hand, during NT, stratified water

column due to low tidal activity, with higher water transparency along with nutrients enhanced the PP growth in the middle estuary. During MON, the variation in the PP abundance and community structure was independent of the tidal phases and dependent on the rainfall intensity that regulates freshwater discharge thus modulating the estuarine environment. During PM, both tidal activity and freshwater discharge along with accumulated nutrients regulated the PP growth along the transect. However, with higher tidal activity during NT till December there was no particular trend in PP distribution between the two tidal phases. Higher PP abundance was observed when the estuarine hydrography was completely governed by tides (January). During this period, higher PP abundance during ST was possibly due to higher nutrients and lower grazing pressure. Among the PP groups, *SYN*-PC was the most sensitive group showing prominent difference in the response to hydrographic changes during the two tidal phases (ST and NT), irrespective of seasons whereas *SYN*-PE group showed significant response only during PrM. Thus, the intensity of tidal phases and freshwater discharge controlled the spatial and temporal distribution pattern of PP. Therefore, highlighting the importance of hydrodynamics in monsoonal estuaries and corroborate our hypothesis that water column conditions during NT favour the growth of PP as compared to ST.

2B Dynamics of size fractionated phytoplankton biomass in a monsoonal estuary: Patterns and drivers for seasonal and spatial variability

2B.1. Introduction

Amongst the coastal ecosystems, estuaries are important as they provide nursery ground for many microorganisms and macroorganisms including fishes thereby supporting higher biodiversity (Qasim, 2003; Nobre, 2009; Flo et al., 2011). Indian estuaries are highly productive in terms of fisheries (Jha et al., 2008) which is the main source of livelihood. For sustaining good fishery yields, the entire biological community of the food web needs to function efficiently. Estuarine regions are influenced by a wide variety of environmental factors, such as nutrient inputs, salinity, turbidity and freshwater flow (Bec et al., 2011; Liu et al., 2015; Patil and Anil, 2015). Freshwater discharge is the main source of nutrient input and salinity gradients, and therefore, is considered as a major stressor causing significant changes in the biological community (Paerl et al., 2006). However, in the tropical regions, especially the Indian monsoonal estuaries, freshwater discharges intensify the rapid changes in the water column properties due to monsoonal activities (Shetye and Murty, 1987; Anand et al., 2014) which subsequently influences the seasonal variation of the biological communities in these waters (Qasim, 2003).

Phytoplankton are one of the important components of the biological community fuelling the food webs of aquatic ecosystems through primary productivity. The studies on phytoplankton community structures are well documented for the coastal and estuarine regions (Lemaire et al., 2002; Jouenne et al., 2007; Madhu et al., 2007; Marshall, 2009; Patil and Anil, 2011; Pednekar et al., 2011; Rochelle-Newall et a., 2011; Bazin et al., 2014) and were mostly focused on larger phytoplankton (> 3 µm). In recent years, smaller phytoplankton i.e., picophytoplankton (cell size < 3 µm; PP)

are being highlighted as an important component of phytoplankton community in coastal and estuarine regions (Gaulke et al., 2010; Qiu et al., 2010; Mitbavkar and Anil, 2011; Contant and Pick, 2013; Mitbavkar et al., 2015).

The measurement of phytoplanktonic biomass is critical to understand the carbon flow dynamics in a particular ecosystem. In this regard, size structure of the phytoplankton community is an important factor controlling the carbon cycle and food web dynamics in pelagic ecosystems (Richardson and Jackson, 2007). Oceanic oligotrophic regions are dominated by the PP in terms of chlorophyll, cell abundance and primary production (Partensky et al., 1999). On the contrary, nano- (3 to 20 μm) and micro-phytoplankton (20 to 200 μm) dominate the phytoplankton community of coastal waters where the environment is comparatively more variable (Guenther et al., 2015). However, PP dominance has been reported in some regions occasionally (Qiu et al., 2010; Bec et al., 2011). Since phytoplankton form the base of food webs, the variations in its size fractionated biomass in an ecosystem determines the type of prevailing food web. When the larger phytoplankton biomass (> 3 μm) dominates, the herbivores food web prevails whereas it is the microbial food web when the PP biomass (< 3 μm) dominates (Azam et al., 1983). Amongst the studies on the contribution of larger phytoplankton (> 3 μm) and picophytoplankton (< 3 μm) size fractions to the bulk chlorophyll biomass, although information is available from temperate regions, there is still scarcity of information from the tropical estuarine regions (Sin et al., 2000; Caroppo, 2000; Madhu et al., 2009; Gaulke et al., 2010; Qiu et al., 2010; Guenther et al., 2015; Purcell-Meyerink et al., 2017).

In the monsoonal estuaries where the seasonal hydrography is controlled by the freshwater runoff and tides, the estuarine characteristics evolve from stratified to partially mixed conditions. This is intermingled with ephemeral stabilized

environmental conditions depending on the monsoonal precipitation intensity. These estuaries are characterized by high annual runoff with a distinctly higher run off during monsoon season as compared to non-monsoon season resulting in rapid changes in physico-chemical conditions throughout the year (Vijith et al., 2009; Anand et al., 2014). Larger phytoplankton are known to proliferate in such highly dynamic estuarine conditions whereas smaller PP prefer stabilized conditions. Earlier study in this estuary revealed the influence of tides and freshwater run off on the abundance of PP (Mitbavkar et al., 2015) and microphytoplankton (Patil and Anil, 2011; Patil and Anil, 2015) on a seasonal scale. However, there are no combined studies which assessed the size fractionated biomass contribution to the total phytoplankton biomass across the salinity gradient of this estuary. The aim of this study was to assess the spatial and temporal variations in size fractionated chlorophyll biomass of > 3 µm and < 3 µm phytoplankton along with the controlling environmental factors. The information obtained from such studies can be useful in understanding the biomass dynamics of these two important phytoplankton size groups and also to predict the type of food web prevailing in estuarine ecosystems based on the environmental conditions.

2B.2 Materials and methods

2B.2.1 Description of the study region

Please refer chapter 2A, section 2A.2.1.

2B.2.2 Sampling

Samples were collected from ten stations [S1 to S10; surface and near bottom waters (NBW)] in the Zuari estuary, along a salinity gradient of 0 to 35 (Fig. 2B.1; Table 2B.1) on a monthly basis from October 2010 to September 2011 during flood tide with occasional sampling during ebb tide (Table 2B.2). The sampled transect was

demarcated as the estuarine mouth (S1 to S4; salinity > 30), middle estuary (S5 to S8; salinity between 30 and 0.5) and upstream (S9 and S10; salinity < 0.5). Portable Seabird CTD (SBE 19 plus) was deployed to measure the temperature and salinity. Salinity was measured in practical salinity unit. Stratification parameter (ΔS) was calculated from the difference between surface and NBW salinity for the entire study period. Water transparency was measured with a secchi disk (SD). The data of rainfall and tidal phase for the study period were acquired from IMD (Table 2B.2). Water samples for analysis of nutrients, size fractionated biomass (> 3 μm and < 3 μm) and PP groups were collected using 5 L of Niskin sampler. For the analyses of dissolved inorganic nutrients [nitrate (NO_3^-), nitrite (NO_2^-), phosphate (PO_4^{3-}), and silicate (SiO_4^{4-})], samples were collected in 5 mL cryo vials and analyzed in the laboratory

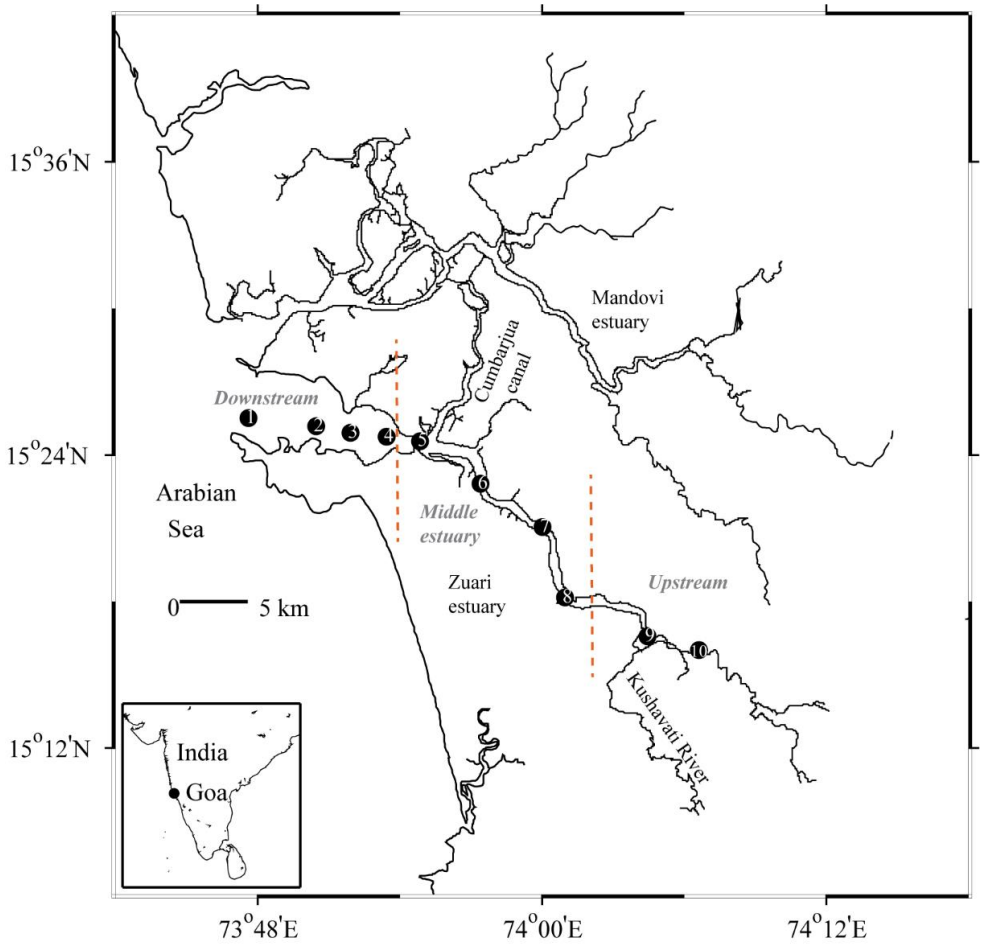

Fig. 2B.1 Sampling stations located in the Zuari estuary, west coast of India.

Table 2B.1 Rainfall data and tidal phase for the sampling days (Rainfall data includes the previous day). LT - low tide and HT- high tide.

Sr No.	Sampling dates (d-m-y)	Rainfall (mm)	Tidal phase
1	23-10-2010	55.4	LT (spring tide)
2	06-11-2010	13.0	HT (spring tide)
3	06-12-2010	0	HT (spring tide)
4	10-01-2011	0	HT (spring tide)
5	11-02-2011	0	LT (neap tide)
6	21-03-2011	0	HT (spring tide)
7	19-04-2011	0	HT (spring tide)
8	27-05-2011	0	LT (neap tide)
9	16-06-2011	99.5	HT (spring tide)
10	15-07-2011	92.2	HT (spring tide)
11	25-08-2011	15.4	HT (spring tide)
12	22-09-2011	6.4	HT (spring tide)

2B.2.3 Size- fractionated chlorophyll a and phaeopigments

In the laboratory, known amount of seawater samples were filtered through Whatman GF/F filters (0.7 µm porosity) to estimate the total chlorophyll *a* (chl *a*) and phaeopigment concentrations. For determining chl *a* and phaeopigment concentrations of < 3 µm size fraction, initially subsamples were filtered through 3.0 µm porosity nucleopore polycarbonate membrane filters and then filtrate was filtered through Whatman GF/F filters. Size fraction filtration was carried out under gentle vacuum. Each filter paper was placed separately in a dark vial containing 90% acetone. After extraction in the dark at 4^{o}C for 24 h (Parsons et al., 1984), chl *a* and phaeopigments were determined on a Turner Design Triology fluorometer calibrated with commercial chl *a*. Subsequently, > 3 µm chl *a* and phaeopigment concentrations were calculated by subtracting < 3 µm chl *a* from the total concentration.

2B.2.4 Flow cytometric analysis of picophytoplankton

Refer chapter 2A, section 2A.2.3. In order to calculate the percentage contribution of each PP group to the total PP chl *a*, the bead normalized mean coefficient value of chl red fluorescence obtained from flow cytometric analyses was multiplied by the cell abundance of each group. Bead normalized mean chl and PE fluorescence intensities of each PP group were obtained from FCM statistics.

2B.2.5. Data analyses

Two-way analysis of variance (ANOVA) was conducted to assess the monthly, spatial and vertical variations in < 3 µm chl *a* and > 3 µm chl *a*, and between the size classes, followed by Tukey's Post-Hoc test to observe the pair wise comparisons of size classes between the seasons. In order to understand the relationship between < 3 µm chl *a*, > 3 µm chl *a*, total chl *a* and flow cytometric chl fluorescence, Pearson correlation was performed. Regression analysis was performed to observe the relationship of < 3 µm and > 3 µm chl *a* with salinity and temperature.

Factor analysis was performed for abiotic and biotic data to examine the relationships among a set of variables. In this analysis, the relationship between the variables are explained by two major factors. The varimax rotation distributes the factor loadings having maximum dispersion by reducing the number of larger and smaller coefficients. The correlation matrix obtained, indicates that the factors show the relationships between variables by calculating correlations between them and the correlations between factors and variables. The most important variables are loaded on the factor 1 (x axis). The value obtained for each variable indicates the importance of the variable. Values <0.4 are not considered, 0.4 to 0.5 considered as weak factors, 0.5 to 0.75 moderate factors, > 0.75 is strong factor (Liu et al., 2003). The above analysis was done through SPSS Multi-variate Statistical Package (Windows Ver. 16).

The contour plots for biotic and abiotic parameters were plotted using Ferret programme.

2B.3 Results

2B.3.1 Environmental parameters

During PM and MON, temperature was almost similar at both ends of the estuary with lowest temperature in January (26.33 ± 0.53^{o}C). During PrM, the river water (30.14 ± 2.38^{o}C) was warmer than the seawater (29.64 ± 1.45^{o}C; Fig. 2B.2a and b). In October (PM), continuation of monsoonal rainfall and freshwater influx led to a difference of 9.47 ± 3.92 salinity between the surface and NBW up to middle estuary, leading to a stratified water column (Fig. 2B.2c - e). During the following PM and PrM months, intrusion of seawater towards upstream resulted in a partially mixed water column. During MON, with the onset of rainfall and consequent freshwater influx, the lower saline riverine water flowing in at the surface and saltier water entering the estuary at the bottom resulted in a vertically stratified water column in the middle and lower estuary. This salt wedge characteristic lasted throughout the MON with stronger stratification from July to September (Fig. 2B.2e). Stratification was also observed in May (S6 to S8). Water transparency was high (1.14 ± 0.49 m) during PM (especially in January) and PrM. During heavy monsoonal precipitation, it was < 1 m and increased in August and September with reduced precipitation (Fig. 2B.2f).

NO_3^- concentrations ranged between 0.66 and 9.92 µM (Fig. 2B.2g and h) with highest values during MON (June: 8.42 ± 5.43 µM) coinciding with the highest rainfall (Table 2B.2). This was followed by PM with highest values in October (7.48 ± 2.09 µM) coinciding with high rainfall. PO_4^{3-} concentrations ranged between 0.24 and 4.3 µM (Fig. 2B.2i and j) with highest values during MON (September: 4.3 ± 1.73 µM) and PM (October: 4.69 ± 1.03 µM). NO_2^- concentrations were high (0.97 ±

0.94 µM) during PrM with higher concentration at the upstream (Fig. 2B.2k and l). SiO_4^{4-} concentrations (33.63 ± 21.39 µM) increased from the middle estuary to upstream during PM, followed by a decline during PrM and increase during MON (Fig. 2B.2m and n).

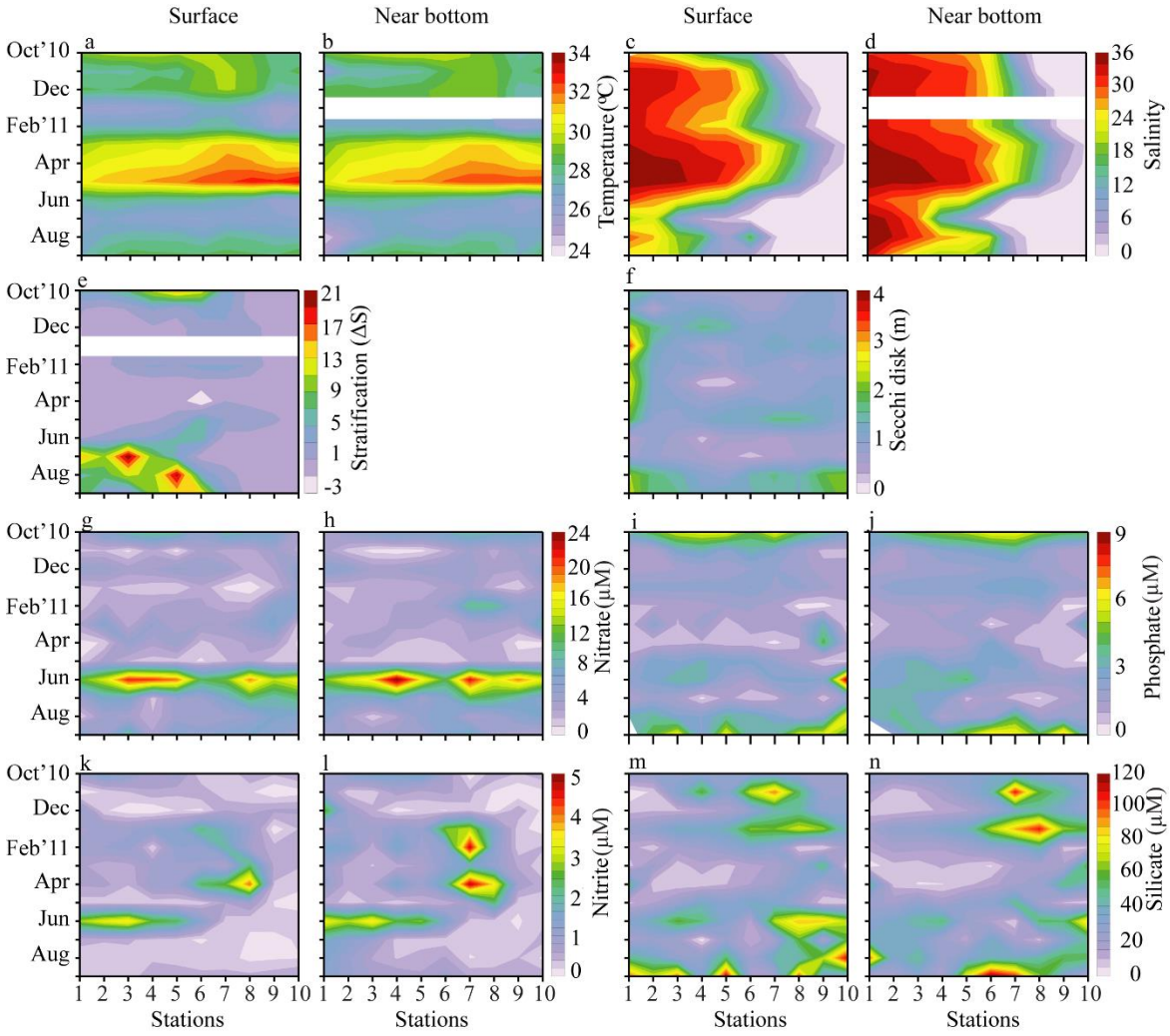

Fig. 2B.2 Temporal and spatial variations in (a, b) temperature, (c, d) salinity, (e) stratification parameter, (f) secchi disk depth, (g, h) nitrate, (i, j) phosphate, (k, l) nitrite and (m, n) silicate in the Zuari estuary.

2B.3.2 Phytoplankton biomass size structure

During PM, the total phytoplankton biomass concentration was relatively higher downstream (3.1 ± 2.01 µg L^{-1}) and middle (3.79 ± 1.9 µg L^{-1}) estuary than upstream (2.76 ± 1.6 µg L^{-1}). The > 3 µm fraction was the major contributor (71.75 ± 1.9%, 66.69 ± 21.73% and 53.41 ± 26.38%, respectively) with highest biomass in January

(surface: 4.61 ± 2.1 µg L^{-1}; NBW: 3.76 ± 1.5 µg L^{-1}) (Fig. 2B.3a and b). The highest < 3 µm biomass concentration was observed from S6 to upstream (0.28 to 2.74 µg L^{-1}) with PEUK-II as the major contributor (Fig. 2B.3c and d, $5m^{-}$ and n^{-}). The higher contribution of < 3 µm biomass was observed in the middle estuary (from S6) and upstream during October (71 ± 18%) and at the estuarine mouth during December (48 ± 20%; Fig. 2B.4a).

During PrM, total phytoplankton biomass concentration was higher in the upstream (3.99 ± 2.47 µg L^{-1}) and middle estuary (3.62 ± 1.9 µg L^{-1}) followed by downstream (3.14 ± 1.86 µg L^{-1}). The > 3 µm fraction was the major contributor (71.66 ± 22.45%, 70.45 ± 27.07% and 66.92 ± 29.21%, respectively) with highest biomass in March and May (surface: 3.05 ± 1.85 µg L^{-1}; NBW: 3.91 ± 2.32 µg L^{-1}) (Fig. 2B. 3a and b). The highest < 3 µm biomass concentration was higher downstream and middle estuary in May (2.40 ± 1.05 µg L^{-1}) with PEUK-I as the major contributor (87 ± 7%; S1 to S6) downstream and *SYN*-PC (44 ± 14%) upstream (Fig. 2B.5k^{-} and l^{-}). During this period, the < 3 µm biomass contribution was highest in the surface waters of estuarine mouth and middle estuary (up to S6; 65 ± 18%) whereas in the NBW, it was observed at the middle estuary (from S5 to S8; 65 ± 28%; Fig. 2B.4b). The higher contribution (57 ± 28%) of < 3 µm biomass was also observed in February in the surface waters of estuarine mouth and middle estuary.

During MON, biomass concentration of both size fractions declined after the onset of rainfall (< 3 µm biomass: < 0.65 µg L^{-1}; > 3 µm biomass: < 1.90 µg L^{-1}). An increase occurred in > 3 µm (August and September) and < 3 µm biomass concentration (September) coinciding with low rainfall intensity and high water transparency. The higher contribution (43 ± 22%) of < 3 µm biomass was observed in

September in the upstream (Fig. 2B.4c). *SYN*-PEI and *SYN*-PEII were the major contributors during this

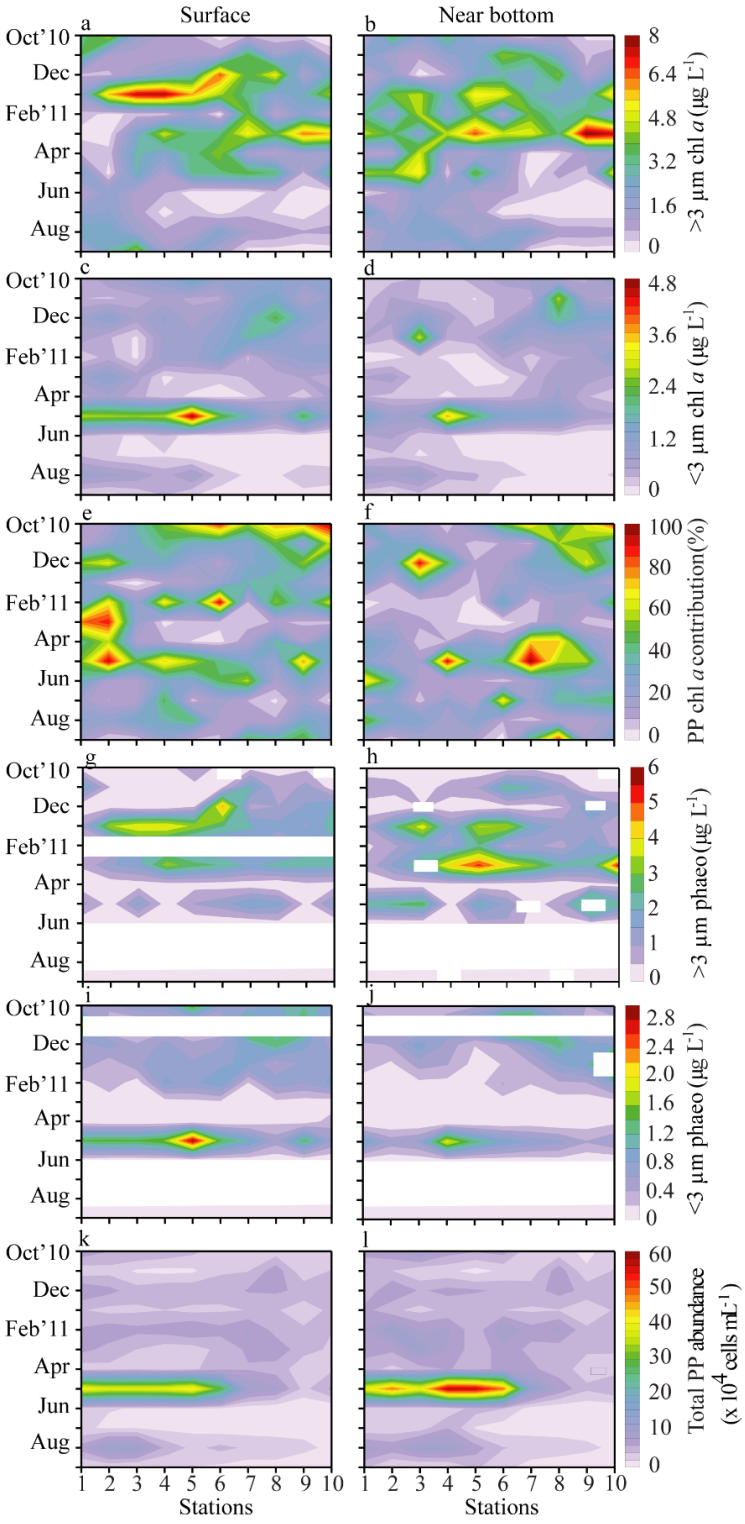

Fig. 2B.3 Temporal and spatial variations in (a, b) larger phytoplankton biomass (>3 µm chl *a*), (c, d) PP biomass (<3 µm chl *a*), (e, f) PP contribution to the total chl *a*, (g, h) Phaeopigment concentrations of larger phytoplankton (>3 µm), (i, j) Phaeopigment concentrations of PP and (k, l) total PP abundance.

season (54 ± 14%) with higher contribution of *SYN*-PEI in the NBW compared to that in the surface waters (Fig. 2B.5a- - d-).

Higher phaeopigment concentrations in the > 3 µm fraction were observed in January (2.34 ± 1.11 µg L^{-1}), March (2.58 ± 1.28 µg L^{-1}) and May (1.58 ± 1.24 µg L^{-1}; Fig. 2B.3g and h). in the < 3 µm fraction, higher phaeopigment concentrations were observed in January (0.64 ± 0.59 µg L^{-1}) and May (1.11 ± 0.63 µg L^{-1}; Fig. 3i and j).

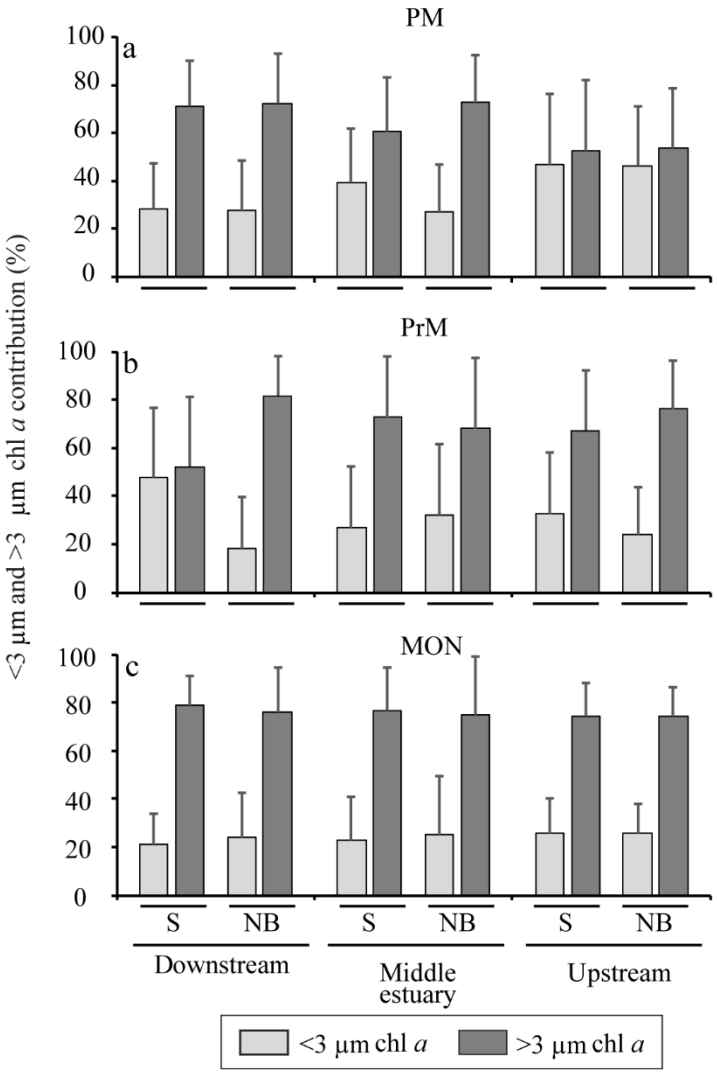

Fig. 2B.4 Seasonal variations in <3 µm and >3 µm biomass contribution to the total chl biomass in the surface (S) and near bottom (NB) waters of the Zuari estuary. (a) Post-monsoon, (b) Pre-monsoon, and (c) Monsoon seasons.

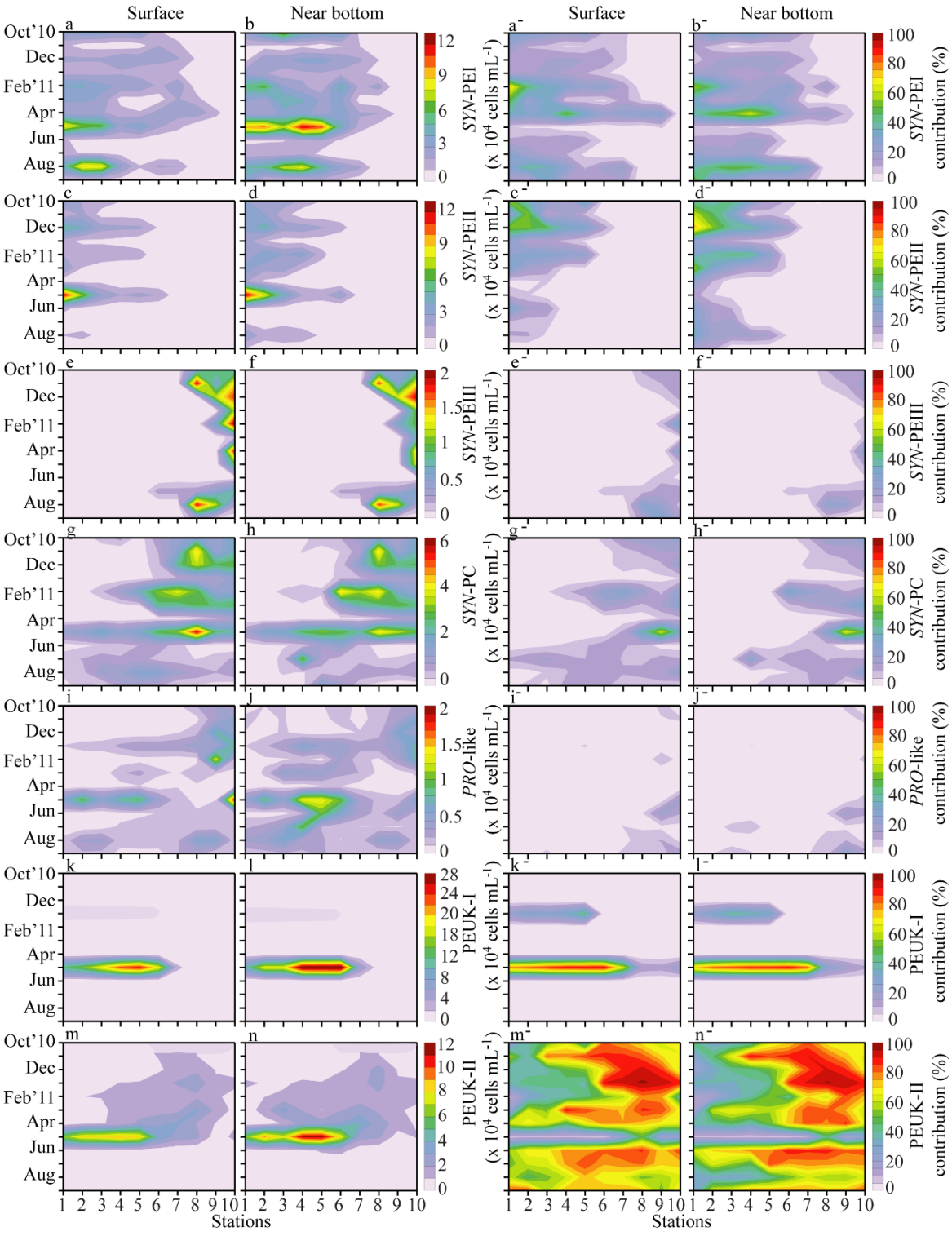

Fig. 2B.5 Temporal and spatial variations in (a, b and a$^-$, b$^-$) *SYN*-PEI, (c, d and c$^-$, d$^-$) *SYN*-PEII, (e, f and e$^-$, f$^-$) *SYN*-PEIII, (g, h and g$^-$, h$^-$) *SYN*-PC, (i, j and i$^-$, j$^-$) *PRO*-like cells, (k, l and k$^-$, l$^-$) PEUK-I and (m, n and m$^-$, n$^-$) PEUK-II abundance and its contribution to the total PP biomass.

2B.3.3. Factors affecting the phytoplankton biomass size structure

Two-way ANOVA indicated significant temporal variations in > 3 µm and < 3 µm biomass in the surface and NBW ($p < 0.01$). There was a significant seasonal variation ($p < 0.001$) between the size classes, and they varied significantly between MON and non-MON seasons, with higher biomass of > 3 µm during PrM and PM seasons (ANOVA, Tukey's Post hoc test, $p < 0.01$). Within the non-MON season, < 3 µm biomass was higher during PrM, especially in the surface waters (ANOVA, Tukey's Post hoc test, $p < 0.01$). Pearson correlation analysis revealed that, irrespective of season and depth, > 3 µm biomass positively correlated with total biomass concentration (Table 2B.2). Regression analysis showed < 3 µm biomass negatively correlated with salinity during PrM and positively correlated during MON (Fig. 2B.6). It was positively correlated with temperature during PrM. > 3 µm biomass was negatively correlated with temperature during PM and positively correlated with salinity during MON.

In factor analyses, two main factors for three seasons explained > 45% of total variance among the variables (Table 2B.3). During PM, < 3 µm chl *a* in the surface waters negatively correlated with salinity and water transparency whereas in the NBW, it was negatively correlated with salinity and NO_2^-. A positive correlation of < 3 µm chl *a* with SiO_4^{4-} was observed in the surface and NBW. *SYN*-PC, *SYN*-PEIII, PEUK-II and *PRO*-like biomass exhibited a similar relation with these abiotic factors whereas *SYN*-PEI and II biomass exhibited an opposite relation at both depths. In surface waters, > 3 µm chl *a* negatively correlated with temperature, PO_4^{3-} and NO_3^-. During PrM, < 3 µm chl *a* positively correlated with temperature, PO_4^{3-} and SiO_4^{4-} (only surface). In surface waters, PEUK-I and II showed a similar relation with these

abiotic factors whereas *SYN*-PEI and II exhibited an opposite relation. *SYN*-PC, *SYN*-PEIII and *PRO*-like biomass were negatively correlated with salinity and SD and *SYN*-PEI and II were positively correlated. In surface waters, > 3 µm chl *a* negatively correlated with salinity and SD. During MON, both size fraction biomass positively correlated with salinity,

PO_4^{3-}, temperature, water transparency and NO_2^-, and negatively with NO_3^- in the surface waters. In the NBW, both size fraction biomass positively correlated with salinity and NO_2^-. In the surface and NBW, *SYN*-PEI and II positively associated with the above abiotic factors. *SYN*-PEIII and *PRO*-like biomass negatively correlated with salinity and NO_2^-. PEUK-II biomass positively correlated with NO_3^- and negatively correlated with PO_4^{3-}, temperature and water transparency in the surface waters, whereas in the NBW, it was positively correlated with NO_3^-, PO_4^{3-} and temperature, and negatively with NO_2^-. In the NBW, *SYN-PC*, *SYN*-PEIII, *PRO*-like cells and PEUK-II biomass negatively correlated with salinity and NO_2^-. *SYN*-PEIII biomass negatively correlated with temperature, salinity, NO_3^- and PO_4^{3-}.

Table 2B.3 Results of Pearson correlation analysis for the PP biomass (< 3 µm chl *a*), larger phytoplankton biomass (> 3 µm chl *a*), flow cytometric (FCM) chl fluorescence and total chl *a*

	Surface			Near bottom		
Parameter	<3 µm chl *a*	>3 µm chl *a*	FCM chl fluorescence	<3 µm chl *a*	>3 µm chl *a*	FCM chl fluorescence
Post-monsoon						
<3 µm chl *a*	-	-0.107	0.733**	-	0.134	0.336*
>3 µm chl *a*	-	-	-	-	-	-
Total chl *a*	0.103	0.978**	-	0.467**	0.939**	-
Pre-monsoon						
<3 µm chl *a*	-	-0.111	0.768**	-	-0.185	0.704**
>3 µm chl *a*	-	-	-	-	-	-
Total chl *a*	0.420**	0.856**	0.495**	0.134	0.949**	-
Monsoon						
<3 µm chl *a*	-	0.474**	0.653**	-	0.321*	0.521**
>3 µm chl *a*	-	-	-	-	-	-
Total chl *a*	0.631**	0.982**	-	0.531**	0.973**	-

Table 2B.4 Results of factor analysis. Rotated component matrix with varifactors [factors (F)] extracted in different seasons. Bold text denotes significant loading of the variables.

Parameters	Post-monsoon				Pre-monsoon				Monsoon			
	Surface water		Near bottom water		Surface water		Near bottom water		Surface water		Near bottom water	
	F1	F2	F1	F2	F1	F2	F1	F2	F1	F2	F1	F2
Abiotic factors												
Temperature	0.084	**0.860**	-0.154	**0.827**	**0.625**	-0.057	0.022	**0.576**	0.094	**0.485**	-0.194	**0.623**
Salinity	**0.894**	-0.261	**-0.959**	-0.111	0.103	**0.821**	**-0.939**	0.079	**0.903**	0.215	**0.958**	0.103
SD	**0.404**	-0.249			0.023	**0.540**			-0.159	**0.859**		
NO_3^-	0.048	**0.801**	0.139	**0.765**	-0.217	-0.300	**0.448**	-0.316	0.140	**-0.616**	-0.177	**0.475**
NO_2^-	0.167	-0.270	**-0.580**	0.385	-0.266	-0.019	0.001	-0.335	**0.620**	**-0.409**	**0.538**	**0.530**
PO_4^{3-}	0.125	**0.586**	0.034	**0.849**	**0.664**	0.184	-0.179	**0.614**	-0.192	**0.457**	0.124	**0.694**
SiO_4^{4-}	**-0.443**	-0.281	**0.481**	0.373	**0.463**	0.089	0.281	0.384	-0.255	0.266	0.009	0.329
Biotic factors												
< 3 µm chl *a*	**-0.443**	0.288	**0.508**	-0.085	**0.730**	0.164	0.014	**0.800**	**0.521**	**0.586**	**0.778**	-0.198
> 3 µm chl *a*	0.158	**-0.663**	-0.176	0.184	0.350	**-0.456**	0.127	-0.072	**0.489**	**0.635**	**0.655**	0.035
SYN-PEI	**0.880**	0.168	**-0.758**	**0.471**	**-0.618**	**0.682**	**-0.643**	**-0.500**	**0.753**	-0.046	**0.844**	-0.200
SYN-PEII	**0.852**	0.219	**-0.852**	-0.218	**-0.492**	**0.654**	**-0.595**	-0.365	**0.731**	**0.516**	**0.864**	-0.265
SYN-PEIII	**-0.689**	0.169	**0.806**	-0.126	-0.159	**-0.483**	**0.559**	-0.003	**-0.665**	0.110	**-0.551**	**-0.455**
SYN-PC	**-0.779**	0.320	**0.894**	0.096	-0.102	**-0.650**	**0.734**	0.036	-0.307	-0.038	**-0.588**	-0.258
PEUK-I	0.216	**-0.719**	-0.102	0.002	**0.852**	0.253	-0.205	**0.935**				
PEUK-II	**-0.727**	-0.004	**0.667**	0.022	**0.811**	-0.200	**0.467**	**-0.574**	-0.314	**-0.579**	**-0.720**	**0.565**
PRO-like	**-0.515**	**-0.422**	**0.688**	-0.183	-0.116	**-0.577**	**0.589**	-0.175	**-0.686**	0.075	**-0.470**	0.043
Eigenvalues	4.86	3.43	5.42	2.57	3.89	3.32	3.44	3.34	5.74	3.79	6.85	2.37
% of Variance	30.34	21.44	38.70	18.37	24.28	20.76	22.92	22.26	30.22	19.94	38.08	13.19
Cumulative %	30.34	51.78	38.70	57.07	24.28	45.05	22.92	45.18	30.22	50.16	38.08	51.27

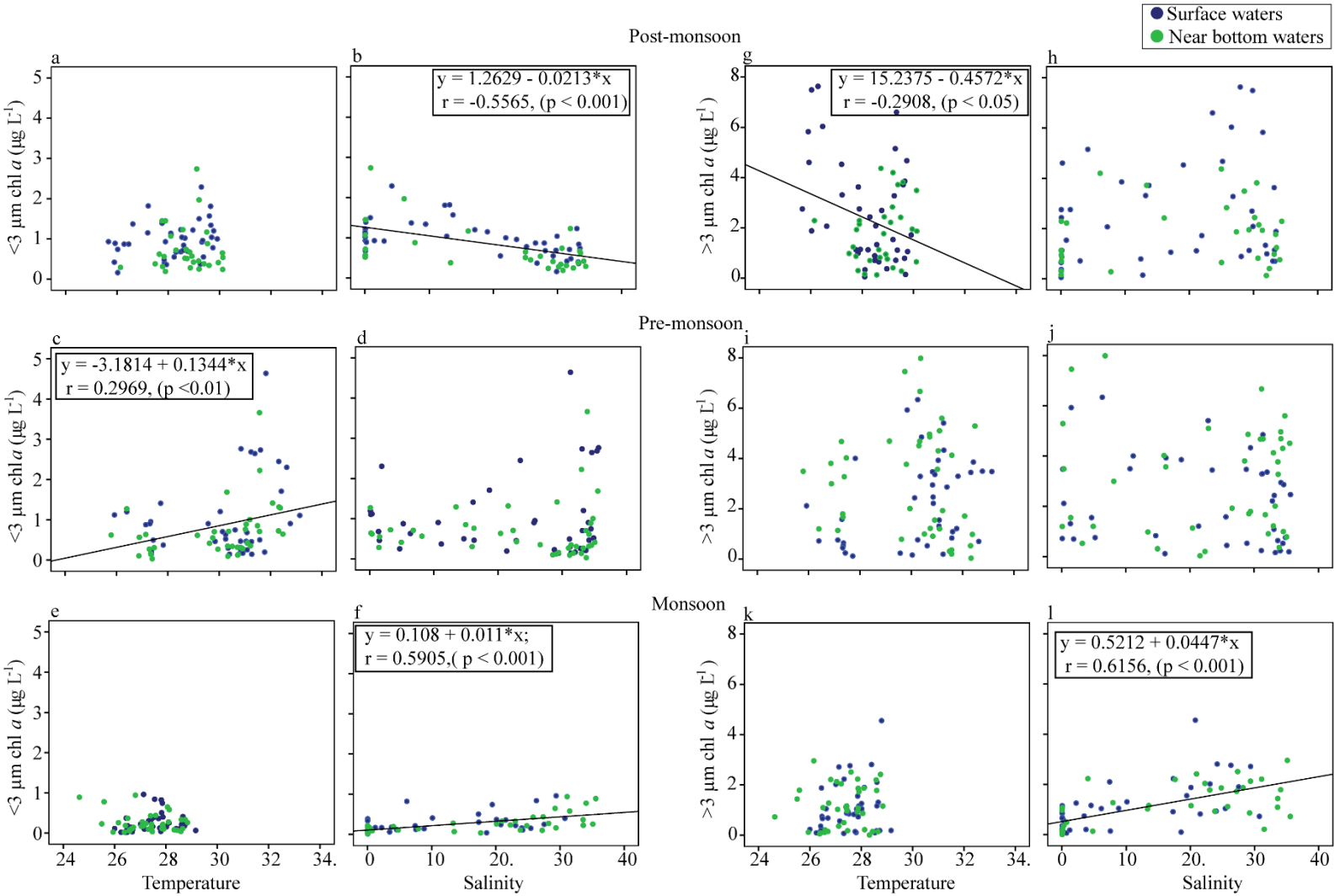

Fig. 2B.6 Regression analysis of < 3 µm and > 3 µm chl *a* with salinity and temperature during different seasons.

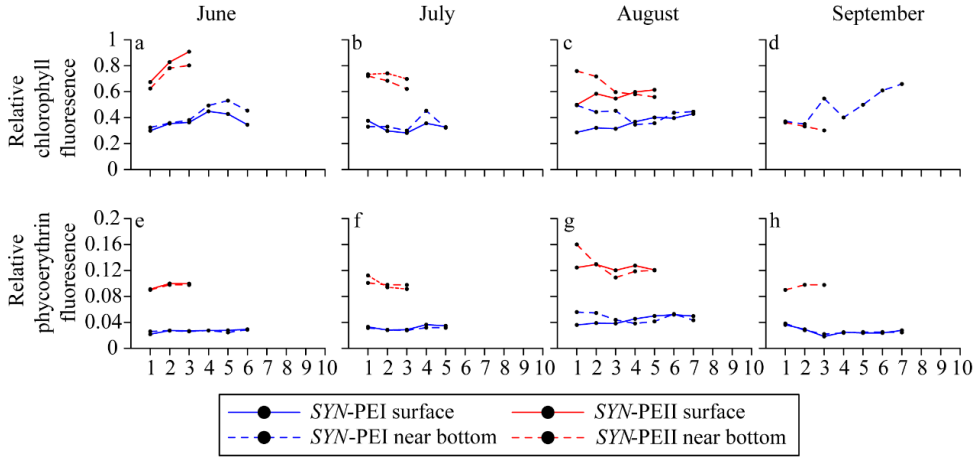

Fig. 2B.7 Variations in mean phycoerythrin and chlorophyll fluorescence intensity of *SYN*-PEI and *SYN*-PEII during monsoon season.

2B.4. Discussion

The results revealed a size dependent and a size independent response of the phytoplankton biomass during the non-monsoon and monsoon seasons, respectively with inter- and intraseasonal variations in the intensity of these responses. The relatively stronger relationship between total chl *a* and > 3 µm chl *a* concentrations than < 3 µm chl *a* indicate their major contribution in the estuarine waters on most occasions. The SW monsoon was the main meteorological driver of the biomass response during MON season. Heavy rainfall intensity during the beginning phase of MON, accompanied by low light intensity due to cloud cover, low saline waters and high turbidity due to freshwater influx induced the lowering of phytoplankton biomass as a whole (Madhu et al., 2007; Sarma et al., 2009; Patil and Anil, 2015). The phytoplankton growth is also influenced by the reduced residence time of water masses and the high particle transport due to flushing (Patil and Anil, 2011; Lu and Gan, 2015). Although in the Zuari estuary, residence time has not been calculated, the residence time of the waters in the neighboring estuary (Mandovi) is 5 to 6 days during MON and about 50 days during non-MON seasons (Qasim and Gupta, 1981). The reduction in rainfall intensity towards the later phase of MON accompanied with reduction in freshwater influx and simultaneous increase in tidal intensity led to stabilization of the water column. These

conditions along with increasing solar radiation, salinity and high water transparency could be responsible for an increase in phytoplankton biomass downstream. A minimum of 50 cm depth of light penetration was reported to be essential for phytoplankton bloom formation in nutrient rich waters of this estuary (Patil and Anil, 2015). During August, when *SYN*-PEI and II abundance was highest, they exhibited high mean chl and PE fluorescence intensity in the NBW, which probably suggests the influence of light intensity on the physiological properties of *SYN*-PEI and II (Fig. 2B.7c - g; Palenik, 2001).

With reduced rainfall progressing into the PM season (October), the marked increase in larger phytoplankton biomass downstream implies the sumptuous use of nutrients accumulated through the MON processes. Due to the unstable conditions during MON, the nutrients are utilized after the cessation of rainfall when water column stabilizes, and light intensity increases (Patil and Anil, 2011; Mitbavkar et al., 2015). Nutrient availability is an important factor controlling phytoplankton biomass (Agawin et al., 2000). The switching over of dominance towards the PP biomass at the middle and upstream estuary with the low saline form, *SYN*-PC as the major contributor suggests salinity as the controlling factor. Further into the PM season (November to December), the complete absence of rainfall and dominance of tidal effect favored the larger phytoplankton biomass across the estuary. This scenario underwent a change towards the end of PM (January) wherein the highest phytoplankton biomass (downstream) coincided with the lowest water temperatures recorded for the study period and lower water transparency. The simultaneous presence of high SiO_4^{4-} concentrations indicate water turbulence. Such intermittent vertical mixing promotes phytoplankton growth, especially of diatoms (Devassy and Goes, 1989; Patil and Anil, 2011). As zooplankton abundance is high during this period (Nair, 1980), the high NO_2^-

concentrations could be a product of nitrification process as reported earlier (Patil and Anil, 2011). Also, the low NO_3^- concentrations could suggest its utilization by phytoplankton blooms. Due to their ability to store nutrients in large intracellular vacuoles and high maximum growth rates, episodic inputs of nutrients into the euphotic layer lead to an increase in diatom population, with comparatively little response of PP (Cermeno et al., 2005).

During the PrM, the intra-seasonal waxing and waning trend in phytoplankton biomass could be attributed to two reasons. The waning in February and April could be due to exhaustion of nutrients resulting in reduced growth rates or the grazing pressure (as evident from higher NO_2^- concentrations) superseding the growth rates as copepods are reported in high numbers during this period (Achuthankutty et al., 1998). The intermittent waxing (March, May) in phytoplankton biomass reveals preference for prevalent environmental conditions such as high temperature, salinity and water transparency. Also, the high PO_4^{3-} concentrations, resulting from sediment resuspension due to the high tidal well-mixed water column (Anand et al., 2014) could be responsible for the high phytoplankton biomass. However, a switch over towards the dominance of PP biomass during May coinciding with the highest water temperature (31.87 ± 0.72^oC) during the study period suggests an influence of high temperatures on PP growth. In sub-tropical and temperate estuaries, PP contribution was restricted to < 10% when water temperature was < 20^oC and subsequently increased to > 50% at higher temperatures (> 20^oC; Ray et al., 1989; Caroppo, 2000; Buchanan et al., 2005; Qiu et al., 2010). Phytoplankton size structure, among other factors, also depends on the maximum growth rate of the different groups of phytoplankton (Irwin et al., 2006). A general trend of an increase in relative *SYN* and PEUK abundance with increasing water temperature due to the higher activation energy of their growth rates than that of larger

phytoplankton has been reported (Chen et al., 2014). Similarly, in this study *SYN*-PC and PEUK groups which are generally present in lower abundance, attained higher abundance (10^4 and 10^5 cells ml^{-1}, respectively) at the estuarine mouth (salinity > 30) in May where highest temperature was recorded. Also, the increase in growth rates of these PP groups corresponds with an increase in chl *a* and nutrient concentrations as observed in this study where abundance peaks occurred at higher concentrations of PO_4^{3-} and SiO_4^{4-}. The higher NH_4^+ concentrations (Ram, 2002) which are better utilized by PP than the larger phytoplankton (Stolte and Riegman, 1995) could also result in higher PP biomass. Also, the dominance of *SYN*-PE at lower temperatures and PEUK-I at higher temperatures suggests a temperature regulated shift in the community structure. This further implies that PP increase was due to a combination of factors such as temperature and nutrients leading to higher growth rates. These observations show that *SYN*-PE can dominate both, stratified as well as mixed waters (Xia et al., 2015). The possibility of different strains inhabiting these conditions cannot be ruled out. Similarly, the PEUK-I which was observed downstream could be a high saline form.

However, the restriction of PP dominance only up to the middle estuary which coincided with temperatures below 32^{o}C and tilt of balance towards the higher phytoplankton biomass above this temperature could be due to increased grazing pressure or lowering growth rates of PP. Grazing is likely to affect larger phytoplankton less severely due to the longer generation times of mesozooplankton while the PP in spite of their effective light and nutrient utilization are tightly controlled by microzooplankton, with growth rates similar to their own (Landry et al., 1997). The high < 3 µm phaeopigment concentrations show that grazing on this biomass fraction was prevalent. Blooms of larger phytoplankton have been reported earlier from this estuary resulting in high chl *a* and oxygen saturation (> 100%) showing maximum

production (Patil and Anil, 2011). From the size fractionated biomass, it can be hypothesized that a majority of this contribution during this period is from the PP.

These inter- and intraseasonal size-fractionated phytoplankton biomass responses to environmental perturbations can provide some clues about the dominant type of functioning food web. During MON, the size independent response with dominance of larger phytoplankton biomass implies the prevalence of herbivorous food web. During non-MON seasons, intra-seasonal and spatial variations in the size dependent response suggests intermittent prevalence of either herbivorous or microbial food web. Although, the former is said to be more efficient in energy transfer due to the lower number of links as compared to the latter, the contribution of the microbial food web cannot be ignored in estuarine ecosystems.

2B.5. Conclusions

The larger phytoplankton biomass fraction dominated the total biomass on most occasions. Size dependent response during the non-monsoon seasons revealed dominance of larger phytoplankton biomass downstream during the lowest recorded annual temperature coinciding with high SiO_4^{4-} concentrations indicating vertical mixing. Highest PP biomass was observed at low salinity upstream and high salinity-highest temperature recorded from downstream to middle estuary. During MON, size independent response led to simultaneous decrease and increase in biomass of both size fractions downstream during the heavy rainfall and rainfall break, respectively. Community composition differences were revealed with PEUK during high temperature, *SYN*-PC at low salinity and *SYN*-PEI at higher salinity downstream during MON. This study reveals seasonal and spatial variations in size fractionated phytoplankton biomass influenced by the hydrography and environmental factors which will in turn influence the higher trophic community structure.

Chapter 3

Picophytoplankton community structure under different environmental settings along the coast of India

3.1 Introduction

Coastal ecosystems are productive and serve as breeding or nursery areas for a wide range of coastal and marine organisms. These ecosystems are mainly vulnerable to anthropogenic pressures because of ease of access to people and industry. This is particularly visible in the port areas, where the activities such as dredging, oil discharge, petroleum wastes and out-fall of a variety of cargo handled by the port disturb the port environment (Bailey et al., 2004; Tripathy et al., 2005). The ports located in the estuaries and rivers have additional sources of anthropogenic pressure such as sewage or municipal runoff and terrestrial runoff during monsoons (Musale et al., 2014).

The present study was carried out under a port biological baseline survey of the major ports of India, as part of a ballast water management programme. V.O. Chidambaranar (V.O.C.; Tuticorin), Chennai, New Mangalore, Cochin and Kolkata ports are the major ports situated along the east and west coast of India having different ecosystems. V.O.C., Chennai, and New Mangalore ports are situated in the marine environments, Cochin port is situated in the estuarine environment, and Kolkata port is situated in the riverine environment. In recent years, eutrophication is one of the serious problems in the port waters having an impact on the biotic communities. Several studies have been carried out to understand the biotic communities in ports, which are dynamic and have high anthropogenic pressure such as the Visakhapatnam, Cochin and Marmugoa ports (Menon et al., 2000; Tripathy et al., 2005; Madhu et al., 2009; D'Silva et al., 2012, 2013). However, very few studies are carried out in the Chennai (Duraisamy and Latha, 2011; Ramanibai, 2015), Kolkata (Dasgupta et al., 2013), V.O.C. (Pitchaikani et al., 2010) and New Mangalore ports (Shankar and Karbassi, 1991). Cochin port area has been studied in detail.

Location of the Cochin port accelerated the industrial growth in Cochin, making it one of the fastest growing cities in India. As a consequence, eutrophication becomes a threat for trophic dynamics and functioning of the ecosystem (Madhu et al., 2007; Kaladharan et al., 2011). For the efficient functioning, such ecosystems should be in a healthy state which can be easily detected through regular monitoring of the base of the food web i.e., phytoplankton. At the base of the food web, the smallest group of phytoplankton, i.e., picophytoplankton (PP; < 3 µm), which forms a major component of phytoplankton in the aquatic ecosystems, both marine, and freshwater, including nutrient rich to poor ecosystems, was selected as the study organism (Stockner and Antia, 1986; Shiomoto et al., 1997). PP are significant contributors to primary productivity and total phytoplankton biomass in various ecosystems (Paerl, 1977; Platt et al., 1983). PP forms an important component of the marine microbial food web by creating a linkage with the higher trophic levels (Chiang et al., 2013).

The port waters are influenced by southwest monsoon (SWM) and/or northeast monsoon (NEM). However, their impact depends on the location of the port. These monsoonal activities bring excess nutrient input from the landmass, especially in the estuarine waters. Studies conducted in tropical (Qiu et al., 2010; Mitbavkar et al., 2015) and subtropical (Lin et al., 2010; Qiu et al., 2010; Zhang et al., 2013) regions, which come under the influence of monsoonal rainfall, have suggested that riverine runoff influences the PP growth. In coastal and estuarine waters, phytoplankton shows wide seasonal changes in species composition and abundance (Patil and Anil, 2011; Pednekar et al., 2011). Some studies are also available on the PP community structure in such environments (Anas et al., 2015; Mohan et al., 2016), which shows that salinity variation, water column stability, and freshwater discharge affect the PP growth, community structure, and its distribution. The present study was carried out

on a seasonal basis to characterize the main environmental factors, which control the spatial distribution pattern of PP groups and consequently whether these organisms can serve as ecological indicators. Since *SYN*-PE is known to prefer clear waters and *SYN*-PC turbid waters (Stomp et al., 2007), we hypothesize that these organisms can serve as good indicators of the trophic status of the water column.

3.2 Materials and Methods

3.2.1 Description of the study region

3.2.1.1 V.O. Chidambaranar port (Tuticorin)

V.O. C. port is located (8° 44' N, 78° 13' E) in Tuticorin, an industrial city of the state of Tamil Nadu, situated along the east coast of India. This port is one of the 12 major ports in India, connecting the Gulf of Mannar in Tuticorin district (Fig. 3.1). It is an artificial deep-sea port formed with rubble mound-type parallel breakwaters projecting into the sea for about 4 km. The length of south breakwater and north breakwater are 3873.37 m and 4098.66 m long respectively, with the distance between them is 1275 m. The harbour has an approach channel of 2400 m length and 183 m width (http://www.vocport.gov.in/portlayout.aspx).

This port has 14 berths with a total length of almost 3000 m and depths ranging from 5.85 to 10.9 m. Based on the location, stations (S) are demarcated as inner (S17 to S21), middle (S8, S9, S14 to S16 and S22) and outer stations (S1 to S7 and S10 to S13). This port imports mainly thermal coal, industrial coal, fertilizer, timber logs, fire-retardant materials, container, copper concentrate, wheat, petroleum products and liquefied petroleum gas. Exports container, construction materials, ilmenite sand, phosphoric acid, cement, sulphuric acid, granite, and sugar, (http://www.vocport.gov.in/port/userinterface/statisticals.aspx). This area has a

tropical climate with an annual air temperature variation from 22°C to 39°C with the minimum and maximum in January and May to June, respectively. The study region experiences three seasons, pre-monsoon (PrM; March to May), SWM (June to September), and NEM (November to February). October month is considered as a transition period (TP) between SWM and NEM. The annual rainfall varies from 762 mm to 1270 mm with moderate to heavy rainfall from October to mid-December [Indian Meteorological Department (IMD)]. Thus, NEM contributes higher proportion towards annual rainfall than that during SWM. Tides are diurnal with a maximum tidal height of 0.81 m during spring tide (ST) and a minimum of 0.2 m during neap tide (NT).

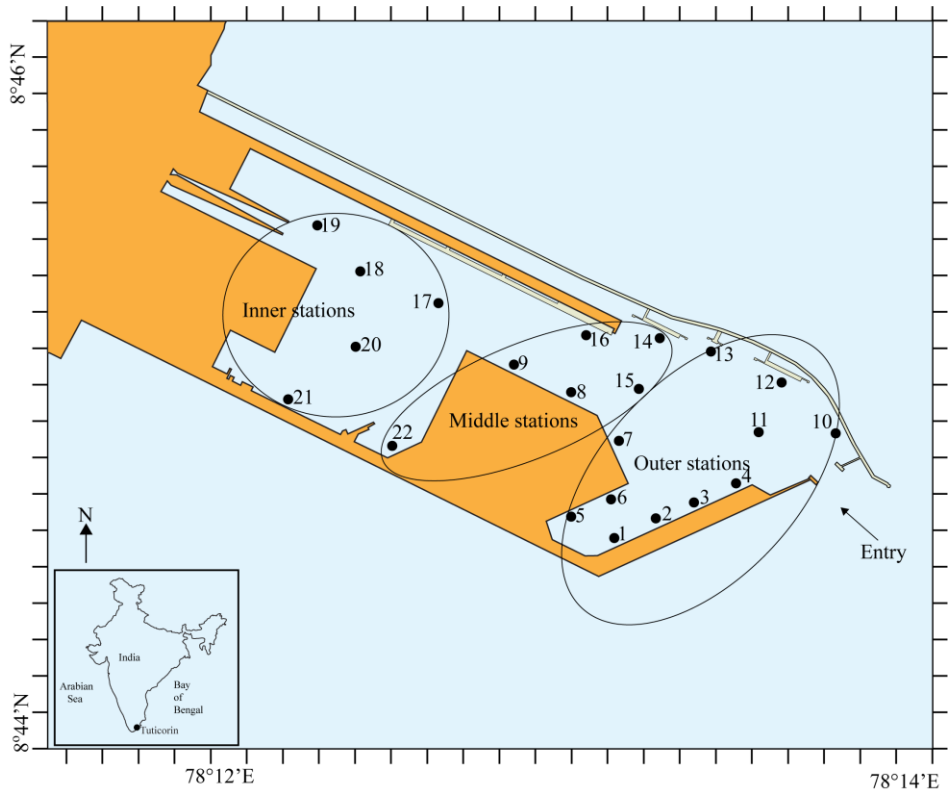

Fig. 3.1 Location of sampling stations in V.O.C. port (Tuticorin), east coast of India.

Table 3.1 Sampling details for each sampled station in V.O.C. port (Tuticorin) along the east coast of India. S- stations; Est- estimated.

					South west monsoon (July)				Transition period (October)				North east monsoon (December)				Pre-monsoon (March)			
S. No.	S. Name	Latitude (N)	Longitude (E)	Average depth (m)	Date (d-m-y)	Time (h)	Est. tidal height (m)	Rainfall (mm)	Date (d-m-y)	Time (h)	Est.tidal height (m)	Rainfall (mm)	Date (d-m-y)	Time (h)	Est.tidal height (m)	Rainfall (mm)	Date (d-m-y)	Time (h)	Est.tidal height (m)	Rainfall (mm)
1	Berth-1	8° 44' 34''	78° 13' 19''	10.81	09-07-2012	09:09	0.52	0	08-10-2012	07:57	0.65	0	05-12-2012	10:00	0.49	0	17-03-2013	15:29	0.74	0
2	Berth-2	8° 44' 38''	78° 13' 26''	10.89	09-07-2012	08:10	0.60	0	08-10-2012	09:00	0.60	0	05-12-2012	07:30	0.69	0	16-03-2013	08:40	0.49	1
3	Berth-3	8° 44' 38''	78° 13' 30''	12.38	09-07-2012	10:14	0.44	0	08-10-2012	09:40	0.58	0	05-12-2012	08:10	0.64	0	16-03-2013	08:19	0.52	1
4	Berth-4	8° 44' 45''	78° 13' 40''	12.92	09-07-2012	10:42	0.40	0	08-10-2012	10:13	0.55	0	05-12-2012	09:10	0.55	0	16-03-2013	07:52	0.57	1
5	Berth-5	8° 44' 38''	78° 13' 15''	10.79	09-07-2012	07:24	0.66	0	08-10-2012	07:35	0.67	0	04-12-2012	09:10	0.50	0	16-03-2013	09:05	0.44	1
6	Berth-6	8° 44' 42''	78° 13' 19''	10.63	09-07-2012	07:06	0.68	0	08-10-2012	07:01	0.69	0	04-12-2012	09:30	0.47	0	15-03-2013	09:21	0.37	0
7	Berth-7	8° 44' 52''	78° 13' 22''	15.21	08-07-2012	09:59	0.36	0	07-10-2012	08:00	0.67	0	04-12-2012	07:40	0.64	0	14-03-2013	10:01	0.34	0
8	Berth-8	8° 45' 00''	78° 13' 12''	15.09	08-07-2012	08:17	0.52	0	07-10-2012	07:37	0.70	0	04-12-2012	07:00	0.71	0	14-03-2013	11:04	0.45	0
9	Berth-9	8° 45' 03''	78° 13' 01''	15.27	08-07-2012	07:43	0.57	0	07-10-2012	07:20	0.71	0	04-12-2012	06:35	0.75	0	14-03-2013	11:18	0.48	0
10	Eastern Point	8° 45' 00''	78° 13' 51''	15.30	11-07-2012	06:30	0.54	0	10-10-2012	07:11	0.66	0	06-12-2012	07:00	0.73	0	17-03-2013	07:28	0.69	0
11	Mid-Point-1	8° 45' 52''	78° 13' 44''	15.29	09-07-2012	07:35	0.40	0	09-10-2012	06:46	0.68	0	06-12-2012	09:25	0.53	0	16-03-2013	07:31	0.60	1
12	Coal Jetty-1	8° 45' 03''	78° 13' 51''	15.24	10-07-2012	07:41	0.69	0	09-10-2012	07:09	0.68	0	06-12-2012	07:20	0.71	0	15-03-2013	10:32	0.35	0
13	Oil Jetty	8° 45'10''	78° 13' 37''	15.26	10-07-2012	08:18	0.65	0	09-10-2012	07:40	0.67	0	05-12-2012	08:00	0.65	0	15-03-2013	09:58	0.31	0
14	Coal Jetty-2	8° 45'10''	78° 13' 30''	14.50	10-07-2012	08:54	0.61	0	07-10-2012	10:01	0.54	0	04-12-2012	08:30	0.56	0	16-03-2013	06:45	0.68	1
15	Mid-Point-2	8° 45' 03''	78° 13' 19''	15.16	08-07-2012	10:25	0.34	0	07-10-2012	09:09	0.59	0	05-12-2012	06:40	0.76	0	16-03-2013	07:05	0.65	1
16	North Container Berth-1	8° 45'10''	78° 13' 19''	15.03	08-07-2012	10:49	0.37	0	07-10-2012	09:36	0.56	0	04-12-2012	07:30	0.66	0	15-03-2013	08:01	0.51	0
17	Mid-Point-3	8° 45' 14''	78° 12' 50''	6.31	08-07-2012	06:55	0.64	0	06-10-2012	10:57	0.38	0	03-12-2012	08:20	0.53	0	15-03-2013	07:35	0.55	0
18	Mid-Point-4	8° 45'18''	78° 12' 39''	5.29	09-07-2012	11:39	0.50	0	06-10-2012	08:37	0.53	0	03-12-2012	07:45	0.59	0	15-03-2013	07:06	0.60	0
19	Mid-Point-5	8° 45' 25''	78° 12' 32''	4.70	09-07-2012	11:35	0.45	0	06-10-2012	09:01	0.50	0	03-12-2012	08:00	0.57	0	15-03-2013	06:45	0.64	0
20	Mid-Point-6	8° 45'07''	78° 12' 43''	4.00	09-07-2012	11:53	0.42	0	06-10-2012	08:16	0.56	0	03-12-2012	07:30	0.62	0	14-03-2013	11:55	0.55	0
21	Lash Jetty	8° 45' 00''	78° 12' 25''	4.23	09-07-2012	11:58	0.40	0	06-10-2012	07:48	0.60	0	03-12-2012	07:15	0.65	0	14-03-2013	12:06	0.57	0
22	Shallow Berth-1	8° 45'52''	78° 12' 39''	5.90	09-07-2012	12:53	0.54	0	06-10-2012	10:23	0.39	0	03-12-2012	08:30	0.51	0	14-03-2013	12:30	0.61	0

3.2.1.2 Chennai port

Chennai port is located (13° 05’ N, 80° 17’ E) in the state of Tamil Nadu, along the east coast of India bearing the status of the second largest port in India (Fig. 3.2). It is an artificial seaport with 26 berths and port area spreads over 407.51 hectares and contains mainly three docks (Jawahar, Ambedkar, and Bharathi) and a timber pond; where Jawahar dock and timber pond are situated inside the port. The width of the main entrance channel where seawater entry and exit occurs, varies between 244 m and 410 m. Entrance width of Ambedkar and Bharathi docks (125 m and 350 m, respectively) is greater than that of Jawahar dock and timber pond (< 50 m). Based on the location, stations are demarcated as inner (S1, S2 and S13 to S15), middle (S3 to S12) and outer stations (S16 to S25). This port handles (export and import) a variety of cargo including iron ore, coal, granite, fertilizers, petroleum products, containers, automobiles and several other types of general cargo items (http://www.chennaiport.gov.in).

The occurrence of tides in these regions is semidiurnal with a maximum height of 1.26 m during ST. The mean tidal range varies from 0.91 m to 1.22 m during spring tide and from 0.61 m to 0.80 m during NT. Climatic condition in this region is tropical maritime climate with air temperature ranging from 24°C in January to 39°C in May (IMD). The study region experiences three seasons, PrM (March to May), SWM (June to September) and NEM (November to February). October is considered as a TP between SWM and NEM. This region receives an annual rainfall of 1250 mm with 60% during NEM and 30% during SWM (Shanthi and Ramanibai, 2011).

Table 3.2 Sampling details for each sampled station in the Chennai port along the east coast of India. S- stations; Est- estimated.

					South west monsoon (June)				Transition period (October)				Pre-monsoon (April)			
S. No.	S. Name	Latitude (N)	Longitude (E)	Average depth (m)	Date (d-m-y)	Time (h)	Est. tidal height (m)	Rainfall (mm)	Date (d-m-y)	Time (h)	Est. tidal height (m)	Rainfall (mm)	Date (d-m-y)	Time (h)	Est. tidal height (m)	Rainfall (mm)
1	Timber Pond	13° 5' 38"	80° 17' 42"	3.73	25-06-2012	07:34	0.52	0	18-10-2012	09:31	1.21	35.60	25-04-2013	07:10	0.98	0.20
2	Boat Basin	13° 5' 49"	80° 17' 45"	16:19	25-06-2012	09:20	0.75	0	19-10-2012	10:09	1.08	31.20	25-04-2013	07:20	1.01	0.20
3	West Quay-4	13° 5' 56"	80° 17' 49"	13.75	25-06-2012	09:55	0.83	0	19-10-2012	10:17	1.10	31.20	25-04-2013	07:53	1.10	0.20
4	West Quay, C.B.	13° 6' 3"	80° 17' 52"	14.75	25-06-2012	10:45	0.94	0	19-10-2012	10:25	1.12	31.20	25-04-2013	08:44	1.06	0.20
5	West Quay-1	13° 6' 10"	80° 17' 52"	14.01	25-06-2012	11:15	1.00	0	19-10-2012	10:34	1.14	31.20	25-04-2013	09:06	1.01	0.20
6	North Quay	13° 6' 14"	80° 17' 59"	20.88	26-06-2012	11:16	0.89	0	19-10-2012	11:21	1.07	31.20	25-04-2013	09:35	0.93	0.20
7	Chokani International	13° 6' 14"	80° 18' 7"	10.51	28-06-2012	09:01	0.46	0	21-10-2012	07:32	0.54	32.90	25-04-2013	10:02	0.86	0.20
8	A.D. Turning Circle	13° 5' 59"	80° 18' 7"	13.22	28-06-2012	10:09	0.56	0	21-10-2012	10:33	0.86	32.90	27-04-2013	09:41	1.20	0
9	2nd CT-I	13° 6' 3"	80° 18' 18"	16.07	28-06-2012	08:06	0.47	0	21-10-2012	09:49	0.78	32.90	27-04-2013	09:04	1.14	0
10	2nd CT-III	13° 5' 52"	80° 18' 14"	14.66	28-06-2012	09:38	0.52	0	21-10-2012	08:07	0.60	32.90	27-04-2013	08:47	1.09	0
11	South Quay-2	13° 5' 49"	80° 18' 7"	12.21	26-06-2012	09:33	0.69	0	19-10-2012	09:14	0.95	31.20	27-04-2013	08:33	1.04	0
12	South Quay-1	13° 5' 52"	80° 17' 56"	11.86	26-06-2012	10:32	0.81	0	19-10-2012	09:44	1.02	31.20	27-04-2013	08:27	1.02	0
13	Jawahar Dock-3	13° 5' 42"	80° 17' 49"	13.47	26-06-2012	08:03	0.52	0	19-10-2012	08:10	0.81	31.20	27-04-2013	07:16	0.79	0
14	Jawahar Dock-4	13° 5' 38"	80° 17' 52"	15.65	26-06-2012	09:09	0.64	0	19-10-2012	07:47	0.76	31.20	27-04-2013	07:02	0.75	0
15	Jawahar Dock Southern end	13° 5' 34"	80° 17' 45"	14.62	26-06-2012	07:16	0.43	0	19-10-2012	07:25	0.71	31.20	27-04-2013	06:48	0.70	0
16	B.D. Container Terminal-1	13° 6' 21"	80° 17' 59"	15.62	27-06-2012	10:52	0.73	0	20-10-2012	10:38	0.96	53.10	26-04-2013	09:24	1.10	0
17	B.D. Container Terminal-2	13° 6' 32"	80° 18' 3"	16.26	27-06-2012	10:19	0.68	0	20-10-2012	10:07	0.90	53.10	26-04-2013	08:55	1.19	0
18	B.D. Container Terminal-3	13° 6' 43"	80° 18' 7"	19.22	27-06-2012	09:45	0.62	0	20-10-2012	09:43	0.86	53.10	26-04-2013	08:06	1.06	0
19	B.D. Berth-II	13° 6' 50"	80° 18' 10"	19.64	27-06-2012	09:17	0.57	0	20-10-2012	09:17	0.81	53.10	26-04-2013	07:49	1.01	0
20	B.D. Northern end	13° 6' 54"	80° 18' 18"	9.27	27-06-2012	08:36	0.50	0	20-10-2012	08:55	0.77	53.10	26-04-2013	07:38	0.98	0
21	Oil Berth-I	13° 6' 46"	80° 18' 21"	20.06	27-06-2012	08:17	0.47	0	20-10-2012	07:59	0.66	53.10	26-04-2013	07:17	0.91	0
22	Oil Berth-III	13° 6' 35"	80° 18' 18"	20.63	27-06-2012	07:08	0.40	0	20-10-2012	07:45	0.63	53.10	26-04-2013	06:50	0.83	0
23	B.D. Turning Circle	13° 6' 21"	80° 18' 14"	30.13	29-06-2012	07:05	0.68	43.2	22-10-2012	07:45	0.55	18.50	28-04-2013	06:38	0.54	0
24	B.D. entrance-N	13° 6' 18"	80° 18' 25"	9.81	28-06-2012	07:11	0.55	0.6	21-10-2012	09:04	0.70	32.90	28-04-2013	07:08	0.64	0
25	B.D. entrance-S	13° 1' 47"	80° 18' 21"	6.52	28-06-2012	07:37	0.51	0.6	21-10-2012	09:27	0.74	32.90	28-04-2013	07:28	0.70	0

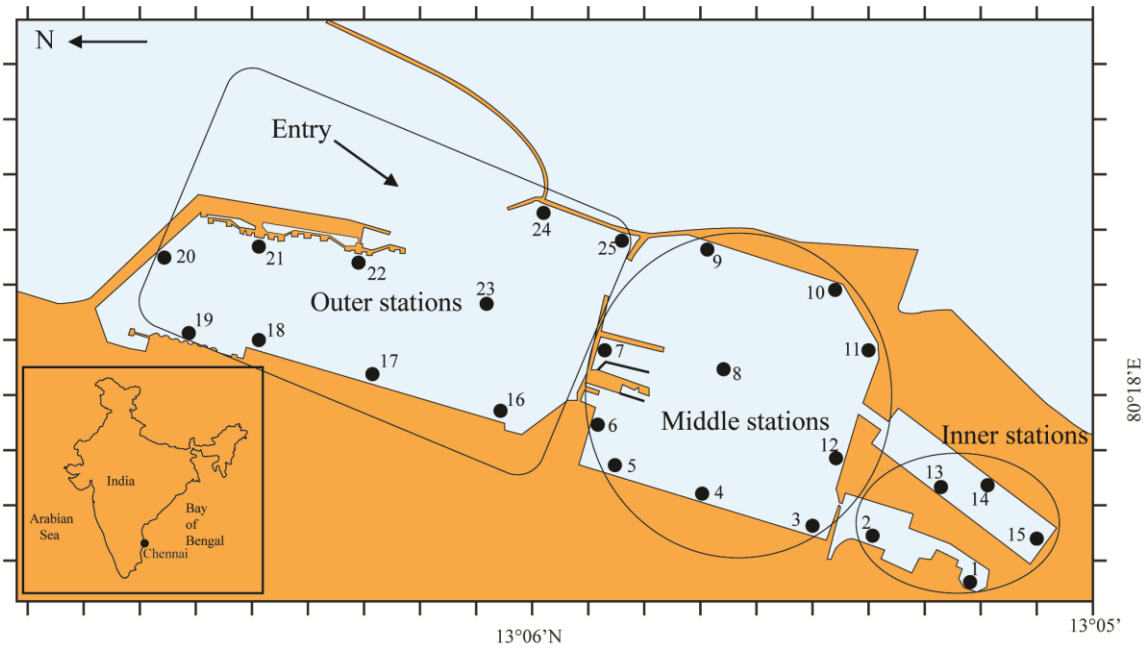

Fig. 3.2 Location of sampling stations in Chennai port, east coast of India.

3.2.1.3 New Mangalore port

New Mangalore port is located (12° 55' N; 74° 48' E) at Panambur, Mangalore in the state of Karnataka, along the west coast of India (Fig. 3.3). It is a modern all weather port consisting of 14 berths for both dry and liquid cargo vessels, with over 3.5 km of berthing space. The port is a lagoon port completed in 1974. Based on the location, stations are demarcated as inner (S1 to S9), middle (S15 to S19) and outer stations (S10 to S14). The major cargoes exported through this port includes iron ore concentrates and pellets, iron ore fines, Petroleum Oil Lubricants (POL) Products, granite stones and containerized cargo. The crude and POL products, coal, limestone, timber logs, finished fertilizers, phosphoric acid, other liquid chemicals, liquid ammonia, and containerized cargo are the major imports (http://www.newmangalore-port.com). Mangalore has a tropical MON climate with air temperatures ranging from 20°C to 38°C (IMD). It experiences three seasons, PrM (February to May), SWM (June to September) and post-monsoon (PM; October to January). This region receives an annual rainfall of 3,479 mm out of which 95% occurs during SWM, while

the remaining period (December to May) is extremely dry (IMD). New Mangalore port experiences semidiurnal tides with a mean tidal range of 0.03 m to 1.68 m during ST and 0.26 m to 1.26 m during NT.

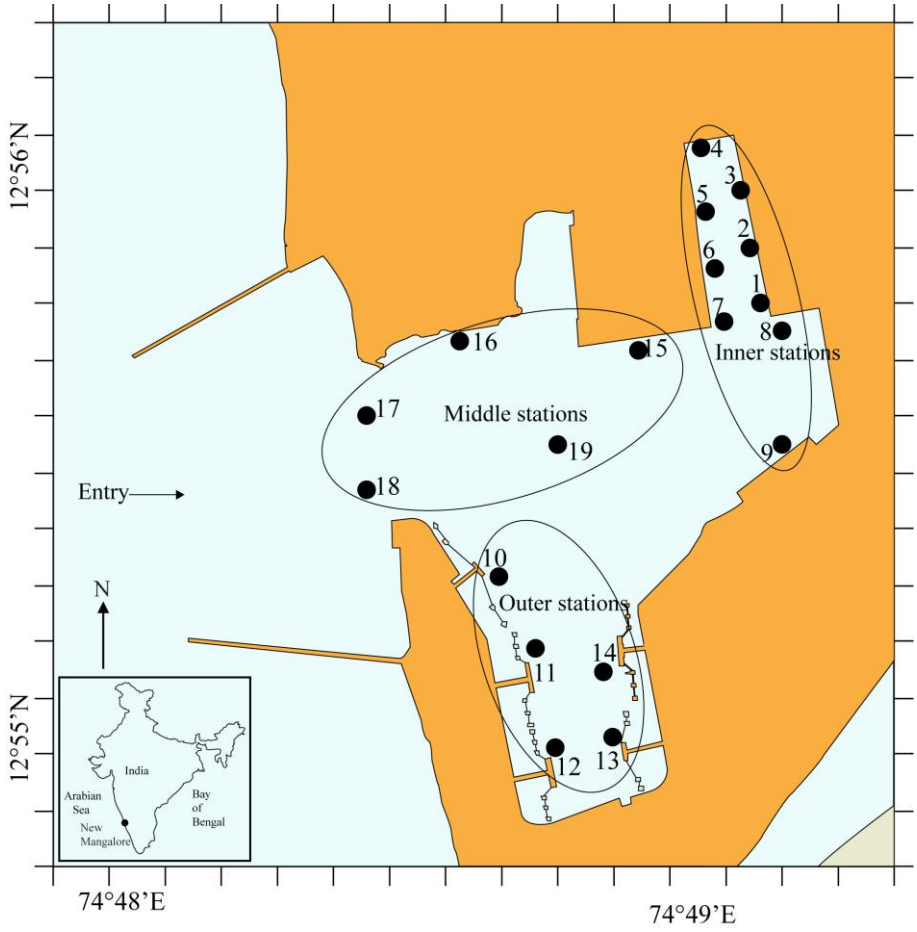

Fig. 3.3 Location of sampling stations in New Mangalore port, west coast of India.

3.2.1.4 Cochin port

Cochin port is located (9° 56' N, 76° 15' E) at the mouth of Cochin backwaters (CB) along the northern part of Kerala state, running parallel to the west coast of India with two permanent openings to the Arabian Sea (AS, Fig. 3.4). One opening is at the Cochin port and another further north at Azhikode, where the estuary is flushed during ebb tide, and seawater intrudes during flood tide. Periyar and Muvattupuzha rivers along with four others and their tributaries bring a large volume of freshwater into the CB through the Vembanad Lake, which has an active influence on the

Table 3.3 Sampling details for each sampled station in the New Mangalore port along the west coast of India. S- stations; Est- estimated.

					Post-monsoon I (November)				Pre-monsoon (May)				South west monsoon (September)				Post-monsoon II (December)			
S No.	S. Name	Latitude (N)	Longitude (E)	Average depth (m)	Date (d-m-y)	Time (h)	Est. tidal height (m)	Rainfall (mm)	Date (d-m-y)	Time (h)	Est. tidal height (m)	Rainfall (mm)	Date (d-m-y)	Time (h)	Est. tidal height (m)	Rainfall (mm)	Date (d-m-y)	Time (h)	Est. tidal height (m)	Rainfall (mm)
1	Berth No.1	12º 55' 44"	74º 49' 12"	8.76	21-11-2011	09:45	0.94	0	16-05-2012	11:37	0.99	0	26-09-2012	07:20	1.17	141.4	16-12-2012	08:04	0.81	0
2	Berth No.2	12º 55' 48"	74º 49' 8"	10.74	21-11-2011	10:00	0.90	0	16-05-2012	12:04	0.95	0	26-09-2012	08:05	1.11	141.4	16-12-2012	08:29	0.88	0
3	Berth No.3	12º 55' 55"	74º 49' 8"	10.83	21-11-2011	10:45	0.78	0	16-05-2012	08:24	1.16	0	26-09-2012	08:33	1.07	141.4	16-12-2012	08:54	0.94	0
4	Berth No.4	12º 56' 2"	74º 49' 5"	11.48	21-11-2011	11:10	0.74	0	17-05-2012	08:50	1.14	0	26-09-2012	09:13	1.02	141.4	16-12-2012	09:15	0.99	0
5	Northern Return	12º 56' 2"	74º 49' 5"	10.47	21-11-2011	11:25	0.67	0	17-05-2012	08:24	1.08	0	26-09-2012	09:57	0.96	141.4	16-12-2012	09:53	1.08	0
6	Berth No.5	12º 55' 59"	74º 49' 1"	10.99	21-11-2011	11:50	0.60	0	17-05-2012	07:57	1.02	0	27-09-2012	07:54	1.10	68.2	16-12-2012	10:13	1.13	0
7	Berth No.6	12º 55' 55"	74º 49' 1"	12.58	21-11-2011	12:05	0.56	0	17-05-2012	11:41	1.12	0	27-09-2012	07:25	1.17	68.2	16-12-2012	10:49	1.22	0
8	Berth No.7	12º 55' 48"	74º 49' 12"	12.25	21-11-2011	12:20	0.52	0	17-05-2012	11:19	1.16	0	27-09-2012	06:56	1.25	68.2	16-12-2012	11:19	1.29	0
9	Berth No.8	12º 55' 30"	74º 49' 8"	16.71	21-11-2011	14:25	0.53	0	16-05-2012	10:05	1.11	0	27-09-2012	08:42	1.21	68.2	17-12-2012	11:20	1.10	0
10	Berth No.9	12º 55' 19"	74º 48' 40"	13.28	23-11-2011	09:30	1.18	0	18-05-2012	08:08	0.98	0	27-09-2012	09:23	1.14	68.2	17-12-2012	10:45	1.02	0
11	Berth No.10	12º 55' 8"	74º 48' 47"	14.15	23-11-2011	10:30	0.97	0	18-05-2012	08:48	1.08	0	27-09-2012	09:24	1.12	68.2	16-12-2012	11:51	1.37	0
12	Berth No.11	12º 54' 58"	74º 48' 47"	15.52	23-11-2011	11:55	0.67	0	18-05-2012	09:47	1.25	0	27-09-2012	09:47	1.10	68.2	16-12-2012	12:16	1.43	0
13	Berth No.12	12º 55' 1"	74º 48' 54"	15.44	23-11-2011	12:25	0.56	0	18-05-2012	12:03	1.21	0	27-09-2012	10:12	1.06	68.2	16-12-2012	12:37	1.45	0
14	Berth No.13	12º 55' 12"	74º 48' 54"	13.27	23-11-2011	12:45	0.49	0	18-05-2012	12:52	1.13	0	28-09-2012	06:45	0.96	37.6	16-12-2012	12:53	1.39	0
15	Berth No. 14	12º 55' 41"	74º 48' 58"	14.52	21-11-2011	13:00	0.42	0	17-05-2012	10:56	1.19	0	28-09-2012	07:27	1.08	37.6	17-12-2012	07:30	0.71	0
16	Berth No. 15	12º 55' 37"	74º 48' 43"	14.98	21-11-2011	13:10	0.39	0	17-05-2012	10:13	1.26	0	28-09-2012	07:55	1.16	37.6	17-12-2012	07:54	0.63	0
17	Channel Marker Buoy-1	12º 55' 34"	74º 48' 29"	12.85	21-11-2011	13:30	0.40	0	17-05-2012	09:20	1.22	0	28-09-2012	08:21	1.23	37.6	17-12-2012	12:24	1.25	0
18	Channel Marker Buoy-2	12º 55' 26"	74º 48' 29"	10.38	21-11-2011	13:45	0.44	0	17-05-2012	09:52	1.29	0	28-09-2012	08:49	1.31	37.6	17-12-2012	11:58	1.19	0
19	Turning circle	12º 55' 30"	74º 48' 50"	15.39	21-11-2011	14:00	0.47	0	19-05-2012	07:36	0.81	0	29-09-2012	07:36	0.99	59.3	16-12-2012	14:07	1.12	0

prevailing salinity of the estuarine system (Jyothibabu et al., 2006).

CB is a very important estuarine system of Kerala in terms of fishing and extensive transportation of goods. It is also used for dumping industrial as well as domestic wastes. It has three dredged channels where the selected S are located, one being the approach channel (S1, S9 to S12, S21 to S23) of around 10 km length and 500 m width and the two inner channels located on either side of the Willingdon Island, i.e. Ernakulam channel (S13 to S20) of around 5 km length with a width of 250 to 500 m and Mattancherry channel (S2 to S8) of 3 km length with a width of around 170 to 250 m (Menon et al., 2000). This port is equipped with pipelines and flexible hoses for handling liquid cargoes including cashew nut shell liquid, chemicals, crude oil, and petroleum products, general cargo, one boat-train pier, and two jetties for various cargoes. This port receives a lot of organic and inorganic substances from several industries like oil refineries, fertilizer plants and chemical industries. From these industries, acids, alkalis, suspended solids, fluorides, free ammonium, insecticides, dyes, trace and heavy metals and radioactive nuclei are the major contaminants (Menon et al., 2000; Martin et al., 2012; Anu et al., 2014), which create a polluted environment in this port.

Tides in this region are mixed semidiurnal with a range of about 1 m (Qasim and Gopinathan, 1969). Annual air temperature ranges from 20^{o}C to 35^{o}C with maximum values from February to May (IMD). Annually this region experiences three seasons i.e., SWM (June to September), PM (October to January) and PrM (February to May). It has a hot and humid climate with an average annual rainfall of about 3500 mm, most of which is contributed by the SWM and rest by NEM (IMD). During SWM this estuary receives large amounts of freshwater (~3500 m^3 s^{-1}), which leads to a salt wedge condition in the CB during August to October, whereas during November to

May it changes to partially mixed condition due to a reduction in freshwater discharge. In June, moderately stratified to partially mixed waters are observed (Menon et al., 2000).

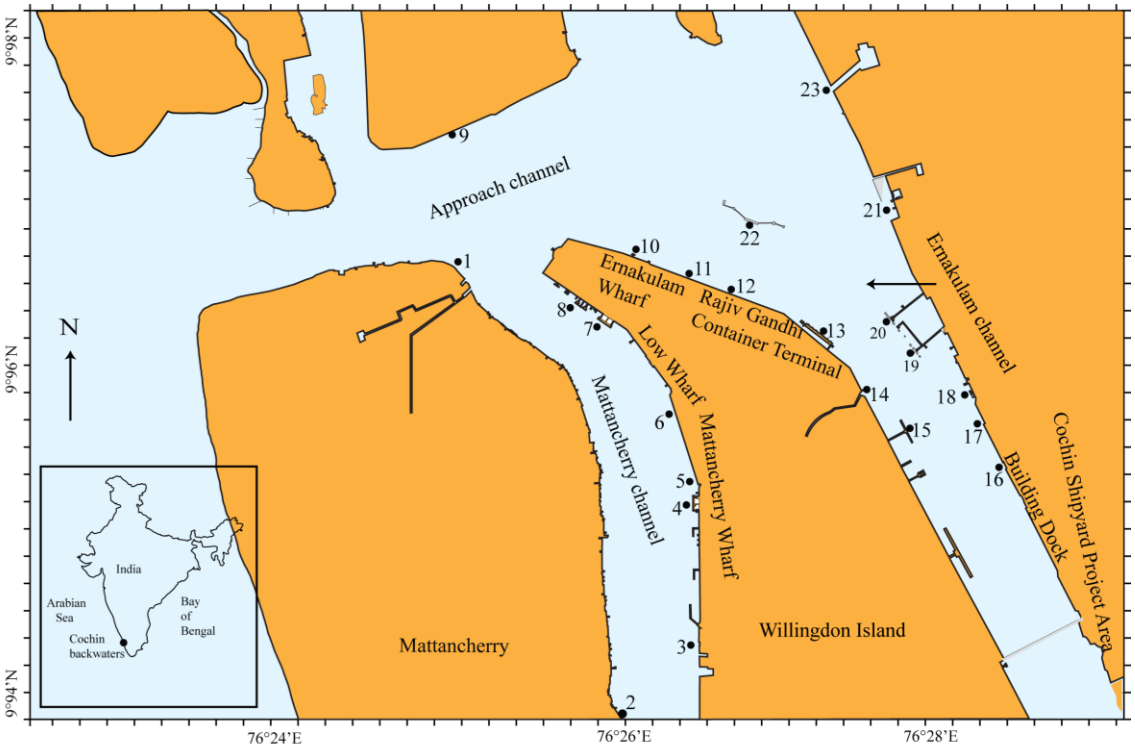

Fig. 3.4 Location of sampling stations in Cochin port, west coast of India.

3.2.1.5 Kolkata port

Kolkata port is one of the key ports in India situated (22° 32' N, 88° 18' E) on the left bank of the Hooghly River in the state of West Bengal. It is about 203 km upstream from the Sea (Fig. 3.5). It is the only riverine port in India. Hooghly River is an extension of the river Ganges, which flows south and east through the Gangetic plain of north India for about 260 km and empties into the Bay of Bengal. The Ganges is one of the world's biggest river, largest by discharge and also considered as most polluted. Hooghly River flows through a heavily industrialized area with more than one-half of West Bengal's population. The river's lower reaches are fed by the Ajay, Damodar, Rupnarayan, and Haldi (Kasai) rivers. It serves as a navigable channel for

Table 3.4 Sampling details for each sampled station in the Cochin port along the west coast of India. S- stations; Est- estimated.

					Post-monsoon I (October)				Pre-monsoon (May)				South west monsoon (August)				Post-monsoon II (November)			
S. No.	S. Name	Latitude (N)	Longitude (E)	Average depth (m)	Date (d-m-y)	Time (h)	Est. tidal height (m)	Rainfall (mm)	Date (d-m-y)	Time (h)	Est. tidal height (m)	Rainfall (mm)	Date (d-m-y)	Time (h)	Est. tidal height (m)	Rainfall (mm)	Date (d-m-y)	Time (h)	Est. tidal height (m)	Rainfall (mm)
1	Custom Buoy	9º 58' 05''	76º 15' 11''	4.88	11-10-2011	07:30	0.56	0	27-05-2012	12:08	0.54	5.4	12-08-2012	08:07	0.64	6.1	24-11-2012	09:19	0.78	1.0
2	Fishery Harbour	9º 56' 24''	76º 15' 47''	5.60	11-10-2011	12:45	0.72	0	28-05-2012	11:12	0.46	10.6	13-08-2012	07:20	0.56	7.2	24-11-2012	07:06	0.55	1.0
3	L-Jetty/Dry Dock	9º 56' 42''	76º 16' 01''	5.05	11-10-2011	11:30	0.78	0	26-05-2012	10:44	0.44	0.6	13-08-2012	08:18	0.62	7.2	24-11-2012	07:28	0.52	1.0
4	South coal berth	9º 57'11''	76º 16' 01''	6.91	11-10-2011	10:45	0.80	0	26-05-2012	12:17	0.58	0.6	13-08-2012	09:30	0.69	7.2	24-11-2012	07:51	0.50	1.0
5	Qua-1	9º 57' 14''	76º 16' 01''	7.01	11-10-2011	09:45	0.74	0	26-05-2012	11:31	0.51	0.6	13-08-2012	10:51	0.73	7.2	21-11-2012	08:32	0.76	0.0
6	Qua-4	9º 57'29''	76º 15' 54''	8.33	11-10-2011	09:00	0.68	0	26-05-2012	11:01	0.46	0.6	13-08-2012	11:42	0.71	7.2	21-11-2012	10:25	0.63	0.0
7	North Coal Berth	9º 57' 50''	76º 15' 40''	11.69	11-10-2011	08:15	0.62	0	26-05-2012	10:10	0.38	0.6	12-08-2012	09:57	0.69	6.1	21-11-2012	10:59	0.59	0.0
8	Boat Train Pier	9º 57'54''	76º 15' 36''	6.85	12-10-2011	07:00	0.54	0	28-05-2012	08:40	0.44	10.6	12-08-2012	09:16	0.70	6.1	21-11-2012	09:41	0.68	0.0
9	Container Terminal	9º 58' 30''	76º 15' 07''	11.25	12-10-2011	07:45	0.59	0	28-05-2012	09:15	0.41	10.6	12-08-2012	07:36	0.61	6.1	24-11-2012	09:56	0.73	1.0
10	DC Jetty	9º 58'08''	76º 15' 14''	9.27	12-10-2011	08:30	0.65	0	28-05-2012	07:52	0.48	10.6	12-08-2012	06:49	0.57	6.1	23-11-2012	10:19	0.69	56.1
11	Qua-6	9º 58' 01''	76º 16' 01''	9.25	12-10-2011	09:30	0.71	0	28-05-2012	07:29	0.47	10.6	11-08-2012	09:33	0.65	29.0	23-11-2012	09:52	0.72	56.1
12	Qua-8	9º 57'58''	76º 16' 12''	11.44	10-10-2011	07:30	0.60	0	27-05-2012	06:55	0.45	5.4	11-08-2012	08:56	0.66	29.0	23-11-2012	09:20	0.75	56.1
13	Qua-10	9º 57' 50''	76º 16' 30''	9.19	10-10-2011	08:00	0.65	0	27-05-2012	11:03	0.45	5.4	11-08-2012	08:07	0.67	29.0	23-11-2012	09:02	0.77	56.1
14	Ro-Ro Jetty	9º 57'36''	76º 16' 41''	8.88	10-10-2011	08:45	0.71	0	27-05-2012	10:37	0.41	5.4	11-08-2012	07:22	0.66	29.0	23-11-2012	06:59	0.86	56.1
15	Naval Jetty	9º 57' 25''	76º 16' 52''	2.69	10-10-2011	09:30	0.77	0	29-05-2012	09:56	0.49	0.0	11-08-2012	06:57	0.64	29.0	23-11-2012	06:35	0.84	56.1
16	Cochin Shipyard	9º 57'18''	76º 17' 10''	7.22	10-10-2011	10:15	0.81	0	29-05-2012	10:03	0.49	0.0	10-08-2012	10:03	0.58	31.9	22-11-2012	06:43	0.91	0.0
17	Bunker Oil Jetty	9º 57' 29''	76º 17' 06''	8.57	10-10-2011	11:15	0.74	0	27-05-2012	10:34	0.42	5.4	10-08-2012	10:30	0.57	31.9	22-11-2012	07:20	0.86	0.0
18	IFP Jetty	9º 57'36''	76º 17' 02''	3.75	09-10-2011	12:30	0.66	0	29-05-2012	08:45	0.53	0.0	10-08-2012	09:18	0.60	31.9	22-11-2012	07:54	0.82	0.0
19	South Tanker Berth	9º 57' 43''	76º 16' 48''	10.69	09-10-2011	11:30	0.70	0	29-05-2012	11:38	0.51	0.0	10-08-2012	08:42	0.62	31.9	22-11-2012	08:45	0.77	0.0
20	North Tanker Berth	9º 57'50''	76º 16' 44''	10.37	09-10-2011	10:45	0.77	0	27-05-2012	10:57	0.44	5.4	10-08-2012	07:50	0.64	31.9	22-11-2012	09:27	0.72	0.0
21	Ernakulam Ferry Jetty	9º 58' 16''	76º 16' 44''	2.28	09-10-2011	10:00	0.79	0	29-05-2012	07:58	0.56	0.0	15-08-2012	10:43	0.74	28.2	25-11-2012	06:40	0.78	0.0
22	Cochin Oil Terminal	9º 58'12''	76º 16' 12''	11.11	12-10-2011	11:00	0.77	0	27-05-2012	12:27	0.57	5.4	11-08-2012	10:12	0.64	29.0	22-11-2012	10:46	0.63	0.0
23	Ernakulam Creek mouth	9º 58'41''	76º 16' 30''	1.71	09-10-2011	09:00	0.73	0	27-05-2012	07:07	0.43	5.4	10-08-2012	07:04	0.66	31.9	22-11-2012	10:12	0.66	0.0

shipping activity to Haldia and Kolkata ports. Navigation is facilitated by constant dredging and the scour of a tidal bore that rushes inland at high tide (Rudra, 2011). It is an essential lifeline for the people of Kolkata. The fish from the river is important to the local economy (Bhaumik and Sharma, 2011).

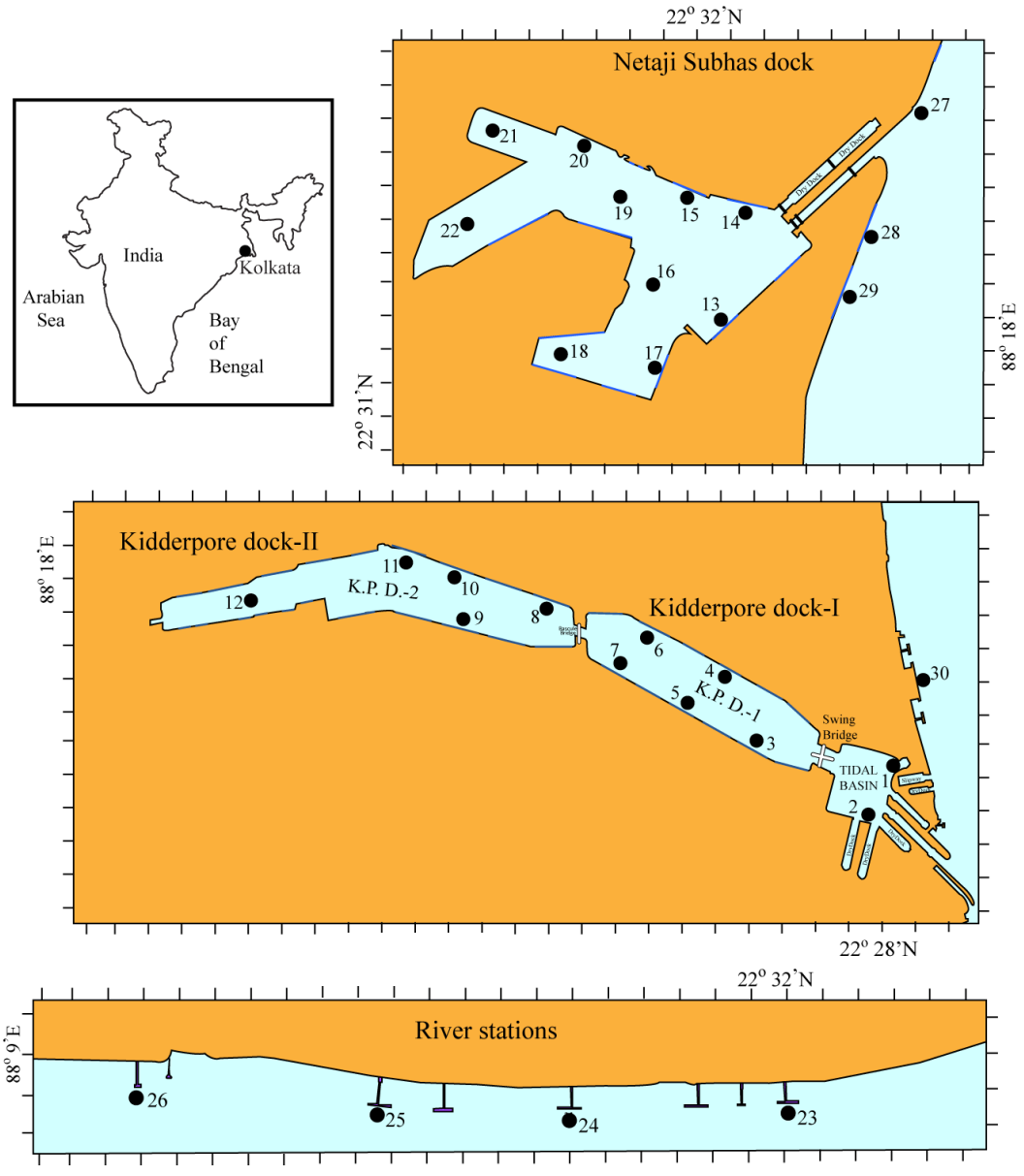

Fig. 3.5 Location of sampling stations in Kolkata port, east coast of India.

Table 3.5 Sampling details for each sampled station in the Kolkata port along the east coast of India. S- stations; Est- estimated.

					South west monsoon (September)				Pre-monsoon-I (February)				Pre-monsoon-II (February)				Post-monsoon (December)			
S. No.	S. Name	Latitude (N)	Longitude (E)	Average depth (m)	Date (d-m-y)	Time (h)	Est. tidal height (m)	Rainfall (mm)	Date (d-m-y)	Time (h)	Est. tidal height (m)	Rainfall (mm)	Date (d-m-y)	Time (h)	Est. tidal height (m)	Rainfall (mm)	Date (d-m-y)	Time (h)	Est. tidal height (m)	Rainfall (mm)
1	K.P.D. Tidal basin-1	22° 32' 43"	88° 19' 07"	5.70	20-09-2013	09:17	4.38	12	09-02-2014	08:32	2.95	0	03-02-2015	11:58	4.15	0	14-12-2015	09:00	2.09	0
2	K.P.D. Tidal basin-2	22° 32' 48"	88° 19' 03"	6.13	20-09-2013	09:38	4.80	12	09-02-2014	08:55	2.85	0	03-02-2015	12:08	4.07	0	14-12-2015	09:10	2.23	0
3	K.P.D. Berth-3	22° 32' 33"	88° 18' 54"	7.66	20-09-2013	10:07	5.39	12	09-02-2014	09:19	2.76	0	03-02-2015	10:05	3.82	0	14-12-2015	08:20	1.53	0
4	K.P.D. Berth-6	22° 32' 25"	88° 18' 50"	7.93	20-09-2013	10:42	6.11	12	09-02-2014	10:08	2.55	0	03-02-2015	10:42	4.29	0	14-12-2015	10:30	3.35	0
5	K.P.D. Berth-7	22° 32' 35"	88° 19' 01"	8.04	20-09-2013	11:18	6.03	12	09-02-2014	10:32	2.46	0	03-02-2015	11:05	4.58	0	14-12-2015	10:00	2.93	0
6	K.P.D.Berth-10	22° 32' 27"	88° 18' 57"	7.23	20-09-2013	11:05	5.87	12	09-02-2014	10:53	2.37	0	03-02-2015	09:31	3.40	0	14-12-2015	10:50	3.63	0
7	K.P.D.Berth-11	22° 32' 21"	88° 18' 53"	7.09	20-09-2013	12:35	4.95	12	09-02-2014	11:20	2.26	0	03-02-2015	09:03	3.05	0	14-12-2015	11:15	3.98	0
8	K.P.D.Berth-15	22° 32' 14"	88° 18' 46"	5.69	21-09-2013	08:22	2.61	0	06-02-2014	09:12	1.49	0	30-01-2015	08:53	3.39	0	11-12-2015	09:20	3.82	0
9	K.P.D.Berth-24	22° 32' 06"	88° 18' 48"	8.65	21-09-2013	09:04	3.43	0	06-02-2014	09:37	1.29	0	30-01-2015	09:35	3.16	0	11-12-2015	10:15	4.52	0
10	K.P.D.Berth-17	22° 32" 05"	88° 18' 44"	8.23	21-09-2013	09:50	4.32	0	06-02-2014	10:13	1.15	0	30-01-2015	10:15	2.95	0	11-12-2015	11:00	4.78	0
11	K.P.D.Berth-19	22° 31' 55"	88° 18' 42"	8.35	21-09-2013	10:17	4.85	0	06-02-2014	10:34	1.37	0	30-01-2015	10:36	2.83	0	11-12-2015	11:20	4.60	0
12	K.P.D.Berth-28	22° 31' 46"	88° 18' 46"	8.87	21-09-2013	11:00	5.68	0	06-02-2014	10:54	1.59	0	30-01-2015	11:00	2.70	0	11-12-2015	12:00	4.24	0
13	N.S.D.Berth-1-14	22° 32' 40"	88° 18' 01"	7.66	24-09-2013	11:00	4.11	0	07-02-2014	09:42	1.69	0	01-02-2015	12:33	3.05	0	12-12-2015	08:00	2.36	0
14	N.S.D..Berth-2	22° 32' 41"	88° 17' 56"	7.28	24-09-2013	12:07	4.74	0	07-02-2014	10:13	1.48	0	01-02-2015	09:13	3.83	0	12-12-2015	09:30	3.57	0
15	N.S.D.Berth-13	22° 32' 36"	88° 17' 54"	7.66	24-09-2013	15:55	3.71	0	07-02-2014	10:52	1.52	0	01-02-2015	11:01	3.68	0	12-12-2015	15:20	2.76	0
16	N.S.D.Dolphin mooring-1	22° 32' 30"	88° 18' 05"	6.41	24-09-2013	10:40	3.92	0	07-02-2014	12:03	2.10	0	01-02-2015	11:24	3.52	0	13-12-2015	08:20	2.09	0
17	N.S.D..Berth-3	22° 32' 33"	88° 18' 12"	9.24	24-09-2013	06:56	1.83	0	07-02-2014	12:24	2.28	0	01-02-2015	09:45	4.12	0	12-12-2015	10:20	4.24	0
18	N.S.D..Berth-5-6	22° 32' 23"	88° 18' 10"	6.97	24-09-2013	07:19	2.04	0	07-02-2014	16:13	4.07	0	01-02-2015	10:18	3.97	0	12-12-2015	11:30	4.93	0
19	N.S.D.Berth-7-12-	22° 32' 28"	88° 17' 54"	8.96	23-09-2013	17:32	2.51	0	08-02-2014	06:28	3.19	0	02-02-2015	08:34	3.13	0	12-12-2015	13:40	3.70	0
20	N.S.D.Ship breaking-1	22° 32' 25"	88° 17' 50"	7.28	24-09-2013	13:51	4.88	0	07-02-2014	17:18	3.53	0	02-02-2015	10:32	4.37	0	13-12-2015	08:40	2.37	0
21	N.S.D.Ship breaking-2	22° 32' 14"	88° 17' 49"	6.27	24-09-2013	15:22	4.02	0	08-02-2014	07:00	3.03	0	02-02-2015	10:56	4.20	0	13-12-2015	08:55	2.58	0
22	N.S.D.Dolphin mooring-2	22° 32' 17"	88° 17' 57"	6.15	23-09-2013	17:05	3.96	0	07-02-2014	16:38	3.86	0	02-02-2015	09:12	3.53	0	12-12-2015	13:00	4.08	0
23	Budge Budge Jetty-1	22° 29' 10"	88° 10' 36"	10.09	23-09-2013	10:30	3.04	0	08-02-2014	13:39	2.49	0	02-02-2015	14:35	2.52	0	15-12-2015	09:35	1.99	0
24	Budge Budge Jetty-3	22° 29' 17"	88° 10' 42"	9.44	23-09-2013	10:55	2.66	0	08-02-2014	13:49	2.55	0	02-02-2015	15:05	2.29	0	15-12-2015	09:55	2.27	0
25	Budge Budge Jetty-7	22° 29' 23"	88° 10' 49"	9.15	23-09-2013	11:20	2.27	0	08-02-2014	14:15	2.70	0	02-02-2015	15:35	2.06	0	15-12-2015	10:15	2.54	0
26	Budge Budge Jetty-8	22° 29' 33"	88° 11' 36"	8.45	23-09-2013	11:45	1.89	0	08-02-2014	14:35	2.82	0	02-02-2015	16:10	1.79	0	15-12-2015	10:40	2.87	0
27	HPCL Jetty	22° 33' 02"	88° 17' 37"	8.50	22-09-2013	13:00	5.19	0	08-02-2014	09:28	2.25	0	31-01-2015	13:23	2.35	0	13-12-2015	15:10	3.23	0
28	G.R. Jetty-4	22° 32' 55"	88° 17' 57"	10.46	22-09-2013	12:31	5.51	0	08-02-2014	09:07	2.36	0	31-01-2015	13:03	2.47	0	13-12-2015	14:55	3.37	0
29	G.R. Jetty-3	22° 32' 53"	88° 18' 04"	7.75	22-09-2013	12:07	5.78	0	08-02-2014	09:50	2.13	0	31-01-2015	12:24	2.70	0	13-12-2015	14:45	3.47	0
30	River Jetty	22° 32' 52"	88° 18' 52"	5.77	22-09-2013	11:26	5.32	0	08-02-2014	10:11	2.02	0	31-01-2015	12:00	2.85	0	13-12-2015	15:25	3.08	0

The Kolkata port manages two separate docks i.e, Kidderpore docks (KOPT-I and KOPT-II) which consist of 18 berths and 3 dry docks and Netaji Subhas Dock (NSD) with 10 berths 2 dry docks. Four berths are located on the river, outside the KOPT docks. Budge Budge river moorings have 6 petroleum wharves. The length and width of the KOPT docks are 405 m and 19.33 m, respectively; and NSD is 172.21 m and 22.86 m, respectively. This port handles chemicals, crude oil, petroleum products, automobiles, several other types of general cargo, coal, timber, containers and pulses (http://www.kolkataporttrust.gov.in).

Tidal variation at the mouth is 6.5 m during ST and 4.2 m during NT (IMD). Saline water intrusion is limited to 70 km from the mouth (Sadhuram et al., 2005). The average depth of this river is about 6 m. The average values of freshwater discharge are 3000 m^3 s^{-1} during SWM season (June to September) and 1000 m^3 s^{-1} during the dry season (November to May; Sadhuram et al., 2005). This region experiences a tropical savannah climate with a hot and dry season from March to early June (28 to 38°C), hot and wet season from mid-June to September and a cold season from October to February (9 to 16°C) (IMD).

3.2.2 Sampling

Altogether four samplings were conducted in each port except Chennai port where three samplings were carried out. Within each port, 19 to 25 stations were selected for sample collection including ship berths and channels. Details of sampling stations, seasons, date, time and depth of the stations are presented in table 3.1 (V.O.C), 3.2 (Chennai), 3.3 (New Mangalore), 3.4 (Cochin) and 3.5 (Kolkata). Sampling was carried out between 06:30 to 17:00. Rainfall and tidal range data were collected from the IMD. Tidal height was estimated from the tidal range for the respective sampling time. Water temperature was determined using multi parameter

Sonde DS5X (Hydrolab). Surface and near bottom water (NBW) samples were collected with a 5 L Niskin sampler. Salinity was measured with an autosal (Guildline Autosal 8400B). For chlorophyll *a* (chl *a*) estimation, seawater samples (250 mL) were filtered through Whatman GF/F filter papers. Filters were preserved with $MgCO_3$ and stored at -20ºC until analysis. In the laboratory, each filter paper was placed separately in a dark vial containing 90% acetone. After extraction in the dark at 4°C for 24 h, chl *a* concentration was determined on a Turner Design 10-AU fluorometer calibrated with commercial chl *a* (Parsons et al., 1984). Nutrients such as nitrate (NO_3^-), phosphate (PO_4^{3-}), nitrite (NO_2^-), ammonium (NH_4^+) and silicate (SiO_4^{4-}) were analyzed by SKALAR SANplus ANALYSER. Dissolved oxygen (DO) and biological oxygen demand (BOD) were analyzed following standard methods (Parsons et al., 1984). For PP analysis, duplicate samples were preserved with paraformaldehyde (0.2% final concentration, Campbell, 2001) in 2 mL cryovials, flash frozen in liquid nitrogen and stored at -80°C until analysis.

3.2.3 Flow cytometric analysis of picophytoplankton

Refer chapter 2A, section 2A.2.3. From the V.O.C, Chennai and New Mangalore port waters, four groups of PP were distinguished i. e., *SYN*-PEI, *SYN*-PEII, PEUK and *PRO*-like cells. From Cochin port waters, five groups of PP were distinguished i. e., *SYN*-PEI, *SYN*-PEII, *SYN*-PC, PEUK and *PRO*-like cells. PE-rich *SYN* observed in the freshwater (Kolkata port) was designated as *SYN*-PEIII (see chapter 2A, section 2A.2.3). Along with this, *SYN*-PC, PEUK and *PRO*-like cells were also distinguished in Kolkata port waters.

3.2.4 Trophic status of the water column

For coastal waters, multivariate index of trophic state (TRIX) method was used to evaluate the trophic status of port waters (Vollenweider et al., 1998; Sin et al., 2013),

which was then used to assess the relationship with the PP groups. TRIX was calculated using the equation TRIX= (log10 (chl *a* × a%O_2 × DIN × DIP) - k)/m, where chl *a* is in mg m^{-3}, a%O_2 is absolute value of the percentage of DO saturation (abs |100 - %O_2| = %O_2), DIN is dissolved inorganic nitrogen including NO_3^-, NO_2^-, NH_4^+ in mg m^{-3} and DIP is dissolved inorganic PO_4^{3-} in mg m^{-3}. The constants k- 3.5 and m- 0.8 are scale values obtained from Vollenweider et al. (1998) to adjust TRIX scale values (reads from 0 to 10) with a level of eutrophication in the ports. According to this method, TRIX scores lesser than 4 indicate high state of water quality with low eutrophication; scores between 4 and 5 indicate good state of water quality with medium eutrophication; scores between 5 and 6 indicate bad state of water quality with high eutrophication and scores greater than 6 indicate poor state of water quality with elevated levels of eutrophication. For freshwater (Kolkata port), Carlson trophic Index method was used to measure the trophic status of water column (Carlson, 1977). Carlson trophic Index was calculated based on the chl *a* concentration, using the equation TSI(chl) = 30.6 + 9.81 ln(chl) where ln is natural log. According to this method, TSI(chl) value < 40 indicate oligotrophic, between 40 and 50 indicate mesotrophic and > 50 indicate eutrophic waters.

3.2.5 Data analyses

In each port, linear regression analysis was performed in order to understand the relationship of PP abundance (*SYN*-PEI, *SYN*-PEII, *SYN*-PEIII, *SYN*-PC, PEUK and *PRO*-like; log [x+1]) and TRIX scores (except for Kolkata port). Multiple regression analysis was carried out between TRIX scores and environmental variables (DO, chl *a*, NO_3^-, NO_2^-, PO_4^{3-}, and NH_4^+) used to extract TRIX scores, for different ports except for Kolkata port. Principal Component Analysis (PCA) was applied to the ecological variables: salinity, temperature, DO, BOD, NO_3^-, NO_2^-, PO_4^{3-}, NH_4^+ and

SiO_4^{4-}. This analysis was done using SPSS statistics software (windows 22.0) with a significance level of $p < 0.05$ in order to assess the ecological variables which are major influencing factors in the ports. Principal components (PC) having eigen values > 1 were considered for further analysis. Subsequently, linear regression analysis was performed between the PC scores and cell abundance [log (x+1)] of individual PP groups in order to evaluate the relationship of PP groups with the environmental variables.

3.3 Results

3.3.1 Environmental parameters

3.3.1.1 V.O.C. port

Precipitation was not observed during any of the sampling periods, except a day during PrM (Table 3.1). Tidal height ranged from 0.31 to 0.76 m during the study period (Table 3.1). Distinct seasonal variation ($p < 0.05$) in environmental variables were observed. Water temperature was highest (29.46 ± 0.18^{o}C) during SWM and PrM; and lowest (27.69 ± 0.12^{o}C) during NEM (Fig. 3.6a and b). Salinity in inner, middle and outer stations was > 35 during SWM and TP, whereas during NEM and PrM, it was < 35 at most of the stations (Fig. 3.6c and d). DO concentrations were higher (4.5 to 7.1 mg L^{-1}) during TP and lower during NEM (3.4 to 6.3 mg L^{-1}; Fig. 3.6e and f). BOD concentrations ranged from 0.2 to 5.6 mg L^{-1} during the study period (Fig. 3.6g and h). On an average, BOD values were higher during NEM (2.73 ± 1.22 mg L^{-1}), especially at the inner stations followed by SWM (1.72 ± 0.85 mg L^{-1}), PrM (1.56 ± 1.66 mg L^{-1}) and TP (1.38 ± 0.9 mg L^{-1}). There was not much difference ($p > 0.05$) between the surface and NBW temperature, salinity, DO and BOD values. Chl *a* concentrations were higher (0.5 to 32.06 µg L^{-1}) during TP,

particularly at the inner stations (Fig. 3.6i and j). During rest of the seasons, chl *a* concentrations ranged from 0.01 to 7.43 µg L^{-1}. There was not much difference ($p > 0.05$) between the surface and NBW chl *a* concentration.

NO_3^- concentrations were higher (3.7 to 34.15 µM) during NEM at the inner and middle stations (Fig. 3.6k and l) and were lower (0.03 to 4.57 µM) during SWM. NO_2^- concentrations ranged from 0.01 to 2.8 µM, except during NEM where higher concentrations (2.92 to 25.60 µM) were observed (Fig. 3.6m and n). NH_4^+ concentrations were higher (9.54 to 47.89 µM) during NEM especially at the inner stations, followed by TP, whereas during SWM and PrM, it was lower (Fig. 3.6o and p). PO_4^{3-} concentrations ranged from 0.66 to 4.08 µM during the study period with higher concentrations during NEM and TP, especially at the outer stations. PO_4^{3-} concentrations were lower during SWM except at S1 and S22 (Fig. 3.6q and r). SiO_4^{4-} concentrations ranged from 2.51 to 23.44 µM with higher values during SWM (Fig. 3.6s and t). There was not much difference ($p > 0.05$) in NO_3^-, NO_2^-, NH_4^+, PO_4^{3-} and SiO_4^{4-} concentrations between the surface and NBW. TRIX scores for the study region ranged from 1.1 to 6.08 during all the seasons (Fig. 3.6u and v). TRIX scores were higher during TP (2.5 to 6.08) compared to other seasons, especially at the inner stations. There was not much difference ($p > 0.05$) in TRIX scores between the surface and NBW. Chl *a* was the major factor contributing to the TRIX scores followed by PO_4^{3-} and DO (Table 3.6).

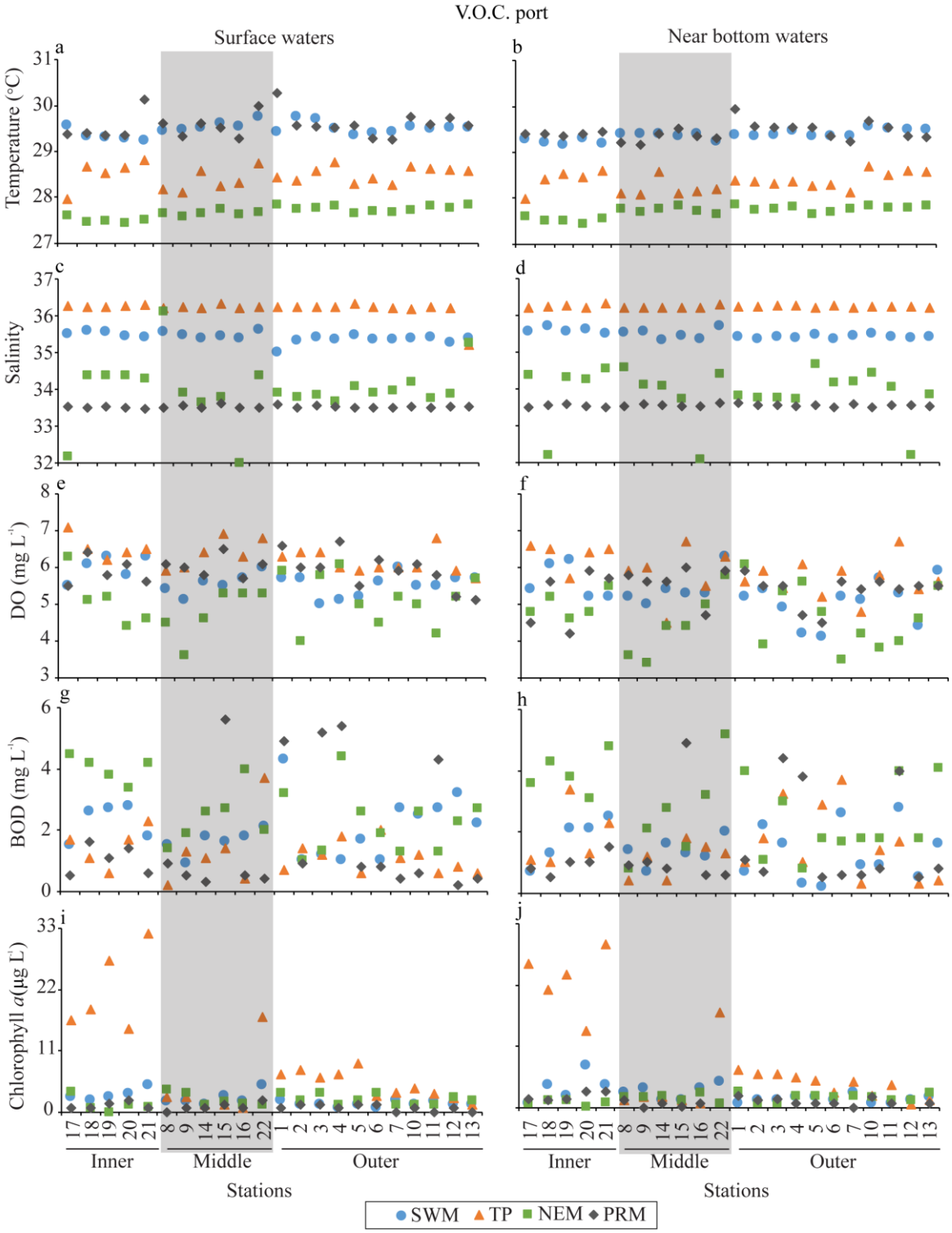

Fig. 3.6 Seasonal and spatial variations in (a, b) temperature, (c, d) salinity, (e, f) dissolved oxygen, (g, h) biological oxygen demand, (i, j) chl *a*, (k, l) nitrate, (m, n) nitrite, (o, p) ammonium, (q, r) phosphate, (s, t) silicate and (u, v) TRIX scores in the surface and near bottom waters of the V.O.C. port.

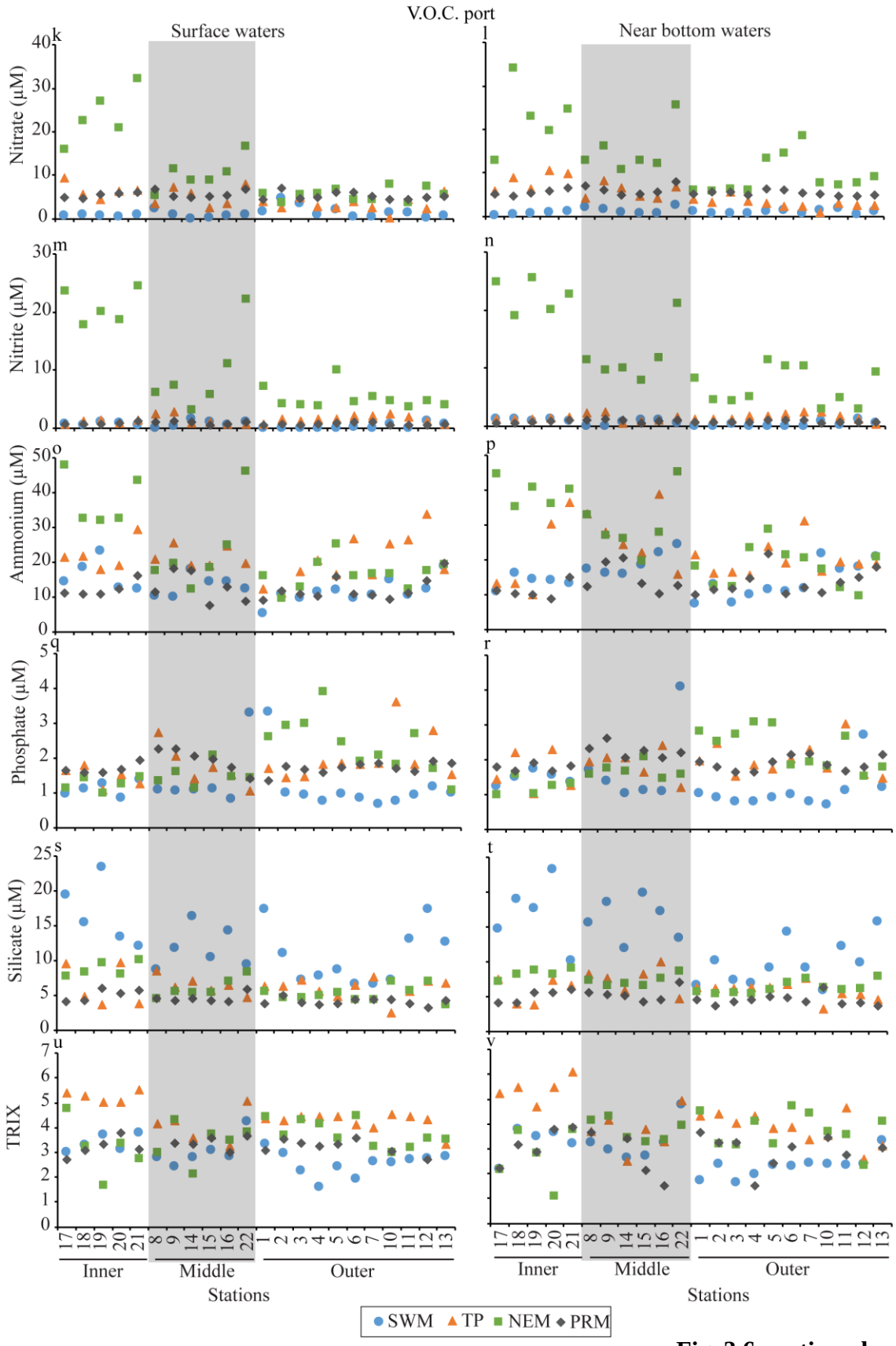

Fig. 3.6 continued

3.3.1.2 Chennai port

During TP, the study region experienced heavy rainfall (Table 3.2). During SWM, tidal height varied between 0.40 and 1.00 m whereas, during TP and PrM, it varied from 0.54 to 1.2 m (Table 3.2). Distinct seasonal variation ($p < 0.05$) in environmental variables were observed. During SWM, the average temperature was 27.28 ± 0.3ºC, which was lower than that in the TP (29.09 ± 0.3ºC) and PrM (28.49 ± 0.3ºC) (Fig. 3.7a and b). During TP, lower salinity (23.62 to 33.34) was observed compared to SWM and PrM (32.5 to 34.6) which coincided with heavy precipitation (Fig. 3.7c and d; Table 3.2). During TP, DO concentration varied seasonally, ranging from 1.39 to 6.3 mg L^{-1} with lower concentration during SWM and higher during TP, especially at the outer stations (Fig. 3.7e and f). BOD concentrations were higher during PrM (0.2 to 3.7 mg L^{-1}) especially in the surface waters of outer stations followed by SWM and TP (Fig. 3.7g and h). Overall, there was not much difference ($p > 0.05$) in temperature, salinity, DO and BOD values between the surface and NBW. Chl *a* concentrations ranged from 0.6 to 10.2 µg L^{-1} with higher values during PrM, especially in the surface waters of outer stations (Fig. 3.7i and j). During TP, higher chl *a* concentrations were observed at the outer stations. There was not much difference ($p > 0.05$) in chl *a* concentrations between the surface and NBW.

NO_3^- concentrations were higher (1.8 to 56.2 µM) during SWM and TP (in the surface waters of some stations, Fig. 3.7k and l). The highest concentration was observed in the surface waters of S15 (56.2 µM) during TP. NO_2^- concentrations were higher (0.4 to 4.1 µM) during SWM at all the stations and only inner stations (surface waters) during TP (Fig. 3.7m and n). NH_4^+ concentrations were higher (10.8 to 177.2 µM) during TP at the inner and middle stations and lower during PrM (5.9 to 27.86 µM; Fig. 3.7o and p). PO_4^{3-} concentrations ranged from 0.9 to 17.4 µM during the

study period with higher concentrations (1.1 to 17.4 µM) during SWM, especially at the outer stations (Fig. 3.7q and r). SiO_4^{4-} concentrations were higher (8.9 to 93.6 µM) during SWM especially at S11 and S16 (surface and NBW) followed by TP and PrM (Fig. 3.7s and t). There was not much difference ($p > 0.05$) in NO_3^-, NO_2^-, NH_4^+, PO_4^{3-} and SiO_4^{4-} values between the surface and NBW. TRIX scores were higher during SWM (2.95 to 5.99) followed by PrM (2.56 to 5.08) and TP (2.01 to 5.39). Overall TRIX scores suggest that the water quality was good (Fig. 3.7u and v). Generally, TRIX scores were higher at the outer stations (S17 to S25). There was not much difference ($p > 0.05$) in TRIX scores between the surface and NBW. DO was the major factor, which negatively contributed to the TRIX scores followed by chl *a*, PO_4^{3-} and NO_2^- (Table 3.6).

3.3.1.3 New Mangalore port

During the SWM, the study region experienced heavy rainfall (Table 3.3). Tidal height during sampling period ranged from 0.39 to 1.45 m. During PM-I, sampling was carried out during low tide at most of the stations. Distinct seasonal variation ($p < 0.05$) in environmental variables were observed. Water temperature was lower (25.56 ± 0.62ºC) during SWM compared to other seasons (29.14 ± 0.52ºC; Fig. 3.8a and b). During PrM, temperature difference between surface and NBW was 1.5ºC. There was not much difference ($p > 0.05$) in temperature between the surface and NBW, except during SWM. Higher salinity (35.2 to 36.7) was observed during PM-I and PrM compared to SWM and PM-II (33.8 to 35.0) (Fig. 3.8c and d). There was not much difference ($p > 0.05$) in salinity between the surface and NBW. DO concentrations varied seasonally, ranging from 0.1 to 7.8 mg L^{-1} with higher values in the surface waters of the outer stations and middle stations during PrM (Fig. 3.8e and f). During SWM in the NBW, DO concentration was < 1 mg L^{-1} at most of the stations whereas,

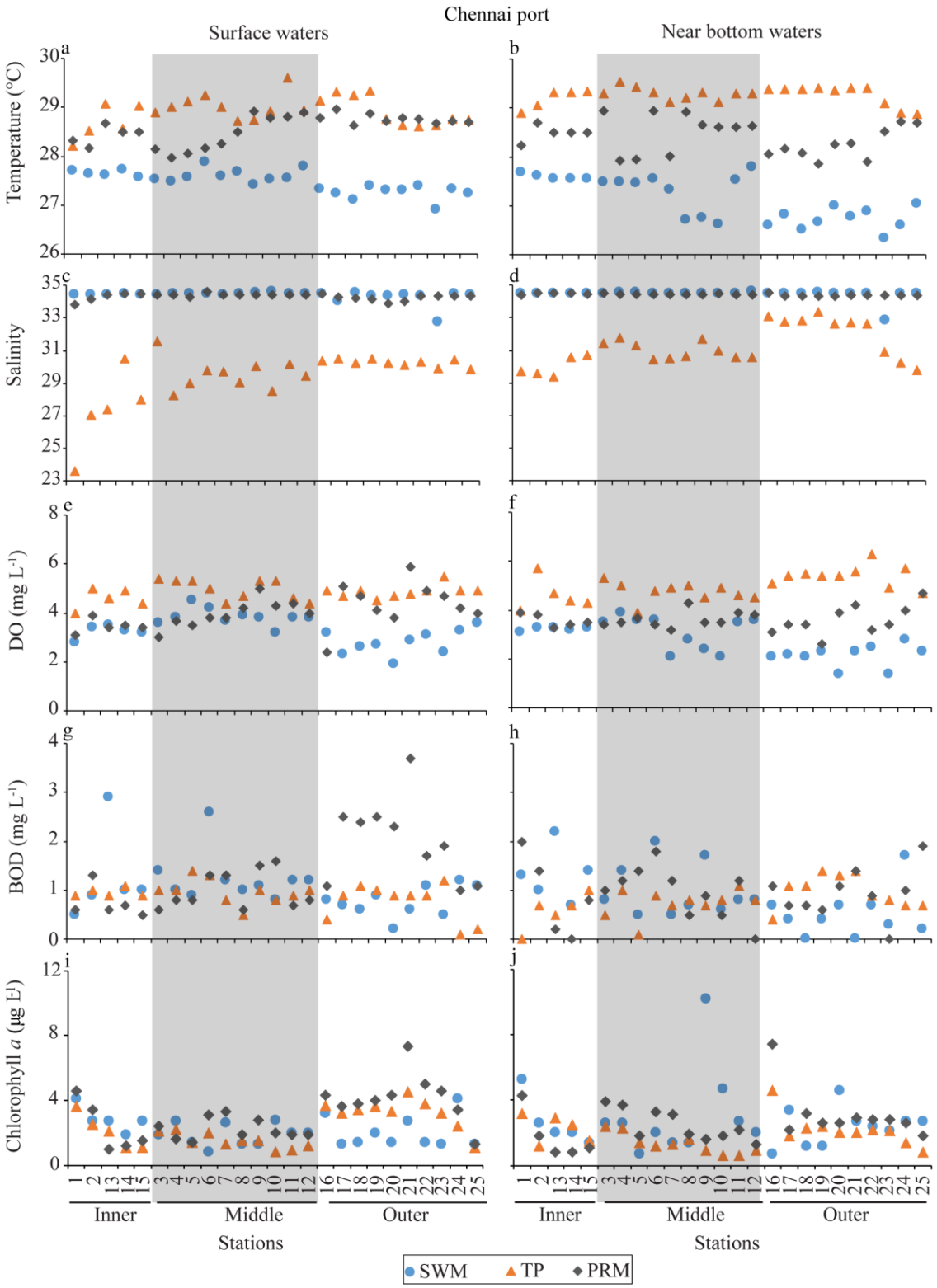

Fig. 3.7 Seasonal and spatial variations in (a, b) temperature, (c, d) salinity, (e, f) dissolved oxygen, (g, h) biological oxygen demand, (i, j) chl *a*, (k, l) nitrate, (m, n) nitrite, (o, p) ammonium, (q, r) phosphate, (s, t) silicate and (u, v) TRIX scores in the surface and near bottom waters of the Chennai port.

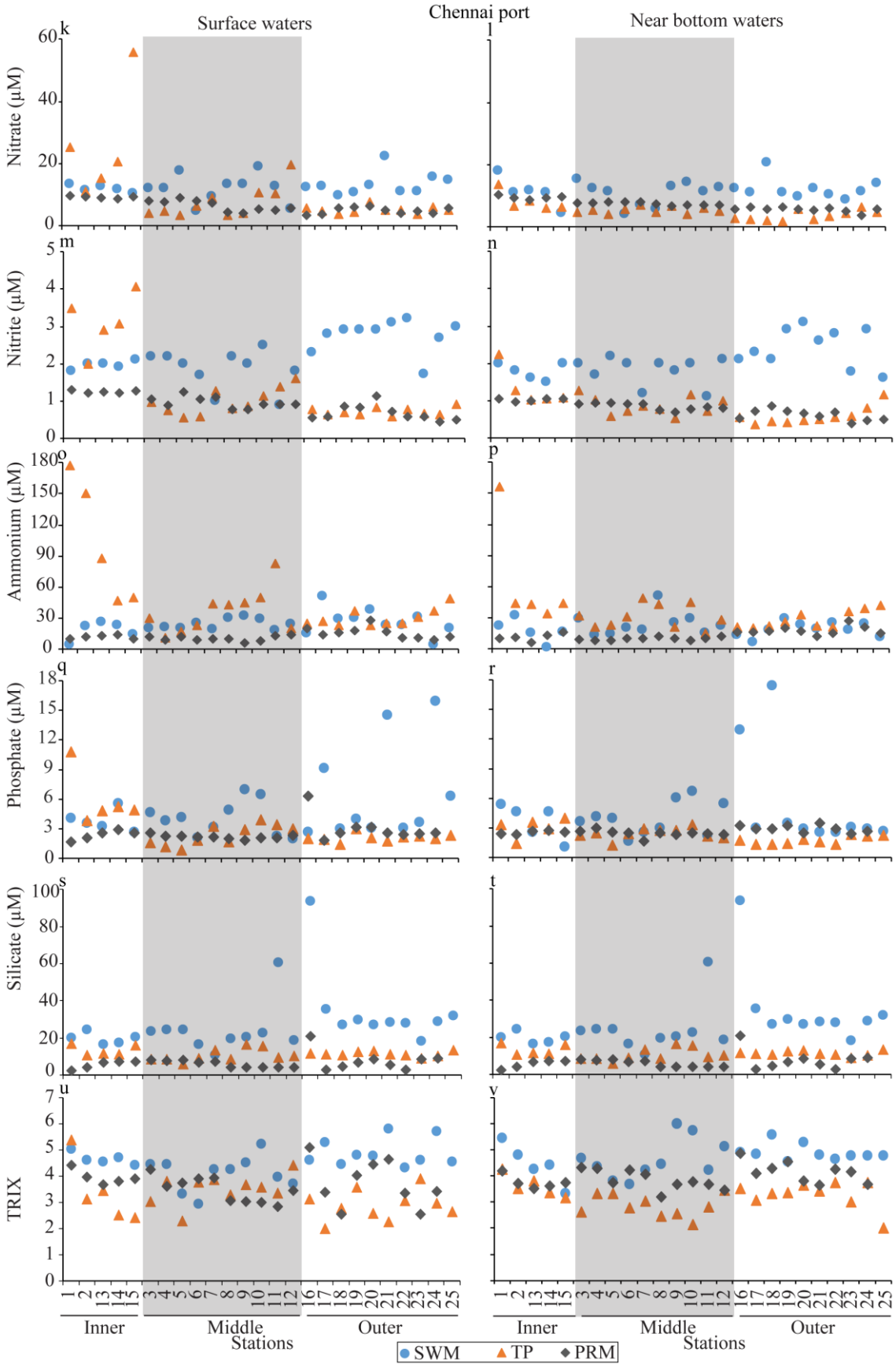

Fig. 3.7 continued

it was higher (1.7 to 6.2 mg L^{-1}) in the surface waters. Higher DO concentrations (3.4 to 6.2 mg L^{-1}) were observed during PM-II compared to that during PM-I (1.7 to 4.8 mg L^{-1}). There was not much difference ($p > 0.05$) in DO concentrations between the surface and NBW during PM's. BOD concentrations were higher during SWM (0.01 to 4.8 mg L^{-1}) in the surface waters of inner stations and during PM-II (0.01 to 3.8 mg L^{-1}) at the outer and middle stations (surface and NBW) (Fig. 3.8g and h). Chl *a* concentrations were higher (0.9 to 47.1 µg L^{-1}) in the surface waters of inner stations during PrM and SWM and in the NBW of some stations (S1 to 2, S6 to 8, and S13 to 19; Fig. 3.8i and j). Highest chl *a* concentration (47.1 µg L^{-1}) was observed at S5 in the surface waters during PrM. During PM-I, low chl *a* concentrations (< 2 µg L^{-1}) were recorded across the study region. There was not much difference ($p > 0.05$) in salinity between the surface and NBW during PM-I and PM-II.

Maximum NO_3^- concentrations (0.7 to 28.7 µM) were found during PM-I, especially at the inner and middle stations of surface and inner and outer stations in the NBW, followed by PrM and PM-II. NO_3^- concentrations were lower (0.1 to 3.1 µM) during SWM (Fig. 3.8k and l). Overall, higher NO_3^- concentrations were observed in the NBW compared to that in the surface waters during PrM and some stations during PM-I . NO_2^- concentrations were higher (0.5 to 13.2 µM) during PMs and lowest during SWM (0.3 to 1.1 µM) (Fig. 3.8m and n). NH_4^+ concentrations ranged from 8.6 to 52.5 µM with higher values during PM-I and lowered during PM-II (Fig. 3.8o and p). There was not much difference ($p > 0.05$) in NO_2^- and NH_4^+, concentrations between the surface and NBW. PO_4^{3-} concentrations ranged from 0.3 to 9.19 µM during the study period with higher concentrations (1.8 to 5.3 µM) during SWM, especially in the NBW (Fig. 3.8q and r). Highest PO_4^{3-} concentration was observed in the surface waters of S19 (9.19 µM) during PrM and also during PM-I at

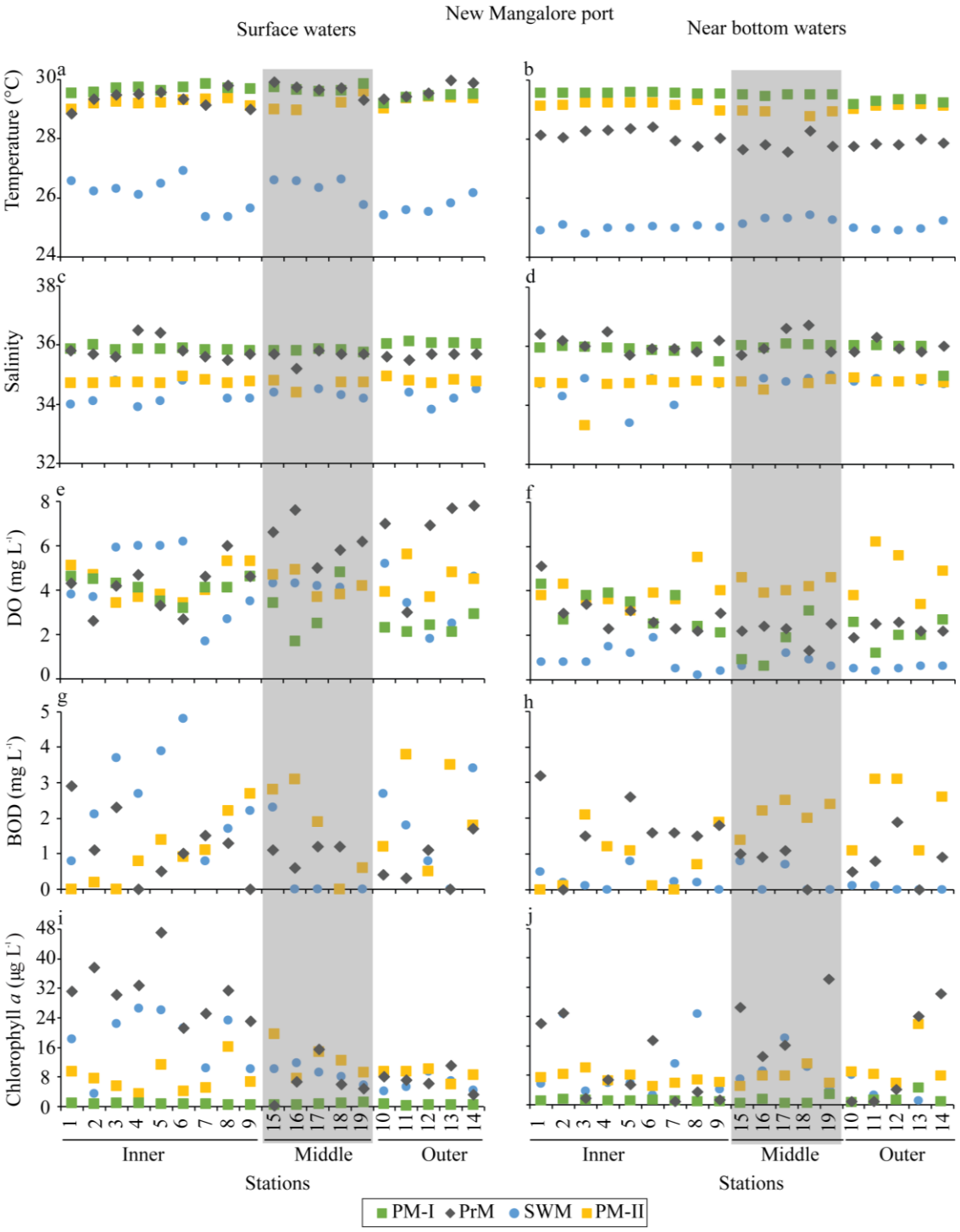

Fig. 3.8. Seasonal and spatial variations in (a, b) temperature, (c, d) salinity, (e, f) dissolved oxygen, (g, h) biological oxygen demand, (i, j) chl *a*, (k, l) nitrate, (m, n) nitrite, (o, p) ammonium, (q, r) phosphate, (s, t) silicate and (u, v) TRIX scores in the surface and near bottom waters of the New Mangalore port.

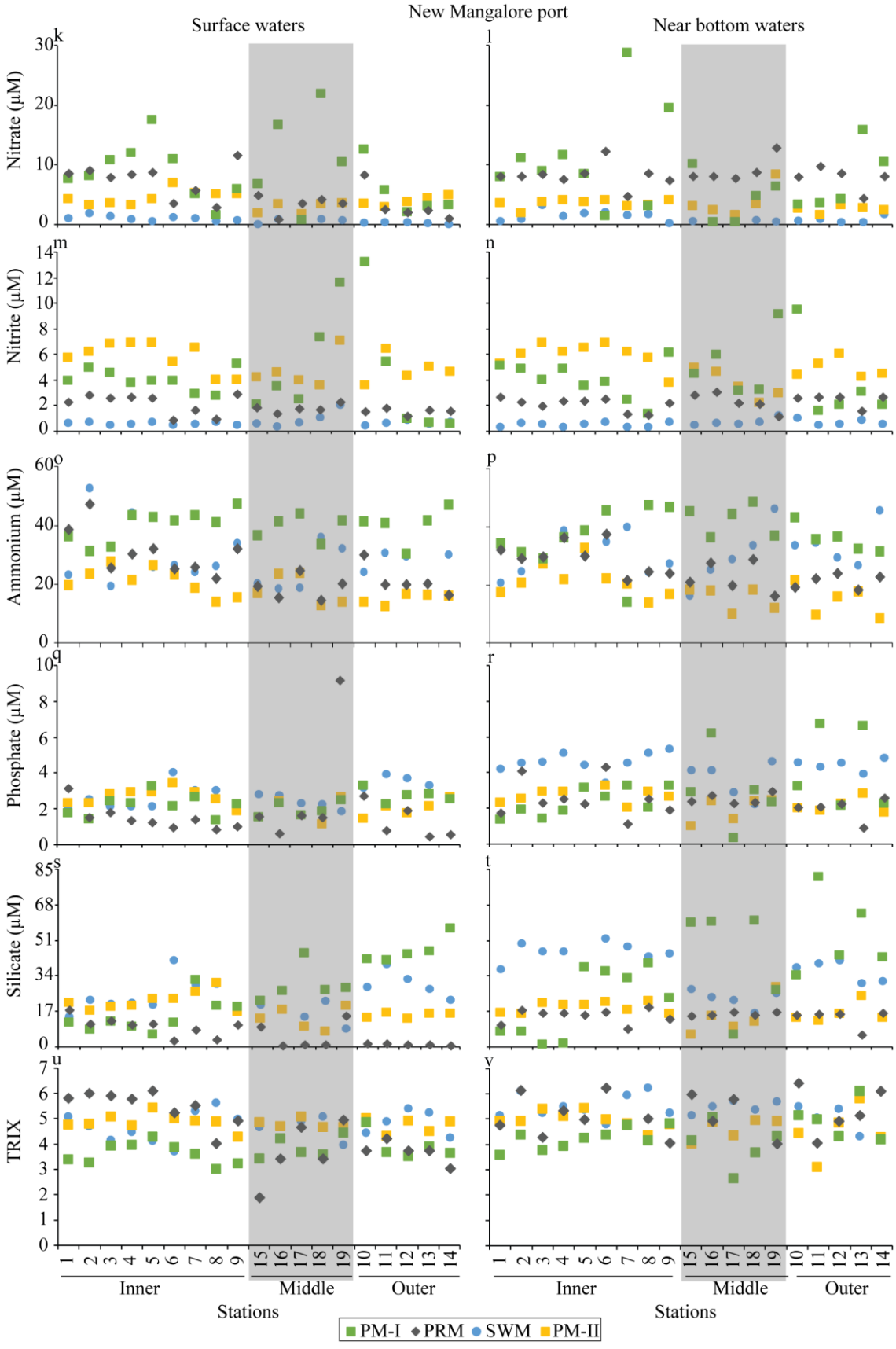

Fig. 3.8 continued

S11, S13, and S16 in the NBW. There was not much difference ($p > 0.05$) in PO_4^{3-} concentrations between the surface and NBW, except during SWM. SiO_4^{4-} concentrations were higher at middle and outer stations during PM-I (5.5 to 81.1 µM) and in the NBW across the study region during SWM (16.2 to 51.5 µM; Fig. 3.8s and t). SiO_4^{4-} concentrations (0.22 to 18.74 µM) were lower during PrM. There was not much difference ($p > 0.05$) in SiO_4^{4-} concentrations between the surface and NBW, except during SWM. Higher TRIX (4.02 to 6.22) scores were observed during PrM at the inner stations and across the study region during SWM (3.74 to 6.24) in the NBW suggesting bad water quality during this period (Fig. 3.8u and v). Overall, TRIX scores revealed that the New Mangalore port waters showed a good state of water quality. TRIX scores were significantly ($p < 0.05$) higher in NBW. Chl *a* was the major factor contributing to the TRIX scores followed by DO, NO_2^-, NH_4^+ and PO_4^{3-} (Table 3.6).

3.3.1.4 Cochin port

Heavy precipitation was observed during SWM (total 102.4 mm). PrM showers (total 22 mm) were observed at the end of May 2012 (Table 3.4). During the study period, tidal amplitude ranged from 0.38 to 0.91m. PrM sampling was carried out during low tide and during mid to high tide during the other seasons (Table 3.4). Station depths varied from ~1.71 m (S23) to ~11.69 m (S9). Temperature ranged from 24 to 31.3ºC with the lowest temperature during SWM compared to PM and PrM in surface and NBW (Fig. 3.9a and b). The study region was partially mixed during PrM and PM and stratified during SWM (Salinity 2 to 14 of surface waters and 4 to 34.8 of NBW) due to a significant amount of freshwater discharge. During PM-I, surface water salinity was higher than that during PrM at the approach channel stations (Fig.

3.9c and d), as PrM sampling was carried out during low tide (Table 3.4). Higher salinity was observed across the Cochin port during PM-II, which was carried out during high tide. Salinity and temperature showed significant variation ($p < 0.05$) between surface and NBW. DO concentrations were high in PM-I (0.55 to 9.34 mg L^{-1}) followed by PrM, PM-II and SWM with significantly ($p < 0.05$) higher values in the surface waters (Fig. 3.9e and f). BOD values ranged between 0.02 and 7.45 mg L^{-1} during all the seasons and did not show much difference ($p > 0.05$) between surface and NBW (Fig. 3.9g and h). On an average, BOD values were higher during PM-I (0.02 to 7.45 mg L^{-1}) and PM-II (0.05 to 4.05 mg L^{-1}) and lower during PrM (0.026 to 4.78 mg L^{-1}) and SWM (0.04 to 2.74 mg L^{-1}). Chl *a* concentrations during the four seasons varied from 2.25 to 107.08 µg L^{-1} across the Cochin port (Fig. 3.9i and j). Compared to the mouth of the Cochin port, chl *a* concentrations were higher at the Ernakulam (S2 to S8) and Mattancherry channel (S11 to S23) stations. During SWM and PrM, higher chl *a* concentrations were observed in the surface waters compared to that in the NBW whereas during PM-I and PM-II higher chl *a* concentrations were observed in the NBW.

High NO_3^- concentrations (0.55 to 28.42 µM) were recorded during SWM followed by PM-II (1.14 to 14.11 µM), PrM (1.85 to 7.54 µM), and PM-I (0.01 to 11.91 µM) with higher values in the surface waters. NO_3^- concentrations did not differ ($p > 0.05$) much between the stations except during PM-II, where Ernakulam (S14 and S15) and Mattancherry channel (S4 and S6) stations had higher NO_3^- concentrations (Fig. 3.9k and l). NO_2^- concentrations were lower (0.01 to 1.21 µM) during two successive PMs (Fig. 3.9m and n). NO_2^- concentrations were higher during SWM (0.45 to 3.20 µM), especially in the Ernakulam channel. NH_4^+ concentrations were higher during PrM followed by PM-I and SWM (10 to 66 µM, Fig. 3.9o and p).

There was not much difference ($p > 0.05$) in NO_2^- and NH_4^+ concentrations between the surface and NBW. Higher PO_4^{3-} concentrations were recorded in the surface waters during PrM (2.17 to 6.69 µM) followed by SWM (2.27 to 6.55 µM) and PM (1.15 to 5.09 µM; Fig. 3.9q and r). SiO_4^{4-} concentrations ranged from 9.76 to 93.53 µM and were higher during PM-I in the surface waters, particularly at Ernakulam channel (S15 to S19) (Fig. 3.9s and t). TRIX scores for the study region ranged from 1.64 to 7.37 during all the seasons (Fig. 3.9u and v). During PrM and SWM, most of the stations showed elevated conditions of eutrophication. Only during the PM-I medium level of eutrophication with a good state of water quality was observed for the surface waters. Overall, TRIX scores revealed that the Cochin port water quality is poor. There was not much difference ($p > 0.05$) in TRIX scores in the surface and NBW. Chl *a* was the major factor contributing to the TRIX score followed by DO, NO_2^-, NH_4^+ and PO_4^{3-} (Table 3.6).

3.3.1.5 Kolkata port

Precipitation was not observed during any of sampling periods, except for a day during SWM (Table 3.5). A wide tidal height difference (1.15 to 6.11 m) was observed in this port. During PrM-I, stations located in the closed docks were sampled during low tide. Distinct seasonal variation ($p < 0.05$) in environmental variables were observed. Water temperature was higher (31.12 ± 0.38^{o}C) during SWM followed by PM and lowest (20.59 ± 0.75^{o}C) during PrM-I and PrM-II (Fig. 3.10a and b). Salinity ranged from 0.17 to 0.35 during the study period with higher salinity at NSD and riverine station during PM and PrM-I (Fig. 3.10c and d). There was not much difference ($p > 0.05$) in temperature and salinity between the surface and NBW. DO concentration ranged from 3.32 to 9.94 mg L^{-1} with lower concentration during SWM (5.8±1.4 mg L^{-1}), especially at KOPT docks (Fig. 3.10e and f). DO concentrations

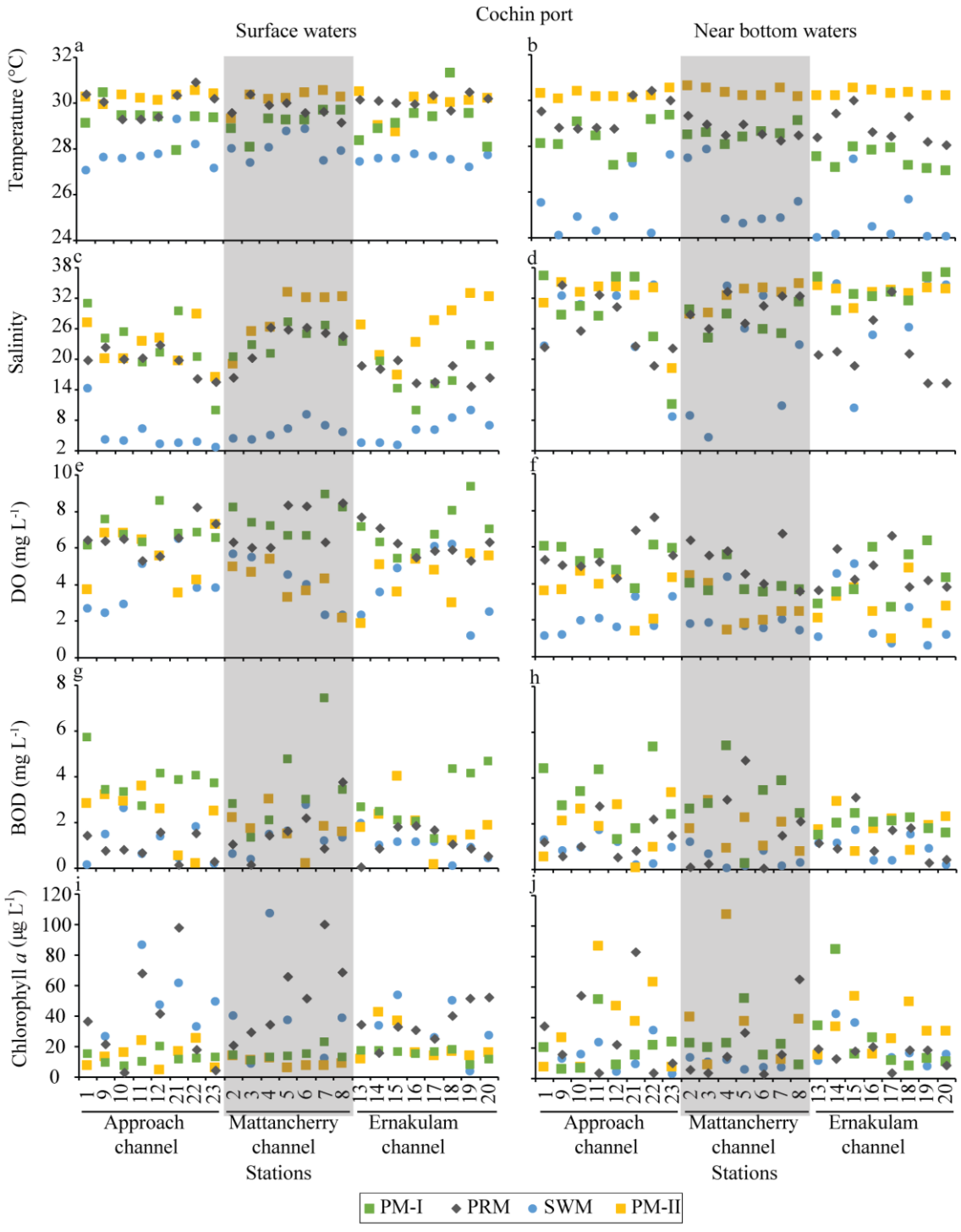

Fig. 3.9 Seasonal and spatial variations in (a, b) temperature, (c, d) salinity, (e, f) dissolved oxygen, (g, h) biological oxygen demand, (i, j) chl *a*, (k, l) nitrate, (m, n) nitrite, (o, p) ammonium, (q, r) phosphate, (s, t) silicate and (u, v) TRIX scores in the surface and near bottom waters of the Cochin port.

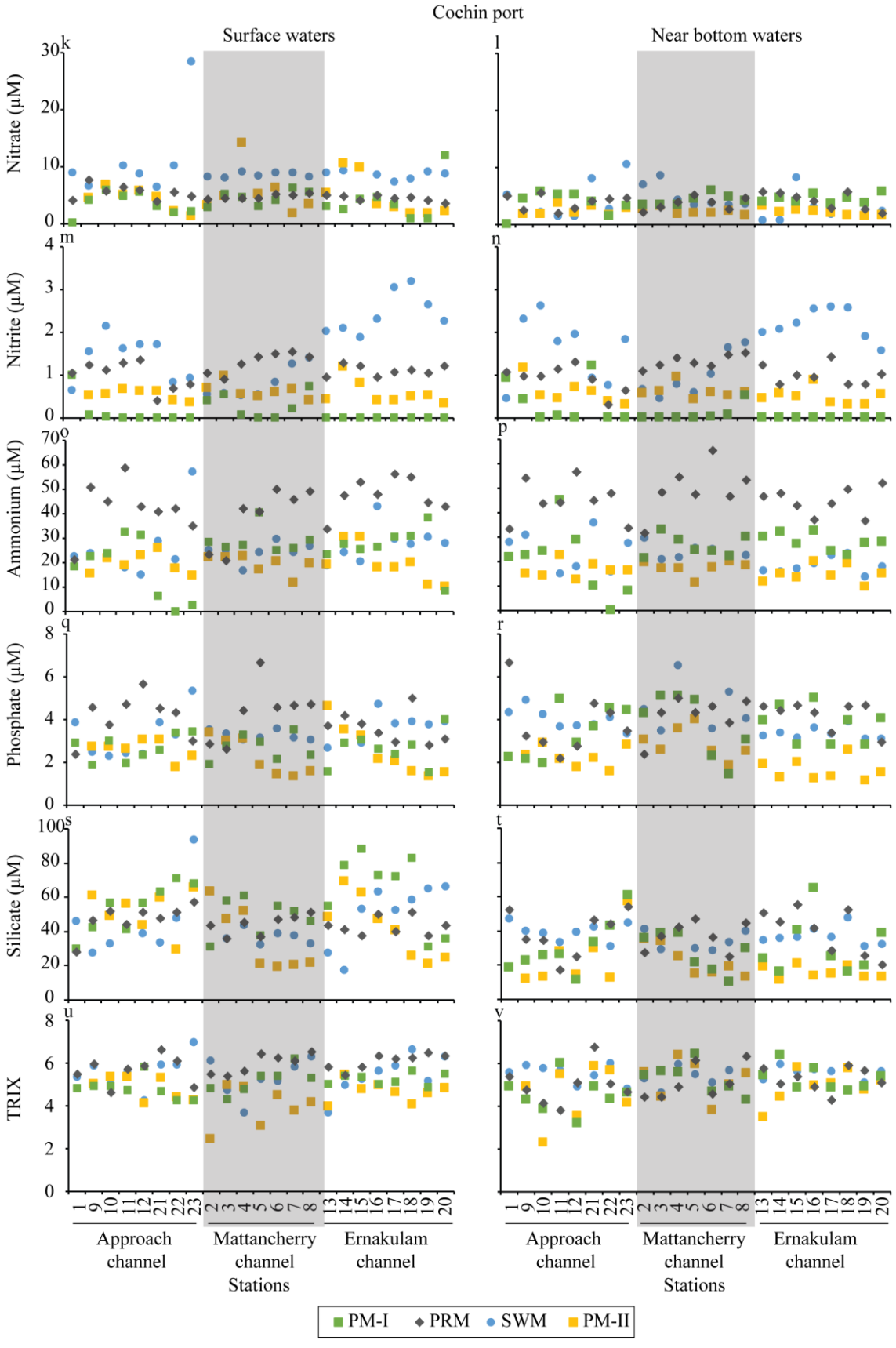

Fig. 3.9 continued

were higher in the surface waters compared to that in the NBW during PrM-I and PrM-II. High values of BOD were observed during SWM (3.23 to 6.86 mg L^{-1}) followed by PrM-I (1.44 to 7.30 mg L^{-1}), PrM-II (1.89 to 5.42 mg L^{-1}), and PM (1.04 to 6.36 mg L^{-1}) (Fig. 3.10g and h). BOD concentrations were higher in the surface waters compared to that in the NBW during SWM. Chl *a* concentrations ranged from 0.14 to 46.23 µg L^{-1} in the study area with higher values during PrM-I (3.42 to 46.23 µg L^{-1}), especially at the riverine stations. During SWM, higher concentrations (9.4 to 28.96 µg L^{-1}) were observed at NSD (Fig. 3.10i and j). During PrM-II and PM, chl *a* concentrations were lower (2.89 ± 2.20 µg L^{-1}). Chl *a* concentrations were higher in the surface waters compared to that in the NBW during SWM and PrM-I.

Among the studied ports, the highest nutrient concentration was observed in this port, especially for NO_3^-. Maximum NO_3^- concentration was found during the PM especially at KOPT docks (17.66 to 205.85 µM), followed by SWM (9.54 to 42.59 µM), PrM-II (11.77 to 42.86 µM), and PrM-I (0.20 to 22.93 µM). In NSD relatively lower NO_3^- concentrations were observed during the study period (Fig. 3.10k and l). NO_2^- concentrations ranged from 2.54 to 15.7 µM with highest during PM at NSD stations (Fig. 3.10m and n). NH_4^+ concentrations (1.8 to 43.18 µM) were higher during PrM-I in the NSD and riverine stations and lowest during SWM (0.5 to 8.48 µM) (Fig. 3.10o and p). PO_4^{3-} concentrations were higher during PM (5.58 to 12.52 µM) followed by PrM-I, SWM and PrM-II (0.43 to 7.27 µM; Fig. 3.10q and r). Generally, PO_4^{3-} and SiO_4^{4-} concentrations were high at the riverine stations compared to closed docks. Peak values of SiO_4^{4-} were observed during PM across the study region (14.07 to 190.88 µM) and at riverine stations during PrM-II (107.51 to 480.41 µM) (Fig. 3.10s and t). There was not much difference ($p > 0.05$) in NO_3^-, NO_2^-, NH_4^+, PO_4^{3-} and SiO_4^{4-} values between the surface and NBW. Carlson index indicated

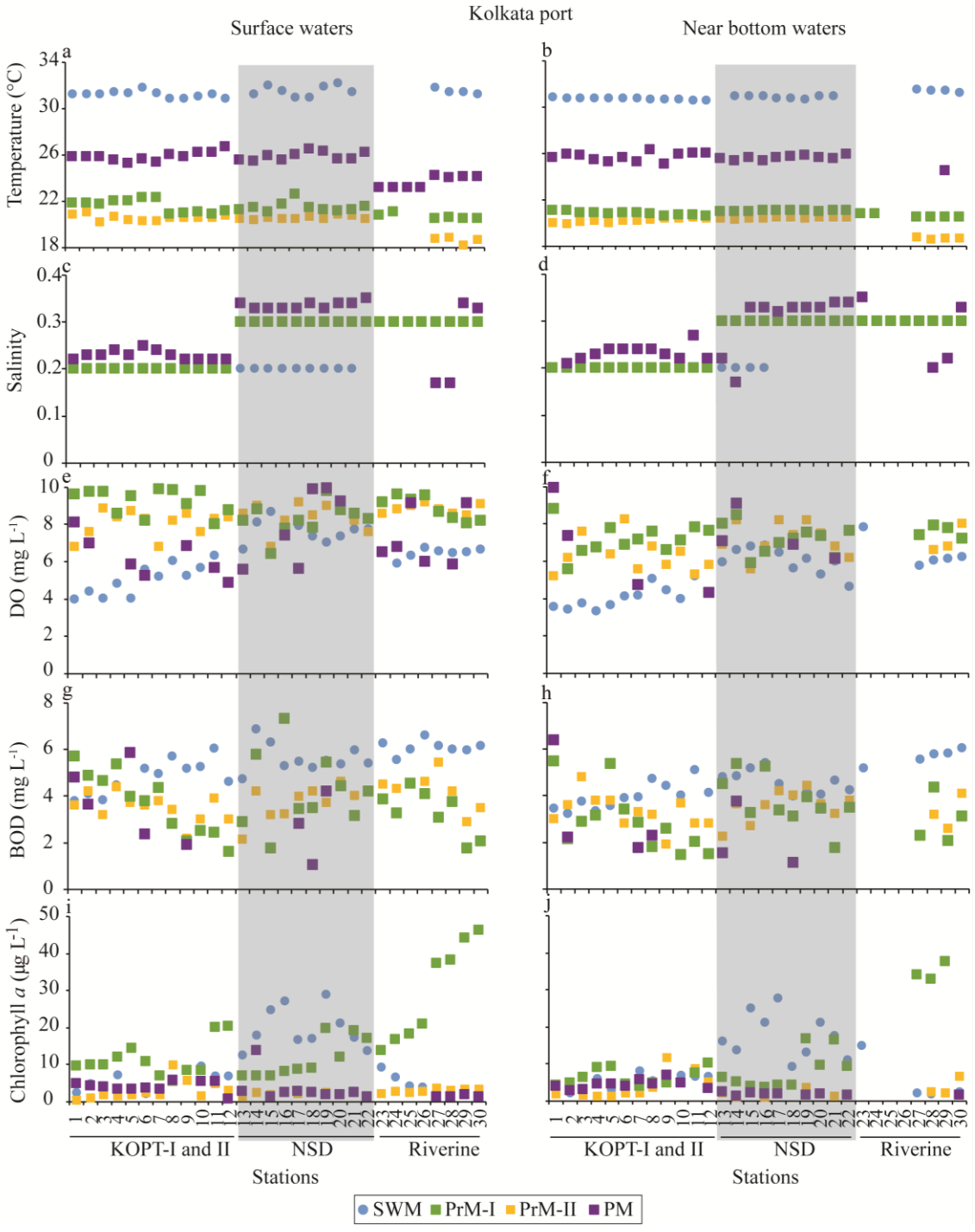

Fig. 3.10 Seasonal and spatial variations in (a, b) temperature, (c, d) salinity, (e, f) dissolved oxygen, (g, h) biological oxygen demand, (i, j) chl *a*, (k, l) nitrate, (m, n) nitrite, (o, p) ammonium, (q, r) phosphate, (s, t) silicate and (u, v) TRIX scores in the surface and near bottom waters of the Kolkata port.

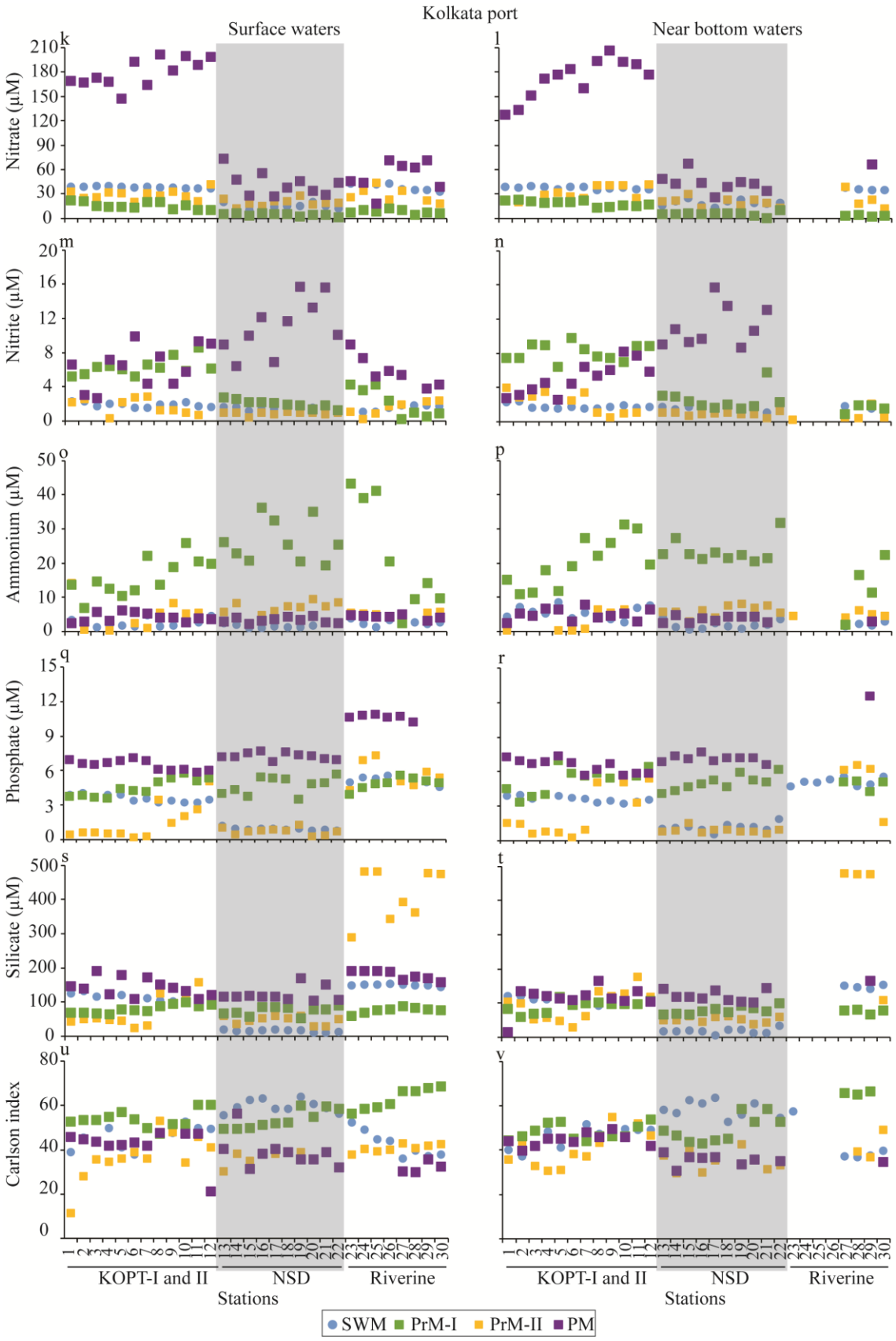

Fig. 3.10 continued

eutrophicated waters during SWM (36 to 64) and PrM-I (43 to 68) (especially at NSD docks; Fig. 3.10u and v). Mesotrophic waters were observed during PM and PrM-II.

3.3.2 Interseasonal and spatial variation of picophytoplankton

3.3.2.1 V.O.C. port

Total PP abundance ranged from 0.3 to 12.2 × 10^4 cells mL^{-1} during the study period with higher abundance during PrM at the middle and outer stations and inner stations during SWM (Fig. 3.11a and b). Highest cell abundance was recorded at S21 (12.2 × 10^4 cells mL^{-1} and 8.1 × 10^4 cells mL^{-1} in surface and NBW, respectively) during SWM. During TP, cell abundance was high (4 to 8 × 10^4 cells mL^{-1}) in the surface waters of outer stations (S10 to S12) and NBW of inner stations (S17 to S19). Among the PP groups, *SYN*-PEI was dominant. During PrM, *SYN*-PEI abundance ranged from 0.29 to 5.4 × 10^4 cells mL^{-1} in the surface and NBW with higher abundance at the outer and middle stations (Fig. 3.11c and d). During TP, cell abundance was high (2.4 to 3.4 × 10^4 cells mL^{-1}) in the surface waters of outer stations (S10 to S12) and NBW of the inner stations (S17 to S19). Highest cell abundance was recorded at S21 (7.9 × 10^4 cells mL^{-1} and 6.1 × 10^4 cells mL^{-1} in surface and NBW, respectively) during SWM. *SYN*-PEII abundance ranged from 0.02 to 4.4 × 10^4 cells mL^{-1} with higher abundance during TP at the outer stations (S10 to S12), especially in the surface waters and during SWM at S21 and S16 (Fig. 3.11e and f). *PRO*-like cells abundance was low (< 0.7 × 10^4 cells mL^{-1}) throughout sampling with comparatively higher abundance during TP and PrM in the NBW (Fig. 3.11g and h). PEUK cell abundance ranged from 0.01 to 1.5 × 10^4 cells mL^{-1} during the study period with higher abundance (0.17 to 1.55 × 10^4 cells mL^{-1}) during PrM. During SWM and TP, cell abundance was relatively higher at the inner stations (Fig. 3.11i and j). To the total PP abundance, the dominant contributor was *SYN*-PEI (49 ±

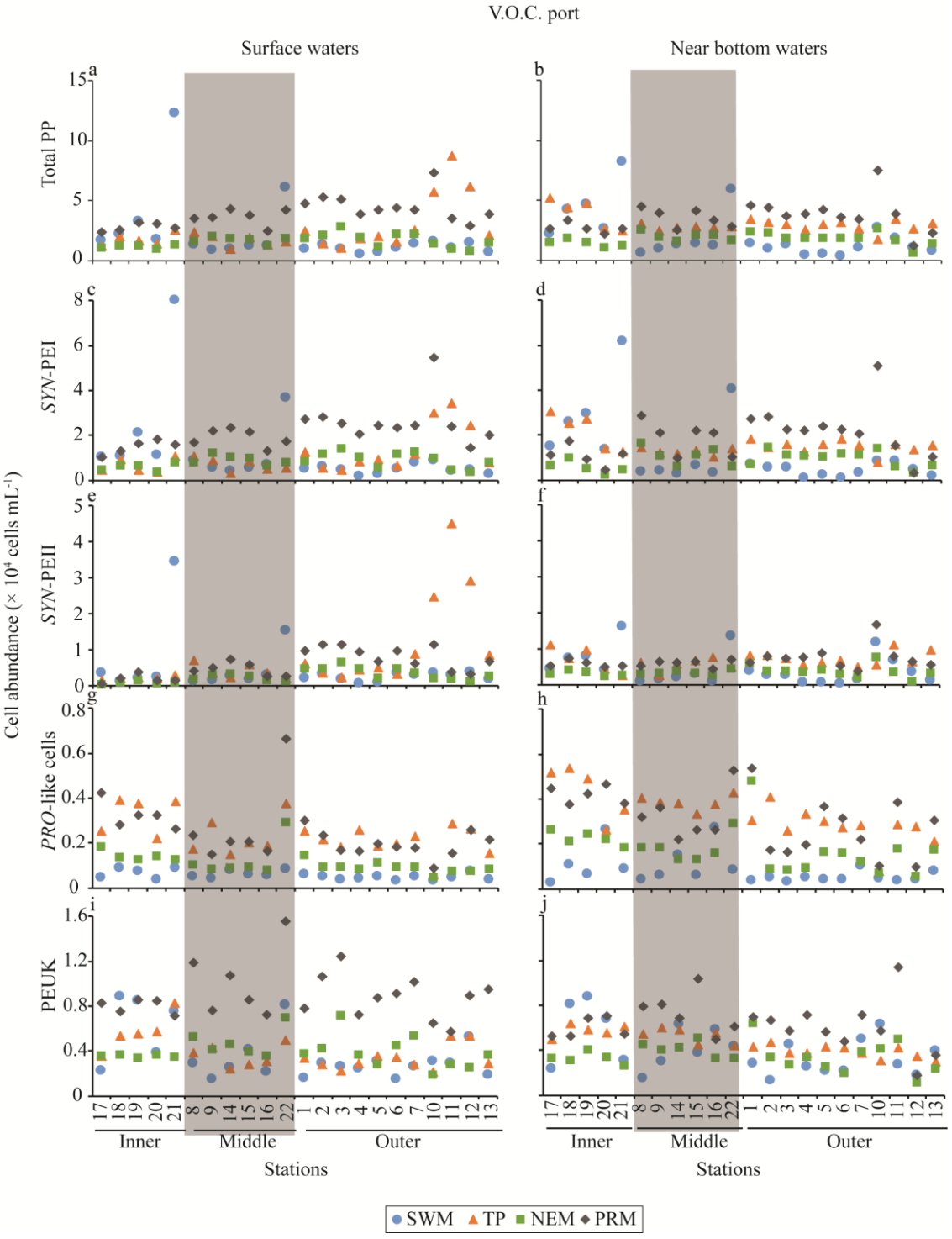

Fig. 3.11 Seasonal and spatial variations in (a, b) total picophytoplankton, (c, d) *SYN*-PEI, (e, f) *SYN*-PEII, (g, h) *PRO*- like cells, and (i, j) PEUK cell abundance in the surface and near bottom waters of the V.O.C. port.

7%) followed by *SYN*-PEII (20 ± 3%), PEUK (21 ± 6%) and *PRO*-like (10 ± 4%) (Fig. 3.16a and b).

3.3.2.2 Chennai port

Total PP abundance ranged from 0.2 to 4.0 × 10^4 cells mL^{-1} with higher abundance during SWM at the outer stations (S17 to S25), and from S1 to S5 during TP (Fig. 3.12a and b). At middle stations, cell abundance was low in all the seasons. *SYN*-PEI was the dominant group, with higher abundance (1.2 to 2.9 × 10^4 cells mL^{-1}) during SWM in surface and NBW of outer stations (S17 to S25) and during TP in the surface waters and NBW from S1 to S5 and S23 to S25 (Fig. 3.12c and d). *SYN*-PEII abundance showed a similar trend with low abundance (< 1.0 × 10^4 cells mL^{-1}; Fig. 3.12e and f). *PRO*-like cells abundance was low (< 0.3 × 10^4 cells mL^{-1}) during the study period (Fig. 3.12g and h). PEUK abundance ranged from 0.03 to 1.22 × 10^4 cells mL^{-1} with high abundance during SWM and PrM (Fig. 3.12i and j).

SYN-PEI contributed up to 49 ± 15% to the total PP abundance during the study period with highest during TP (65 ± 9%) (Fig. 3.16c and d). *SYN*-PEII contribution was restricted to < 37% (Fig. 3.16c and d). *PRO*-like cells was the least contributing (< 13%) group to the total PP abundance. PEUK contribution (up to 70%) was significant during SWM and PrM, especially at the inner stations (S1 to S5; Fig. 3.16c and d). During TP, PEUK contribution was restricted to < 23%.

3.3.2.3 New Mangalore port

Total PP abundance ranged from 0.02 to 11 × 10^4 cells mL^{-1} during the study period with higher abundance during PrM and PM-I particularly at the middle stations and lowest during PM-II (Fig. 3.13a and b). *SYN*-PEI was the dominant PP group with higher abundance (0.03 to 7.7 × 10^4 cells mL^{-1}) during PM-I and PrM. During PM-I and PrM, cell abundance was high in the middle stations (S15 to S18; Fig. 3.13c

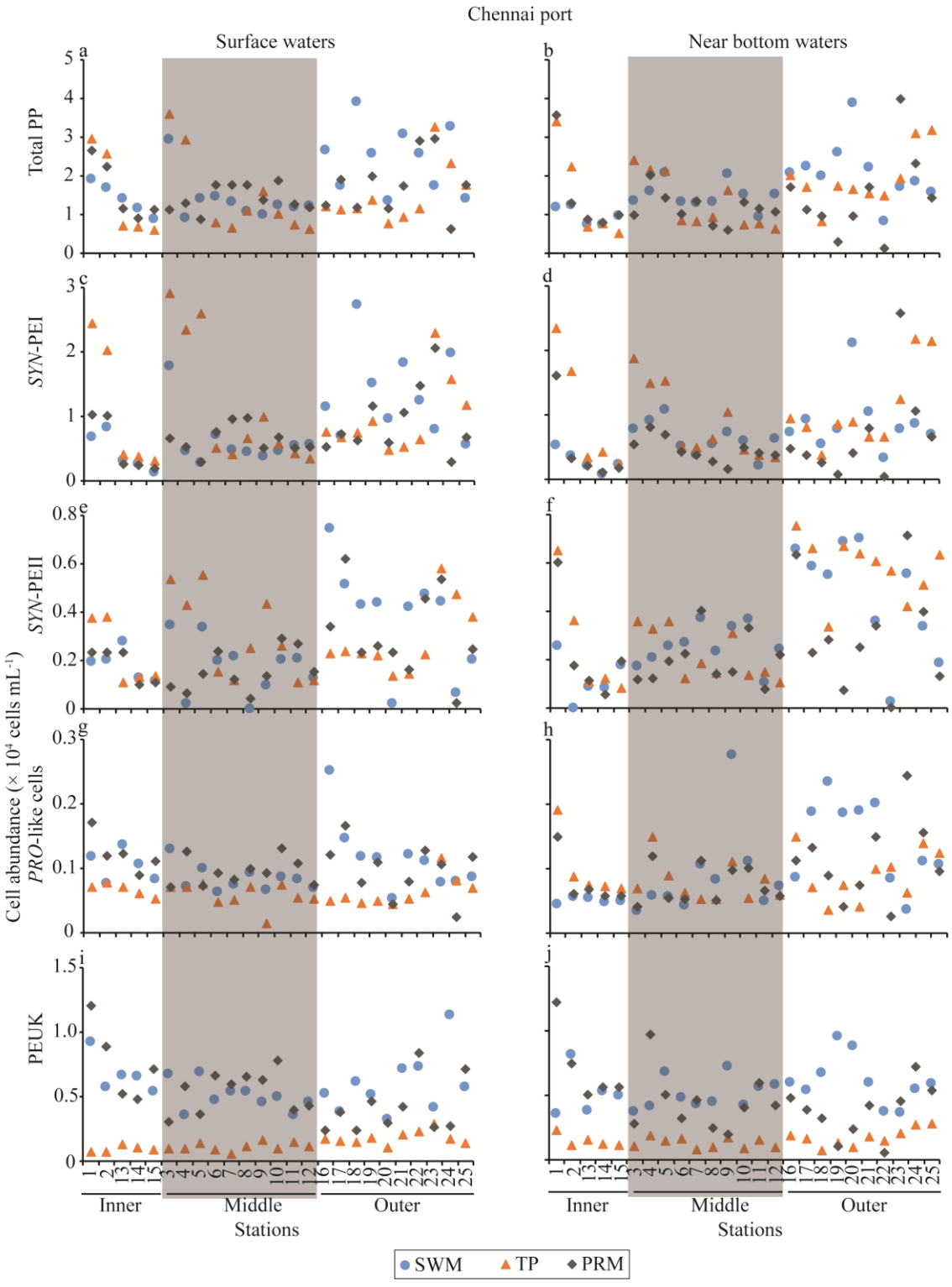

Fig. 3.12 Seasonal and spatial variations in (a, b) total picophytoplankton, (c, d) *SYN*-PEI, (e, f) *SYN*-PEII, (g, h) *PRO*- like cells, and (i, j) PEUK cell abundance in the surface and near bottom waters of the Chennai port.

and d). During this period, cell abundance in the surface waters was higher than that in the NBW. *SYN*-PEI abundance was lower (< 0.34 × 10^4 cells mL^{-1}) during SWM which further decreased (< 0.11 × 10^4 cells mL^{-1}) during PM-II. *SYN*-PEII abundance during PM-I ranged from 0.7 to 2.23 × 10^4 cells mL^{-1}, which decreased (0.4 ± 0.3 × 10^4 cells mL^{-1}) during PrM. Abundance increased during SWM, especially in the NBW with the highest abundance (4.3 × 10^4 cells mL^{-1}) detected at S16 (Fig. 3.13e and f). *PRO*-like cells abundance was low (< 2.1 × 10^4 cells mL^{-1}) in the study region with comparatively higher abundance during PM-I and PrM (Fig. 3.13g and h). PEUK cell abundance ranged from 0.03 to 3.2 × 10^4 cells mL^{-1} during the study period with higher abundance during PrM (Fig. 3.13i and j). Higher PEUK abundance was also observed in the surface waters of inner stations and NBW of S10, S14 and S15 during SWM. PEUK abundance was low (< 1.01 × 10^4 cells mL^{-1}) during both the PM seasons. *SYN*-PEI contributed 55 to 81% to the total PP abundance during PM-I and PrM (Fig. 3.16e and f). Their contribution decreased to < 52% during SWM and PM-II. *SYN*-PEII contribution ranged from 3 to 35% during PM-I and PrM with higher contribution in the NBW compared to surface waters. Its contribution increased (21 to 46%) during SMW especially in the NBW. *PRO*-like cells contribution to the total PP abundance was low (< 12%) irrespective of seasons. PEUK contributed 8 to 28% to the total PP abundance during the study period with higher contribution in the surface waters of inner stations during SWM and in the surface and NBW during PM-II .

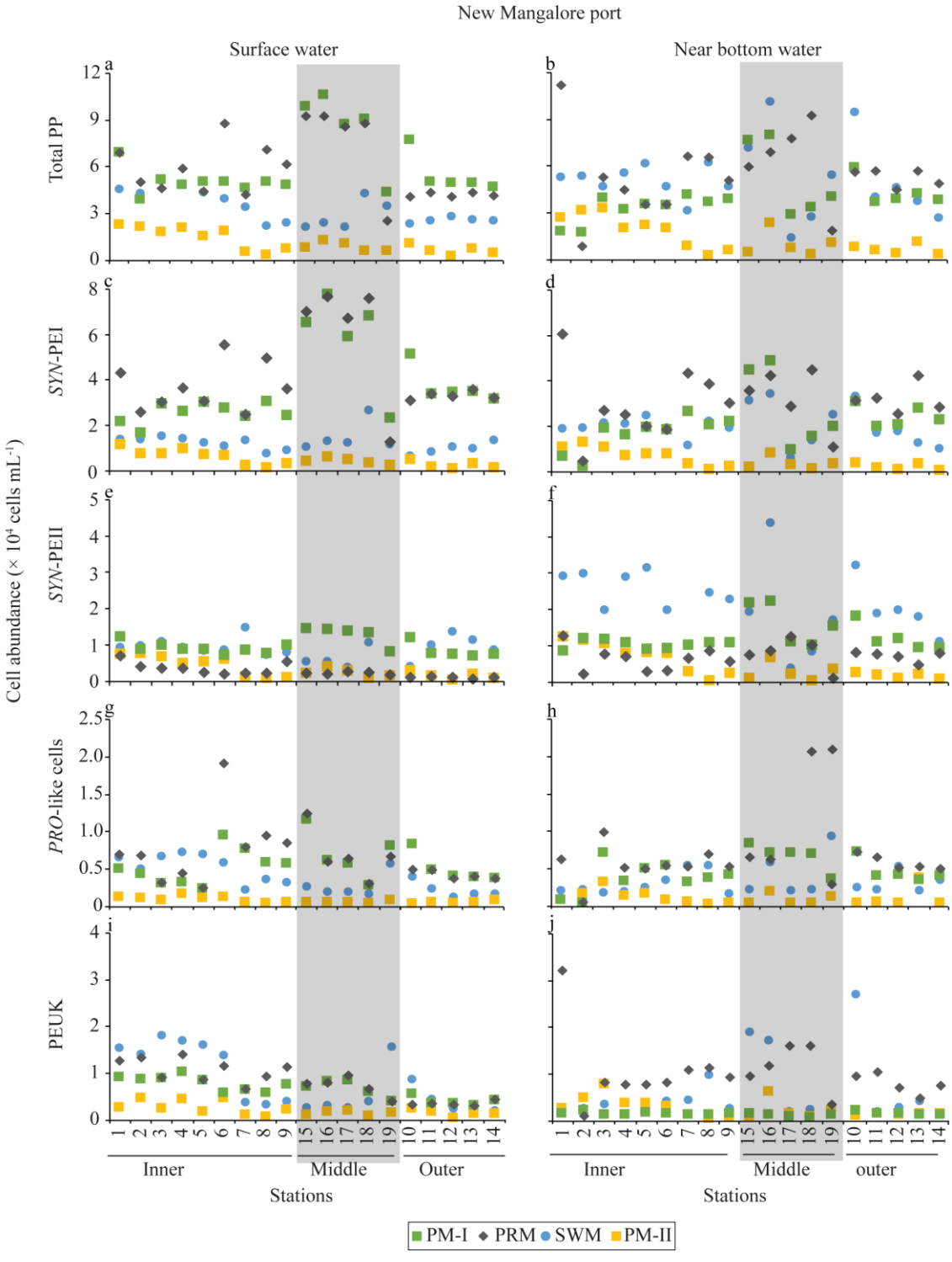

Fig. 3.13 Seasonal and spatial variations in (a, b) total picophytoplankton, (c, d) *SYN*-PEI, (e, f) *SYN*-PEII, (g, h) *PRO*- like cells, and (i, j) PEUK cell abundance in the surface and near bottom waters of the New Mangalore port.

3.3.2.4 Cochin port

During PM-I, total PP abundance ranged from 0.1 to 29.2 × 10^4 cells mL^{-1}. During PrM, a prominent increase in PP abundance was observed across the Cochin port (1.4 to 46.09 × 10^4 cells mL^{-1}), which decreased during SWM (1.02 to17.18 × 10^4 cells mL^{-1}) and increased during PM-II (3.31 to 28.84 × 10^4 cells mL^{-1}; Fig. 3.14a and b). During PrM and SWM, *SYN*-PEI abundance was low (< 4.6 × 10^4 cells mL^{-1}). Highest cell abundance was recorded in NBW of S7 (28.6 × 10^4 cells mL^{-1}) and S1 (20 × 10^4 cells mL^{-1}) during PM-I, compared to all other seasons (Fig. 3.14c and d). During PM-II, higher *SYN*-PEI abundance (0.8 to 11.46 × 10^4 cells mL^{-1}) was observed at Ernakulam channel stations (surface waters and NBW) where salinity was > 29. During PM-I, *SYN*-PEII group was absent where salinity was < 20 and during PrM it was completely absent (Fig. 3.14e and f). This group was observed in the NBW during SWM with very low cell abundance (< 0.05 × 10^4 cells mL^{-1}). During PM-II, *SYN*-PEII was detected only at salinities > 26, with low cell abundance (< 1.96 × 10^4 cells mL^{-1}). Being second dominant group during PM-I, *SYN*-PC abundance (0 to 3.41 × 10^4 cells mL^{-1}) was high in the Ernakulam channel stations compared to the stations near the mouth of Cochin port (Fig. 3.14g and h). Throughout the season, cell abundance was higher in the surface waters than NBW, except at some stations where NBW salinity was < 29. A steep increase in *SYN*-PC abundance (0.8 to 37.71 × 10^4 cells mL^{-1}) was observed during the PrM, with maximum cell abundance at NBW of S21 (37.71 × 10^4 cells mL^{-1}). During SWM, the dominance of *SYN*-PC group continued with comparatively higher cell abundance (0.1 to 11.12 × 10^4 cells mL^{-1}) than that during PrM. During PM-II, *SYN*-PC dominated low saline waters (< 24) with the highest cell abundance in surface waters of S9 (21.64 × 10^4 cells mL^{-1}) and in NBW of S23 (16.24 × 10^4 cells mL^{-1}). *PRO*-like cells showed a remarkable increase

during SWM ((0.17 to 4.19 × 10^4 cells mL^{-1}) with higher cell abundance in the surface waters compared to NBW, except at Mattancherry channel stations (Fig. 3.14i and j). PEUK abundance was high (0.09 to 4.95 × 10^4 cells mL^{-1}) during SWM exhibiting a decreasing trend from S2 to S23 (Fig. 3.14k and l). In the surface waters, cell abundance was higher than in the NBW, except at Mattancherry channel stations. Highest cell abundance (4.95 × 10^4 cells mL^{-1}) was recorded in the NBW of S7. PEUK abundance was reduced by an order of magnitude during PM-II. During PrM increased abundance was observed compared to PM-I. Generally, their abundance was high in the surface waters compared to the NBW, except during PrM.

SYN-PEI was the dominant group and contributed substantially (42 ± 17%) to total PP during PM-I and PM-II, especially in NBW (55 ± 9%; Fig. 3.16g and h). *SYN*-PEII contribution to total PP abundance was higher in the NBW, especially at S20 (46%) during PM-I whereas during other seasons it was < 26% (Fig. 3.16g and h). During PrM and SWM, *SYN*-PC was the dominant group contributing 67 ± 18% and 52 ± 22% respectively, to the total PP abundance across the Cochin port (Fig. 3.16g and h). *PRO*-like cells contribution to total PP abundance was high (17±4%) during SWM and decreased (10 ± 3%) during PM-II. Even though PEUK abundance was high during SWM, their contribution to total PP was 15 ± 6%. During PM-I, PEUK contribution to total PP abundance in the surface waters was 28 ± 15%.

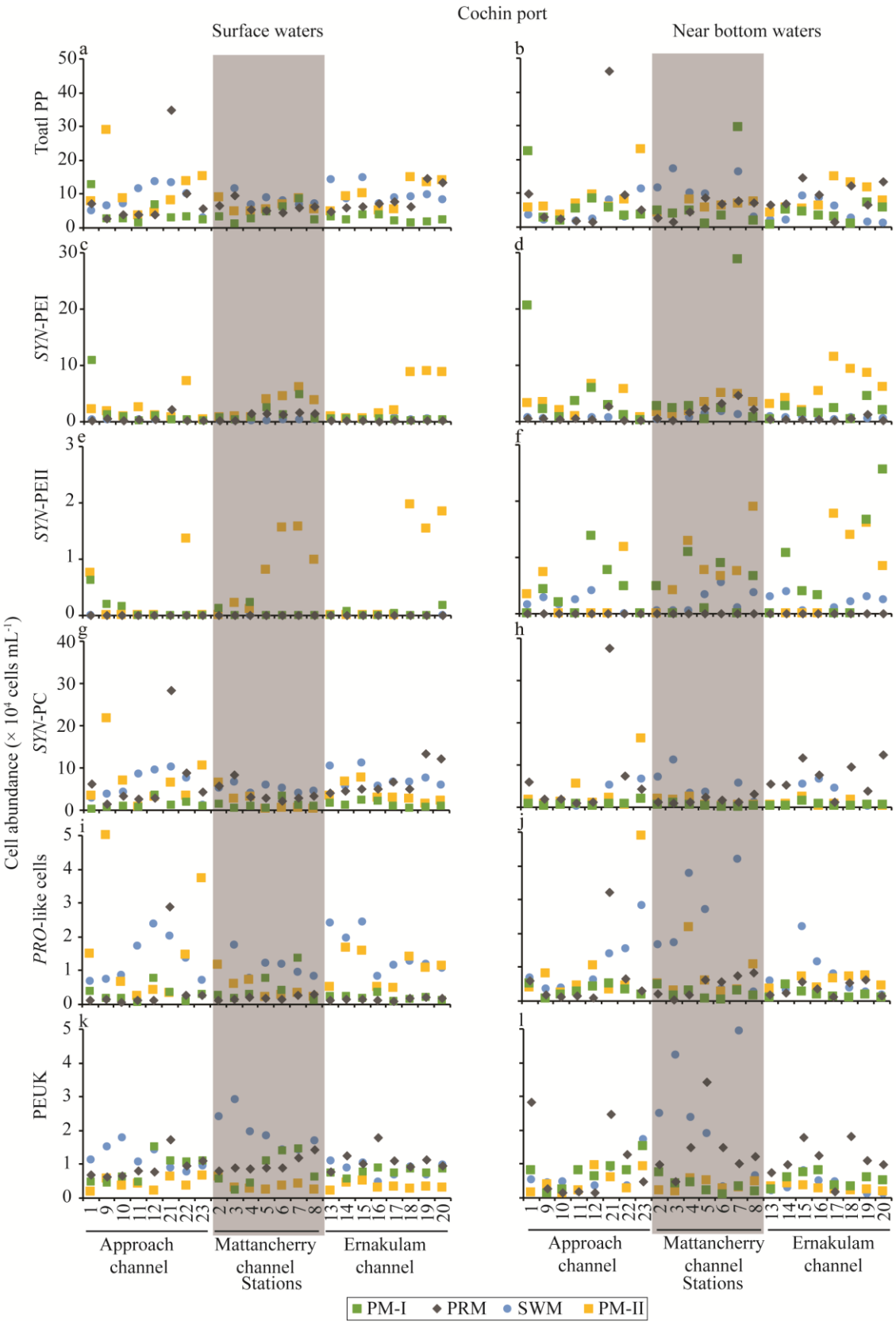

Fig. 3.14 Seasonal and spatial variations in (a, b) total picophytoplankton, (c, d) *SYN*-PEI, (e, f) *SYN*-PEII, (g, h) *SYN*-PC, (i, j) *PRO*- like cells, and (k, l) PEUK cell abundance in the surface and near bottom waters of the Cochin port.

3.3.2.5 Kolkata port

Among all the studied ports, highest (1.24 to 110.7 × 10^4 cells mL^{-1}) PP abundance was observed in this port with higher abundance during SWM (Fig. 3.15a and b). Overall, the PP abundance was low in the riverine waters compared to closed docks. *SYN*-PEIII abundance was high (0.01 to 11.83 × 10^4 cells mL^{-1}) during SWM, especially in the surface waters followed by PrM-I (0.04 to 4.70 × 10^4 cells mL^{-1}), PrM-II (0.09 to 2.69 × 10^4 cells mL^{-1}) and PM (0.02 to 3.21 × 10^4 cells mL^{-1}) (Fig. 3.15c and d). *SYN*-PEIII abundance was high at NSD compared to KOPT docks and riverine stations except in the NBW during PrM where higher abundance was observed in the KOPT docks. *SYN*-PC abundance was highest (11.4 to 97.4 × 10^4 cells mL^{-1}) during SWM, especially at the NSD. During PrM-I, *SYN*-PC abundance was high (2.41 to 20.5 × 10^4 cells mL^{-1}) at KOPT-I and II docks compared to NSD (Fig. 3.15e and f) whereas, during PrM-II, it was relatively high at NSD (2.45 to 8.57 × 10^4 cells mL^{-1}). Significant variation ($p < 0.05$) of *SYN*-PEIII and *SYN*-PC abundance was observed between surface and NBW. *PRO*-like cells were higher (0.04 to 2.52 × 10^4 cells mL^{-1}) during SWM at NSD whereas during other seasons their abundance was higher at KOPT docks. During PM, *PRO*-like cells abundance was low (Fig. 3.15g and h). PEUK showed higher abundance during PM (0.4 to 2.45 × 10^4 cells mL^{-1}) followed by PrM-I (0.01 to 4.00 × 10^4 cells mL^{-1}) and PrM-II (0.4 to 2.3 × 10^4 cells mL^{-1}) (Fig. 3.15i and j). During SWM, its abundance was low in the docks compared to riverine stations. During PM, higher abundance was observed, especially at KOPT-I. There was no significant variation in PEUK abundance between surface and NBW.

SYN-PC was the dominant group (contributed 62 ± 18% to the total PP) in these waters followed by PEUK (19 ± 10%), *SYN*-PEIII (12 ± 8%), and *PRO*-like cells (8 ±

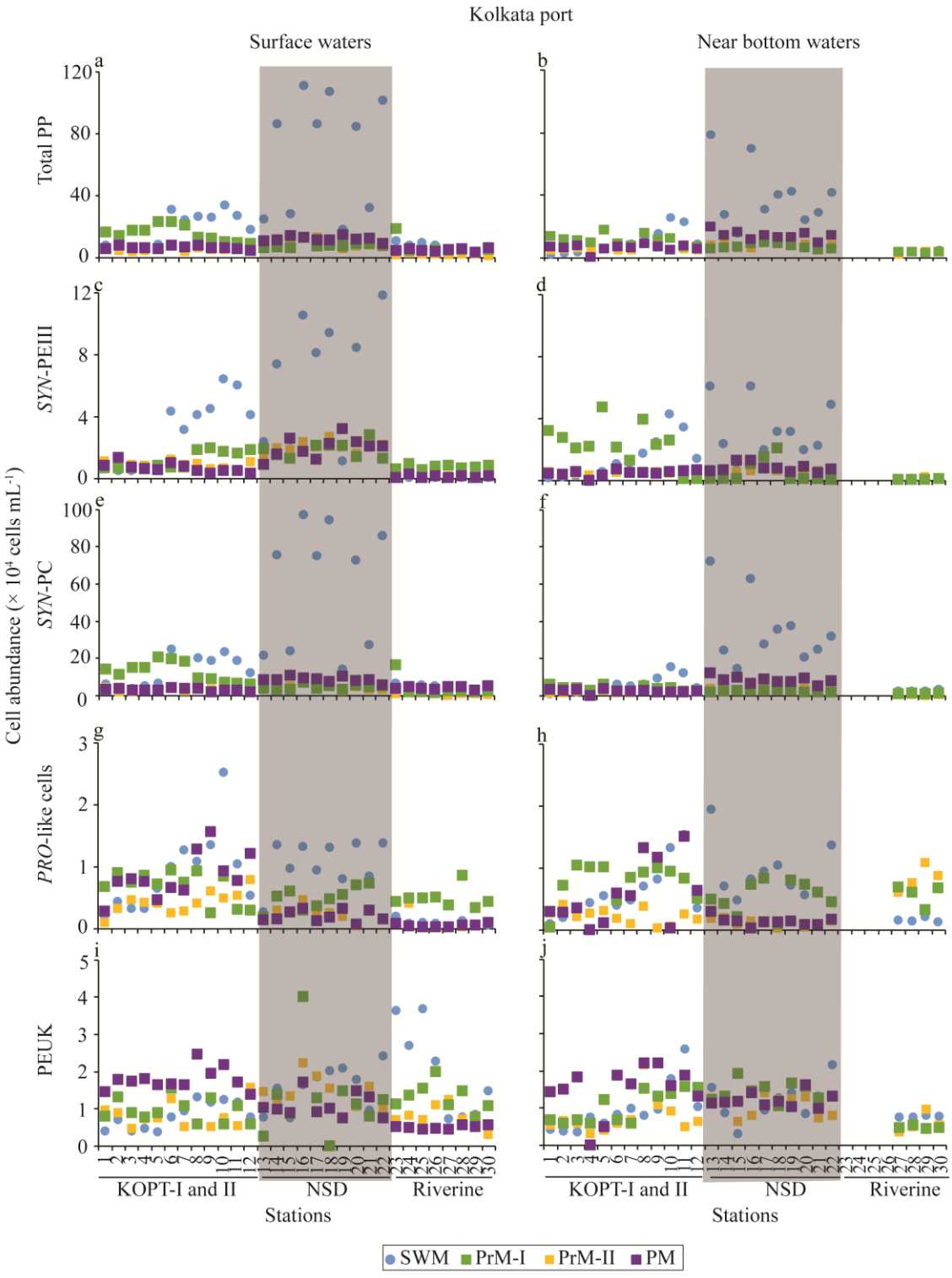

Fig. 3.15 Seasonal and spatial variations in (a, b) total picophytoplankton, (c, d) *SYN*-PEIII, (e, f) *SYN*-PC, (g, h) *PRO*- like cells, and (i, j), PEUK cell abundance in the surface and near bottom waters of the Kolkata port.

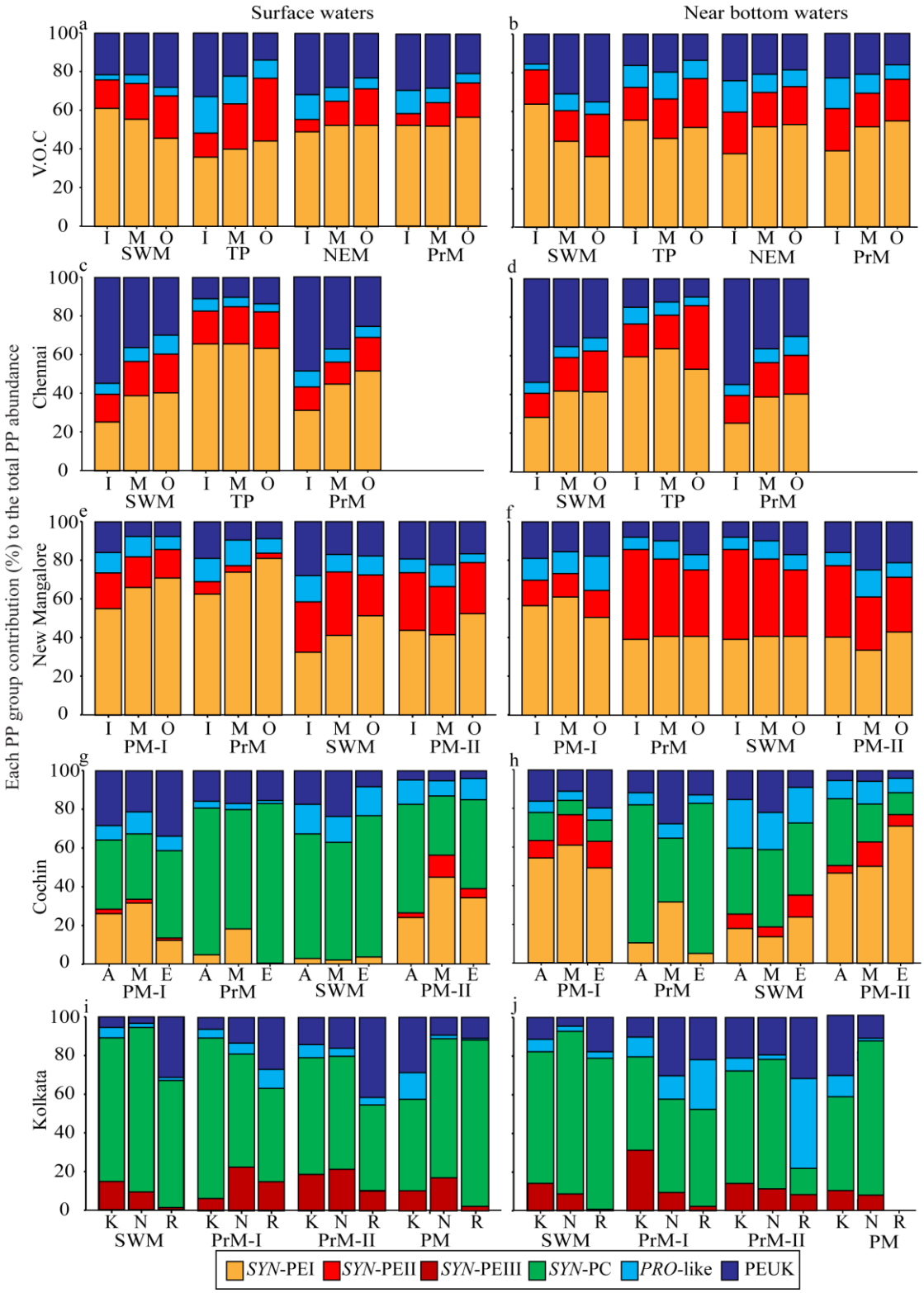

Fig. 3.16 Contribution (%) of individual picophytoplankton group to the total picophytoplankton abundance during different seasons in the surface and near bottom waters of the (a, b) V.O.C. port (I-inner, M-miidle and O-outer stations), (c, d) Chennai port (I-inner, M-miidle and O-outer stations), (e, f) New Mangalore port (I-inner, M-miidle and O-outer stations), (g, h) Cochin port (A-approach, M-Mattancherry, E- Ernakulam channel), and (i, j) Kolkata port (K-KOPT-I and II, N-NSD, R- Riverine stations).

8%) (Fig. 3.16i and j). During SWM, *SYN*-PC contribution to the total PP abundance was up to 86%. Highest contribution (26 ± 13%) of *SYN*-PEIII was observed in the NBW of KOPT docks during PrM-I. During PrM-II, *SYN*-PEIII contributed 18 ± 7% to the total PP abundance in the KOPT dock. *PRO*-like cells contribution was higher (18 ± 5%) at riverine stations during PrM-II. Generally, PEUK contribution was higher at riverine stations.

Table 3.6 Multiple regression analysis between TRIX scores and environmental variable used to extract TRIX scores, for different ports. Values indicate for the variables are correlation coefficient with a significance level of p <0.05 (*) and p <0.01 (**).

	TRIX scores			
	V.O.C	Chennai	New Mangalore	Cochin
R^2	**0.680****	**0.743****	**0.729****	**0.702****
Variables				
DO	**0.244****	**-0.440****	**-0.491****	**-0.325****
NO_3^-	0.059	0.082	0.040	0.039
NO_2^-	0.048	**0.215****	**0.145****	**0.229****
NH_4^+	0.131	0.006	**-0.173****	**0.173****
PO_4^{3-}	**0.393****	**0.248****	**0.295****	**0.129****
Chl *a*	**0.588****	**0.331****	**0.671****	**0.429****

3.3.3 Relationship between environmental factors and picophytoplankton groups

3.3.3.1 V.O.C. port

Linear regression analysis showed that all the PP groups were positively correlated with TRIX scores (Fig. 3.17a-d). In PCA, three major PC's were considered which explained 67.6% variation of the ecological variables. PC1 accounted for 37.1% of the variance with a positive load of NO_3^-, NO_2^-, NH_4^+, and BOD; and a negative load of temperature (Table 3.7). Linear regression analysis showed that *SYN*-PEII was negatively and *PRO*-like cells were positively correlated with PC1 (Table 3.8). All the PP groups were negatively and chl *a* positively correlated with PC2 where positive load of salinity and SiO_4^{4-}, and a negative load of PO_4^{3-} was observed, which explained 17.1% of the variance. Positive load of salinity, DO, and PO_4^{3-} was observed at PC3 which explained 13.4% of the variance. To this component, all the PP groups (except PEUK) and chl *a* were positively correlated.

3.3.3.2 Chennai port

Linear regression analysis showed that PEUK and *PRO*-like cells were positively correlated with TRIX scores (Fig. 3.17e-h). In PCA, three major PC's explained 70.8% variation of the ecological variables. PC1 accounted for 38.2% of the variance with a positive load of NO_3^-, NO_2^-, PO_4^{3-}, SiO_4^{4-} and salinity; and a negative load of temperature and DO (Table 3.7). Positive load of NH_4^+ and negative load of salinity was observed at PC2 which explained 21.3% of the variance. At PC3, BOD was positively loaded. Linear regression analysis showed that PEUK and *PRO*-like cells were positively correlated with PC1 and negatively with PC2 (Table 3.8). Chl *a* was positively correlated with PC3 and negatively with PC2.

3.3.3.3 New Mangalore port

Linear regression analysis showed none of the PP groups and chl *a* were correlated with TRIX scores (Fig. 3.17i-l). In PCA, three major PC's explained 75.4% variation of the ecological variables. PC1 accounted for 45% of the variance with a positive load of temperature, DO, NO_3^-, NO_2^- and salinity; and a negative load of PO_4^{3-}, SiO_4^{4-} and NH_4^+ (Table 3.7). Positive load of salinity, NO_3^- and NH_4^+; negative load of DO and BOD was observed at PC2 which explained 18.2% of the variance. At PC3, NO_2^- was positively loaded. Linear regression analysis showed that *SYN*-PEII was negatively correlated with PC1 (Table 3.8). All the PP groups were positively correlated with PC2. All the PP groups (except *SYN*-PEII) and chl *a* were negatively correlated with PC3.

3.3.3.4 Cochin port

Linear regression analysis showed that *SYN*-PC and *PRO*-like cells abundance correlated positively with TRIX scores, whereas *SYN*-PEI correlated negatively (Fig. 3.17m-q). In PCA, three major PC's were considered which explained 67.4% variation of the ecological variables. PC1 accounted for 28.6% of the variance with a positive load of nutrients and negative load of salinity (Table 3.7). Positive load of DO, BOD, SiO_4^{4-} and temperature; and negative load of NO_2^- were observed at PC2 which explained 25.8% of the variance. Positive load of salinity, PO_4^{3-} and NH_4^+; negative load of NO_3^- was observed at PC3 which explained 13% of the variance. Linear regression analysis showed that *SYN*-PEI and *SYN*-PEII correlated negatively with PC1 and PC2 scores, whereas *SYN*-PC, PEUK, and *PRO*-like cells correlated positively, except *PRO*-like cells which correlated negatively with PC2 (Table 3.8). Chl *a* correlated positively with PC1.

Table 3.7 Principal component analysis with varifactors (PC's) extracted for the ecological variables. Bold text denotes significant loading.

	V.O.C			Chennai			New Mangalore			Cochin			Kolkata		
	PC1	PC2	PC3	PC1	PC2	PC3	PC1	PC2	PC3	PC1	PC2	PC3	PC1	PC2	PC3
Temperature	**-0.79**	-0.02	-0.34	**-0.68**	0.16	0.09	**0.94**	0.04	0.23	-0.33	**0.69**	0.06	**-0.80**	0.27	-0.01
Salinity	-0.30	**0.69**	**0.50**	**0.47**	**-0.81**	0.05	**0.44**	**0.75**	-0.15	**-0.68**	-0.31	**0.51**	0.37	-0.36	**0.64**
DO	-0.34	0.25	**0.50**	**-0.80**	0.33	0.27	**0.75**	**-0.43**	-0.27	0.08	**0.89**	0.13	**0.61**	-0.39	-0.08
BOD	**0.51**	0.16	-0.24	-0.21	-0.30	**0.90**	0.33	**-0.42**	-0.37	-0.36	**0.59**	0.01	**-0.54**	-0.24	0.19
NO_3^-	**0.87**	-0.02	-0.05	**0.68**	0.38	0.25	**0.51**	**0.71**	0.12	**0.69**	0.20	**-0.40**	-0.23	**0.71**	-0.01
NO_2^-	**0.94**	0.11	-0.12	**0.84**	0.30	0.19	**0.56**	-0.14	**0.73**	**0.55**	**-0.55**	-0.04	**0.48**	**0.55**	**-0.48**
NH_4^+	**0.77**	0.35	0.30	-0.05	**0.87**	0.03	**-0.55**	**0.42**	-0.32	**0.53**	0.19	**0.68**	**0.74**	-0.15	-0.15
PO_4^{3-}	0.10	**-0.55**	**0.59**	**0.66**	0.16	0.15	**-0.84**	0.04	0.31	**0.67**	-0.09	**0.51**	**0.50**	**0.71**	0.20
SiO_4^{4-}	-0.14	**0.73**	-0.29	**0.67**	0.17	0.03	**-0.85**	-0.09	0.25	**0.60**	**0.48**	-0.07	0.22	**0.52**	**0.67**
Eigenvalues	3.34	1.54	1.20	3.43	1.92	1.02	4.05	1.64	1.09	2.57	2.32	1.17	2.57	2.00	1.20
% of Variance	37.1	17.1	13.4	38.2	21.3	11.3	45.0	18.2	12.1	28.6	25.8	13.0	28.5	22.3	13.3
Cumulative %	37.1	54.2	67.6	38.2	59.5	70.8	45.0	63.2	75.4	28.6	54.4	67.4	28.5	50.8	64.1

Table 3.8 Regression analysis between PP groups and chl *a* with principal component scores (PC) for the entire data set of ecological variables. Values indicate are correlation coefficient with significance level of $p < 0.05$ (*) and $p < 0.01$ (**)

	V.O.C			Chennai			New Mangalore			Cochin			Kolkata		
	PC1	PC2	PC3	PC1	PC2	PC3	PC1	PC2	PC3	PC1	PC2	PC3	PC1	PC2	PC3
SYN-PEI	-0.12	**-0.35****	**0.25****	-0.08	0.15	0.07	-0.12	**0.54****	**-0.45****	**-0.61****	**-0.20****	0.07			
SYN-PEII	**-0.22****	**-0.25****	**0.40****	-0.08	0.03	0.01	**-0.74****	**0.12***	0.02	**-0.44****	**-0.37****	-0.06			
SYN-PEIII													**-0.16***	-0.15	**-0.47****
SYN-PC										**0.52****	**0.15***	-0.09	**-0.40****	**-0.18***	**-0.51****
PEUK	-0.12	**-0.29****	0.05	**0.52****	**-0.58****	0.09	-0.08	**0.39****	**-0.47****	**0.53****	**0.25****	0.00	-0.01	-0.03	-0.06
PRO-like	**0.18***	**-0.23****	**0.40****	**0.25****	**-0.19***	-0.03	-0.15	**0.48****	**-0.55****	**0.18***	**-0.21****	**-0.41****	-0.08	0.08	**-0.35****
Total PP	**-0.15***	**-0.34****	**0.31****	0.11	-0.12	0.05	**-0.27****	**0.48****	**-0.44****	0.09	0.08	**-0.18***	**-0.35****	**-0.16***	**-0.45****
Chl *a*	-0.04	**0.25****	**0.38****	-0.01	**-0.35****	**0.26****	0.14	0.18	**-0.25****	**0.16***	0.02	0.07	0.07	**-0.28****	-0.08

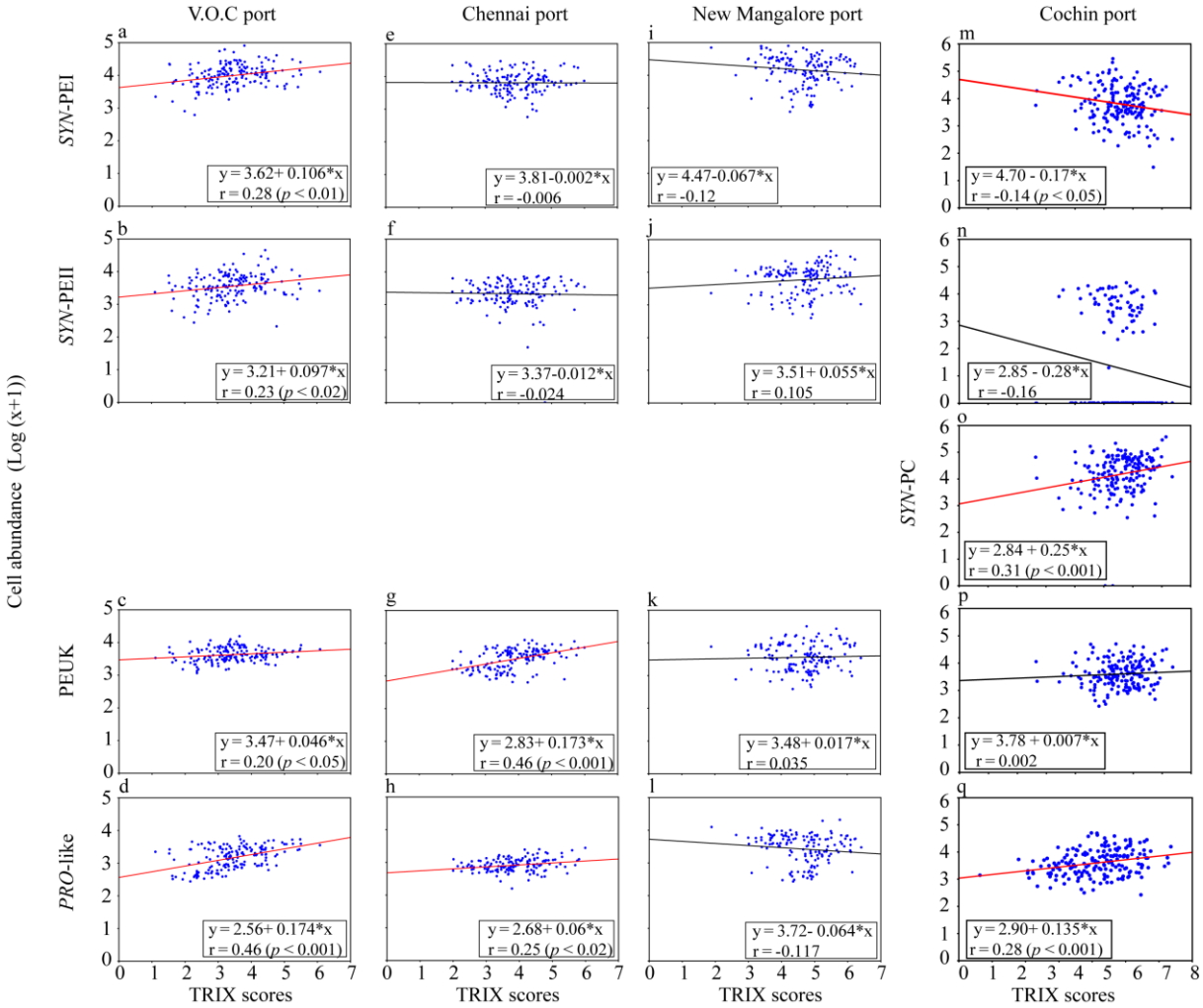

Fig. 3.17 Linear regression analyses of picophytoplankton group abundance with TRIX scores. (a-d) V.O.C port, (e-h) Chennai port, (i-l) New Mangalore port, and (m-q) Cochin port.

3.3.3.5 Kolkata port

In PCA, three major PC's were considered which explained 64.1% variation of the ecological variables. PC1 accounted for 28.5% of the variance with a positive load of NH_4^+, DO, NO_2^- and PO_4^{3-}. Negative load of temperature and BOD was observed in PC1 (Table 3.7). Positive load of NO_2^-, PO_4^{3-}, NO_3^- and SiO_4^{4-} were observed at PC2 which explained 22.3% of the variance. Positive load of salinity and SiO_4^{4-}; negative load of NO_2^- was observed at PC3 which explained 13.3% of the variance. Linear regression analysis showed that *SYN*-PEIII correlated negatively with PC1 and PC3. *SYN*-PC correlated negatively with all the components (Table 3.8). *PRO*-like cells correlated negatively with PC3. Chl *a* correlated negatively with PC2.

3.4 Discussion

3.4.1 Hydrography of port waters

Over the past few years, investigators have revealed that the major ports are contaminated by anthropogenic activities; Cochin port (Balachandran et al., 2005; Martin et al., 2012; Anu et al., 2014); New Mangalore (Rao et al., 2004; Shirodkar et al., 2010); Chennai (Sudhakar et al., 2007); V.O.C. (Ramasamy and Murugan, 2003) and Kolkata (Dasgupta et al., 2013) ports. There is evidence for the waste discharge in large quantity, which has an impact on the local ecosystem in the world wide ports (Herz and Davis, 2002). Since, Cochin port is situated at the mouth of the Cochin backwaters, the port waters are contaminated by industrialization (10^4 million liters of partially treated and untreated industrial effluents are discharged every day by a large number of industries), agriculture, transportation and domestic sewage effluent discharge (Unnithan et al., 1975; Vijayan et al., 1976; Menon et al., 2000; Qasim, 2003). As a consequence, the concentration of toxic metals in the surficial sediments

has been reported in moderate to heavily polluted condition (Martin et al., 2012). Discharging sewage from the anchored ship and recycling of existing nutrient could be the major sources and processes contributing to maintaining higher nutrient levels in the water column during different seasons. Loading of nutrient from human sewage was the problem observed throughout the history of Visakhapatnam port (Ganapati and Raman, 1973, Raman, 1995; D'Silva et al., 2013). The impact of organic pollution in this harbour has resulted in periodic outbursts of phytoplankton blooms and fish mortality (Bharati et al., 2001; Raman, 1995).

Distinct seasonal variation in environmental factors was observed along the west and east coastal ports. Hydrography of the port waters reflected typical tropical conditions where temperature gradually increased from SWM to PrM season. However, during June and July, the temperature was high in east coast ports (V.O.C. and Chennai) compared to west coast ports due to ineffective SWM in the east coast (IMD). Earlier studies have reported that the coastal waters of the east coast are warmer compared to the west coast (Prasanna Kumar et al., 2002) due to stratified water on the east coast and mixed water column in the west coast. Kolkata port, situated in the north eastern part experiencing a subtropical climate, showed the higher temperature range (Mandal et al., 2013).

Ports situated along the east coast had lower salinity compared to the west coast and varied according to monsoonal activities, except Cochin and Kolkata ports. East coast receives enormous riverine flux as compared to the west coast (Qasim, 1977). In the AS (west coast) the annual variation in temperature is more as compared to salinity, but in the Bay of Bengal (east coast), annual salinity variation is more as compared to temperature (Wyrtki, 1973). In the estuarine Cochin port during SWM, stratification developed due to increased freshwater influx and formed a decreasing

salinity gradient from the mouth towards upstream. During the non-MON period, as freshwater influx reduced, water column was partially mixed as observed in estuaries influenced by monsoonal rainfall (Joseph and Kurup, 1989; Shetye, 1999). Recently, Jacob et al. (2013) reported that during non-MON high tide, saltwater intrudes up to 40 km in Cochin backwaters. Thus, in the present study, stations located in all three channels of Cochin port were influenced by the incoming high saline waters during the high tide. Since Kolkata is a freshwater port, there was no variation in salinity.

The most prominent feature of the port that makes the system unique is the presence of high nutrient concentrations (D'Silva et al., 2013), which is also observed in all the studied ports. This is also reflected in the phytoplankton biomass in all the ports. The highest biomass in Cochin port compared to other ports suggests that the estuarine ecosystem is most productive. Several studies have been conducted on the biological aspects in the Cochin backwater (Madhu et al., 2007; Martin et al., 2008; Madhu et al., 2009). These studies emphasize that irrespective of the season, Cochin backwater facilitates the luxurious growth of phytoplankton due to excess level of nutrient availability (Balachandran et al., 2005; Madhu et al., 2007). In the study region, maximum phytoplankton biomass recorded was higher (average 17.05 µg L^{-1}; ranged up to 107 µg L^{-1}) than that reported in previous studies in Cochin backwaters (49 µg L^{-1}; Madhu et al., 2007; Madhu et al., 2009; Martin et al., 2011) and also in the Mandovi and Zuari estuaries located along the west coast of India (Pednekar et al., 2011; Patil and Anil, 2011). This could be due to the nutrient enrichment by anthropogenic activities, which triggers the massive growth of nanoplankton (< 20 µm; Madhu et al., 2007; Martin et al., 2011) and phytoplankton blooms which are common in the Cochin backwaters when the intermediate salinity condition exists (Devassy, 1974; Madhu et al., 2010; Martin et al., 2013). Another reason could be the

weeds and water hyacinths, which proliferate in the upstream waters that severely restrict the natural flushing (Shivaprasad et al., 2012) and enter the CB during SWM due to the influx of low saline waters. In the PrM and PM-II seasons the higher chl *a* concentration in the surface and NBW of some of the S, could be the result of showers that occurred during the sampling period, which probably drive the weeds and water hyacinths into the CB or from stirred up sediments. Also, during PM-II, the highest chl *a* concentration recorded at S4 (107.06 µg L^{-1}) one day after heavy showers confirms that the incoming freshwater is a source of the high chl biomass.

Higher phytoplankton biomass also observed in Kolkata port, irrespective of season, could be related to high nutrient concentration. The unique feature of Kolkata port water is that; it is an enclosed water body which is connected to Hooghly River only during high tides when ship movements take place. However, Kolkata port operational management creates zero water masses exchange with outside river waters (Kumar, 2011). Therefore, the water circulation in this area is believed to be low. However, higher nutrient concentrations detected in the study region during different seasons could be from sewage discharge from the anchored ships and recycling of existing nutrients. Among the marine ports, New Mangalore port showed the highest biomass followed by V.O.C. and Chennai. Generally, the Bay of Bengal (East coast) is less productive region than its counterpart, AS (Qasim, 1977; Radhakrishna et al., 1978; Prasanna Kumar et al., 2002). Even though it receives high riverine nutrient flux, nutrient scavenging to deeper sediment (Qasim, 1977), strong stratification (Wyrtki, 1973), the lack of upwelling and convective mixing results in low productivity. In New Mangalore port, higher biomass in the inner stations during PrM and SWM coincided with the high tide during the sampling. Similarly, high biomass in Chennai port was observed during PrM in the outer stations during high tide. Such

observation was not noticed in V.O.C. port due to low tidal amplitude (see Materials and methods).

3.4.2 Picophytoplankton community structure in the marine ports (New Mangalore, V.O.C. and Chennai)

Generally, in the coastal waters, PP community dynamics is controlled by several environmental variables (Ning and Vaulot, 1992; Chiang et al., 2002; Qiu et al., 2010). Total PP abundance (0.02 to 12.2 × 10^4 cells mL^{-1}) was low in these coastal ports compared to other coastal waters (0.04 to 52 × 10^4 cells mL^{-1}; Ning et al., 2000; Gin et al., 2003). The lower PP abundance in ports could be due to a higher nutrient condition which is known to support the growth of larger phytoplankton thus suppressing the PP (Malone, 1992; Granli et al., 1993; Gin et al. 2003).

In marine ports (salinity > 30) four groups of PP were observed, i.e., *SYN*-PEI, *SYN*-PEII, PEUK and *PRO*-like cells. *SYN*-PC which is a low saline group was absent in these port waters (Murel and Lores, 2004). Among these groups *SYN*-PE was observed as a dominant group (60 to 80% of PP abundance). However, their abundance range was lower compared to other studied coastal regions (Ning et al., 2000; Xia et al., 2015). The dominance of *SYN*-PE was also observed in Singapore port waters where it contributed 70% to the total PP abundance (Gin et al., 2003). Generally, *SYN* grows even well in oligotrophic/mesotrophic condition due to the higher surface area to volume ratio, lower subsistence quota and high growth rate (Chisholm, 1992). It is generally a poor competitor in eutrophic ecosystems (Gin, 1996).

In the present study, the two types of *SYN*-PE (*SYN*-PEI and *SYN*-PEII) observed are also reported earlier in the north Atlantic and Pacific Oceans (Olson et al., 1990) and the western AS (Campbell et al., 1998). The higher abundance of *SYN*-PEI during

PrM compared to other seasons could be attributed to higher temperature. The growth of *SYN* exceeds its grazing mortality in summer, resulting in its high abundance (Tsai et al., 2008). Among the marine ports, the abundance was relatively higher in the New Mangalore port which could be due to higher temperature and salinity whereas in V.O.C. port even though the temperature was high the salinity was low whereas in Chennai port lower temperature was observed. Along with low temperature, the port activity and port structure (lower water circulation) may have also resulted in lower *SYN*-PEI abundance in Chennai port waters. Port structure also influences the abundance where Chennai port mouth is perpendicular to sea whereas V.O.C. and New Mangalore ports mouth are opened to the seaward side which influenced the water circulation due to the entry of seawater. In Ceuta port (North Africa), water movement is limited in the inner port area due to the port structure, which is not affected by the currents. This has negatively influenced the benthic community (Guerra-Garcia and García-Góme, 2003). Higher nutrient concentrations in the Chennai port supports this assumption of low circulation.

Similarly, PEUK, the less abundant group compared to *SYN*, showed relatively higher abundance during PrM in all the marine ports. Generally, PEUK prefers higher nutrient for their efficient growth (Pan et al., 2007). Thus, higher nutrient concentration coupled with increased water temperature could be the reason for higher PEUK abundance during PrM. PEUK also showed a positive relation with temperature, and it preferred 27 to 30^{o}C. This is consistent with the previous studies where PEUK abundance and growth rate were higher during summer months in subtropical estuaries (Qiu et al., 2010; Pan et al., 2007; Bec et al., 2005). However, in some region of subtropical and temperate estuaries, the winter season caused the peak

of PEUK abundance (Qiu et al., 2010; Charpy and Blanchot, 1998). The reason behind this variation is mainly the difference in the loading of nutrients.

SWM was characterized by the lowest temperature and salinity due to the effect of rainfall, which resulted in the low PP abundance. Besides the effect of these abiotic factors, the lower light condition due to the monsoonal cloud also influences the PP abundance (Patil and Anil, 2008). Light is considered a first order factor in controlling phytoplankton biomass and also partly controls the nutrient uptake which is an energy-demanding process (Kooistra et al., 2007). Thus, low light can restrict the build-up of phytoplankton biomass, and could be one of the reasons for the low PP abundance during the SWM. Generally, the monsoon brings nutrients to the water bodies through heavy riverine discharge and land drainage (Hung and Huang, 2005; Liu et al., 2009). However, in the ports, relatively low nutrient concentration was observed suggesting that the source of nutrients is not dependent on rainfall rather on other sources such as human activity involving shipping. This effect was better seen in west coast because of the ineffectiveness of SWM monsoon in the east coast. However, low PP abundance during this season on the east coast could be attributed to lower temperature and the factors observed during PrM. In New Mangalore port in the NBW, relative *SYN*-PEII and *SYN*-PEI abundance were high when DO concentration was lowest. Low DO concentration suggests higher decomposition activity releasing high nutrients (especially PO_4^{3-}) in the water column thus supporting PP. Generally, PEUK shows lower abundance during SWM in the estuarine region (Chapter 1). In New Mangalore port, PEUK showed higher abundance in the right wing which could be categorized as low circulation area. The higher PO_4^{3-} and SiO_4^{4-} could have played a role in increasing the SiO_4^{4-} preferring PEUK during this period (Vaulot et al., 2008). Also, low grazing pressure has been

reported during this period in the other studied region (Madhu et al., 2009), due to which the growth rate exceeds the grazing rate. However, in Chennai and V.O.C. ports, PrM conditions prevailed during this season as SWM effect was less on the east coast. This could be the reason for higher PEUK abundance during SWM.

The PM season is conducive for phytoplankton growth due to increased light conditions and higher nutrient concentrations. In New Mangalore port, *SYN*-PEI abundance increased during PM's especially PM-I; whereas during PM-II the abundance was lowest which could be attributed to higher temperature and higher salinity. Fluctuations in the SWM can also impact the phytoplankton community in the PM season (D'Costa and Anil, 2010). In New Mangalore port, 2012 (PM-II) had lower rainfall compared to 2011 (PM-I), in fact, 16% less than normal rainfall (IMD). In Chennai port, higher rainfall was observed during TP wherein the relatively higher abundance of *SYN*-PEI was observed especially inner station. Even though there was rainfall, higher temperature and NH_4^+ concentration could have supported the *SYN*-PEI during this period. In contrast, V.O.C. port had a lower abundance of *SYN*-PEI during TP period, which coincides with lower temperature. Further reduction in abundance was observed during NEM with lowering temperature. During low temperature conditions, low growth rates make the PP unable to keep pace with grazing, and as a result, *SYN* abundance becomes low (Xia et al., 2015; Tsai et al., 2008). PEUK abundance was lowest during TP and NEM periods suggesting that temperature was limiting factor for this group in the port waters. Higher chl biomass during PM-II compared to PM-I suggests the utilization of nutrients as its concentration was low compared to PM-I. To support this a strong positive correlation of chl *a* with nutrient concentration was observed. In the earlier study, PO_4^{3-} was found to be a limiting factor for phytoplankton growth (Elser et al., 2007). However,

in the port area, the higher nutrient concentration was reflected in the higher chl. In V.O.C. port, in both TP and NEM seasons even though the nutrient concentration was high, PP abundance was low which could be attributed to lower temperature.

3.4.3 Picophytoplankton community structure in Cochin port

Consistently high PP abundance (10^5 cells mL^{-1}) during all the seasons indicates that PP could be an important component of the phytoplankton community in Cochin port. During SWM the prevailing environmental factors influenced the distribution of PP groups, especially *SYN*-PE and *SYN*-PC, wherein the former is known to be abundant in high saline waters and latter in low saline waters (Murrell and Lores, 2004). During non-MON seasons, tide controls the salinity distribution in Cochin port (George and Kartha, 1963). Salinity variation due to tidal impact clearly influenced *SYN*-PC and *SYN*-PE distribution in the Cochin port, both horizontally and vertically. PM-II sampling was carried out during high tide. This could be the reason for high salinity in Ernakulam channel where *SYN*-PEI was the dominant group in the surface and NBW. PrM sampling was carried out during low tide which resulted in low surface salinity across the estuary where *SYN*-PC was dominant. These observations suggest that tide is also an influential factor for *SYN* distribution in the Cochin port wherein *SYN*-PE enters the Cochin port from the coastal waters during high tide and *SYN*-PC during the low tide from the upstream end. This is substantiated by observations from the monsoonal Zuari estuary (Chapter 2), wherein during the non-MON period due to high tidal activity, *SYN*-PE showed higher abundance upstream whereas, during SWM, *SYN*-PC abundance was higher downstream due to strong freshwater runoff. The significant positive relation of *SYN*-PE abundance and negative relation of *SYN*-PC and PEUK abundance with salinity and estimated tidal height indicates that tide is a prominent controller of PP community structure in

Cochin port. The significant relationship of PP groups with salinity is consistent with studies carried out in subtropical and temperate regions (Ray et al., 1989; Murrell and Lores, 2004), especially for *SYN*. Transition in dominance from *SYN*-PC to *SYN*-PE at salinities of ~20 to 25 found in this study, was previously observed in subtropical estuaries (Ray et al., 1989; Murrell and Lores, 2004; Zhang et al., 2013). Also, higher abundance of *SYN*-PC and *SYN*-PE in surface and NBW, respectively indicate that higher salinity in the NBW favors *SYN*-PE groups. This was well reflected in SWM when the high saline waters harboring *SYN*-PE were capped by the low saline waters harboring *SYN*-PC in the approach channel stations. These findings suggest that *SYN* distribution pattern can serve as an indicator of the seasonal water column hydrography (stratified or mixed) influenced by physical forces such as tides and freshwater runoff. The presence of an additional group of *SYN*-PE with high PE intensity at higher salinities (*SYN*-PEII) in the estuarine waters indicates that this group could have been introduced from the offshore waters during high tide. This observation is consistent with previous reports from the Zuari estuary, North western Arabian coast, Mississippi river plume and the Pearl River estuary (Campbell et al., 1998; Liu et al., 1998; Liu et al., 2004; Lin et al., 2010; Mitbavkar et al., 2015). *PRO*-like cells detected in the low saline waters of the Cochin port were also observed in the Zuari estuary along the south west coast of India (Chapter 2A). Shang et al. (2007) reported *PRO*-like cells in brackish and in freshwater. Similarly, in the present study, *PRO*-like cells were higher in the low saline waters as seen from the negative correlation with salinity. However, work on *PRO*-like cells is very limited and effect of environmental condition on these cells is still not clear. Recently, Liu et al. (2013) identified a previously suggested group of *PRO*-like cells as *SYN*-PC based on

laboratory experiments. However, to confirm the strain in the Cochin port, molecular approaches are required.

Variation in the spectral light quality is one of the factors altering the PP composition in oceanic, coastal and estuarine waters (Wood, 1985; Scanlan, 2003). In coastal and estuarine waters, *SYN*-PE group abundance is high in clear waters where the green light predominates due to the low concentrations of suspended particles and dissolved organic matter concentrations (Li et al., 1983; Wood, 1985; Stomp et al., 2007). *SYN*-PC is higher in turbid waters loaded with dissolved particulate organic matter or rich in chl where the spectral light quality is altered from green to red (Stomp et al., 2007). In Cochin port, water is highly turbid throughout the year and comparatively higher during the SWM (Qasim and Reddy, 1967). Hence, this could be one of the factors responsible for the predominance of *SYN*-PC in the Cochin port throughout the year, due to its better ability to utilize the red wavelength along with its ability to proliferate at lower salinities. Also, the positive correlation of *SYN*-PC with chl *a* suggests that this group is not only dominant but also significantly contributes to total phytoplankton biomass in the Cochin port. Increasing temperature, irradiance, salinity and comparatively lower turbidity could be responsible for the higher abundance of *SYN*-PE groups during PM.

The temperature in the tropical regions does not show much annual variation (24 to 32^{o}C in the present study) as in temperate regions (10 to 24^{o}C). As a consequence, PP abundance was high throughout the year in the tropics as compared to the temperate regions where abundance peaks are observed only during summer (Agawin et al., 1998; Chiang et al., 2002; Murrell and Lores, 2004). This suggests that seasonal temperature exercises a latitudinal variation on the PP distribution (Murphy and Haugen, 1985). Significant positive relation of total PP abundance with temperature is

a profound characteristic of tropical, subtropical and temperate estuaries (Ray et al., 1989; Agawin et al., 1998; Qiu et al., 2010; Wang et al., 2011). However, in the present study, only *SYN*-PC showed a positive correlation ($p < 0.05$) with temperature. Some studies conducted in tropical and subtropical estuaries showed that PP negatively correlated with nutrients (Qiu et al., 2010; Zhang et al., 2013). However, these studies considered total *SYN* (*SYN*-PC and *SYN*-PE) abundance to evaluate the relationship with nutrients. In the present study, although the positive relation of *SYN*-PC, PEUK and the negative relation of *SYN*-PE groups with NO_3^-, PO_4^{3-}, and NH_4^+ may not be cause and effect relationships, it indicates that nutrient concentrations could influence the seasonal variations of these groups. Similar results were obtained from the Zuari estuary, India (Chapter 2). In the Uchiumi Bay, Japan, PO_4^{3-} addition showed seasonal variations in the growth rates of *SYN* and PEUK (Katano et al., 2005). They presumed that the *in situ* nutrient concentrations or difference in species could be responsible for such a seasonal response. Though PEUK are the most competitive among PP groups (Pan et al., 2007), it was not the dominant group in Cochin port, even in high nutrient concentrations. Previous studies in tropical and subtropical regions have reported that this group dominated the nutrient-rich conditions (Jiao et al., 2005; Qiu et al., 2010). Probably, this group abundance was controlled by the high microzooplankton grazing rates which we did not consider in the present study (Wetz et al., 2011).

SYN-PE groups attained higher abundance during PM-I and PM-II seasons indicating its preference for increased temperature after SWM. Along with temperature, irradiance is also known to influence the seasonal distribution of *SYN* abundance and biomass (Agawin et al., 1998; Tsai et al., 2008). It is believed that there are multifactor, which are controlling the *SYN*-PE growth in coastal and

estuarine ecosystems (Chang et al., 2003; Zhang et al., 2013). Decreasing temperature and salinity during SWM and tide induced lower salinity during PrM could be the reason for low abundance during these periods. *SYN*-PC was the dominant group present in the Cochin port with the highest abundance in PrM, and their contribution was substantial to total PP. Similarly, studies carried out in the subtropical and temperate estuaries have shown that abundance of *SYN*-PC was greatest during warm periods (Ray et al., 1989; Murrell and Lores, 2004). The temperature was the limiting factor for PEUK in the previous studies where temperature varied between 20 to 27^{o}C (Pan et al., 2007). However, in the present study area, where the temperature range was 24 to 32^{o}C, PEUK were not significantly affected by temperature.

As the PM-I sampling was carried out in October soon after the SWM, the freshwater influence was still felt in the Cochin port as compared to that during PM-II sampling which was held in November. As a result, salinity and temperature were comparatively lower during PM-I. This was reflected in the PP distribution wherein higher PP abundance was observed during the PM-II. The dominance of *SYN*-PC over *SYN*-PEI during PM-II in some of the stations was mainly due to salinity < 25 as a result of rainfall that occurred on the sampling day. Higher salinity in the NBW during PM-II favored higher *SYN*-PEI and *SYN*-PEII abundance in the Cochin port.

3.4.4 Picophytoplankton community structure in Kolkata port

The information on PP community structure in the enclosed water bodies of the freshwater port are rare and it is not available in this part of the world. The results suggest that *SYN*-PC was the potent dominant species observed over *SYN*-PE and PEUK, irrespective of the seasons. The dominance of *SYN*-PC in freshwater has been reported earlier (Pick, 1991, Camacho et al., 2003, Murrell and Lores, 2004), but it was largely outnumbered in the present study. Its maximum abundance (10×10^5 cells

mL^{-1}) recorded in the present study was higher than the other studied freshwater ecosystems such as Zuari River (chapter 2), Pearl River (Ni et al., 2015), Pagan River (Davis et al., 1997), Wujian reservoir (Wang et al., 2008), Rimov reservoir (Simek et al., 1997) and some of the lake ecosystem such as lake Maggiore, Mascardi, Moreno, Gutierrez, Espejo, Correntoso and Nahuel Huapi (1×10^5 cells mL^{-1}; Callieri et al., 2007). Sardis reservoir, Mississippi, USA had the same range of abundance during summer at temperature ~24ºC (Ochs and Rhew, 1997). Highest PP abundance was recorded during summer, when temperature was ~25ºC (maximum) in nutrient rich waters of lake Aydat, (2.3×10^6 cells mL^{-1}) and La Cruz hypertrophic lake (7×10^6 cells mL^{-1}; Camacho et al., 2003). There was a distinct seasonal variation of PP groups observed during the study period. The highest abundance of *SYN*-PC and *SYN*-PE was observed during SWM. As observed in marine ports, temperature played a major role along with nutrients. PCA showed that temperature was the significant factor in this port. Several studies have established temperature as the key factor influencing the seasonal dynamics of *SYN* from tropics to temperate lakes, rivers, reservoirs, estuaries and coastal waters (Callari et al., 2007; Ochs and Rhew, 1997; Wang et al., 2008; Qiu et al., 2010; Wang et al., 2011; Ning et al., 2000; Murrell and Lores, 2004; Mitbavkar et al., 2009). These studies showed that warm period is favorable for *SYN*. Similarly, in the present study, *SYN* abundance showed significant positive correlation with temperature where temperature range was wider (18 to 32°C) compared to other studied ports (24 to 34°C). The optimum temperature range of 27 to 30°C was found to be favorable for *SYN* in the present study. As the temperature dropped below 23°C in February, the abundance decreased. The decrease in temperature is known to reduce the activation energy of their growth rate (Chen et al., 2014), and along with high grazing pressure results in low PP abundance (Xia et al.,

2015). Even though the temperature was 26°C during PM, the low abundance could be linked to suppression of their growth by very high nutrient concentrations (Agawin et al., 2000). This is particularly observed in the KOPT-I and KOPT-II docks, whereas higher abundance was observed in the NSD when nutrient concertation was lower compared to other two docks. Overall PEUK abundance was low compared to other studied regions (Li et al., 2016; Mozes et al., 2006). However, during PM, when high nutrient concentrations were observed in KOPT-I, and KOPT-II docks comparatively higher abundance of PEUK was observed with positive correlation with NO_3^- suggesting that nutrients play a role in the spatial and temporal variation of different PP groups. In hypertrophic waters, the community structure of phytoplankton in the water body was determined by the dominant species in competition for nutrients (Zhu et al., 2010). *PRO*-like cells were encountered earlier in the Zuari estuary (Chapter 2), Cochin backwaters (in the present study), Rhone River (Vaulot et al., 1990), Suruga Bay (Shimada et al., 1995) and Changjiang estuary (Shang et al., 2007). However, in the present study, their abundance was low. PCA analysis showed that *PRO*-like cells were not a strong group loaded on the first two components which suggest that this group is less important in relation to environmental factors (Table 3.8). Indeed, the effect of environmental condition on these cells is still not clear.

Clear spatial variation of *SYN*-PC was observed in the present study. KOPT-I and KOPT-II showed low abundance where higher nutrient concentration was recorded; whereas NSD dock recorded higher abundance when the nutrient concentration was lower except during PrM-I. This observation clearly points out that nutrients are being utilized by *SYN*-PC for causing bloom like conditions in NSD dock during SWM. PCA also showed the strong negative relation of *SYN* with NO_3^- and PO_4^{3-} suggesting

the efficient utilization of nutrients. Generally, *SYN*-PC and *SYN*-PE showed low abundance in the NBW compared to surface waters. The higher biomass in the surface water could have restricted the light penetration till the NBW resulting in suppression of the PP growth in the NBW. Shipping activities can also negatively affect the growth of PP in the NBW due to increased turbidity induced a decrease in light penetration. Stations located in the river showed very low abundance due to higher flow rate. Low cell abundance at higher flow rate was observed earlier during monsoon months in the Zuari estuary (Chapter 2). Higher abundance of *SYN-PC* in these eutrophic waters is consistent with a previous study (Stomp et al., 2007). The reason behind the unusual higher abundance of PP in NSD could be the consequences of shipping activities which helps in the maintenance of higher nutrients throughout the seasons. NSD is the busiest dock compared to KOPT-I and KOPT-II with more berths facilities. Therefore, a large number of anchored ships might release untreated sewage. In the present study region, there is no possibility of supply of nutrients from the river waters. High nutrient concentrations through a diel cycle was an indication of maintenance of high nutrients in the study region (personal observation). Although it is a closed ecosystem, water movement helps in the easy access of nutrients for the PP. Therefore, the shape of the dock could play a major role in the water movements and circulation of nutrient within the water column. NSD is broader dock whereas, other docks are narrow and long. Therefore, water masses are easily circulated in the broader dock rather than the narrow and longer docks. This might also be a reason of higher abundance in NSD. Also, the higher abundance was observed where the station located at the corner or end of the dock. Those stations are also described as ship breakage and repairing berths. These observations corroborate our hypothesis that the undisturbed closed ecosystem promotes the excessive growth of which could lead to

the ecological imbalance in the microbial food web. Therefore, the present study depicts the best example for the consequences of human interference in the modification of ecosystem and it could cause serious problems.

3.4.5 Variation of picophytoplankton community with trophic index of water column.

TRIX scores indicated that the marine port waters exhibit a good state of water quality except on some occasions. In these waters, there was no significant relation between PP groups and TRIX scores, except at V.O.C. port waters. When the TRIX scores were > 5 in V.O.C. and New Mangalore port waters, PP abundance correspondingly decreased, especially of *SYN*-PE. This indicates that clear water is favorable for their growth as observed in an earlier study (Bell and kalff, 2001). In the estuarine port waters (Cochin port), the negative relationship of TRIX with the estimated tidal height and salinity suggests that low tide causes a higher trophic index due to higher influence of freshwater rich in anthropogenic contaminants from the upstream whereas, high tide brings offshore waters into the Cochin port, which leads to dilution of eutrophic waters. The positive and negative relation of *SYN*-PC and *SYN*-PE, respectively, with TRIX scores, suggests that these groups occupy contrasting ecological niches. In the hypertrophic waters of French Mediterranean lagoon, which was described as an anthropogenically influenced eutrophicated area, abundance of *SYN*-PC was higher than that of *SYN*-PE (Bec et al., 2011). The negative relation of *SYN*-PEIII with TRIX scores indicates that they are poor competitors in eutrophic waters (Gin, 1996). Munawar and Weisse (1989) reported that autotrophic picoplankton avoided contaminated environments but was high in contaminated eutrophicated areas. They attributed this to the availability of excess nutrients, which may have complexing effects resulting in the detoxification of

contaminants. Aneeshkumar and Sujatha (2012) reported that zeaxanthin pigment indicative of cyanobacteria was found more in the sediments of sites influenced by anthropogenic activities (near to S23) in the Cochin port. Since zeaxanthin is a marker pigment of both *SYN*-PE and *SYN*-PC and we found *SYN*-PC > *SYN*-PE throughout the study period at S23, which is a sewage discharge point, we assume that *SYN*-PC was the dominant group found in this area by Aneeshkumar and Sujatha (2012). Carlson's index showed that the riverine port (Kolkata port) waters also exhibited eutrophic condition during SWM and PM-I as seen in estuarine port (Cochin port). During these periods, *SYN*-PC was the dominant and highly abundant group in these waters. These observations corroborate our findings and suggest that *SYN* could serve as a potential indicator of the trophic status of water bodies.

3.5 Conclusion

The present study shows clear temporal and spatial variations in the PP abundance and community structure with respect to different ecosystems. The highest PP abundance was observed in the closed riverine port (Kolkata port), where PP community was strongly correlated with temperature and nutrient concentrations. Comparatively lower abundance of PP was detected in the estuarine port (Cochin port), and lowest in the marine ports (V.O.C., Chennai, and New Mangalore ports). The dominance pattern also varied among these ports. *SYN*-PEI was dominant in marine ports, and high saline waters of estuarine port whereas *SYN*-PC was dominant in low saline waters of estuarine port and riverine port. Temperature and nutrients played a major role in the seasonal and spatial variations of PP in these ports. The effect of monsoons (SWM and NEM) was also well reflected in the variation of PP community structure and its abundance along the west and east coasts. TRIX showed that the marine ports exhibited a lower level of eutrophication compared to estuarine

and riverine ports (Carlson index). In these waters, distribution of *SYN*-PE and *SYN*-PC groups highlight that they occupy contrasting ecological niches, where former was higher in the lower eutrophic waters and latter in the higher eutrophic waters. Therefore, PP distribution pattern can serve as an indicator of the trophic status of coastal water bodies.

Chapter 4

Picophytoplankton community structure from eastern Arabian Sea

4.1 Introduction

The Arabian Sea (AS) constitutes the north-western part of the Indian Ocean and its semi-enclosed feature leads to an unusual climate, hydrography, and biogeochemical processes (Naqvi et al., 2003). As a result of the semiannual reversal of monsoon winds, seasonal variation of water column characteristics is also observed (Qasim, 1982; Banse, 1987). During the south west monsoon (SWM), coastal upwelling is a common phenomenon (Banse, 1968; Banse and McClain, 1986; Shetye et al., 1994) whereas during the north-east monsoon (NEM) convective mixing is prominent in the northern AS (Madhupratap et al., 1996) with decreasing intensity of mixing towards the southern AS (Prasanna Kumar et al., 2000). Additionally, during this period downwelling is also observed (Rao et al., 2008). Monsoonal forcing results in seasonal variations in the mixed layer depth, flux of nutrients to the upper mixed layer and thereby on pelagic food web structure and production (Madhupratap et al., 1996; Morrison et al., 1998; Prasanna Kumar et al., 2000; Wiggert et al., 2000; Shankar et al., 2005).

In the AS, phytoplankton biomass and primary productivity are high during the SWM and the NEM (Marra et al., 1998; Prasanna Kumar et al., 2000). During the NEM, interannual variations in the phytoplankton biomass and primary production are significant along the eastern (Bhattathiri et al., 1996; Sawant and Madhupratap, 1996; Parab et al., 2006; Ahmed et al., 2016) and the western AS (Campbell et al., 1998; Brown et al., 1999; Garrison et al., 2000). Only a few of the above studies have dealt with the smaller sized phytoplankton groups in the eastern AS (Roy et al., 2015; Ahmed et al., 2016).

During the last decades, the importance of picophytoplankton (PP; < 3 µm) has been demonstrated in the marine environment as major contributors to the

phytoplankton biomass (Worden et al., 2004; Richardson and Jackson, 2007). PP comprises of three major groups, *Prochlorococcus* (*PRO*), *Synechococcus* (*SYN*) and picoeukaryotes (PEUK). *PRO* dominates the oligotrophic waters and is encountered down to 150 m depth (Chisholm et al., 1988; Partensky et al., 1999; Johnson et al., 2006; Fuller et al., 2006). *SYN* is abundant in mesotrophic waters with a shallower vertical distribution than that of *PRO* (Bouman et al., 2006; Zwirglmaier et al., 2007; Flombaum et al., 2013). PEUK, along with *SYN* dominate the nutrient-rich coastal ecosystems (Blanchot et al., 2001; Jiao et al., 2005; Sharples et al., 2009). Although limited information is available on the PP community from the eastern AS, short-term variability which can impart an in-depth understanding of the PP dynamics still remains unknown.

The present study was focused on the short-term vertical variations (every 3 h for 9 days) in the PP community structure at a fixed location over the continental slope in the eastern AS, off Goa, India. The objective of this study was to assess the influence of different hydrographic conditions such as stratification and mixing on the PP distribution pattern. Along with this study, a transect observation was carried out from the coast towards the offshore so as to gain an understanding of the PP spatial distribution pattern in the cross-shelf region during the NEM. In this study, it was hypothesized that in the eastern AS, the PP community structure and carbon biomass varies in response to the short-term hydrographic variability resulting from coastal advection and vertical water column mixing. This study will also serve as a basis for understanding the response of phytoplankton community as a whole with chlorophyll biomass as the proxy.

4.2. Materials and methods

4.2.1 Sampling

Sampling was conducted in the cross-shelf region of the eastern AS, off Goa coast, onboard the ocean research vessel ORV Sindhu Sankalp (SSK-27) during the early NEM season (18-27 November 2011). Five stations along the coastal to offshore transect were sampled for the spatial variability studies on the PP community structure. For the temporal variability, one fixed station i.e. station (S) 6 was sampled every 3 h for 9 days (D) (Fig. 4.1). Details of the sampling are given in table 4.1. Temperature, salinity and dissolved oxygen (DO) data profiles were taken from precalibrated CTD. The calculation of mixed layer (ML) depth was based on sigma-t criteria. Water samples for nutrients and PP analyses were collected from 7 to 10 depths in the upper 0 to 200 m (depending on the water column depth) with 12 L Niskin bottles (General Oceanics, Miami, FL, USA) mounted on a CTD (Sea- Bird electronics) rosette sampler. Nutrient samples were analyzed [nitrite (NO_2^-) nitrate (NO_3^-), phosphate (PO_4^{3-}), ammonium (NH_4^+), and silicate (SiO_4^{4-})] with a SKALAR SAN^{plus} auto-analyzer. For analysis of PP, water samples were preserved in paraformaldehyde (final concentration 0.2%; Campbell, 2001). After 15 min dark incubation, the samples were quick-frozen in liquid nitrogen and stored at -80^oC until analysis. For chlorophyll *a* analysis, water samples (~3 to 4 L) were filtered through GF/F filter followed by extraction of pigments in 90% acetone which were measured using High Performance Liquid Chromatography (LC 1200 series, Agilent Technologies, USA; Acharyya et al., 2012).

4.2.2 Flow cytometric analyses of picophytoplankton

In the laboratory, samples were thawed and analyzed through FacsVerse flow cytometer configured with 20 mW and 40 mW air-cooled lasers exciting at 488 nm

(blue) and 664 nm (red), respectively. Sample acquisition was set for 10000 events. Flow rates were calibrated before analysis using the equation, $R= (W_i- W_f)/ (T \times d)$ where W_i = initial weight of the sample (mg), W_f = final weight of the sample (mg), T = time (minutes), and d = density of the sample (seawater = 1.03) (Marie et al., 2005). Forward angle light scatter (FALS; proxy for cell size) and right angle light scatter (RALS), orange (564 to 606 nm) and red (> 650 nm) fluorescence intensities were collected from each particle and analyzed with Facs Suite™ software. Yellow-green fluoresbrite fluorescent beads (Polysciences co., USA) of 2 µm diameter were added to the samples as an internal standard. Cell fluorescence emission and light scatter signals of each PP group were normalized to that of the beads (mean cell values/ mean bead values) to distinguish the different PP groups based on their autofluorescence properties and size. Three major groups of PP were determined (Fig. 4.2a-c). *SYN* was identified based on the orange fluorescence of the pigment phycoerythrin. PEUK were differentiated from *PRO* based on the relatively higher red chl *a* fluorescence and largest FALS.

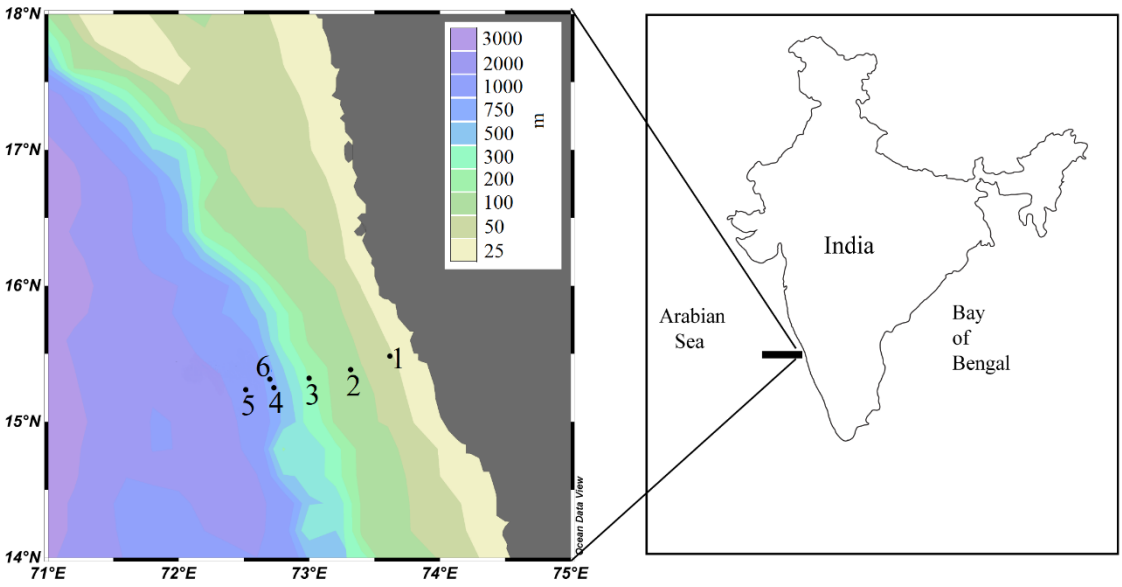

Fig. 4.1 Locations of sampling stations in the eastern Arabian Sea.

Table 4.1 Details of sampling in the eastern Arabian Sea.

Stations	Latitude (ºN)	Longitude (ºE)	Sampling date (d/m/y)	Approx. distance from station 1 (miles)
1	15º 28’ 56”	73º 37’ 00”	27/11/2011	0
2	15º 23’ 57”	73º 19’ 57”	27/11/2011	19.86
3	15º 19’ 14”	72º 59’ 53”	27/11/2011	42.87
4	15º 15’ 00”	72º 43’ 47”	26/11/2011	60.89
5	15º 14’ 6”	72º 30’ 50”	26/11/2011	75.18
6 (time series)	15º 18’ 46”	72º 41’ 53”	18-26/11/ 2011	62.13

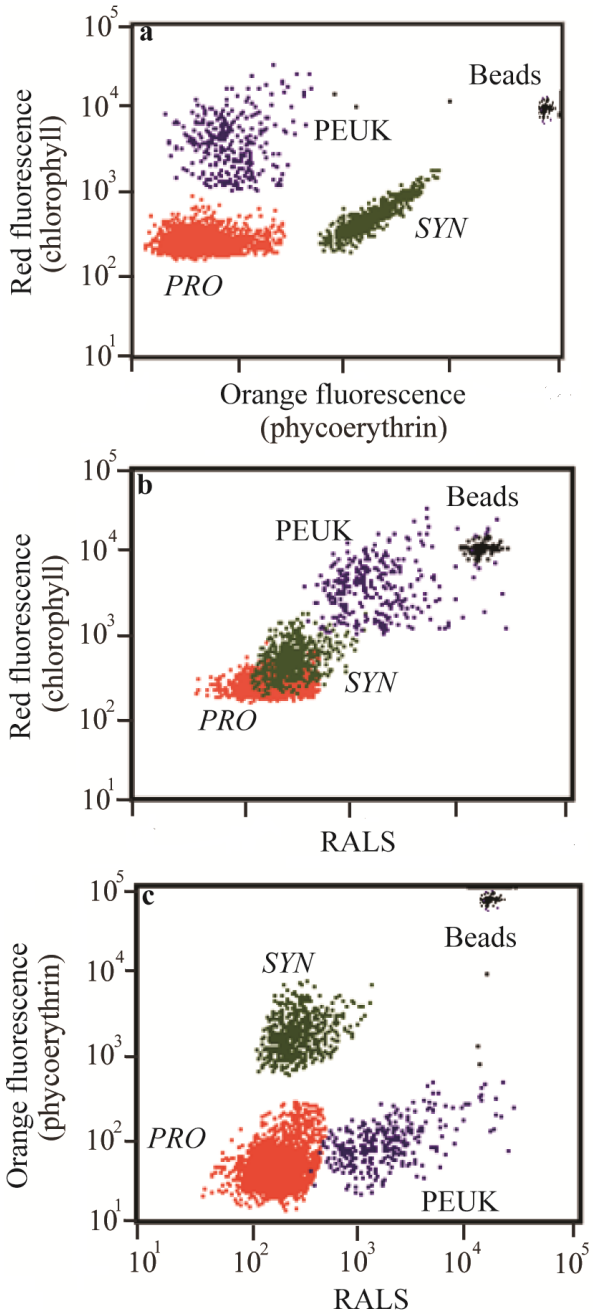

Fig. 4.2 Dot plot of flow cytometric analysis showing PP groups from the eastern Arabian Sea.

4.2.3. Carbon biomass estimation

Phytoplankton carbon biomass was derived from chl *a* using a carbon: chl *a* ratio of 140 and 83 µg C: µg chl^{-1} for the phase-I and phase-II ML depths, respectively (Shalapyonok et al., 2001). A C: chl *a* ratio of 52 was used for depths below the ML (Brown et al., 1999; Garrison et al., 2000). Carbon biomass of *SYN*, *PRO* (Garrison et al., 2000; Shalapyonok et al., 2001) and PEUK (Shalapyonok et al., 2001) were estimated using conversion factors as given in Table 4.2. For PEUK, the biovolume calculated from FALS was converted to carbon per cell (Shalapyonok et al., 2001).

Table 4.2 Conversion factors used to estimate carbon biomass of PP groups (fg C $cell^{-1}$) and total phytoplankton (µg C $µg^{-1}$ chl *a*) in the mixed layer (ML) and below mixed layer during phase I and phase II.

	Phase I		Phase-II	
	ML	Below ML	ML	Below ML
SYN	106.2	185.1	101.0	152.0
PRO	34.2	84.5	32.0	72.0
PEUK	601.0	647.0	522.0	528.0
C:Chl *a*	140.0	52.0	83.0	52.0

4.2.4. Data analyses

The depth of euphotic zone ($Z_{1\%}$) was estimated from chl *a* concentration of surface layer using the chl centered approach (Lee et al., 2007). The percentage contribution of PP to total phytoplankton carbon biomass and individual PP group contribution to total PP carbon biomass were estimated from the phytoplankton and PP carbon values. PP carbon biomass was depth integrated by trapezoidal method and its percentage contribution to the total phytoplankton biomass was also calculated.

PERMANOVA analysis (Wood et al., 2016) was performed using PRIMER 6 software to assess the variation in the biotic (*SYN*, *PRO*, PEUK, PP carbon biomass, chl *a*, phytoplankton carbon biomass, and PP carbon contribution) and abiotic (nutrients, temperature, salinity, and DO) parameters between phase I (stratified water

column) and phase II (mixed water column) samplings in the surface (0 m), ML and below ML. Path analysis was used to explain the linear relationships (R^2 = coefficient of determination) between the biological and the contextual physicochemical parameters in the ML (phase I and phase II) and below ML (50 m, 75 m and 100 m depths). It was conducted as a hierarchical multiple regression analysis and the obtained results were used to establish a path diagram (SPSS Amos). The D5 data (ML and below ML) was also treated separately in order to assess the PP response to environmental conditions during the transition phase.

4.3 Results

4.3.1 Spatial variation of environmental variables

Along the transect, the ML increased from nearshore (23 to 27 m) to offshore (37 to 40 m) stations. The ML water temperature was 28.6 ± 0.1^{o}C at all the stations (Fig. 4.3a). The surface salinity in the nearest coastal station (S1) was 34.19 ± 0.06 and gradually increased towards the offshore (35.23 ± 0.29; Fig. 4.3b). DO concentrations ranged from 4 to 4.2 mg L^{-1} in the ML and decreased below 50 m (Fig. 4.3c). Chl *a* concentrations in the surface waters were high (0.69 ± 0.12 µg L^{-1}) in the nearshore station (S1) and gradually decreased (0.19 ± 0.04 µg L^{-1}) in the offshore stations. Subsurface chl *a* maxima was observed at 50 m for S2 to S5 (Fig. 4.3d).

4.3.2 Spatial variation of picophytoplankton community structure

SYN was the dominant PP group observed in the nearshore waters (S1 and S2), and its abundance decreased at the subsequent stations except, at 25 m of S4 (Fig. 4.4a). In contrast to *SYN*, *PRO* was the dominant group observed at offshore stations with the highest abundance (17.5 × 10^4 cells mL^{-1}) recorded at 10 m of S5 (Fig. 4.4b). In the offshore stations, *SYN* and *PRO* abundance decreased with increasing depth. The PEUK abundance was lower (0.8 ± 0.9 × 10^4 cells mL^{-1}) at all the stations, except

at station located at the edge of the continental shelf (S3; 3 to 17.1 × 10^4 cells mL^{-1}; Fig. 4.4c).

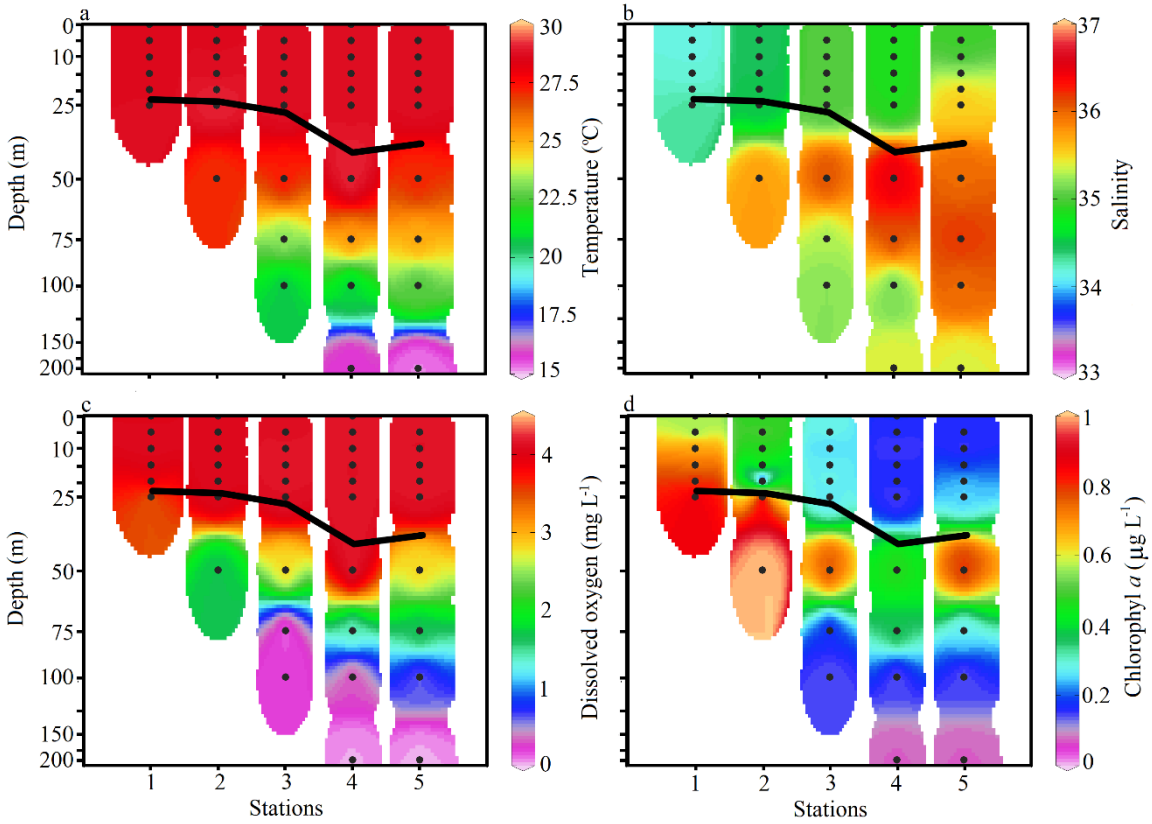

Fig. 4.3 Vertical profiles of spatial variation in (a) temperature, (b) salinity, (c) disolved oxygen, and (d) chlorophyll *a* in the continental shelf and slope of the eastern Arabian Sea. Black line indicates mixed layer depth.

4.3.3 Environmental variables

During the time series sampling, based on the ML depth, the sampling period was divided into two phases: phase I (from D1 to D5) was characterized by a shallow ML (25.58 ± 4.85 m) with high temperature (29.39 ± 0.2°C) and low salinity (34.34 ± 2.8) water mass, and phase II (D6 to D9) was characterized by a deep ML (51.44 ± 5.50 m) with lower temperature (28.62 ± 0.2°C) and higher salinity (35.15± 0.43) water mass (Fig. 4.5a and b). DO concentration ranged from 3.9 to 6.1 mg L^{-1} in the ML (Fig. 4.5c). Nutrient concentrations within the ML were significantly higher during phase II. NO_3^- and PO_4^{3-} concentrations were < 1 µM within the ML during

phase I whereas during phase II, it increased (>1 µM; Fig. 4.5d, Fig. 4.5f). PO_4^{3-} concentration started increasing from the end of phase I (D4 to D5; Fig. 4.5f). NO_2^-

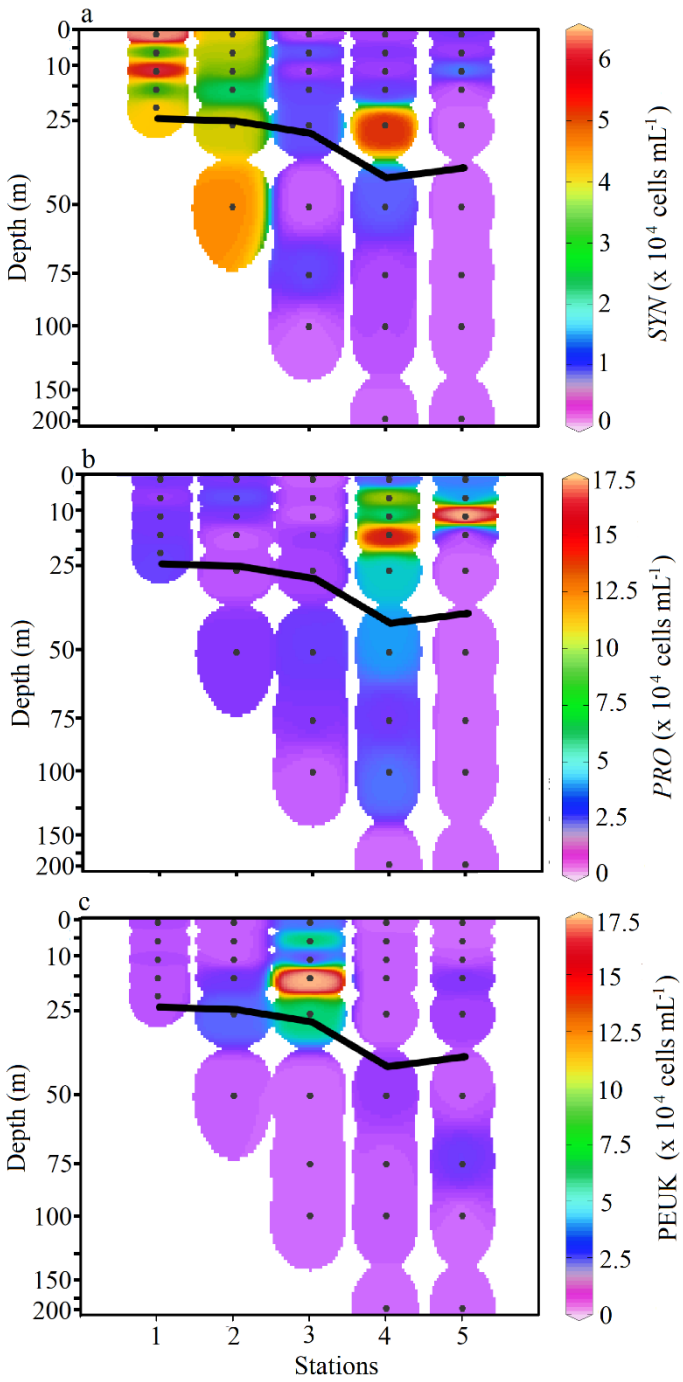

Fig. 4.4 Vertical profiles of spatial variation in (a) *SYN*, (b) *PRO* and (c) PEUK abundance in the continental shelf and slope of the eastern Arabian Sea. Black line indicates mixed layer depth.

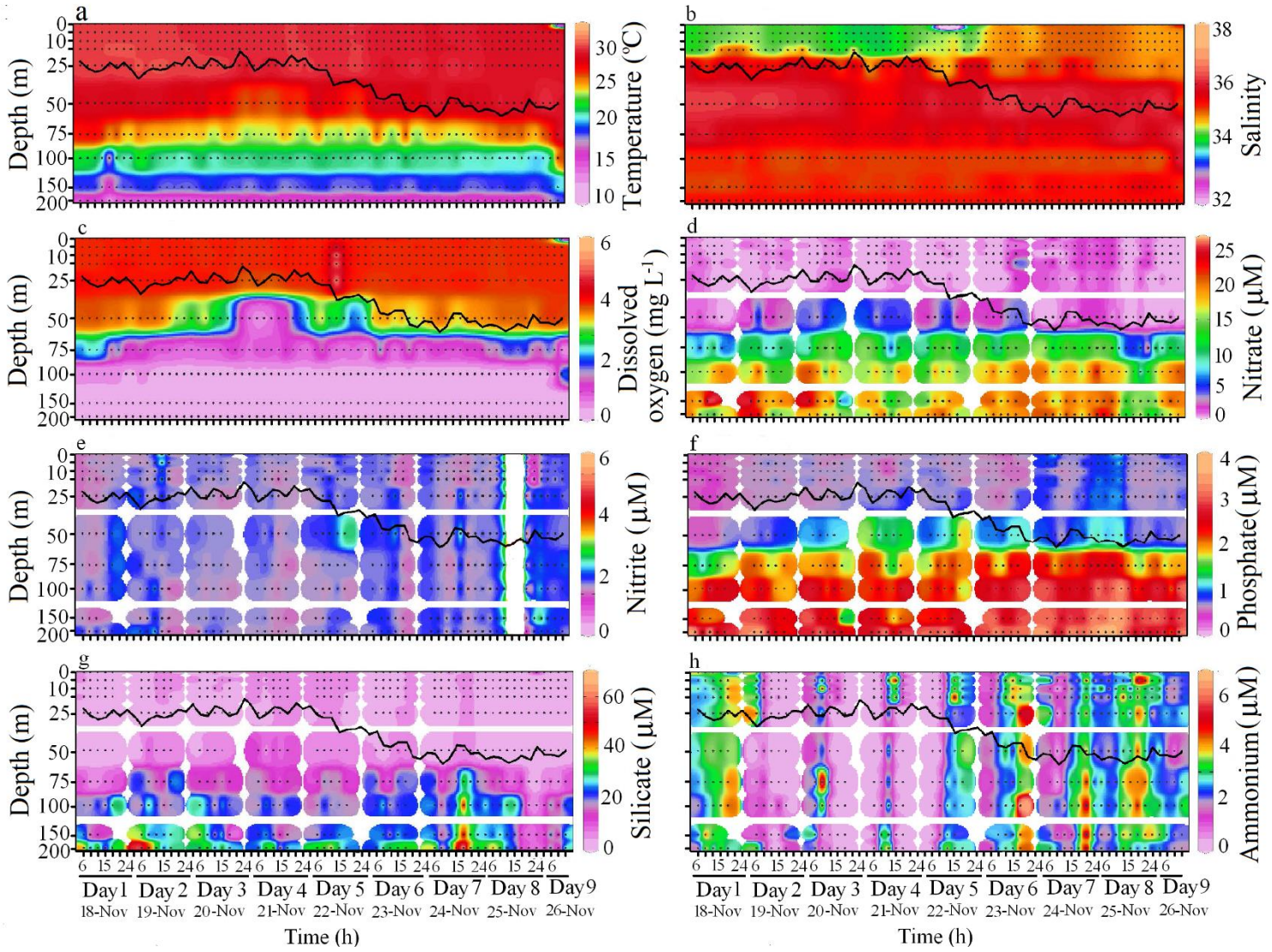

Fig. 4.5 Vertical profiles of temporal variation in (a) temperature, (b) salinity, (c) dissolved oxygen, (d) nitrate, (e) nitrite, (f) phosphate, (g) silicate, and (h) ammonium over the continental slope of the eastern Arabian Sea. Black line indicates mixed layer depth.

concentration ranged from 0.02 to 0.97 µM in the water column (Fig. 4.5e). SiO_4^{4-} concentration in the ML ranged from 1.05 to 6.54 µM (Fig. 4.5g). In the ML, NH_4^+ concentration ranged from 0.01 to 5.95 µM (Fig. 4.5h). Nutricline deepened during the beginning of phase I and during phase II, whereas it was shallower during end of phase I (D4 to D5). The depth of euphotic layer ranged between 60 and 70 m during the study period.

4.3.4 Picophytoplankton community structure

Variations of hydrographic conditions during the two phases were well reflected in the PP community structure and its abundance, especially in the ML. At the beginning of phase I, *SYN* abundance was higher in the upper 75 m water column, with maximum abundance at 50 m (6.4×10^4 cells mL^{-1}). Its abundance reduced during the later part of phase I (except on D4 at 25 m; 9.8×10^4 cells mL^{-1}) and phase II (Fig. 4.6a). At the beginning of phase I, *PRO* was the dominant PP group in the water column. *PRO* population was observed down to 200 m depth with maximum abundance in the ML and occasionally in deeper waters (100 m; Fig. 4.6b). By the end of phase I, PEUK was the dominant PP group, especially between 25 m and 75 m depths (Fig. 4.6c). On D5 and D6, dominance of PEUK extended to deeper waters (75 m). PEUK had a higher abundance at 50 m, except on D2 and D3. During phase II, the abundance of all PP groups (*PRO* > PEUK > *SYN*) reduced by an order of magnitude in the water column. Overall, PP abundance was higher during phase I (Fig. 4.6d).

Pronounced diel variation was observed in the PP community during the study period. Generally, *SYN*, *PRO*, and PEUK showed higher cell abundance during the afternoon and night (12:00 to 24:00) and the time of attaining maximum cell

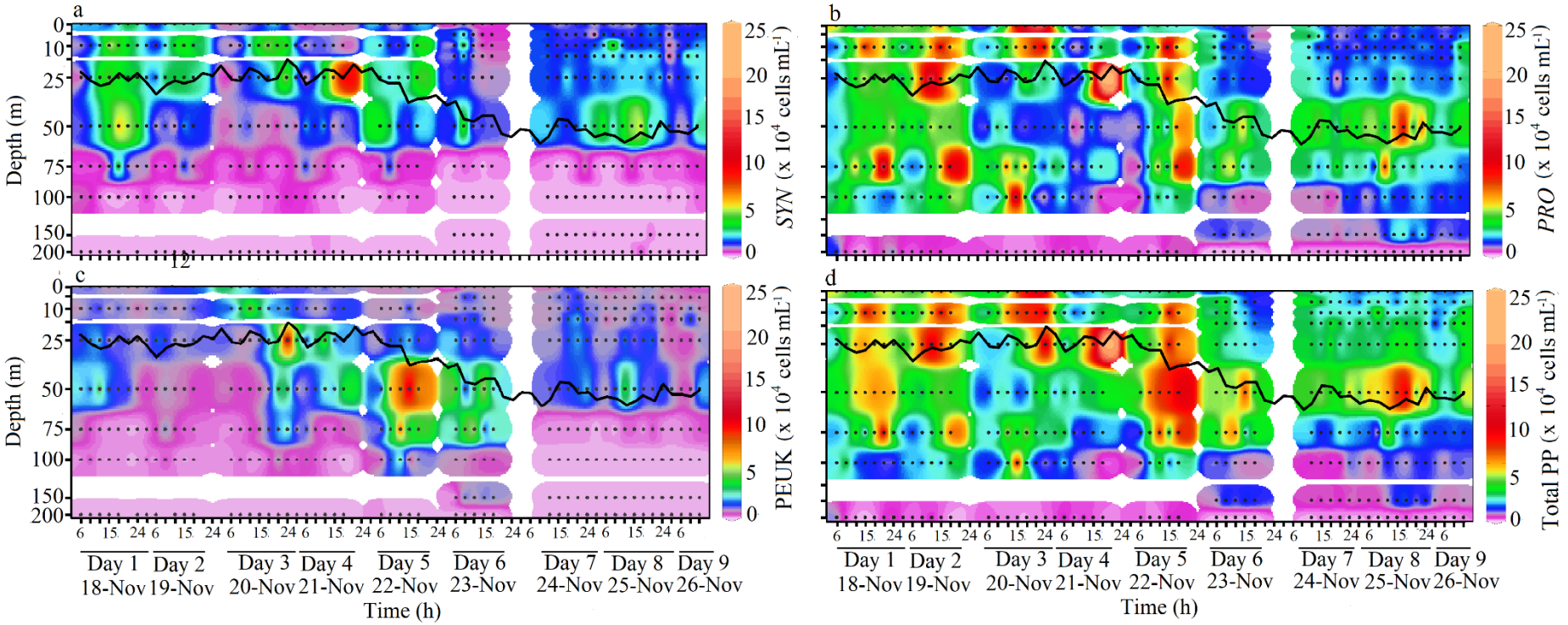

Fig. 4.6 Vertical profiles of temporal variation in cell abundance of (a) *SYN*, (b) *PRO*, (c) PEUK, and (d) total PP over the continental slope of the eastern Arabian Sea. Black line indicates mixed layer depth.

abundance showed variation between the two phases. In particular, during phase I (D1 to D3) the abundance of *SYN*, *PRO*, and PEUK was higher at 18:00, 15:00, and 12:00, respectively, which remained high till 24:00 (Fig. 4.6a-c). At the end of phase I, PEUK cell abundance was higher at 9:00 but *SYN* and *PRO* did not show any change in the pattern. During phase II, in the ML, higher abundance of *SYN* and *PRO* was observed at 12:00 and PEUK at 15:00 (Fig. 4.6a-c). In both phases, higher abundance of *SYN* and PEUK was only observed in the upper 50 m (Fig. 4.6a, Fig. 4.6c). *PRO* abundance was higher in the shallower depths (upper 50 m) from evening to night (after 15:00) and below 50 m depth before 15:00 during phase I, whereas, during phase II, higher cell abundance was observed only in the upper 50 m (Fig. 4.6b).

4.3.5 Contribution of picophytoplankton to the total phytoplankton carbon biomass

Chl *a* concentration ranged from 0.07 to 1.09 µg L^{-1} with peak values just below the ML (50 m; Fig. 4.7a). Chl *a* concentrations were high during afternoon and night followed by lower values in the early morning. Phytoplankton carbon biomass varied from 2.5 to 203.1 µg L^{-1} in the water column with higher concentrations below the ML. Phytoplankton carbon biomass concentration was significantly ($p < 0.05$) higher during phase I than phase II in the ML and also below ML. PP carbon biomass varied from 0.1 to 98.32 µg L^{-1} in the water column during the entire study period (Fig. 4.7b). PP contribution to the total phytoplankton carbon in the entire water column ranged from 13 to 70% during phase I and 15 to 47% during phase II. Higher PP carbon contribution was observed during phase I, especially on D5 (26 to 70%, entire water column, Fig. 4.7c). Depth-integrated PP carbon biomass concentration was significantly ($p < 0.05$) higher during phase I than phase II in surface, ML and below ML. Depth-integrated PP carbon biomass contribution to the total phytoplankton carbon ranged from 9 to 58% in the ML during the entire study period. However,

there was not much difference in their contribution to total phytoplankton carbon biomass in surface and ML; whereas below ML, PP carbon contribution to total carbon biomass was higher during phase I than phase II.

At the end of phase I, the PP carbon biomass was higher especially at 25 m and 50 m depth with a major contribution by PEUK (Fig. 4.8c). The major contributor to PP carbon biomass was PEUK (35 - 90%) followed by *SYN* (4 - 44%) and *PRO* (1-39%) in the upper 50 m during both phases (Fig. 4.8a-c). In the deeper waters, *PRO* carbon biomass was dominant except at the end of phase I, where PEUK was dominant down to 100 m depth. However, on some occasions, *PRO* dominated the PP carbon biomass in the ML. There was no consistent diel pattern of PP carbon biomass and its contribution to the total phytoplankton carbon biomass. Generally, PP contribution was higher in the upper 50 m depth but at the end of phase I, higher PP carbon contribution was observed down to 100 m, and extended down to 150 m in the early phase II.

4.3.6 Relationship between picophytoplankton and environmental variables

PERMANOVA analysis revealed significant variations ($p < 0.01$) in temperature, DO, PO_4^{3-}, SiO_4^{4-}, chl *a* concentration, PEUK abundance, *PRO* abundance, phytoplankton carbon biomass, and PP carbon biomass between phase I and phase II samplings in the surface waters (0 m) whereas salinity, NH_4^+, NO_2^-, NO_3^- and PP contributions showed insignificant variations (Table 4.3). In ML, significant variations ($p < 0.01$) were observed in temperature, nutrient concentrations, chl *a* concentration, PP group cell abundances, phytoplankton carbon biomass, and PP carbon biomass between phase I and phase II samplings whereas salinity, DO and PP contributions showed insignificant variations (Table 4.3). Below ML, DO, nutrients (except SiO_4^{4-}), chl *a* concentration, *SYN*, PEUK, phytoplankton carbon biomass, PP carbon biomass and its

contribution to total phytoplankton carbon biomass showed significant variation ($p < 0.01$) between phase I and phase II samplings, whereas temperature, salinity, *PRO* abundance and SiO_4^{4-} showed insignificant variations (Table 4.3).

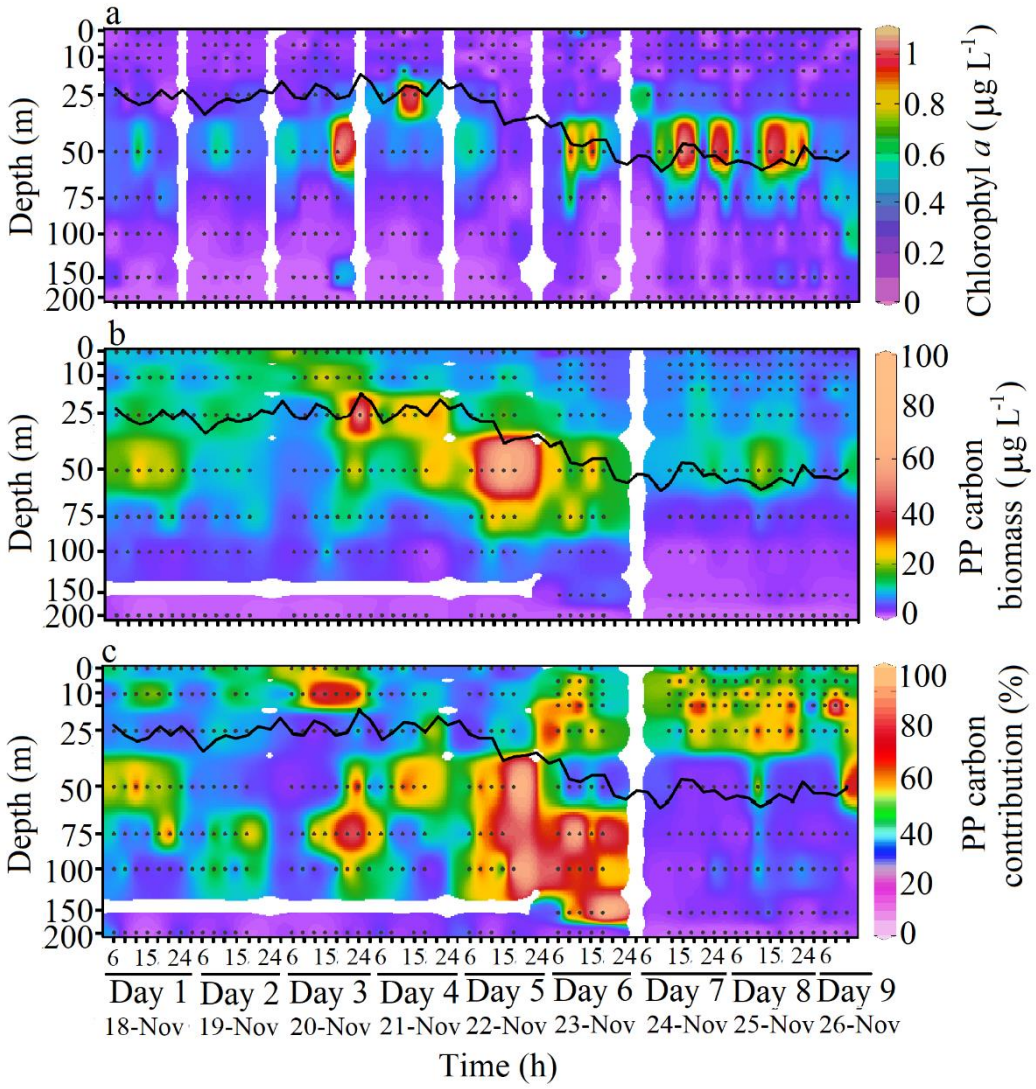

Fig.4.7 Vertical profiles of temporal variation in (a) chlorophyll *a*, (b) PP carbon, and (c) PP carbon contribution (%) to the total phytoplankton carbon biomass over the continental slope of the eastern Arabian Sea. Black line indicates mixed layer depth.

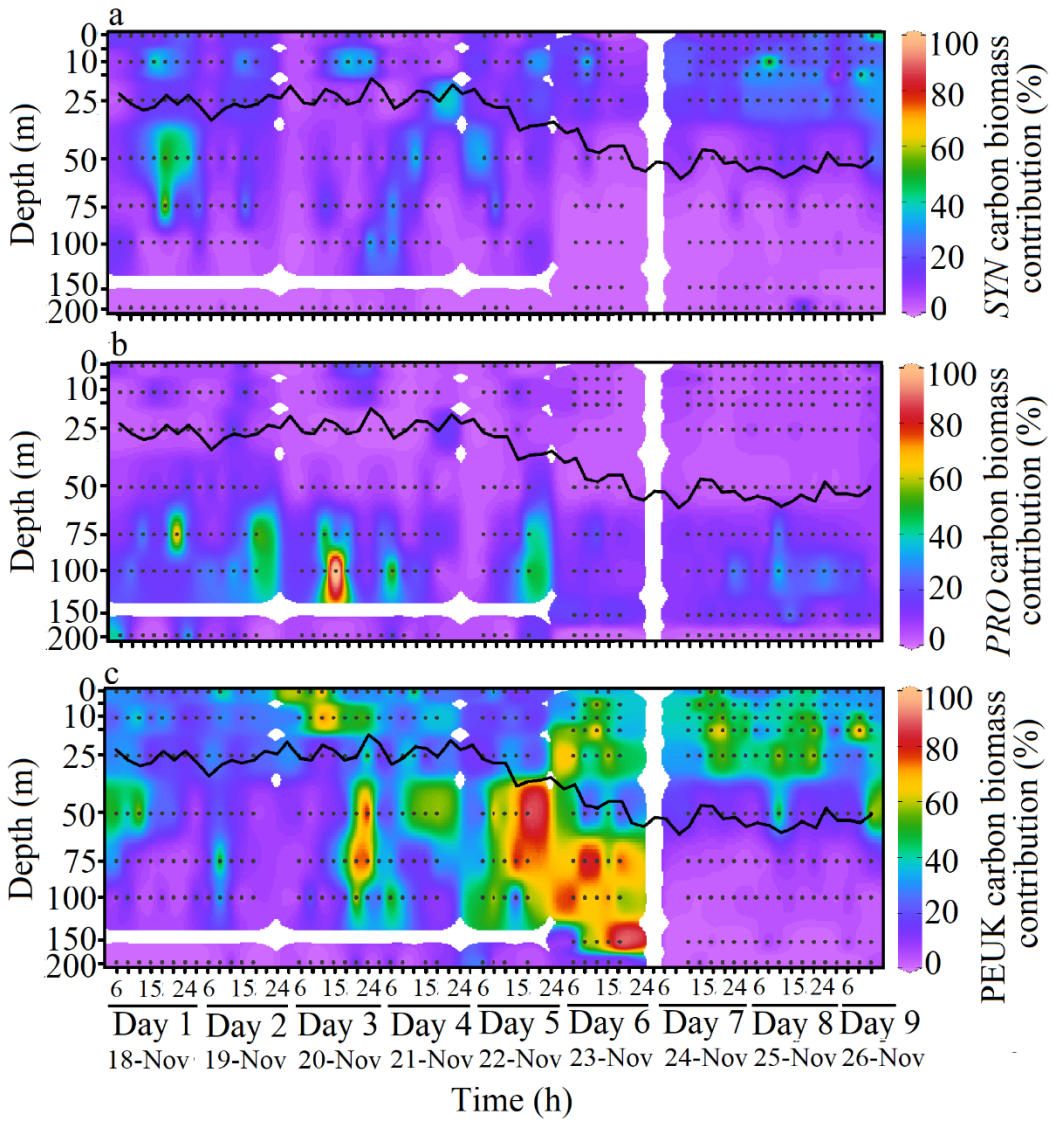

Fig. 4.8 Vertical profiles of temporal variation in (a) *SYN*, (b) *PRO* and (c) PEUK carbon contribution to the total PP carbon biomass over the continental slope of the eastern Arabian Sea. Black line indicates mixed layer depth.

In the ML, variability of *SYN* abundance was partially explained by the positive correlation with temperature and NO_3^- during phase I (R^2 = 0.17, P < 0.05) and PO_4^{3-} during phase II (R^2 = 0.12, p < 0.05) (Fig. 4.9a and b). The variation of PEUK abundance was partially explained by negative correlation with temperature, and positive correlation with PO_4^{3-} and NO_3^- during phase I (R^2 = 0.33, p < 0.05) and positive correlation with NH_4^+, salinity, and temperature during phase II (R^2 = 0.28, p < 0.05). *PRO* abundance variation was partially explained by the positive correlation with temperature and NO_2^- during phase I (R^2 = 0.23, p < 0.05) and negative correlation with NH_4^+ and positive correlation with PO_4^{3-} during phase II (R^2 = 0.12, p < 0.05). The variability of PP carbon biomass was largely explained by positive correlation with *SYN*, PEUK, temperature and nutrient concentrations (NH_4^+, PO_4^{3-}, NO_2^- and NO_3^-) during phase I (R^2 = 0.93, p < 0.05) and positive correlation with PEUK, *PRO*, PO_4^{3-}, and NO_3^-; and negative correlation with NH_4^+ and temperature during phase II (R^2 = 0.83, p < 0.05). The variation in phytoplankton carbon biomass was largely explained by positive correlation with PP carbon biomass and PO_4^{3-} and negative correlation with salinity, SiO_4^{4-} and NO_2^- during phase I (R^2 = 0.67, p < 0.05) and positive correlation with PP carbon biomass and salinity during phase II (R^2 = 0.73, p < 0.05) (Fig. 4.9a, and b).

At 50 m depth, variation in *SYN* abundance was largely explained by the positive correlation with temperature (R^2 = 0.32, p < 0.05), at 75 m, partially explained by the negative correlation with NH_4^+ (R^2 = 0.16, p < 0.05) and at 100 m depth, largely explained by the positive correlation with salinity, NO_2^- and NO_3^- and negative correlation with temperature and PO_4^{3-}, (R^2 = 0.47, p < 0.05; Fig. 4.9c-e). The variation in PEUK abundance at 50 m depth was largely explained by the positive correlation with NH_4^+, SiO_4^{4-}, and PO_4^{3-}, and negative correlation with NO_3^- (R^2 =

0.51, $p < 0.05$), at 75 m by the positive correlation with salinity and negative correlation with temperature and PO_4^{3-} ($R^2 = 0.33$, $p < 0.05$) and 100 m depth, partially by the positive correlation with NO_3^- ($R^2 = 0.14$, $p < 0.05$). The variation in *PRO* abundance was largely explained by the positive correlation with temperature and NH_4^+ at 50 m depth ($R^2 = 0.53$, $p < 0.05$), whereas at 75 m by the positive correlation with temperature ($R^2 = 0.13$, $p < 0.05$). At 50 m, variation in PP carbon biomass was largely explained by the positive correlation with PEUK, NO_3^- and NH_4^+ and negative correlation with SiO_4^{4-} ($R^2 = 0.73$, $p < 0.05$), at 75 m, largely explained by the negative correlation with salinity and positive correlation with PEUK abundance and temperature ($R^2 = 0.65$, $p < 0.05$) and at 100 m, largely explained by the positive correlation with PEUK abundance ($R^2 = 0.41$, $p < 0.05$). At 50 m, the positive correlation with PP carbon biomass largely explained the variation in phytoplankton carbon biomass ($R^2 = 0.42$, $p < 0.05$), at 75 m, largely explained by the positive correlation with PP carbon biomass and negative correlation with NO_3^- ($R^2 = 0.43$, $p < 0.05$) and at 100 m depth, largely explained by the positive correlation with salinity and PP carbon biomass ($R^2 = 0.40$, $p < 0.001$).

On D5, variability of *SYN* abundance was largely explained by the positive correlation with temperature, PO_4^{3-} and NO_3^- in ML ($R^2 = 0.82$, $p < 0.05$; Fig. 4.9f), whereas below ML by the positive influence of salinity, temperature and NO_3^- and negative correlation with PO_4^{3-} ($R^2 = 0.96$, $p < 0.05$; Fig. 4.9g). The variation in PEUK abundance was largely explained by the positive correlation with temperature, NH_4^+, PO_4^{3-}, and NO_3^- and negative correlation with NO_2^- in ML ($R^2 = 0.88$, $p < 0.05$); whereas below ML by the positive correlation with temperature, NH_4^+, SiO_4^{4-}, and PO_4^{3-} and negative correlation with salinity, NO_2^-, and NO_3^- ($R^2 = 1.00$, $p < 0.05$).

Table 4.3 PERMANOVA analysis of environmental variables, PP groups, total phytoplankton carbon biomass, PP carbon biomass, and PP carbon contribution to the total phytoplankton carbon biomass between phase I and phase II samplings in surface waters (0 m), mixed layer (ML) and below mixed layer. Bold text denotes significant variation between the two phases.

	Surface waters					MLD					Below MLD				
Source	df	SS	MS	Pseudo-F	*P*	df	SS	MS	Pseudo-F	*P*	df	SS	MS	Pseudo-F	*P*
Temperature	1	112.6	112.6	3.09	**0.00**	1	93.6	93.6	11.5	**0.01**	1	294.1	294.1	2.7	0.09
Salinity	1	91.3	91.3	1.17	0.38	1	14.3	14.3	0.8	0.36	1	0.3	0.3	1.5	0.23
DO	1	337.1	337.1	1.64	**0.00**	1	78.4	78.4	1.4	0.36	1	11965.0	11965.0	5.3	**0.01**
NO_3^-	1	3734.4	3734.4	2.13	0.09	1	13175.0	13175.0	8.8	**0.01**	1	5385.5	5385.5	5.7	**0.01**
NO_2^-	1	1132.9	1132.9	1.05	0.32	1	8364.6	8364.6	7.5	**0.01**	1	12118.0	12118.0	10.6	**0.01**
PO_4^{3-}	1	799.8	799.8	9.91	**0.00**	1	4564.1	4564.1	40.0	**0.01**	1	7061.2	7061.2	19.0	**0.01**
NH_4^+	1	729.2	729.2	1.09	0.30	1	4110.1	4110.1	6.8	**0.01**	1	11460.0	11460.0	15.9	**0.01**
SiO_4^{4-}	1	3313.8	3313.8	4.84	**0.00**	1	2867.8	2867.8	4.1	**0.04**	1	775.3	775.3	0.8	0.45
Chl *a*	1	1224.0	1224.0	6.4	**0.01**	1	3499.6	3499.6	6.2	**0.01**	1	8887.5	8887.5	7.6	**0.01**
SYN	1	59.3	59.3	3.08	0.09	1	5026.9	5026.9	5.4	**0.01**	1	29312.0	29312.0	12.3	**0.01**
PEUK	1	113.7	113.7	13.01	**0.00**	1	3886.3	3886.3	6.0	**0.01**	1	16992.0	16992.0	6.2	**0.01**
PRO	1	170.2	170.2	8.24	**0.01**	1	23308.0	23308.0	27.4	**0.01**	1	2315.9	2315.9	1.2	0.28
Phytoplankton carbon	1	1549.5	1549.5	78.9	**0.00**	1	5029.7	5029.7	25.4	**0.01**	1	4256.2	4256.2	15.8	**0.01**
PP carbon	1	2490.3	2490.3	28.2	**0.00**	1	7797.3	7797.3	7.8	**0.01**	1	22374.0	22374.0	16.3	**0.01**
PP contribution (%)	1	55.5	55.5	1.6	0.23	1	115.1	115.1	0.45	0.64	1	4167.7	4167.7	12.1	**0.01**

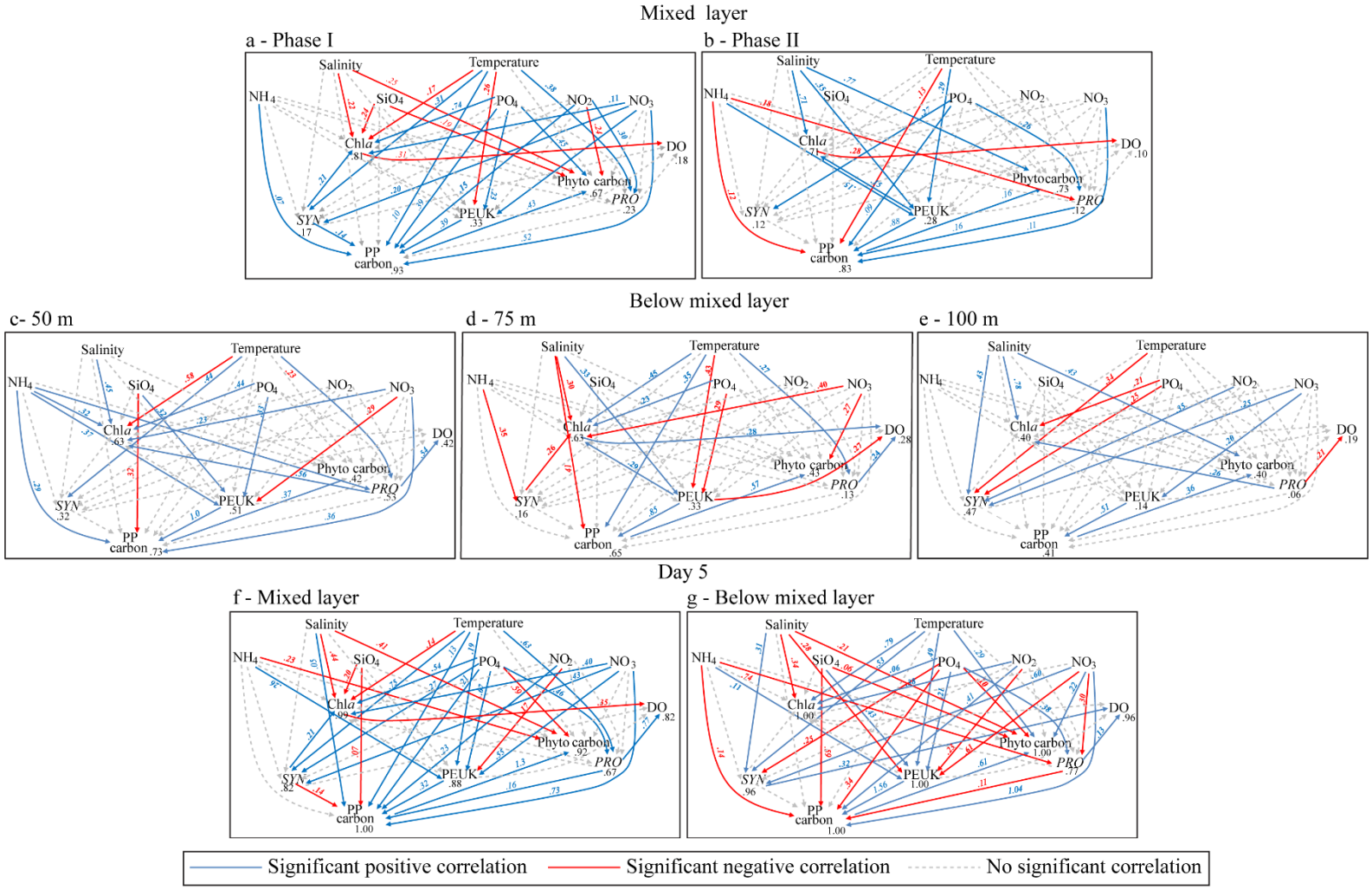

Fig. 4.9 Path diagrams showing the relationships between the environmental variables and PP groups, total phytoplankton carbon biomass, PP carbon biomass, and chl *a* within the mixed layer of (a) phase I, (b) phase II, below mixed layer at (c) 50 m, (d) 75 m, (e) 100 m, and on day 5 (f) within mixed layer, and (g) below mixed layer. Bold values are the coefficient of determination of the linear regression (R^2) and colored values are the regression coefficients for the specific standardized independent variables.

The variation in *PRO* abundance in the ML was largely explained by the positive correlation with PO_4^{3-} and temperature (R^2 = 0.67, $p < 0.05$) whereas below ML, by the positive correlation with PO_4^{3-}, and negative correlation with NO_3^- and NH_4^+ (R^2 = 0.77, $p < 0.05$). The variability of PP carbon biomass was largely explained by the positive correlation with salinity, temperature, PO_4^{3-}, NO_2^-, NO_3^-, PEUK and *PRO* and negative correlation with *SYN* and SiO_4^{4-} in the ML (R^2 = 1.00, $p < 0.05$) whereas below ML by a positive correlation with NO_2^-, NO_3^-, and PEUK and negative correlation with NH_4^+, SiO_4^{4-}, PO_4^{3-} and *PRO* (R^2 = 1.00, $p < 0.05$). The variation in phytoplankton carbon biomass (R^2 = 0.92, $p < 0.05$) was largely explained by the positive correlation with PP carbon biomass and negative correlation with salinity, PO_4^{3-} and NH_4^+ in the ML, whereas below ML, by the positive correlation with PP carbon biomass, temperature and NO_3^- and negative correlation with salinity, SiO_4^{4-} and PO_4^{3-} (R^2 = 1.00, $p < 0.05$).

4.4 Discussion

4.4.1 Variations in picophytoplankton community structure

Clear spatial variation was observed in the distribution of PP groups along the cross-shelf region, with higher abundance of *SYN* in the coastal waters and *PRO* in the slope waters. Although *SYN* is abundant at high concentrations of nitrogenous nutrients, their nurient requirement is lesser compared to eukaryotic PP (Olson et al., 1990; Campbell and Vaulot, 1993; Campbell et al., 1998; Jiao et al., 2005). In contrast, *PRO* cells are better adapted to high temperature, low nutrient and stratified water column (Campbell et al., 1998; Liu et al., 1998; Zubkov et al., 1998; Agawin et al., 2000; Jiao et al., 2005) which is characteristic of the offshore waters. At S3, located at the edge of the continental shelf (continental shelf break) and referred to as a zone of interaction between offshore and coastal waters, the PP community structure

was unique with the dominance of PEUK. From the literature, it is evident that nutrient concentrations are relatively higher in this part of the eastern AS (Naqvi et al., 2000; 2010). However, the increased PEUK abundance was not accompanied by a simultaneous increase in chl *a* biomass in the ML. On the contrary, higher chl *a* biomass below ML (50 m) where PEUK were low suggests that in the ML, total chl *a* was contributed by PP whereas below ML, larger phytoplankton dominated. The non-response of chl *a* in the ML could be either due to a lag in the response of larger phytoplankton to increased nutrient concentrations (Finkel et al., 2009) or grazing pressure by heterotrophic nanoflagellates (Landry et al., 1998).

The high resolution study at a fixed station (S6) was thus carried out in order to better understand the evolution of PP community dynamics in such regions on shorter time scales. There is a scarcity of information on the short-term variability in PP (Jacquet et al., 2002), especially in the AS where monsoonal winds influence the hydrography. During this study, the dynamic hydrography was well reflected in the PP community structure. The ML depth evolved from shallow to deep with relatively lower salinity surface waters (34) during phase I as compared with phase II (37). This could be attributed to the advection of low saline coastal waters leading to a shallower (25 m) mixed layer (Shankar et al. 2005). The resultant oligotrophic conditions during phase I favored *PRO* and *SYN* growth within the mixed layer (Anderson et al., 2008; Dongen-Vogels et al., 2012), with *PRO* as the dominant group. In the north western AS and Alboran Sea, *SYN* and PEUK dominated the mesotrophic conditions whereas oligotrophic conditions were dominated by *PRO* (Campbell et al., 1998; Jacquet et al., 2002). Generally, in surface waters, *PRO* cells are better adapted to high temperature, low nutrient and stratified water column (Campbell et al., 1998; Liu et al., 1998; Zubkov et al., 1998; Agawin et al., 2000; Jiao et al., 2005). This is also supported by

path analysis where *PRO* positively correlated with temperature but showed an insignificant relation with NO_3^- and PO_4^{3-} within the mixed layer. The degree of mixing in euphotic layer of the water column was also associated with differences in temperature of around 30°C in the mixed layer compared with 25°C at 50-75 m. Hence, the temperature of each layer could have influenced the *PRO* populations in the euphotic layer. Below the mixed layer, the positive correlation of *PRO* with the prevailing temperature at 50 m and 75 m suggests the influence of this parameter on its vertical distribution. Different ecotypes of *PRO* such as high light (HL) and low light (LL) adapted have been reported in the oceanic waters (Partensky et al., 1993; Moore and Chisholm, 1999). Depending on their ability to adapt to different light optima for growth, HL ecotype dominates in the surface waters and LL ecotype in the deeper waters (Partensky et al., 1999). Similar observations have been reported from the NEAS (Roy and Anil, 2015). As the euphotic depth in the present study area ranged between 60 and 70 m, vertical distribution of light could have played an important role in the distribution of HL and LL adapted *PRO* strains.

SYN, the next abundant group during phase I, which correlated positively with the prevailing temperature within the mixed layer (30°C) and at 50 m (25°C) suggests a temperature maxima regulating its vertical distribution in the water column. In the deeper waters (75 to 100 m), its minimal abundance in spite of the high nutrient concentrations could be due to lowered growth rates. Since *SYN* is a mesotrophic form, its vertically decreasing trend shows that temperature and irradiance effect overrides the nutrient needs to optimize growth (Mouriño-Carballido et al., 2016). Another loss factor resulting in its lower abundance could be the high grazing pressure exerted by the small heterotrophic nanoflagellates (Reckermann and Veldhuis, 1997). The vertical distribution of the least abundant group, PEUK, were

generally controlled by the nutrients as seen from the positive correlation. PEUK are the main carbon source for the microzooplankton (Reckermann and Veldhuis, 1997). However, the role of grazers as the controller of PEUK in the open oceans is unclear (Hirose et al., 2008). PEUK mortality losses (50 to 100%) due to viral lysis was also reported with rates ranging from 0.1 to 0.8 d^{-1} (Baudoux et al., 2007).

With the initiation of vertical mixing during the transition phase (D5) at the end of phase I, increased abundance of the PP groups within the mixed layer, with *SYN* dominating the community, suggests a positive influence of increased nutrient concentrations. This was supported by the positive correlation with the prevailing temperature, NO_3^- and PO_4^{3-}. Below the ML, the highest PEUK abundance at the subsurface chl *a* maxima where *SYN* and *PRO* exhibited relatively lower numbers, coincided with increased nutrient concentrations. This was supported by the positive correlation of PEUK with nutrients (SiO_4^{4-}, PO_4^{3-}, and NH_4^+). During this period, PEUK cell abundance peaked earlier than that of *PRO* and *SYN*, implying cell division, which could be mainly driven by variations in nutrient concentrations. This also suggests that during pulses of nutrient inputs, PEUK are the fastest to respond amongst the PP groups, followed by *PRO*. Amongst the larger phytoplankton, diatoms respond to pulsed nutrient inputs (Ornolfsdottir et al., 2004). Some diatom species such as *Chaetoceros throndsenii* which attain a minimum size of 1.5 µm have also been observed in the PP community (Vaulot et al., 2008). Not et al. (2008) also reported the presence of Ocean picoplanktonic diatom in Indian Ocean. *Minutocellus* species, strains RCC703 which belongs to Bacillariophyceae was isolated from Indian ocean (Giovagnetti et al., 2012). Samanta and Bhadury (2014) have reported picoplanktonic diatom signature in the northern Bay of Bengal. However, till date, there is no published data suggesting that pico-diatoms are an important fraction of

the PP in the present study area. The positive correlation of PEUK with SiO_4^{4-} implies representation by some smaller diatoms that are quick in responding to nutrient pulses due to their greater capacity for assimilation of nutrients at high concentrations (Agawin et al., 2000; Jiao et al., 2005; Paulsen et al., 2015). The present study area was located above the continental slope, and usually, at the continental shelf break and slope, formation of internal tides and nonlinear waves (Smith and Sandstrom, 1988; Shenoi and Antony, 1991; Shankar et al., 2005), cause churning of water column (Wolanski and Pickard, 1983; Kurapov et al., 2010) that results in nutrient influx from the sediment to the upper water column yielding high productivity (Sharples et al., 2001). In the shelf edge of north east Atlantic Ocean complete dominance of PEUK was observed due to the supply of NO_3^- from bottom waters, whereas *SYN* and *PRO* were dominant in the NO_3^- depleted continental shelf region (Sharples et al., 2009). Dongen-Vogels et al. (2011) observed that the mixing process decreases the light irradiance and increases the nutrient input which led to a proliferation of eukaryotes and decline of prokaryotes. The PEUK abundance was the highest recorded for the entire study period and also coincided with the higher chl *a* biomass below the ML. Their contribution to the total phytoplankton biomass (26 to 70%) implies that PEUK were the major contributors. Sharples et al. (2009) reported a higher rate of primary production in the shelf edge, which can support higher trophic levels including fishes, thereby serving as a potential fishery zone. The short life span of PEUK abundance peak could be attributed to the grazing by heterotrophic nanoflagellates whose growth response is as quick as the PP (Eccleston-Parry and Leadbeater, 1994; Landry et al., 1998) leading to a succession of the phytoplankton community by diatoms. However, lack of such a response from PEUK during spatial sampling at S4 (station close to S6), although *SYN* and *PRO* were abundant above

ML, implies an effect of deepening ML, similar to phase II. The high resolution vertical sampling strategy allowed us to capture such refined transient observations *in situ* which are essential for further understanding of the microbial loop functioning in such dynamic ecosystems.

The vertical mixing of water column during phase II caused deepening of the mixed layer leading to a uniform distribution of PP within the ML, with significantly lower PP abundance and biomass compared to phase I. On the other hand, phytoplankton biomass did not vary much during this period. This suggests that during vertical mixing, increased nutrient concentration favored larger phytoplankton. However, the prevalence of lower numbers of PP for a longer period of time (4 days) suggests lowered growth rates due to certain unfavorable environmental perturbation due to deepening of ML. In addition to the physical factors, the observed diel patterns in *SYN*, *PRO* and PEUK abundance could be attributed to biological factors such as cell division (Mitbavkar and Saino, 2015), cell death and loss factors such as grazing, viral infection and parasitism (Crumpton and Wetzel, 1982; Banse, 1994; Vaulot and Marie, 1999; Behrenfeld, 2010). The biological processes are in turn driven by nutrient or irradiance availability. The dephased abundance peaks for the three PP groups during the day time could be attributed to the cell division and the decreasing cell abundance during the night to higher grazing pressure (Reckermann and Veldhuis, 1997; Partensky et al., 1999; Gauns et al., 2005). As the cells divide their reduced size makes them more vulnerable to predation (Tsai et al., 2005).

4.4.2 Picophytoplankton carbon biomass

The appropriate selection of the C:Chl *a* ratios and carbon cell conversion factors for PP from that reported in literature is a challenging task as they are known to vary with growth conditions (Booth et al., 1993; Buck et al., 1996; Taylor et al., 1997). As

such, the values determined in the open ocean are more realistic than in cultures. Taking into consideration the contrasting conditions under which the sampling was conducted, the closest match was found in Garrison et al. (2000) and Shalapyonok et al. (2001). This study was carried out in the AS during NEM wherein carbon cell^{-1} for both *PRO* and *SYN* varied significantly between cells from within and below ML, which was in the range observed in our study (< 50 m). For the C:Chl *a* ratios in ML, we used the upper (for phase I) and lower (for phase II) limits of the average value (112 ± 29; Shalapyonok et al., 2001). For below ML, we used a factor (52) suggested by Brown et al. (1999) and Garrison et al. (2000) for the AS when the ML was > 50 m. The relative contribution of the PP carbon to total phytoplankton carbon biomass (up to 70%) obtained by this approach was consistent with the previous studies carried out in the AS during NEM (Shalapyonok et al., 2001). Using lower factors led to over estimation of the carbon values. Thus, these biomass assessments can be considered reliable and useful for further PP studies in these waters.

The PP carbon biomass contribution to total carbon biomass increases in these waters when stratified conditions prevail. On the other hand, the vertical mixing and the associated deepening of the surface layer lead to a decrease of PP carbon biomass indicating that increasing mixed layer depth is less supportive for PP growth (Lindell and Post, 1995). This tendency suggests that mixing of the water column contributes to the maintenance of large cells such as diatoms in the water column, since diatoms are otherwise subjected to high sinking losses, as observed earlier in the AS (Campbell et al., 1998). These variations were driven by the gradual increase in nutrient concentration due to vertical mixing, from phase I to II as was evident from the positive correlation of chl *a* and phytoplankton carbon biomass with nutrients. Higher abundance of *SYN* and PEUK coincided with the maximum chl *a* peak

signifying that the total phytoplankton biomass was largely contributed by PP. This is also evident from a significant positive relation between total phytoplankton carbon biomass and PP carbon biomass. The major component of PP carbon biomass was PEUK (35 - 90%) even though their abundance was low. This is mainly due to their larger size compared to *PRO* and *SYN* (Buitenhuis et al., 2012). Through this study it is evident that transient bursts in PP abundance can be captured *via* high resolution sampling which can be missed during the spatial observations depending on the sampling time. The short duration of these abundance peaks suggest incorporation of this biomass into higher trophic levels. Future high resolution studies at different regions in the continental margin encompassing the other components of the food web will help in validating and better elucidating the PP responses under varying environmental conditions.

Chapter 5

Influence of salinity on the picophytoplankton groups through laboratory experiments

5.1 Introduction

Salinity is one of the important environmental factor influencing aquatic biota, especially in the estuarine habitat. It is known to affect the physiological functions, size, growth rate and survival of organisms (Gardner and Thompson, 2001; Westerbom et al., 2002). In the estuarine environment, the salinity of the water constantly changes, mainly due to salt water intrusion by tidal activity and dilution by freshwater runoff. In the monsoon-influenced estuaries, monsoon is an additional factor for salinity variations. Such frequent changes in salinity have a considerable effect on the organism inhabiting this area thus affecting the species diversity and trophodynamics (Short and Neckles, 1999; Li et al., 2010). To survive and grow in such conditions, organisms must be able to respond quickly to drastic changes in salinity.

Phytoplankton, the base of the aquatic food chain, are key primary producers (Nixon, 1986) and are known to respond quickly to the environmental changes (Paerl et al., 2007). The phytoplankton abundance and community structure are known to exhibit diel variation in response to tidal activity (Litaker et al., 1993) and also over tidal phases (Zhou et al., 2016). Previous studies have shown higher phytoplankton abundance and diversity during neap tides when lower salinity and higher nutrients were observed compared to the spring phase (Domingues et al., 2010; Zhou et al., 2016), which suggests that salinity plays a significant role in these variations. Nutrients are also required for the growth of phytoplankton, and under nutrient limiting conditions the phytoplankton growth is severely affected (Yin et al., 2000; Patil and Anil, 2011). Till date, most of the studies in the estuarine waters focuses on the larger phytoplankton, excluding the picophytoplankton (PP) size class. In recent years, the studies on PP are increasing in coastal and estuarine regions which

highlight their importance in these environments (Murell and Lores, 2004; Gaulke et al., 2010; Qiu et al., 2010; Contant and Pick, 2013).

The studies have shown that in coastal and estuarine regions phycoerythrin rich *Synechococcus* (*SYN*-PE) is recognized as higher salinity species whereas phycocyanin rich *Synechococcus* (*SYN*-PC) as lower salinity (Murell and Lores, 2004). Picoeukaryotes (PEUK) also shows higher abundance in the low saline waters (Mitbavkar et al., 2015). Tidal water movement can result in their distribution across the estuary. Thus, it was hypothesis that the presence of these species throughout the estuary albeit at lower numbers in non-native salinities could be a result of changes in their cellular growth. In order to assess the changes in cellular properties such as growth, size and pigment fluorescence, *SYN*-PC and PEUK from the low and *SYN*-PE from high salinities were isolated; and their growth pattern was observed under different salinities.

5.2 Materials and methods

Field observation showed that the salinity was the major influencing factor for PP groups distribution in the estuarine region. Thus, *SYN*-PE, *SYN*-PC and PEUK strains were isolated from Zuari estuary. Further they were grown under different salinity conditions to assess their growth pattern.

5.2.1 Culture isolation

SYN-PE was isolated from higher salinity (S1; salinity ~31; 15° 25' 16.9" N, 73° 47' 36.9" E), whereas *SYN*-PC and PEUK were isolated from low salinities (S5; salinity ~15; 15° 25' 32.0" N, 73° 47' 50.2" E). Strains were initially sorted through FACS ARIA flow cytometer and then subjected to repeated spread and streak plate method on agar plate (1.5%) containing f/2 medium (Guillard and Ryther, 1962) for further purification. The purified strains were isolated and maintained in f/2 media

having native salinity at ~28°C under constant illumination of ~150 µmol m^{-2} s^{-1} provided by white light fluorescent tubes with a light: dark cycle of 12:12 h.

5.2.2 Identification of picophytoplankton strains

Genomic DNA was extracted from exponentially growing cells (*SYN*-PE, *SYN*-PC, and PEUK) using a purelink DNA mini kit (Invitrogen) following the manufacturer's instructions. Initially, for cell lysis, cells were treated in bead beater by suspending the cells in lysis buffer which was provided with the kit. In PCR amplification, 16S rRNA sequences were amplified using specific cyanobacterial primers CYA359Fc (5'-GGGGAATYTTCCGCAATGGG-3') and CYA781R (3'-GACTACTGGGGTATCTAATC CCATT-5') for *SYN* (Nubel et al., 1997) and PEUK strains. To determine the approximate phylogenetic affiliation, the sequenced 16S rRNA gene was subjected to a BLASTn search at the National Center for Biotechnology Information (Altschul et al., 1997). ClustalW (Thompson et al., 1994) and neighbour-joining (Saitou and Nei, 1987) method were used to align the sequences and construct an unrooted phylogenetic tree, respectively with MEGA version 7 (Tamura et al., 2011). Branches corresponding to partitions reproduced in less than 50% bootstrap replicates are collapsed. The evolutionary distances were computed using the Maximum Composite Likelihood method and are in the units of the number of base substitutions per site. The bootstrap analysis with 500 replications was used to estimate the topology of the phylogenetic trees (Felsenstein, 1985).

5.2.3 Experimental design

The three cultures (in triplicate) were maintained separately in 700 mL of f/2 media (SiO_4^{4-} omitted) with salinities of 0, 5, 10, 15, 20, 25, 30, 35 and 40. Dilutions were prepared from 0.22 µm filtered, autoclaved aged natural freshwater and

seawater. Flasks were inoculated initially with 5×10^4 cells mL^{-1} from the exponentially growing cultures, maintained at 28°C under constant illumination at ~150 µmol m^{-2} s^{-1} provided by white light fluorescent tubes with light: dark cycle of 12:12 h. To minimize the salinity variation due to evaporation, experimental flask mouth was tightly covered with aluminum foil and swirled twice a day. Transfer of media, cultures, and sampling were done under the laminar flow to minimize contamination. Samples were collected every alternate day for analysis of cell abundance (preserved in 0.2 % paraformaldehyde), nutrients (NO_3^- and PO_4^{3-}) and chl *a*. Chl *a* concentration was measured at an interval of 4 days.

5.2.4 Nutrient analyses

The nutrient (NO_3^- and PO_4^{3-}) concentrations were analyzed through SKALAR SANplus auto-analyzer. Before analysis, samples were filtered through 0.45 µm pore size cellulose paper.

5.2.5 Chlorophyll a analysis

A known amount of sample was filtered through a Whatman GF/F filter and filter paper was immediately placed in a dark vial containing 90% acetone for extraction. The details of chl *a* analysis is explained in chapter 2A, section 2A.2.2.

5.2.6 Flow cytometric analysis

The details of sample analysis through FACS Aria flow cytometer (FCM) are given in chapter 2A, section 2A.2.3. Samples were vortexed well before analysis to reduce the clumps. Yellow green latex beads of 2 µm (polysciences co., USA) were added to the sample as internal standards to calculate the relative size (forward angle light scatter (FALS) and right angle light scatter (RALS)) and pigment fluorescence properties [red fluorescence from chl (> 650 nm) and phycocyanin (630 nm) and orange fluorescence from phycoerythrin (564-606 nm)] of all three species in

different salinities. FALS and RALS signals measure the size and granularity of the cells, respectively. Therefore, it is a good sizing parameter for studies on cell size (Phinney and Cucci, 1989) and in recent years many phytoplankton studies have adopted this method (Read et al., 2014; McFarland et al., 2015).

5.2.7 Statistical analyses

Two-way analysis of variance (ANOVA) was used to assess the significant variation in growth under different salinities and experimental days. The level of significance considered was $p \leq 0.05$. Before analyses, the data was checked for normality and homogeneity of variances. Pearson correlation was implemented to find the relation between FALS, RALS, chl, PE, PC fluorescence intensities and growth rates for the entire data and individual salinity treatments. All the statistical analyses were performed using SPSS 22 software.

5.3 Results

5.3.1 Identification of picophytoplankton strains

The cell shape of *SYN*-PE strain isolated from the high saline waters appeared round with size approximately 1.8 µm in diameter (Fig. 5.1a). Cells were found to be non-motile with bright orange fluorescence of PE (Fig. 5.1b). The 16S rRNA gene sequence obtained from this strain was found to be closely related to genus *SYN*. Neighbour-joining phylogenetic analysis based on 16S rRNA gene sequences revealed that this strain formed a phylogenetic lineage with *SYN* sp. RS9901 (AY172811) and uncultured cyanobacterium clone MWLSC91 (bootstrap value 55; Fig. 5.1c) with sequence similarities of 98%.

Cells of the low saline *SYN*-PC strain, appeared coccoid shaped with size approximately 1.5 µm (Fig. 5.2a). Cells were found to be non-motile with bright red fluorescence of PC (Fig. 5.2b). The 16S rRNA gene sequence obtained from this

strain was found to be closely related to genus *SYN*. Neighbour-joining phylogenetic analysis based on 16S rRNA gene sequences revealed that this strain formed a phylogenetic lineage with *SYN* UBR (AF448063) and uncultured cyanobacterium clone MWLSC91 (bootstrap value 100; Fig. 5.2c) with sequence similarities of 99%.

Cells of the PEUK strain appeared oval shaped with size approximately 2.5 µm (Fig. 5.3a). Cells were found to be non-motile with bright red fluorescence of chl (Fig. 5.3b). The 16S rRNA gene sequence obtained from this strain was found to be closely related to division Chlorophyta. Neighbour-joining phylogenetic analysis based on 16S rRNA gene sequences revealed that this strain formed a phylogenetic lineage with *Choricystis parasitica* (bootstrap value 57; Fig. 5.3c) with sequence similarities of 98%. However, this percentage sequence similarity is below the threshold considered necessary for species delineation (Stackebrandt and Goebel, 1994). Further studies are required to confirm this species.

5.3.2 Influence of salinity on picophytoplankton strains

5.3.2.1 Synechococcus-PE

The high saline *SYN*-PE strain showed a lag phase of 2 days in all the salinity treatments (Fig. 5.4a). The abundance was significantly highest at salinity 30 and lowest at salinity 15 and 10 ($p < 0.05$). On day 2, maximum abundance was found in native salinity 30 ($1.62 \pm 0.12 \times 10^5$ cells mL^{-1}) followed by 35 ($1.20 \pm 0.05 \times 10^5$ cells mL^{-1}), 25 ($1.08 \pm 0.25 \times 10^5$ cells mL^{-1}), 20 ($1.04 \pm 0.14 \times 10^5$ cells mL^{-1}), 40 ($0.97 \pm 0.20 \times 10^5$ cells mL^{-1}), 15 ($0.95 \pm 0.06 \times 10^5$ cells mL^{-1}) and 10 ($0.74 \pm 0.08 \times 10^5$ cells mL^{-1}). This strain did not grow in salinities < 5. This trend was also reflected in the growth rate of this species with significantly ($p < 0.05$) higher growth rate at salinity 30 (0.49 ± 0.04 d^{-1}), followed by 35 (0.43 ± 0.02 d^{-1}), 20 (0.45 ± 0.07 d^{-1}), 25 (0.29 ± 0.11 d^{-1}), 15 (0.34 ± 0.04 d^{-1}), 10 (0.18 ± 0.04 d^{-1}), and 40 (0.33 ± 0.11 d^{-1};

Fig. 5.5a). The exponential phase duration was similar in salinities 25 to 40 (12 days). In salinity 20, exponential phase duration was shorter (till day 8) and in salinity 15, exponential phase duration was longer (till day 14). At salinity 10, exponential phase continued till the end of experiment. The abundance was significantly highest at salinity 40 and lowest at salinity 20 ($p < 0.05$). Maximum abundance was observed at

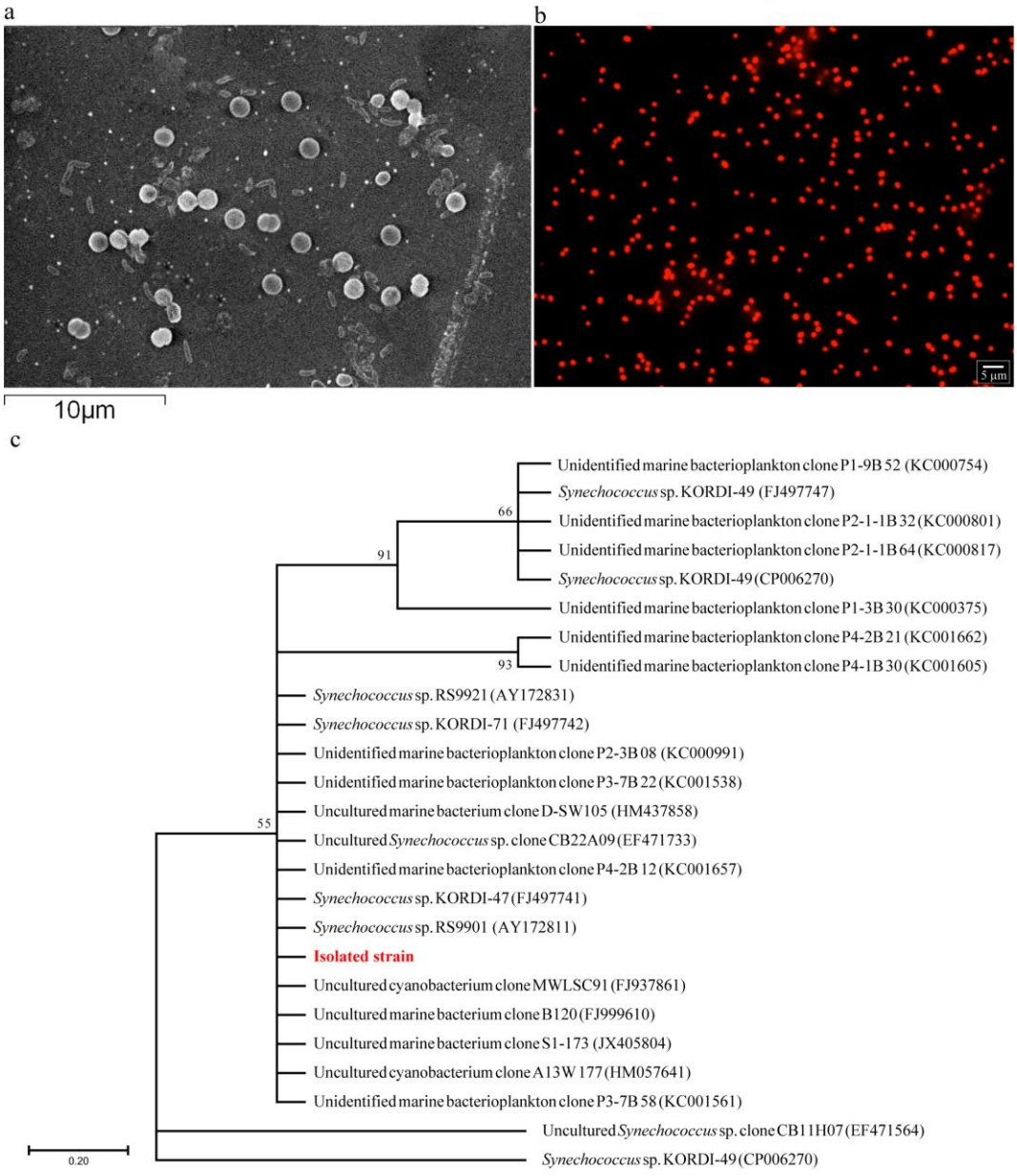

Fig. 5.1 *SYN*-PE strain, (a) scanning electronic microscope image (b) epifluorescence microscope image and (c) Neighbour-joining tree showing the phylogenetic relationship of isolated *SYN*-PE strain and phylogenetically related species based on 16S rRNA gene sequences.

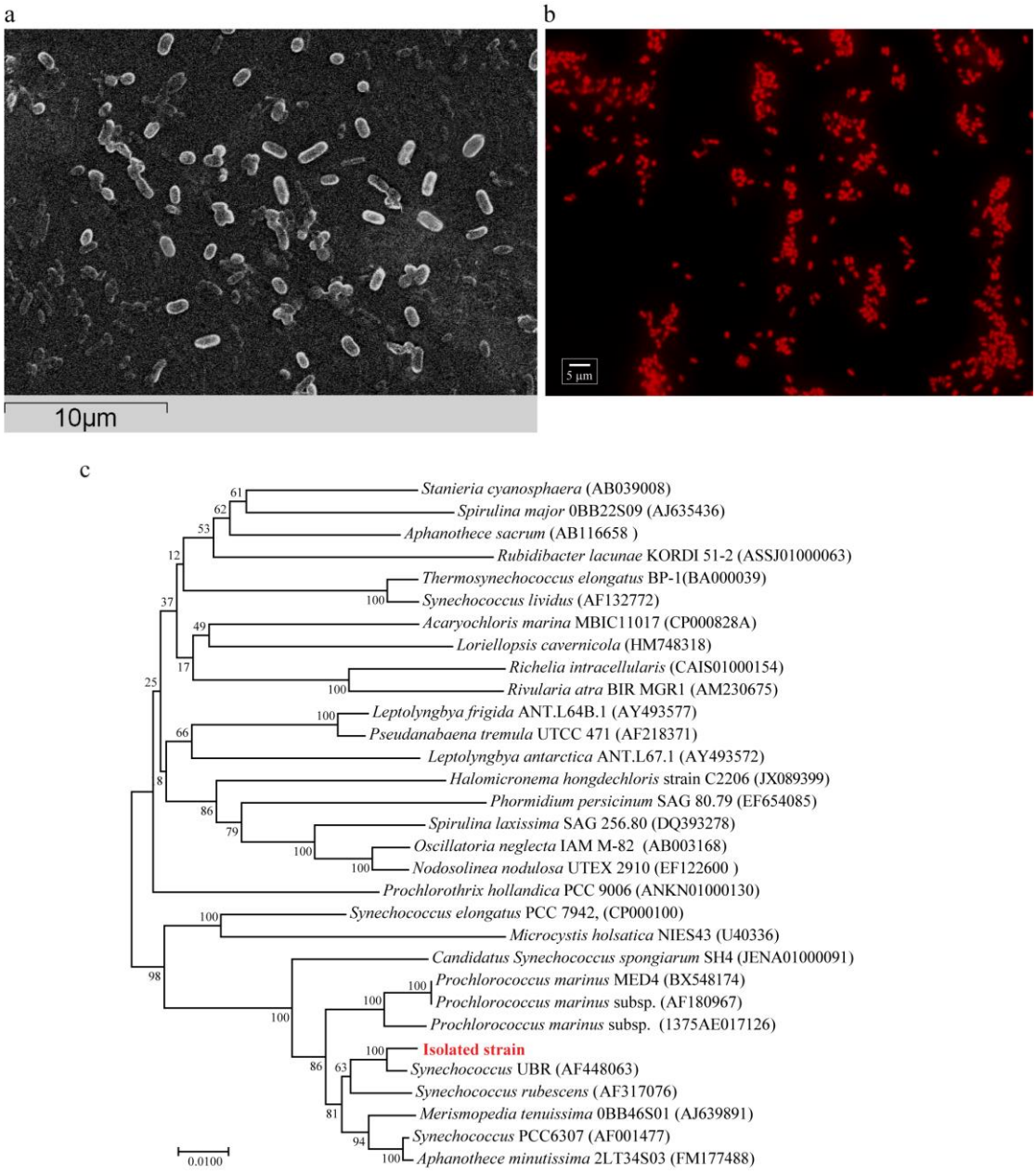

Fig. 5.2 *SYN*-PC strain, (a) scanning electronic microscope image (b) epifluorescence microscope image and (c) Neighbour-joining tree showing the phylogenetic relationship of isolated *SYN*-PC strain and phylogenetically related species based on 16S rRNA gene sequences.

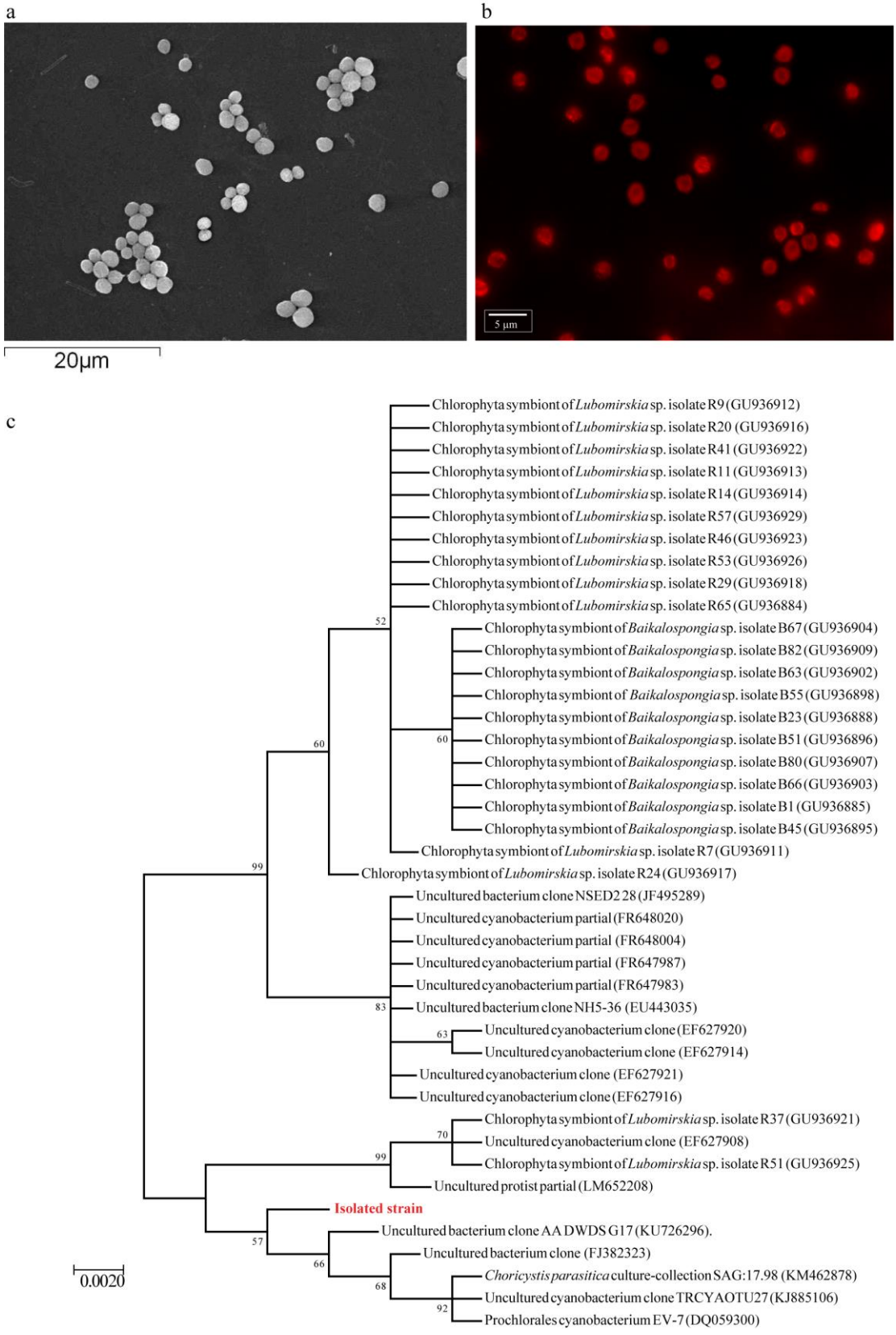

Fig. 5.3 PEUK strain, (a) scanning electronic microscope image (b) epifluorescence microscope image and (c) Neighbour-joining tree showing the phylogenetic relationship of isolated PEUK strain and phylogenetically related species based on 16S rRNA gene sequences.

salinity 40 (552.66 ± 16.48 × 10^5 cells mL^{-1}) followed by 30 (481.12 ± 46.88 × 10^5 cells mL^{-1}), 35 (410.67 ± 66.63 × 10^5 cells mL^{-1}), 25 (315.46 ± 41.46 × 10^5 cells mL^{-1}), 15 (322.36 ± 6.22 × 10^5 cells mL^{-1}), and 20 (265.82 ± 80.94 × 10^5 cells mL^{-1}). During exponential phase, significantly ($p < 0.05$) highest growth rates were observed at salinity 20 (0.64 ± 0.01 d^{-1}), followed by 40 (0.49 ± 0.01 d^{-1}), 35 (0.43 ± 0.02 d^{-1}), 30 (0.43 ± 0.01 d^{-1}), 25 (0.43 ± 0.01 d^{-1}), 15 (0.35 ± 0.01 d^{-1}) and 10 (0.13 ± 0.02 d^{-1}). In stationary phase, there was no significant variation in the cell abundance and growth rate ($p > 0.05$). However, highest abundance was observed at native salinity 30 (306.29 ± 38.92 × 10^5 cells mL^{-1}) followed by 35 (261.06 ± 53.23 × 10^5 cells mL^{-1}), 40 (246.23 ± 43.27 × 10^5 cells mL^{-1}), 25 (215.18 ± 40.88 × 10^5 cells mL^{-1}), 20 (116.99 ± 51.26 × 10^5 cells mL^{-1}), and 15 (171.40 ± 25.44 × 10^5 cells mL^{-1}). In the stationary phase, growth rate was relatively higher at 30 compared to other salinity treatments.

During lag phase salinity stress was reflected in increasing cell size (FALS) and granularity (RALS) with decreasing salinity along with a corresponding increase in the fluorescence properties (chl $cell^{-1}$ and PE $cell^{-1}$ derived from FCM) (Fig. 5.6a-d). Higher growth rates resulted in smaller cell size (lower FALS) and less granularity (lower RALS) in all the salinities. Chl $cell^{-1}$ remained unchanged between lag and exponential phase, whereas PE $cell^{-1}$ fluorescence values increased in the exponential phase at salinities 20 to 40. During the stationary period, cell size (FALS) and granularity (RALS) increased along with an increase in PE $cell^{-1}$ and chl $cell^{-1}$ fluorescence.

Regression analysis showed a positive correlation between FCM derived chl $cell^{-1}$ and fluorometrically derived chl *a* $cell^{-1}$ (Table 5.2). *SYN*-PE chl *a* $cell^{-1}$ varied (0.6 to 3.70 fg $cell^{-1}$) with salinity and growth phases (Fig. 5.7a). *SYN*-PE chl *a* $cell^{-1}$ initially

ranged between 2.29 and 3.70 fg cell^{-1} which decreased with decreasing salinity treatment on day 4 which was the beginning of exponential phase. Lowest chl *a* cell^{-1} was observed at salinity 35 and 40. On day 8, not much difference in the chl *a* cell^{-1} at salinity 25 to 35 was observed when compared to day 4 whereas at < 20, chl *a* cell^{-1} decreased and at salinity 40 it increased. Chl *a* cell^{-1} increased in all the treatments on day 12 and day 16, which was the stationary phase. The growth rate of *SYN*-PE was negatively correlated ($p < 0.05$) with cell size (FALS), granularity (RALS), chl cell^{-1} and PE fluorescence values. FALS and RALS values showed a significant ($p < 0.05$) positive relation with chl cell^{-1} and PE cell^{-1} fluorescence (Table 5.2). NO_3^- (initial 1008 ± 77 µM and final 114 ± 76 µM) and PO_4^{3-} (initial 39.05 ± 0.33 µM and final 8.01 ± 1.16 µM) were utilized efficiently by *SYN*-PE at salinities > 25 (Fig. 5.8a and b).

5.3.2.2 Synechococcus-PC

The low saline *SYN*-PC strain showed a lag phase of 2 days in all the salinity treatments except salinity 40 where it lasted till day 6 (Fig. 5.4b). During the lag phase, the abundance was significantly highest at salinity 15 and lowest at salinity 40 ($p < 0.05$). The maximum abundance was found in native salinity 15 (0.75 ± 0.02 × 10^5 cells mL^{-1}) followed by 10 (0.63 ± 0.23 × 10^5 cells mL^{-1}), 5 (0.56 ± 0.10 × 10^5 cells mL^{-1}), 20 (0.36 ± 0.16 × 10^5 cells mL^{-1}), 30 (0.34 ± 0.08 × 10^5 cells mL^{-1}), 25 (0.33 ± 0.12 × 10^5 cells mL^{-1}), 0 (0.29 ± 0.04 × 10^5 cells mL^{-1}), 35 (0.29 ± 0.03 × 10^5 cells mL^{-1}), and 40 (0.26 ± 0.12 × 10^5 cells mL^{-1}). This trend was also reflected in growth rate of this species with significantly ($p < 0.05$) higher growth rate at salinity 15 (0.42 ± 0.01 d^{-1}) followed by 10 (0.27 ± 0.19 d^{-1}), 5 (0.26 ± 0.08 d^{-1}), 20 (0.14 ± 0.13 d^{-1}), 30 (0.04 ± 0.13 d^{-1}), 25 (-0.04 ± 0.03 d^{-1}), 0 (-0.11 ± 0.08 d^{-1}), 35 (-0.01 ± 0.03 d^{-1}), and 40 (-0.01 ± 0.01 d^{-1}; Fig. 5.5b). In salinity 0 and 5 exponential phase

continued till the end of experiment. At salinity 10 and 20 exponential phase duration was shorter (day 8) and at salinities 15, 25 and 30 exponential phase duration was till day 12. At salinity 35 and 40 exponential phase duration was till day 14 and day 16, respectively. There was no significant variation in the cell abundance with respect to salinity ($p > 0.05$). However, maximum abundance was observed at salinity 5 ($1257.25 \pm 69.54 \times 10^5$ cells mL^{-1}) followed by 30 ($763.40 \pm 114.25 \times 10^5$ cells mL^{-1}), 35 ($684.01 \pm 314.85 \times 10^5$ cells mL^{-1}), 15 ($641.54 \pm 129.02 \times 10^5$ cells mL^{-1}), 25 ($461.19 \pm 142.98 \times 10^5$ cells mL^{-1}), 10 ($413.04 \pm 135.54 \times 10^5$ cells mL^{-1}), 20 ($400.60 \pm 143.40 \times 10^5$ cells mL^{-1}), 0 ($319.52 \pm 5.31 \times 10^5$ cells mL^{-1}) and 40 ($229.40 \pm 145.37 \times 10^5$ cells mL^{-1}). During exponential phase, significantly ($p < 0.05$) highest growth rates were observed at salinity 20 (1.14 ± 0.01 d^{-1}), 15 (1.09 ± 0.01 d^{-1}) and 10 (1.08 ± 0.08 d^{-1}), followed by 25 (0.72 ± 0.05 d^{-1}), 30 (0.67 ± 0.13 d^{-1}), 35 (0.64 ± 0.03 d^{-1}), 40 (0.62 ± 0.02 d^{-1}), 5 (0.30 ± 0.01 d^{-1}) and 0 (0.27 ± 0.01 d^{-1}). In stationary phase, there was no significant variation in the cell abundance with respect to salinity ($p > 0.05$). However, highest abundance was observed at native salinity 15 ($348.37 \pm 134.09 \times 10^5$ cells mL^{-1}) followed by 30 ($336.06 \pm 165.91 \times 10^5$ cells mL^{-1}), 25 ($300.02 \pm 104.42 \times 10^5$ cells mL^{-1}), 10 ($281.98 \pm 97.24 \times 10^5$ cells mL^{-1}), 20 ($94.96 \pm 59.60 \times 10^5$ cells mL^{-1}), 40 ($151.85 \pm 39.74 \times 10^5$ cells mL^{-1}) and 35 ($88.01 \pm 38.93 \times 10^5$ cells mL^{-1}). At stationary phase growth rates were up to 0.32 d^{-1} among the salinity treatments.

During the lag phase, the cell size (FALS) increased with increasing salinity treatments whereas granularity (RALS) did not vary much (Fig. 5.6e-h). Similar to *SYN*-PE, *SYN*-PC showed higher growth rates in exponential phase resulting in smaller cell size (FALS) and lower granularity (RALS) but the variations were smaller compared to that in the *SYN*-PE. Chl $cell^{-1}$ and PC $cell^{-1}$ did not show much

variation in lag and exponential phase except at high salinity (> 20?) where its value increased during the exponential phase. During stationary phase and also with increasing salinity, FALS, RALS, PC and chl cell^{-1} values increased.

Chl *a* cell^{-1} varied between the salinity and days. Initially, chl *a* cell^{-1} was 1.1 ± 0.07 fg cell^{-1} which increased on day 4 in most of the salinity treatments (Fig. 5.7b). Further it increased on day 8 in the salinity 0, 10, 15, 20, and 40. Chl *a* cell^{-1} decreased on day 12 in all the salinity treatments (except 25 and 30). On day 16, chl *a* cell^{-1} increased in all the salinity treatments (except salinity 10). *SYN*-PC growth rate was ($p < 0.05$) negatively related to FALS, RALS, and chl cell^{-1} values for the entire data and in different salinity treatments except salinity 40, 5 and 0 (Table 5.2). FALS and RALS values showed significant ($p < 0.05$ or 0.01) positive relation with chl cell^{-1} and PC cell^{-1} in most of the salinity treatments (Table 5.2). NO_3^- (initial 974 ± 30 µM and final 369 ± 191 µM) and PO_4^{3-} (initial 36 ± 2 µM and final 17 ± 1.9 µM) were utilized efficiently by *SYN*-PC at salinities < 25 (Fig. 5.8c-d). However, the nutrients were not exhausted (except in salinity 5) in the culture media as observed for *SYN*-PE and PEUK.

5.3.2.3 Picoeukaryotes

The growth pattern PEUK was different compared to both *SYN* strains (Fig. 5.4c). PEUK strain grew well in lower salinities and could not tolerate higher salinity (35 and 40) stress. The growth curve of this strain exhibited a lag phase for 2 days in salinities 20, 25 and 30. During this phase, there was no significant variation in the cell abundance with respect to salinity. The maximum abundance and growth rates were observed in salinities 20 (0.90 ± 0.13 × 10^5 cells mL^{-1}, 0.30 ± 0.07 d^{-1}), 25 (0.77 ± 0.13 × 10^5 cells mL^{-1}, 0.23 ± 0.08 d^{-1}) and 30 (0.60 ± 0.11 × 10^5 cells mL^{-1}, 0.12 ± 0.07 d^{-1}) (Fig. 5.4c and Fig. 5.5c). Compared to *SYN* strains, longer exponential phase

(till day 30) was observed in the PEUK strain in salinities 0, 5, 10, 15, 25, and 30. At salinity 20, exponential phase lasted for 32 days. The abundance was significantly higher at salinities 5 (534.73 ± 13.75 × 10^5 cells mL^{-1}) and 10 (560.21 ± 40.50 × 10^5 cells mL^{-1}) and lowest at salinity 25 (103.38 ± 6.14 × 10^5 cells mL^{-1}) and 30 (94.26 ± 3.70 × 10^5 cells mL^{-1}) ($p < 0.05$). This trend was also reflected in the growth rates of this strain with significantly ($p < 0.05$) higher growth rates at 10 (0.24 ± 0.01 d^{-1}), 5 (0.23 ± 0.001 d^{-1}), 15 (0.23 ± 0.01 d^{-1}), 20 (0.22 ± 0.001 d^{-1}), 0 (0.22 ± 0.01 d^{-1}), 25 (0.18 ± 0.01 d^{-1}) and 30 (0.18 ± 0.01 d^{-1}). In the stationary phase, the abundance was significantly higher in salinities 5 and 10 and lower at salinities 25 and 30 ($p < 0.05$). Highest abundance was observed in native salinities 10 (504.34 ± 11.90 × 10^5 cells mL^{-1}), 5 (520.70 ± 12.18 × 10^5 cells mL^{-1}) and 15 (404.71 ± 3.17 × 10^5 cells mL^{-1}) followed by 20 (388.53 ± 5.91 × 10^5 cells mL^{-1}), 0 (291.71 ± 6.08 × 10^5 cells mL^{-1}), 25 (89.79 ± 10.47 × 10^5 cells mL^{-1}), and 30 (92.85 ± 5.35 × 10^5 cells mL^{-1}). Overall, PEUK strain showed similar growth rates at salinities 35 and 40 ($p > 0.05$) with lower abundance and were significantly different from other salinities ($p < 0.05$).

In the PEUK strain, cell size (FALS), granularity (RALS) and chl $cell^{-1}$ values were higher than that of the *SYN* strains. In the lag phase, cell size, granularity and chl $cell^{-1}$ were higher in salinity 30 than in salinity 20 (Fig. 5.6i-k). In the exponential phase, cell size showed an increasing trend from salinity 0 to salinity 30. Granularity and chl $cell^{-1}$ values were similar at salinities 0, 5 and 10 and it increased from salinity 15 to 30. In the stationary phase, the cell size and granularity values did not differ much from exponential phase. Cell size showed an increasing trend from salinity 0 to salinity 30 and granularity values from 15 to 30 salinities. Chl $cell^{-1}$ showed an increasing trend in salinity 0 to 30 during the stationary phase and was comparatively higher than that in the exponential phase.

Chl *a* cell^{-1} varied between the salinities and days. Initially, chl *a* cell^{-1} was 6.78 ± 0.36 fg cell^{-1} which increased on day 4 in all the salinity treatments and further increased on day 8 (Fig. 5.7c). During this period, chl cell^{-1} values were similar at salinity 0, 5 and 10 and it increased from salinity 15 to 30. Chl *a* cell^{-1} decreased on day 12 and further decreased on day 16, but values were similar at salinity 0, 5 and 10 and it increased from salinity 15 to 30. In the stationary phase (day 32), chl *a* cell^{-1} increased with increasing salinity treatment (except at salinity 30). PEUK growth rate showed significant ($p < 0.05$) negative relation with FALS, RALS and chl cell^{-1} values for the entire data whereas in different salinity treatments it showed significant ($p < 0.05$) positive relationship with FALS, RALS, and chl cell^{-1} values. FALS and RALS values showed significant ($p < 0.05$ or 0.01) positive relation with chl cell^{-1} in all the salinity treatments (Table 5.2). NO_3^- (initial 976.3 ± 9.6 µM and final 11.1 ± 4.3 µM) and PO_4^{3-} (initial 40.3±1.76 µM and final 0.2 ± 0.01 µM) were utilized faster at salinity 5 and 10 (Fig. 5.8e and f).

Table 5.1 Two-way analysis of variance (ANOVA) to assess the significant variation in growth of *SYN*-PE, *SYN*-PC and PEUK under different salinities and days. The level of significance considered was $p \leq 0.05$.

Variables	SS	df	MS	f	*p*
SYN-PE					
Salinity	11.2	6	1.86	11.0	**0.01**
Days	140.4	18	7.80	380.8	**0.01**
Salinity x days	8.9	108	0.08	4.0	**0.01**
Error	5.2	252	0.02		
SYN-PC					
Salinity	41.7	8	5.21	46.5	**0.01**
Days	393.4	13	30.26	1049.3	**0.01**
Salinity x days	42.3	104	0.41	14.1	**0.01**
Error	6.7	234	0.03		
PEUK					
Salinity	1223.4	8	152.9	932.1	**0.01**
Days	91.8	18	5.1	406.0	**0.01**
Salinity x days	374.5	144	2.6	207.0	**0.01**
Error	4.1	324	0.0		

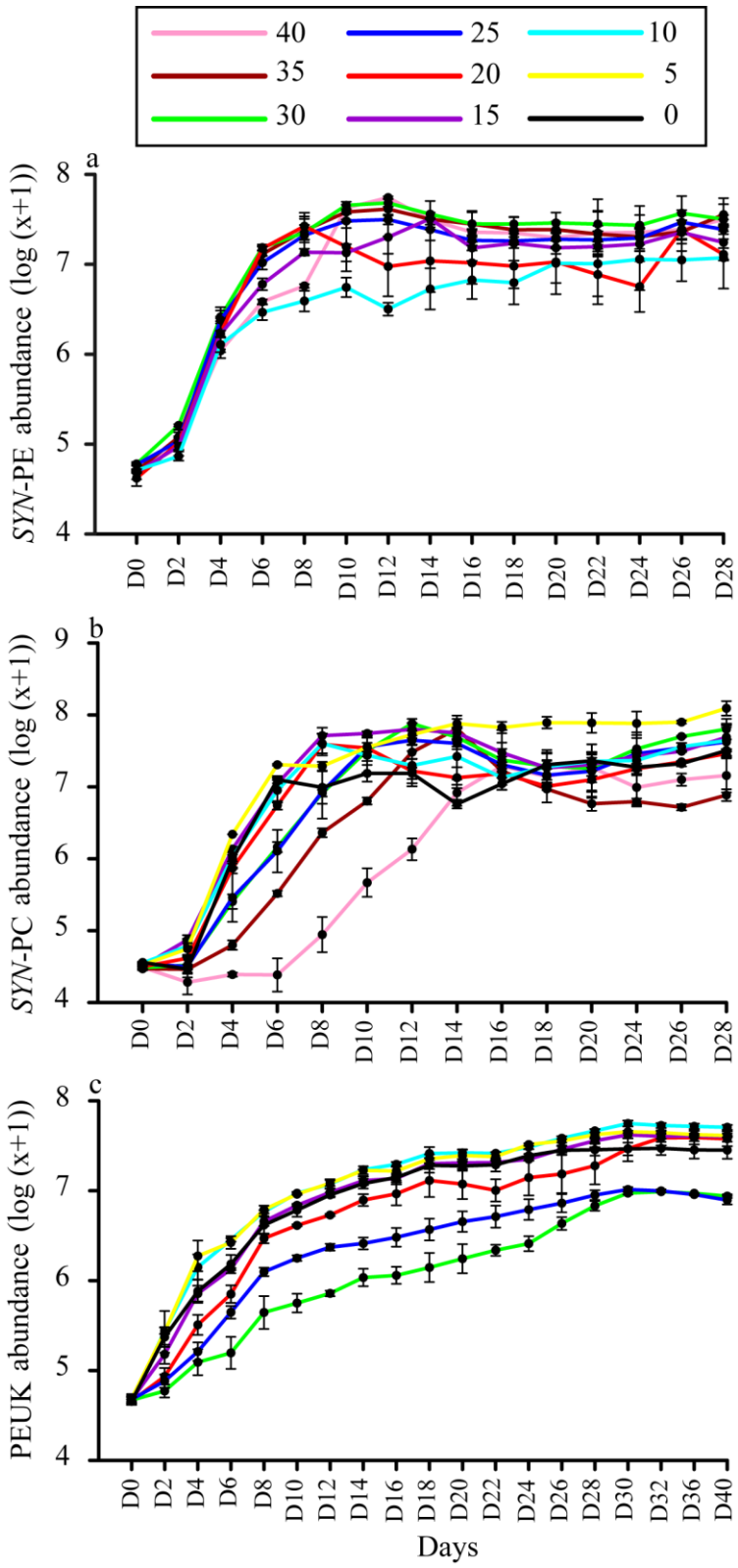

Fig. 5.4 Growth curve of the isolated strains (a) *SYN*-PE, (b) *SYN*-PC and (c) PEUK. Abundance expressed in log (x+1).

Table 5.2 Pearson correlation between FALS, RALS, chl, PE, PC fluorescence and growth rate for the entire data and individual salinity treatments for *SYN*-PE, *SYN*-PC and PEUK. *p*-values *< 0.05 and **< 0.01 are statistically significant and are highlighted in bold.

	Growth rate				FALS			RALS	
Salinity	FALS	RALS	Chl	PE	RALS	Chl	PE	Chl	PE
SYN-PE									
Entire data	**-0.282****	**-0.216****	**-0.272****	**-0.281****	**0.919****	**0.220****	**0.271****	**0.126****	**0.191****
40	**-0.472****	**-0.398****	**-0.482****	**-0.335***	**0.683****	**0.441****	**0.299***	**0.465****	**0.342****
35	**-0.267***	-0.191	**-0.427****	**-0.414****	**0.719****	**0.683****	**0.634****	**0.476****	**0.394****
30	**-0.387****	-0.221	**-0.389****	**-0.336***	**0.747****	**0.687****	**0.638****	**0.592****	**0.501****
25	-0.246	-0.162	**-0.392****	**-0.284***	**0.643****	**0.643****	**0.625****	**0.496****	**0.375****
20	**-0.325***	-0.201	**-0.426****	**-0.392****	**0.726****	**0.604****	**0.523****	**0.588****	**0.363****
15	**-0.277***	-0.162	**-0.422****	**-0.441****	**0.724****	**0.433****	0.054	**0.338***	0.003
10	0.006	0.02	0.195	-0.065	**0.859****	**0.336***	0.172	**0.340****	0.158
5	**-0.299***	-0.294	-0.059	-0.092	**0.943****	0.213	**0.261***	**0.321***	**0.341****
0									
SYN-PC				PC			PC		PC
Entire data	**-0.354****	**-0.372****	**-0.213****	0.010	**0.921****	**0.656****	**0.436****	**0.526****	**0.288****
40	-0.230	**-0.319***	0.030	0.090	**0.965****	**0.691****	**0.496****	**0.600****	**0.365***
35	**-0.499****	**-0.495****	**-0.529****	-0.260	**0.981****	**0.829****	**0.628****	**0.818****	**0.600****
30	**-0.578****	**-0.595****	**-0.520****	-0.230	**0.971****	**0.745****	**0.477****	**0.666****	**0.412****
25	**-0.447****	**-0.452****	-0.210	0.110	**0.995****	**0.586****	**0.323***	**0.608****	**0.338***
20	**-0.532****	**-0.520****	**-0.405****	-0.160	**0.981****	**0.786****	**0.529****	**0.774****	**0.523****
15	**-0.514****	**-0.453****	0.240	**0.305***	**0.910****	0.140	-0.020	**0.308***	0.160
10	**-0.581****	**-0.481****	-0.100	0.060	**0.961****	**0.399****	0.225	**0.494****	**0.338***
5	-0.220	-0.22	0.020	0.220	**0.992****	**-0.385***	**-0.616****	**-0.411****	**-0.626****
0	-0.280	-0.30	-0.180	0.290	**0.963****	**-0.363***	**-0.410****	**-0.346***	**-0.428****
PEUK									
Entire data	**-0.283****	**-0.160****	**-0.119***		**0.872****	**0.742****		**0.732****	
40	-0.067	-0.153	0.072		**0.750****	**0.510****		**0.537****	
35	-0.266	-0.117	-0.146		**0.730****	**0.737****		**0.516****	
30	**0.332***	**0.383****	**0.416****		**0.896****	**0.809****		**0.796****	
25	**0.631****	**0.678****	**0.278***		**0.891****	**0.819****		**0.697****	
20	**0.605****	**0.599****	**0.322***		**0.859****	**0.689****		**0.821****	
15	**0.430****	**0.564****	**0.463****		**0.906****	**0.770****		**0.918****	
10	0.256	**0.602****	**0.286***		**0.816****	**0.726****		**0.851****	
5	**0.554****	**0.597****	**0.400****		**0.928****	**0.930****		**0.885****	
0	0.178	**0.586****	**0.367****		**0.686****	**0.804****		**0.896****	

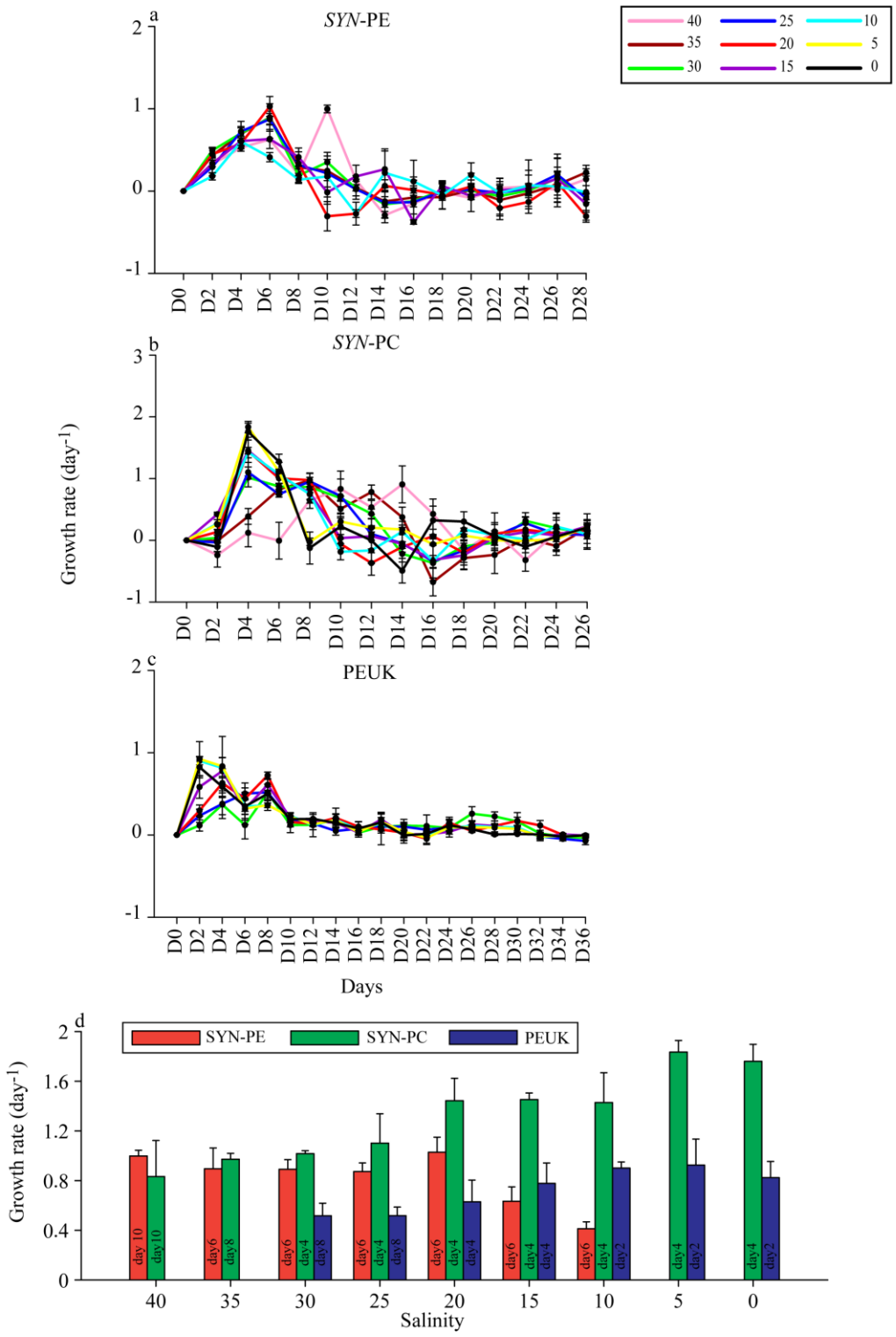

Fig. 5.5 Growth rate of the isolated strains (a) *SYN*-PE, (b) *SYN*-PC and (c) PEUK; and (d) Maximum growth attained by the isolated strains in different salinities.

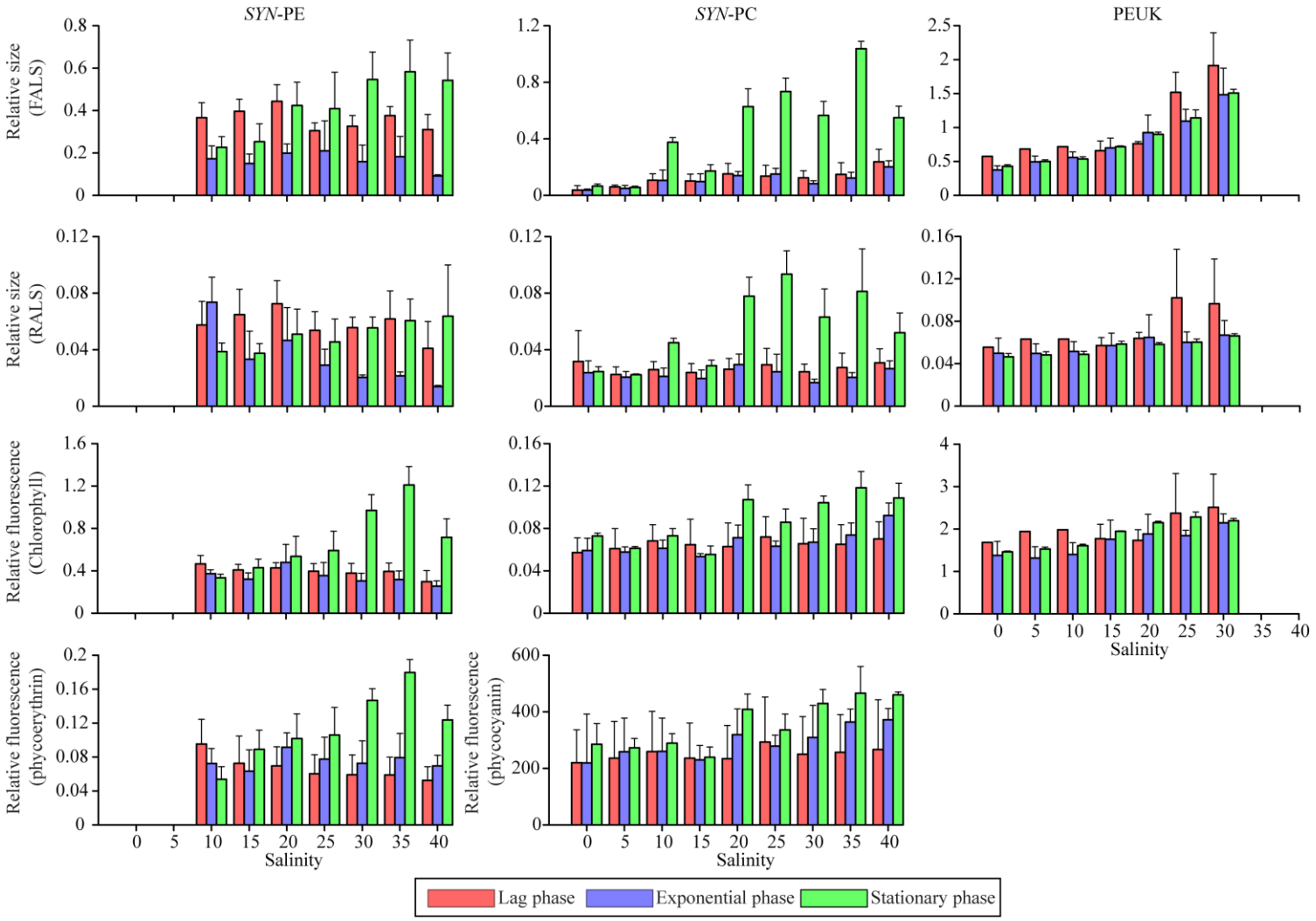

Fig. 5.6 Variation in relative size and fluorescence properties during lag, exponential and stationary phase for (a-d) *SYN*-PE, (e-h) *SYN*-PC and (i-k) PEUK.

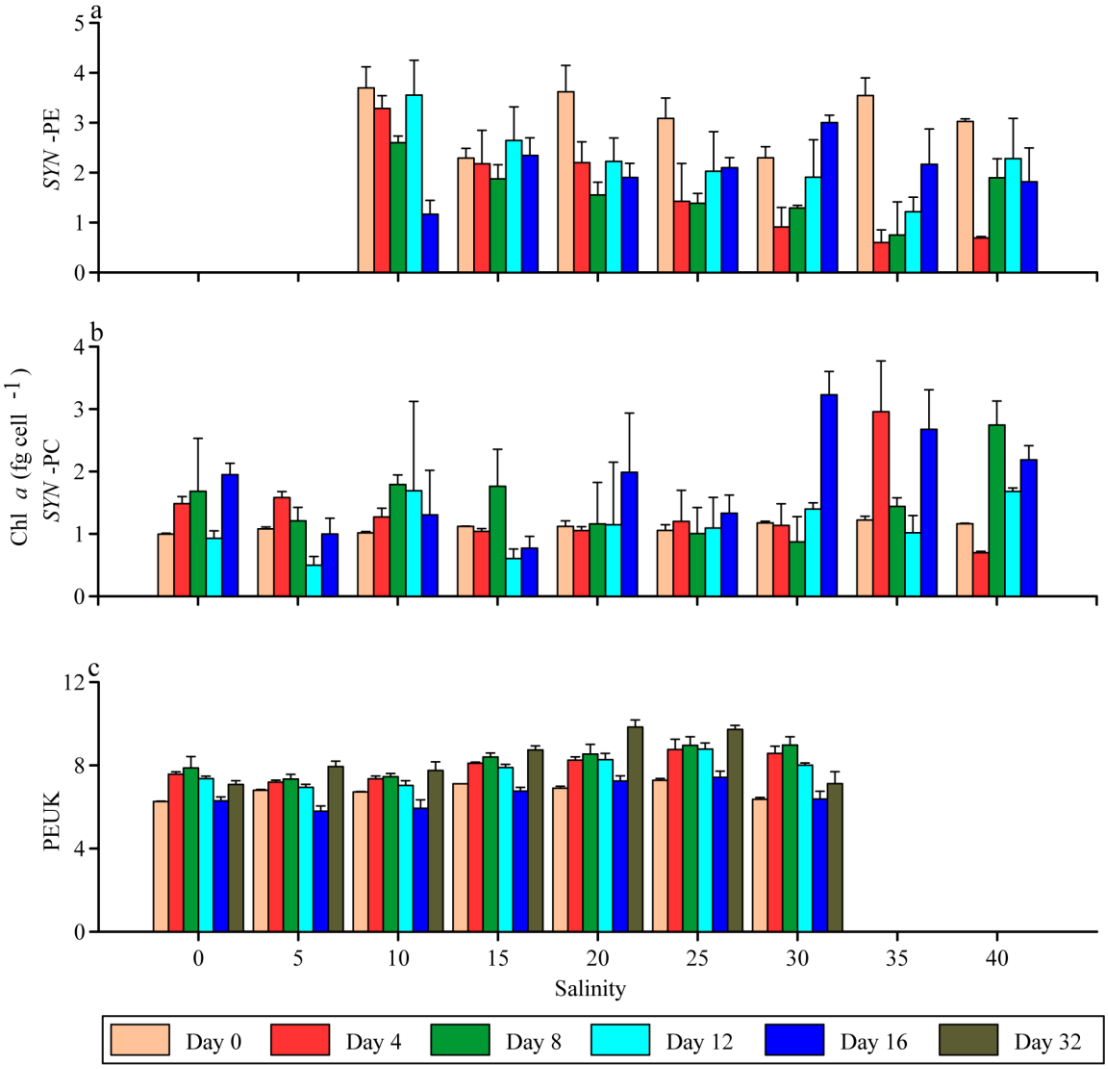

Fig. 5.7 Chl *a* cell^{-1} of the isolated strains (a) *SYN*-PE, (b) *SYN*-PC and (c) PEUK in different salinities with interval of 4 days.

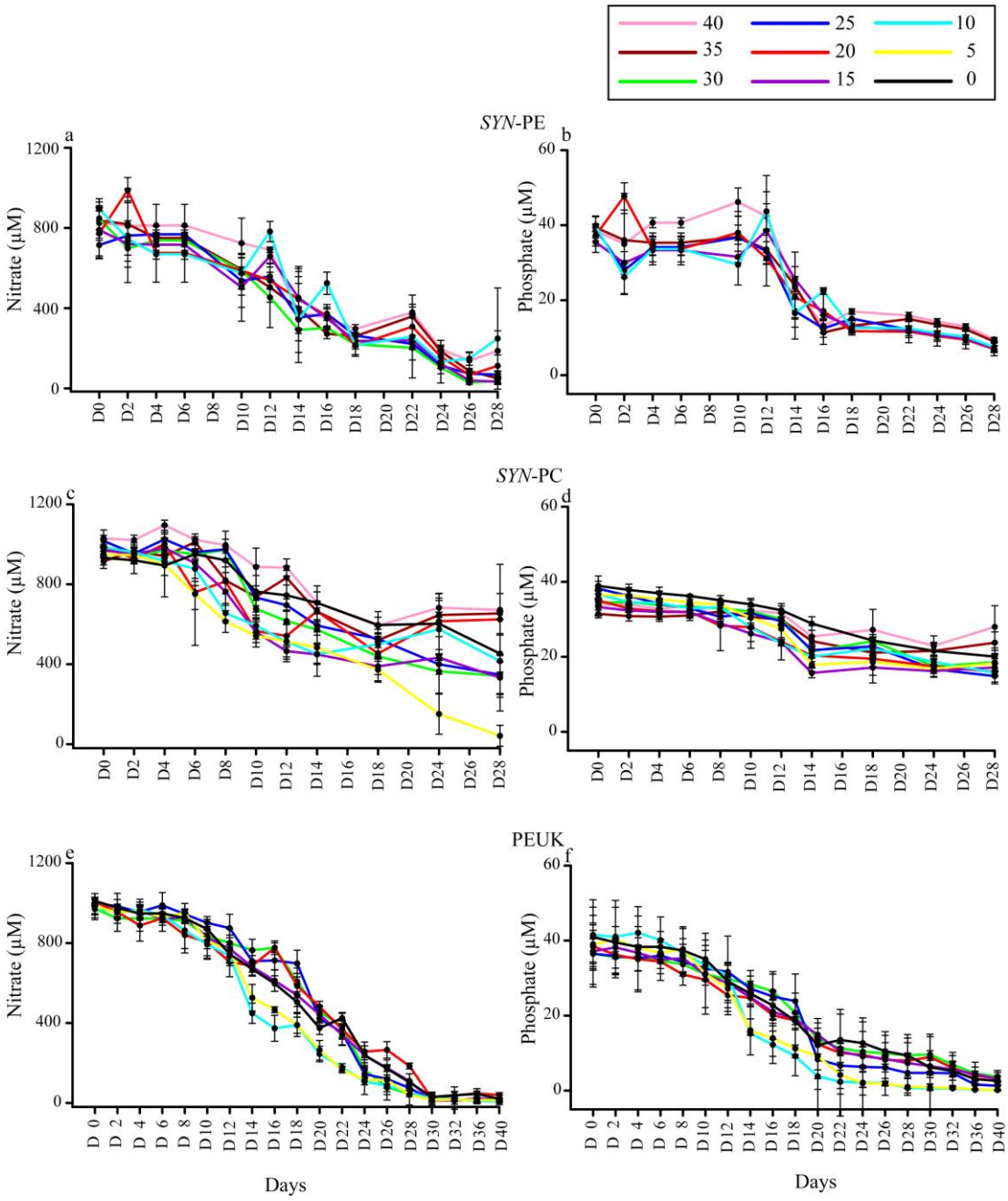

Fig. 5.8 Variation in NO_3^- and PO_4^{3-} concentrations during the experiment. (a, b) *SYN*-PE, (c, d) *SYN*-PC and (e, f) PEUK in different salinities.

5.4 Discussion

Exposure of *SYN*-PC and PEUK strains to higher salinity gradient and *SYN*-PE strain to lower salinity gradient caused significant modifications in their physiology such as cell size, pigment fluorescence intensity and growth characteristics. When an aquatic organism is exposed to higher or lower saline stress, different adaptation features have been reported earlier. Freshwater species under salt stress accumulate disaccharide and glucosyl glycerol in response to osmotic stress, whereas higher saline organisms accumulate glycine betaine under lower salinities (Blumwald et al., 1983; Mackay et al., 1984; Reed et al., 1984). Several studies have been conducted on adaptation processes in cyanobacteria including *SYN* (Lefort-Tran et al., 1988; Ladas and Papageorgiou, 2001; Sheng et al., 2006; Ozturk and Aslim, 2010;). Sheng et al., (2006) reported that microorganisms could protect themselves under high salt concentrations by increasing biosynthesis of exopolysaccharides. Fatty acid desaturation was also one of the proposed mechanisms to adapt to high-salinity environments (Allakhverdiev et al., 1999; Sing et al., 2002).

Transfer of cells to non-native haline conditions (low to high or high to low salinities) causes a stress condition which was evidenced by a lag phase in the growth. In the present study, during lag phase, decrease in abundance of *SYN*-PC and PEUK with increasing salinity, and *SYN*-PE with decreasing salinity and at salinity 40, suggests that these species take a longer time to adapt with the given stress conditions. This is well reflected in the growth rate of each group. Slowing of the growth rate is the major physiological response of the cells to the salt shock (Lefort-Tran et al., 1988). During lag phase cell burst due to osmotic pressure could be the reason for cell loss (Agrawal, 1999). These observations could be related to their adaptation to the natural environments. In the natural environment, as observed earlier (chapter 2A),

salinity in the estuarine waters varied regularly, due to the tidal activity and freshwater flow. Thus, seasonal variation is also pronounced in monsoon influenced estuaries. During non-MON, *SYN*-PE, *SYN*-PC, and PEUK abundance were high during NT when tidal activity is low which resulted in the stratified waters in the lower and upper middle estuary. Whereas, when water column was mixed during ST, these groups abundance reduced. Even though there are multiple factors influencing these groups, salinity was found to be the most significant. This is further confirmed during MON season. During this period, increased *SYN*-PC abundance till estuarine mouth suggests that this group is transported from upstream due to freshwater influx. On the other hand, *SYN*-PE abundance decreases. Thus, *SYN*-PC and PEUK shows high growth in the lower salinity and *SYN*-PE in the salinity > 20. In the experiment, *SYN*-PE growth was identical in salinity > 20 but growth rates were slightly higher in salinity 20 at exponential phase. In addition, *SYN*-PE did not grow in < 5 which suggests that abundance detected in < 5 salinity in field studies were freshwater strains. These observations indicate that PP growth was strongly coupled with variation in the salinity rather than the other parameters in the estuarine transect.

Among the PP strains, the growth pattern and magnitude of response varied throughout the experiment. *SYN*-PE and *SYN*-PC showed two days of lag phase in most of the salinity treatments with higher growth rate and abundance of *SYN*-PE in the salinity 20 to 30. *SYN*-PC did not show significant variation in abundance during exponential phase but growth rate varied significantly in different salinities suggesting that this low saline species is adapted to wide range of salinities compared to *SYN*-PE. At higher salinity, *SYN*-PC showed longer lag phase but attained similar abundance as observed in native salinity (10 to 20). At native salinity, cells showed good growth but due to the limiting factors such as light and nutrients (Brauer et al., 2012; Verspagen

et al., 2014) it reached stationary phase. Therefore, the maximum abundance at exponential phase at different salinities was similar but the time reaching the stationary phase differed among the salinity treatments. In contrast, low saline PEUK strain did not show lag phase for salinity 0 to 20 and longer exponential phase in all the salinity treatments suggest that requirement of energy for maintenance of non-scalable cellular components such as membranes and chromosomes in PEUK strain is lower than that of *SYN* strains (Zubkov et al., 2014). Therefore, PEUK growth rates were low compared to *SYN* species.

Physiological variations of an organism under salinity stress is common. Similarly, in the present study, *SYN*-PC and PEUK showed increased size in higher salinity whereas decreased in lower salinity for *SYN*-PE and remained unchanged in their native salinity within 48 h of treatment. This suggests that biochemical processes take place during this period to adapt to salinity stress which is reflecting in the variations in the size. The variation in cell size could be related to intrusion (increased cell size) and extrusion (decreased cell size) of NaCl from the cell when exposed to higher and lower salinities, respectively. The former was more prominent in the *SYN*-PC and PEUK culture. In cyanobacteria, adaptation processes start within 10 min and acclimated within 24 h to salt concentration (Apte et al., 1989). Blumwald (1983) reported that the cell volume of *SYN* 6311 changes within 200 milliseconds, indicating that salt adaptation is accompanied by changes in cell membrane properties. Increased or decreased FALS signature was well reflected in the variations of granularity (RALS) and fluorescence properties of respective culture, where RALS and fluorescence signals also followed the FALS pattern. These changes occurred mostly during lag phase in all three cultures. Subsequently, cell size declined sharply in the exponential phase in all three cultures. This is mainly due to faster cell division

and rapid synthesis of new cytoplasm and organelles. Generally, this is the phase where the cells attain maximum healthy state which is supported by the increased growth rate and not much changes in fluorescence intensity of the cells.

In the stationary phase, increasing FALS and RALS signals with decreasing growth rate suggests the cessation of cell division as the specific requirement were limiting, consequently resulting in increased cell size in all three cultures. This was reflected in the increased pigment fluorescence intensity cell^{-1} (obtained from FCM) and chl *a* concentration cell^{-1} in all cultures suggesting that cells increase their light-harvesting pigment content to match the larger cells requirements (Finkel et al., 2009). Reason for higher chl *a* concentration cell^{-1} at higher salinity could be that salt affects cellular morphology due to osmotic stress, while pigmentation is likely affected by ionic toxicity (Singh and Montgomery, 2013). The cyanobacteria are known to enhance the zeaxanthin pigment production as protective xanthophyll against osmotic stress (Chakraborty et al., 2011).

The cell size increases from *SYN*-PC < *SYN*-PE < PEUK showing a similar trend in Chl *a* concentration cell^{-1}. However, chl *a* is the major pigment in PEUK. When these species were in their native salinity, the physiological change was not much evident throughout the growth phases. The highest growth rate for *SYN*-PE, *SYN*-PC and PEUK were observed at salinities 20-35, < 5 and 0 to 10, respectively. This indicates that the optimum salinity for *SYN*-PE, *SYN*-PC and PEUK is 20 to 35, < 5 and 5 to 10, respectively. However, these groups can adapt to a wide range of salinity variation in the natural environment, but cannot dominate the non-native conditions. This could be due to inability of these cells to compete with other groups due to their slower growth rate and also mortality due to grazing.

Chapter 6

Summary

In recent years, increasing research on PP in the worldwide aquatic ecosystems revealed their significant role in food web dynamics. Thus, their importance is being highlighted around the world, especially in the oceanic region. Tropical monsoonal influenced region i.e., Indian continent is quite different from the subtropical, temperate and polar regions in terms of hydrographic conditions due to monsoonal activities. These regions can unravel some important roles of PP in the aquatic trophodynamics. In view of this, the present study was undertaken to investigate the PP community structure and its response to hydrographic conditions on temporal (Diel, fortnightly, monthly and seasonal) and spatial basis around the Indian waters. This study encompassed different environments such as oceanic, coastal, estuarine and riverine ecosystems with varying trophic status of waters such as oligotrophic, mesotrophic, eutrophic and hypertrophic.

In the estuarine environment, the strong coupling of spatio-temporal variation in PP abundance and community structure with hydrographic variations induced by physical processes such as tide and freshwater discharge during two tidal phases (ST and NT) was observed (Fig. 6.1). *SYN* was the dominant group observed over the sampling period with the occasional dominance of PEUK. During PrM, due to low freshwater discharge, tidal activity played major role in the variations of the hydrography thus consequently influencing the spatial variation of PP groups during the two tidal phases. During ST, salt water intruded up to upstream, whereas during NT it was restricted up to the upper middle estuary. This was well reflected in the spatial variation of PP during ST and NT with relatively higher abundance during NT. This suggests that during ST, high salt water intrusion and high tidal activity led to a well-mixed water column, which negatively influenced the PP growth. On the other hand, during NT, stratified water column due to low tidal activity, with higher water

transparency along with higher nutrient concentrations enhanced the PP growth in the middle estuary. During MON, variation in the PP abundance and community structure was independent of the tidal phases and dependent on the rainfall intensity that regulates freshwater discharge thus modulating the estuarine environment. This creating a temporal-spatial niche segregation of *SYN* groups thereby serving as indicator organisms of the estuarine hydrodynamics. During PM, both tidal activity and freshwater discharge along with accumulated nutrients regulated the PP growth along the transect. However, with higher tidal activity during NT till December there was no particular trend in PP distribution between the two tidal phases. Higher PP abundance was observed when the estuarine hydrography was completely governed by tides (January). During this period, higher PP abundance during ST was possibly due to higher nutrients and lower grazing pressure. Among the PP groups, *SYN*-PC was the most sensitive group showing the prominent difference in response to hydrographic changes during the two tidal phases (ST and NT), irrespective of seasons whereas *SYN*-PE group showed significant response only during PrM. This suggests that the intensity of tidal phases and freshwater discharge controlled the spatial and temporal distribution pattern of PP. Thus, highlighting the importance of hydrodynamics in monsoonal estuaries and corroborate our hypothesis that water column conditions during NT favor the growth of PP as compared to ST.

Phytoplankton size fractionated biomass is an important determinant of the type of food web functioning in aquatic ecosystems. Knowledge about the effect of seasonal salinity gradient on the size fractionated biomass dynamics is still lacking, especially in tropical estuaries experiencing monsoons. The phytoplankton size-fractionated chlorophyll biomass (> 3 μm and < 3 μm) and PP community structure

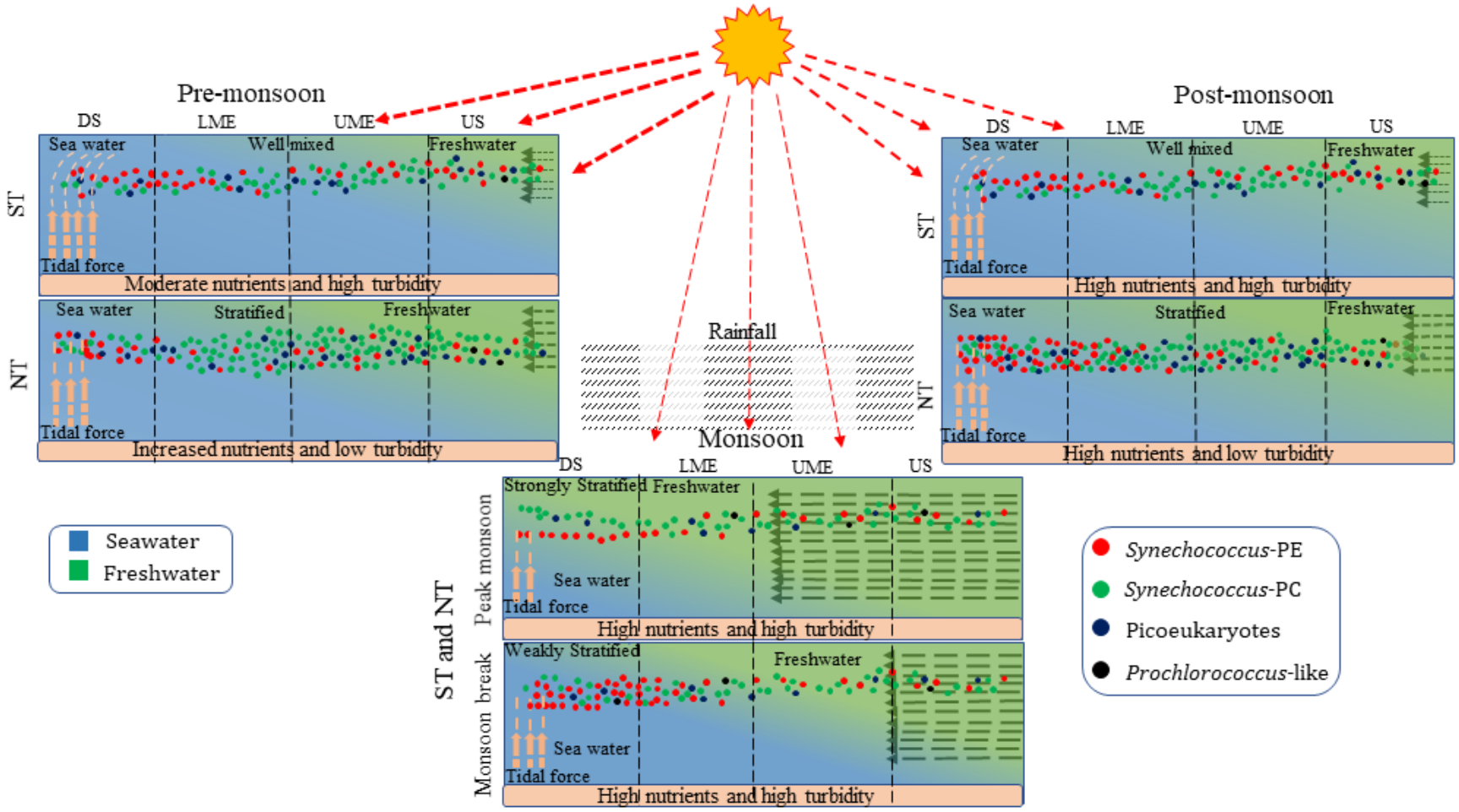

Fig. 6.1. Schematic representation of temporal and spatial variations of PP groups during spring and neap tide in the Zuari estuary. DS-Downstream, LME- Lower middle estuary, UME- Upper middle estuary and US-Upstream.

were characterized in the present study. On an annual scale, >3 µm size fraction contributor to the total phytoplankton biomass with the ephemeral dominance of < 3 µm size fraction. During MON season, freshwater runoff and shorter water residence time resulted in a size-independent response. The lowest annual biomass concentration of both size fractions during this period showed signs of recovery with increasing salinity downstream towards the end of MON. In contrast, the biomass response was size-dependent during the non-MON seasons with the sporadic dominance (> 50%) of < 3 µm biomass during high water temperature episodes from downstream to middle estuary during PrM and at low salinity and high nutrient conditions upstream during PM (Fig. 6.2). These conditions also influenced the PP community structure with *SYN*-PE dominating during MON, *SYN*-PC during PM and PEUK during the PrM. This study highlights switching over of dominance in size fractionated phytoplankton biomass at intra, inter-seasonal and spatial scales which will likely govern the estuarine trophodynamics.

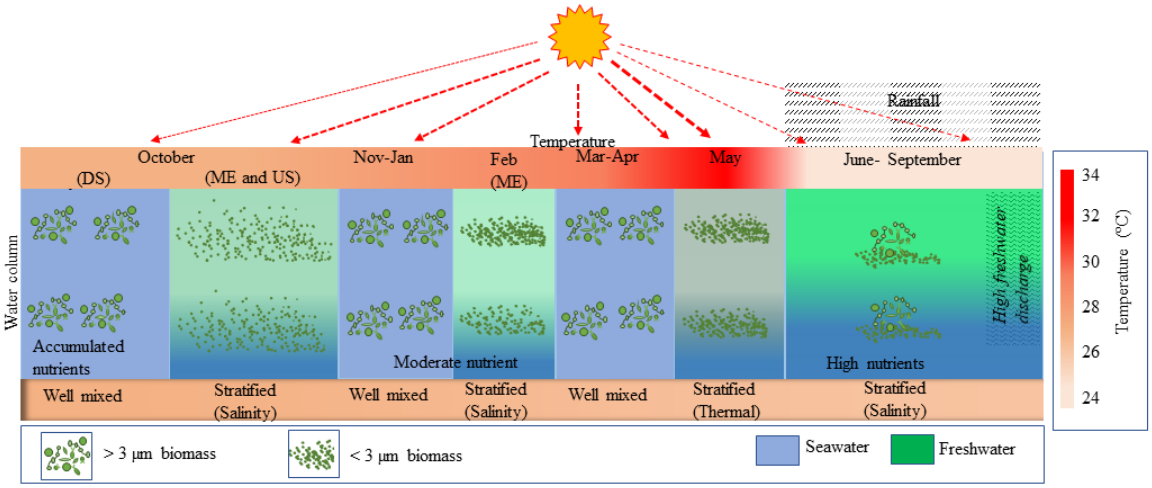

Fig. 6.2. Schematic representation of temporal variations of < 3 µm and > 3 µm chl *a* in the Zuari estuary. DS- Downstream, ME- Middle estuary and US-Upstream

A comparative study of PP abundance and community structure in different coastal ecosystems (marine, estuarine and freshwater) depicted clear temporal and spatial variations. The highest PP abundance was observed in the closed riverine port

(Kolkata port), and comparatively lower abundance of PP was detected in the estuarine port (Cochin port). Lowest PP abundance was observed in marine ports (V.O.C., Chennai, and New Mangalore ports). The dominance pattern also varied among these ports. *SYN*-PEI was dominant in marine ports and high saline waters of the estuarine port whereas, *SYN*-PC was dominant in low saline waters of the estuarine port and in the riverine port. Temperature and nutrient concentrations played a major role in the seasonal and spatial variation of PP in these port waters. The effect of monsoons (SWM and NEM) was also well reflected in the variation of PP community structure and its abundance along the west and east coasts. The trophic index showed that the marine ports exhibited a lower level of eutrophication compared to estuarine and riverine ports. In these waters, distribution of *SYN*-PE and *SYN*-PC groups highlight that they occupy contrasting ecological niches, wherein former was higher in the lower eutrophic waters and latter in the higher eutrophic waters. Therefore, PP distribution pattern can serve as an indicator of the trophic status of coastal water bodies.

Continental margin of the AS is a dynamic region subjected to variability in hydrography as a result of various physical forcing such as coastal advection and vertical mixing. Across the continental margin, *SYN* was abundant in the shelf waters and *PRO* in slope waters. Based on the temperature and salinity distribution, the study period was divided into phase I representing a stratified water column and phase II representing a vertically mixed water column. Phase I had higher PP abundance with the initial dominance of *PRO* which was later taken over by PEUK. Towards the end of phase I, with the initiation of vertical mixing, PEUK were the first to respond to the nutrient influx. As the vertical mixing intensified during phase II, the PP abundance declined. PP carbon biomass and their contribution to total phytoplankton biomass

was relatively higher during phase I with PEUK as the major contributors. These transient variations in PP abundance highlights the importance of high frequency observations at the single cell level for better understanding the population dynamics in such environments. The short-term variability in the hydrographic conditions mainly nutrient availability and water column stability regulate the variations in the PP community structure.

The above field observations depicted distinct spatial variation in PP community structure in the oceanic, estuarine, coastal and riverine waters. *SYN* groups were dominant in the estuarine, coastal and riverine waters whereas *PRO* was dominant in the oceanic waters. PEUK were dominant during some occasions in the estuarine waters and oceanic sub surface regions.

Field observations highlight salinity as the major environmental factor influencing the distribution of different PP groups. This raises a question why these strains cannot dominate the non-native salinity. In the view of this, experiments were conducted on isolated PP strains i.e., *SYN*-PC (low saline), *SYN*-PE (high saline) and PEUK (low saline) to observe their growth pattern under different salinities. Results revealed a significant influence of salinity on the growth of different PP strains. *SYN*-PE grew well in salinities ranging between 20 and 30. They did not grow in salinity ≤ 5. *SYN*-PC grew in all salinity treatments with a higher growth rate at salinity 0-15. PEUK grew well in salinities ≤ 30 with higher growth rates in salinities ranging between 0-15. These observations suggest that the three strains adapt to a wide range of salinity variations in the natural environment, but cannot dominate the non-native conditions due to lowering growth rates resulting in a prolonged lag phase thereby, hampering their ability to compete with other groups. This leads to their lower abundance in the non-native salinities.

Bibliography

Acharyya, T., Sarma, V.V.S.S., Sridevi, B., Venkataramana, V., Bharathi, M.D., Naidu, S.A., Kumar, B.S.K., Prasad, V.R., Bandyopadhyay, D., Reddy, N.P.C., Kumar, M.D., 2012. Reduced river discharge intensifies phytoplankton bloom in Godavari estuary, India. Mar. Chem., 132, 15-22.

Achuthankutty, C., Ramaiah, N., Padmavati, G., 1998. Zooplankton variability and copepod assemblage in the coastal and estuarine waters of Goa along the central-west coast of India. IOC Workshop Report, 142.

Agawin, N.S., Duarte, C.M., Agusti, S., 1998. Growth and abundance of *Synechococcus* sp. in a Mediterranean Bay: seasonality and relationship with temperature. Mar. Ecol. Prog. Ser., 170, 45-53.

Agawin, N.S., Duarte, C.M., Agusti, S., 2000. Nutrient and temperature control of the contribution of picoplankton to phytoplankton biomass and production. Limnol. Oceanogr., 45, 591-600.

Agrawal, S.C., 1999. Limnology. A.P.H Publishing corporations, New Delhi, India.

Ahmed, A., Kurian, S., Gauns, M., Chndrasekhararao, A.V., Mulla, A., Naik, B., Naik, H., Naqvi, S.W., 2016. Spatial variability in phytoplankton community structure along the eastern Arabian Sea during the onset of south-west monsoon. Cont. Shelf Res., 119, 30-39.

Allakhverdiev, S.I., Nishiyama, Y., Suzuki, I., Tasaka, Y., Murata, N., 1999. Genetic engineering of the unsaturation of fatty acids in membrane lipids alters the tolerance of *Synechocystis* to salt stress. Proc. Nation. Acad. Sci., 96, 5862-5867.

Anand, S.S., Sardesai, S., Muthukumar, C., Mangala, K., Sundar, D., Parab, S., Kumar, M. D., 2014. Intra-and inter-seasonal variability of nutrients in a tropical monsoonal estuary (Zuari, India). Cont. Shelf. Res., 82, 9-30.

Anas, A., Jasmin, C., Sheeba, V., Gireeshkumar, T., Nair, S., 2015. Heavy metals pollution influence the community structure of Cyanobacteria in nutrient rich tropical estuary. Oceanography, 3, 137.

Anderson, C.R., Siegel, D.A., Brzezinski, M.A., Guillocheau, N., 2008. Controls on temporal patterns in phytoplankton community structure in the Santa Barbara Channel, California. J. Geophys. Res., 113, 1-16.

Aneeshkumar, N., Sujatha, C., 2012. Biomarker pigment signatures in Cochin backwater system–A tropical estuary south west coast of India. Estuar. Coast. Shelf. Sci., 99, 182-190.

Anu, P., Jayachandran, P., Sreekumar, P., Nandan, S.B., 2014. A Review on Heavy Metal Pollution in Cochin Backwaters, Southwest Coast of India. Int. J. Mar. Sci., 4, 92-98.

Apte, S.K., Bhagwat, A.A., 1989. Salinity-stress-induced proteins in two nitrogen-fixing Anabaena strains differentially tolerant to salt. J. Bacter., 171, 909-915.

Azam, F., Fenchel, T., Field, J.G., Gray, J., Meyer-Reil, L., Thingstad, F., 1983. The ecological role of water-column microbes in the sea. Mar. Ecol. Prog. Ser., 10, 257-263.

Bailey, D., Plenys, T., Solomon, G.M., Campbell, T.R., Feuer, G.R., Masters, J., Tonkonogy, B., 2004. Harboring pollution: The dirty truth about US ports. San Francisco, California: Natural Resources Defense Council, 29.

Balachandran, K., Raj, L., Nair, M., Joseph, T., Sheeba, P., Venugopal, P., 2005. Heavy metal accumulation in a flow restricted, tropical estuary. Estuar. Coast. Shelf. Sci., 65, 361-370.

Balch, W.M., 1981. An apparent lunar tidal cycle of phytoplankton blooming and community succession in the Gulf of Maine. J. Exp. Mar. Biol. Ecol., 55, 65-77.

Banse, K., 1968. Hydrography of the Arabian Sea shelf of India and Pakistan and effects on demersal fishes. Deep Sea Res. Oceanogr. Abstr., 15, 45-79.

Banse, K., McClain, C., 1986. Winter blooms of phytoplankton in the Arabian Sea as observed by the Coastal Zone Color Scanner. Mar. Ecol. Prog. Ser., 34, 201-211.

Banse, K., 1987. Seasonality of phytoplankton chlorophyll in the central and northern Arabian Sea. Deep Sea Res. Pt I., 34, 713-723.

Banse, K., 1994. Grazing and zooplankton production as key controls of phytoplankton production in the open ocean. Oceanography, 7, 13-20.

Baudoux, A.C., Veldhuis, M.J., Witte, H.J., Brussaard, C.P., 2007. Viruses as mortality agents of picophytoplankton in the deep chlorophyll maximum layer during IRONAGES III. Limnol. Oceanogr., 52, 2519-2529.

Bazin, P., Jouenne, F., Friedl, T., Deton-Cabanillas, A.F., Le Roy, B. and Véron, B., 2014. Phytoplankton diversity and community composition along the estuarine gradient of a temperate macrotidal ecosystem: combined morphological and molecular approaches. PloS one, 9, 805-825.

Bec, B., Collos, Y., Souchu, P., Vaquer, A., Lautier, J., Fiandrino, A., Benau, L., Orsoni, V., Laugier, T., 2011. Distribution of picophytoplankton and nanophytoplankton along an anthropogenic eutrophication gradient in French Mediterranean coastal lagoons. Aquat. Microb. Ecol., 63, 29-45.

Bec, B., Husseini-Ratrema, J., Collos, Y., Souchu, P., Vaquer, A., 2005. Phytoplankton seasonal dynamics in a Mediterranean coastal lagoon: emphasis on the picoeukaryote community. J. Plankton Res., 87, 881-894.

Becker, A., Whitfield, A., Cowley, P., Cole, V., Taylor, M., 2016. Tidal amplitude and fish abundance in the mouth region of a small estuary. J. Fish Biol., 89, 1851-1856.

Behrenfeld, M.J., 2010. Abandoning Sverdrup's critical depth hypothesis on phytoplankton blooms. Ecology, 91, 977-989.

Bell, T., Kalff, J., 2001. The contribution of picophytoplankton in marine and freshwater systems of different trophic status and depth. Limnol.Oceanogr., 46, 1243–1248.

Bharati, V.R., Kalavati, C., Raman, A.V., 2001. Planktonic flagellates in relation to pollution in Visakhapatnam harbour, east coast of India. Indian J. Mar. Sci., 30, 25–32.

Bhattathiri, P., Pant, A., Sawant, S., Gauns, M., Matondkar, S.G.P., Mahanraju, R., 1996. Phytoplankton production and chlorophyll distribution in the eastarn and central Arabian Sea in 1994-1995. Curr. Sci., 71, 857-862.

Bhaumik, U., Sharma, A.P., 2011. The fishery of Indian Shad (Tenualosa ilisha) in the Bhagirathi-Hooghly river system. Fish. Chimes, 31, 21-27.

Biller, S.J., Berube, P.M., Lindell, D., Chisholm, S.W., 2015. *Prochlorococcus*: the structure and function of collective diversity. Nature Rev. Microbiol., 13, 1-15.

Blanchot, J., André, J.M., Navarette, C., Neveux, J., Radenac, M.H., 2001. Picophytoplankton in the equatorial Pacific: vertical distributions in the warm pool and in the high nutrient low chlorophyll conditions. Deep Sea Res. Pt I, 48, 297-314.

Blauw, A.N., Beninca, E., Laane, R.W., Greenwood, N., Huisman, J., 2012. Dancing with the tides: fluctuations of coastal phytoplankton orchestrated by different oscillatory modes of the tidal cycle. PloS One, 7, 1-14.

Blumwald, E., Mehlhorn, R.J., Packer, L., 1983. Ionic osmoregulation during salt adaptation of the cyanobacterium *Synechococcus* 6311. Plant physiol., 73, 377-380.

Booth, B.C., Lewin, J., Postel, J.R., 1993. Temporal variation in the structure of autotrophic and heterotrophic communities in the subarctic Pacific. Prog. Oceanogr., 32, 57-99.

Bouman, H.A., Ulloa, O., Scanlan, D.J., Zwirglmaier, K., Li, W.K., Platt, T., Lutz, V., 2006. Oceanographic basis of the global surface distribution of *Prochlorococcus* ecotypes. Science, 312, 918-921.

Brauer, V.S., Stomp, M., Huisman, J., 2012. The nutrient-load hypothesis: patterns of resource limitation and community structure driven by competition for nutrients and light. Am. Nat., 179, 721–740.

Brown, S.L., Landry, M.R., Barber, R.T., Campbell, L., Garrison, D.L., Gowing, M.M., 1999. Picophytoplankton dynamics and production in the Arabian Sea during the 1995 Southwest Monsoon. Deep Sea Res. Pt II, 46, 1745-1768.

Buchanan, C., Lacouture, R.V., Marshall, H.G., Olson, M., Johnson, J.M., 2005. Phytoplankton reference communities for Chesapeake Bay and its tidal tributaries. Estuaries, 28, 138-159.

Buck, K.R., Chavez, F.P., Campbell, L., 1996. Basin-wide distributions of living carbon components and the inverted trophic pyramid of the central gyre of the North Atlantic Ocean, summer 1993. Aquat. Microb. Ecol., 10, 283-298.

Buitenhuis, E.T., Li, W.K., Vaulot, D., Lomas, M.W., Landry, M.R., Partensky, F., Karl, D.M., Ulloa, O., Campbell, L., Jacquet, S., Lantoine, F., Chavez, F., Macias, D., Gosselin, M., McManus, G.B., 2012. Picophytoplankton biomass distribution in the global ocean. Earth Sys. Sci. Data, 4, 37-46.

Callieri, C., 2007. Picophytoplankton in freshwater ecosystems: the importance of small-sized phototrophs. Freshw. Rev., 1, 1–28.

Camacho, A., Picazo, A., Miracle, M.R., Vicente, E., 2003. Spatial distribution and temporal dynamics of picocyanobacteria in a meromictic karstic lake. Algol. Stud., 109, 171-184.

Campbell, L., Carpenter, E.J., 1987. Characterisation of phycoerythrin-containing *Synechococcus* spp. populations by immunofluorescence. J. Plankton Res., 9, 1167-1181.

Campbell, L., Vaulot, D., 1993. Photosynthetic picoplankton community structure in the subtropical North Pacific Ocean near Hawaii (station ALOHA). Deep Sea Res. Pt I, 40, 2043-2060.

Campbell, L., Landry, M., Constantinou, J., Nolla, H.A., Brown, S.L., Liu, H., Caron, D. A., 1998. Response of microbial community structure to environmental forcing in the Arabian Sea. Deep Sea Res. Pt II, 45, 2301-2325.

Campbell, L., 2001. Flow cytometric analysis of autotrophic picoplankton. Methods in microbiology, 30, 317-343.

Carlson, R.E., 1977. A trophic state index for lakes. Limnol. Oceanogr., 22, 361-369.

Caroppo, C., 2000. The contribution of picophytoplankton to community structure in a Mediterranean brackish environment. J. Plankton Res., 22, 381-397.

Cermeno, P., Maranon, E., Rodríguez, J., Fernandez, E., 2005. Large-sized phytoplankton sustain higher carbon specific photosynthesis than smaller cells in a coastal eutrophic ecosystem. Mar. Ecol. Prog. Ser., 297, 51–60.

Chakraborty, P., Acharyya, T., Babu, P.R., Bandyopadhyay, D., 2011. Impact of salinity and pH on phytoplankton communities in a tropical freshwater system: An investigation with pigment analysis by HPLC. J. Environ. Monit., 13, 614-620.

Chang, J., Lin, K.H., Chen, K.M., Gong, G.C., Chiang, K.P., 2003. *Synechococcus* growth and mortality rates in the East China Sea: range of variations and correlation with environmental factors. Deep-Sea Res. Pt II, 50, 1265-1278.

Charpy, L., Blanchot, J., 1998. Photosynthetic picoplankton in French Polynesian atoll lagoons: estimation of taxa contribution to biomass and production by flow cytometry. Mar. Ecol. Prog. Ser., 162, 57-70.

rayChen, B., Liu, H., Huang, B., Wang, J., 2014. Temperature effects on the growth rate of marine picoplankton. Mar. Ecol. Prog. Ser., 505, 37.

Chen, X., Shen, Z., Yang, Y., 2016. Response of the turbidity maximum zone in the Yangtze River Estuary due to human activities during the dry season. Environ. Sci. Pollut. R., 23, 18466-18481.

Chiang, K.P., Kuo, M.C., Chang, J., Wang, R.H., Gong, G.C., 2002. Spatial and temporal variation of the *Synechococcus* population in the East China Sea and its contribution to phytoplankton biomass. Cont. Shelf. Res., 22, 3-13.

Chiang, K.P., Tsai, A.Y., Tsai, P.J., Gong, G.C., Tsai, S.F., 2013. Coupling of the spatial dynamic of picoplankton and nanoflagellate grazing pressure and carbon flow of the microbial food web in the subtropical pelagic continental shelf ecosystem. Biogeosc. Discus., 10, 233-263.

Chisholm, S.W., Olson, R.J., Zettler, E.R., Goericke, R., Waterbury, J.B., Welschmeyer, N.A., 1988. A novel free-living prochlorophyte abundant in the oceanic euphotic zone. Nature, 334, 340-343.

Chisholm, S.W., 1992. Phytoplankton size. Primary productivity and biogeochemical cycles in the sea, 213, 213-237.

Cloern, J.E., Nichols, F.H., 1985. Time scales and mechanisms of estuarine variability, a synthesis from studies of San Francisco Bay. Hydrobiologia, 129, 229-237.

Contant, J., Pick, F.R., 2013. Picophytoplankton during the ice-free season in five temperate-zone rivers. J. Plankton Res., 35, 553-565.

Copeland, B., 1966. Effects of decreased river flow on estuarine ecology. J. Water Pollut. Control Fed., 38, 1831-1839.

Crumpton, W.G., Wetzel, R.G., 1982. Effects of differential growth and mortality in the seasonal succession of phytoplankton populations in Lawrence Lake, Michigan. Ecology, 63, 1729-1739.

Dasgupta, D., Ghosh, R., Sengupta, T.K., 2013. Biofilm-mediated enhanced crude oil degradation by newly isolated *Pseudomonas* species. ISRN Biotech., 2013, 1-13.

Davis, L.N., Phillips, K.A., Marshall, H.G., 1997. Seasonal abundance of autotrophic picoplankton in the Pagan River, a nutrient enriched subestuary of the James River, Virginia. Virginia J. Sci., 48, 211-218.

D'Costa, P.M., Anil, A.C., 2010. Diatom community dynamics in a tropical, monsoon-influenced environment: West coast of India. Cont. Shelf. Res., 30, 1324-1337.

Devassy, V., 1974. Observations on the bloom of a diatom *Fragilaria Oceanica* Cleve. Mahasagar, 7, 101-105.

Devassy, V., Goes, J., 1988. Phytoplankton community structure and succession in a tropical estuarine complex (central west coast of India). Estuar. Coast. Shelf. Sci., 27, 671-685.

Devassy, V., Goes, J., 1989. Seasonal patterns of phytoplankton biomass and productivity in a tropical estuarine complex (west coast of India). Proc. Plant Sci., 99, 485-501.

Domingues, R.B., Anselmo, T.P., Barbosa, A.B., Sommer, U., Galvao, H.M., 2010. Tidal variability of phytoplankton and environmental drivers in the freshwater reaches of the Guadiana Estuary (SW Iberia). Int. Rev. Hydrobiol., 95, 352-369.

Dongen-Vogels, V., Seymour, J.R., Middleton, J.F., Mitchell, J.G., Seuront, L., 2011. Influence of local physical events on picophytoplankton spatial and temporal dynamics in South Australian continental shelf waters. J. Plankton Res., 20, 1-16.

Dongen-Vogels, V., Seymour, J.R., Middleton, J.F., Mitchell, J.G., Seuront, L., 2012. Shifts in picophytoplankton community structure influenced by changing upwelling conditions. Estuar. Coast. Shelf Sci., 109, 81-90.

D'Silva, M.S., Anil, A.C., Borole, D.V., Nath, B.N., Singhal, R.K., 2012. Tracking the history of dinoflagellate cyst assemblages in sediments from the west coast of India. J. Sea Res., 73, 86-100.

D'Silva, M.S., Anil, A.C., Sawant, S.S., 2013. Dinoflagellate cyst assemblages in recent sediments of Visakhapatnam harbour, east coast of India: Influence of environmental characteristics. Mar. Pollut. Bull., 66, 59-72.

Duraisamy, A., Latha, S., 2011. Impact of pollution on marine environment-A case study of coastal Chennai. Indian J. Sci.Technol., 4, 259-262.

Eccleston-Parry, J.D., Leadbeater, B.S., 1994. A comparison of the growth kinetics of six marine heterotrophic nanoflagellates fed with one bacterial species. Mar. Ecol. Prog. Ser., 105, 167-177.

Elser, J.J., Bracken, M.E., Cleland, E.E., Gruner, D.S., Harpole, W.S., Hillebrand, H., Smith, J.E., 2007. Global analysis of nitrogen and phosphorus limitation of primary producers in freshwater, marine and terrestrial ecosystems. Ecol. Lett., 10, 1135-1142.

Falkowski, P.G., 1994. The role of phytoplankton photosynthesis in global biogeochemical cycles.Photosynthesis research, 39, 235-258.

Fatema, K., Omar, W., Isa, M., Omar, A., 2016. Effects of Water Quality Parameters on Abundance and Biomass of Zooplankton in Merbok Estuary Malaysia. J. Environ. Sci. Nat. R., 9, 117-122.

Felsenstein, J., 1985. Conference limits on phylogenies: an approach using the bootstrap. Evolution, 39, 783–789.

Finkel, Z.V., Beardall, J., Flynn, K.J., Quigg, A., Rees, T.A.V., Raven, J.A., 2009. Phytoplankton in a changing world: cell size and elemental stoichiometry. J. Plankton Res., 32, 119-137.

Flo, E., Garcés, E., Manzanera, M., Camp, J., 2011. Coastal inshore waters in the NW Mediterranean: Physicochemical and biological characterization and management implications. Estuar. Coast. Shelf Sci., 1-11

Flombaum, P., Gallegos, J.L., Gordillo, R.A., Rincón, J., Zabala, L.L., Jiao, N., Karl, D.M., Li, W.K., Lomas, M.W., Veneziano, D., Vera, C.S., 2013. Present and future global distributions of the marine Cyanobacteria *Prochlorococcus* and *Synechococcus*. Proc. Natl. Acad. Sci., 110, 9824-9829.

Fuller, N.J., Tarran, G.A., Yallop, M., Orcutt, K.M., Scanlan, D.J., 2006. Molecular analysis of picocyanobacterial community structure along an Arabian Sea transect reveals distinct spatial separation of lineages. Limnol. Oceanogr., 51, 2515-2526.

Ganapati, P.N., Raman, A.V., 1973. Pollution in Visakhapatnam harbour. Curr. Sci., 42, 490-492.

Gardner, J.P., Thompson, R.J., 2001. The effects of coastal and estuarine conditions on the physiology and survivorship of the mussels *Mytilus edulis*, *M. trossulus* and their hybrids. J. Exp. Mar. Biol. Ecol., 265, 119-140.

Garrison, D.L., Gowing, M.M., Hughes, M.P., Campbell, L., Caron, D.A., Dennett, M.R., Shalapyonok, A., Olson, R.J., Landry, M.R., Brown, S.L., Liu, H.B., 2000. Microbial food web structure in the Arabian Sea: a US JGOFS study. Deep Sea Res. Pt II, 47, 1387-1422.

Gaulke, A.K., Wetz, M.S., Paerl, H.W., 2010. Picophytoplankton: a major contributor to planktonic biomass and primary production in a eutrophic, river-dominated estuary. Estuar. Coast. Shelf Sci., 90, 45-54.

Gauns, M., Madhupratap, M., Ramaiah, N., Jyothibabu, R., Fernandes, V., Paul, J.T., Kumar, S.P., 2005. Comparative accounts of biological productivity characteristics and estimates of carbon fluxes in the Arabian Sea and the Bay of Bengal. Deep Sea Res. Pt II, 52, 2003-2017.

George, M., Kartha, K., 1963. Surface salinity of Cochin backwater with reference to tide. J. Mar. Biol. Ass. India, 5, 178-184.

Gianesella, S., Saldanha-Corrêa, F., Teixeira, C., 2000. Tidal effects on nutrients and phytoplankton distribution in Bertioga Channel, São Paulo, Brazil. Aquat. Ecosyst. Health Manag., 3, 533-544.

Gillanders, B., Able, K., Brown, J., Eggleston, D., Sheridan, P., 2003. Evidence of connectivity between juvenile and adult habitats for mobile marine fauna: an important component of nurseries. Mar. Ecol. Progr. Ser., 247, 281-295.

Gin, K., 1996. Microbial size spectra from diverse marine ecosystems. Ph.D. thesis, Massachusetts Institute of Technology and Woods Hole Oceanographic Institute.

Gin, K.Y.H., Zhang, S., Lee, Y.K., 2003. Phytoplankton community structure in Singapore's coastal waters using HPLC pigment analysis and flow cytometry. J. Plankton Res., 25, 1507-1519.

Giovagnetti, V., Cataldo, M.L., Conversano, F., Brunet, C., 2012. Growth and photophysiological responses of two picoplanktonic *Minutocellus* species, strains RCC967 and RCC703 (Bacillariophyceae). Eur. J. Phycol., 47, 408-420.

Glazer, A.N., 1985. Light harvesting by phycobilisomes. Ann. Rev. Biophys. Chem., 14, 47-77.

Goericke, R., Repeta, D.J., 1992. The pigments of *Prochlorococcus* marinus: the presence of divinyl chlorophyll *a* and *b* in a marine procaryote. Limnol. Oceanogr., 37, 425–433.

GranÍi, E., Granéli, W., Rabbani, M.M., Daugbjerg, N., Fransz, G., Roudy, J.C., Alder, V. A., 1993. The influence of copepod and krill grazing on the species composition of phytoplankton communities from the Scotia Weddell sea. Polar Biol., 13, 201-213.

Guenther, M., Araújo, M., Flores-Montes, M., Gonzalez-Rodriguez, E., Neumann-Leitao, S. 2015. Eutrophication effects on phytoplankton size-fractioned biomass and production at a tropical estuary. Mar. Pollut. Bull., 91, 537-547.

Guerra-García, J.M., García-Gómez, J.C., 2005. Assessing pollution levels in sediments of a harbour with two opposing entrances. Environmental implications. J. Environ. Manag., 77, 1-11.

Guillard, R.R., Ryther, J.H., 1962. Studies of marine planktonic diatoms: I. *Cyclotella Nana* Hustedt, and *Detonula Confervacea* (CLEVE) Gran. Can. J. Microbiol., 8, 229-239.

Harrison, P.J., Yin, K., Lee, J.H.W., Gan, J., Liu, H., 2008. Physical–biological coupling in the Pearl River Estuary. Cont. Shelf. Res., 28, 1405-1415.

Herz, M., Davis, J. 2002. Cruise control: A report on how cruise ships affect the marine environment. A Report on How Cruise Ships Affect the Marine Environment. Washington, DC: The Ocean Conservancy.

Hirose, M., Katano, T., Nakano, S.I., 2008. Growth and grazing mortality rates of *Prochlorococcus, Synechococcus* and eukaryotic picophytoplankton in a bay of the Uwa Sea, Japan. J. Plankton Res., 30, 241-250.

Holligan, P., Harbour, D., 1977. The vertical distribution and succession of phytoplankton in the western English Channel in 1975 and 1976. J. Mar. Biol. Assoc. U.K., 57, 1075-1093.

Holt, J.G., Krieg, N.R., Sneath, P.H.A., Staley, J.T. Williams, S.T., 1994. Oxygenic phototrophic bacteria. In Bergey's Manual of Determinative Bacteriology. 9th edn, edited by J. G. Holt. Baltimore: Williams & Wilkins, 377–425.

Hung, J.J., Huang, M.H., 2005. Seasonal variations of organic-carbon and nutrient transport through a tropical estuary (Tsengwen) in southwestern Taiwan. Environ. Geochem. Health, 27, 75-95.

Hynes, H.B.N., 1970. The ecology of running waters. Liverpool University Press Liverpool.

Irwin, A.J., Finkel, Z.V., Schofield, O.M., Falkowski, P.G., 2006. Scaling-up from nutrient physiology to the size-structure of phytoplankton communities. J. Plankton Res., 28, 459-471.

Iturriaga, R., Mitchell, B.G., 1986. Chroococcoid cyanobacteria: a significant component in the food web dynamics of the open ocean. Mar. Ecol. Prog. Ser., 28, 291-297.

Jacob, B., Revichandran, C., NaveenKumar, K., 2013. Salt intrusion study in Cochin estuary-using empirical models. Indian J. Geo. Mar. Sci., 42, 304-313.

Jacquet, S., Prieur, L., Avois-Jacquet, C., Lennon, J.F., Vaulot, D., 2002. Short-timescale variability of picophytoplankton abundance and cellular parameters in surface waters of the Alboran Sea (western Mediterranean). J. Plankton Res., 24, 635-651.

Jeffrey, S.W., Vesk, M., 1997. Introduction to marine phytoplankton and their pigment signatures. In: Jeffrey SW, Mantoura RFC, Wright SW (eds.) Phytoplankton pigments in oceanography: guidelines to modern methods. Monographs on oceanographic methodology 10, UNESCO Publishing, France, 37-84.

Jha, B., Nath, D., Srivastava, N., Satpathy, B., 2008. Estuarine Fisheries Management-Options and Strategies. CIFRI Policy paper, 3, 1-23.

Jiao, N., Yang, Y., Hong, N., Ma, Y., Harada, S., Koshikawa, H., Watanabe, M., 2005. Dynamics of autotrophic picoplankton and heterotrophic bacteria in the East China Sea. Cont. Shelf. Res., 25, 1265-1279.

Jing, H., Liu, H., Bird, D.F., Wong, T.H., Chen, X., Chen, B., 2010. Composition and seasonal variability of picoeukaryote communities at two subtropical coastal sites with contrasting trophic conditions. J. Plankton Res., 32, 565-573.

Johnson, M., 2000. Physical control of plankton population abundance and dynamics in intertidal rock pools. Hydrobiologia, 440,145-152.

Johnson, P.W., Sieburth, J.M., 1982. In-situ morphology and occurrence of eucaryotic phototrophs of bacterial size in the picoplankton of estuarine and oceanic waters. J. Phycol., 18, 318-327.

Johnson, Z.I., Zinser, E.R., Coe, A., McNulty, N.P., Woodward, E.M.S., Chisholm, S.W., 2006. Niche partitioning among *Prochlorococcus* ecotypes along ocean-scale environmental gradients. Science, 311, 1737-1740.

Joseph, J., Kurup, P., 1989. Volume transport and estuarine features at Cochin inlet. Mahasagar, 22, 165-172.

Jyothibabu, R., Madhu, N., Jayalakshmi, K., Balachandran, K., Shiyas, C., Martin, G., Nair, K., 2006. Impact of freshwater influx on microzooplankton mediated food web in a tropical estuary (Cochin backwaters–India). Estuar. Coast. Shelf. Sci., 69, 505-518.

Jyothibabu, R., Mohan, A.P., Jagadeesan, L., Anjusha, A., Muraleedharan, K.R., Krishna Kiran, L., Ullas, N., 2013. Ecology and trophic preference of picoplankton and nanoplankton in the Gulf of Mannar and the Palk Bay, southeast coast of India. J. Mar. Sys., 112, 29-44.

Jouenne, F., Lefebvre, S., Véron B, Lagadeuc Y (2007) Phytoplankton community structure and primary production in small intertidal estuarine-bay ecosystem (eastern English Channel, France). Mar Biol., 151, 805–825.

Kaladharan, P., Krishnakumar, P., Prema, D., Nandakumar, A., Khambadkar, L., Valsala, K., 2011. Assimilative capacity of Cochin inshore waters with reference to contaminants received from the backwaters and the upstream areas. Ind. J. Fish., 58, 75-83.

Kasai, A., Kurikawa, Y., Ueno, M., Robert, D., Yamashita, Y., 2010. Salt-wedge intrusion of seawater and its implication for phytoplankton dynamics in the Yura Estuary, Japan. Estuar. Coast. Shelf. Sci., 86, 408-414.

Katano, T., Nakano, S.I., Ueno, H., Mitamura, O., Anbutsu, K., Kihira, M., Satoh, Y., Drucker, V., Sugiyama, M., 2005. Abundance, growth and grazing loss rates of picophytoplankton in Barguzin Bay, Lake Baikal. Aquat. Ecol., 39, 431-438.

Kazuhiko, M., Ken, F., Takeshi, K., 2004. Association of picophytoplanktonn distribution with ENSO events in the equatorial Pacific between 145°E and 160°W. Deep-Sea Res. Pt I, 51, 1851–1871.

Khandeparker, L., Anil, A.C., Naik, S.D., Gaonkar, C.C., 2015. Daily variations in pathogenic bacterial populations in a monsoon influenced tropical environment. Mar. Pollut. Bull., 96, 337–343.

Khandeparker, L., Ranjith, E., Laxman, G., Nishanth, K., Kaushal, M., Sneha, D.N., Anil, A.C., 2017. Elucidation of the tidal influence on bacterial populations in a monsoon influenced estuary through simultaneous observations. Environ. Monit. Assess., 189, 1-17.

Kooistra, W.H.C.F., Gersonde, R.R., Medlin, L.K., Mann, D.G., 2007. The origin and evolution of the diatoms: their adaptation to a planktonic existence. Evolution of primary producers in the sea, ed. P.G. Falkowski, A.H. Knoll, Academic Press, Inc., 207-249.

Kumar, U., 2011. Study of Port Activities and Ship Scheduling Problem at Haldia Dock Complex. Ph.D. dissertation, Indian Institute of Technology, Kharagpur, India.

Kurapov, A., Allen, J., Egbert, G., 2010. Combined effects of wind-driven upwelling and internal tide on the continental shelf. J. Phys. Oceanogr., 40, 737-756.

Ladas, N.P., Papageorgiou, G.C., 2001. The salinity tolerance of freshwater cyanobacterium *Synechococcus* sp. PCC 7942 is determined by its ability for osmotic adjustment and presence of osmolyte sucrose. Photosynthetica, 38, 343-348.

Lallu, K., Fausia, K., Vinita, J., Balachandran, K., Kumar, K.N., Rehitha, T., 2014. Transport of dissolved nutrients and chlorophyll *a* in a tropical estuary, southwest coast of India. Environ. Monit. Assess., 186, 4829-4839.

Lemaire, E., Abril, G., De Wit, R., Etcheber, H., 2002. Distribution of phytoplankton pigmentsin nine European estuaries and implications for an estuarine typology, Biogeochemistry, 59, 5–23.

Landry, M.R., Barber, R.T., Bid, R.R., Chai, F., Coale, K.H., Dam, H.G., Lewis, M.R., Lindley, S.T., McCarthy, J.J., Roman, M.R., 1997. Iron and grazing constraints on primary production in the central equatorial Pacific: an EqPac synthesis. Limnol. Oceanogr., 42, 405-418.

Landry, M.R., Brown, S.L., Campbell, L., Constantinou, J., Liu, H. 1998. Spatial patterns in phytoplankton growth and microzooplankton grazing in the Arabian Sea during monsoon forcing. Deep Sea Res. Pt II, 45, 2353-2368.

Lantoine, F., Neveux, J., 1997. Spatial and seasonal variations in abundance and spectral characteristics of phycoerythrins in the tropical northeastern Atlantic Ocean. Deep Sea Res. Pt I, 44, 223-246.

Lee, Z., Weidemann, A., Kindle, J., Arnone, R., Carder, K.L., Davis, C., 2007. Euphotic zone depth: Its derivation and implication to ocean-color remote sensing. J. Geophysic. Res., Oceans, 112, 1-11.

Lefort-Tran, M., Pouphile, M., Spath, S., Packer, L., 1988. Cytoplasmic membrane changes during adaptation of the fresh water cyanobacterium *Synechococcus* 6311 to salinity. Plant physiol., 87, 767-775.

Li, W., Rao, S., Harrison, W., Smith, J., Cullen, J., Irwin, B., Platt, T., 1983. Autotrophic picoplankton in the tropical ocean. Science(Washington), 219, 292-295.

Li, W.K.W., Dickie, P.M., Irwin, B.D., Wood, A.M., 1992. Biomass of bacteria, cyanobacteria, prochlorophytes and photosynthetic eukaryotes in the Sargasso Sea. Deep-Sea Res., 39, 501-519.

Li, W.K.W., 1994. Primary production of prochlorophytes, cyanobacteria, and eukaryotic ultraphytoplankton: measurements from flow cytometric sorting. Limnol. Oceanogr., 39, 169-175.

Li, K.Z., Huang, L.M., Zhang, J.L., Yin, J.Q., Luo, L., 2010. Characteristics of phytoplankton community in the Pearl River Estuary during saline water intrusion period. J. Tropic. Oceanogr., 1, 1-10.

Li, S., Shi, X., Lepère, C., Liu, M., Wang, X., Kong, F., 2016. Unexpected predominance of photosynthetic picoeukaryotes in shallow eutrophic lakes. J. Plankton Res., 38, 830-842.

Lin, D., Zhu, A., Xu, Z., Huang, L., Fang, H., 2010. Dynamics of photosynthetic picoplankton in a subtropical estuary and adjacent shelf waters. J. Mar. Biol. Assoc. U.K., 90, 1319-1329.

Lindell, D., Post, A.F., 1995. Ultraphytoplankton succession is triggered by deep winter mixing in the Gulf of Aqaba (Eilat), Red Sea. Limnol. Oceanogr., 40, 1130-1141.

Litaker, W., Duke, C.S., Kenney, B.E., Ramus, J., 1993. Short-term environmental variability and phytoplankton abundance in a shallow tidal estuary. Mar. Ecol. Prog. Ser., 94, 141-141.

Liu, H., Campbell, L., Landry, M., Nolla, H., Brown, S., Constantinou, J., 1998. *Prochlorococcus* and *Synechococcus* growth rates and contributions to production in the Arabian Sea during the 1995 Southwest and Northeast Monsoons. Deep Sea Res. Pt II, 45, 2327-2352.

Liu, C.W., Lin, K.H., Kuo, Y.M., 2003. Application of factor analysis in the assessment of groundwater quality in a blackfoot disease area in Taiwan. Sci. Total Environ., 313, 77-89.

Liu, H., Dagg, M., Campbell, L., Urban-Rich, J., 2004. Picophytoplankton and bacterioplankton in the Mississippi River plume and its adjacent waters. Estuar. Coast., 27, 147-156.

Liu, S.M., Hong, G.H., Zhang, J., Ye, X.W., Jiang, X.L., 2009. Nutrient budgets for large Chinese estuaries. Biogeosciences, 6, 2245-2263.

Liu, H., Jing, H., Wong, T.H., Chen, B., 2013. Co-occurrence of phycocyanin-and phycoerythrin-rich *Synechococcus* in subtropical estuarine and coastal waters of Hong Kong. Env. Microbiol. Rep., 6, 90-99.

Liu, J., Fu, B., Yang, H., Zhao, M., He, B., Zhang, X.H., 2015. Phylogenetic shifts of bacterioplankton community composition along the Pearl Estuary: the potential impact of hypoxia and nutrients. Frontier. Microb., 6, 1-13.

Long, A., Sun, L., Shi, R., Zhou, W., Dang, A., 2012. Saltwater intrusion induced by a complete neap tide and its effect on nutrients variation in the Estuary of Pearl River, China. J. Coast. Res., 29, 1158-1168.

Lu, Z., Gan, J., 2014. Controls of seasonal variability of phytoplankton blooms in the Pearl River Estuary. Deep Sea Res. Pt II, 13, 86-96.

Mackay, M.A., Nortan, R.S., Borowitzka, L.J., 1984. Organic osmo-regulatory solutes in cyanobacteria. Microbiology, 130, 2177-2191.

Madhu, N., Jyothibabu, R., Balachandran, K., Honey, U., Martin, G., Vijay, J., Shiyas, C., Gupta, G., Achuthankutty, C., 2007. Monsoonal impact on planktonic standing stock and abundance in a tropical estuary (Cochin backwaters–India). Estuar. Coast. Shelf. Sci., 73, 54-64.

Madhu, N.V., Jyothibabu, R., Balachandran, K.K., 2009. Monsoon-induced changes in the size-fractionated phytoplankton biomass and production rate in the estuarine and coastal waters of southwest coast of India. Environ. Monit. Assess., 166, 521-528.

Madhu, N., Balachandran, K., Martin, G., Jyothibabu, R., Thottathil, S.D., Nair, M., Joseph, T., Kusum, K., 2010. Short-term variability of water quality and its implications on phytoplankton production in a tropical estuary (Cochin backwaters, India). Environ. Monit. Assess., 170, 287-300.

Madhupratap, M., Kumar, S.P., Bhattathiri, P., Kumar, D.M., Raghukumar, S., Nair, K.K. C., Ramaiah, N., 1996. Mechanism of the biological response to winter cooling in the northeastern Arabian Sea. Nature, 384, 549-552.

Malone, T.C., 1992. Effects of water column processes on dissolved oxygen, nutrients, phytoplankton and zooplankton. Oxygen dynamics in the Chesapeake Bay. A synthesis of recent research, 61-112.

Mandal, S., Choudhury, B.U., Mondal, M., Bej, S., 2013. Trend analysis of weather variables in Sagar Island, West Bengal, India: a long-term perspective (1982–2010). Curr. Sci., 105, 947-953.

Mann, K.H., 2009. Ecology of coastal waters: with implications for management. John Wiley & Sons, Hoboken, NJ.

Manoj, N., Unnikrishnan, A., 2009. Tidal circulation and salinity distribution in the Mandovi and Zuari estuaries: case study. J. Waterw. Port Coast., 135, 278-287.

Manoj, N., 2012. Estimation of flushing time in a monsoonal estuary using observational and numerical approaches. Nat. hazards, 64, 1323-1339.

Marie, D., Simon, N., Vaulot, D., 2005. Phytoplankton cell counting by flow cytometry. Algal Cultur. Techniq., 1, 253-267.

Marra, J., Dickey, T., Ho, C., Kinkade, C.S., Sigurdson, D.E., Weller, R.A., Barber, R.T., 1998. Variability in primary production as observed from moored sensors in the central Arabian Sea in 1995. Deep Sea Res. Pt II, 45, 2253-2267.

Marshall, H.G., 2009. Phytoplankton of the York River. J. Coastal Res., 57, 59-65.

Martin, G., Vijay, J., Laluraj, C., Madhu, N., Joseph, T., Nair, M., Gupta, G., Balachandran, K., 2008. Fresh water influence on nutrient stoichiometry in a tropical estuary, South West coast of India. Appl. Ecol. Env. Res., 6, 57-64.

Martin, G., Nisha, P., Balachandran, K., Madhu, N., Nair, M., Shaiju, P., Joseph, T., Srinivas, K., Gupta, G., 2011. Eutrophication induced changes in benthic community structure of a flow-restricted tropical estuary (Cochin backwaters), India. Environ. Monit. Assess., 176, 427-438.

Martin, G., George, R., Shaiju, P., Muraleedharan, K., Nair, S., Chandramohanakumar, N., 2012. Toxic metals enrichment in the surficial sediments of a eutrophic tropical estuary (Cochin Backwaters, Southwest coast of India). Sci. World J., 2012, 1-17.

Martin, G., Jyothibabu, R., Madhu, N., Balachandran, K., Nair, M., Muraleedharan, K., Arun, P., Haridevi, C., Revichandran, C., 2013. Impact of eutrophication on the occurrence of *Trichodesmium* in the Cochin backwaters, the largest estuary along the west coast of India. Environ. Monit. Assess., 185, 1237-1253.

Massana, R., 2011. Eukaryotic picoplankton in surface oceans. Annu. Rev. Microbiol., 65, 91-110.

McFarland, M.N., Rines, J., Sullivan, J., Donaghay, P., 2015. Impact of phytoplankton size and physiology on particulate optical properties determined with scanning flow cytometry. Mar. Ecol. Prog. Ser., 531, 43-61.

Menon, N., Balchand, A., Menon, N., 2000. Hydrobiology of the Cochin backwater system–a review. Hydrobiol., 430, 149-183.

Mitbavkar, S., Saino, T., Horimoto, N., Kanda, J., Ishimaru, T., 2009. Role of environment and hydrography in determining the picoplankton community structure of Sagami Bay, Japan. J. Oceanogr., 65, 195-208.

Mitbavkar, S., Anil, A.C., 2011. Tiniest primary producers in the marine environment: an appraisal from the context of waters around India. Curr. Sci., 100, 986-988.

Mitbavkar, S., Patil, J.S., Rajaneesh, K.M., 2015. Picophytoplankton as Tracers of Environmental Forcing in a Tropical Monsoonal Bay. Microb. Ecol., 7, 1-18.

Mitbavkar, S., Saino, T., 2015. Diurnal variability of *Synechococcus* abundance in Sagami Bay, Japan. Hydrobiologia, 747, 133–145.

Mohan, A.P., Jyothibabu, R., Jagadeesan, L., Lallu, K., Karnan, C., 2016. Summer monsoon onset-induced changes of autotrophic pico-and nanoplankton in the largest monsoonal estuary along the west coast of India. Environ. Monit. Assess., 188, 1-15.

Montani, S., Magni, P., Shimamoto, M., Abe, N., Okutani, K., 1998. The effect of a tidal cycle on the dynamics of nutrients in a tidal estuary in the Seto Inland Sea, Japan. J. Oceanogr., 54, 65-76.

Moore, L.R., Chisholm, S.W., 1999. Photophysiology of the marine cyanobacterium *Prochlorococcus*: Ecotypic differences among cultured isolates. Limnol. Oceanogr., 44, 628-638.

Moreira, D., López-García, P., 2002. The molecular ecology of microbial eukaryotes unveils a hidden world. Trend. Microbiol., 10, 31-38.

Morel, A., Ahn, Y., Partensky, F., Vaulot, D., Claustre, H., 1993. *Prochlorococcus* and *Synechococcus*: A comparative study of their optical properties in relation to their size and pigmentation. J. Mar. Res., 51, 617–649.

Morrison, J.M., Codispoti, L., Gaurin, S., Jones, B., Manghnani, V., Zheng, Z., 1998. Seasonal variation of hydrographic and nutrient fields during the US JGOFS Arabian Sea Process Study. Deep Sea Res. Pt II, 45, 2053-2101.

Mouriño-Carballido, B., Hojas, E., Cermeño, P., Chouciño, P., Fernández-Castro, B., Latasa, M., Marañón, E., Morán, X.A., Vidal, M., 2016. Nutrient supply controls picoplankton community structure during three contrasting seasons in the northwestern Mediterranean Sea. Mar. Ecol. Prog. Ser., 543, 1-19.

Mózes, A., Présing, M., Vörös, L., 2006. Seasonal dynamics of picocyanobacteria and picoeukaryotes in a large shallow lake (Lake Balaton, Hungary). Int. Rev. Hydrobiol., 91, 38-50.

Munawar, M., Weisse, T., 1989. Is the 'microbial loop'an early warning indicator of anthropogenic stress?. Hydrobiologia, 188, 163-174.

Murphy, L.S., Haucen, E.M., 1985. The distribution and abundance of phototrophic ultraplankton in the North Atlantic. Eimnoi. Oceanogr., 30, 47-58.

Murrell, M.C., Lores, E.M., 2004. Phytoplankton and zooplankton seasonal dynamics in a subtropical estuary: importance of cyanobacteria. J. Plankton Res., 26, 371-382.

Musale, A.S., Desai, D.V., Sawant, S.S., Venkat, K., Anil, A.C., 2015. Distribution and abundance of benthic macroorganisms in and around Visakhapatnam Harbour on the east coast of India. J. Mar. Biol. Assoc. U.K., 95, 215-231.

Nair, V.R., 1980. Production and associations of zooplankton in estuarine and nearshore Waters of Goa. Indian J. Mar. Sci., 9, 116-119.

Naqvi, S.W.A., Jayakumar, D.A., Narvekar, P.V., Naik, H., Sarma, V.V.S.S., D'Souza, W., Joseph, S., George, M.D., 2000. Increased marine production of N_2O due to intensifying anoxia on the Indian continental shelf. Nature, 408, 346-349.

Naqvi, S., Naik, H., Narvekar, P., 2003. The Arabian Sea. in: Biogeochemistry of Marine Systems, edited by: Black, K. and Shimmield, G., Blackwell, Oxford, U.K.,157-207.

Naqvi, S., Moffett, J.W., Gauns, M., Narvekar, P.V., Pratihary, A.K., Naik, H., Shenoy, D. M., Jayakumar, D.A., Goepfert T.J., Patra, P.K., Al-Azri, A., 2010. The Arabian Sea as a high-nutrient, low-chlorophyll region during the late southwest monsoon. Biogeosciences, 7, 2091-2100.

Ni, Z., Huang, X., Zhang, X., 2015. Picoplankton and virioplankton abundance and community structure in Pearl River Estuary and Daya Bay, South China. J. Environ. Sci., 32, 146-154.

Ning X, Vaulot D., 1992. Estimating *Synechococcus* spp. growth rates and grazing pressure by heterotrophic nano-picoplankton in the English Channel and the Celtic Sea. Acta. Oceanol. Sinica., 11, 255-273.

Ning, X., Cloern, J.E., Cole, B.E., 2000. Spatial and temporal variability of picocyanobacteria *Synechococcus* sp. in San Francisco Bay. Limnol. Oceanogr., 45, 695-702.

Nixon, S.W., 1986. Nutrient dynamics and the productivity of marine coastal waters. In D. Clayton and M. Beh-behani (eds.), Coastal Eutrophication. The Alden Press, Oxford, U.K., 97-115.

Nobre, A.M., 2009. An ecological and economic assessment methodology for coastal ecosystem management. Env. Manag. 44, 185–204.

Not, F., Latasa, M., Scharek, R., Viprey, M., Karleskind, P., Balagué, V., Ontoria-Oviedo, I., Cumino, A., Goetze, E., Vaulot, D., Massana, R., 2008. Protistan assemblages across the Indian Ocean, with a specific emphasis on the picoeukaryotes. Deep Sea Res. Pt I, 55, 1456-1473.

Nubel, U., Garcia-Pichel, F., Muyzer, G., 1997. PCR primers to amplify 16S rRNA genes from cyanobacteria. App. Environ. Microb., 63, 3327-3332.

Ochs, C.A., Rhew, K., 1997. Population dynamics of autotrophic picoplankton in a southeastern US reservoir. Int. Rev. Hydrobiol., 82, 293-313.

Olson, R.J., Chisholm, S., Zettler, E.R., Altabet, M., Dusenberry, J.A., 1990. Spatial and temporal distributions of prochlorophyte picoplankton in the North Atlantic Ocean. Deep Sea Res. Part A, Oceanogr. Res., 37, 1033–1051.

Örnólfsdóttir, E.B., Lumsden, S.E., Pinckney, J.L., 2004. Phytoplankton community growth-rate response to nutrient pulses in a shallow turbid estuary, Galveston Bay, Texas. J. Plankton Res., 26, 325-339.

Ozturk, S., Aslim, B., 2010. Modification of exopolysaccharide composition and production by three cyanobacterial isolates under salt stress. Environ. Sci. Pollut. Res., 17, 595-602.

Padmavati, G., Goswami., S.C., 1996. Zooplankton ecology in the Mandovi-Zuari estuarine system of Goa, west coast of India. Indian J. Geo. Mar. Sci., 25, 268-273.

Paerl, H.W., 1977. Ultraphytoplankton biomass and production in some New Zealand lakes. New Zeal. J. Mar. Fresh., 11, 297-305.

Paerl, H.W., Valdes, L.M., Peierls, B.L., Adolf, J.E., Harding Jr., L., 2006. Anthropogenic and climatic influences on the eutrophication of large estuarine ecosystems. Limnol. Oceanogr., 51, 448-462.

Paerl, H.W., Valdes-Weaver, L.M., Joyner, A.R., Winkelmann, V., 2007. Phytoplankton indicators of ecological change in the eutrophying Pamlico Sound system, North Carolina. Ecol. App., 17, 88-101.

Palenik, B., 2001. Chromatic Adaptation in Marine Synechococcus Strains. Appl. Environ. Microb., 67, 991-994.

Pan, L., Zhang, J., Zhang, L., 2007. Picophytoplankton, nanophytoplankton, heterotrohpic bacteria and viruses in the Changjiang Estuary and adjacent coastal waters. J. Plank. Res., 29, 187-197.

Parab, S.G., Matondkar, S.P., Gomes, H.D.R., Goes, J.I., 2006. Monsoon driven changes in phytoplankton populations in the eastern Arabian Sea as revealed by microscopy and HPLC pigment analysis. Cont. Shelf Res., 26, 2538-2558.

Parsons, T., Maita, Y., Lalli, C., 1984. A manual of chemical and biological methods for seawater analysis. Pergamon Press, Oxford.

Partensky, F., Hess, W.R., Vaulot, D., 1999. *Prochlorococcus*, a marine photosynthetic prokaryote of global significance. Microbiol. Mol. Biol. Rev., 63, 106–426.

Partensky, F., Hoepffner, N., Li, W.K., Ulloa, O., Vaulot, D., 1993. Photoacclimation of *Prochlorococcus* sp. (Prochlorophyta) strains isolated from the North Atlantic and the Mediterranean Sea. Plant Physiol., 101, 285-296.

Patil, J.S., Anil, A.C., 2008. Temporal variation of diatom benthic propagules in a monsoon influenced tropical estuary. Cont. Shelf Res., 28, 2404-2416.

Patil, J.S., Anil, A.C., 2011. Variations in phytoplankton community in a monsoon-influenced tropical estuary. Environ. Monit. Assess., 182, 291-300.

Patil, J.S., Anil, A.C., 2015. Effect of monsoonal perturbations on the occurrence of phytoplankton blooms in a tropical bay. Mar. Ecol. Prog. Ser., 530, 77-92.

Paulsen, M.L., Riisgaard, K., Frede, T., St John, M., Nielsen, T.G., 2015. Winter-spring transition in the subarcticAtlantic: microbial response to deep mixing and pre-bloom production. Aquat. Microb. Ecol., 76, 49–69.

Pednekar, S.M., Matondkar, S.G.P., Gomes, H.D.R., Goes, J.I., Parab, S., Kerkar, V., 2011. Fine-scale responses of phytoplankton to freshwater influx in a tropical monsoonal estuary following the onset of southwest monsoon. J. Earth. Syst. Sci., 120, 545-556.

Peters, H., 1997. Observations of stratified turbulent mixing in an estuary: Neap-to-spring variations during high river flow. Estuar. Coast. Shelf. Sci., 45: 69-88.

Phinney, D.A., Cucci, T.L., 1989. Flow cytometry and phytoplankton. Cytometry, 10, 511-521.

Phlips, E.J., Badylak, S., Hart, J., Haunert, D., Lockwood, J., O'Donnell, K., Sun, D., Viveros, P., Yilmaz, M., 2012. Climatic influences on autochthonous and allochthonous phytoplankton blooms in a subtropical estuary, St. Lucie Estuary, Florida, USA. Estuar. Coast., 35, 335-352.

Pick, F.R., 1991. The abundance and composition of freshwater picocyanobacteria in relation to light penetration. Limnol. Oceanogr., 36, 1457-1462.

Pitchaikani, J.S., Ananthan, G., Sudhakar, M., 2010. Studies on the effect of coolant water effluent of tuticorin thermal power station on hydro biological characteristics of Tuticorin Coastal Waters, South East Coast of India. Curr. Res. J. Biol. Sci., 2, 118-123.

Platt, T., Rao, D.S., Irwin, B., 1983. Photosynthesis of picoplankton in the oligotrophic ocean. Nature, 301, 702-704.

Pomeroy, L.R., 1974. The ocean's food web, a changing paradigm. Bioscience, 24, 499-504.

Prasanna Kumar, S., Madhupratap, M., Dileep Kumar, M., Gauns, M., Muraleedharan, P. M., Sarma, V.V.S.S., De Souza, S.N., 2000. Physical control of primary productivity on a seasonal scale in central and eastern Arabian Sea. J. Earth. Syst. Sci., 109, 433-441.

Prasanna Kumar, S., Muraleedharan, P.M., Prasad, T.G., Gauns, M., Ramaiah, N., DeSouza, S.N., Madhupratap, M., 2002. Why is the Bay of Bengal less productive during summer monsoon compared to the Arabian Sea?. Geophys. Res. Lett., 29, 88-91.

Purcell-Meyerink, D., Fortune, J. and Butler, E.C.V., 2017. Productivity dominated by picoplankton in a macro-tidal tropical estuary, Darwin Harbour. New Zealand J. Bot., 55, 47-63.

Qasim, S., Reddy, C., 1967. The estimation of plant pigments of Cochin Backwater during the monsoon months. Bull. Mar. Sci., 17, 95-110.

Qasim, S., Gopinathan, C., 1969. Tidal cycle and the environmental features of Cochin Backwater (a tropical estuary). Proc. Indian Acad. Sci., 336-353.

Qasim, S.Z., 1977. Biological productivity of the Indian Ocean. Indian J. Mar. Sci., 6, 122-137.

Qasim, S., Sen Gupta, R., 1981. Environmental characteristics of the Mandovi-Zuari estuarine system in Goa. Estuar. Coast. Shelf. Sci., 13, 557-578.

Qasim, S.Z., 1982. Oceanography of the northern Arabian Sea. Deep Sea Res. Pt I, 29, 1041-1068.

Qasim, S.Z., 2003. Indian estuaries. Allied publishers.

Qiu, D., Huang, L., Zhang, J., Lin. S., 2010. Phytoplankton dynamics in and near the highly eutrophic Pearl River Estuary, South China Sea. Cont. Shelf Res., 30, 177-186.

Radhakrishna, K., Bhattathiri, P.M.A., Devassy, V.P., 1978. Primary productivity of Bay of Bengal during AugustSeptember 1976. Indian J. Mar. Sci., 7, 94–98.

Ram, A., 2002. Studies on the role of bacteria in the assimilation of organic inputs in coastal waters. Ph.D. dissertation, Goa University, Goa, India.

Raman, A.V., 1995. Pollution effects in Visakhapatnam harbour, India: an overview of 23 years of investigations and monitoring. Helgol. Meeresunters., 49, 633–645.

Ramanibai, R., 2015. Marine Species Conservation in India with special reference to Zooplankton. Magazine of Zoo Outreach Organization, 5, 2-8.

Ramasamy, M.S., Murugan, A., 2003. Chemical defense in ascidians Eudistoma viride and Didemnum psammathodes in Tuticorin, southeast coast of India: Bacterial epibiosis and fouling deterrent activity. Ind. J. Mar. Sci., 32, 337-339.

Rao, A.D., Joshi, M., Ravichandran, M., 2008. Oceanic upwelling and downwelling processes in waters off the west coast of India. Ocean Dynam., 58, 213-226.

Rao, S., Shirlal, K.G., Radheshyam, B., Mahaganesha, K., 2004. Study of littoral transport along Dakshina Kannada coast, Karnataka. INCHOE, 1, 89-95.

Raven, J.A., 1998. The twelfth Tansley Lecture. Small is beautiful: the picophytoplankton. Funct. Ecol., 12, 503-513.

Ray, R.T., Haas, L.W., Sieracki, M.E., 1989. Autotrophic picoplankton dynamics in a Chesapeake Bay sub-estuary. Mar. Ecol. Prog. Ser., 52, 273-285.

Read, D.S., Bowes, M.J., Newbold, L.K., Whiteley, A.S., 2014. Weekly flow cytometric analysis of riverine phytoplankton to determine seasonal bloom dynamics. Environ. Sci., 16, 594-603.

Reckermann, M., Veldhuis, M.J., 1997. Trophic interactions between picophytoplankton and micro-and nanozooplankton in the western Arabian Sea during the NE monsoon 1993. Aquat. Microb. Ecol., 12, 263-273.

Reed, R.H., Richardson, D.L., Warr, S.R., Stewart, W.D., 1984. Carbohydrate accumulation and osmotic stress in cyanobacteria. Microbiology, 130, 1-4.

Richardson, T.L., Jackson, G.A., 2007. Small phytoplankton and carbon export from the surface ocean. Science, 315, 838-840.

Rochelle-Newall, E. J., Chu, V. T., Pringault, O., Amouroux, D., Arfi, R., Bettarel, Y., et al. (2011). Phytoplankton diversity and productivity in a highly turbid, tropical coastal system (Bach Dang Estuary, Vietnam). Mar. Pollut. Bullet., 62, 2317–2329.

Roy, R., Chitari, R., Kulkarni, V., Krishna, M.S., Sarma, V.V.S.S., Anil, A.C., 2015. CHEMTAX-derived phytoplankton community structure associated with temperature fronts in the northeastern Arabian Sea. J. Mar. Res., 144, 81-91.

Roy, R., Anil, A.C., 2015. Complex interplay of physical forcing and *Prochlorococcus* population in ocean. Prog. Oceanogr., 137, 250-260.

Rudra, K., 2011. The Encroaching Ganga and Social Conflicts: The Case of West Bengal, India. Department of Geography, Habra S.C. Mahavidyalaya (College), West Bengal, India, 1-38.

Sadhuram, Y., Sarma, V.V., Murthy, T.V.R., Rao, B.P., 2005. Seasonal variability of physico-chemical characteristics of the Haldia channel of Hooghly estuary, India. J. Earth Syst. Sci., 114, 37-49.

Samanta, B., Bhadury, P., 2014. Analysis of diversity of chromophytic phytoplankton in a mangrove ecosystem using rbcL gene sequencing. J. Phycol., 50, 328-340.

Saitou, N., Nei, M., 1987. The neighbor-joining method: a new method for reconstructing phylogenetic trees. Mol. Biol. Evol., 4, 406-425.

Sarma, V., Gupta, S., Babu, P., Acharya, T., Harikrishn achari, N., Vishnuvardhan, K., Rao, N., Reddy, N., Sarma, V., Sadhuram, Y., 2009. Influence of river discharge on plankton metabolic rates in the tropical monsoon driven Godavari estuary, India. Estuar. Coast. Shelf Sci., 85, 515-524.

Sawant, S., Madhupratap, M., 1996. Seasonality and composition of phytoplankton in the Arabian Sea. Curr. Sci., 71, 869-873.

Scanlan, D.J., 2003. Physiological diversity and niche adaptation in marine *Synechococcus.* Adv. Microb. Physiol., 47, 1-64.

Schattenhofer, M., Fuchs, B.M., Amann, R., Zubkov, M.V., Tarran, G.A., Pernthaler, J., 2009. Latitudinal distribution of prokaryotic picoplankton populations in the Atlantic Ocean. Environ. Microbiol., 11, 2078-2093.

Shalapyonok, A.,R.J., Olson, L.S., Shalapyonok, 2001. Arabian Sea phyto-plankton during southwest and northeast monsoons 1995: Composition,size structure and biomass from individual cell properties measured by flow cytometry. Deep Sea Res., Part II, 48, 1231-1261.

Shang, X., Zhang, L., Zhang, J., 2007. *Prochlorococcus*-like populations detected by flow cytometry in the fresh and brackish waters of the Changjiang Estuary. J. Mar. Biol. Assoc. U.K., 87, 643-648.

Shankar, R., Karbassi, A.R., 1991. Geocbemistry and Magnetic Susceptibility of Surficial Sediments of the New Mangalore Port. J. Geol. Soc. India, 38, 412-417.

Shankar, D., Shenoi, S., Nayak, R., Vinayachandran, P.N., Nampoothiri, G., Almeida, A.M., Michael, G.S., Ramesh Kumar, M.R., Sundar, D., Sreejith, O.P., 2005. Hydrography of the eastern Arabian Sea during summer monsoon 2002. J. Earth. Syst. Sci., 114, 459-474.

Shanthi, M., Ramanibai, R., 2011. Studies on copepods from chennai coast (Cooum and Adyar), bay of Bengal-during the cruise. Curr. Res. J. Biol. Sci., 3, 32-136.

Shapiro, L.P., Guillard, R.R.L., 1986. Physiology and ecology of the marine eukaryotic ultraplankton. Can. Bull. Fish. Aquat. Sci., 214, 371-389.

Sharples, J., Moore, C.M., Abraham, E.R., 2001. Internal tide dissipation, mixing, and vertical nitrate flux at the shelf edge of NE New Zealand. J. Geophys. Res., 106, 14069–14081.

Sharples, J., Moore, C.M., Hickman, A.E., Holligan, P.M., Tweddle, J.F., Palmer, M.R., Simpson, J.H., 2009. Internal tidal mixing as a control on continental margin ecosystems. Geophys. Res. Lett., 36, 1-5.

Sheng, G.P., Yu, H.Q., Yue, Z., 2006. Factors influencing the production of extracellular polymeric substances by *Rhodopseudomonas acidophila*. Int. Biodeter. Biodegr., 58, 89–93.

Shenoi, S.C., Antony M.K., 1991. Current measurements over the western continental shelf of India. Cont. Shelf Res., 11, 81-93.

Shetye, S., Murty, C., 1987. Seasonal variation of the salinity in the Zuari estuary, Goa, India. J. Earth. Syst. Sci., 96, 249-257.

Shetye, S., Gouveia, A., Shenoi, S., 1994. Circulation and water masses of the Arabian Sea. Proceed. Indian Academ. Sci. Earth Planet. Sci., 103, 107-123.

Shetye, S.R., 1999. Propagation of tides in the Mandovi and Zuari estuaries. Sadhana (Academy Proceedings in Engineering Sciences). Ind. Acad. Sci., 24, 5-16.

Shetye, S., Shankar, D., Neetu, S., Suprit, K., Michael, G., Chandramohan, P., 2007. The environment that conditions the Mandovi and Zuari estuaries. The Mandovi and Zuari Estuaries. NIO, Dona Paula, Goa, India, 29–38.

Shimada, A., Nishijima, M., Maruyama, T., 1995. Seasonal appearance of *Prochlorococcus* in Suruga Bay, Japan in 1992–1993. J. Oceanogr., 51, 289-300.

Shiomoto, A., Tadokoro, K., Monaka, K., Nanba, M., 1997. Productivity of picoplankton compared with that of larger phytoplankton in the subarctic region. J. Plank. Res., 19, 907-916.

Shirodkar, P.V., Pradhan, U.K., Vethamony, P., 2010. Impact of water quality changes on harbour environment due to port activities along the west coast of India. In: Proc. 2nd Int. Conf. on Coastal Zone Eng. and Management, Muscat, Oman, 2010, 1–3.

Shivaprasad, A., Vinita, J., Revichandran, C., Manoj, N., Srinivas, K., Reny, P., Ashwini, R., Muraleedharan, K., 2012. Influence of Saltwater Barrage on Tides, Salinity, and Chlorophyll a in Cochin Estuary, India. J. Coast. Res., 29, 1382-1390.

Short, F.T., Neckles, H.A., 1999. The effects of global climate change on seagrasses. Aquat. Botany, 63, 169-196.

Shynu, R., Purnachandra, R.V., Parthiban, G., Balakrishnan, S., Tanuja, N., Pratima, M.K., 2013. REE in suspended particulate matter and sediment of the Zuari estuary and adjacent shelf, western India: Influence of mining and estuarine turbidity. Mar. Geol., 346, 326–342.

Simek, K., Hartman, P., Nedoma, J., Pernthaler, J., Springmann, D., Vrba, J., Psenner, R., 1997. Community structure, picoplankton grazing and zooplankton control of heterotrophic nanoflagellates in a eutrophic reservoir during the summer phytoplankton maximum. Aquat. Microb. Ecol., 12, 49-63.

Sin, Y., Wetzel, R.L., Anderson, I.C., 2000. Seasonal variation of size-fractionated phytoplankton along the salinity gradient in the York River estuary, Virginia (USA). J. Plank. Res., 22, 1945-1960.

Sin, Y., Hyun, B., Jeong, B., Soh, H.Y., 2013. Impacts of eutrophic freshwater inputs on water quality and phytoplankton size structure in a temperate estuary altered by a sea dike. Mar. Environ. Res., 85, 54-63.

Singh, S.C., Sinha, R.P., Hader, D.P., 2002. Role of lipids and fatty acids in stress tolerance in cyanobacteria. Acta Protozool., 41, 297-308.

Singh, S.P., Montgomery, B.L., 2013. Salinity impacts photosynthetic pigmentation and cellular morphology changes by distinct mechanisms in *Fremyella diplosiphon*. Biochem. Biophys. Res. Commun., 433, 84-89.

Smith, P.C., Sandstrom, H., 1988. Physical processes at the shelf edge in the Northwest Atlantic. J. Northwest Atlantic Fish. Sci., 8, 5-13.

Stephens, R., Imberger, J., 1996. Dynamics of the Swan River Estuary: the seasonal variability. Mar. Freshwater Res., 47, 517-529.

Stockner, J.G., Antia, N.J., 1986. Algal picoplankton from marine and freshwater ecosystems: a multidisciplinary perspective. Can. J. Fish. Aquat. Sci., 43, 2472-2503.

Stolte, W., Riegman, R., 1995. Effect of phytoplankton cell size on transient-state nitrate and ammonium uptake kinetics. Microbiology, 141, 1221-1229.

Stomp, M., Huisman, J., Voros, L., Pick, F.R., Laamanen, M., Haverkamp, T., Stal, L.J., 2007. Colourful coexistence of red and green picocyanobacteria in lakes and seas. Ecol. Lett.,10, 290-298.

Sudhakar, M., Trishul, A., Doble, M., Kumar, K.S., Jahan, S.S., Inbakandan, D., Viduthalai, R.R., Umadevi, V.R., Murthy, P.S., Venkatesan, R., 2007. Biofouling and biodegradation of polyolefins in ocean waters. Polym. Degrad. Stab., 92, 1743-1752.

Suja, S., Pratima, M.K, Shynu, R., Purnachandra, R.V., Lina, L.F., 2016. Spatial distribution of suspended particulate matter in the Mandovi and Zuari estuaries: inferences on the estuarine turbidity maximum. Cur. Sci., 110, 1165-1168.

Sundar, D., Unnikrishnan, A., Michael, G., Kankonkar, A., Nidheesh, A., Subeesh, M., 2015. Observed variations in stratification and currents in the Zuari estuary, west coast of India. Environ. Earth Sci., 74, 6951-6965.

Tamura, K., Peterson, D., Peterson, N., Stecher, G., Nei, M., Kumar, S., 2011. MEGA5: molecular evolutionary genetics analysis using maximum likelihood, evolutionary distance, and maximum parsimony methods. Mol. Biol. Evol., 28, 2731–2739.

Taylor, A.H., Geider, R.J., Gilbert, F.J., 1997. Seasonal and latitudinal dependencies of phytoplankton carbon-to-chlorophyll *a* ratios: results of a modelling study. Mar. Ecol. Prog. Ser., 152, 51-66.

Telesh, I.V., Schubert, H., Skarlato, S.O., 2011. Revisiting Remane's concept: evidence for high plankton diversity and a protistan species maximum in the horohalinicum of the Baltic Sea. Mar. Ecol. Prog. Ser., 421, 1-11.

Ter Braak, C.J., Smilauer, P., 2002. CANOCO reference manual and CanoDraw for Windows user's guide: software for canonical community ordination (version 4.5).

Thompson, J.D., Higgins, D.G., Gibson, T.J., 1994. CLUSTAL W: improving the sensitivity of progressive multiple sequence alignment through sequence weighting, position-specific gap penalties and weight matrix choice. Nucleic Acids Res., 22, 4673–4680.

Ting, C.S., Rocap, G., King, J. Chisholm, S.W., 2002. Cyanobacterial photosynthesis in the oceans: the origins and significance of divergent light-harvesting strategies. Trends Microbiol., 10, 134-142.

Tripathy, S.C., KusumaKumari, B.A.V.L., Sarma, V.V., Murty, T.R., 2005. Evaluation of trophic state and plankton abundance from the environmental parameters of Visakhapatnam harbour and near-shore waters, east coast of India. Asian J. Microbiol. Biotechnol. Environ. Sci., 7, 831–838.

Tsai, A.Y., Chiang, K.P., Chang, J., Gong, G.C., 2005. Seasonal diel variations of picoplankton and nanoplankton in a subtropical western Pacific coastal ecosystem. Limnol. Oceanogr., 50, 1221-1231.

Tsai, A.Y., Chiang, K.P., Chang, J., Gong, G.C., 2008. Seasonal variations in trophic dynamics of nanoflagellates and picoplankton in coastal waters of the western subtropical Pacific Ocean. Aquat. Microb. Ecol., 51, 263-274.

Unnithan, R., Vijayan, M., Remani, K., 1975. Organic pollution in Cochin backwaters. Indian J. Mar. Sci., 4, 39-42.

Vaulot, D., Partensky, F., Neveux, J., Mantoura, R.F.C., Llewellyn, C.A., 1990. Winter presence of prochlorophytes in surface waters of the northwestern Mediterranean Sea. Limnol. Oceanogr., 35, 1156-1164.

Vaulot, D., Marie, D., 1999. Diel variability of photosynthetic picoplankton in the equatorial Pacific. J. Geophys. Res., 104, 3297-3310.

Vaulot, D., Eikrem, W., Viprey, M., Moreau, H., 2008. The diversity of small eukaryotic phytoplankton (≤ 3 μm) in marine ecosystems. FEMS Microbiol. Rev., 32, 795-820.

Verspagen, J.M., Van de Waal, D.B., Finke, J.F., Visser, P.M., Huisman, J., 2014. Contrasting effects of rising CO_2 on primary production and ecological stoichiometry at different nutrient levels. Ecol. Lett., 17, 951–960.

Vijayan, M., Ramani, K., Unnithan, R., 1976. Effects of organic pollution on some hydrographic features of Cochin backwaters. J. Mar. Sci., 5, 196-200.

Vijith, V., Sundar, D., Shetye, S., 2009. Time-dependence of salinity in monsoonal estuaries. Estuar. Coast. Shelf Sci., 85, 601-608.

Vinita, J., Shivaprasad, A., Manoj, N., Revichandran, C., Naveenkumar, K., Jineesh, V., 2015. Spatial tidal asymmetry of Cochin estuary, West Coast, India. J. Coast. Conserv., 19, 537-551.

Vollenweider, R., Giovanardi, F., Montanari, G., Rinaldi, A., 1998. Characterization of the trophic conditions of marine coastal waters, with special reference to the NW Adriatic Sea: proposal for a trophic scale, turbidity and generalized water quality index. Environmetrics, 9, 329-357.

Wang, B., Liu, C.Q., Wang, F., Yu, Y., Zhang, L., 2008. The distributions of autumn picoplankton in relation to environmental factors in the reservoirs along the Wujiang River in Guizhou Province, SW China. Hydrobiologia, 598, 35-45.

Wang, K., Wommack, K.E., Chen, F., 2011. Abundance and distribution of *Synechococcus* spp. and cyanophages in the Chesapeake Bay. Appl. Environ. Microb., 77, 7459-7468.

Waterbury, J.B., Watson, S.W., Guillard, R.R., Brand, L.E., 1979. Widespread occurrence of a unicellular, marine, planktonic, cyanobacterium . Nature, 277, 293-294.

Waterbury, J.B., Rippka, R., 1989. Subsection I. Order Chroococcales Wettstein 1924, emend. Rippka et al. 1979. In Bergey's Manual of Systematic Bacteriology, 1728–1746. Edited by J. T. Staley, M. P. Bryant, N. Pfennig & J. G. Holt. Baltimore: Williams & Wilkins.

Westerbom, M., Kilpi, M., Mustonen, O., 2002. Blue mussels, *Mytilusedulis*, at the edge of the range: population structure, growth and biomass along a salinity gradient in the north-eastern Baltic Sea. Mar. Biol., 140, 991-999.

Wetz, M.S., Paerl, H.W., Taylor, J.C., Leonard, J.A., 2011. Environmental controls upon picophytoplankton growth and biomass in a eutrophic estuary. Aquat. Microb. Ecol., 63, 133.

Wiggert, J., Jones, B., Dickey, T., Brink, K.H., Weller, R.A., Marra, J., Codispoti, L.A., 2000. The Northeast Monsoon's impact on mixing, phytoplankton biomass and nutrient cycling in the Arabian Sea. Deep Sea Res. Pt II, 47, 1353-1385.

Wolanski, E., Pickard, G., 1983. Upwelling by internal tides and Kelvin waves at the continental shelf break on the Great Barrier Reef. Mar. Freshwater Res., 34, 65-80.

Wood, A.M., 1985. Adaptation of photosynthetic apparatus of marine ultraphytoplankton to natural light fields. Nature, 316, 253-255.

Wood, H.L., Sundell K., Almroth, B.C., Sköld, H.N., Eriksson, S.P., 2016. Population-dependent effects of ocean acidification. Proc. R. Soc. B, 283, 1-7.

Worden, A.Z., Nolan, J.K., Palenik, B., 2004. Assessing the dynamics and ecology of marine picophytoplankton: the importance of the eukaryotic component. Limnol. Oceanogr., 49, 168–179.

Worden, A.Z., 2006. Picoeukaryote diversity in coastal waters of the Pacific Ocean. Aquat. Microb. Ecol., 43, 165–175.

Wyrtki, K., 1973. Physical oceanography of the Indian Ocean. In The biology of the Indian Ocean, B. Zeitzschel (ed.). Springer Berlin Heidelberg, 18-36.

Xia, X., Vidyarathna, N.K., Palenik, B., Lee, P., Liu, H., 2015. Comparison of the Seasonal Variations of *Synechococcus* Assemblage Structures in Estuarine Waters and Coastal Waters of Hong Kong. Appl. Environ. Microbiol., 81, 7644-765.

Yin, K., Qian, P.Y., Chen, J.C., Hsieh, D.P., Harrison, P.J., 2000. Dynamics of nutrients and phytoplankton biomass in the Pearl River estuary and adjacent waters of Hong Kong during summer: preliminary evidence for phosphorus and silicon limitation. Mar. Ecol. Prog. Ser., 194, 295-305.

Yves, D., Awa, N., 2007. Assemblages of phytoplankton pigments along a shipping line through the North Atlantic and tropical Pacific. Prog. Oceanogr., 73, 127–144.

Zhang, X., Shi, Z., Ye, F., Zeng, Y., Huang, X., 2013. Picophytoplankton abundance and distribution in three contrasting periods in the Pearl River Estuary, South China. Mar. Fresh. Res., 64, 692-705.

Zhou, W., Gao, J., Liao, J., Shi, R., Li, T., Guo, Y., Long, A., 2016. Characteristics of Phytoplankton Biomass, Primary Production and Community Structure in the Modaomen Channel, Pearl River Estuary, with Special Reference to the Influence of Saltwater Intrusion during Neap and Spring Tides. PloS One, 11, 1-19.

Zhu, W., Wan, L., Zhao, L., 2010. Effect of nutrient level on phytoplankton community structure in different water bodies. J. Environ. Sci., 22, 32-39.

Zinser, E.R., Lindell, D., Johnson, Z.I., Futschik, M.E., Steglich, C., Coleman, M.L., Wright, M.A., Rector, T., Steen, R., McNulty, N., Thompson, L.R., 2009. Choreography of the transcriptome, photophysiology, and cell cycle of a minimal photoautotroph, *Prochlorococcus*. PLoS One, 4, 1-18.

Zubkov, M.V., Sleigh, M.A., Tarran, G.A., Burkill, P.H., Leakey, R.J., 1998. Picoplanktonic community structure on an Atlantic transect from 50^{o}N to 50^{o}S. Deep Sea Res. Pt I, 45, 1339-1355.

Zubkov, M.V., Sleigh, M.A., Burkill, P.H., Leakey, R.J.G., 2000. Picoplankton community structure on the Atlantic Meridional Transect: a comparison between seasons. Prog. Oceanogr., 45, 369–386.

Zubkov, M.V., 2014. Faster growth of the major prokaryotic versus eukaryotic CO_2 fixers in the oligotrophic ocean. Nat. Commun., 5, 1-6.

Zwirglmaier, K., Heywood, J.L., Chamberlain, K., Woodward, E.M.S., Zubkov, M.V., Scanlan, D.J., 2007. Basin-scale distribution patterns of picocyanobacterial lineages in the Atlantic Ocean. Env. Microb., 9, 1278-1290.

http://www.vocport.gov.in/portlayout.aspx

http://www.vocport.gov.in/port/userinterface/statisticals.aspx

http://www.chennaiport.gov.in

http://www.newmangalore-port.com

http://www.kolkataporttrust.gov.in

Publications

Continental Shelf Research 146 (2017) 28–36

Contents lists available at ScienceDirect

Continental Shelf Research

journal homepage: www.elsevier.com/locate/csr

Research papers

Influence of short-term hydrographic variations during the north-east monsoon on picophytoplankton community structure in the eastern Arabian Sea

K.M. Rajaneesh, Smita Mitbavkar*, A.C. Anil

Council of Scientific and Industrial Research, National Institute of Oceanography, Dona Paula, Goa 403004, India

ARTICLE INFO

Keywords:
Eastern Arabian Sea
Picophytoplankton
Community structure
Hydrography
High resolution sampling
Environmental factors

ABSTRACT

The eastern Arabian Sea over the continental margin is a dynamic region subjected to short-term variability in hydrography as a result of various physical forcing such as coastal advection and vertical mixing. In order to assess the influence of hydrography on the picophytoplankton community, a temporal high resolution (every 3 h for nine days) study was carried out at a fixed location (15° 18′ 46″N, 72° 41′ 53″E) in the eastern Arabian Sea during the early north-east monsoon (November 2011). The picophytoplankton community comprised of *Synechococcus*, *Prochlorococcus*, and picoeukaryotes. Based on the temperature and salinity distribution, the study period was divided into phase I representing a stratified water column and phase II representing a vertically mixed water column. Phase I had higher picophytoplankton abundance with the initial dominance of *Prochlorococcus* which was later taken over by picoeukaryotes. Towards the end of phase I, with the initiation of vertical mixing, picoeukaryotes were the first to respond to the nutrient influx. As the vertical mixing intensified during phase II, the picophytoplankton abundance declined. Picophytoplankton carbon biomass and their contribution to total phytoplankton biomass was relatively higher during phase I with picoeukaryotes as the major contributors. These transient variations in picophytoplankton abundance highlights the importance of high frequency observations at the single cell level for better understanding the population dynamics in such environments.

1. Introduction

The Arabian Sea (AS) constitutes the north-western part of the Indian Ocean and its semi-enclosed feature leads to an unusual climate, hydrography, and biogeochemical processes (Naqvi et al., 2003). As a result of the semiannual reversal of monsoon winds, seasonal variation of water column characteristics is also observed (Qasim, 1982; Banse, 1987). During the south west monsoon (SWM), coastal upwelling is a common phenomenon (Banse, 1968; Banse and McClain, 1986; Shetye et al., 1994) whereas during the north-east monsoon (NEM) convective mixing is prominent in the northern AS (Madhupratap et al., 1996) with decreasing intensity of mixing towards the southern AS (Prasanna Kumar et al., 2000). Additionally, during this period downwelling is also observed (Rao et al., 2008). Monsoonal forcing results in seasonal variations in the mixed layer depth, flux of nutrients to the upper mixed layer and thereby on pelagic food web structure and production (Madhupratap et al., 1996; Morrison et al., 1998; Prasanna Kumar et al., 2000; Wiggert et al., 2000; Shankar et al., 2005).

In the AS, phytoplankton biomass and primary productivity are high during the SWM and the NEM (Marra et al., 1998; Prasanna Kumar et al., 2000). During the NEM, interannual variations in the phytoplankton biomass and primary production are significant along the eastern (Bhattathiri et al., 1996; Sawant and Madhupratap, 1996; Parab et al., 2006; Ahmed et al., 2016) and the western AS (Campbell et al., 1998; Brown et al., 1999; Garrison et al., 2000). Only a few of the above studies have dealt with the smaller sized phytoplankton groups in the eastern AS (Roy et al., 2015; Ahmed et al., 2016).

During the last decades, the importance of picophytoplankton (PP; < 3 μm) has been demonstrated in the marine environment as major contributors to the phytoplankton biomass (Worden et al., 2004; Richardson and Jackson, 2007). PP comprises of three major groups, *Prochlorococcus* (*PRO*), *Synechococcus* (*SYN*) and picoeukaryotes (PEUK). *PRO* dominates the oligotrophic waters and is encountered down to 150 m depth (Chisholm et al., 1988; Partensky et al., 1999; Johnson et al., 2006; Fuller et al., 2006). *SYN* is abundant in mesotrophic waters with a shallower vertical distribution than that of *PRO* (Bouman et al., 2006; Zwirglmaier et al., 2007; Flombaum et al., 2013). PEUK, along with *SYN* dominate the nutrient-rich coastal ecosystems

* Corresponding author.
E-mail address: mitbavkars@nio.org (S. Mitbavkar).

http://dx.doi.org/10.1016/j.csr.2017.08.008
Received 18 November 2016; Received in revised form 14 July 2017; Accepted 14 August 2017
Available online 17 August 2017

(Blanchot et al., 2001; Jiao et al., 2005; Sharples et al., 2009). Although limited information is available on the PP community from the eastern AS, short-term variability which can impart an in-depth understanding of the PP dynamics still remains unknown.

In this study, we focused on the short-term vertical variations (every 3 h for 9 days) in the PP community structure at a fixed location over the continental slope in the eastern AS, off Goa, India. The objective of this study was to assess the influence of different hydrographic conditions such as stratification and mixing on the PP distribution pattern. We hypothesize that in the eastern AS, the PP community structure and carbon biomass varies in response to the short-term hydrographic variability resulting from coastal advection and vertical water column mixing. This study will also serve as a basis for understanding the response of phytoplankton community as a whole with chlorophyll biomass as the proxy.

2. Materials and methods

2.1. Sampling

Sampling was conducted for 9 days (D) at an interval of 3 h at one fixed location over the continental slope of the eastern AS (15° 18′ 46″N, 72° 41′ 53″E) (Fig. 1), onboard the ocean research vessel ORV Sindhu Sankalp (SSK-27) during the early NEM season (18–26 November 2011). Temperature, salinity and dissolved oxygen (DO) data profiles were taken from precalibrated CTD. Mixed layer (ML) depth was derived from the sigma-t criteria, as the depth at which a change from the surface sigma-t of 0.125 has occurred. Water samples for nutrients and PP analyses were collected from 7 to 10 depths in the upper 0–200 m water column with 12 dm^3 Niskin bottles (General Oceanics, Miami, FL, USA) mounted on a CTD (Sea- Bird electronics) rosette sampler. Nutrient samples were analyzed [nitrite (NO_2^-) nitrate (NO_3^-), orthophosphate (PO_4^{3-}), ammonium (NH_4^+), and silicate (SiO_4^{4-})] with a SKALAR SAN^{plus} auto-analyzer. For analysis of PP, water samples were preserved in paraformaldehyde (final concentration 0.2%; Campbell, 2001). After 15 min dark incubation, the samples were quick-frozen in liquid nitrogen and stored at −80 °C until analysis. For chlorophyll *a* analysis, water samples (~ 3–4 L) were filtered through GF/F filter followed by extraction of pigments in 90% acetone which were measured using High Performance Liquid Chromatography (LC 1200 series, Agilent Technologies, USA; Acharyya et al., 2012).

2.2. Flow cytometric analyses of picophytoplankton

In the laboratory, samples were thawed and analyzed through FacsVerse flow cytometer configured with 20 mW and 40 mW air-cooled lasers exciting at 488 nm (blue) and 664 nm (red), respectively. Sample acquisition was set for 10,000 events. Flow rates were calibrated before analysis using the equation, $R = (W_i - W_f)/ (T \times d)$ where W_i = initial weight of the sample (mg), W_f = final weight of the sample (mg), T = time (minutes), and d = density of the sample (seawater = 1.03) (Marie et al., 2005). Forward angle light scatter (FALS; proxy for cell size) and right angle light scatter (RALS), orange (564–606 nm) and red (> 650 nm) fluorescence intensities were collected from each particle and analyzed with Facs Suite™ software. Yellow-green fluoresbrite fluorescent beads (Polysciences co., USA) of 2 μm diameter were added to the samples as an internal standard. Cell fluorescence emission and light scatter signals of each PP group were normalized to that of the beads (mean cell values/mean bead values) to distinguish the different PP groups based on their autofluorescence properties and size. Three major groups of PP were determined (Fig. 2a–c). *SYN* was identified based on the orange fluorescence of the pigment phycoerythrin. PEUK were differentiated from *PRO* based on the relatively higher red chl *a* fluorescence and largest FALS.

2.3. Carbon biomass estimation

Phytoplankton carbon biomass was derived from chl *a* using a carbon: chl *a* ratio of 140 and 83 μg C: μg chl^{-1} for the phase-I and phase-II ML depths, respectively (Shalapyonok et al., 2001). A C: chl *a* ratio of 52 was used for depths below the ML (Brown et al., 1999; Garrison et al., 2000). Carbon biomass of *SYN*, *PRO* (Garrison et al., 2000; Shalapyonok et al., 2001) and PEUK (Shalapyonok et al., 2001) were estimated using conversion factors as given in Table 1. For PEUK, the biovolume calculated from FALS was converted to carbon per cell (Shalapyonok et al., 2001).

2.4. Data analyses

The depth of euphotic zone ($Z_{1\%}$) was estimated from chl *a* concentration of surface layer using the chl centered approach (Lee et al., 2007). The percentage contribution of PP to total phytoplankton carbon biomass and individual PP group contribution to total PP carbon biomass were estimated from the phytoplankton and PP carbon values. PP carbon biomass was depth integrated by trapezoidal method and its percentage contribution to the total phytoplankton biomass was also calculated.

PERMANOVA analysis (Wood et al., 2016) was performed using PRIMER 6 software to assess the variation in the biotic (*SYN*, *PRO*, PEUK, PP carbon biomass, chl *a*, phytoplankton carbon biomass, and PP carbon contribution) and abiotic (nutrients, temperature, salinity, and DO) parameters between phase I (stratified water column) and phase II

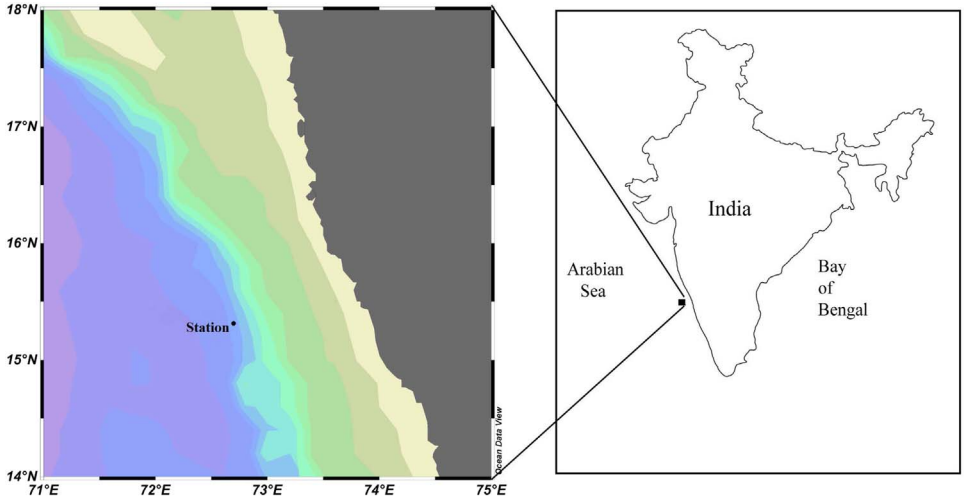

Fig. 1. Location of sampling station in the eastern Arabian Sea.

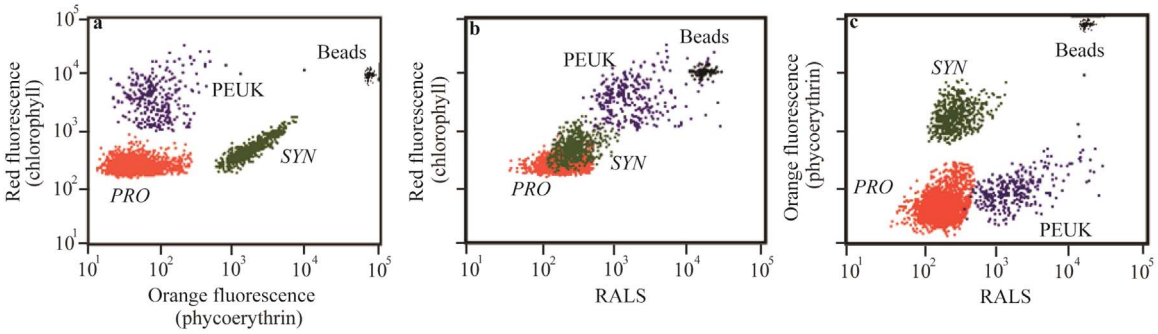

Fig. 2. Dot plot of flow cytometric analysis showing PP groups from the eastern Arabian Sea.

Table 1
Conversion factors used to estimate carbon biomass of PP groups (fg C cell^{-1}) and total phytoplankton (μg C μg^{-1} chl *a*) in the mixed layer (ML) and below mixed layer during phase I and phase II.

	Phase I		Phase-II	
	ML	Below ML	ML	Below ML
SYN	106.2	185.1	101.0	152.0
PRO	34.2	84.5	32.0	72.0
PEUK	601.0	647.0	522.0	528.0
C:Chl *a*	140.0	52.0	83.0	52.0

(mixed water column) samplings in the surface (0 m), ML and below ML. Path analysis was used to explain the linear relationships (R^2 = coefficient of determination) between the biological and the contextual physicochemical parameters in the ML (phase I and phase II) and below ML (50 m, 75 m and 100 m depths). It was conducted as a hierarchical multiple regression analysis and the obtained results were used to establish a path diagram (SPSS Amos). The D5 data (ML and below ML) was also treated separately in order to assess the PP response to environmental conditions during the transition phase.

3. Results

3.1. Environmental variables

Based on the ML depth, the sampling period was divided into two phases: phase I (from D1 to D5) was characterized by a shallow ML (25.58 ± 4.85 m) with high temperature (29.39 ± 0.2 °C) and low salinity (34.34 ± 2.8) water mass, and phase II (D6 to D9) was characterized by a deep ML (51.44 ± 5.50 m) with lower temperature (28.62 ± 0.2 °C) and higher salinity (35.15 ± 0.43) water mass (Fig. 3a and b). DO concentration ranged from 3.9 to 6.1 mg dm^{-3} in the ML (Fig. 3c). Nutrient concentrations within the ML were significantly higher during phase II. NO_3^- and PO_4^{3-} concentrations were < 1 μM within the ML during phase I whereas during phase II, it increased (> 1 μM; Fig. 3d and f). PO_4^{3-} concentration started increasing from the end of phase I (D4-D5; Fig. 3f). NO_2^- concentration ranged from 0.02 to 0.97 μM in the water column (Fig. 3e). SiO_4^{4-} concentration in the ML ranged from 1.05 to 6.54 μM (Fig. 3g). In the ML, NH_4^+ concentration ranged from 0.01 to 5.95 μM (Fig. 3h). Nutricline deepened during the beginning of phase I and during phase II, whereas it was shallower during end of phase I (D4-D5). The depth of euphotic layer ranged between 60 and 70 m during the study period.

3.2. Picophytoplankton community structure

Variations of hydrographic conditions during the two phases were well reflected in the PP community structure and its abundance, especially in the ML. At the beginning of phase I, *SYN* abundance was higher in the upper 75 m water column, with maximum abundance at 50 m (6.4 × 10^4 cells cm^{-3}). Its abundance reduced during the later part of phase I (except on D4 at 25 m; 9.8 × 10^4 cells cm^{-3}) and phase II (Fig. 4a). At the beginning of phase I, *PRO* was the dominant PP group in the water column. *PRO* population was observed down to 200 m depth with maximum abundance in the ML and occasionally in deeper waters (100 m; Fig. 4b). By the end of phase I, PEUK was the dominant PP group, especially between 25 m and 75 m depths (Fig. 4c). On D5 and D6, dominance of PEUK extended to deeper waters (75 m). PEUK had a higher abundance at 50 m, except on D2 and D3. During phase II, the abundance of all PP groups (*PRO* > PEUK > *SYN*) reduced by an order of magnitude in the water column. Overall, PP abundance was higher during phase I (Fig. 4d).

Pronounced diel variation was observed in the PP community during the study period. Generally, *SYN*, *PRO*, and PEUK showed higher cell abundance during the afternoon and night (12:00 to 24:00) and the time of attaining maximum cell abundance showed variation between the two phases. In particular, during phase I (D1 to D3) the abundance of *SYN*, *PRO*, and PEUK was higher at 18:00, 15:00, and 12:00, respectively, which remained high till 24:00 (Fig. 4a–c). At the end of phase I, PEUK cell abundance was higher at 9:00 but *SYN* and *PRO* did not show any change in the pattern. During phase II, in the ML, higher abundance of *SYN* and *PRO* was observed at 12:00 and PEUK at 15:00 (Fig. 4a–c). In both phases, higher abundance of *SYN* and PEUK was only observed in the upper 50 m (Fig. 4a and c). *PRO* abundance was higher in the shallower depths (upper 50 m) from evening to night (after 15:00) and below 50 m depth before 15:00 during phase I, whereas, during phase II, higher cell abundance was observed only in the upper 50 m (Fig. 4b).

3.3. Contribution of picophytoplankton to the total phytoplankton carbon biomass

Chl *a* concentration ranged from 0.07 to 1.09 μg dm^{-3} with peak values just below the ML (50 m; Fig. 5a). Chl *a* concentrations were high during afternoon and night followed by lower values in the early morning. Phytoplankton carbon biomass varied from 2.5 to 203.1 μg dm^{-3} in the water column with higher concentrations below the ML. Phytoplankton carbon biomass concentration was significantly ($P < 0.05$) higher during phase I than phase II in the ML and also below ML. PP carbon biomass varied from 0.1 to 98.32 μg dm^{-3} in the water column during the entire study period (Fig. 5b). PP contribution to the total phytoplankton carbon in the entire water column ranged from 13% to 70% during phase I and 15 to 47% during phase II. Higher PP carbon contribution was observed during phase I, especially on D5 (26–70%, entire water column, Fig. 5c). Depth-integrated PP carbon biomass concentration was significantly ($P < 0.05$) higher during phase I than phase II in surface, ML and below ML. Depth-integrated PP carbon biomass contribution to the total phytoplankton carbon ranged from 9% to 58% in the ML during the entire study period. However, there was not much difference in their contribution to total

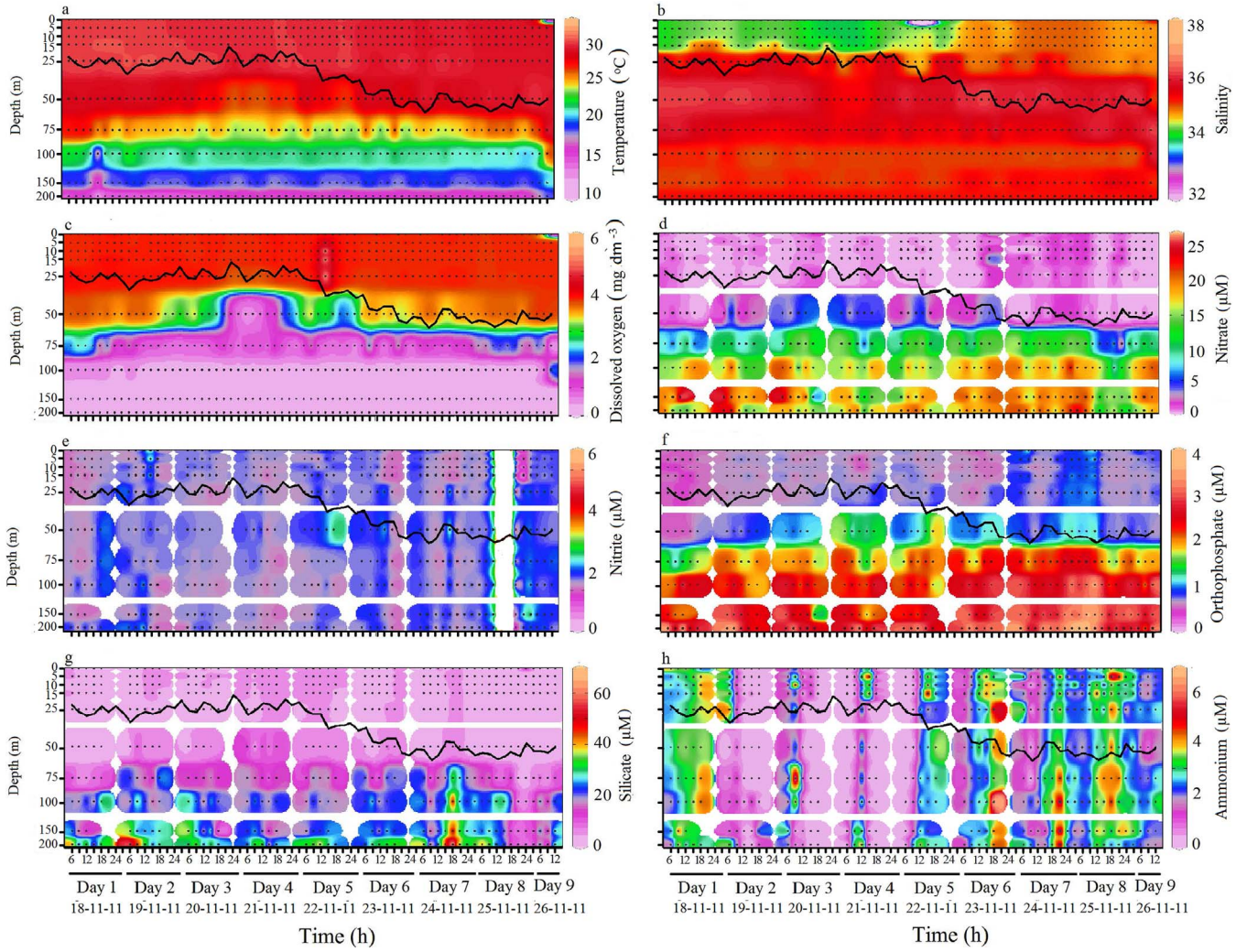

Fig. 3. Vertical profiles of temporal variation in (a) temperature, (b) salinity, (c) dissolved oxygen, (d) nitrate, (e) nitrite, (f) orthophosphate, (g) silicate, and (h) ammonium over the continental slope of the eastern Arabian Sea. Black line indicates mixed layer depth.

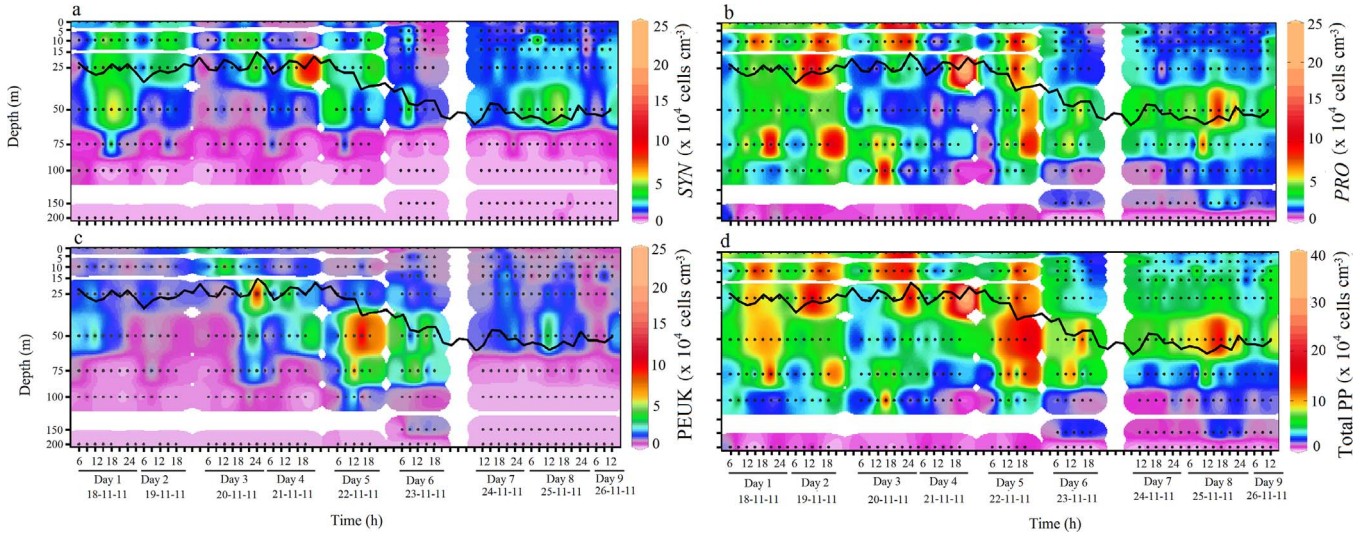

Fig. 4. Vertical profiles of temporal variation in cell abundance of (a) *SYN,* (b) *PRO,* (c) PEUK, and (d) total PP over the continental slope of the eastern Arabian Sea. Black line indicates mixed layer depth.

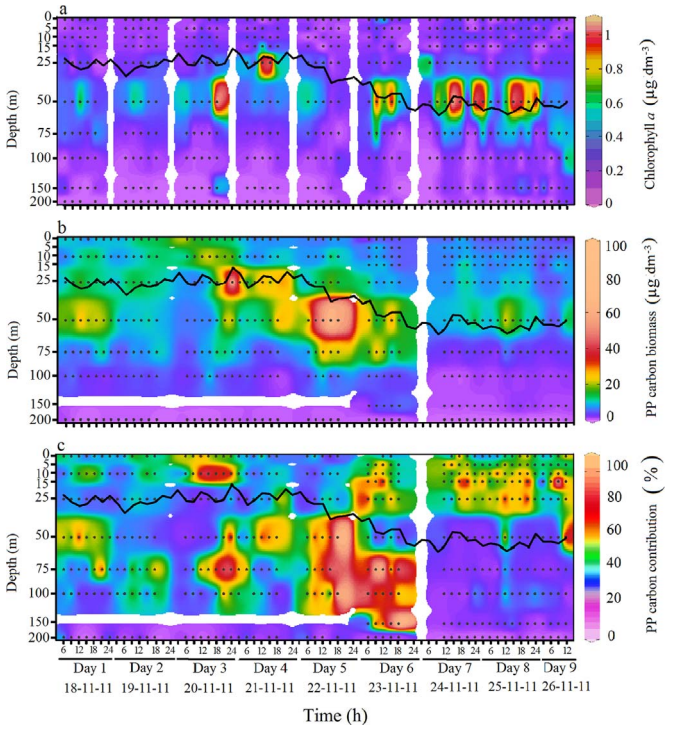

Fig. 5. Vertical profiles of temporal variation in (a) chlorophyll *a,* (b) PP carbon, and (c) PP carbon contribution (%) to the total phytoplankton carbon biomass over the continental slope of the eastern Arabian Sea. Black line indicates mixed layer depth.

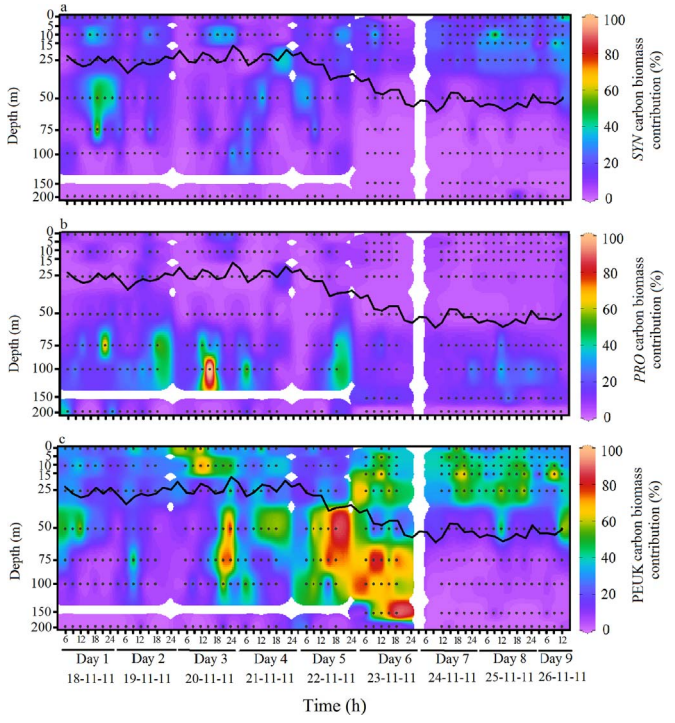

Fig. 6. Vertical profiles of temporal variation in (a) *SYN,* (b) *PRO* and (c) PEUK carbon contribution to the total PP carbon biomass over the continental slope of the eastern Arabian Sea. Black line indicates mixed layer depth.

phytoplankton carbon biomass in surface and ML; whereas below ML, PP carbon contribution to total carbon biomass was higher during phase I than phase II.

At the end of phase I, the PP carbon biomass was higher especially at 25 m and 50 m depth with a major contribution by PEUK (Fig. 6c). The major contributor to PP carbon biomass was PEUK (35–90%) followed by *SYN* (4–44%) and *PRO* (1–39%) in the upper 50 m during both phases (Fig. 6a–c). In the deeper waters, *PRO* carbon biomass was dominant except at the end of phase I, where PEUK was dominant down to 100 m depth. However, on some occasions, *PRO* dominated the PP carbon biomass in the ML. There was no consistent diel pattern of PP carbon biomass and its contribution to the total phytoplankton carbon biomass. Generally, PP contribution was higher in the upper 50 m depth but at the end of phase I, higher PP carbon contribution was observed down to 100 m, and extended down to 150 m in the early phase II.

3.4. Relationship between picophytoplankton and environmental variables

PERMANOVA analysis revealed significant variations ($P < 0.01$) in temperature, DO, PO_4^{3-}, SiO_4^{4-}, chl *a* concentration, PEUK abundance, *PRO* abundance, phytoplankton carbon biomass, and PP carbon biomass between phase I and phase II samplings in the surface waters (0 m) whereas salinity, NH_4^+, NO_2^-, NO_3^- and PP contributions showed insignificant variations (Table 2). In ML, significant variations ($P < 0.01$) were observed in temperature, nutrient concentrations, chl *a* concentration, PP group cell abundances, phytoplankton carbon biomass, and PP carbon biomass between phase I and phase II samplings whereas salinity, DO and PP contributions showed insignificant variations (Table 2). Below ML, DO, nutrients (except SiO_4^{4-}), chl *a* concentration, *SYN*, PEUK, phytoplankton carbon biomass, PP carbon biomass and its contribution to total phytoplankton carbon biomass showed significant variation ($P < 0.01$) between phase I and phase II samplings, whereas temperature, salinity, *PRO* abundance and SiO_4^{4-} showed insignificant variations (Table 2).

In the ML, variability of *SYN* abundance was partially explained by the positive correlation with temperature and NO_3^- during phase I ($R^2 = 0.17$, $P < 0.05$) and PO_4^{3-} during phase II ($R^2 = 0.12$, $P < 0.05$) (Fig. 7a and b). The variation of PEUK abundance was partially explained by negative correlation with temperature, and positive correlation with PO_4^{3-} and NO_3^- during phase I ($R^2 = 0.33$, $P < 0.05$) and positive correlation with NH_4^+, salinity, and temperature during phase II ($R^2 = 0.28$, $P < 0.05$). *PRO* abundance variation was partially explained by the positive correlation with temperature and NO_2^- during phase I ($R^2 = 0.23$, $P < 0.05$) and negative correlation with NH_4^+ and positive correlation with PO_4^{3-} during phase II ($R^2 = 0.12$, $P < 0.05$). The variability of PP carbon biomass was largely explained by positive correlation with *SYN*, PEUK, temperature and nutrient concentrations (NH_4^+, PO_4^{3-}, NO_2^- and NO_3^-) during phase I ($R^2 = 0.93$, $P < 0.05$) and positive correlation with PEUK, *PRO*, PO_4^{3-}, and NO_3^-; and negative correlation with NH_4^+ and temperature during phase II ($R^2 = 0.83$, $P < 0.05$). The variation in phytoplankton carbon biomass was largely explained by positive correlation with PP carbon biomass and PO_4^{3-} and negative correlation with salinity, SiO_4^{4-} and NO_2^- during phase I ($R^2 = 0.67$, $P < 0.05$) and positive correlation with PP carbon biomass and salinity during phase II ($R^2 = 0.73$, $P < 0.05$) (Fig. 7a and b).

At 50 m depth, variation in *SYN* abundance was largely explained by the positive correlation with temperature ($R^2 = 0.32$, $P < 0.05$), at 75 m, partially explained by the negative correlation with NH_4^+ ($R^2 = 0.16$, $P < 0.05$) and at 100 m depth, largely explained by the positive correlation with salinity, NO_2^- and NO_3^- and negative correlation with temperature and PO_4^{3-}, ($R^2 = 0.47$, $P < 0.05$; Fig. 7c–e). The variation in PEUK abundance at 50 m depth was largely explained by the positive correlation with NH_4^+, SiO_4^{4-}, and PO_4^{3-}, and negative correlation with NO_3^- ($R^2 = 0.51$, $P < 0.05$), at 75 m by the positive correlation with salinity and negative correlation with temperature and PO_4^{3-} ($R^2 = 0.33$, $P < 0.05$) and 100 m depth, partially by the positive correlation with NO_3^- ($R^2 = 0.14$, $P < 0.05$). The variation in *PRO* abundance was largely explained by the positive correlation with temperature and NH_4^+ at 50 m depth ($R^2 = 0.53$, $P < 0.05$), whereas at 75 m by the positive correlation with temperature ($R^2 = 0.13$, $P < 0.05$). At 50 m,

Table 2
PERMANOVA analysis of environmental variables, PP groups, total phytoplankton carbon biomass, PP carbon biomass, and PP carbon contribution to the total phytoplankton carbon biomass between phase I and phase II samplings in surface waters (0 m), mixed layer (ML) and below mixed layer. Bold text denotes significant variation between the two phases.

	Surface waters (0 m)					ML					Below ML				
Source	df	SS	MS	Pseudo-F	*P*	df	SS	MS	Pseudo-F	*P*	df	SS	MS	Pseudo-F	*P*
Temperature	1	112.6	112.6	3.09	**0.00**	1	93.6	93.6	11.5	**0.01**	1	294.1	294.1	2.7	0.09
Salinity	1	91.3	91.3	1.17	0.38	1	14.3	14.3	0.8	0.36	1	0.3	0.3	1.5	0.23
DO	1	337.1	337.1	1.64	**0.00**	1	78.4	78.4	1.4	0.36	1	11,965.0	11,965.0	5.3	**0.01**
NO_3^-	1	3734.4	3734.4	2.13	0.09	1	13,175.0	13,175.0	8.8	**0.01**	1	5385.5	5385.5	5.7	**0.01**
NO_2^-	1	1132.9	1132.9	1.05	0.32	1	8364.6	8364.6	7.5	**0.01**	1	12,118.0	12,118.0	10.6	**0.01**
PO_4^{3-}	1	799.8	799.8	9.91	**0.00**	1	4564.1	4564.1	40.0	**0.01**	1	7061.2	7061.2	19.0	**0.01**
NH_4^+	1	729.2	729.2	1.09	0.30	1	4110.1	4110.1	6.8	**0.01**	1	11,460.0	11,460.0	15.9	**0.01**
SiO_4^{4-}	1	3313.8	3313.8	4.84	**0.00**	1	2867.8	2867.8	4.1	**0.04**	1	775.3	775.3	0.8	0.45
Chl *a*	1	1224.0	1224.0	6.4	**0.01**	1	3499.6	3499.6	6.2	**0.01**	1	8887.5	8887.5	7.6	**0.01**
SYN	1	59.3	59.3	3.08	0.09	1	5026.9	5026.9	5.4	**0.01**	1	29,312.0	29,312.0	12.3	**0.01**
PEUK	1	113.7	113.7	13.01	**0.00**	1	3886.3	3886.3	6.0	**0.01**	1	16,992.0	16,992.0	6.2	**0.01**
PRO	1	170.2	170.2	8.24	**0.01**	1	23,308.0	23,308.0	27.4	**0.01**	1	2315.9	2315.9	1.2	0.28
Phytoplankton carbon	1	1549.5	1549.5	78.9	**0.00**	1	5029.7	5029.7	25.4	**0.01**	1	4256.2	4256.2	15.8	**0.01**
PP carbon	1	2490.3	2490.3	28.2	**0.00**	1	7797.3	7797.3	7.8	**0.01**	1	22,374.0	22,374.0	16.3	**0.01**
PP contribution (%)	1	55.5	55.5	1.6	0.23	1	115.1	115.1	0.45	0.64	1	4167.7	4167.7	12.1	**0.01**

variation in PP carbon biomass was largely explained by the positive correlation with PEUK, NO_3^- and NH_4^+ and negative correlation with SiO_4^{4-} ($R^2 = 0.73$, $P < 0.05$), at 75 m, largely explained by the negative correlation with salinity and positive correlation with PEUK abundance and temperature ($R^2 = 0.65$, $P < 0.05$) and at 100 m, largely explained by the positive correlation with PEUK abundance ($R^2 = 0.41$, $P < 0.05$). At 50 m, the positive correlation with PP carbon biomass largely explained the variation in phytoplankton carbon biomass ($R^2 = 0.42$, $P < 0.05$), at 75 m, largely explained by the positive correlation with PP carbon biomass and negative correlation with NO_3^- ($R^2 = 0.43$, $P < 0.05$) and at 100 m depth, largely explained by the positive correlation with salinity and PP carbon biomass ($R^2 = 0.40$, $P < 0.001$).

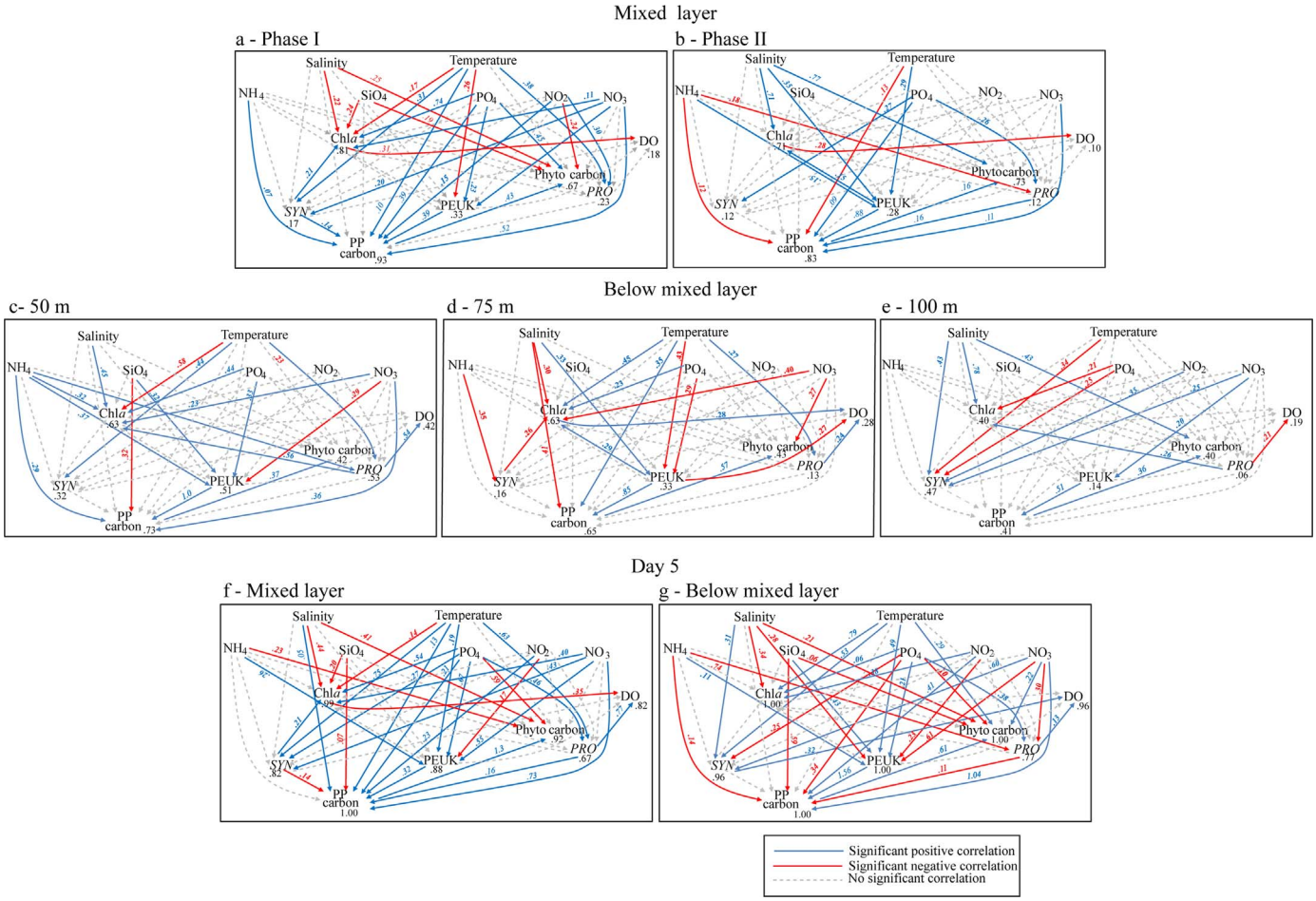

Fig. 7. Path diagrams showing the relationships between the environmental variables and PP groups, total phytoplankton carbon biomass, PP carbon biomass, and chl *a* within the mixed layer of (a) phase I, (b) phase II, below mixed layer at (c) 50 m, (d) 75 m, (e) 100 m, and on day 5 (f) within mixed layer and (g) below mixed layer. Bold values are the coefficient of determination of the linear regression (R^2) and colored values are the regression coefficients for the specific standardized independent variables. (For interpretation of the references to color in this figure legend, the reader is referred to the web version of this article.)

On D5, variability of *SYN* abundance was largely explained by the positive correlation with temperature, PO_4^{3-} and NO_3^- in ML (R^2 = 0.82, $P < 0.05$; Fig. 7f), whereas below ML by the positive influence of salinity, temperature and NO_3^- and negative correlation with PO_4^{3-} (R^2 = 0.96, $P < 0.05$; Fig. 7g). The variation in PEUK abundance was largely explained by the positive correlation with temperature, NH_4^+, PO_4^{3-}, and NO_3^- and negative correlation with NO_2^- in ML (R^2 = 0.88, $P < 0.05$); whereas below ML by the positive correlation with temperature, NH_4^+, SiO_4^{4-}, and PO_4^{3-} and negative correlation with salinity, NO_2^-, and NO_3^- (R^2 = 1.00, $P < 0.05$). The variation in *PRO* abundance in the ML was largely explained by the positive correlation with PO_4^{3-} and temperature (R^2 = 0.67, $P < 0.05$) whereas below ML, by the positive correlation with PO_4^{3-}, and negative correlation with NO_3^- and NH_4^+ (R^2 = 0.77, $P < 0.05$). The variability of PP carbon biomass was largely explained by the positive correlation with salinity, temperature, PO_4^{3-}, NO_2^-, NO_3^-, PEUK and *PRO* and negative correlation with *SYN* and SiO_4^{4-} in the ML (R^2 = 1.00, $P < 0.05$) whereas below ML by a positive correlation with NO_2^-, NO_3^-, and PEUK and negative correlation with NH_4^+, SiO_4^{4-}, PO_4^{3-} and *PRO* (R^2 = 1.00, $P < 0.05$). The variation in phytoplankton carbon biomass (R^2 = 0.92, $P < 0.05$) was largely explained by the positive correlation with PP carbon biomass and negative correlation with salinity, PO_4^{3-} and NH_4^+ in the ML, whereas below ML, by the positive correlation with PP carbon biomass, temperature and NO_3^- and negative correlation with salinity, SiO_4^{4-} and PO_4^{3-} (R^2 = 1.00, $P < 0.05$).

4. Discussion

4.1. Variations in picophytoplankton community structure

There is a scarcity of information on the short-term variability in PP (Jacquet et al., 2002), especially in the AS where monsoonal winds influence the hydrography. Hence a high resolution study at a fixed station over the continental slope of the eastern AS was carried out to better understand the impact of short-term variability in hydrography and environmental conditions on the PP community dynamics. During this study, the dynamic hydrography was well reflected in the PP community structure. The ML depth evolved from shallow (phase I) to deep (phase II). The relatively lower salinity (34) surface waters during phase I could be attributed to the advection of low saline coastal waters (Shankar et al., 2005). The resultant oligotrophic conditions during phase I favored *PRO* and *SYN* growth within the mixed layer (Anderson et al., 2008; Dongen-Vogels et al., 2012), with *PRO* as the dominant group. In the north-western AS and Alboran Sea, *SYN* and PEUK dominated the mesotrophic conditions whereas oligotrophic conditions were dominated by *PRO* (Campbell et al., 1998; Jacquet et al., 2002). Generally, in surface waters, *PRO* cells are better adapted to high temperature, low nutrient and stratified water column (Campbell et al., 1998; Liu et al., 1998; Zubkov et al., 1998; Agawin et al., 2000; Jiao et al., 2005). This is also supported by path analysis where *PRO* positively correlated with temperature but showed an insignificant relation with NO_3^- and PO_4^{3-} within the mixed layer. The degree of mixing in euphotic layer of the water column was also associated with differences in temperature of around 30 °C in the mixed layer compared with 25 °C at 50–75 m. Hence, the temperature of each layer could have influenced the *PRO* populations in the euphotic layer. Below the mixed layer, the positive correlation of *PRO* with the prevailing temperature at 50 m and 75 m suggests the influence of this parameter on its vertical distribution. Different ecotypes of *PRO* such as high light (HL) and low light (LL) adapted have been reported in the oceanic waters (Partensky et al., 1993; Moore and Chisholm, 1999). Depending on their ability to adapt to different light optima for growth, HL ecotype dominates in the surface waters and LL ecotype in the deeper waters (Partensky et al., 1999). Similar observations have been reported from the NEAS (Roy and Anil, 2015). As the euphotic depth in the present study area ranged between 60 and 70 m, vertical distribution of light could have played an important role in the distribution of HL and LL adapted *PRO* strains.

SYN, the next abundant group during phase I, which correlated positively with the prevailing temperature within the mixed layer (30 °C) and at 50 m (25 °C) suggests a temperature maxima regulating its vertical distribution in the water column. In the deeper waters (75–100 m), its minimal abundance in spite of the high nutrient concentrations could be due to lowered growth rates. Since *SYN* is a mesotrophic form, its vertically decreasing trend shows that temperature and irradiance effect overrides the nutrient needs to optimize growth (Mouriño-Carballido et al., 2016). Another loss factor resulting in its lower abundance could be the high grazing pressure exerted by the small heterotrophic nanoflagellates (Reckermann and Veldhuis, 1997). The vertical distribution of the least abundant group, PEUK, were generally controlled by the nutrients as seen from the positive correlation. PEUK are the main carbon source for the microzooplankton (Reckermann and Veldhuis, 1997). However, the role of grazers as the controller of PEUK in the open oceans is unclear (Hirose et al., 2008). PEUK mortality losses (50–100%) due to viral lysis was also reported with rates ranging from 0.1 to 0.8 d^{-1} (Baudoux et al., 2007).

With the initiation of vertical mixing during the transition phase (D5) at the end of phase I, increased abundance of the PP groups within the mixed layer, with *SYN* dominating the community, suggests a positive influence of increased nutrient concentrations. This was supported by the positive correlation with the prevailing temperature, NO_3^- and PO_4^{3-}. Below the ML, the highest PEUK abundance at the subsurface chl *a* maxima where *SYN* and *PRO* exhibited relatively lower numbers, coincided with increased nutrient concentrations. This was supported by the positive correlation of PEUK with nutrients (SiO_4^{4-}, PO_4^{3-}, and NH_4^+). During this period, PEUK cell abundance peaked earlier than that of *PRO* and *SYN,* implying cell division, which could be mainly driven by variations in nutrient concentrations. This also suggests that during pulses of nutrient inputs, PEUK are the fastest to respond amongst the PP groups, followed by *PRO*. Amongst the larger phytoplankton, diatoms respond to pulsed nutrient inputs (Ornolfsdottir et al., 2004). Some diatom species such as *Chaetoceros throndsenii* which attain a minimum size of 1.5 μm have also been observed in the PP community (Vaulot et al., 2008). Not et al. (2008) also reported the presence of picoplanktonic diatom in Indian ocean. *Minutocellus* species, strains RCC703 which belongs to Bacillariophyceae was isolated from Indian ocean (Giovagnetti et al., 2012). However, till date there is no published data suggesting that pico-diatoms are an important fraction of the PP in the present study area. The positive correlation of PEUK with SiO_4^{4-} implies representation by some smaller diatoms that are quick in responding to nutrient pulses due to their greater capacity for assimilation of nutrients at high concentrations (Agawin et al., 2000; Jiao et al., 2005; Paulsen et al., 2015). The present study area was located above the continental slope, and usually, at the continental shelf break and slope, formation of internal tides and nonlinear waves (Smith and Sandstrom, 1988; Shenoi and Antony, 1991; Shankar et al., 2005), cause churning of water column (Wolanski and Pickard, 1983; Kurapov et al., 2010) that results in nutrient influx from the sediment to the upper water column yielding high productivity (Sharples et al., 2001). In the shelf edge of north-east Atlantic Ocean complete dominance of PEUK was observed due to the supply of NO_3^- from bottom waters, whereas *SYN* and *PRO* were dominant in the NO_3^- depleted continental shelf region (Sharples et al., 2009). Dongen-Vogels et al. (2011) observed that the mixing process decreases the light irradiance and increases the nutrient input which led to a proliferation of eukaryotes and decline of prokaryotes. The PEUK abundance was the highest recorded for the entire study period and also coincided with the higher chl *a* biomass below the ML. Their contribution to the total phytoplankton biomass (26–70%) implies that PEUK were the major contributors. Sharples et al. (2009) reported a higher rate of primary production in the shelf edge, which can support higher trophic levels including fishes, thereby serving as a potential fishery zone. The short life span of PEUK abundance peak could be attributed to the grazing by

heterotrophic nanoflagellates whose growth response is as quick as the PP (Eccleston-Parry and Leadbeater, 1994; Landry et al., 1998) leading to a succession of the phytoplankton community by diatoms. The high resolution vertical sampling strategy allowed us to capture such refined transient observations *in situ* which are essential for further understanding of the microbial loop functioning in such dynamic ecosystems.

The vertical mixing of water column during phase II caused deepening of the mixed layer leading to a uniform distribution of PP within the ML, with significantly lower PP abundance and biomass compared to phase I. On the other hand, phytoplankton biomass did not vary much during this period. This suggests that during vertical mixing, increased nutrient concentration favored larger phytoplankton. However, the prevalence of lower numbers of PP for a longer period of time (4 days) suggests lowered growth rates due to certain unfavorable environmental perturbation due to deepening of ML. In addition to the physical factors, the observed diel patterns in *SYN*, *PRO* and PEUK abundance could be attributed to biological factors such as cell division (Mitbavkar and Saino, 2015), cell death and loss factors such as grazing, viral infection and parasitism (Crumpton and Wetzel, 1982; Banse, 1994; Vaulot and Marie, 1999; Behrenfeld, 2010). The biological processes are in turn driven by nutrient or irradiance availability. The dephased abundance peaks for the three PP groups during the day time could be attributed to the cell division and the decreasing cell abundance during the night to higher grazing pressure (Reckermann and Veldhuis, 1997; Partensky et al., 1999; Gauns et al., 2005). As the cells divide their reduced size makes them more vulnerable to predation (Tsai et al., 2005).

4.2. Picophytoplankton carbon biomass

The appropriate selection of the C: Chl *a* ratios and carbon cell conversion factors for PP from that reported in literature is a challenging task as they are known to vary with growth conditions (Booth et al., 1993; Buck et al., 1996; Taylor et al., 1997). As such, the values determined in the open ocean are more realistic than in cultures. Taking into consideration the contrasting conditions under which the sampling was conducted, the closest match was found in Garrison et al. (2000) and Shalapyonok et al. (2001). This study was carried out in the AS during NEM wherein carbon cell^{-1} for both *PRO* and *SYN* varied significantly between cells from within and below ML, which was in the range observed in our study (< 50 m). For the C: Chl *a* ratios in ML, we used the upper (for phase I) and lower (for phase II) limits of the average value (112 ± 29; Shalapyonok et al., 2001). For below ML, we used a factor (52) suggested by Brown et al. (1999) and Garrison et al. (2000) for the AS when the ML was > 50 m. The relative contribution of the PP carbon to total phytoplankton carbon biomass (up to 70%) obtained by this approach was consistent with the previous studies carried out in the AS during NEM (Shalapyonok et al., 2001). Using lower factors led to over estimation of the carbon values. Thus, these biomass assessments can be considered reliable and useful for further PP studies in these waters.

The PP carbon biomass contribution to total carbon biomass increases in these waters when stratified conditions prevail. On the other hand, the vertical mixing and the associated deepening of the surface layer lead to a decrease of PP carbon biomass indicating that increasing mixed layer depth is less supportive for PP growth (Lindell and Post, 1995). This tendency suggests that mixing of the water column contributes to the maintenance of large cells such as diatoms in the water column, since diatoms are otherwise subjected to high sinking losses, as observed earlier in the AS (Campbell et al., 1998). These variations were driven by the gradual increase in nutrient concentration due to vertical mixing, from phase I to II as was evident from the positive correlation of chl *a* and phytoplankton carbon biomass with nutrients. Higher abundance of *SYN* and PEUK coincided with the maximum chl *a* peak signifying that the total phytoplankton biomass was largely contributed by PP. This is also evident from a significant positive relation between total phytoplankton carbon biomass and PP carbon biomass. The major component of PP carbon biomass was PEUK (35–90%) even though their abundance was low. This is mainly due to their larger size compared to *PRO* and *SYN* (Buitenhuis et al., 2012). Through this study it is evident that transient bursts in PP abundance can be captured *via* high resolution sampling which can be missed during the spatial observations depending on the sampling time. The short duration of these abundance peaks suggest incorporation of this biomass into higher trophic levels. Future high resolution studies at different regions in the continental margin encompassing the other components of the food web will help in validating and better elucidating the PP responses under varying environmental conditions.

Acknowledgements

The authors would like to thank the Director of Council of Scientific and Industrial Research (CSIR)-National Institute of Oceanography for his support. The authors wish to acknowledge Mr. Sundar D., chief scientist of the SSK-27 cruise and Mr. Michael G.S., for providing CTD data. We thank Dr. V.V.S.S. Sarma for providing chlorophyll *a* (HPLC derived) data. We thank Dr. Shankar D. for the support and encouragement. We thank Mr. S. Subha Anand for providing nutrient data and our project team members for their help and suggestions during sampling. We would also like to thank the officers and crew of the SSK-27 cruise for onboard help. We thank the anonymous reviewers for their valuable comments. Rajaneesh K.M. acknowledges CSIR for the award of Senior Research Fellowship. This work was funded by the project Ocean Finder (PSC 0105). This is NIO contribution (no. 6090).

References

Acharyya, T., Sarma, V.V.S.S., Sridevi, B., Venkataramana, V., Bharathi, M.D., Naidu, S.A., Kumar, B.S.K., Prasad, V.R., Bandyopadhyay, D., Reddy, N.P.C., Kumar, M.D., 2012. Reduced river discharge intensifies phytoplankton bloom in Godavari estuary, India. Mar. Chem. 132, 15–22.

Agawin, N.S., Duarte, C.M., Agusti, S., 2000. Nutrient and temperature control of the contribution of picoplankton to phytoplankton biomass and production. Limnol. Oceanogr. 45, 591–600.

Ahmed, A., Kurian, S., Gauns, M., Chndrasekhararao, A.V., Mulla, A., Naik, B., Naik, H., Naqvi, S.W., 2016. Spatial variability in phytoplankton community structure along the eastern Arabian Sea during the onset of south-west monsoon. Cont. Shelf Res. 119, 30–39.

Anderson, C.R., Siegel, D.A., Brzezinski, M.A., Guillocheau, N., 2008. Controls on temporal patterns in phytoplankton community structure in the Santa Barbara Channel, California. J. Geophys. Res. 113, 1–16.

Banse, K., 1968. Hydrography of the Arabian Sea shelf of India and Pakistan and effects on demersal fishes. Deep Sea Res. 15, 45–79.

Banse, K., 1987. Seasonality of phytoplankton chlorophyll in the central and northern Arabian Sea. Deep Sea Res. Part A 34, 713–723.

Banse, K., 1994. Grazing and zooplankton production as key controls of phytoplankton production in the open ocean. Oceanography 7, 13–20.

Banse, K., McClain, C., 1986. Winter blooms of phytoplankton in the Arabian Sea as observed by the Coastal Zone Color Scanner. Mar. Ecol. Prog. Ser. 34, 201–211.

Baudoux, A.C., Veldhuis, M.J., Witte, H.J., Brussaard, C.P., 2007. Viruses as mortality agents of picophytoplankton in the deep chlorophyll maximum layer during IRONAGES III. Limnol. Oceanogr. 52, 2519–2529.

Behrenfeld, M.J., 2010. Abandoning Sverdrup's critical depth hypothesis on phytoplankton blooms. Ecology 91, 977–989.

Bhattathiri, P., Pant, A., Sawant, S., Gauns, M., Matondkar, S.G.P., Mahanraju, R., 1996. Phytoplankton production and chlorophyll distribution in the eastern and central Arabian Sea in 1994–1995. Curr. Sci. 71, 857–862.

Blanchot, J., André, J.-M., Navarette, C., Neveux, J., Radenac, M.H., 2001. Picophytoplankton in the equatorial Pacific: vertical distributions in the warm pool and in the high nutrient low chlorophyll conditions. Deep Sea Res. I 48, 297–314.

Booth, B.C., Lewin, J., Postel, J.R., 1993. Temporal variation in the structure of autotrophic and heterotrophic communities in the subarctic Pacific. Prog. Oceanogr. 32, 57–99.

Bouman, H.A., Ulloa, O., Scanlan, D.J., Zwirglmaier, K., Li, W.K., Platt, T., Lutz, V., 2006. Oceanographic basis of the global surface distribution of *Prochlorococcus* ecotypes. Science 312, 918–921.

Brown, S.L., Landry, M.R., Barber, R.T., Campbell, L., Garrison, D.L., Gowing, M.M., 1999. Picophytoplankton dynamics and production in the Arabian Sea during the 1995 Southwest Monsoon. Deep Sea Res. II 46, 1745–1768.

Buck, K.R., Chavez, F.P., Campbell, L., 1996. Basin-wide distributions of living carbon components and the inverted trophic pyramid of the central gyre of the North Atlantic Ocean, summer 1993. Aquat. Microb. Ecol. 10, 283–298.

Buitenhuis, E.T., Li, W.K., Vaulot, D., Lomas, M.W., Landry, M.R., Partensky, F., Karl, D.M., Ulloa, O., Campbell, L., Jacquet, S., Lantoine, F., Chavez, F., Macias, D., Gosselin, M., McManus, G.B., 2012. Picophytoplankton biomass distribution in the

global ocean. Earth Syst. Sci. Data 4, 37–46.
Campbell, L., 2001. Flow cytometric analysis of autotrophic picoplankton. Methods Microbiol. 30, 317–343.
Campbell, L., Landry, M., Constantinou, J., Nolla, H.A., Brown, S.L., Liu, H., Caron, D.A., 1998. Response of microbial community structure to environmental forcing in the Arabian Sea. Deep Sea Res. II 45, 2301–2325.
Chisholm, S.W., Olson, R.J., Zettler, E.R., Goericke, R., Waterbury, J.B., Welschmeyer, N.A., 1988. A novel free-living prochlorophyte abundant in the oceanic euphotic zone. Nature 334, 340–343.
Crumpton, W.G., Wetzel, R.G., 1982. Effects of differential growth and mortality in the seasonal succession of phytoplankton populations in Lawrence Lake, Michigan. Ecology 63, 1729–1739.
Dongen-Vogels, V., Seymour, J.R., Middleton, J.F., Mitchell, J.G., Seuront, L., 2011. Influence of local physical events on picophytoplankton spatial and temporal dynamics in South Australian continental shelf waters. J. Plankton Res. 20, 1–16.
Dongen-Vogels, V., Seymour, J.R., Middleton, J.F., Mitchell, J.G., Seuront, L., 2012. Shifts in picophytoplankton community structure influenced by changing upwelling conditions. Estuar. Coast. Shelf Sci. 109, 81–90.
Eccleston-Parry, J.D., Leadbeater, B.S., 1994. A comparison of the growth kinetics of six marine heterotrophic nanoflagellates fed with one bacterial species. Mar. Ecol. Prog. Ser. 105, 167–177.
Flombaum, P., Gallegos, J.L., Gordillo, R.A., Rincón, J., Zabala, L.L., Jiao, N., Karl, D.M., Li, W.K., Lomas, M.W., Veneziano, D., Vera, C.S., 2013. Present and future global distributions of the marine cyanobacteria *Prochlorococcus* and *Synechococcus*. Proc. Natl. Acad. Sci. 110, 9824–9829.
Fuller, N.J., Tarran, G.A., Yallop, M., Orcutt, K.M., Scanlan, D.J., 2006. Molecular analysis of picocyanobacterial community structure along an Arabian Sea transect reveals distinct spatial separation of lineages. Limnol. Oceanogr. 51, 2515–2526.
Garrison, D.L., Gowing, M.M., Hughes, M.P., Campbell, L., Caron, D.A., Dennett, M.R., Shalapyonok, A., Olson, R.J., Landry, M.R., Brown, S.L., Liu, H.B., 2000. Microbial food web structure in the Arabian Sea: a US JGOFS study. Deep Sea Res. II 47, 1387–1422.
Gauns, M., Madhupratap, M., Ramaiah, N., Jyothibabu, R., Fernandes, V., Paul, J.T., Kumar, S.P., 2005. Comparative accounts of biological productivity characteristics and estimates of carbon fluxes in the Arabian Sea and the Bay of Bengal. Deep Sea Res. II 52, 2003–2017.
Giovagnetti, V., Cataldo, M.L., Conversano, F., Brunet, C., 2012. Growth and photophysiological responses of two picoplanktonic *Minutocellus* species, strains RCC967 and RCC703 (Bacillariophyceae). Eur. J. Phycol. 47, 408–420.
Hirose, M., Katano, T., Nakano, S.I., 2008. Growth and grazing mortality rates of *Prochlorococcus, Synechococcus* and eukaryotic picophytoplankton in a bay of the Uwa Sea, Japan. J. Plankton Res. 30, 241–250.
Jacquet, S., Prieur, L., Avois-Jacquet, C., Lennon, J.F., Vaulot, D., 2002. Short-timescale variability of picophytoplankton abundance and cellular parameters in surface waters of the Alboran Sea (western Mediterranean). J. Plankton Res. 24, 635–651.
Jiao, N., Yang, Y., Hong, N., Ma, Y., Harada, S., Koshikawa, H., Watanabe, M., 2005. Dynamics of autotrophic picoplankton and heterotrophic bacteria in the East China Sea. Cont. Shelf Res. 25, 1265–1279.
Johnson, Z.I., Zinser, E.R., Coe, A., McNulty, N.P., Woodward, E.M.S., Chisholm, S.W., 2006. Niche partitioning among *Prochlorococcus* ecotypes along ocean-scale environmental gradients. Science 311, 1737–1740.
Kurapov, A., Allen, J., Egbert, G., 2010. Combined effects of wind-driven upwelling and internal tide on the continental shelf. J. Phys. Oceanogr. 40, 737–756.
Landry, M.R., Brown, S.L., Campbell, L., Constantinou, J., Liu, H., 1998. Spatial patterns in phytoplankton growth and microzooplankton grazing in the Arabian Sea during monsoon forcing. Deep Sea Res. II 45, 2353–2368.
Lee, Z., Weidemann, A., Kindle, J., Arnone, R., Carder, K.L., Davis, C., 2007. Euphotic zone depth: its derivation and implication to ocean-color remote sensing. J. Geophys. Res. Oceans 112, 1–11.
Lindell, D., Post, A.F., 1995. Ultraphytoplankton succession is triggered by deep winter mixing in the Gulf of Aqaba (Eilat), Red Sea. Limnol. Oceanogr. 40, 1130–1141.
Liu, H., Campbell, L., Landry, M., Nolla, H.A., Brown, S.L., Constantinou, J., 1998. *Prochlorococcus* and *Synechococcus* growth rates and contributions to production in the Arabian Sea during the 1995 Southwest and Northeast Monsoons. Deep Sea Res. II 45, 2327–2352.
Madhupratap, M., Kumar, S.P., Bhattathiri, P., Kumar, D.M., Raghukumar, S., Nair, K.K.C., Ramaiah, N., 1996. Mechanism of the biological response to winter cooling in the northeastern Arabian Sea. Nature 384, 549–552.
Marie, D., Simon, N., Vaulot, D., 2005. Phytoplankton cell counting by flow cytometry. Algal Cultur. Tech. 1, 253–267.
Marra, J., Dickey, T., Ho, C., Kinkade, C.S., Sigurdson, D.E., Weller, R.A., Barber, R.T., 1998. Variability in primary production as observed from moored sensors in the central Arabian Sea in 1995. Deep Sea Res. II 45, 2253–2267.
Mitbavkar, S., Saino, T., 2015. Diurnal variability of *Synechococcus* abundance in Sagami Bay, Japan. Hydrobiologia 747, 133–145.
Moore, L.R., Chisholm, S.W., 1999. Photophysiology of the marine cyanobacterium *Prochlorococcus*: ecotypic differences among cultured isolates. Limnol. Oceanogr. 44, 628–638.
Morrison, J.M., Codispoti, L., Gaurin, S., Jones, B., Manghnani, V., Zheng, Z., 1998. Seasonal variation of hydrographic and nutrient fields during the US JGOFS Arabian Sea process study. Deep Sea Res. II 45, 2053–2101.
Mouriño-Carballido, B., Hojas, E., Cermeño, P., Chouciño, P., Fernández-Castro, B., Latasa, M., Marañón, E., Morán, X.A., Vidal, M., 2016. Nutrient supply controls picoplankton community structure during three contrasting seasons in the northwestern Mediterranean Sea. Mar. Ecol. Prog. Ser. 543, 1–19.
Naqvi, S., Naik, H., Narvekar, P., 2003. The Arabian Sea. In: Black, K., Shimmield, G. (Eds.), Biogeochemistry of Marine Systems. Blackwell, Oxford, UK, pp. 157–207.
Not, F., Latasa, M., Scharek, R., Viprey, M., Karleskind, P., Balagué, V., Ontoria-Oviedo, I., Cumino, A., Goetze, E., Vaulot, D., Massana, R., 2008. Protistan assemblages across the Indian Ocean, with a specific emphasis on the picoeukaryotes. Deep Sea Res. Part A 55, 1456–1473.
Ornolfsdottir, E.B., Lumsden, S.E., Pinckney, J.L., 2004. Phytoplankton community growth-rate response to nutrient pulses in a shallow turbid estuary, Galveston Bay, Texas. J. Plankton Res. 26, 325–339.
Parab, S.G., Matondkar, S.P., Gomes, H.D.R., Goes, J.I., 2006. Monsoon driven changes in phytoplankton populations in the eastern Arabian Sea as revealed by microscopy and HPLC pigment analysis. Cont. Shelf Res. 26, 2538–2558.
Partensky, F., Hoepffner, N., Li, W.K., Ulloa, O., Vaulot, D., 1993. Photoacclimation of *Prochlorococcus* sp. (Prochlorophyta) strains isolated from the North Atlantic and the Mediterranean Sea. Plant Physiol. 101, 285–296.
Partensky, F., Hess, W., Vaulot, D., 1999. *Prochlorococcus*, a marine photosynthetic prokaryote of global significance. Microbiol. Mol. Biol. Rev. 63, 106–127.
Paulsen, M.L., Riisgaard, K., Frede, T., St John, M., Nielsen, T.G., 2015. Winter-spring transition in the subarctic Atlantic: microbial response to deep mixing and pre-bloom production. Aquat. Microb. Ecol 76, 49–69.
Prasanna Kumar, S., Madhupratap, M., Dileep Kumar, M., Gauns, M., Muraleedharan, P.M., Sarma, V.V.S.S., De Souza, S.N., 2000. Physical control of primary productivity on a seasonal scale in central and eastern Arabian Sea. J. Earth Syst. Sci. 109, 433–441.
Qasim, S., 1982. Oceanography of the northern Arabian Sea. Deep Sea Res. 29, 1041–1068.
Rao, A.D., Joshi, M., Ravichandran, M., 2008. Oceanic upwelling and downwelling processes in waters off the west coast of India. Ocean Dyn. 58, 213–226.
Reckermann, M., Veldhuis, M.J., 1997. Trophic interactions between picophytoplankton and micro-and nanozooplankton in the western Arabian Sea during the NE monsoon 1993. Aquat. Microb. Ecol. 12, 263–273.
Richardson, T.L., Jackson, G.A., 2007. Small phytoplankton and carbon export from the surface ocean. Science 315, 838–840.
Roy, R., Anil, A.C., 2015. Complex interplay of physical forcing and *Prochlorococcus* population in ocean. Prog. Oceanogr. 137, 250–260.
Roy, R., Chitari, R., Kulkarni, V., Krishna, M.S., Sarma, V.V.S.S., Anil, A.C., 2015. CHEMTAX-derived phytoplankton community structure associated with temperature fronts in the northeastern Arabian Sea. J. Mar. Syst. 144, 81–91.
Sawant, S., Madhupratap, M., 1996. Seasonality and composition of phytoplankton in the Arabian Sea. Curr. Sci. 71, 869–873.
Shalapyonok, A., Olson, R.J., Shalapyonok, L.S., 2001. Arabian Sea phyto-plankton during southwest and northeast monsoons 1995: composition, size structure and biomass from individual cell properties measured byflow cytometry. Deep Sea Res. II 48, 1231–1261.
Shankar, D., Shenoi, S., Nayak, R., Vinayachandran, P.N., Nampoothiri, G., Almeida, A.M., Michael, G.S., Ramesh Kumar, M.R., Sundar, D., Sreejith, O.P., 2005. Hydrography of the eastern Arabian Sea during summer monsoon 2002. J. Earth Syst. Sci. 114, 459–474.
Sharples, J., Moore, C.M., Abraham, E.R., 2001. Internal tide dissipation, mixing, and vertical nitrate flux at the shelf edge of NE New Zealand. J. Geophys. Res. 106, 14069–14081.
Sharples, J., Moore, C.M., Hickman, A.E., Holligan, P.M., Tweddle, J.F., Palmer, M.R., Simpson, J.H., 2009. Internal tidal mixing as a control on continental margin ecosystems. Geophys. Res. Lett. 36, 1–5.
Shenoi, S.C., Antony, M.K., 1991. Current measurements over the western continental shelf of India. Cont. Shelf Res. 11, 81–93.
Shetye, S., Gouveia, A., Shenoi, S., 1994. Circulation and water masses of the Arabian Sea. Proc. Indian Acad. Sci. Earth Planet. Sci. 103, 107–123.
Smith, P.C., Sandstrom, H., 1988. Physical processes at the shelf edge in the Northwest Atlantic. J. Northwest Atl. Fish. Sci. 8, 5–13.
Taylor, A.H., Geider, R.J., Gilbert, F.J., 1997. Seasonal and latitudinal dependencies of phytoplankton carbon-to-chlorophyll *a* ratios: results of a modelling study. Mar. Ecol. Prog. Ser. 152, 51–66.
Tsai, A.Y., Chiang, K.P., Chang, J., Gong, G.C., 2005. Seasonal diel variations of picoplankton and nanoplankton in a subtropical western Pacific coastal ecosystem. Limnol. Oceanogr. 50, 1221–1231.
Vaulot, D., Marie, D., 1999. Diel variability of photosynthetic picoplankton in the equatorial Pacific. J. Geophys. Res. 104, 3297–3310.
Vaulot, D., Eikrem, W., Viprey, M., Moreau, H., 2008. The diversity of small eukaryotic phytoplankton ($\leq$ 3 μm) in marine ecosystems. FEMS Microbiol. Rev. 32, 795–820.
Wiggert, J., Jones, B., Dickey, T., Brink, K.H., Weller, R.A., Marra, J., Codispoti, L.A., 2000. The northeast monsoon's impact on mixing, phytoplankton biomass and nutrient cycling in the Arabian Sea. Deep Sea Res. II 47, 1353–1385.
Wolanski, E., Pickard, G., 1983. Upwelling by internal tides and Kelvin waves at the continental shelf break on the Great Barrier Reef. Mar. Freshw. Res. 34, 65–80.
Wood, H.L., Sundell, K., Almroth, B.C., Sköld, H.N., Eriksson, S.P., 2016. Population-dependent effects of ocean acidification. Proc. R. Soc. B 283, 1–7.
Worden, A.Z., Nolan, J.K., Palenik, B., 2004. Assessing the dynamics and ecology of marine picophytoplankton: the importance of the eukaryotic component. Limnol. Oceanogr. 49, 168–179.
Zubkov, M.V., Sleigh, M.A., Tarran, G.A., Burkill, P.H., Leakey, R.J., 1998. Picoplanktonic community structure on an Atlantic transect from 50°N to 50°S. Deep Sea Res. I 45, 1339–1355.
Zwirglmaier, K., Heywood, J.L., Chamberlain, K., Woodward, E.M.S., Zubkov, M.V., Scanlan, D.J., 2007. Basin-scale distribution patterns of picocyanobacterial lineages in the Atlantic Ocean. Environ. Microbiol. 9, 1278–1290.

Ecological Indicators 55 (2015) 118–130

Contents lists available at ScienceDirect

Ecological Indicators

journal homepage: www.elsevier.com/locate/ecolind

Synechococcus as an indicator of trophic status in the Cochin backwaters, west coast of India

K.M. Rajaneesh, Smita Mitbavkar*, A.C. Anil, S.S. Sawant

Council of Scientific and Industrial Research, National Institute of Oceanography, Dona Paula, Goa 403 004, India

ARTICLE INFO

Article history:
Received 23 July 2014
Received in revised form 16 February 2015
Accepted 21 February 2015

Keywords:
Picophytoplankton
Cochin backwaters
Eutrophication
Monsoon
Trophic status indicators
Synechococcus

ABSTRACT

Eutrophication is a major problem in coastal water bodies. Information about the trophic status of water bodies will enable proper management of coastal ecosystems. In this regard, biological organisms which are sensitive to environmental changes can serve as indicators of ecosystem trophic status. In this study, seasonal and spatial variations of picophytoplankton (PP; <3 μm size) community structure was assessed in the Cochin backwaters (CB) with respect to the prevailing environmental conditions during three seasons, post-monsoon (PM-I; October 2011 and PM-II; November 2012), pre-monsoon (PrM; May 2012) and monsoon (MON; August 2012). CB, along the west coast of India, receives continuous load of nutrients throughout the year through anthropogenic wastes. Trophic status index (TRIX) scores showed that CB is highly eutrophic with a high phytoplankton biomass. *Synechococcus* was the dominant PP observed in the study area. Seasonal and spatial salinity variations influenced the PP distribution, especially *Synechococcus* where PE-rich *Synechococcus* (*SYN*-PE) were dominant in higher saline (>30) and PC-rich *Synechococcus* (*SYN*-PC) in lower saline (<30) waters. *SYN*-PC showed a significant positive relation with chlorophyll *a* suggesting that this group contributes substantially to the total phytoplankton biomass. TRIX scores and *SYN*-PC: *SYN*-PE abundance ratio were negatively correlated with salinity suggesting an influence of the tidal amplitude. *SYN*-PC correlated positively and *SYN*-PE negatively with TRIX scores suggesting that these groups occupy contrasting ecological niches. These findings imply that PP distribution pattern can serve as an indicator of the trophic status of coastal water bodies.

1. Introduction

Backwaters are interlinked bodies of waterways, rivers, inlets, lakes and natural canals. These are the largest and the most complex ecosystems in the world. These locations are highly productive and play a distinct role in the livelihood and sustenance of the local people. Physical and chemical variables are the crucial factors supporting the higher productivity. The Cochin backwaters (CB), one of the such estuarine systems along the west coast of India, is considered to be highly productive, where phytoplankton plays an important role in the food web and serves as nursery grounds for fishes and other ecologically and economically important organisms (Qasim, 2003).

Eutrophication is one of the serious problems which CB is facing presently, resulting from the increasing anthropogenic activity. This is mainly due to the location of the Cochin port in the CB, which has accelerated the industrial growth in Cochin, making it one of the fastest growing cities in India. As a consequence, eutrophication becomes a threat for trophic dynamics and functioning of the ecosystem (Madhu et al., 2007; Kaladharan et al., 2011). CB receives a lot of organic and inorganic substances from several industries like oil refineries, fertilizer plants and chemical industries. From these industries, acids, alkalis, suspended solids, fluorides, free ammonium, insecticides, dyes, trace and heavy metals and radioactive nuclei are the major contaminants (Menon et al., 2000; Martin et al., 2012; Anu et al., 2014), which create a polluted environment in CB. For its efficient functioning, such ecosystems should be in a healthy state which can be easily detected through regular monitoring of the base of the food web i.e., phytoplankton.

At the base of the food web, the smallest group of phytoplankton, i.e., picophytoplankton (PP; <3 μm; Sieburth et al., 1978), which forms a major component of phytoplankton in the aquatic ecosystems, both marine and freshwater, including nutrient rich to

Abbreviations: CB, Cochin backwaters; PP, picophytoplankton; *SYN*, *Synechococcus*; PE, phycoerythrin; PC, phycocyanin; *PRO*-like, *Prochlorococcus*-like; PEUK, picoeukaryotes; PM, post-monsoon; PrM, pre-monsoon; MON, monsoon; NBW, near bottom waters; TRIX, trophic status index; SW, south-west; S, station; Chl *a*, chlorophyll *a*; IMD, Indian Meteorological Department; RALS, right angle light scatter; FALS, forward angle light scatter; DO, dissolved oxygen; BOD, biological oxygen demand; DIN, dissolved inorganic nitrogen; DIP, dissolved inorganic phosphate.

* Corresponding author. Tel.: +91 832 2450376; fax: +91 832 2450615.
E-mail address: mitbavkars@nio.org (S. Mitbavkar).

http://dx.doi.org/10.1016/j.ecolind.2015.02.033
1470-160X/

poor ecosystems, was selected as the study organism (Stockner and Antia, 1986; Shiomoto et al., 1997). PP are significant contributors to primary productivity and total phytoplankton biomass in various ecosystems (Paerl, 1977; Platt et al., 1983). PP forms an important component of the marine microbial food web by creating a linkage with the higher trophic levels (Chiang et al., 2013). PP comprises of three groups; two of cyanobacteria i.e., *Synechococcus* (*SYN*) and *Prochlorococcus* (*PRO*) and a group of picoeukaryotes (PEUK). *SYN* is the major group of PP in well-lit coastal and estuarine waters (Jochem, 1988) with comparatively lower numbers in oligotrophic waters where *PRO* are abundant (Partensky et al., 1999). PEUK are most competitive in nutrient rich waters (Jiao et al., 2005). Although *PRO* is considered to be an oceanic group, recently researchers have reported *PRO*-like cells in low saline waters (Shang et al., 2007; Mitbavkar et al., 2012) and it is still speculative whether this group of cells is actually growing in these waters or is being carried from the offshore waters (Partensky et al., 1999). *SYN* is further differentiated based on phycobilisome composition into phycoerythrin (PE) rich and phycocyanin (PC) rich in estuarine and coastal ecosystems (Murrell and Lores, 2004). Previous studies have suggested that salinity plays an important role in the spatial distribution of *SYN* where PE rich *SYN* dominates high saline waters whereas, PC rich *SYN* are abundant in lower saline waters (Murrell and Lores, 2004; Rajaneesh and Mitbavkar, 2013). Based on PE fluorescence intensity, different clades of PE rich *SYN* have been observed in the Mississippi river plume (Liu et al., 2004), Pearl River estuary (Lin et al., 2010) and the Zuari estuary (Mitbavkar et al., 2012).

CB is influenced by the south-west (SW) monsoon (MON). Generally, estuaries influenced by monsoonal rainfall are highly productive due to excess nutrient input from the landmass. Studies conducted in tropical (Qiu et al., 2010; Rajaneesh and Mitbavkar, 2013) and subtropical (Lin et al., 2010; Qiu et al., 2010; Zhang et al., 2013) regions, which come under the influence of monsoonal rainfall, have suggested that riverine runoff influences the PP growth. Physico-chemical and biological characteristics of the CB (Menon et al., 2000; Madhu et al., 2009) have suggested that this region is highly eutrophic and productive, where nanoplankton are the major component of phytoplankton (Madhu et al., 2007) and is also a perfect breeding ground for economically important fishes and other organisms (Qasim, 2003). In the monsoonal Zuari estuary along the west coast of India, rainfall intensity was found to regulate freshwater runoff, which controls the estuarine environment thereby resulting in temporal and spatial niche segregation of *SYN* groups (Rajaneesh and Mitbavkar, 2013). The present study was carried out on a seasonal basis to characterize the main environmental factors, which control the spatial distribution pattern of PP groups and consequently whether these organisms can serve as ecological indicators. Since *SYN*-PE is known to prefer clear waters and *SYN*-PC turbid waters (Stomp et al., 2007), we hypothesize that these organisms can serve as good indicators of the trophic status of the water column.

2. Materials and methods

2.1. Study area

Sampling was carried out in an area within the CB, along the west coast (9°34′48″N, 76°08′24″E) of India (Fig. 1). It is situated along

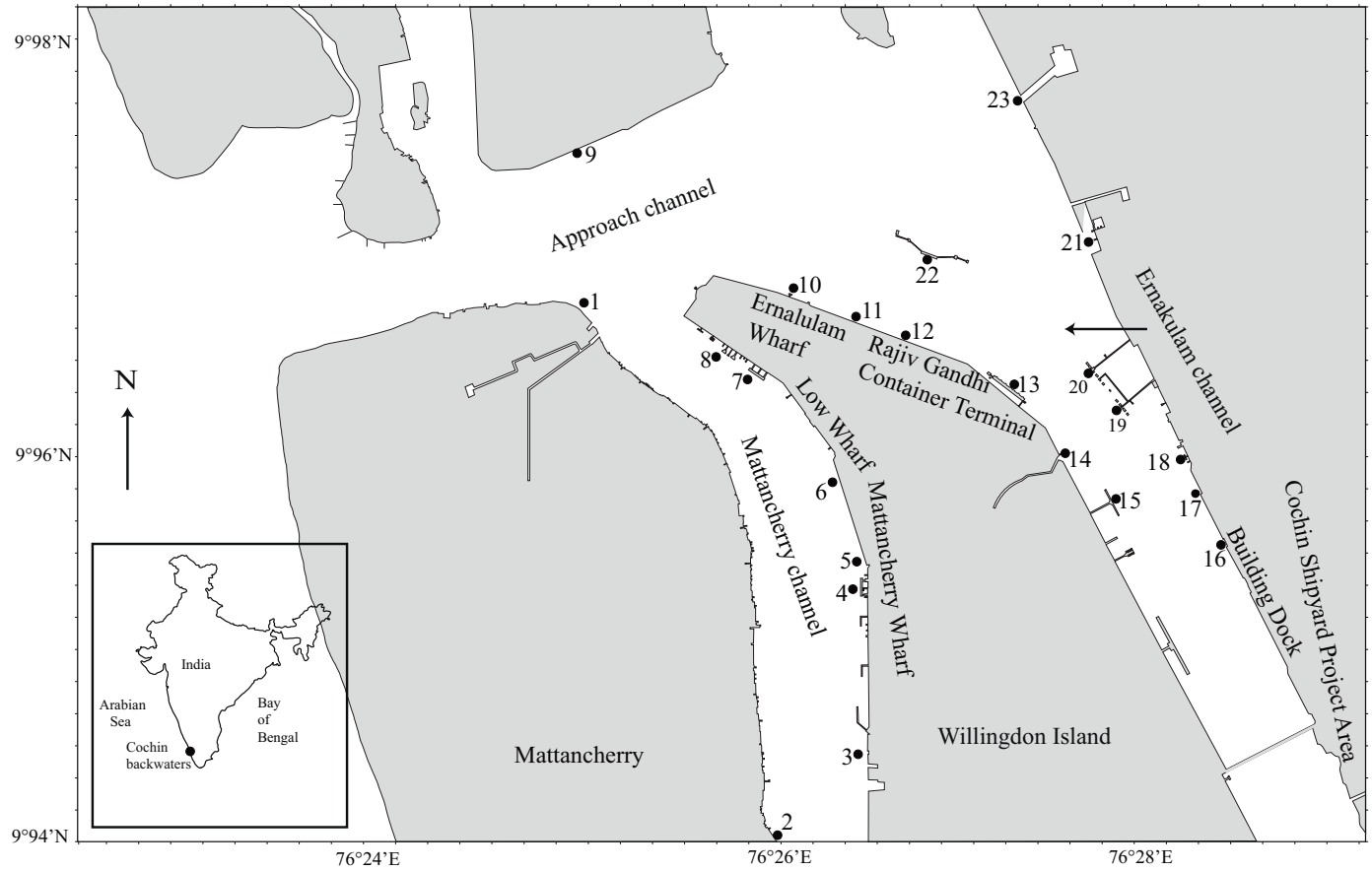

Fig. 1. Sampling stations located in the Cochin backwaters, west coast of India. (1) Custom buoy, (2) fishery harbor, (3) dry dock, (4) south coal berth, (5) Quay-1, (6) Quay-2, (7) north coal berth, (8) boat train pier, (9) container terminal, (10) DC jetty, (11) Quay-6, (12) Quay-8, (13) Quay-10, (14) Ro-Ro jetty, (15) naval jetty, (16) Cochin shipyard, (17) bunker oil jetty, (18) integrated fisheries project jetty, (19) south tanker berth, (20) north tanker berth, (21) Ernakulam ferry jetty, (22) Cochin oil terminal, (23) Ernakulam creek mouth.

the northern part of Kerala state, running parallel to the coastline with two permanent openings to the Arabian Sea. One opening is at the Cochin Port and another further north at Azhikode, where the estuary is flushed during ebb tide and seawater intrudes during flood tide. Periyar and Muvattupuzha rivers along with 4 others and their tributaries bring large volume of freshwater into the CB through the Vembanad Lake, which has an active influence on the prevailing salinity of the estuarine system (Jyothibabu et al., 2006). CB is a very important estuarine system of Kerala in terms of fishing and extensive transportation of goods. It is also used for dumping industrial as well as domestic wastes. It has three dredged channels where the selected stations are located, one being the approach channel (S1, S9–12, S21–23) of around 10 km length and 500 m width and the two inner channels located on either side of the Willingdon Island, i.e. Ernakulam channel (S13–20) of around 5 km length with a width of 250–500 m and Mattancherry channel (S2–8) of 3 km length with a width of around 170–250 m (Menon et al., 2000). Tides in this region are mixed semidiurnal with a range of about 1 m (Qasim and Gopinathan, 1969). Annual air temperature range is 20 °C to 35 °C with maximum temperature during February to May. Annually this region experiences three seasons i.e., SW MON (June to September), post-monsoon (October to January; PM) and pre-monsoon (February to May; PrM). It has a hot and humid climate with an average annual rainfall of about 350 cm, most of which is contributed by the SW MON and rest by north-east MON. During SW MON this estuary receives large amounts of freshwater, which leads to a salt wedge condition in the CB during August to October, whereas during November to May it changes to partially mixed condition due to reduction in freshwater discharge. In June, moderately stratified to partially mixed waters are observed (Menon et al., 2000).

2.2. Sampling

All together four samplings were conducted which included two PM seasons during the consecutive years i.e., 9th to 12th October, 2011 (PM-I) and 21st to 25th November, 2012 (PM-II), one MON season, (10th to 15th August, 2012; MON) and one PrM season (26th to 29th May, 2012; PrM). Within the CB, twenty three stations were selected for sample collection including ship berths and channels (Table A1). Sampling was carried out between 06:30 and 13:00 h for four days. Rainfall and tidal range data were collected from the Indian Meteorological Department (IMD; Table A2). Tidal height was estimated from the tidal range for the respective sampling time. Temperature was determined using multiparameter Sonde DS5X (Hydrolab). Surface and near bottom water (NBW) samples were collected with a 5 l Niskin sampler. Salinity was measured with an autosal (Guildline Autosal 8400B). For chlorophyll *a* (chl *a*) estimation, seawater samples (250 ml) were filtered through Whatman GF/F filter papers. Filters were preserved with $MgCO_3$ and stored at −20 °C until analysis. In the laboratory, each filter paper was placed separately in a dark vial containing 90% acetone. After extraction in the dark at 4 °C for 24 h, chl *a* concentration was determined on a Turner Design 10-AU fluorometer calibrated with commercial chl *a* (Parsons et al., 1984). Nutrients such as nitrate (NO_3), phosphate (PO_4), nitrite (NO_2), ammonium (NH_4) and silicate (SiO_4) were analyzed by SKALAR SAN^{plus} ANALYSER. Dissolved oxygen (DO) and biological oxygen demand (BOD) were analyzed following standard methods (Parsons et al., 1984). For PP analysis, duplicate samples were preserved with paraformaldehyde (0.2% final concentration) in 2 ml cryovials, flash frozen in liquid nitrogen and stored at −80 °C until analysis.

2.3. Flow cytometric analysis of picophytoplankton

In the laboratory, frozen samples were thawed and yellow green latex beads of 2 μm (Polysciences Co., USA) were added to 1 ml of sample as an internal standard to calibrate cell fluorescence emission and light scatter signals. Samples were analyzed with FACS Aria II flow cytometer equipped with blue (488 nm) and red (630 nm) lasers. *Prochlorococcus*-like (*PRO*-like) cells, *SYN* and PEUK were distinguished based on the forward and right angle light scatter (FALS and RALS, respectively, which serve as proxies for cell size), red fluorescence from chlorophyll (>650 nm) and phycocyanin (630 nm) and orange fluorescence from phycoerythrin (578 nm; Fig. 2). Two groups of *SYN* were distinguished based on their specific fluorescence characteristics; one rich in phycoerythrin (*SYN*-PE) with orange fluorescence and the other in phycocyanin (*SYN*-PC) with

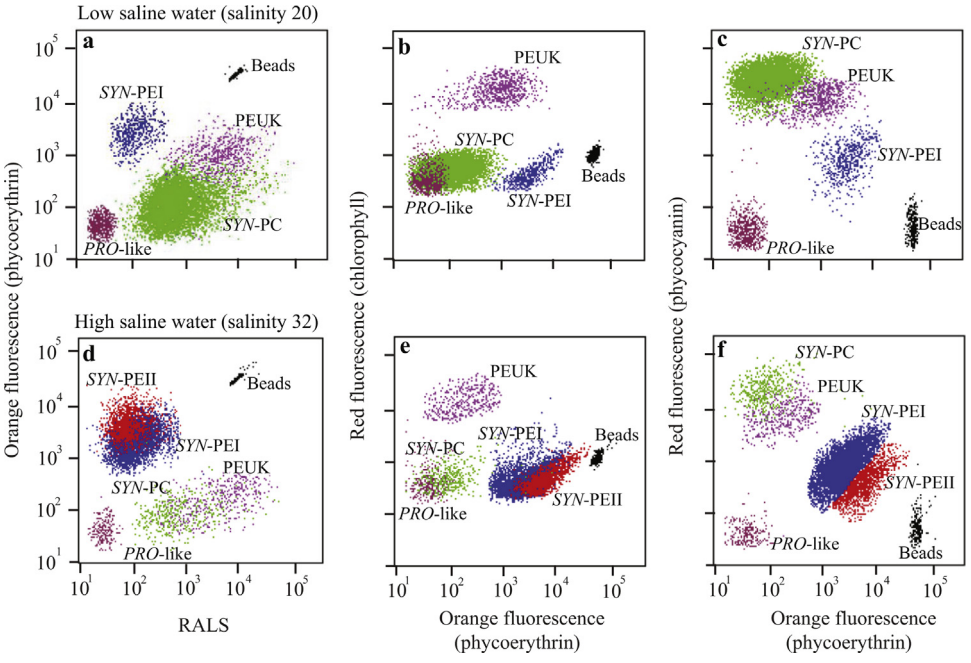

Fig. 2. Flow cytometric analysis of picophytoplankton community from (a–c) low saline and (d–f) high saline water samples.

red fluorescence. PEUK and *PRO*-like cells were identified based on their larger and smaller RALS along with higher and lower red fluorescence characteristics, respectively. *SYN*-PE group comprised two sub-groups, one with a lower PE fluorescence (*SYN*-PEI) than the other (*SYN*-PEII).

2.4. Trophic status of the water column

The multivariate index of trophic state (TRIX) method was used to evaluate the trophic status of CB (Vollenweider et al., 1998; Sin et al., 2013), which was then used to assess the relationship between PP groups and trophic status of water. TRIX was calculated using the equation $TRIX = (\log_{10}(\text{chl } a \times a\%O_2 \times DIN \times DIP) + k)/m$, where chl *a* is in mg m^{-3}, a%O_2 is absolute value of the percentage of DO saturation (abs $|100 - \%O_2| = \%O_2$), DIN is dissolved inorganic nitrogen including NO_3, NO_2, NH_4 in mg m^{-3} and DIP is dissolved inorganic PO_4 in mg m^{-3}. The constants k—3.5 and m—0.8 are scale values obtained from Vollenweider et al. (1998) to adjust TRIX scale values (reads from 0 to 10) with a level of eutrophication in the CB. According to this method, TRIX scores lesser than 4 indicate high state of water quality with low eutrophication; scores between 4 and 5 indicate good state of water quality with medium eutrophication; scores between 5 and 6 indicate bad state of water quality with high eutrophication and scores greater than 6 indicate poor state of water quality with elevated levels of eutrophication.

2.5. Data analyses

Linear regression analysis was performed in order to understand the relationship of PP abundance (*SYN*-PEI, *SYN*-PEII, *SYN*-PC, PEUK and *PRO*-like; log [x + 1]) with the environmental variables (salinity, temperature, estimated tidal height, depth, DO, BOD, nutrients and chl *a*) and TRIX scores. Linear regression analysis was also performed to assess the relation of *SYN*-PC: *SYN*-PE abundance ratio with salinity. Principle Component Analysis (PCA) was applied to the ecological variables: DO, BOD, nitrate, nitrite, phosphate, ammonium and silicate (log [x + 1]), which are indicators of anthropogenic pressure. This analysis was done using SPSS statistics software (windows 16.0) with a significance level of 0.05 in order to evaluate the ecological variables which are major indicators of anthropogenic pressure in the CB. Principle components (PC) having eigen values >1 were considered for further analysis. Subsequently, linear regression analysis was performed between the PC1 scores and cell abundance (log [x + 1]) of individual PP groups in order to evaluate the relationship of PP groups with the indicators of anthropogenic pressure.

3. Results

3.1. Environmental parameters

Lowest temperature was recorded during MON (24 to 29 °C; Fig. 3a and b) and it varied from 27 to 31.3 °C during PrM and PM in surface and NBW. Heavy precipitation was observed during MON season (total 195 mm). During PM-II, 56 mm precipitation was recorded on November 23, 2012. PrM showers were observed at the end of May 2012 (Table A2). During PM-I and PM-II, tidal amplitude difference was 0.50–0.91 m. During PrM and MON, tidal amplitude difference was 0.41–0.58 m and 0.56–0.74 m, respectively (Table A2). Station depths varied from ~1.71 m (S23) to ~11.69 m (S9). CB was partially mixed during PrM and PM and stratified during MON (Salinity 2 to 14 of surface waters and 4 to 34.8 of NBW) due to large amount of freshwater discharge. During PM-I, surface water salinity was higher than that during PrM at the approach channel stations (Fig. 3c and d), as PrM sampling was carried out during low tide (Table A1). Higher salinity was observed across the CB during PM-II sampling which was carried out during high tide. Vertically, salinity and temperature showed differences only at those stations where the depth was >5 m. DO concentration was high in PM-I (up to 8.4 mg l^{-1}) followed by PrM, PM-II and MON (Fig. 3e and f). DO concentrations were lower in the NBW than in the surface waters. BOD values were >1 mg l^{-1} during all the seasons and did not show much difference between surface and NBW. On an average, BOD values were high during PM-I (3.14 mg l^{-1}) and PM-II (1.58 mg l^{-1}) and low during PrM and MON (Fig. 3g and h).

High NO_3 concentrations (up to 28.42 μM) were recorded during MON followed by PM-II, PrM and PM-I with higher values in the surface waters. NO_3 concentrations did not differ much between the stations except during PM-II, when inner stations (S4–6, S14–15) had higher NO_3 concentrations (Fig. 3i and j). Higher PO_4 concentrations were recorded in the surface waters during PrM followed by MON and PM (up to 6.69 μM; Fig. 3k and l). NO_2 concentrations were lower during two successive PM seasons. NH_4 concentrations were high during PrM followed by PM-I and MON (10 to 66 μM). SiO_4 concentration ranged from 9.76 to 93.53 μM and were higher during PM-I in the surface waters, particularly at S15 to S19 (Fig. 3q and r). Vertically, not much difference was observed in PO_4, NH_4 and NO_2 concentrations (Fig. 3k–p). Average chl *a* concentrations during the four seasons varied from 1.4 to 32.46 μg l^{-1} across the CB. Compared to the mouth of the CB, chl *a* concentrations were higher at the inner stations (S2–8 and S11–23) with occasionally high concentrations in the surface waters during PrM (~59.92 μg l^{-1}; S7), PM-II (~107.1 μg l^{-1}; S4) and in the NBW during PM-I (~63.23 μg l^{-1}; S22), PrM (~64.77 μg l^{-1}; S7) and MON (~84.60 μg l^{-1}; S7; Fig. 3s and t).

3.2. Interseasonal and spatial variation of picophytoplankton

Total PP abundance ranged from 0.1 to 2.29×10^5 cells ml^{-1} in surface and NBW during PM-I. During PrM, a prominent increase in PP abundance was observed across the CB (up to 4.06×10^5 cells ml^{-1}), which decreased during MON (<1.71×10^5 cells ml^{-1}) and increased during PM-II (<2.8×10^5 cells ml^{-1}; Fig. 4k and l). Seasonal and spatial variation of PP groups abundance is shown in Fig. 4a–l. *SYN*-PEI was the dominant group observed during PM-I (surface waters of S1, S5, S7, S9 and NBW of S1–22) and PM-II (surface waters of S5–8, S11, S18–20, S22 and NBW of S1, S5–22; Fig. 4a and b). During PrM and MON, *SYN*-PEI abundance was low (<0.46×10^5 cells ml^{-1}). During PM-I, contribution of *SYN*-PEI to total PP was higher (~85%) in the NBW compared to the surface waters (Fig. 5a and b). Highest cell abundance was recorded in NBW of S1 (2.0×10^5 cells ml^{-1}) and S7 (2.86×10^5 cells ml^{-1}) compared to all other seasons. During PM-II, higher *SYN*-PEI abundance was observed at Ernakulam channel stations (surface waters and NBW) where salinity was >29 (Fig. 4a and b). Being second dominant group during PM-I, *SYN*-PC abundance was high in the Ernakulam channel stations compared to the stations near the mouth of CB (Fig. 4e and f). Throughout the season, cell abundance was higher in the surface waters than NBW, except at some stations where NBW salinity was <29. A steep increase in *SYN*-PC abundance was observed during the PrM, with maximum cell abundance at S21 (Fig. 4e and f). This was the dominant group contributing up to 92% to the total PP abundance across the CB (Fig. 5c and d). During MON, dominance of *SYN*-PC group continued with comparatively higher cell abundance than that during PrM (Fig. 4e and f). During PM-II, *SYN*-PC dominated low saline waters (<24) with the highest cell abundance at S9. At S23, higher cell abundance was recorded as observed during MON (Fig. 4e and f). During PM-I, *SYN*-PEII group was absent where salinity was <20 and during PrM it was completely absent. This group was observed in the NBW during MON with very low cell abundance. During PM-II, *SYN*-PEII was detected only at salinities

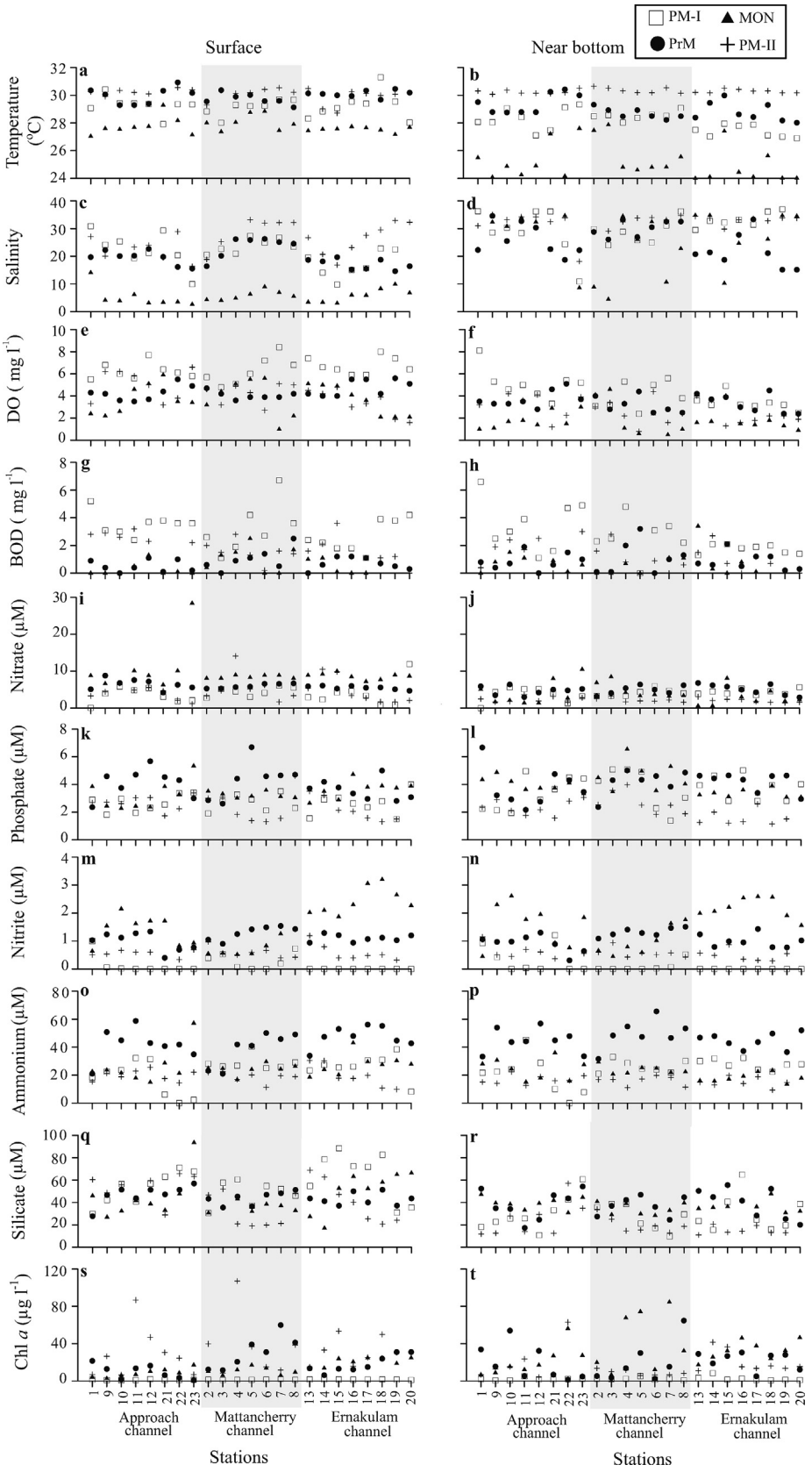

Fig. 3. Seasonal and spatial variations in (a and b) temperature, (c and d) salinity, (e and f) dissolved oxygen, (g and h) biological oxygen demand, (i and j) nitrate, (k and l) phosphate, (m and n) nitrite, (o and p) ammonium, (q and r) silicate and (s and t) chlorophyll *a* in the Cochin backwaters.

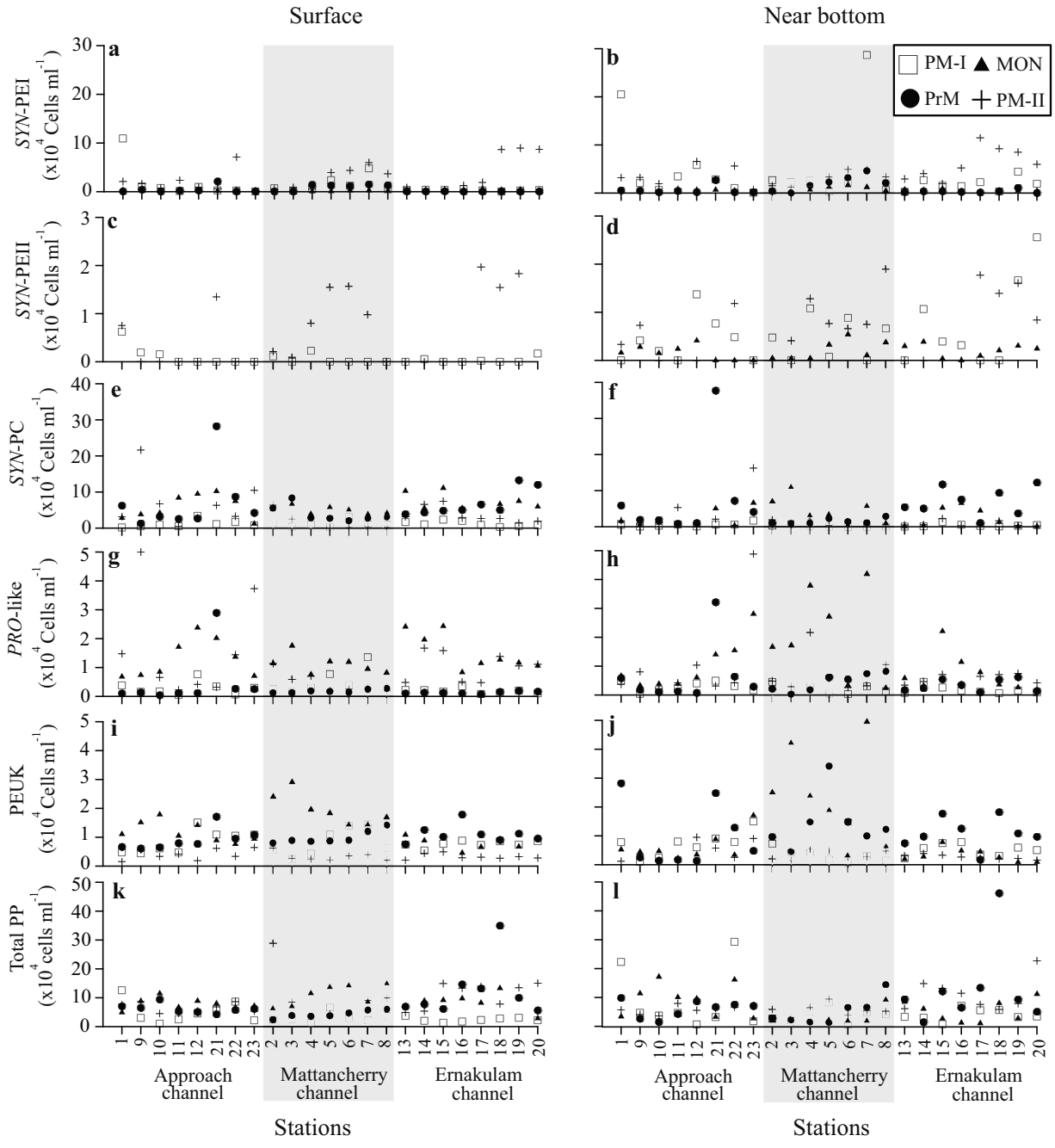

Fig. 4. Seasonal and spatial variations in the picophytoplankton community structure in the Cochin backwaters. (a and b) *SYN*-PEI, (c and d) *SYN*-PEII, (e and f) *SYN*-PC, (g and h) *PRO*-like cells, (i and j) PEUK and (k and l) total picophytoplankton cell abundance.

>26, with low cell abundance (Fig. 4c and d). Their contribution to total PP abundance was higher in the NBW, especially at S20 (46%) during PM-I whereas during other seasons it was <26% (Fig. 5a–h).

PRO-like cells showed remarkable increase during MON with higher cell abundance in the surface waters than that in the NBW, except at Mattancherry channel stations (Fig. 4g and h). Contribution to total PP abundance was high (~40%) during this season and decreased (<27%) during PM-II (Fig. 5a–h). PEUK abundance was high during MON exhibiting a decreasing trend from S2 to S23. In the surface waters, cell abundance was higher than in the NBW, except at Mattancherry channel stations. Highest cell abundance (0.49×10^5 cells ml^{-1}) was recorded in the NBW of S7. Even though their abundance was high, their contribution to total PP was <33%. PEUK abundance was reduced by an order of magnitude during PM-II. However, during PrM increased abundance was observed compared to PM-I (Fig. 4i and j). During PM-I, PEUK contribution to total PP abundance in the surface waters ranged up to 64% (Fig. 5a and b). Generally, their abundance was high in the surface waters compared to the NBW, except during PrM.

3.3. Intraseasonal variation of picophytoplankton

During PM-II, total PP abundance was higher compared to that during PM-I (Fig. 4k and l). *SYN*-PEI and *SYN*-PEII abundance were significantly higher during PM-II compared to that during PM-I at S22, S5–8 and S18–20 (Fig. 4a–d) where salinity was comparatively higher (Fig. 3c and d). *SYN*-PC showed higher cell abundance during PM-II at most of the stations compared to that during PM-I (Fig. 4e

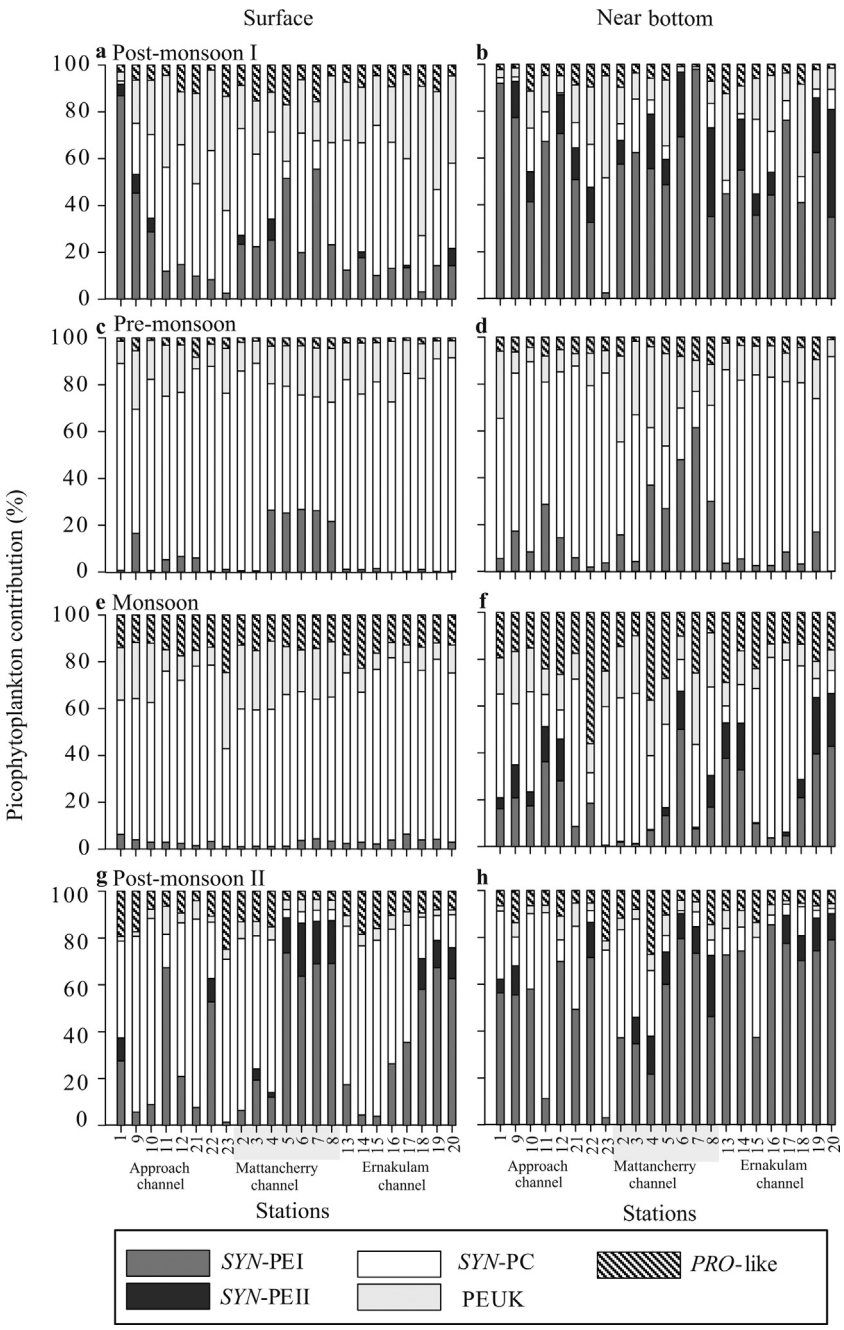

Fig. 5. Contribution (%) of individual picophytoplankton groups to the total picophytoplankton abundance during (a and b) post-monsoon I, (c and d) pre-monsoon, (e and f) monsoon and (g and h) post-monsoon II seasons.

and f). The spatial distribution of *SYN*-PEI and *SYN*-PC differed during PM-II wherein the latter dominated in the surface waters of S13–17, S1–4, S9–10, S12 and S21 and NBW of S11, S23 and S2–4 (Fig. 4a–f).

3.4. TRIX scores for Cochin backwaters

The average values of TRIX (5.15) for the study period revealed that the CB is highly eutrophic with a bad state of water quality. TRIX scores for the study region ranged from 1.64 to 7.37 during all the seasons (Fig. 6a and b). During PrM and MON, most of the stations showed elevated conditions of eutrophication. Only during PM-I medium level of eutrophication with good state of water quality was observed for the surface waters.

3.5. Relationship between environmental parameters and picophytoplankton groups

Linear regression analysis showed that TRIX scores correlated negatively with salinity and estimated tidal height (Table 1). *SYN*-PEI and *SYN*-PEII correlated positively with salinity, estimated tidal height and station depth, whereas *SYN*-PC and PEUK correlated negatively. *PRO*-like cells correlated negatively with salinity. *SYN*-PC correlated positively with temperature whereas *SYN*-PEII and *PRO*-like cells correlated negatively (Table 1). DO correlated negatively with station depth. *SYN*-PC and PEUK correlated positively with nutrients whereas, *SYN*-PEI and *SYN*-PEII correlated negatively (Table 1). *SYN*-PC and *PRO*-like cells correlated positively with total chl *a*. *SYN*-PC correlated positively with TRIX scores, whereas

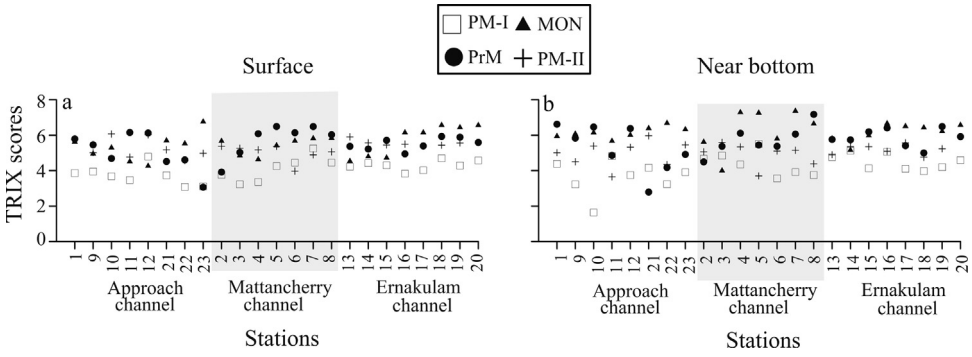

Fig. 6. TRIX scores during different seasons for Cochin backwaters. (a) surface and (b) Near bottom waters.

Table 1
Results of linear regression analysis for the environmental variables, TRIX scores and picophytoplankton abundance.

Variables	Temperature	Salinity	Est. tidal height	Station depth	TRIX	DO	BOD	NO_3	NO_2	NH_4	PO_4	SiO_4	Chlorophyll *a*
Salinity	0.11												
Est. tidal height	−0.14	**0.20****											
Station depth	**−0.25****	**0.43****	0.03										
TRIX	**−0.21****	**−0.18***	**−0.20****	0.06									
DO	**0.46****	**−0.19****	−0.07	**−0.50****	**−0.36****								
Chlorophyll *a*	−0.08	0.02	−0.13	0.05	**0.54****	**−0.43****	**−0.40****	0.11	**0.58****	0.12	0.14	−0.01	
SYN-PEI	0.06	**0.26****	**0.36****	**0.33****	**−0.24****	−0.10	**0.18***	**−0.40****	**−0.30****	**−0.28****	**−0.25****	**−0.31****	−0.06
SYN-PEII	**−0.24****	**0.20****	**0.33****	**0.28****	−0.16	−0.13	**0.15***	**−0.29****	**−0.23****	**−0.34****	**−0.17***	**−0.24****	−0.01
SYN-PC	**0.19***	**−0.35****	**−0.20****	**−0.43****	**0.34****	0.06	**−0.25****	**0.36****	**0.36****	**0.16***	**0.22****	**0.38****	**0.34****
PEUK	−0.11	**−0.32****	**−0.32****	**−0.20****	0.14	0.13	−0.06	**0.20****	**0.29****	**0.27****	**0.25****	**0.27****	−0.09
PRO-like	**−0.27****	**−0.19****	−0.07	−0.01	0.02	**−0.30****	**−0.25****	−0.09	**0.33****	−0.10	−0.11	−0.08	**0.31****

* $p < 0.05$.
** $p < 0.01$.

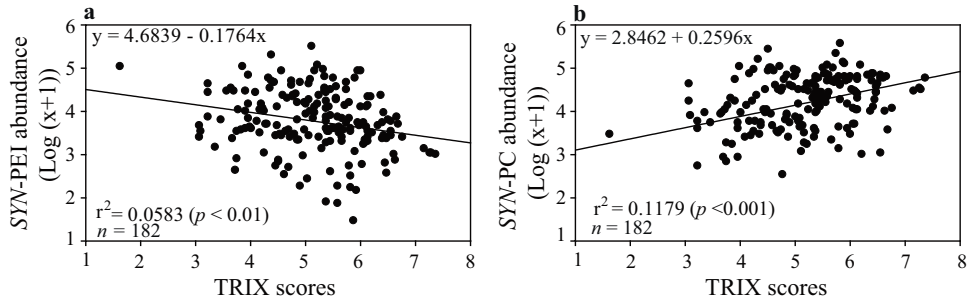

Fig. 7. Linear regression analysis of (a) *SYN*-PEI and (b) *SYN*-PC abundance with TRIX scores.

SYN-PE correlated negatively (Fig. 7a and b; Table 1). *SYN*-PC: *SYN*-PE abundance ratio correlated negatively with salinity (Fig. 8).

PCA exhibited 2 PC's which explained 65% variation of the ecological variables (DO, BOD, nitrate, nitrite, phosphate, ammonium and silicate) which are indicators of anthropogenic pressure. The first factor, PC1 accounted for 37% of the variance with a positive load of PO_4, NH_4, SiO_4, NO_2, and NO_3. NH_4 and PO_4 were the most significant variables. Weak negative loading of the BOD was observed in PC1 (Table 2). Positive load of the DO and BOD

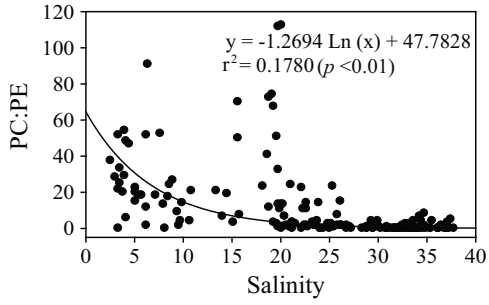

Fig. 8. Linear regression analysis between *SYN*-PC:*SYN*-PE abundance ratio and salinity in the Cochin backwaters. The curve was fitted under the logarithmic equation model.

Table 2
Principle component analysis with varifactors (PC's) extracted for the ecological variables. Bold text denotes significant loading.

Variables	PC1	PC2
DO	−0.239	**0.868**
BOD	**−0.460**	**0.739**
NO_3	**0.590**	0.299
NO_2	**0.634**	**−0.440**
NH_4	**0.739**	0.206
PO_4	**0.781**	0.209
SiO_4	**0.639**	0.524
Eigenvalues	2.58	1.94
% of variance	36.9	27.8
Cumulative %	36.9	64.7

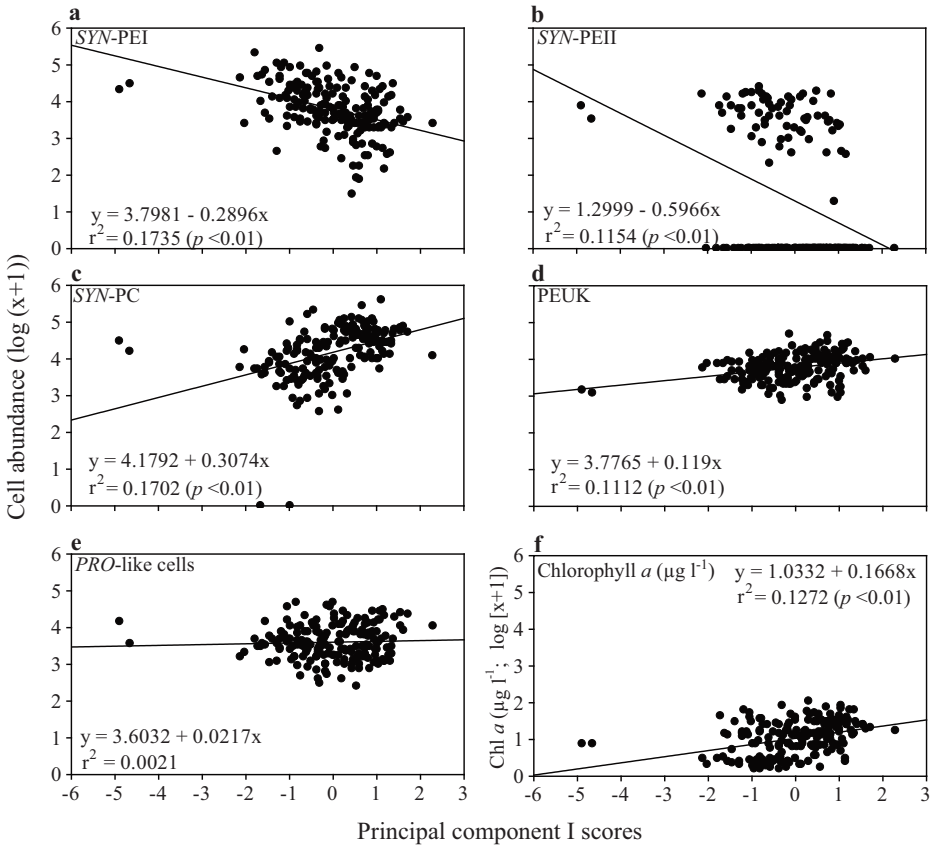

Fig. 9. Linear regression analysis of (a) *SYN*-PEI, (b) *SYN*-PEII, (c) *SYN*-PC, (d) PEUK, (e) *PRO*-like cells and (f) chl *a* with principle component scores (PC1) for the ecological variables (Dissolved oxygen, biological oxygen demand, nitrate, phosphate, nitrite, ammonium and silicate).

was observed at PC2 which explained 27% of the variance. Linear regression analysis showed that *SYN*-PEI and *SYN*-PEII correlated negatively with PC1 scores, whereas *SYN*-PC, PEUK and chl *a* correlated positively (Fig. 9a–f).

4. Discussion

4.1. Hydrography of Cochin backwaters

Over the past few years, investigators have revealed that CB is contaminated by anthropogenic activities (Balachandran et al., 2005; Martin et al., 2012; Anu et al., 2014) such as industrialization (10^4 million liters of partially treated and untreated industrial effluents are discharged everyday by a large number of industries), agriculture, transportation and domestic sewage effluent discharge (Unnithan et al., 1975; Vijayan et al., 1976; Menon et al., 2000; Qasim, 2003). As a consequence, concentration of toxic metals in the surficial sediments has been reported in moderate to heavily polluted condition (Martin et al., 2012). In the present study, TRIX scores showed that CB is highly eutrophic.

Hydrography of the CB reflected typical tropical estuarine conditions where temperature gradually increased from PM to PrM season and subsequently decreased during MON. During MON, stratification developed due to increased freshwater influx and formed a decreasing salinity gradient from the mouth toward upstream of the CB. During non-MON period, as freshwater influx reduced, water column was partially mixed as is observed in estuaries influenced by monsoonal rainfall (Joseph and Kurup, 1989; Shetye, 1999). Recently, Jacob et al. (2013) reported that during non-MON high tide, saltwater intrudes up to 40 km in CB. Thus, in the present study, stations located in all three channels were influenced by the incoming high saline waters during the high tide.

An unique feature of CB is the surplus amount of nutrient load that it receives throughout the year via land drainage, agricultural activities and river discharge during MON (Devi et al., 1991; Madhu et al., 2007), when annual discharge of freshwater is $20{,}000 \times 10^6$ m^3 (Srinivas et al., 2003). High nutrient supply during MON is a profound characteristic of estuaries influenced by monsoonal rainfall (Qasim and Sen Gupta, 1981). High PO_4 concentrations were observed during the PrM as reported in earlier studies (Sankaranarayanan and Qasim, 1969). Martin et al. (2012) has reported a steady increase in PO_4 concentration from December to April. This is believed to be the result of high salinity/pH combined with tidal activity during the PrM, which causes desorption of phosphate from the suspended particles (Reddy and Sankaranarayanan, 1972; Martin et al., 2008). In this study, PCA suggested that PO_4 and NH_4 are the major indicators of the eutrophicated environment in the CB.

Comparatively lower concentrations of DO in the NBW than that in the surface waters indicated higher utilization of oxygen than production. This observation was consistent with previous reports (Madhu et al., 2009; Martin et al., 2011) and was substantiated by the BOD values of >1.5 mg l^{-1} at most of the stations suggesting that respiration by aquatic animals, decomposition by bacteria and various chemical reactions were active in the CB.

4.2. Interseasonal variation of picophytoplankton in Cochin backwaters

Several studies have been conducted on the biological aspects in the CB (Madhu et al., 2007, 2009; Martin et al., 2008). These studies emphasize that irrespective of the season, CB facilitates luxurious growth of phytoplankton due to excess level of nutrient availability (Balachandran et al., 2005; Madhu et al., 2007). In the study region, maximum phytoplankton biomass recorded was higher (average 17.05 $\mu g\,l^{-1}$; ranged up to 107 $\mu g\,l^{-1}$) than that reported in previous studies in CB (49 $\mu g\,l^{-1}$; Madhu et al., 2007, 2009; Martin et al., 2011) and also in the Mandovi and Zuari estuaries located along the west coast of India (Pednekar et al., 2011; Patil and Anil, 2011). This could be due to the nutrient enrichment by anthropogenic activities, which triggers the massive growth of nanoplankton (<20 μm; Madhu et al., 2007; Martin et al., 2011) and phytoplankton blooms which are common in the CB when the intermediate salinity condition exists (Devassy, 1974; Madhu et al., 2010; Martin et al., 2013). Another reason could be the weeds and water hyacinths, which proliferate in the upstream waters that severely restrict the natural flushing (Shivaprasad et al., 2012) and enter the CB during MON due to influx of low saline waters. In the PrM and PM-II seasons the higher chl *a* concentration in the surface (64.77 $\mu g\,l^{-1}$; S7) and NBW (59.99 $\mu g\,l^{-1}$; S8), could be the result of showers that occurred during the sampling period (Table A2), which probably drive the weeds and water hyacinths into the CB or from stirred up sediments. In addition, during PM-II, the highest chl *a* concentration recorded at S4 (104 $\mu g\,l^{-1}$) one day after heavy showers confirms that the incoming freshwater is a source of the high chl biomass.

Consistently high PP abundance (10^5 cells ml^{-1}) during all the seasons indicates that PP could be an important component of the phytoplankton community in CB. During MON the prevailing environmental factors influenced the distribution of PP groups, especially *SYN*-PE and *SYN*-PC, wherein the former is known to be abundant in high saline waters and latter in low saline waters (Murrell and Lores, 2004). During non-MON seasons, tide controls the salinity distribution in CB (George and Kartha, 1963). Salinity variation due to tidal impact clearly influenced *SYN*-PC and *SYN*-PE distribution in the CB, both horizontally and vertically. PM-II sampling was carried out during high tide. This could be the reason for high salinity in Ernakulam channel where *SYN*-PEI was the dominant group in the surface and NBW. PrM sampling was carried out during low tide which resulted in low surface salinity across the estuary where *SYN*-PC was dominant. These observations suggest that tide is also an influential factor for *SYN* distribution in the CB wherein *SYN*-PE enters the CB from the coastal waters during high tide and *SYN*-PC during the low tide from the upstream end. This is substantiated by observations from the monsoonal Zuari estuary (Rajaneesh and Mitbavkar, 2013), wherein during the non-MON period due to high tidal activity, *SYN*-PE showed higher abundance upstream whereas, during MON, *SYN*-PC abundance was higher downstream due to strong freshwater runoff. The significant positive relation of *SYN*-PE abundance and negative relation of *SYN*-PC and PEUK abundance with salinity and estimated tidal height (Table A1) indicates that tide is a prominent controller of PP community structure in CB. Significant relationship of PP groups with salinity is consistent with studies carried out in subtropical and temperate regions (Ray et al., 1989; Murrell and Lores, 2004), especially for *SYN*. Transition in dominance from *SYN*-PC to *SYN*-PE at salinities of ~20–25 found in this study (Fig. 8), was previously observed in subtropical estuaries (Ray et al., 1989; Murrell and Lores, 2004; Zhang et al., 2013) and tropical estuaries (Rajaneesh and Mitbavkar, 2013). In addition, negative relation of *SYN*-PC and positive relation of *SYN*-PE with the station depths indicate that higher salinity in the NBW favors *SYN*-PE groups. This was well reflected in MON when the high saline waters harboring *SYN*-PE were capped by the low saline waters harboring *SYN*-PC in the approach channel stations (Fig. 5c and d). These findings suggest that *SYN* distribution pattern can serve as an indicator of the seasonal water column hydrography (stratified or mixed) influenced by physical forces such as tides and freshwater runoff. The presence of an additional group of *SYN*-PE with high PE intensity at higher salinities (*SYN*-PEII) in the estuarine waters indicates that this group could have been introduced from the offshore waters during high tide. This observation is consistent with previous reports from the Zuari estuary, North western Arabian coast, Mississippi river plume and the Pearl River estuary (Campbell et al., 1998; Liu et al., 1998, 2004; Lin et al., 2010; Rajaneesh and Mitbavkar, 2013). *PRO*-like cells detected in the low saline waters of the CB were also observed recently in the Zuari estuary along the south west coast of India (Mitbavkar et al., 2012). Shang et al. (2007) reported *PRO*-like cells in brackish and in freshwater. Similarly in the present study, *PRO*-like cells were higher in the low saline waters as seen from the negative correlation with salinity. However, work on *PRO*-like cells is very limited and effect of environmental condition on these cells is still not clear. Recently, Liu et al. (2013) identified a previously suggested group of *PRO*-like cells as *SYN*-PC based on laboratory experiments. However, to confirm the strain in the CB, molecular approaches are required.

Variation in the spectral light quality is one of the factors altering the PP composition in oceanic, coastal and estuarine waters (Wood, 1985; Scanlan, 2003). In coastal and estuarine waters, generally, *SYN*-PE group abundance is high in clear waters where the green light predominates due to the low concentrations of suspended particles and dissolved organic matter concentrations (Li et al., 1983; Wood, 1985; Stomp et al., 2007). *SYN*-PC is higher in turbid waters loaded with dissolved particulate organic matter or rich in chlorophyll where the spectral light quality is altered from green to red (Stomp et al., 2007). In CB, water is highly turbid throughout the year and comparatively higher during the MON (Qasim and Reddy, 1967). Hence, this could be one of the factors responsible for the predominance of *SYN*-PC in the CB throughout the year, due to its better ability to utilize the red wavelength along with its ability to proliferate at lower salinities. In addition, the positive correlation of *SYN*-PC with chl *a* suggests that this group is not only dominant, but also significantly contributes to total phytoplankton biomass in the CB. Increasing temperature, irradiance, salinity and comparatively lower turbidity could be responsible for the higher abundance of *SYN*-PE groups during PM.

The negative relationship of TRIX with the estimated tidal height and salinity suggests that low tide causes a higher trophic index due to more influence of freshwater rich in anthropogenic contaminants from the upstream whereas, high tide brings offshore waters in to the CB, which leads to dilution of eutrophic waters (Table 1). The positive and negative relation of *SYN*-PC and *SYN*-PE, respectively, with TRIX scores suggests that these groups occupy contrasting ecological niches (Fig. 7a and b). In the hypertrophic waters of French Mediterranean lagoon, which was described as an anthropogenically influenced eutrophicated area, abundance of *SYN*-PC was higher than that of *SYN*-PE (Bec et al., 2011). Munawar and Weisse (1989) reported that autotrophic picoplankton avoided contaminated environments but were high in contaminated eutrophicated areas. They attributed this to availability of excess nutrients, which may have complexing effects resulting in the detoxification of contaminants. Aneeshkumar and Sujatha (2012) reported that zeaxanthin pigment indicative of cyanobacteria was found more in the sediments of sites influenced by anthropogenic activities (near to S23) in the CB. Since zeaxanthin is a marker pigment of both *SYN*-PE and *SYN*-PC and we found *SYN*-PC > *SYN*-PE throughout the study period at S23, which is a sewage discharge point, we assume that *SYN*-PC was the dominant group found in this area by Aneeshkumar and Sujatha (2012). These observations corroborate our findings and suggest that *SYN*

could serve as a potential indicator of the trophic status of water bodies.

Temperature in the tropical regions does not show much annual variation (8 °C in the present study) as in temperate regions (14 °C). As a consequence, PP abundance was high throughout the year in the tropics as compared to the temperate regions where abundance peaks are observed only during summer (Agawin et al., 1998; Chiang et al., 2002; Murrell and Lores, 2004). This suggests that seasonal temperature exercises a latitudinal variation on the PP distribution. Significant positive relation of total PP abundance with temperature is a profound characteristic of tropical, subtropical and temperate estuaries (Ray et al., 1989; Agawin et al., 1998; Qiu et al., 2010; Wang et al., 2011). However, in the present study, only *SYN*-PC showed a positive correlation ($p < 0.05$) with temperature. Some studies conducted in tropical and subtropical estuaries showed that PP negatively correlated with nutrients (Qiu et al., 2010; Zhang et al., 2013). However, these studies considered total *SYN* (*SYN*-PC and *SYN*-PE) abundance in order to evaluate the relationship with nutrients. In the present study, although the positive relation of *SYN*-PC, PEUK and negative relation of *SYN*-PE groups with NO_3, PO_4 and NH_4 may not be cause and effect relationships, it indicates that nutrient concentrations could influence the seasonal variations of these groups. Similar results were obtained from the Zuari estuary, India (Rajaneesh and Mitbavkar, 2013). In the Uchiumi Bay, Japan, PO_4 addition showed seasonal variations on the growth rates of *SYN* and PEUK (Katano et al., 2005). They presumed that the in situ nutrient concentrations or difference in species could be responsible for such a seasonal response. Though PEUK are the most competitive among PP groups (Pan et al., 2007), it was not the dominant group in CB, even in high nutrient concentrations. Previous studies in tropical and subtropical regions have reported that this group dominated the nutrient rich conditions (Jiao et al., 2005; Qiu et al., 2010). Probably, this group abundance was controlled by the high microzooplankton grazing rates which we did not consider in the present study (Wetz et al., 2011).

SYN-PE groups attained higher abundance during PM-I and PM-II seasons indicating its preference for increased temperature after MON. Along with temperature, irradiance is also known to influence the seasonal distribution of *SYN* abundance and biomass (Agawin et al., 1998; Tsai et al., 2008). It is believed that there are multifactors, which are controlling the *SYN*-PE growth in coastal and estuarine ecosystems (Chang et al., 2003; Zhang et al., 2013). Increasing temperature during PrM and decreasing temperature and salinity during MON could be the reason for low abundance during these periods. *SYN*-PC was the dominant group present in the CB with highest abundance in PrM and their contribution was substantial to total PP. Similarly, studies carried out in the subtropical and temperate estuaries have shown that abundance of *SYN*-PC was greatest during warm periods (Ray et al., 1989; Murrell and Lores, 2004). Temperature was the limiting factor for PEUK in the previous studies where temperature varied between 20 and 27 °C (Pan et al., 2007). However, in the present study area, where the temperature range was 24 to 32 °C, PEUK were not significantly affected by temperature.

4.3. Intraseasonal variation of picophytoplankton in Cochin backwaters

As the PM-I sampling was carried out in October soon after the MON, the freshwater influence was still observed in the CB as compared to that during PM-II sampling which was carried out in November. As a result, salinity and temperature were comparatively lower during PM-I. This was reflected in the PP distribution wherein higher PP abundance was observed during the PM-II. The dominance of *SYN*-PC over *SYN*-PEI during PM-II in some of the stations was maily due to salinity <25 as a result of rainfall that occurred on the sampling day (Table A2). Higher salinity in the NBW during PM-II favored higher *SYN*-PEI and *SYN*-PEII abundance in the CB.

5. Conclusion

Hydrography of the CB reflected typical tropical estuarine conditions with stratification during MON and partially mixed condition during non-MON seasons. Irrespective of the season, high concentrations of nutrients were recorded in the estuary. TRIX scores showed that this estuary is highly eutrophic. Consistently high PP abundance (10^5 cells ml^{-1}) during all the seasons indicates that PP is an important component of the phytoplankton community in the CB. During non-MON, tide was an influential factor for *SYN* distribution wherein *SYN*-PE was found to be high during high tide and *SYN*-PC during the low tide suggesting their influx from the coastal waters and upstream, respectively. During MON, due to stratification by freshwater influx, surface waters dominated by *SYN*-PC capped the *SYN*-PE dominated NBW of inner stations. Along with low salinity, high turbidity that affects the light penetration with predominance of red light could be another factor favoring the *SYN*-PC abundance in the low saline waters. *SYN*-PC showed a significant positive relation with chl *a* suggesting its significant contribution to total biomass. Although the relation of *SYN*-PC and *SYN*-PE groups with nutrients may not be cause and effect relationships, it indicates that nutrient concentrations could influence the seasonal variations of these groups. *SYN*-PE groups attained higher abundance during PM-I and PM-II seasons indicating its preference for higher temperature. *SYN*-PC and PEUK showed positive and *SYN*-PE showed negative relation with TRIX scores which suggests that these groups occupy contrasting ecological niches. These findings suggest that PP distribution pattern can serve as an indicator of the trophic status of coastal water bodies.

Acknowledgements

The authors would like to thank The Director, Council of Scientific and Industrial Research (CSIR)– National Institute of Oceanography for his support. This work was supported by the Ballast Water Management Programme India, funded by Directorate General of Shipping, Government of India. We thank Dr. Dattesh and Mr. K. Venkat for their support and guidance. We thank our project team members for their help and suggestions during sampling. We thank the anonymous reviewers for their valuable comments. Rajaneesh K.M. acknowledges CSIR for the award of Senior Research Fellowship (SRF). This is a NIO contribution # 5729.

Appendix A. Supplementary data

Supplementary data associated with this article can be found, in the online version, at http://dx.doi.org/10.1016/j.ecolind.2015.02.033. These data include Google maps of the most important areas described in this article.

References

Agawin, N.S., Duarte, C.M., Agusti, S., 1998. Growth and abundance of *Synechococcus* sp. in a Mediterranean Bay: seasonality and relationship with temperature. Mar. Ecol. Prog. Ser. 170, 45–53.

Aneeshkumar, N., Sujatha, C., 2012. Biomarker pigment signatures in Cochin backwater system—a tropical estuary south west coast of India. Estuarine Coastal Shelf Sci. 99, 182–190.

Anu, P., Jayachandran, P., Sreekumar, P., Nandan, S.B., 2014. A review on heavy metal pollution in Cochin backwaters, Southwest Coast of India. Int. J. Mar. Sci. 4, 92–98.

Balachandran, K., Raj, L., Nair, M., Joseph, T., Sheeba, P., Venugopal, P., 2005. Heavy metal accumulation in a flow restricted, tropical estuary. Estuarine Coastal Shelf Sci. 65, 361–370.

Bec, B., Collos, Y., Souchu, P., Vaquer, A., Lautier, J., Fiandrino, A., Benau, L., Orsoni, V., Laugier, T., 2011. Distribution of picophytoplankton and nanophytoplankton along an anthropogenic eutrophication gradient in French Mediterranean coastal lagoons. Aquat. Microb. Ecol. 63, 29–45.

Campbell, L., Landry, M., Constantinou, J., Nolla, H., Brown, S., Liu, H., Caron, D., 1998. Response of microbial community structure to environmental forcing in the Arabian Sea. Deep Sea Res., II: Top. Stud. Oceanogr. 45, 2301–2325.

Chang, J., Lin, K.H., Chen, K.M., Gong, G.C., Chiang, K.P., 2003. *Synechococcus* growth and mortality rates in the East China Sea: range of variations and correlation with environmental factors. Deep Sea Res., II: Top. Stud. Oceanogr. 50, 1265–1278.

Chiang, K.P., Kuo, M.C., Chang, J., Wang, R.H., Gong, G.C., 2002. Spatial and temporal variation of the *Synechococcus* population in the East China Sea and its contribution to phytoplankton biomass. Cont. Shelf Res. 22, 3–13.

Chiang, K.P., Tsai, A.Y., Tsai, P.J., Gong, G.C., Tsai, S.F., 2013. Coupling of the spatial dynamic of picoplankton and nanoflagellate grazing pressure and carbon flow of the microbial food web in the subtropical pelagic continental shelf ecosystem. Biogeosci. Discuss. 10, 233–263.

Devi, K.S., Sankaranarayanan, V., Venugopal, P., 1991. Distribution of nutrients in the Periyar river estuary. Indian J. Mar. Sci. 20, 49–54.

Devassy, V., 1974. Observations on the bloom of a diatom *Fragilaria Oceanica* Cleve. Mahasagar 7, 101–105.

George, M., Kartha, K., 1963. Surface salinity of Cochin backwater with reference to tide. J. Mar. Biol. Assoc. India 5, 178–184.

Jacob, B., Revichandran, C., NaveenKumar, K., 2013. Salt intrusion study in Cochin estuary-using empirical models. Indian J. Geo-Mar. Sci. 42, 304–313.

Jiao, N., Yang, Y., Hong, N., Ma, Y., Harada, S., Koshikawa, H., Watanabe, M., 2005. Dynamics of autotrophic picoplankton and heterotrophic bacteria in the East China Sea. Cont. Shelf Res. 25, 1265–1279.

Jochem, F., 1988. On the distribution and importance of picocyanobacteria in a boreal inshore area (Kiel Bight, Western Baltic). J. Plankton Res. 10, 1009–1022.

Joseph, J., Kurup, P., 1989. Volume transport and estuarine features at Cochin inlet. Mahasagar 22, 165–172.

Jyothibabu, R., Madhu, N., Jayalakshmi, K., Balachandran, K., Shiyas, C., Martin, G., Nair, K., 2006. Impact of freshwater influx on microzooplankton mediated food web in a tropical estuary (Cochin backwaters—India). Estuarine Coastal Shelf Sci. 69, 505–518.

Kaladharan, P., Krishnakumar, P., Prema, D., Nandakumar, A., Khambadkar, L., Valsala, K., 2011. Assimilative capacity of Cochin inshore waters with reference to contaminants received from the backwaters and the upstream areas. Indian J. Fish. 58, 75–83.

Katano, T., Nakano, S.I., Ueno, H., Mitamura, O., Anbutsu, K., Kihira, M., Satoh, Y., Drucker, V., Sugiyama, M., 2005. Abundance, growth and grazing loss rates of picophytoplankton in Barguzin Bay, Lake Baikal. Aquat. Ecol. 39, 431–438.

Li, W., Rao, S., Harrison, W., Smith, J., Cullen, J., Irwin, B., Platt, T., 1983. Autotrophic picoplankton in the tropical ocean. Science(Washington) 219, 292–295.

Lin, D., Zhu, A., Xu, Z., Huang, L., Fang, H., 2010. Dynamics of photosynthetic picoplankton in a subtropical estuary and adjacent shelf waters. J. Mar. Biol. Assoc. U.K. 90, 1319–1329.

Liu, H., Campbell, L., Landry, M., Nolla, H., Brown, S., Constantinou, J., 1998. *Prochlorococcus* and *Synechococcus* growth rates and contributions to production in the Arabian Sea during the 1995 Southwest and Northeast Monsoons. Deep Sea Res., II: Top. Stud. Oceanogr. 45, 2327–2352.

Liu, H., Dagg, M., Campbell, L., Urban-Rich, J., 2004. Picophytoplankton and bacterioplankton in the Mississippi River plume and its adjacent waters. Estuaries Coasts 27, 147–156.

Liu, H., Jing, H., Wong, T.H., Chen, B., 2013. Co-occurrence of phycocyanin- and phycoerythrin-rich *Synechococcus* in subtropical estuarine and coastal waters of Hong Kong. Environ. Microbiol. Rep. 6, 90–99.

Madhu, N., Jyothibabu, R., Balachandran, K., Honey, U., Martin, G., Vijay, J., Shiyas, C., Gupta, G., Achuthankutty, C., 2007. Monsoonal impact on planktonic standing stock and abundance in a tropical estuary (Cochin backwaters—India). Estuarine Coastal Shelf Sci. 73, 54–64.

Madhu, N.V., Jyothibabu, R., Balachandran, K.K., 2009. Monsoon-induced changes in the size-fractionated phytoplankton biomass and production rate in the estuarine and coastal waters of southwest coast of India. Environ. Monit. Assess. 166, 521–528.

Madhu, N., Balachandran, K., Martin, G., Jyothibabu, R., Thottathil, S.D., Nair, M., Joseph, T., Kusum, K., 2010. Short-term variability of water quality and its implications on phytoplankton production in a tropical estuary (Cochin backwaters—India). Environ. Monit. Assess. 170, 287–300.

Martin, G., Vijay, J., Laluraj, C., Madhu, N., Joseph, T., Nair, M., Gupta, G., Balachandran, K., 2008. Fresh water influence on nutrient stoichiometry in a tropical estuary. South West coast of India. Appl. Ecol. Environ. Res. 6, 57–64.

Martin, G., Nisha, P., Balachandran, K., Madhu, N., Nair, M., Shaiju, P., Joseph, T., Srinivas, K., Gupta, G., 2011. Eutrophication induced changes in benthic community structure of a flow-restricted tropical estuary (Cochin backwaters), India. Environ. Monit. Assess. 176, 427–438.

Martin, G., George, R., Shaiju, P., Muraleedharan, K., Nair, S., Chandramohanakumar, N., 2012. Toxic metals enrichment in the surficial sediments of a eutrophic tropical estuary (Cochin Backwaters Southwest coast of India)<. Sci. World J. 2012.

Martin, G., Jyothibabu, R., Madhu, N., Balachandran, K., Nair, M., Muraleedharan, K., Arun, P., Haridevi, C., Revichandran, C., 2013. Impact of eutrophication on the occurrence of *Trichodesmium* in the Cochin backwaters, the largest estuary along the west coast of India. Environ. Monit. Assess. 185, 1237–1253.

Menon, N., Balchand, A., Menon, N., 2000. Hydrobiology of the Cochin backwater system—a review. Hydrobiol 430, 149–183.

Mitbavkar, S., Rajaneesh, K., Anil, A., Sundar, D., 2012. Picophytoplankton community in a tropical estuary: detection of *Prochlorococcus*-like populations. Estuarine Coastal Shelf Sci. 107, 159–164.

Munawar, M., Weisse, T., 1989. Is the 'microbial loop'an early warning indicator of anthropogenic stress? Hydrobiologia 188, 163–174.

Murrell, M.C., Lores, E.M., 2004. Phytoplankton and zooplankton seasonal dynamics in a subtropical estuary: importance of cyanobacteria. J. Plankton Res. 26, 371–382.

Paerl, H.W., 1977. Ultraphytoplankton biomass and production in some New Zealand lakes. N.Z. J. Mar. Freshwater Res. 11, 297–305.

Pan, L., Zhang, J., Zhang, L., 2007. Picophytoplankton, nanophytoplankton, heterotrohpic bacteria and viruses in the Changjiang Estuary and adjacent coastal waters. J. Plankton Res. 29, 187–197.

Parsons, T., Maita, Y., Lalli, C., 1984. A Manual of Chemical and Biological Methods for Seawater Analysis. Pergamon Press, Oxford.

Partensky, F., Hess, W., Vaulot, D., 1999. *Prochlorococcus*, a marine photosynthetic prokaryote of global significance. Microbiol. Mol. Biol. Rev. 63, 106–127.

Patil, J.S., Anil, A.C., 2011. Variations in phytoplankton community in a monsoon-influenced tropical estuary. Environ. Monit. Assess. 182, 291–300.

Pednekar, S.M., Matondkar, S.G.P., Gomes, H.D.R., Goes, J.I., Parab, S., Kerkar, V., 2011. Fine-scale responses of phytoplankton to freshwater influx in a tropical monsoonal estuary following the onset of southwest monsoon. J. Earth Syst. Sci. 120, 545–556.

Platt, T., Rao, D.S., Irwin, B., 1983. Photosynthesis of picoplankton in the oligotrophic ocean. Nature 301, 702–704.

Qasim, S., Gopinathan, C., 1969. Tidal cycle and the environmental features of Cochin backwater (a tropical estuary). Proc. Indian Acad. Sci., 336–353.

Qasim, S., Reddy, C., 1967. The estimation of plant pigments of Cochin backwater during the monsoon months. Bull. Mar. Sci. 17, 95–110.

Qasim, S., Sen Gupta, R., 1981. Environmental characteristics of the Mandovi–Zuari estuarine system in Goa. Estuarine Coastal Shelf Sci. 13, 557–578.

Qasim, S.Z., 2003. Indian Estuaries. Allied Publishers.

Qiu, D., Huang, L., Zhang, J., Lin, S., 2010. Phytoplankton dynamics in and near the highly eutrophic Pearl River Estuary, South China Sea. Cont. Shelf Res. 30, 177–186.

Rajaneesh, K., Mitbavkar, S., 2013. Factors controlling the temporal and spatial variations in *Synechococcus* abundance in a monsoonal estuary. Mar. Environ. Res. 92, 133–143.

Ray, R.T., Haas, L.W., Sieracki, M.E., 1989. Autotrophic picoplankton dynamics in a Chesapeake Bay sub-estuary. Mar. Ecol. Prog. Ser. 52, 273–285.

Reddy, C., Sankaranarayanan, V., 1972. Phosphate regenerative activity in the muds of a tropical estuary. Indian J. Mar. Sci. 1, 57–60.

Sankaranarayanan, V., Qasim, S., 1969. Nutrients of the Cochin backwater in relation to environmental characteristics. Mar. Biol. 2, 236–247.

Sieburth, J.M., Smetacek, V., Lenz, J., 1978. Pelagic ecosystem structure, heterotrophic compartments of the plankton and their relationship to plankton size fractions. Limnol. Oceanogr. 23, 1256–1263.

Sin, Y., Hyun, B., Jeong, B., Soh, H.Y., 2013. Impacts of eutrophic freshwater inputs on water quality and phytoplankton size structure in a temperate estuary altered by a sea dike. Mar. Environ. Res. 85, 54–63.

Scanlan, D.J., 2003. Physiological diversity and niche adaptation in marine *Synechococcus*. Adv. Microb. Physiol. 47, 1–64.

Shang, X., Zhang, L., Zhang, J., 2007. Prochlorococcus-like populations detected by flow cytometry in the fresh and brackish waters of the Changjiang Estuary. J. Mar. Biol. Assoc. U.K. 87, 643–648.

Shetye, S.R., 1999. Propagation of tides in the Mandovi and Zuari estuaries. Sadhana (Academy Proceedings in Engineering Sciences). Indian Acad. Sci., 5–16.

Shiomoto, A., Tadokoro, K., Monaka, K., Nanba, M., 1997. Productivity of picoplankton compared with that of larger phytoplankton in the subarctic region. J. Plankton Res. 19, 907–916.

Shivaprasad, A., Vinita, J., Revichandran, C., Manoj, N., Srinivas, K., Reny, P., Ashwini, R., Muraleedharan, K., 2012. Influence of saltwater barrage on tides, salinity, and chlorophyll *a* in Cochin estuary, India. J. Coast. Res. 29, 1382–1390.

Srinivas, K., Revichandran, C., Maheswaran, P., Asharaf, T.M., Murukesh, N., 2003. Propagation of tides in the Cochin estuarine system, southwest coast of India. J. Mar. Sci. 32, 14–24.

Stockner, J.G., Antia, N.J., 1986. Algal picoplankton from marine and freshwater ecosystems: a multidisciplinary perspective. Can. J. Fish. Aquat. Sci. 43, 2472–2503.

Stomp, M., Huisman, J., Voros, L., Pick, F.R., Laamanen, M., Haverkamp, T., Stal, L.J., 2007. Colourful coexistence of red and green picocyanobacteria in lakes and seas. Ecol. Lett. 10, 290–298.

Tsai, A.Y., Chiang, K.P., Chang, J., Gong, G.C., 2008. Seasonal variations in trophic dynamics of nanoflagellates and picoplankton in coastal waters of the western subtropical Pacific Ocean. Aquat. Microb. Ecol. 51, 263–274.

Unnithan, R., Vijayan, M., Remani, K., 1975. Organic pollution in Cochin backwaters. Indian J. Mar. Sci. 4, 39–42.

Vijayan, M., Ramani, K., Unnithan, R., 1976. Effects of organic pollution on some hydrographic features of Cochin backwaters. J. Mar. Sci. 5, 196–200.

Vollenweider, R., Giovanardi, F., Montanari, G., Rinaldi, A., 1998. Characterization of the trophic conditions of marine coastal waters, with special reference to the NW Adriatic Sea: proposal for a trophic scale, turbidity and generalized water quality index. Environmetrics 9, 329–357.

Wang, K., Wommack, K.E., Chen, F., 2011. Abundance and distribution of *Synechococcus* spp. and cyanophages in the Chesapeake Bay. Appl. Environ. Microbiol. 77, 7459–7468.
Wetz, M.S., Paerl, H.W., Taylor, J.C., Leonard, J.A., 2011. Environmental controls upon picophytoplankton growth and biomass in a eutrophic estuary. Aquat. Microb. Ecol. 63, 133.
Wood, A.M., 1985. Adaptation of photosynthetic apparatus of marine ultraphytoplankton to natural light fields. Nature 316, 253–255.
Zhang, X., Shi, Z., Ye, F., Zeng, Y., Huang, X., 2013. Picophytoplankton abundance and distribution in three contrasting periods in the Pearl River estuary, South China. Mar. Freshwater Res. 64, 692–705.

Estuarine, Coastal and Shelf Science 207 (2018) 325–337

Contents lists available at ScienceDirect

Estuarine, Coastal and Shelf Science

journal homepage: www.elsevier.com/locate/ecss

Dynamics of size-fractionated phytoplankton biomass in a monsoonal estuary: Patterns and drivers for seasonal and spatial variability

K.M. Rajaneesh, Smita Mitbavkar*, Arga Chandrashekar Anil

CSIR-National Institute of Oceanography, Dona Paula, Goa 403 004, India

ARTICLE INFO

Keywords:
Size-fractionated chlorophyll *a* biomass
Picophytoplankton
Zuari estuary
Tropical
Hydrography

ABSTRACT

Phytoplankton size-fractionated biomass is an important determinant of the type of food web functioning in aquatic ecosystems. Knowledge about the effect of seasonal salinity gradient on the size-fractionated biomass dynamics is still lacking, especially in tropical estuaries experiencing monsoon. The phytoplankton size-fractionated chlorophyll *a* biomass (> 3 μm and < 3 μm) and picophytoplankton community structure were characterized in the monsoonal Zuari estuary, along the west coast of India, from October 2010 to September 2011 across the salinity gradient (0–35). On an annual scale, > 3 μm size-fraction was the major contributor to the total phytoplankton chlorophyll *a* biomass with the ephemeral dominance of < 3 μm size-fraction. During monsoon season, freshwater runoff and shorter water residence time resulted in a size-independent response. The lowest annual chlorophyll *a* biomass concentration of both size-fractions showed signs of recovery with increasing salinity downstream towards the end of the monsoon season. In contrast, the chlorophyll *a* biomass response was size-dependent during the non-monsoon seasons with the sporadic dominance (> 50%) of < 3 μm chlorophyll *a* biomass during high water temperature episodes from downstream to middle estuary during pre-monsoon and at low salinity and high nutrient conditions upstream during post-monsoon. These conditions also influenced the picophytoplankton community structure with picoeukaryotes dominating during the pre-monsoon, phycoerythrin containing *Synechococcus* during the monsoon and phycocyanin containing *Synechococcus* during the post-monsoon. This study highlights switching over of dominance in size-fractionated phytoplankton chlorophyll *a* biomass at intra, inter-seasonal and spatial scales which will likely govern the estuarine trophodynamics.

1. Introduction

Among the coastal ecosystems, estuaries play a vitally important role in supporting higher biodiversity by providing nursery grounds for a variety of macroorganisms, including valuable fish species. Indian estuaries are highly productive in terms of fisheries (Jha et al., 2008) which is the main source of income for the local people. In order to sustain good fishery yields, the entire biological community of the food web needs to function efficiently. Estuarine regions are influenced by a wide variety of environmental factors such as nutrient inputs, salinity, turbidity and freshwater flow (Bec et al., 2011; Liu et al., 2015; Patil and Anil, 2015). Indeed, river runoff is the main source of nutrient input and also responsible for the salinity gradient across the estuary and therefore, is considered to be a major stressor causing significant changes in the biological community (Paerl et al., 2006). In the tropical monsoonal estuaries where the seasonal hydrography is controlled by the freshwater runoff and tides, the estuarine characteristics evolve from stratified to partially mixed conditions. This is intermingled with ephemeral stabilized environmental conditions depending on the monsoonal precipitation intensity. These estuaries are characterized by high annual runoff with a distinctly higher run off during monsoon season as compared to non-monsoon seasons resulting in rapid changes in physico-chemical conditions throughout the year (Shetye and Murty, 1987; Vijith et al., 2009; Anand et al., 2014) which subsequently influences the seasonal variation of the biological communities in these waters (Qasim, 2003).

Phytoplankton are one of the important components of the biological community fuelling the food webs of aquatic ecosystems through primary productivity. The studies on phytoplankton community structures are well documented for the coastal and estuarine regions (Madhu et al., 2007; Marshall, 2009; Patil and Anil, 2011) and were mostly focused on larger phytoplankton (> 3 μm). In recent years, smaller phytoplankton i.e., picophytoplankton (cell size < 3 μm; Pico) are being highlighted as an important component of phytoplankton community in coastal and estuarine regions (Gaulke et al., 2010; Qiu et al., 2010; Mitbavkar et al., 2012, 2015; Contant and Pick, 2013; Rajaneesh

* Corresponding author.
E-mail address: mitbavkars@nio.org (S. Mitbavkar).

https://doi.org/10.1016/j.ecss.2018.04.026
Received 3 August 2017; Received in revised form 18 April 2018; Accepted 23 April 2018
Available online 25 April 2018

Nomenclature

Pico	Picophytoplankton
SYN	*Synechococcus*
PE	Phycoerythrin
PC	Phycocyanin
PRO-like	*Prochlorococcus*-like
PEUK	Picoeukaryotes
PoM	Post-monsoon
PrM	Pre-monsoon
SW	Southwest
MON	Monsoon
S	Station
NBW	Near bottom waters
CTD	Conductivity, temperature and depth
ΔS	Stratification parameter
FCM	Flow cytometer
GF/F	glass fiber filter
Chl *a*	Chlorophyll *a*
RALS	Right angle light scatter
FALS	Forward angle light scatter
IMD	Indian meteorological department
SD	Secchi disk
ANOVA	Analysis of variance

and Mitbavkar, 2013).

The measurement of phytoplanktonic biomass is critical to understand the carbon flow dynamics in a particular ecosystem. Phytoplankton biomass can be measured in different ways (eg. chlorophyll, cell abundance, carbon). The spectrometric determination of total chlorophyll *a* (chl *a*) content is a simple and most widely used method to estimate phytoplankton biomass compared to microscopic or any other instrument based measurements. However, phytoplankton abundance may not be directly proportional to chl *a* biomass mostly due to variation in the size of the organisms and photoacclimation (Rodriguez et al., 2006; Alvarez et al., 2017). In this regard, the size structure of the phytoplankton community based on chl *a* biomass is considered an important factor controlling the carbon cycle and food web dynamics in pelagic ecosystems (Richardson and Jackson, 2007). Oceanic oligotrophic regions are dominated by the Pico in terms of chl *a*, cell abundance and primary production (Partensky et al., 1999). On the contrary, in meso or eutrophic coastal waters, nano- (3–20 μm) and micro-phytoplankton (20–200 μm) dominate the phytoplankton community where the environment is comparatively more variable due to the influence of residence time of water, currents, tidal intensity, land runoff and freshwater influx (Guenther et al., 2015). However, Pico dominance has been reported in some coastal regions occasionally (Qiu et al., 2010; Bec et al., 2011). Since phytoplankton forms the base of food webs, the variations in its size-fractionated chl *a* biomass in an ecosystem determines the type of prevailing food web. When the larger phytoplankton biomass (> 3 μm) dominates, the herbivore food web prevails whereas it is the microbial food web when the Pico biomass (< 3 μm) dominates (Azam et al., 1983). Amongst the studies on the contribution of > 3 μm and < 3 μm phytoplankton size-fractions to the bulk chl *a* biomass, although information is available from temperate regions, there is still a scarcity of information from the tropical estuarine regions (Sin et al., 2000; Caroppo, 2000; Madhu et al., 2009; Gaulke et al., 2010; Qiu et al., 2010).

Zuari is a typical tropical monsoonal estuary located in the state of

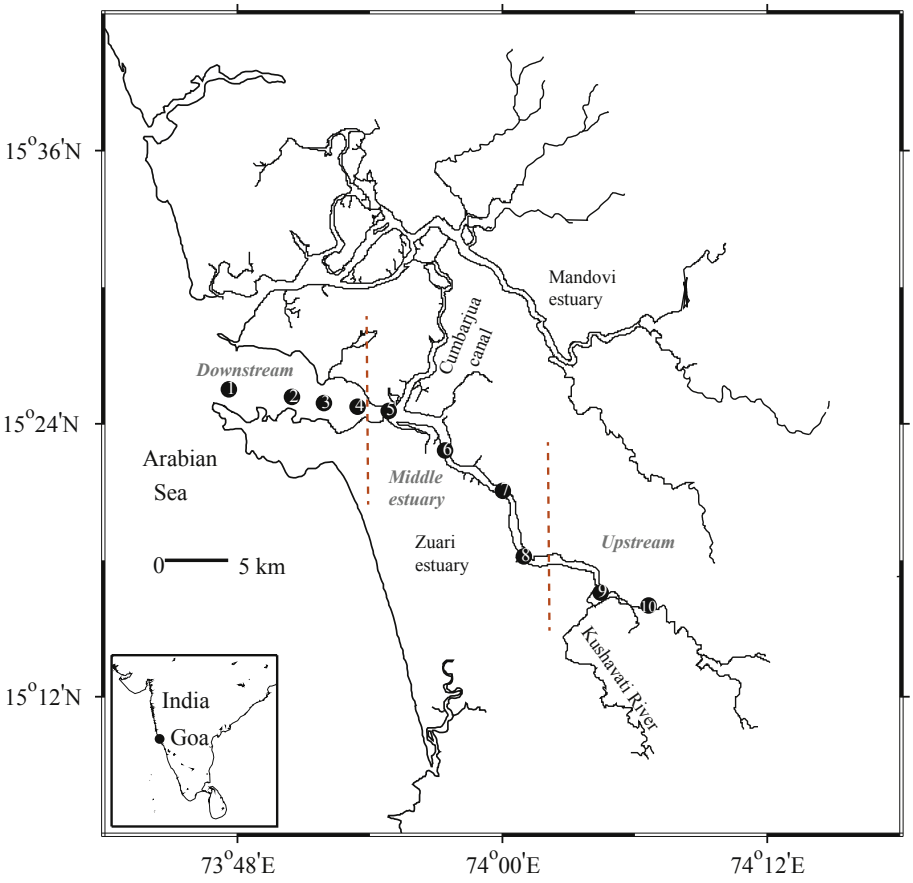

Fig. 1. Locations of sampling stations in the Zuari estuary, west coast of India.

Goa, along the west coast of India (Fig. 1). This estuary is stratified during the monsoon season and ranges from partially to well mixed during the non-monsoon periods depending on the tidal influence and amount of freshwater discharge (Vijith et al., 2009). In such highly dynamic estuarine conditions, > 3 μm phytoplankton are known to proliferate (Patil and Anil, 2011, 2015) whereas < 3 μm are favored by stratified conditions (Rajaneesh and Mitbavkar, 2013). Earlier studies in this estuary revealed the influence of tides and freshwater run off on the abundance of Pico (Mitbavkar et al., 2012, 2015; Rajaneesh and Mitbavkar, 2013) and microphytoplankton (Patil and Anil, 2011, 2015) on a seasonal scale. However, there are no combined studies which assessed the size-fractionated chl *a* biomass contribution to the total chl *a* biomass across the salinity gradient of this estuary. In this regard, the aim of this study was to assess the spatial and temporal variations in size-fractionated chl *a* biomass of > 3 μm and < 3 μm phytoplankton along with the controlling environmental factors. We hypothesized that in the monsoonal estuaries, the intensity of tides and amount of freshwater influx will control the spatial and seasonal variations of phytoplankton chl *a* biomass size structure wherein the > 3 μm chl *a* biomass would dominate the total biomass during most part of the year, with ephemeral dominance by < 3 μm chl *a* biomass depending on the seasonal and spatial water column structure along the estuarine transect. The information obtained from such studies can be useful in understanding the biomass dynamics of these two important phytoplankton size groups and also to predict the type of food web prevailing in estuarine ecosystems based on the environmental conditions.

2. Materials and methods

2.1. Study area

Goa is the smallest state of India with a population of around 2 Million. It is famous for its beaches, natural sanctuaries, places of worship and heritage sites making it a famous tourist destination. The Western Ghats, which form most of eastern Goa, has been internationally recognized as one of the biodiversity hotspots of the world (Myers et al., 2000). Zuari estuary is the backbone of Goa's agriculture and fishing industries (Fig. 1). Its cross-sectional area decreases from mouth to head of the estuary (Shetye and Murty, 1987). The average depth of this estuary is ~5 m with a catchment area of 1152 km^2 (Shetye et al., 2007). This location is strongly influenced by the southwest (SW) monsoon. The huge quantity of freshwater discharge (491 × 10^6 m^3) during this period results in drastic changes in physico-chemical characteristic of the water column (Shetye et al., 2007). Based on the physico-chemical characteristics, a year is classified into three seasons: monsoon (June–September, MON) followed by post-monsoon (October–January, PoM) and pre-monsoon (February–May, PrM). In the study region, a total of 3738.9 mm rainfall was recorded during the study period (from October 2010 to September 2011) (Indian Meteorological Department (IMD), Panaji, Goa). Out of that, 96% of precipitation occurred during the southwest MON. Tides are semidiurnal with the highest height of 2.3 m during spring tide and ~1 m during neap tide (Manoj and Unnikrishnan, 2009).

Table 2
Rainfall data (includes the previous day) and tidal phase for the sampling days. LT-low tide and HT-high tide.

Sampling dates (d-m-y)	Rainfall (mm)	Tidal phase
23-10-2010	55.4	LT (spring tide)
06-11-2010	13.0	HT (spring tide)
06-12-2010	0	HT (spring tide)
10-01-2011	0	HT (spring tide)
11-02-2011	0	LT (neap tide)
21-03-2011	0	HT (spring tide)
19-04-2011	0	HT (spring tide)
27-05-2011	0	LT (neap tide)
16-06-2011	99.5	HT (spring tide)
15-07-2011	92.2	HT (spring tide)
25-08-2011	15.4	HT (spring tide)
22-09-2011	6.4	HT (spring tide)

2.2. Sampling

Surface and near bottom water (NBW; ~1 m above the sea bed) samples were collected from ten stations (S1-S10) in the Zuari estuary, along a salinity gradient of 0–35 (Fig. 1; Table 1) on a monthly basis from October 2010 to September 2011 during flood tide with occasional sampling during ebb tide (Table 2). The sampled transect was demarcated as the estuarine mouth (S1-S4; salinity > 30), middle estuary (S5 to S8; salinity between 30 and 0.5) and upstream (S9-S10; salinity < 0.5). Portable Seabird CTD (SBE 19 plus) was deployed to measure the temperature and salinity. Stratification parameter (ΔS) was calculated from the difference between surface and NBW salinity for the entire study period. Water transparency was measured with a secchi disk (SD). Rainfall and tidal phase data for the study period were acquired from IMD (Table 2). Water samples for analyses of nutrients, size-fractionated chl *a* biomass (> 3 μm and < 3 μm) and Pico abundance were collected using a 5 L Niskin sampler.

2.3. Nutrient analysis

For the analysis of dissolved inorganic nutrients [nitrate (NO_3^-), nitrite (NO_2^-), phosphate (PO_4^{3-}), and silicate (SiO_4^{4-})], samples were collected in 5 mL cryo vials and frozen at −20 °C. Within 2 weeks, samples were analyzed in the laboratory using an autoanalyzer (Skalar SAN^{++} continuous flow analyzer) following the method of Grasshoff et al. (1983). Prior to nutrient analysis, turbid samples were filtered through GF/F (0.7 μm porosity) filters.

2.4. Size-fractionated chlorophyll a and phaeopigments

In the laboratory, measured volumes (250–500 mL) of seawater were filtered through Whatman GF/F filters (0.7 μm porosity) to

Table 1
Details of sampling stations in the Zuari estuary.

Station No.	Station name	Latitude (N)	Longitude (E)	Distance from mouth (km)	Approximate depth (m)
1	Marmugao	15° 25′ 16.9″	73° 47′ 36.9″	0	16
2	Chicalim	15° 25′ 8.5″	73° 47′ 22.4″	5.8	5
3	Island	15° 25′ 57.4″	73° 47′ 57.0″	8.6	5
4	Sancoale	15° 25′ 45.1″	73° 47′ 30.6″	11	7.1
5	Cortalim	15° 25′ 32.0″	73° 47′ 50.2″	13	9.6
6	Loutulim	15° 25′ 54.0″	73° 47′ 24.4″	19.7	10.5
7	Borim	15° 25′ 03.6″	73° 47′ 58.0″	23.9	12.9
8	Shiroda	15° 25′ 12.3″	73° 47′ 55.5″	31.4	9.1
9	Kushavati	15° 25′ 31.7″	73° 47′ 28.3″	38.4	9.9
10	Sanvordem	15° 25′ 01.1″	73° 47′ 36.0″	42.2	4.9

estimate the total chl *a* and phaeopigment concentrations. For determining chl *a* and phaeopigment concentrations of < 3 μm size-fraction, initially subsamples were filtered through 3.0 μm porosity nucleopore polycarbonate membrane filters and then filtrate was filtered through Whatman GF/F filters. Size-fraction filtration was carried out under gentle vacuum. Each filter paper was placed separately in a dark vial containing 90% acetone. After extraction in the dark at 4 °C for 24 h (Parsons et al., 1984), chl *a* and phaeopigments (after acidification by 10% HCl) were determined on a Turner Designs Triology fluorometer complemented with an acidification module (Turner Designs #7200-040) at an emission wavelength of 665 nm. Prior to sample analysis, the instrument was calibrated with commercial chl *a*. Subsequently, > 3 μm chl *a* and phaeopigment concentrations were calculated by subtracting < 3 μm chl *a* from the total concentration.

2.5. Flow cytometric analysis of picophytoplankton

For Pico community structure and abundance analysis, seawater samples were preserved with paraformaldehyde (0.2% final concentration), quick frozen in liquid nitrogen and stored at −80 °C until analysis. Pico abundance was determined on a FACS Aria II flow cytometer (FCM) equipped with blue (488 nm) and red (630 nm) lasers. Data obtained was processed using BD FACSDiva (Version 6.2) software. From the flow cytometer plots, *Synechococcus* (*SYN*), picoeukaryotes (PEUK) and *Prochlorococcus*-like (*PRO*-like) cells were identified by their light scattering [forward angle light scatter (FALS) and right angle light scatter (RALS)] and fluorescence [red fluorescence from chl (> 650 nm) and phycocyanin (630 nm), and orange fluorescence from phycoerythrin (564–606 nm)] properties. Different groups of *SYN*, such as phycocyanin rich *SYN* (*SYN*-PC) and phycoerythrin rich *SYN* (*SYN*-PE), and its subgroups (*SYN*-PEI, *SYN*-PEII, and *SYN*-PEIII) were identified based on flow cytometric signatures as described in Rajaneesh and Mitbavkar (2013). Two sub-groups of PEUK (PEUK-I and PEUK-II) were observed in the estuary, with similar size but unequal chl fluorescence intensity (Fig. 2A to C). The chl fluorescence intensity emitted by PEUK-I was lower than that of PEUK-II. *PRO*-like cells were differentiated based on their smaller size and lower chl fluorescence intensity compared to PEUK. Yellow-green latex size beads of 2 μm (Polysciences Co., USA) were added to the samples as an internal standard to normalize the light scatter signals and fluorescence emission by cells. In order to calculate the chl contribution of each Pico group to the total < 3 μm chl *a*, the mean red fluorescence values obtained from FCM analysis for each group was normalized by the mean bead fluorescence. The normalized mean coefficient value of red fluorescence was then multiplied by the cell abundance of each group.

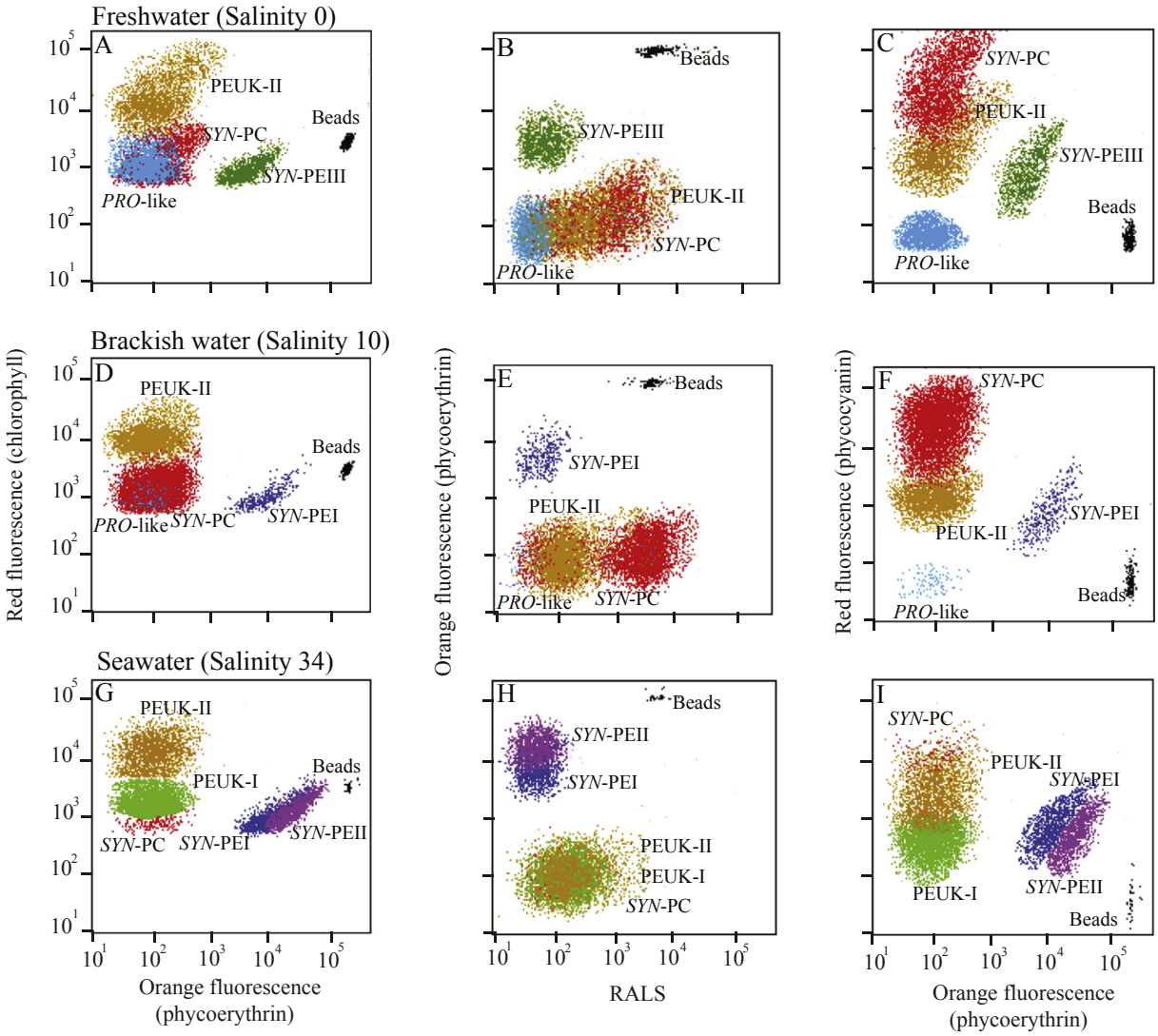

Fig. 2. Flow cytometric plots of picophytoplankton community from (A–C) freshwater, (D–F) brackish water, and (G–I) seawater samples of Zuari estuary.

2.6. Data analyses

Two-way analyses of variance (ANOVA) was conducted to assess the monthly, spatial and vertical variations in > 3 μm chl *a* and < 3 μm chl *a*, and between the size-fractions, followed by Tukey's post-hoc test to observe the pair wise comparisons of size-fractions between the seasons. In order to understand the relationship between total chl *a*, > 3 μm chl *a*, < 3 μm chl *a*, and flow cytometric chl fluorescence, Pearson correlations were performed. Regression analysis was performed to observe the relationship of > 3 μm and < 3 μm chl *a* with salinity and temperature.

Further, a multivariable analytic technique, factor analysis was performed to describe the interrelationships among the set of multiple abiotic and biotic variables. In our analysis, two major factors explained the relationship between the variables. The most important variables are loaded on factor 1 (x axis). The value obtained for each variable indicates the importance of the variable. Values < 0.4 are not considered, between 0.4 and 0.5 are considered as weak factors, between 0.5 and 0.75 as moderate factors and > 0.75 as strong factors (Liu et al., 2003). The above analysis was done through SPSS Multi-variate Statistical Package (Windows Ver. 22). The contour plots for biotic and abiotic parameters were plotted using Ferret programme (Ver. 7.2).

3. Results

3.1. Environmental parameters

During PrM, the river water (S9 to S10) was warmer (30.14 ± 2.38 °C) than the seawater (S1 to S2; 29.64 ± 1.45 °C) (Fig. 3A and B). Temperature lowered (27.42 ± 0.91 °C) during MON. During PoM, the temperature was higher (28.78 ± 0.81 °C) compared to MON except during January when the lowest temperature was recorded (26.33 ± 0.53 °C). During MON and PoM, the temperature did not vary much along the estuary, and statistically significant differences were not observed throughout the study period.

During PrM, the intrusion of seawater towards upstream resulted in a partially mixed water column except in May (S6-S8) when a weak stratification was observed. During MON, with the onset of rainfall and consequent freshwater influx, the lower saline riverine water flowing in at the surface and saltier water entering the estuary at the bottom resulted in a vertically stratified water column in the middle estuary and downstream (Fig. 3C and D). This salt wedge characteristic lasted throughout the MON with stronger stratification from July to September (Fig. 3E). In October (PoM), freshwater influx due to the continuation of monsoonal rainfall led to a salinity difference of 9.47 ± 3.92 between the surface and NBW up to the middle estuary, leading to a stratified water column. During the following PoM months (November to January), a partially mixed water column was observed.

Generally, the water transparency in the entire estuary was low throughout most of the year (< 1 m). Higher values were observed downstream at S1 during most part of the year except during early MON due to heavy rainfall (Fig. 3F). During August to September, water transparency was high even at the upstream end of the estuary. Higher values were also observed in the middle estuary during May.

NO_3^- concentrations ranged between 0.66 and 9.92 μM (Fig. 4A and B) with highest values during MON (June: 8.42 ± 5.43 μM) coinciding with the highest rainfall (Table 2). This was followed by PoM with highest values in October (7.48 ± 2.09 μM) coinciding with high rainfall. PO_4^{3-} concentrations ranged between 0.24 and 4.3 μM (Fig. 4C and D) with highest values during MON (September: 4.3 ± 1.73 μM) and PoM (October: 4.69 ± 1.03 μM). NO_2^- concentrations were high (0.97 ± 0.94 μM) during PrM with a higher concentration at the upstream (Fig. 4E and F). SiO_4^{4-} concentrations (33.63 ± 21.39 μM) increased from the middle estuary to upstream during PoM, followed by a decline during PrM and increase during MON (Fig. 4G and H).

3.2. Phytoplankton biomass size structure

ANOVA revealed that the > 3 μm chl *a* biomass was significantly higher ($p < 0.001$) than the < 3 μm chl *a* biomass throughout the study period. Chl *a* biomass of both the size-fractions exhibited significant seasonal variations ($p < 0.01$) in the surface and NBW, with higher biomass during the PrM ($p < 0.01$). The variations were insignificant between the surface and NBW for both the size-fractions. Hence the surface and NBW data were combined.

Pre-monsoon: The total chl *a* biomass concentration was higher at the upstream and middle estuary followed by downstream (Table 3) with the highest concentration in March (4.84 ± 2.01 μg L^{-1}) and May across the estuary (4.55 ± 1.81 μg L^{-1}; Fig. 5A and B). The highest

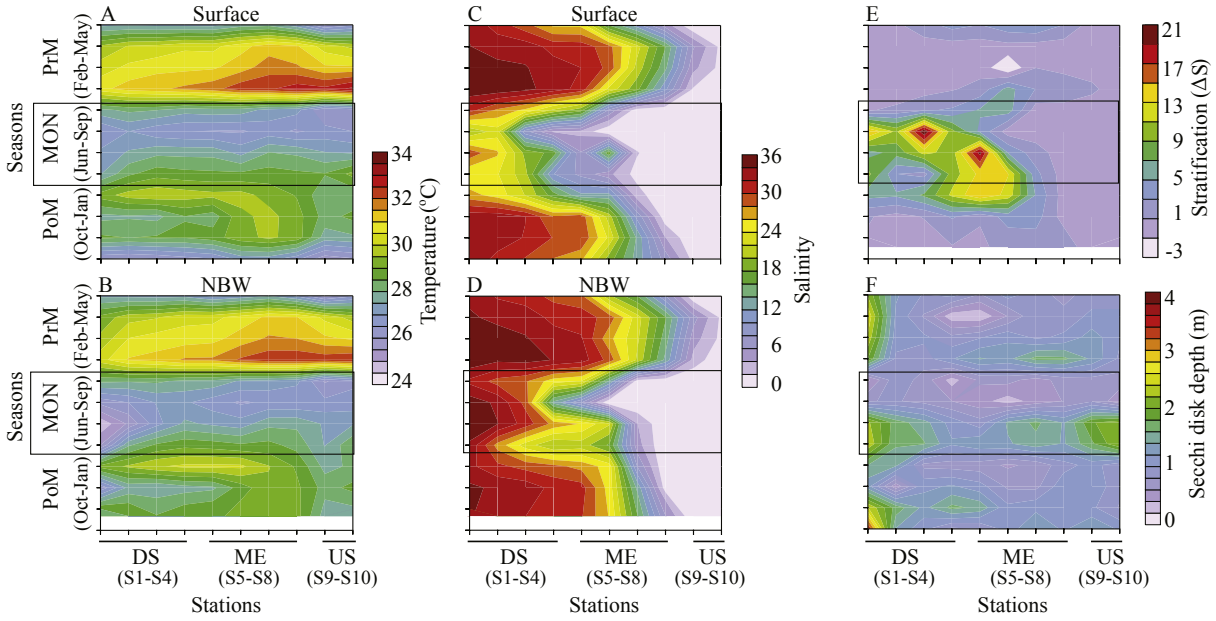

Fig. 3. Temporal and spatial variations in (A, B) temperature, (C, D) salinity, (E) stratification parameter and (F) secchi disk depth (DS-downstream, ME-middle estuary and US-upstream).

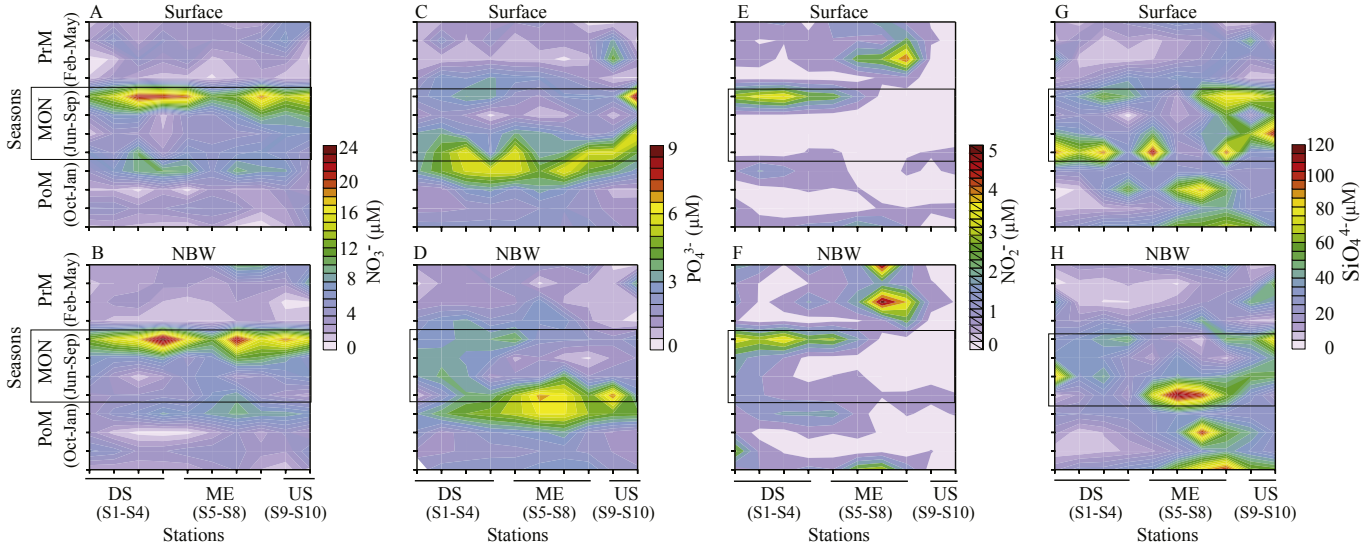

Fig. 4. Temporal and spatial variations in (A, B) NO_3^-, (C, D) PO_4^{3-}, (E, F) NO_2^- and (G, H) SiO_4^{4-} (DS-downstream, ME-middle estuary and US-upstream).

Table 3
Concentration of total, > 3 μm and < 3 μm chl *a* biomass at the downstream, middle estuary and upstream.

Estuarine zones	Total chl *a* (μg L^{-1})	> 3 μm chl *a* (μg L^{-1})	< 3 μm chl *a* (μg L^{-1})
Pre-monsoon			
Downstream	3.14 ± 1.85	2.24 ± 1.77	0.89 ± 0.96
Middle estuary	3.62 ± 1.88	2.77 ± 1.76	0.84 ± 0.91
Upstream	3.99 ± 2.47	3.17 ± 2.59	0.81 ± 0.50
Monsoon			
Downstream	2.04 ± 0.95	1.64 ± 0.90	0.39 ± 0.25
Middle estuary	1.03 ± 0.83	0.87 ± 0.76	0.16 ± 0.15
Upstream	0.48 ± 0.45	0.37 ± 0.36	0.11 ± 0.11
Post-monsoon			
Downstream	3.09 ± 2.01	2.42 ± 1.95	0.67 ± 0.50
Middle estuary	3.78 ± 1.95	2.74 ± 1.79	1.04 ± 0.60
Upstream	2.76 ± 1.63	1.80 ± 1.68	0.98 ± 0.29

concentration of the > 3 μm fraction was observed in March across the estuary (4.34 ± 2.10 μg L^{-1}; 83.00 ± 23.60%) and May at S1 to S3, S5 and S10 (3.43 ± 1.93 μg L^{-1}; 52.75 ± 30.44%) (Fig. 5C and D). This fraction was the major contributor to the total chl *a* biomass (Fig. 6A). The < 3 μm chl *a* biomass concentration was highest at the downstream followed by the middle estuary and upstream (Table 3) with highest concentration and contribution in May (2.40 ± 1.05 μg L^{-1}; 65 ± 18%; Fig. 5E to H). PEUK-I was the major contributor (87 ± 7%; S1 to S6) at the downstream and *SYN*-PC (44 ± 14%) at the upstream (Fig. 7G, H, K, L). Higher contribution (57 ± 28%) of < 3 μm chl *a* biomass was also observed in February in the surface waters of the downstream and middle estuary with significant variation ($p < 0.01$) between surface and NBW concentrations observed only for this month (Fig. 5G and H). However, this higher contribution of < 3 μm chl *a* biomass was due to a decrease in the concentration of > 3 μm chl *a* biomass.

Monsoon: The total chl *a* biomass concentration declined after the onset of rainfall followed by an increase in August and September which coincided with low rainfall intensity and high water transparency (Table 3; Fig. 5A and B). The highest concentration (1.60 ± 0.95 μg L^{-1}) was observed in August and September at the downstream and middle estuary (Table 3; Fig. 5C and D). The > 3 μm fraction was the major contributor to the total chl *a* biomass (Fig. 6B). The highest concentration of < 3 μm fraction (0.76 ± 0.19 μg L^{-1}) was observed in August (Fig. 5E–H). *SYN*-PEI and *SYN*-PEII were the major contributors during this season (54 ± 14%) with higher contribution of *SYN*-PEI in the NBW compared to that in the surface waters (Fig. 7A to D).

Post-monsoon: The total chl *a* biomass concentration was relatively higher at the downstream and middle estuary than upstream (Table 3) with the highest concentration (5.11 ± 1.84 μg L^{-1}) in January across the estuary (Fig. 5A and B). The highest concentration of the > 3 μm chl *a* biomass was recorded in January (4.18 ± 1.83 μg L^{-1}), especially at the downstream and middle estuary (Fig. 5C and D). The > 3 μm fraction was the major contributor to the total chl *a* biomass (Fig. 6C). The contribution of < 3 μm chl *a* biomass was highest at the upstream followed by the middle estuary and downstream (Fig. 6C). The decrease in > 3 μm chl *a* biomass and relatively higher < 3 μm chl *a* biomass resulted in the highest contribution of the latter in October (71 ± 18%) at the middle estuary (from S6) and upstream and in December at the downstream (48 ± 20%; Fig. 5G and H). PEUK-II was the major contributor (Fig. 7M, N).

The phaeopigment concentrations in the > 3 μm fraction were higher in January (2.34 ± 1.11 μg L^{-1}), March (2.58 ± 1.28 μg L^{-1}) and May (1.58 ± 1.24 μg L^{-1}; Fig. 5I and J). In the < 3 μm fraction, higher phaeopigment concentrations were observed in January (0.64 ± 0.59 μg L^{-1}) and May (1.11 ± 0.63 μg L^{-1}; Fig. 5K and L).

3.3. Factors affecting the chlorophyll a biomass size structure

Correlation analysis revealed that irrespective of season and depth, the > 3 μm chl *a* biomass correlated positively with total chl *a* biomass concentration (Table 4). The < 3 μm chl *a* biomass was also positively correlated with the total biomass, although not statistically significant in a couple of interactions. The FCM red fluorescence values positively correlated with the measured < 3 μm chl *a* biomass (Table 4). Regression analysis showed that > 3 μm chl *a* biomass correlated negatively with temperature during PoM whereas the < 3 μm chl *a* biomass correlated positively during PrM (Fig. 8E, G). Chl *a* biomass of both the size-fractions correlated positively with salinity during MON (Fig. 8D, J). The < 3 μm chl *a* biomass correlated negatively with salinity during PoM (Fig. 8F).

In factor analysis, the biomass of two *SYN*-PE subgroups (I + II) and two PEUK subgroups (I + II) were combined as they did not exhibit major differences. Two main factors explained 42%, 46% and 52% of total variance among the variables for PrM, MON and PoM, respectively. During PrM, the < 3 μm chl *a* biomass positively correlated with temperature, PO_4^{3-} and SiO_4^{4-} (Fig. 9A). PEUK (I + II) showed a similar relation with these abiotic factors. *SYN*-PC, *SYN*-PEIII and *PRO-*

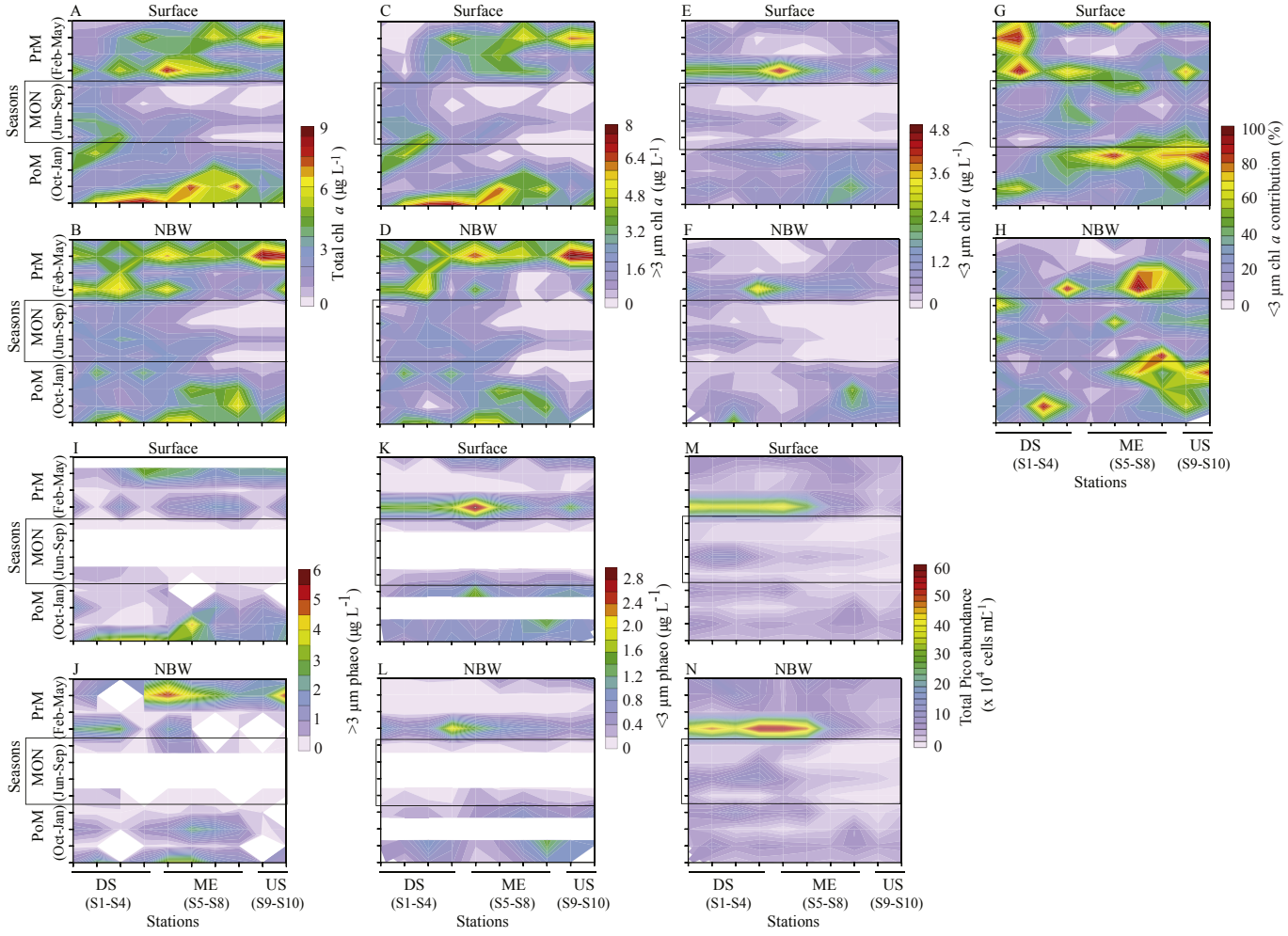

Fig. 5. Temporal and spatial variations in (A, B) total chl *a* biomass, (C, D) > 3 µm chl *a* biomass, (E, F) < 3 µm chl *a* biomass, (G, H) < 3 µm chl *a* contribution to the total chl *a* biomass, (I, J) > 3 µm phaeopigment concentrations, (K, L) < 3 µm phaeopigment concentrations and (M, N) total Pico abundance (DS-downstream, ME-middle estuary and US-upstream).

like biomass were positively correlated with NO_3^- and negatively with salinity and SD whereas, *SYN*-PE (I + II) exhibited an opposite relation. The > 3 µm chl *a* biomass positively correlated with NO_3^- and negatively with salinity and SD. During MON, both size-fractions of chl *a* biomass positively correlated with salinity (Fig. 9B). A similar correlation was observed for *SYN*-PE (I + II). *SYN*-PC, *SYN*-PEIII, PEUK (I + II) and *PRO*-like biomass negatively correlated with salinity. During PoM, < 3 µm chl *a* biomass positively correlated with SiO_4^{4-} and negatively with salinity (Fig. 9C). *SYN*-PC, *SYN*-PEIII, PEUK (I + II) and *PRO*-like biomass exhibited a similar relation with these abiotic factors whereas *SYN*-PE (I + II) biomass exhibited an opposite relation. The > 3 µm chl *a* biomass positively correlated with SD and negatively with temperature, PO_4^{3-} and NO_3^-.

4. Discussion

The study revealed a size-dependent and a size-independent response of the total phytoplankton biomass during the non-MON and MON seasons, respectively with inter- and intraseasonal variations in the intensity of these responses. The relatively stronger relationship between total chl *a* and > 3 µm chl *a* concentrations compared to relationships with < 3 µm chl *a* biomass indicate their major contribution in the estuarine waters on most occasions and appears to control the overall variability in the total phytoplankton community. As reported in earlier studies (Bidigare and Ondrusek, 1996; Binder et al., 1996; Blanchot and Rodier, 1996), a positive correlation between the FCM red fluorescence values and the measured < 3 µm chl *a* was useful for making an estimate of the relative contribution of each Pico group to the measured < 3 µm chl *a* biomass (Table 3).

During the PrM, the intra-seasonal waxing and waning trend in phytoplankton biomass could be attributed to two reasons (Fig. 10). The waning in February and April could be due to exhaustion of nutrients resulting in reduced growth rates or the grazing pressure (as evident from higher NO_2^- concentrations) superseding the growth rates. High abundance of copepods have been reported earlier from this estuary during this period (Achuthankutty et al., 1998). The intermittent waxing (March, May) in phytoplankton biomass reveals favorable environmental conditions such as high temperature, salinity and water transparency. Also, the high PO_4^{3-} concentrations, could be responsible for the high > 3 µm and < 3 µm chl *a* biomass. The sediment resuspension due to the high tidal well-mixed water column is known to introduce high PO_4^{3-} concentrations into the estuarine water column (Anand et al., 2014). However, a switch over towards the dominance of < 3 µm chl *a* biomass during May coinciding with the highest water temperature (31.87 ± 0.72 °C) during the study period suggests an influence of high temperatures on the < 3 µm phytoplankton growth. In sub-tropical and temperate estuaries, < 3 µm chl *a* biomass contribution was restricted to < 10% when water temperature was < 20 °C and subsequently increased to > 50% at higher temperatures (> 20 °C; Ray et al., 1989; Caroppo, 2000; Buchanan et al., 2005; Qiu et al., 2010).

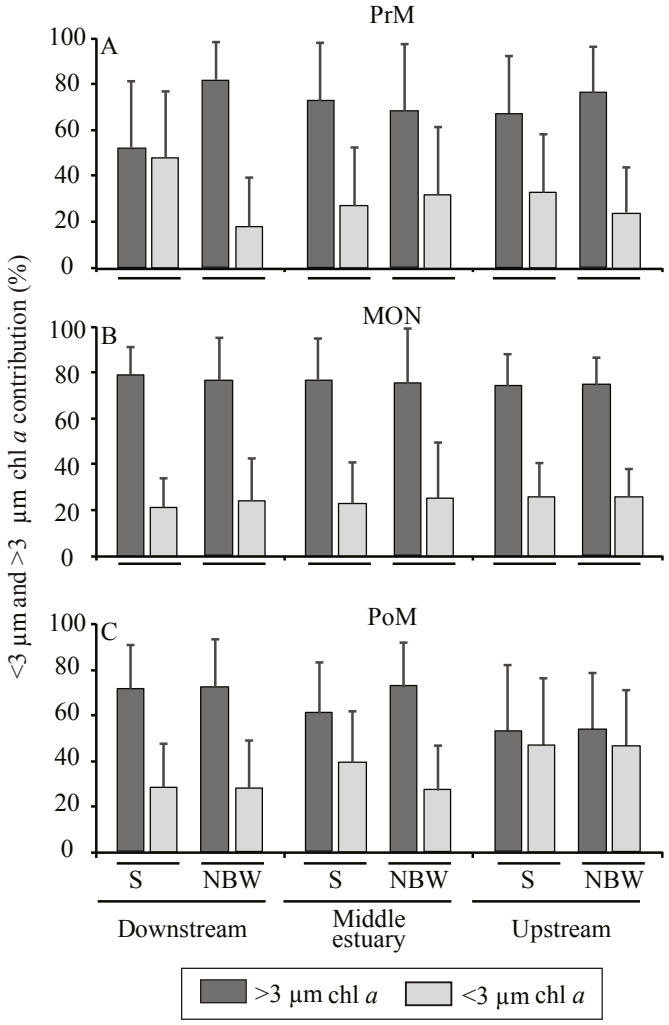

Fig. 6. Seasonal variations in > 3 μm and < 3 μm chl *a* biomass contribution to the total chl *a* biomass in the surface (S) and near bottom (NBW) waters of the Zuari estuary. A) pre-monsoon, B) monsoon, and C) post-monsoon seasons. (Error bars represent the standard deviation (DS- downstream, ME-middle estuary and US- upstream).

Phytoplankton size-structure, among other factors, also depends on the maximum growth rate of the different groups of phytoplankton (Irwin et al., 2006). A general trend of an increase in relative *SYN* and PEUK abundance with increasing water temperature due to the higher activation energy of their growth rates than that of the > 3 μm phytoplankton has been reported (Chen et al., 2014). Similarly, in this study *SYN*-PC and PEUK groups which are generally present in lower abundance, attained higher abundance (10^4 and 10^5 cells mL^{-1}, respectively) downstream (salinity > 30) in May where highest temperature was recorded. Also, the increase in growth rates of these Pico groups corresponds with an increase in chl *a* and nutrient concentrations (Chen et al., 2014) as observed in our study where abundance peaked at higher concentrations of PO_4^{3-} and SiO_4^{4-}. During this period, high NH_4^+ concentrations are also reported from this estuary (Ram, 2002). This could have also favored the < 3 μm phytoplankton which are better utilizers of NH_4^+ than the > 3 μm phytoplankton (Stolte and Riegman, 1995). Also, the dominance of *SYN*-PE at lower temperatures and PEUK-I at higher temperatures suggests a temperature regulated shift in the community structure. This further implies that increase in < 3 μm chl *a* biomass was due to a combination of factors such as temperature and nutrients (PO_4^{3-}, SiO_4^{4-} and NH_4^+) leading to higher growth rates. These observations show that *SYN*-PE can dominate both, stratified as well as mixed waters (Xia et al., 2015). The possibility of different strains inhabiting these conditions cannot be ruled out. Similarly, the PEUK-I which was observed downstream could be a high saline strain. High chl *a* and oxygen saturation (> 100%) showing maximum production have been reported earlier from the downstream of this estuary (Patil and Anil, 2011). From the size-fractionated biomass, it can be hypothesized that a majority of this contribution during this period is from the < 3 μm phytoplankton size fraction.

However, the restriction of < 3 μm chl *a* biomass dominance only up to the middle estuary which coincided with temperatures below 32 °C and tilt of balance towards the > 3 μm chl *a* biomass above this temperature could be due to increased grazing pressure or lowering growth rates of < 3 μm phytoplankton. Grazing is likely to affect > 3 μm phytoplankton less severely due to the longer generation times of mesozooplankton while the < 3 μm phytoplankton, in spite of their effective light and nutrient utilization are tightly controlled by heterotrophic nanoflagellates (HNF), with growth rates similar to their own (Landry et al., 1997). The comparatively higher abundance of HNF than that of micro- and mesozooplankton was reported earlier from this estuary during this period (Gauns et al., 2015). Also, temporal changes in the concentrations of phaeopigments relative to total biomass in the particular size-fraction can be used as rough indicators of changes in the abundance of pigmented faecal pellets and thus in the grazing rates of predators (Tamigneaux et al., 1999). In the present study, the grazing index of < 3 μm chl *a* biomass was comparatively higher (0.570 ± 0.031) than that of > 3 μm chl *a* biomass (0.426 ± 0.240) in May. The decreasing biomass could also be a reflection of the change in community structure due to reducing salinity towards upstream.

The SW MON was the main meteorological driver of the chl *a* biomass response during MON season (Fig. 10). Heavy rainfall intensity during the beginning phase of MON, accompanied by low light intensity due to cloud cover, low saline waters and high turbidity due to freshwater influx contributed to a reduction in the phytoplankton (Madhu et al., 2007; Sarma et al., 2009; Patil and Anil, 2015). Phytoplankton growth is also influenced by the reduced residence time of water masses and the high particle transport due to flushing (Patil and Anil, 2011; Lu and Gan, 2015). Although in the Zuari estuary, residence time has not been calculated, the residence time of the waters in the neighboring estuary (Mandovi) is 5–6 days during MON and about 50 days during non-MON seasons (Qasim and Sen Gupta, 1981). The reduction in rainfall intensity towards the later phase of MON, accompanied with reduction in freshwater influx and a simultaneous increase in tidal intensity, led to stabilization of the water column. These conditions along with increasing solar radiation, salinity and high water transparency could be responsible for an increase in < 3 μm and > 3 μm chl *a* biomass downstream. A minimum of 50 cm depth of light penetration (secchi disk depth) was reported to be essential for phytoplankton bloom formation in nutrient rich waters of this estuary (Patil and Anil, 2015).

With reduced rainfall progressing into the PoM season (October), the marked increase in the > 3 μm chl *a* biomass downstream implies the rapid use of nutrients accumulated through the MON processes (Fig. 10; Devassy and Goes, 1989; Patil and Anil, 2011). Due to the unstable conditions during MON, the nutrients are utilized after the cessation of rainfall when water column conditions return to its original state, and light intensity increases (Patil and Anil, 2011; Rajaneesh and Mitbavkar, 2013; Mitbavkar et al., 2015). Nutrient availability is an important factor controlling the phytoplankton chl *a* biomass (Agawin et al., 2000). The switching over of dominance towards the < 3 μm chl *a* biomass at the middle estuary and upstream with the low saline strain, *SYN*-PC as the major contributor, suggests salinity as the controlling factor. Further into the PoM season (November–December), the complete absence of rainfall and dominance of tidal effect favored the > 3 μm chl *a* biomass across the estuary. This scenario underwent a change towards the end of PoM (January) wherein the highest > 3 μm chl *a* biomass (downstream) coincided with the lowest water temperatures recorded for the study period and lower water transparency.

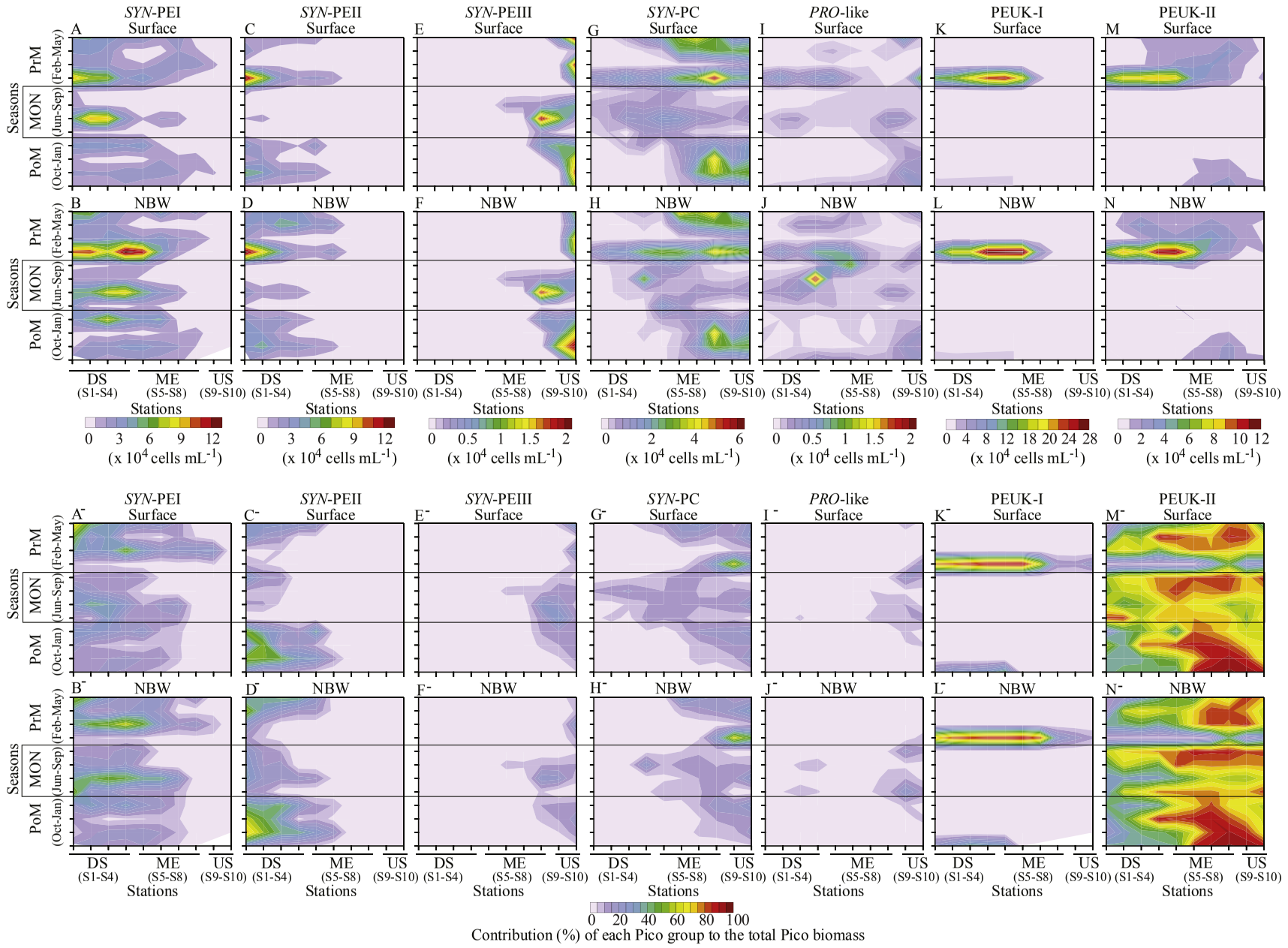

Fig. 7. Temporal and spatial variations in (A, B and A$^-$, B$^-$) *SYN*-PEI, (C, D and C$^-$, D$^-$) *SYN*-PEII, (E, F and E$^-$, F$^-$) *SYN*-PEIII, (G, H and G$^-$, H$^-$) *SYN*-PC, (I, J and I$^-$, J$^-$) *PRO*-like cells, (K, L and K$^-$, L$^-$) PEUK-I and (M, N and M$^-$, N$^-$) PEUK-II abundance and its contribution to the < 3 μm chl *a* biomass (DS- downstream, ME-middle estuary and US- upstream).

Table 4
Results of Pearson correlation analysis for the > 3 μm chl *a* biomass, < 3 μm chl *a* biomass, flow cytometric (FCM) chl fluorescence and total chl *a*.

Parameter	> 3 μm chl *a*	< 3 μm chl *a*	FCM chl fluorescence
Pre-monsoon			
Total chl *a*	0.906**	0.263*	0.328**
> 3 μm chl *a*	–	–	–
< 3 μm chl *a*	−0.170	0.906**	0.690**
Monsoon			
Total chl *a*	0.978**	0.585**	0.580**
> 3 μm chl *a*	–	–	–
< 3 μm chl *a*	−0.404**	–	0.576**
Post-monsoon			
Total chl *a*	0.961**	0.305**	0.181
> 3 μm chl *a*	–	–	–
< 3 μm chl *a*	0.030**	–	0.480**

*p < 0.05, **p < 0.01.

The simultaneous presence of high SiO_4^{4-} concentrations indicate water turbulence. Such intermittent vertical mixing promotes phytoplankton growth, especially of diatoms (Devassy and Goes, 1989; Patil and Anil, 2011). According to Nair (1980), zooplankton abundance is high during this period, suggesting that the high NO_2^- concentrations found in our study could be a product of nitrification processes as reported earlier for this estuary (Patil and Anil, 2011). Also, the low NO_3^- concentrations could suggest its utilization by phytoplankton blooms. Due to their ability to store nutrients in large intracellular vacuoles and high maximum growth rates, episodic inputs of nutrients into the euphotic layer lead to an increase in diatom population, with comparatively little response from the < 3 μm size-fraction (Cermeno et al., 2005). A study carried out at the downstream of the estuary reported an increase in diatom abundance, mainly *Thalassiosira*, *Thalassionema* and *Chaetoceros* during the same season (Patil and Anil, 2011).

These spatial and inter- and intraseasonal size-fractionated chl *a* biomass responses to environmental perturbations can provide some clues about the dominant type of functioning food web (Tamigneaux et al., 1999). During MON, the size-independent response with the dominance of > 3 μm chl *a* biomass implies the prevalence of herbivorous food web. Huge quantity of organic matter load is strongly linked to the volume of freshwater discharge due to monsoonal or anthropogenic activities (Sarma et al., 2012; Krishna et al., 2016). After a reduction in rainfall, there is an enhanced activity of each compartment of the food web, such as higher microbial decomposition, higher phytoplankton biomass and higher microzooplankton biomass (Patil and Anil, 2011; Gauns et al., 2015; Khandeparker et al., 2015). Overall, > 20% contribution of the < 3 μm chl *a* biomass including certain episodes of similar contributions from both size-fractions during the non-MON seasons suggest the prevalence of the herbivorous food web along with the microbial food web. This is substantiated by the earlier reports on high numbers of grazers of both the size-fractions of chl *a* biomass such as HNF, micro- and mesozooplankton during the non-MON seasons (Gauns et al., 2015). HNF, which are the major predators of < 3 μm biomass, are preyed upon by the microzooplankton, thus forming a link between the microbial and herbivorous food web. The microzooplankton, which also grazes on the > 3 μm chl *a* biomass are in turn predated upon by the carnivorous mesozooplankton which are abundant during this period (Padmavati and Goswami, 1996; Gauns et al.,

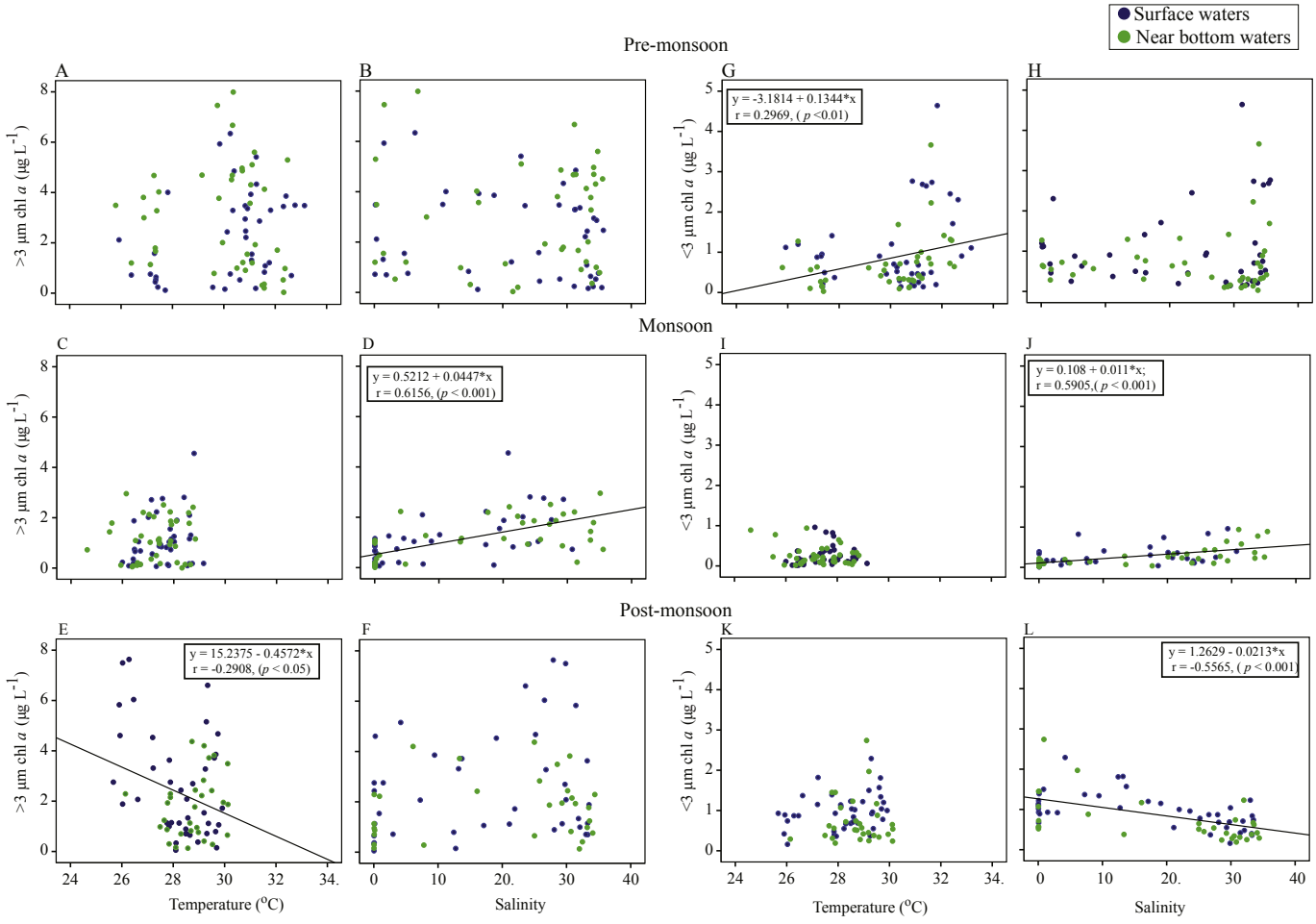

Fig. 8. Regression analysis of > 3 μm and < 3 μm chl *a* biomass with salinity and temperature during different seasons.

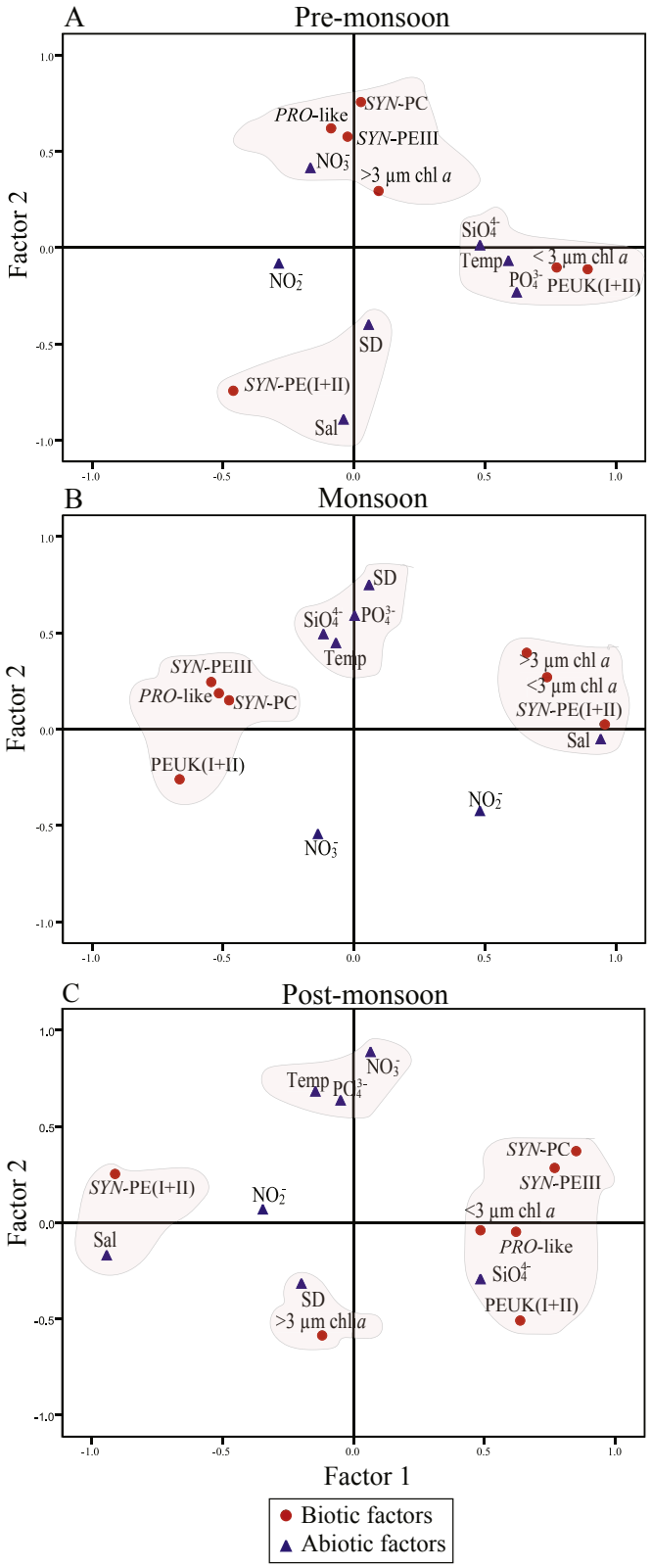

Fig. 9. Diagrammatic representation of factor analysis with two major factors obtained for the (A) pre-monsoon, (B) monsoon and (C) post-monsoon seasons, showing the relationship among the various parameters (temp-temperature, sal-salinity, SD-secchi disk depth, NO_3^-, PO_4^{3-}, NO_2^- and SiO_4^{4-}, < 3 µm chl *a* biomass, > 3 µm chl *a* biomass and contribution of each Pico group to the < 3 µm chl *a* biomass).

2015). The > 3 µm chl *a* biomass is also grazed by the herbivorous mesozooplankton. The presence of the carnivorous mesozooplankton and also the balanced Pico abundance with only ephemeral peaks observed through daily sampling in this region (Mitbavkar et al., 2015) provides an indirect evidence for the high availability of microzooplankton and HNF. Recently, the existence of a multivorous food web was suggested wherein during episodes of lowered > 3 µm chl *a* biomass, the herbivorous mesozooplankton resorts to omnivory, preying upon the microzooplankton when the < 3 µm chl *a* biomass is high (Legendre and Rassoulzadagen, 1995). Hence during non-MON seasons, intra-seasonal and spatial variations in the size-dependent response of chl *a* biomass in the Zuari estuary suggests intermittent functioning between the herbivorous and microbial food webs. Thus, highlighting the significance of both the size-fractions of chl *a* biomass in estuarine food web dynamics although, the herbivorous food web is said to be more efficient in energy transfer due to the lower number of links (Barnes et al., 2010). Multivorous food webs are known to be stable contributing towards a healthy ecosystem functioning (Tamigneaux et al., 1999). Such a scenario can be expected in the Zuari estuary where there is a sizeable contribution from both size-fractions along with the abundant presence of related predators. This is further substantiated by the high abundance of larvae, juveniles, sub-adults, adults and spawners of many commercially important fish species in this estuary during the non-MON seasons (Padmavati and Goswami, 1996; Sreekanth et al., 2017) when food is available in plenty. Hence such estuaries serve as breeding and nursing grounds for a diverse assemblage of fish thereby enhancing the fishery potential, locally and globally.

5. Conclusions

As hypothesized, the > 3 µm chl *a* biomass dominated the total chl biomass on most occasions with the ephemeral dominance of the < 3 µm chl *a* biomass (Fig. 10). During MON, size-independent response led to a decrease and increase in the total phytoplankton biomass downstream during the heavy rainfall and rainfall break, respectively. Size-dependent response during the non-MON seasons revealed the dominance of the > 3 µm chl *a* biomass downstream during the lowest recorded annual temperature coinciding with high SiO_4^{4-} concentrations indicating vertical mixing. Highest < 3 µm chl *a* biomass was observed at high salinity-highest temperature conditions recorded from downstream to middle estuary during PrM and low salinity-high nutrient conditions upstream during PoM. Although some samplings were carried out during ebb tide, the tidal effect was minimal, e.g. October sampling time was dominated by freshwater runoff whereas, in May, temperature effect was dominant on the phytoplankton biomass. The relatively lower biomass in February as compared to March and April could be an exceptional case. Hence, in future studies inclusion of the tidal effects on the phytoplankton biomass size structure needs to be taken into consideration. Community composition differences were revealed with PEUK dominating during PrM, *SYN*-PE at higher salinity downstream during MON and *SYN*-PC at lower salinity upstream during PoM. This study reveals seasonal and spatial variations in size-fractionated chl *a* biomass influenced by the hydrography and environmental factors which will in turn influence the higher trophic community structure.

Acknowledgments

The authors would like to thank the Director, Council of Scientific and Industrial Research (CSIR)-National Institute of Oceanography for his support. This work was conducted under the project OCEAN FINDER (PSC 0105) funded by CSIR. We thank Mr. D. Sundar for providing CTD data. We also thank our project team members for their help and suggestions during sampling. We thank the anonymous reviewers for their valuable comments. Rajaneesh K.M. acknowledges CSIR for

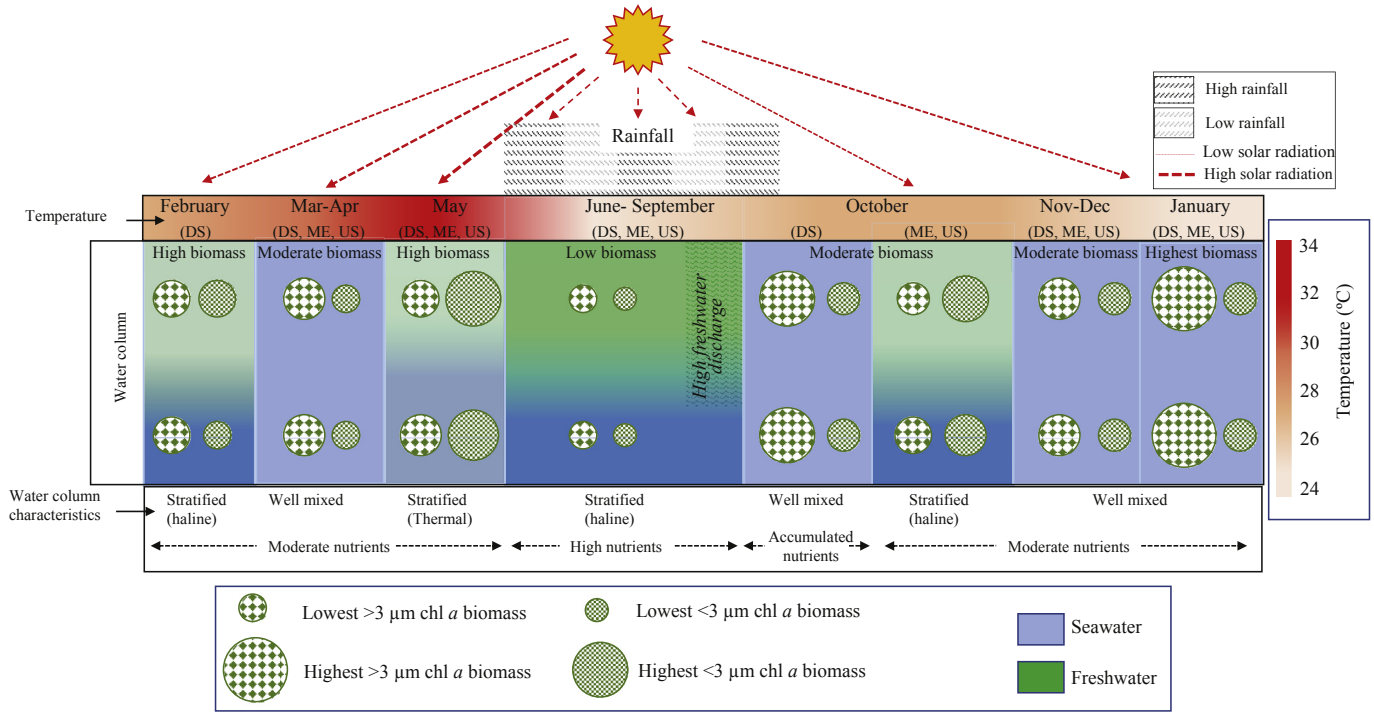

Fig. 10. Schematic representation of the temporal and spatial variations in < 3 µm and > 3 µm chl *a* biomass in the Zuari estuary (DS-Downstream, ME-middle estuary, US-Upstream).

the award of Senior Research Fellowship (SRF). This is a NIO contribution (no. 6211).

References

Achuthankutty, C., Ramaiah, N., Padmavati, G., 1998. Zooplankton Variability and Copepod Assemblage in the Coastal and Estuarine Waters of Goa along the Central-west Coast of India. IOC Workshop Report, 142. .

Agawin, N.S., Duarte, C.M., Agusti, S., 2000. Nutrient and temperature control of the contribution of picoplankton to phytoplankton biomass and production. Limnol. Oceanogr. 45, 591–600.

Alvarez, E., Nogueira, E., Lopez-Urrutia, A., 2017. In vivo single-cell fluorescence and size scaling of phytoplankton chlorophyll content. Appl. Environ. Microbiol. 83 e03317–16. https://doi.org/10.1128/AEM.03317-16.

Anand, S.S., Sardesai, S., Muthukumar, C., Mangala, K., Sundar, D., Parab, S., Kumar, M.D., 2014. Intra-and inter-seasonal variability of nutrients in a tropical monsoonal estuary (Zuari, India). Continent. Shelf Res. 82, 9–30.

Azam, F., Fenchel, T., Field, J.G., Gray, J., Meyer-Reil, L., Thingstad, F., 1983. The ecological role of water-column microbes in the sea. Mar. Ecol. Prog. Ser. 10, 257–263.

Barnes, C., Maxwell, D., Reuman, D.C., Jennings, S., 2010. Global patterns in predator-prey size relationships reveal size dependency of trophic transfer efficiency. Ecology 91, 222–232.

Bec, B., Collos, Y., Souchu, P., Vaquer, A., Lautier, J., Fiandrino, A., Benau, L., Orsoni, V., Laugier, T., 2011. Distribution of picophytoplankton and nanophytoplankton along an anthropogenic eutrophication gradient in French Mediterranean coastal lagoons. Aquat. Microb. Ecol. 63, 29–45.

Bidigare, R.R., Ondrusek, M.E., 1996. Spatial and temporal variability of phytoplankton pigment distributions in the central equatorial Pacific Ocean. Deep Sea Res. Part II 43, 809–833.

Binder, B.J., Chisholm, S.W., Olson, R.J., Frankel, S.L., Worden, A.Z., 1996. Dynamics of picophytoplankton, ultraphytoplankton and bacteria in the central equatorial Pacific. Deep Sea Res. Part II 43, 907–931.

Blanchot, J., Rodier, M., 1996. Picophytoplankton abundance and biomass in the western tropical Pacific Ocean during the 1992 El Niño year: results from flow cytometry. Deep Sea Res. Part I 43, 877–895.

Buchanan, C., Lacouture, R.V., Marshall, H.G., Olson, M., Johnson, J.M., 2005. Phytoplankton reference communities for Chesapeake Bay and its tidal tributaries. Estuaries 28, 138–159.

Caroppo, C., 2000. The contribution of picophytoplankton to community structure in a Mediterranean brackish environment. J. Plankton Res. 22, 381–397.

Cermeno, P., Maranon, E., Rodríguez, J., Fernandez, E., 2005. Large-sized phytoplankton sustain higher carbon specific photosynthesis than smaller cells in a coastal eutrophic ecosystem. Mar. Ecol. Prog. Ser. 297, 51–60.

Chen, B., Liu, H., Huang, B., Wang, J., 2014. Temperature effects on the growth rate of marine picoplankton. Mar. Ecol. Prog. Ser. 505, 37.

Contant, J., Pick, F.R., 2013. Picophytoplankton during the ice-free season in five temperate-zone rivers. J. Plankton Res. 35, 553–565.

Devassy, V., Goes, J., 1989. Seasonal patterns of phytoplankton biomass and productivity in a tropical estuarine complex (west coast of India). Proc. Plant Sci. 99, 485–501.

Gaulke, A.K., Wetz, M.S., Paerl, H.W., 2010. Picophytoplankton: a major contributor to planktonic biomass and primary production in a eutrophic, river-dominated estuary. Estuar. Coast Shelf Sci. 90, 45–54.

Gauns, M., Mochemadkar, S., Patil, S., Pratihary, A., Naqvi, S.W.A., Madhupratap, M., 2015. Seasonal variations in abundance, biomass, and grazing rates of micro-zooplankton in a tropical monsoonal estuary. J. Oceanogr. 71, 345–359.

Grasshoff, K., Ehrhardt, M., Kremling, K., 1983. Methods of Seawater Analysis, vol. 419. Verlag Chemie, New York, NY, pp. 159–223.

Guenther, M., Araújo, M., Flores-Montes, M., Gonzalez-Rodriguez, E., Neumann-Leitao, S., 2015. Eutrophication effects on phytoplankton size fractioned biomass and production at a tropical estuary. Mar. Pollut. Bull. 91, 537–547.

Irwin, A.J., Finkel, Z.V., Schofield, O.M., Falkowski, P.G., 2006. Scaling-up from nutrient physiology to the size structure of phytoplankton communities. J. Plankton Res. 28, 459–471.

Jha, B., Nath, D., Srivastava, N., Satpathy, B., 2008. Estuarine Fisheries Management-options & Strategies, vol. 3. CIFRI Policy paper, pp. 1–23.

Khandeparker, L., Anil, A.C., Naik, S.D., Gaonkar, C.C., 2015. Daily variations in pathogenic bacterial populations in a monsoon influenced tropical environment. Mar. Pollut. Bull. 96, 337–343.

Krishna, M.S., Prasad, M.H.K., Rao, D.B., Viswanadham, R., Sarma, V.V.S.S., Reddy, N.P.C., 2016. Export of dissolved inorganic nutrients to the northern Indian Ocean from the Indian monsoonal rivers during discharge period. Geochem. Cosmochim. Acta 172, 430–443.

Landry, M.R., Barber, R.T., Bid, R.R., Chai, F., Coale, K.H., Dam, H.G., Lewis, M.R., Lindley, S.T., McCarthy, J.J., Roman, M.R., 1997. Iron and grazing constraints on primary production in the central equatorial Pacific: an EqPac synthesis. Limnol. Oceanogr. 42, 405–418.

Legendre, L., Rassoulzadagen, F., 1995. Plankton and nutrient dynamics in coastal waters. Ophelia 41, 153–172.

Liu, C.W., Lin, K.H., Kuo, Y.M., 2003. Application of factor analysis in the assessment of groundwater quality in a Blackfoot disease area in Taiwan. Sci. Total Environ. 313, 77–89.

Liu, J., Fu, B., Yang, H., Zhao, M., He, B., Zhang, X.H., 2015. Phylogenetic shifts of bacterioplankton community composition along the Pearl Estuary: the potential impact of hypoxia and nutrients. Front. Microbiol. 6, 1–13.

Lu, Z., Gan, J., 2015. Controls of seasonal variability of phytoplankton blooms in the Pearl

River Estuary. Deep-Sea Res. Pt II 13, 86–96.
Madhu, N.V., Jyothibabu, R., Balachandran, K.K., 2009. Monsoon-induced changes in the size fractionated phytoplankton biomass and production rate in the estuarine and coastal waters of southwest coast of India. Environ. Monit. Assess. 166, 521–528.
Madhu, N., Jyothibabu, R., Balachandran, K., Honey, U., Martin, G., Vijay, J., Shiyas, C., Gupta, G., Achuthankutty, C., 2007. Monsoonal impact on planktonic standing stock and abundance in a tropical estuary (Cochin backwaters–India). Estuar. Coast Shelf Sci. 73, 54–64.
Manoj, N., Unnikrishnan, A., 2009. Tidal circulation and salinity distribution in the Mandovi and Zuari estuaries: case study. J. Waterw. Port, Coast. 135, 278–287.
Marshall, H.G., 2009. Phytoplankton of the york river. J. Coast Res. 57, 59–65.
Mitbavkar, S., Patil, J.S., Rajaneesh, K.M., 2015. Picophytoplankton as tracers of environmental forcing in a tropical monsoonal bay. Microb. Ecol. 7, 1–18.
Mitbavkar, S., Rajaneesh, K.M., Anil, A.C., Sundar, D., 2012. Picophytoplankton community in a tropical estuary: detection of *Prochlorococcus*-like populations. Estuar. Coast Shelf Sci. 107, 159–164.
Myers, N., Mittermeier, R.A., Mittermeier, C.G., da Fonseca, G.A.B., Kent, J., 2000. Biodiversity hotspots for conservation priorities. Nature 403, 853–858.
Nair, V.R., 1980. Production and associations of zooplankton in estuarine and nearshore Waters of Goa. Indian J. Mar. Sci. 9, 116–119.
Padmavati, G., Goswami, S.C., 1996. Zooplankton ecology in the Mandovi-Zuari estuarine system of Goa, west coast of India. Indian J. Mar. Sci. 25, 268–273.
Paerl, H.W., Valdes, L.M., Peierls, B.L., Adolf, J.E., Harding Jr., L., 2006. Anthropogenic and climatic influences on the eutrophication of large estuarine ecosystems. Limnol. Oceanogr. 51, 448–462.
Parsons, T., Maita, Y., Lalli, C., 1984. A Manual of Chemical and Biological Methods for Seawater Analysis, vol. 173 Pergamon Press, Oxford.
Partensky, F., Hess, W., Vaulot, D., 1999. *Prochlorococcus*, a marine photosynthetic prokaryote of global significance. Microbiol. Mol. Biol. Rev. 63, 106–127.
Patil, J.S., Anil, A.C., 2011. Variations in phytoplankton community in a monsoon-influenced tropical estuary. Environ. Monit. Assess. 182, 291–300.
Patil, J.S., Anil, A.C., 2015. Effect of monsoonal perturbations on the occurrence of phytoplankton blooms in a tropical bay. Mar. Ecol. Prog. Ser. 530, 77–92.
Qasim, S.Z., 2003. Indian Estuaries, vol. 259 Allied publishers.
Qasim, S., Sen Gupta, R., 1981. Environmental characteristics of the Mandovi-Zuari estuarine system in Goa. Estuar. Coast Shelf Sci. 13, 557–578.
Qiu, D., Huang, L., Zhang, J., Lin, S., 2010. Phytoplankton dynamics in and near the highly eutrophic pearl river estuary, south China sea. Continent. Shelf Res. 30, 177–186.
Rajaneesh, K.M., Mitbavkar, S., 2013. Factors controlling the temporal and spatial variations in *Synechococcus* abundance in a monsoonal estuary. Mar. Environ. Res. 92, 133–143.
Ram, A., 2002. Studies on the Role of Bacteria in the Assimilation of Organic Inputs in Coastal Waters. Ph.D. dissertation. Goa University, Goa, India, pp. 49–50 (chapter 4).
Ray, R.T., Haas, L.W., Sieracki, M.E., 1989. Autotrophic picoplankton dynamics in a Chesapeake Bay sub-estuary. Mar. Ecol. Prog. Ser. 52, 273–285.
Richardson, T.L., Jackson, G.A., 2007. Small phytoplankton and carbon export from the surface ocean. Science 315, 838–840.
Rodriguez, F., Chauton, M., Johnsen, G., Andresen, K., Olsen, L.M., Zapata, M., 2006. Photoacclimation in phytoplankton: implications for biomass estimates, pigment functionality and chemotaxonomy. Mar. Biol. 148, 963–971.
Sarma, V.V.S.S., Viswanadham, R., Rao, G.D., Prasad, V.R., Kumar, B.S.K., Naidu, S.A., Kumar, N.A., Rao, D.B., Sridevi, T., Krishna, M.S., Reddy, N.P.C., 2012. Carbon dioxide emissions from Indian monsoonal estuaries. Geophys. Res. Lett. 39, 1239–1242.
Sarma, V.V.S.S., Gupta, S., Babu, P., Acharya, T., Harikrishn achari, N., Vishnuvardhan, K., Rao, N., Reddy, N., Sarma, V., Sadhuram, Y., 2009. Influence of river discharge on plankton metabolic rates in the tropical monsoon driven Godavari estuary, India. Estuar. Coast Shelf Sci. 85, 515–524.
Shetye, S., Murty, C., 1987. Seasonal variation of the salinity in the Zuari estuary, Goa, India. J. Earth Syst. Sci. 96, 249–257.
Shetye, S., Shankar, D., Neetu, S., Suprit, K., Michael, G., Chandramohan, P., 2007. The Environment that Conditions the Mandovi and Zuari Estuaries. The Mandovi and Zuari Estuaries. NIO, Dona Paula, Goa, India, pp. 29–38.
Sin, Y., Wetzel, R.L., Anderson, I.C., 2000. Seasonal variations of size fractionated phytoplankton along the salinity gradient in the York River estuary, Virginia (USA). J. Plankton Res. 22, 1945–1960.
Sreekanth, G.B., Lekshmi, N.M., Chakraborty, S.K., Jaiswar, A.K., Singh, N.P., 2017. Seasonal fish species composition, catch rate and catch value in the small scale fishery of a tropical monsoon estuary along southwest coast of India. J. Environ. Biol. 38, 81.
Stolte, W., Riegman, R., 1995. Effect of phytoplankton cell size on transient-state nitrate and ammonium uptake kinetics. Microbiology 141, 1221–1229.
Tamigneaux, E., Legendre, L., Klein, B., Mingelbier, M., 1999. Seasonal dynamics and potential fate of size-fractionated phytoplankton in a temperate nearshore environment (Western Gulf of St Lawrence, Canada). Estuar. Coast Shelf Sci. 48, 253–269.
Vijith, V., Sundar, D., Shetye, S., 2009. Time-dependence of salinity in monsoonal estuaries. Estuar. Coast Shelf Sci. 85, 601–608.
Xia, X., Vidyarathna, N.K., Palenik, B., Lee, P., Liu, H., 2015. Comparison of the seasonal variations of *Synechococcus* assemblage structures in estuarine waters and coastal waters of Hong Kong. Appl. Environ. Microbiol. 81, 7644–7765.

Estuarine, Coastal and Shelf Science 107 (2012) 159–164

Contents lists available at SciVerse ScienceDirect

Estuarine, Coastal and Shelf Science

journal homepage: www.elsevier.com/locate/ecss

Short communication

Picophytoplankton community in a tropical estuary: Detection of *Prochlorococcus*-like populations

Smita Mitbavkar, K.M. Rajaneesh, A.C. Anil*, D. Sundar

Council of Scientific and Industrial Research, National Institute of Oceanography, Dona Paula, Goa 403 004, India

ARTICLE INFO

Article history:
Received 9 February 2011
Accepted 5 May 2012
Available online 16 May 2012

Keywords:
Zuari estuary
neap tide
picophytoplankton
Prochlorococcus-like cells
spring tide
Synechococcus

Regional index terms:
India
Goa
Zuari estuary

ABSTRACT

The influence of hydrography on the picophytoplankton (PP) abundance in estuaries was studied by sampling along a salinity gradient for the first time in an Indian estuary. *Prochlorococcus*-like cells were detected at salinities ranging from 0.06 to 35, which otherwise is reported from offshore regions, thereby showing that this group is capable of surviving in estuarine waters. PP also comprised picoeukaryotes and two groups of *Synechococcus*, one rich in phycoerythrin (*SYN*-PE) and other in phycocyanin (*SYN*-PC). Salinity played an important role in the picophytoplankton distribution. *SYN*-PE was represented by two sub-groups, one which was found only in saline waters (*SYN*-PEII) and the other throughout the salinity gradient (*SYN*-PEI). *SYN*-PEI and *SYN*-PC dominated downstream and upstream, respectively but were present throughout the salinity gradient unlike in other estuarine regions. Picoeukaryotes abundance showed an increasing trend from saline to brackish water and decreased in freshwater. The entry of seawater into the estuary regulated *SYN*-PE and *Prochlorococcus*-like cells downstream whereas their higher abundance in freshwater could be due to different strains of freshwater origin. The average contribution of PP to the total photosynthetic biomass during spring and neap tides was 43% and 29% respectively, which highlights the importance of PP in estuaries.

1. Introduction

Picophytoplankton (PP; <2 μm), the smallest group representing the phytoplankton community, forms an integral part of the marine microbial food web contributing substantially to primary production especially in oligotrophic ecosystems (Campbell et al., 1998). PP provides food for many protists, large zooplankton and small invertebrates (Richardson and Jackson, 2007; Wilson and Steinberg, 2010). This acts as a pathway for the transfer of PP carbon to the higher trophic levels as well as its vertical flux to the deep sea. PP comprises of two cyanobacteria, *Prochlorococcus* and *Synechococcus* and the picoeukaryotes. Discovery of *Prochlorococcus* (Chisholm et al., 1988) was a breakthrough in biological oceanography research since this is the smallest known phototrophic organism that is capable of flourishing in the oligotrophic regions and the only dominant photosynthetic group found in the waters as deep as 150–200 m (Partensky et al., 1999). *Synechococcus* and picoeukaryotes are abundant in coastal waters as compared to oceanic regions (Pan et al., 2005). Although *Prochlorococcus* is most abundant in oligotrophic waters relative to the other photosynthetic populations, it is by no means restricted to nutrient depleted waters (Partensky et al., 1999). Also this group was thought to be a truly oceanic species, but there are few reports which show their presence in the estuaries, bay and riverine regions (Vaulot et al., 1990; Shimada et al., 1995; Shang et al., 2007; Mitbavkar et al., 2009). However, there is still a question about the existence/origin of this group in such areas regarding whether they are passively advected from the open oceans or they are capable of growth in these areas.

While the importance of PP is well documented in open oceans, their role in coastal waters is not yet well established, especially in the tropical estuaries (Morán, 2007). Moreover, no information is available from the estuaries in the Arabian Sea, although a lot of information is available on the larger groups such as diatoms and dinoflagellates (Patil and Anil, 2008). The objective of this study was to characterize the PP in the Zuari estuary in order to develop an understanding of their prevalence and distribution along a salinity gradient.

2. Materials and methods

The Zuari estuary is a tide-dominated coastal plain estuary located in Goa, on the west coast of India and joins the Arabian Sea in the North Indian Ocean. The main channel of this estuary is about 50 km long and its cross-sectional area decreases towards the

* Corresponding author.
E-mail address: acanil@nio.org (A.C. Anil).

0272-7714/$ – see front matter © 2012 Elsevier Ltd. All rights reserved.
doi:10.1016/j.ecss.2012.05.002

upstream regions (0.5 km) with a width of ~5.5 km at the mouth (Shetye et al., 1995) and an average depth of 5 m (Sundar and Shetye, 2005). The main estuarine channel receives freshwater from a number of streams and rivers (Shetye, 1999). At about 11 km from the mouth, this estuary is joined by the Cumbarjua canal. The general flow pattern in this canal is regulated by the entry of seawater during the incoming tide and during the outgoing tide the flow in the canal is reversed (Qasim and Sen Gupta, 1981) leading to flushing of the estuarine system. Compared to the monsoon season (June to September), November to May is a dry season when the estuary receives comparatively less river discharge and is vertically well mixed throughout the length and the tidal influence reaches up to 50 km from the mouth (Shetye et al., 1995). The increase in elevation of the estuarine channels prevents tides from propagating beyond this distance. Tides in these estuaries are of the mixed semidiurnal type which occurs twice a day raising and lowering the water level by about 2 m and the tidal ranges are about 2.3 and 1.5 m during the spring and neap tides, respectively. Circulation in the channels is forced by oscillatory tidal flow at the mouth and by river discharge at the head (Shetye, 1999).

Ten stations (S) along the estuary were sampled during December 2009 over spring tide (ST; 04 December) and neap tide (NT; 29 December) (Table 1). Samples were collected from the surface and near-bottom (NB) from S1 in the morning subsequently proceeding toward S10. At each station a secchi disk was used to estimate the euphotic zone thickness. Temperature and salinity were recorded in the water column using a conductivity-temperature-depth (CTD) probe. Phytoplankton biomass was estimated as total chlorophyll *a* concentration by filtering 500 ml of seawater through GF/F which was then extracted in 90% acetone overnight and analyzed with fluorometry (Parsons et al., 1984). Water samples for PP analysis were fixed in paraformaldehyde (0.2% final concentration), preserved in liquid nitrogen and later stored at −80 °C until analysis.

For the PP analysis, a BD FACSAria™ II flow cytometer equipped with a blue (488 nm) and a red laser (633 nm) which can distinguish the red fluorescence excited by blue light (produced by chlorophyll) and red light (produced by phycocyanin) was used. Emitted light was collected through the following set of filters: 488/10 band pass (BP) for right angle light scatter (RALS; proxy for cell size), 575/26 BP for orange fluorescence, 695/40 and 660/20 BP for red fluorescence from chlorophyll (blue laser) and phycocyanin (red laser), respectively. Fluorescent beads (2 μm for PP "Fluoresbrite", polysciences) were used as internal standards and for calibration of the above parameters.

Flow cytometry data were processed with the BD FacsDiva software. PP groups were discriminated according to their specific autofluorescence properties and RALS differences. The cellular carbon content for the different PP groups was based on the cell biovolume, estimated by the calibration method of Worden et al. (2004), assuming the PP cells to be spherical. A biovolume to carbon conversion factor of 254 fg C μm^{-3}, 240 fg C μm^{-3} and 239 fg C μm^{-3} for *Synechococcus* (Baudoux et al., 2007), *Prochlorococcus*-like cells and picoeukaryotes (Worden et al., 2004), respectively was used. Linear regression was performed between the PP abundance, temperature and salinity. In order to determine the contribution of PP to the total phytoplankton biomass, the latter was calculated from chl *a* using a carbon-to-chlorophyll ratio of 40 (Gallegos, 2001).

3. Results

During ST and NT, sampling started at S1 during flood and ebb tide, respectively. During ST, by the time S5 was sampled the tide

Table 1
Sampling details for each sampling station in the Zuari estuary during a spring and neap tide.

Stations	Distance from mouth (km)	Station depth (m)	Sampling depth (m)	Spring tide Latitude; Longitude	Sampling time (h)	Z_{eu} (cm)	Temperature		Salinity		Neap tide Latitude; Longitude	Sampling time (h)	Z_{eu} (cm)	Temperature		Salinity	
							Surface	Bottom	Surface	Bottom				Surface	Bottom	Surface	Bottom
1. Marmugao	0	16	14.5	15° 25′ 16.9″; 73° 47′ 36.9″	10:02	215	28.6	28.6	34.4	34.6	15° 25′ 17.5″; 73° 47′ 36.6″	09:28	265	27.9	28.1	34.6	34.7
2. Chicalim	5.8	5	3.5	15° 25″ 08.5‴; 73° 50′ 22.4″	10:49	186	28.5	28.5	34.0	34.0	15° 25″ 03.1‴; 73° 50′ 25.1‴	10:04	200	27.9	27.9	33.0	33.0
3. Island	8.6	5	3.5	15° 24′ 57.4‴; 73° 51′ 57.0″	11:24	144	28.5	28.4	33.1	33.2	15° 24′ 55.4‴; 73° 51′ 56.3‴	10:33	157.2	28.1	28.0	30.7	31.0
4. Sancoale	11	7.1	5.6	15° 24′ 45.1‴; 73° 53′ 30.6‴	11:50	76	28.6	28.6	32.2	32.2	15° 24′ 43.8‴; 73° 53′ 37.4‴	11:01	201.3	28.1	28.1	27.6	30.1
5. Cortalim	13	9.6	8.1	15° 24′ 32.0‴; 73° 54′ 50.2‴	12:10	101	28.7	28.6	31.1	31.5	15° 24′ 36.3‴; 73° 54′ 45.0‴	11:18	185	28.2	28.0	26.6	29.1
6. Loutulim	19.7	10.5	9	15° 22′ 54.0‴; 73° 57′ 24.4″	12:53	104	29.4	28.9	26.8	28.4	15° 22′ 43.0‴; 73° 57′ 24.3‴	12:54	136.8	28.2	28.1	18.8	23.4
7. Borim	23.9	12.9	11.4	15° 21′ 03.6‴; 73° 59′ 58.0‴	13:44	98.5	29.5	29.4	18.2	19.9	15° 21′ 01.2‴; 74° 00′ 03.1‴	13:28	170.1	28.4	28.1	11.9	15.4
8. Shiroda	31.4	9.1	7.6	15° 18′ 12.3‴; 74° 00′ 55.5‴	14:36	113	29.5	29.3	8.5	9.8	15° 18′ 09.6‴; 74° 00′ 59.9‴	14:04	162	27.6	27.6	7.6	9.1
9. Kushavati	38.4	9.9	8.4	15° 16′ 31.7‴; 74° 04′ 28.3‴	15:42	138	28.3	28.3	0.5	0.5	15° 16′ 33.0‴; 74° 04′ 26.6‴	14:54	156.3	27.3	27.3	0.4	0.4
10. Sanvordem	42.2	4.9	3.4	15° 16′ 01.1‴; 74° 06′ 36.0‴	16:22	119	28.2	28.2	0.1	0.1	15° 16′ 02.4‴; 74° 06′ 31.6‴	15:31	123	27.5	27.5	0.1	0.1

had started receding and water from the Cumbarjua canal entered the estuary resulting in a temperature and salinity change from this point onwards (Table 1). From S9, lowest water temperature and salinity were detected due to discharge from the Kushavati River. The estuary was occupied by saline, brackish and freshwater during ST from S1–S5, S6–S8 and S9–S10, respectively and during NT from S1–S3, S4–S8 and S9–S10, respectively.

PP were encountered throughout the estuarine transect during both tides and comprised of *Prochlorococcus*-like cells (*PRO*-like) identified based on their smaller RALS and red autofluorescence, two groups of *Synechococcus*, one rich in phycoerythrin (*SYN*-PE) and the other rich in phycocyanin (*SYN*-PC), identified based on their orange and red autofluorescence, respectively and picoeukaryotes (PEUK) identified based on their larger RALS and red autofluorescence. The group of cells with a higher red autofluorescence than the PEUK was identified as nanoeukaryotes (NEUK) (Annex Table 1; Fig. 1).

SYN-PE group comprised of two sub-groups, one with a lower PE fluorescence (*SYN*-PEI) than the other (*SYN*-PEII). The latter group was observed only up to S3 or S4 (Fig. 1). Their contribution to the total PP abundance during both the tides ranged from 7 to 39% (Fig. 2). *SYN*-PEI showed a decreasing trend up to S8 during both tides and increased from S9 to S10. A significant variation was observed between the surface and NB abundance during both the tides ($P \leq 0.01$ and 0.001, respectively). Higher abundance was observed in saline and freshwater. This group dominated during ST at S1, S2 and S4 and during NT at S1 to S5 and S10. Their contribution to the total PP abundance ranged from 35 to 75% in the saline waters during ST and 58–95% during NT. The percentage contribution decreased in brackish water and freshwater (5%–39%) during both the tides except at S10 during NT. *SYN*-PC abundance increased from seawater to freshwater stations during both tides. The variations in abundance during both the tides were not significant and their contribution to the total PP abundance was low in saline waters (up to S5; 3–30%) and increased from brackish to freshwater (34–75%) except at S10 during NT (15%). A clear spatial pattern was evident in the distribution of *SYN*-PC and *SYN*-PE cells, where they were more abundant upstream and downstream, respectively. There was a sharp transition in dominance from *SYN*-PE to *SYN*-PC at salinities <30 during ST and 25 during NT (Annex Fig. 2).

PRO-like cells showed significant variations between the surface and NB abundance ($P \leq 0.025$ and 0.005, respectively). During ST, their contribution to the total PP abundance ranged from 35 to 46% and 24–27% where salinity was >31 and <0.5, respectively, except at S4 (6–5%). At S7 and S8 (salinity: 8–18), their concentrations were very low, representing <4% of the total. During NT, their contribution to total was comparatively low in saline waters (0.7–2%) and in brackish waters (2.8–3.7%) whereas in freshwaters it was higher (10–14%). Although this group was present at salinities ranging from 35 to 0.06, for the marine samples, comparatively higher values of RALS (0.042–0.11) and chlorophyll fluorescence (0.02–0.21) were observed than for the brackish and freshwater (0.006–0.045 and 0.022–0.149, respectively).

PEUK abundance increased from saline to brackish water and decreased in freshwater. Highest abundance was found at S4, contributing 33% to the total PP abundance. The variations in surface and NB abundance during both the tides were not significant. NEUK abundance was higher in brackish waters than in saline and freshwaters. Their abundance in the surface waters was similar to that of PEUK. Highest abundance was found at S6, contributing 28% to the total PP abundance. During ST, PP contribution to the total photosynthetic biomass ranged from 11 to 85% whereas during NT it ranged from 7 to 60% (Fig. 3).

During ST, temperature showed a significant negative correlation with *SYN*-PEI ($r^2 = 0.61$, $P < 0.001$) and *PRO*-like cells ($r^2 = 0.36$, $P < 0.01$) while with PEUK ($r^2 = 0.19$, $P \leq 0.05$) and NEUK ($r^2 = 0.24$, $P < 0.05$) it showed a positive correlation. Salinity showed a significant positive correlation with *SYN*-PEII ($r^2 = 0.27$, $P < 0.02$) and negative correlation with *SYN*-PC ($r^2 = 0.87$, $P < 0.001$). During NT, salinity showed a significant negative correlation with abundance of *PRO*-like cells ($r^2 = 0.66$, $P < 0.001$), *SYN*-PC ($r^2 = 0.59$, $P < 0.001$), PEUK ($r^2 = 0.81$, $P < 0.001$) and NEUK ($r^2 = 0.63$, $P < 0.001$) whereas it showed a positive correlation with SYN-PEII ($r^2 = 0.41$, $P < 0.01$). Temperature also showed a significant negative correlation with *PRO*-like cells ($r^2 = 0.63$, $P < 0.001$), PEUK ($r^2 = 0.3$, $P < 0.01$) and NEUK ($r^2 = 0.47$, $P < 0.001$).

4. Discussion

Since sampling at S1 started when the ST and NT were at its peak, the sampling at the subsequent stations was not tidally synchronized. Hence the samples, especially from upstream were not typical for the tide assigned. The estuarine circulation played an important role in structuring the community in estuaries because of their dynamic nature as compared to open oceans. Clustering of PP abundance data showed that under calm condition (NT) the estuary was less disturbed when compared to the ST (Annex Fig. 3). There was a clear spatial gradient in the distribution of the PE-rich and PC-rich cells with the former more abundant downstream and the latter upstream. Such a distribution pattern has also been reported in other estuaries. Murrell and Lores (2004) reported that the *SYN*-PC cells were an order of magnitude higher in abundance at the upstream end of the estuary to *SYN*-PE which decreased dramatically as salinity changed from ~20 to 28. The PC:PE ratio of ~11 observed in the Zuari estuary illustrates the importance of *SYN*-PC in estuarine systems. Although it is recognized that *SYN*-PC cells are not observed in oceanic systems, little attention has been accorded to the effect of salinity on the distribution of *SYN*. Waterbury et al. (1986) reported that *SYN*-PE cells have an obligate requirement for elevated concentrations of ions while marine *SYN* isolates that lack PE are halo tolerant and grow equally well in seawater or freshwater. However, in this study we observed two sub-groups of *SYN*-PE, one which is found only in saline waters and the other throughout the salinity gradient, although in low numbers in the brackish waters. Also, although a shift in dominance was observed between *SYN*-PEI and *SYN*-PC groups where each of these groups had a separate ecological niche, they were present throughout the salinity gradient and did not completely disappear as reported in some estuarine regions (Haas and Pearl, 1988). The PC:PE ratio shows that while the upstream end of the estuary is the source for *SYN*-PC, for *SYN*-PEI it is the downstream end. The significant negative correlation observed between *SYN*-PC and salinity was consistent with the observation of an increasing PC:PE ratio progressing upstream which showed that low salinity favored the growth of *SYN*-PC. However, such a significant negative relation was not observed between *SYN*-PEI and salinity because its abundance declined only in brackish water. Such a pattern can arise due to the presence of two different strains of *SYN*-PE abundant in saline and freshwater, which are physiologically/genetically different and cannot flourish in brackish water.

Only a few estuarine regions have reported the presence of *PRO*-like cells in low saline waters. Maximum surface *PRO*-like cell concentrations were similar to that found in the Rhone River of the Mediterranean Sea up to a salinity of 1.2 (Vaulot et al., 1990), Mississippi River plume (Jochem, 2003), Suruga Bay, Japan and Changjiang estuary, China at salinities >20 whereas it was two orders of magnitude lower than that recorded in the Australian coastal lagoon within a salinity range of 1.77–3.54 and >15. In the present study, although *PRO*-like cells were present at salinities

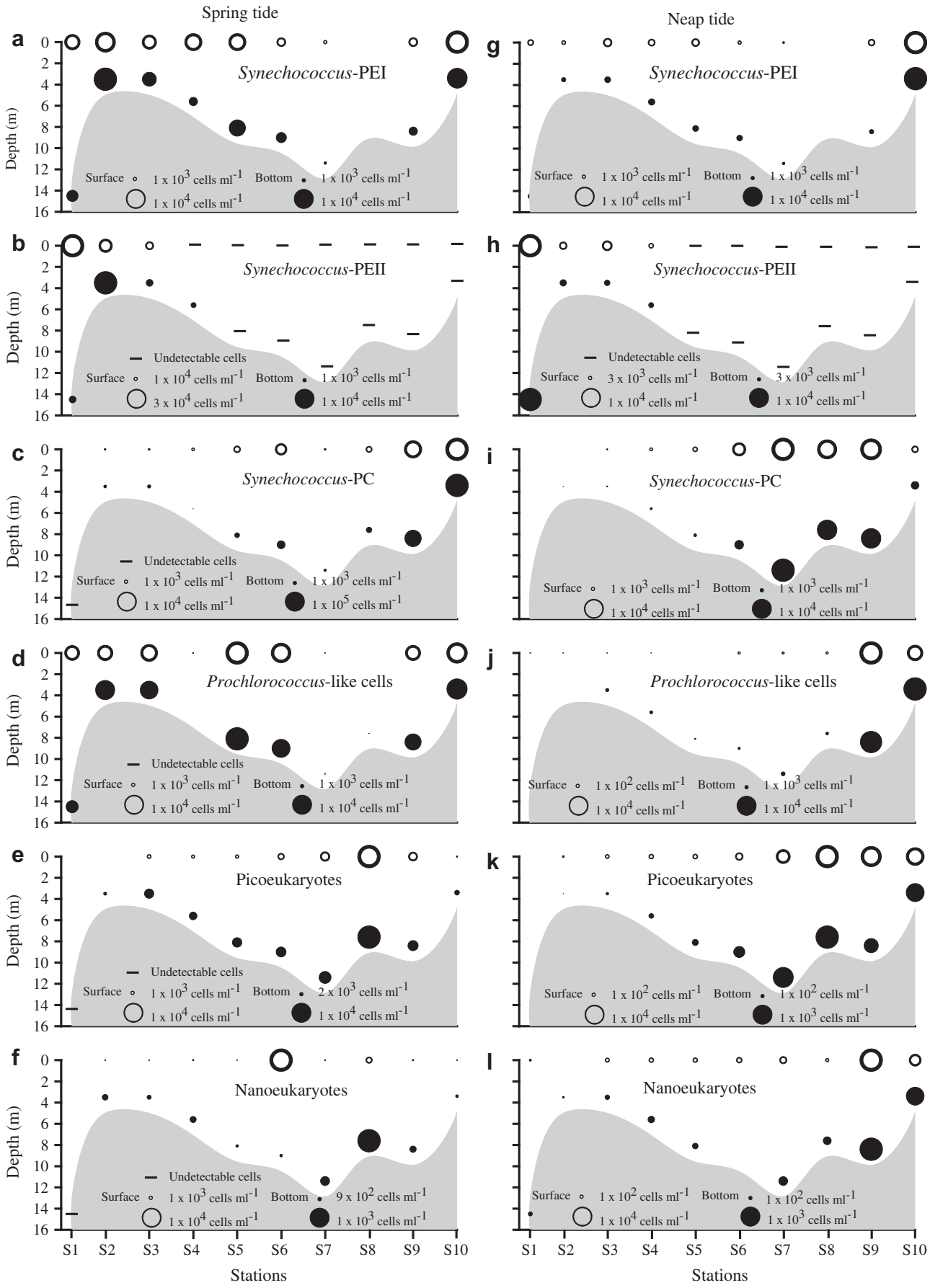

Fig. 1. Distribution of picophytoplankton groups along the Zuari estuary during the spring and neap tide.

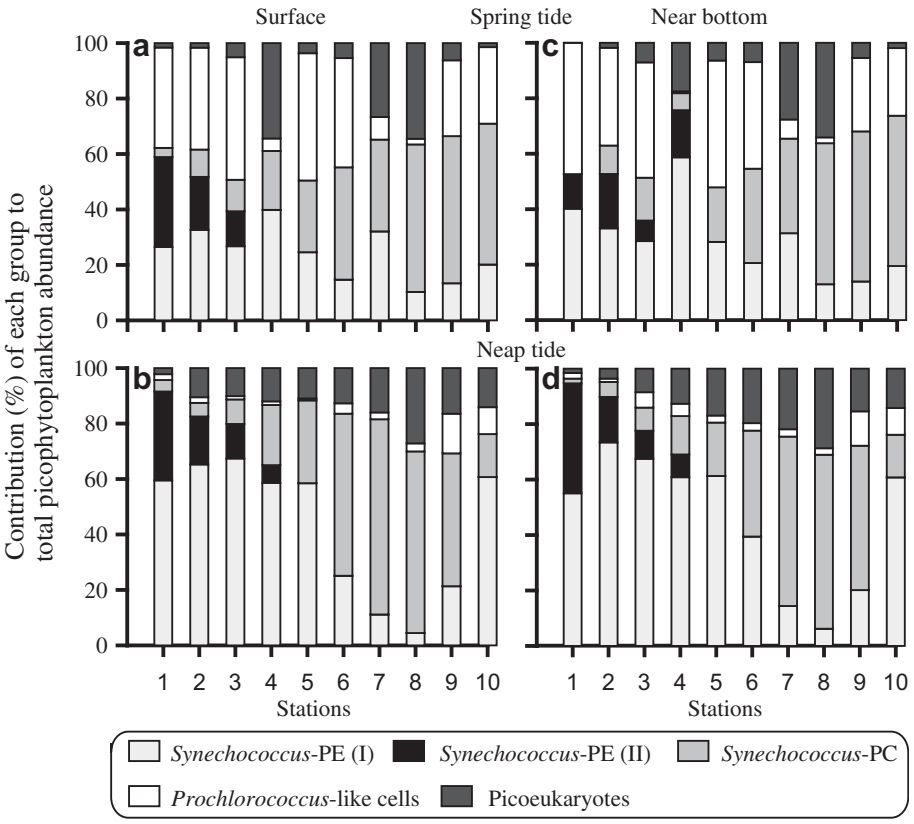

Fig. 2. Contribution (%) of the picophytoplankton groups to the total picophytoplankton abundance during the spring (a, c) and neap tide (b, d).

ranging from 35 to 0.06, differences in their RALS signals and chlorophyll fluorescence is an indication that the cells could be taxonomically and/or physiologically different. Low temperatures are unfavorable for the growth of *PRO*-like cells, with its presence recorded at the lowest surface temperature of about 10 °C and highest of 30 °C in warm equatorial oceanic regions (Partensky et al., 1999). The temperature in the Rhone River, Suruga Bay, Changjiang estuary and in the present study area was within the range for its growth. Nutrient enrichment experiments in the Zuari estuary have shown that *PRO*-like cells cannot only survive but also grow in these waters (S. Mitbavkar, unpublished data). These observations suggest that *PRO*-like cells possess capabilities to

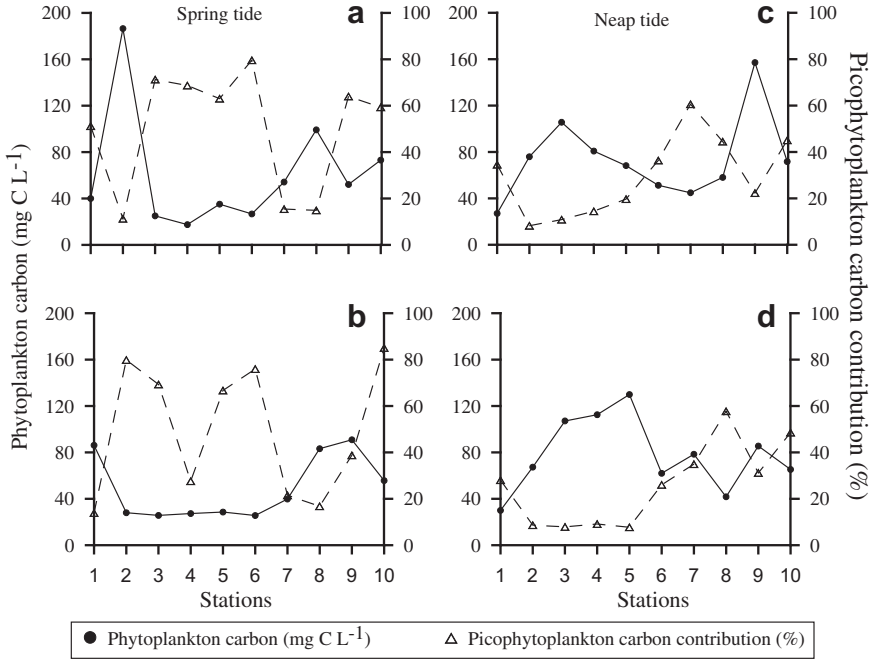

Fig. 3. Contribution of picophytoplankton (%) to the total photosynthetic biomass during the spring (a, b) and neap tide (c, d).

survive in high temperature and low saline estuarine waters. However, these results have to be confirmed through pigment analysis or genetic finger printing. Previous studies based on phytoplankton pigments along the southwest coast of India did not report *PRO*-like cells (Roy et al., 2006) which could be due to their low abundance compared to that in oceanic regions (Campbell et al., 1998). Another reason could be the type of filter paper used for sample collection where there is a possibility of losing the small sized cells. Earlier studies have reported 0.2 μm nylon membranes (Whatman) to be the most suitable for retention of picophytoplankton (Knefelkamp et al., 2007). Taking this observation into consideration, in this study, the total phytoplankton biomass may be underestimated as GF/F was used.

The correlations between environmental parameters and PP abundance may not be a causal one. However, their distribution pattern could be influenced by the entry of water from the Cumbarjua canal into the estuary resulting in flushing out of *SYN*-PE and *PRO*-like cells and influx of *SYN*-PC and PEUK. The rise in *SYN*-PE, *SYN*-PC and *PRO*-like cells at S9 could be due to the Kushavati River discharge. A decrease in the total abundance at S4 was a result of the high turbidity which impacted *PRO*-like cells the most.

The proposition that *PRO*-like cells can be brought to the coastal regions from the offshore regions may explain their higher numbers during ST (up to S5) than during NT. During ST, saline waters (>30 salinity) were present up to S5 whereas during NT, the tide was already receding. The difference in cell abundance between the two tides indicates that the entry of seawater regulates the population at the estuary mouth. However, the role of other factors such as nutrients and grazing, which were not monitored in the present study, cannot be overlooked. The higher abundance in freshwater during both the tides are probably represented by different strains having its origin from the freshwaters. The occurrence of *PRO*-like cells and *SYN*-PE groups along the salinity gradient may indicate presence of different strains which have specific salinity thresholds. This aspect should be confirmed through experimental studies on pure cultures in order to understand their physiology. The average contribution of PP to the total photosynthetic biomass was close to the values reported for other estuaries (Gaulke et al., 2010). However, unlike other estuaries, PP contribution was generally high when the total biomass was low. Similar results have been reported from the monsoonal Arabian Sea (Goericke, 2002) where diatoms and PP dominated the phytoplankton biomass at high and low concentrations of total chl *a*, respectively.

Acknowledgments

The authors are grateful to Dr. Satish Shetye, Director, National Institute of Oceanography for his support and encouragement. We are thankful to the three anonymous reviewers for their valuable suggestions. This is NIO contribution No. 5179.

Appendix A. Supporting information

Supplementary data associated with this article can be found, in the online version, at doi:10.1016/j.ecss.2012.05.002.

References

Baudoux, A.C., Veldhuis, M.J.W., Witte, H.J., Brussaard, P.D., 2007. Viruses as mortality agents of picophytoplankton in the deep chlorophyll maximum layer during IRONAGES III. Limnology and Oceanography 52, 2519–2529.

Campbell, L., Landry, M.R., Constantinou, J., Nolla, H.A., Brown, S.L., Liu, H., Caron, D.A., 1998. Response of microbial community structure to environmental forcing in the Arabian Sea. Deep Sea Research 45, 2301–2325.

Chisholm, S.W., Olson, R.J., Zettler, E.R., Goericke, R., Waterbury, J.B., Welschmeyer, N.A., 1988. A novel free-living prochlorophyte abundance in the oceanic euphotic zone. Nature 334, 340–343.

Gallegos, C.L., 2001. A two-year time series of continuously monitored inherent optical properties in a eutrophic sub-estuary of Chesapeake Bay. Estuarine Coastal Shelf Science 64, 156–170.

Gaulke, A.K., Wetz, M.S., Paerl, H.W., 2010. Picophytoplankton: a major contributor to planktonic biomass and primary production in a eutrophic, river-dominated estuary. Estuarine Coastal Shelf Science 90, 45–54.

Goericke, R., 2002. Top-down control of phytoplankton biomass and community structure in the monsoonal Arabian Sea. Limnology and Oceanography 47, 1307–1323.

Haas, L.W., Pearl, H.W., 1988. The roles of blue-green algae. In: McCoy, S.E. (Ed.), Chesapeake Bay. NOAA Estuary-of-the-Month Seminar Series No. 5. National Oceanic and Atmospheric Administration Estuarine Programs Office, Washington, D.C., pp. 99–113.

Jochem, F.J., 2003. Photo- and heterotrophic pico- and nanoplankton in the Mississippi River plume: distribution and grazing activity. Journal of Plankton Research 25, 1201–1214.

Knefelkamp, B., Carstens, K., Wiltshire, K.H., 2007. Comparison of different filter types on *chlorophyll-a* retention and nutrient measurements. Journal of Experimental Marine Biology and Ecology 345, 61–70.

Mitbavkar, S., Saino, T., Horimoto, N., Kanda, J., Ishimaru, I., 2009. Role of environment and hydrography in determining the picoplankton community structure of Sagami Bay, Japan. Journal of Oceanography 65, 195–208.

Morán, X.A.G., 2007. Annual cycle of picophytoplankton photosynthesis and growth rates in a temperate coastal ecosystem: a major contribution to carbon fluxes. Aquatic Microbial Ecology 49, 267–279.

Murrell, M.C., Lores, E.M., 2004. Phytoplankton and zooplankton seasonal dynamics in a subtropical estuary: importance of cyanobacteria. Journal of Plankton Research 26, 371–382.

Pan, L.A., Zhang, L.H., Zhang, J., Gasol, J.M., Chao, M., 2005. On-board flow cytometric observation of picoplankton community structure in the East China Sea during the fall of different years. FEMS Microbiology Ecology 52, 243–253.

Parsons, T.R., Maita, Y., Lalli, C.M., 1984. A Manual of Chemical and Biological Seawater Analysis. Pergamon, New York.

Partensky, F., Hess, W.R., Vaulot, D., 1999. *Prochlorococcus*, a marine photosynthetic prokaryote of global significance. Microbiology and Molecular Biology Reviews 63, 106–127.

Patil, J.S., Anil, A.C., 2008. Temporal variation of diatom benthic propagules in a monsoon-influenced tropical estuary. Continental Shelf Research 28, 2404–2416.

Qasim, S.Z., Sen Gupta, R., 1981. Environmental characteristics of the Mandovi-Zuari estuarine system in Goa. Estuarine, Coastal and Shelf Science 13, 557–578.

Richardson, T.L., Jackson, G.A., 2007. Small phytoplankton and carbon export from the surface ocean. Science 315, 838–840.

Roy, R., Prathihary, A., Mangesh, G., Naqvi, S.W.A., 2006. Spatial variation of phytoplankton pigments along the southwest coast of India. Estuarine, Coastal and Shelf Science 69, 189–195.

Shang, X., Zhang, L.H., Zhang, J., 2007. Prochlorococcus-like populations detected by flow cytometry in the fresh and brackish waters of the Changjiang estuary. Journal of the Marine Biological Association, UK 87, 643–648.

Shetye, S.R., 1999. Propagation of tides in the Mandovi and Zuari estuaries. Sadhana 24 (Parts 1 & 2), 5–16. February & April 1999, India.

Shetye, S.R., Gouveia, A.D., Singbal, S.Y., Naik, C.G., Sundar, D., Michael, G.S., Nampoothiri, G., 1995. Propagation of tides in the Mandovi-Zuari estuarine network. Proceedings of the Indian Academy of Sciences 104, 682.

Shimada, A., Nishijima, M., Maruyama, T., 1995. Seasonal appearance of *Prochlorococcus* in Suruga bay, Japan in 1992–1993. Journal of Oceanography 51, 289–300.

Sundar, D., Shetye, S.R., 2005. Tides in the Mandovi and Zuari estuaries, Goa, west coast of India. Journal of Earth System Science 114, 493–503.

Vaulot, D., Partensky, F., Neveux, J., Mantoura, R.F.C., Llewellyn, C.A., 1990. Winter presence of prochlorophytes in surface waters of the northwestern Mediterranean Sea. Limnology and Oceanography 35, 1156–1164.

Waterbury, J.B., Watson, S.W., Valois, F.W., Franks, D.G., 1986. Biological and ecological characterization of the marine unicellular cyanobacterium *Synechococcus*. In: Platt, T., Li, W.K. (Eds.), Photosynthetic Picoplankton. Canadian Journal of Fisheries and Aquatic Sciences. Department of Fisheries and Oceans, Ottawa, pp. 71–120.

Wilson, S.E., Steinberg, D.K., 2010. Autotrophic picoplankton in mesozooplankton guts: evidence of aggregate feeding in the mesopelagic zone and export of small phytoplankton. Marine Ecology Progress Series 412, 11–27.

Worden, A.Z., Nolan, J.K., Palenik, B., 2004. Assessing the dynamics and ecology of marine picophytoplankton: the importance of the eukaryotic component. Limnology and Oceanography 49, 168–179.

Marine Environmental Research 92 (2013) 133–143

Contents lists available at ScienceDirect

Marine Environmental Research

journal homepage: www.elsevier.com/locate/marenvrev

Factors controlling the temporal and spatial variations in *Synechococcus* abundance in a monsoonal estuary

Rajaneesh K.M., Smita Mitbavkar*

CSIR-National Institute of Oceanography, Dona Paula, Goa 403 004, India

ARTICLE INFO

Article history:
Received 19 June 2013
Received in revised form
10 September 2013
Accepted 12 September 2013

Keywords:
Estuaries
Monsoon
Picophytoplankton
Salinity
Zuari estuary
Synechococcus

ABSTRACT

Temporal and spatial variations in *Synechococcus* abundance were investigated over an annual cycle (February'10–January'11) along a salinity gradient (0–35) in the tropical Zuari estuary, influenced by south-west monsoons. *Synechococcus* exhibited salinity preferences with phycoerythrin-rich cells at salinities >2 (*Synechococcus*-PEI), >20 (*Synechococcus*-PEII) and <1 (*Synechococcus*-PEIII) whereas phycocyanin-rich (*Synechococcus*-PC) dominant at lower salinities. Downstream stratification during monsoon caused *Synechococcus* group segregation in the surface and near-bottom waters. During monsoon-break and non-monsoon period stabilized waters, increased salinity, temperature, solar radiation and low rainfall favored high *Synechococcus* abundance whereas unstable waters, increased turbidity and low solar radiation during active monsoon lowered abundance. *SYN*-PC positively co-related with nitrate and phosphate and *SYN*-PEI with phosphate. *Synechococcus* contribution to phytoplankton carbon biomass ranged from 9 to 29%. In monsoonal estuaries, rainfall intensity regulates freshwater runoff which modulates the estuarine environment, creating temporal–spatial niche segregation of *Synechococcus* groups thereby serving as indicator organisms of the estuarine hydrodynamics.

1. Introduction

Picophytoplankton (PP; <3 μm) have been recognized as significant contributors to the total phytoplankton biomass and primary production in marine (Platt et al., 1983) and freshwater ecosystems (Paerl, 1977). PP comprises two major groups of cyanobacteria, *Prochlorococcus* and *Synechococcus* (*SYN*) and small eukaryotes known as picoeukaryotes. *Prochlorococcus* is abundant in oligotrophic waters whereas picoeukaryotes are abundant in coastal waters. *SYN* proliferates in well-lit, eutrophic coastal ecosystems (Jochem, 1988) and are present in comparatively lower numbers in oligotrophic open ocean waters at temperatures ranging from 2 °C to 30 °C from tropic, subtropic, temperate and Polar Regions (Partensky et al., 1999). Based on phycobilisome composition, two groups of *SYN* have been identified in estuarine ecosystems; one rich in phycoerythrin (PE) and the other in phycocyanin (PC). These studies revealed that PE rich *SYN* dominates higher saline waters whereas PC rich *SYN* are abundant in lower saline waters (Murrell and Lores, 2004). Sub-groups of PE rich *SYN* were also detected in the Mississippi river plume (Liu et al., 2004), Pearl River estuary (Lin et al., 2010) and the Zuari estuary (Mitbavkar et al., 2012) implying the importance of salinity on the distribution of the *SYN* groups. PP plays an important role in the microbial loop by forming the base of food chain and serving as food for many protists and small invertebrates species (Azam, 1983; Pomeroy, 1974). This carbon transfer through microbial food web creates the important connection between PP and higher trophic levels (Chiang et al., 2013). Studies on PP are well established in the Pacific and Atlantic Oceans whereas comparatively in the Indian Ocean only a few observations have been made (Brown et al., 1999; Campbell et al., 1998). Apart from the open ocean, the importance of PP in coastal regions is now being highlighted (Mitbavkar et al., 2012; Murrell and Lores, 2004).

Estuaries are one of the most productive natural habitats in the world which show wide variation of hydrological characteristics depending on the inputs from upstream rivers. The excess amount of nutrients available in estuarine ecosystems favor the rapid growth of phytoplankton (Madhu et al., 2009; Qiu et al., 2010). Several studies on phytoplankton and PP have been conducted in estuarine region encompassing brackish water to seawater with a wide salinity range (2–35). These studies suggest that salinity plays an important role in the spatial distribution of PP groups (Murrell and Lores, 2004; Ray et al., 1989) and also highlights that PP are

* Corresponding author. Tel.: +91 832 2450376; fax: +91 832 2450615.
E-mail address: mitbavkars@nio.org (S. Mitbavkar).

0141-1136/$ – see front matter © 2013 Elsevier Ltd. All rights reserved.
http://dx.doi.org/10.1016/j.marenvres.2013.09.010

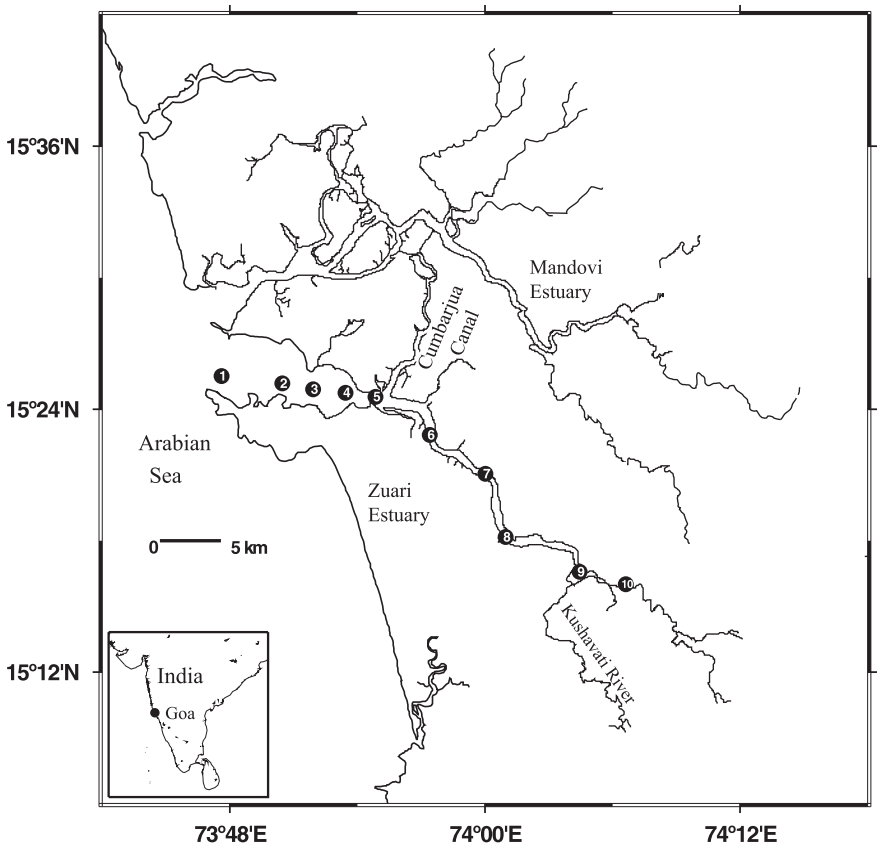

Fig. 1. Location of the study area.

the major component of the phytoplankton community contributing substantially to the total biomass and primary production in estuarine region of subtropical (Sin et al., 2000) and temperate estuaries (Ning et al., 2000). In tropical estuarine regions studies have mostly focused on larger phytoplankton wherein hydrology and nutrients were indicated as the major dynamic factors influencing the phytoplankton biomass and composition (Costa et al., 2009). However, there are few studies on PP especially *SYN* distribution in tropical and subtropical estuarine and coastal environments (Lin et al., 2010; Qiu et al., 2010).

In the tropics, estuaries influenced by monsoons support productive fisheries, which in turn are sustained via a healthy food chain supported by a strong foundation, the phytoplankton. There are few studies conducted on PP in monsoonal estuaries. These findings showed that increase in freshwater discharge influences the PP growth (Lin et al., 2010; Qiu et al., 2010). Such areas serve as good model ecosystems for studying the dynamics of PP on temporal and spatial scales. For the first time we have studied the distribution of this organism in a monsoonal estuary where the tides and freshwater runoff regulate the hydrodynamics on an annual scale and also where short spells of breaks in monsoon are experienced during the monsoon season. The aim of the present study was to assess whether the distribution of *SYN*, the most dominant PP group, is determined by the temporal and spatial variations in environmental factors regulated by the freshwater runoff. We hypothesize that *SYN* population structure is influenced by both, the temporal and spatial variations in environmental factors, with low abundance during monsoon and dominance of different groups along the salinity gradient. As such *SYN* groups can serve as indicator organisms in estuarine regions depicting the hydrodynamics across the estuary.

2. Materials and methods

2.1. Study area

Sampling was carried out in the Zuari estuary (Goa) located along the central west coast of India (Fig. 1, Table 1). It is one of the major estuaries of Goa and important for agriculture, fisheries and transportation of mines (iron and manganese ore). It originates at Hemad-Barshen in the Western Ghats and flows up to Arabian Sea with a length of 65 km. It's cross sectional area decreases from the mouth to head. This location experiences three seasons: the pre-monsoon (PrM; February –May), the southwest monsoon (MON; June–September) and the post-monsoon (PoM; October–January). During the study period, a total of 3723.5 mm rainfall was recorded which was relatively higher than that in previous years (Indian Meteorological Department). Out of that, ~92% of precipitation

Table 1
Details of sampling stations in the Zuari estuary.

Station no.	Station name	Latitude	Longitude	Distance from mouth (km)	Approximate depth (m)
1	Marmugao	15° 25′ 16.9″	73° 47′ 36.9″	0	16
2	Chicalim	15° 25′ 8.5″	73° 47′ 22.4″	5.8	5
3	Island	15° 25′ 57.4″	73° 47′ 57.0″	8.6	5
4	Sancoale	15° 25′ 45.1″	73° 47′ 30.6″	11	7.1
5	Cortalim	15° 25′ 32.0″	73° 47′ 50.2″	13	9.6
6	Loutulim	15° 25′ 54.0″	73° 47′ 24.4″	19.7	10.5
7	Borim	15° 25′ 03.6″	73° 47′ 58.0″	23.9	12.9
8	Shiroda	15° 25′ 12.3″	73° 47′ 55.5″	31.4	9.1
9	Kushavati	15° 25′ 31.7″	73° 47′ 28.3″	38.4	9.9
10	Sanvordem	15° 25′ 01.1″	73° 47′ 36.0″	42.2	4.9

occurred during the southwest MON. Consequently during MON, the main channel receives huge amounts of riverine freshwater through Kushavathi, Sanguem Rivers and small streams at many points along its length. This creates a river runoff exceeding 400 $m^3 s^{-1}$ whereas rest of the year freshwater runoff is <10 $m^3 s^{-1}$ (Shetye and Murty, 1987). Tides occur in this estuary up to a distance of about 50 km and the increase in the elevation of the estuarine channel prevents tides from propagating beyond this distance (Shetye, 1999). Average depth of this estuary is ~5 m with the catchment area of 550 km^2. Tides are semidiurnal, with the highest height of 2.3 m during spring tide and ~1 m during neap tide (Manoj and Unnikrishnan, 2009). Cumbarjua canal, which is at about 11 km distance from the mouth of the estuary, connects the Zuari estuary to the adjacent Mandovi estuary and is also involved in the regulation of the water flow (Qasim and Sen Gupta, 1981).

2.2. Sampling

Monthly sampling was carried out in the Zuari estuary from February 2010 to January 2011 (Table 1). Surface and near-bottom water (NBW) samples were collected from 10 stations with a Niskin sampler (Fig. 1). Vertical profiles of temperature and salinity were determined using portable seabird CTD (SBE 19 plus). Water transparency was measured with a secchi disk (SD). Rainfall data for the study period were acquired from the Indian Meteorological Department (IMD) (Table 2). Chlorophyll *a* (chl *a*) was measured following standard methods (Parsons et al., 1984). Nutrients (nitrate (NO_3–N), phosphate (PO_4–P), nitrite (NO_2–N) and silicate (SiO_4)) were analyzed by SKALAR SAN^{plus} ANALYSER. For PP, seawater samples were preserved with paraformaldehyde (0.2% final concentration), quick frozen in liquid nitrogen and stored at −80 °C until analysis.

2.3. Flow cytometric analysis of Synechococcus

Prior to analysis, frozen samples were thawed and then analyzed by a flow cytometer (FACS Aria II) equipped with blue (488 nm) and red (630 nm) lasers. Forward angle light scatter (FALS), right angle light scatter (RALS), red fluorescence from chlorophyll (>650 nm) and phycocyanin (630 nm) and orange fluorescence from phycoerythrin (564–606 nm) were recorded from each particle after excitation by lasers. Data obtained was processed with the BD FacsDiva (Version 6.2) software. The different *SYN* groups present in the sample could be discriminated according to their specific fluorescence and scattering properties. Yellow green latex beads of 2 μm (polysciences co., USA) were added to the sample as internal standards to calibrate cell fluorescence emission and light scatter signals, which allowed comparison of fluorescence and cell size among different samples. Based on flow cytometric signatures, two groups of *SYN* were distinguished: one rich in phycoerythrin (*SYN*-PE) and the other in phycocyanin (*SYN*-PC) throughout the study period. RALS and FALS (proxy for cell size) signals revealed that the cell size of *SYN*-PC is bigger than *SYN*-PE whereas chlorophyll fluorescence is comparable with *SYN*-PE (Fig. 2). The *SYN*-PE group was further differentiated into 2 subgroups based on the phycoerythrin fluorescence intensity and was designated as *SYN*-PEI which had a lower fluorescence intensity and *SYN*-PEII with a comparatively higher fluorescence intensity. Another group of *SYN*-PE whose flow cytometric signatures were similar to *SYN*-PEI but which was found only in freshwater was designated as *SYN*-PEIII.

Table 2
Rainfall data for the sampling days.

Sr no.	Sampling dates	Rainfall (mm)
1	29-Jan-10	0
2	03-Mar-10	0
3	01-Apr-10	0
4	29-Apr-10	0
5	27-Jun-10	57.8
6	13-Jul-10	0.2
7	11-Aug-10	51.7
8	17-Sep-10	69.8
9	23-Oct-10	55.4
10	06-Nov-10	3
11	06-Dec-10	0
12	10-Jan-11	0

2.4. Carbon biomass estimation

Phytoplankton carbon biomass was derived from chl *a* using a carbon to chlorophyll ratio of 40 (Gallegos, 2001). Choice of this value was based on the fact that the dominant species of diatoms in our study area (Patil and Anil, 2011) were similar to that found in Chesapeake Bay (Marshall et al., 2009).

For calculating the *SYN* carbon biomass, initially RALS data was converted to cell diameter as explained by Worden et al. (2004). Subsequently, the cell diameter was used to estimate the biovolume using the equation, $V = \pi/6\ (d^3)$, assuming *SYN* cells to be spherical. Factors for different *SYN* groups were derived from the biovolume to carbon conversion factor of 254 fg C μm^{-3} (Baudoux et al., 2007). From these estimates, the percentage contribution of *SYN* to the total phytoplankton carbon biomass was calculated.

2.5. Data analysis

Three-way analysis of variance (ANOVA) was used to assess the significant temporal and spatial variations in cell abundance ($\log(x+1)$) of the *SYN* groups. Principal component analysis (PCA) was performed for the environmental data to identify the key factors which influence the *SYN* groups. Principal components (PC's) having eigenvalues greater than 1 were considered for further analysis. Stepwise multiple linear regression analyses were performed between factor scores of PC's and cell abundance ($\log(x+1)$) of different *SYN* groups to evaluate the possible factors that affect the *SYN* abundance. Above statistical analysis was performed using SPSS statistics 16.0 with the significance level of 0.05. Statistica 8 software was used to find the significance among environmental factors, *SYN* carbon biomass (%), phytoplankton carbon biomass and *SYN*-PC: *SYN*-PE.

3. Results

3.1. Environmental parameters

During PrM, surface water temperature was ~27 °C in February and increased gradually to 33 °C in May. Correspondingly, seawater intrusion towards the upstream also increased during this period (Fig. 3g and h). After onset of MON (June), a drop in surface water temperature (<28 °C) and salinity (<21) was observed. During MON the estuary was stratified downstream, with strong stratification in August up to S5 (Fig. 3i and j). In July, when rainfall was low, rise in temperature (29 °C) and salinity (26) was detected at S1. During PoM, temperature was low (<27 °C) (Fig. 3e and f). In October the estuary was stratified as a result of continuing rainfall until November (Table 2). Subsequently (December and January) salinity started increasing as a consequence of cessation in rainfall. There was not much difference in temperature and salinity between surface and NBW during PrM and PoM (except in October). The seasonal trend of chl *a* concentration (surface and NBW) was

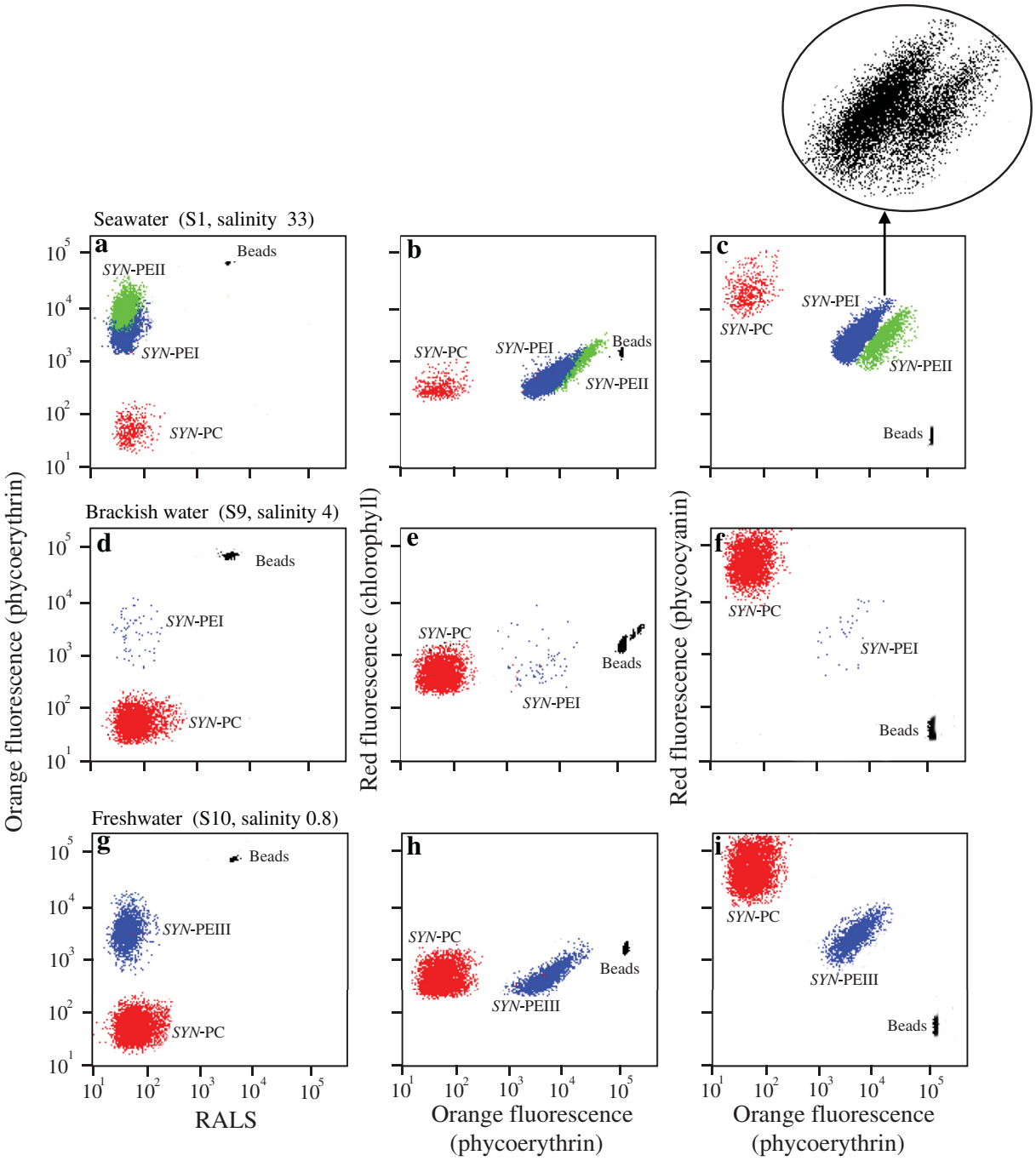

Fig. 2. Flow cytometric analysis of (a–c) seawater, (d–f) brackish water, and (g–i) freshwater samples from the Zuari estuary.

PrM < PoM < MON. During PrM, chl *a* concentration increased along the transect with highest value upstream (3.03 μg l^{-1}). During MON the trend was reversed with highest value downstream (<12 μg l^{-1}). Chl *a* concentration was higher in surface waters in August as compared to NBW whereas the reverse was observed in September (Fig. 3o and p). Chl *a* concentration peaked in January and November with slightly lower concentration in NBW (Fig. 3q and r). During MON, nitrate (22–37.71 μM) and phosphate (3–7.48 μM) concentrations were high. Nitrate concentration showed a decreasing trend from mouth to head of the estuary with higher values at surface than that in the NBW whereas phosphate showed an opposite trend (Fig. 4c, d, i and j). Nitrate and phosphate peaked in May (13.32 μM) and April (4.78 μM). During rest of the months, concentrations in surface and NBW were low (Fig. 4a–i). Nitrite concentration was high in April and May at S6 (Fig. 4m and n) and lowest during MON (Fig. 4o and p). Silicate concentrations showed an increasing trend from downstream to upstream of the estuary except during MON season (Fig. 4s–x). Silicate concentrations were highest in September (44.54–155.29 μM).

3.2. Temporal and spatial variation of Synechococcus

Cell abundance of all *SYN* groups showed distinct temporal variations. Three-way ANOVA indicated significant monthly ($p < 0.001$) and spatial ($p < 0.01$) variations in all *SYN* groups whereas vertical variation was not significant within the stations.

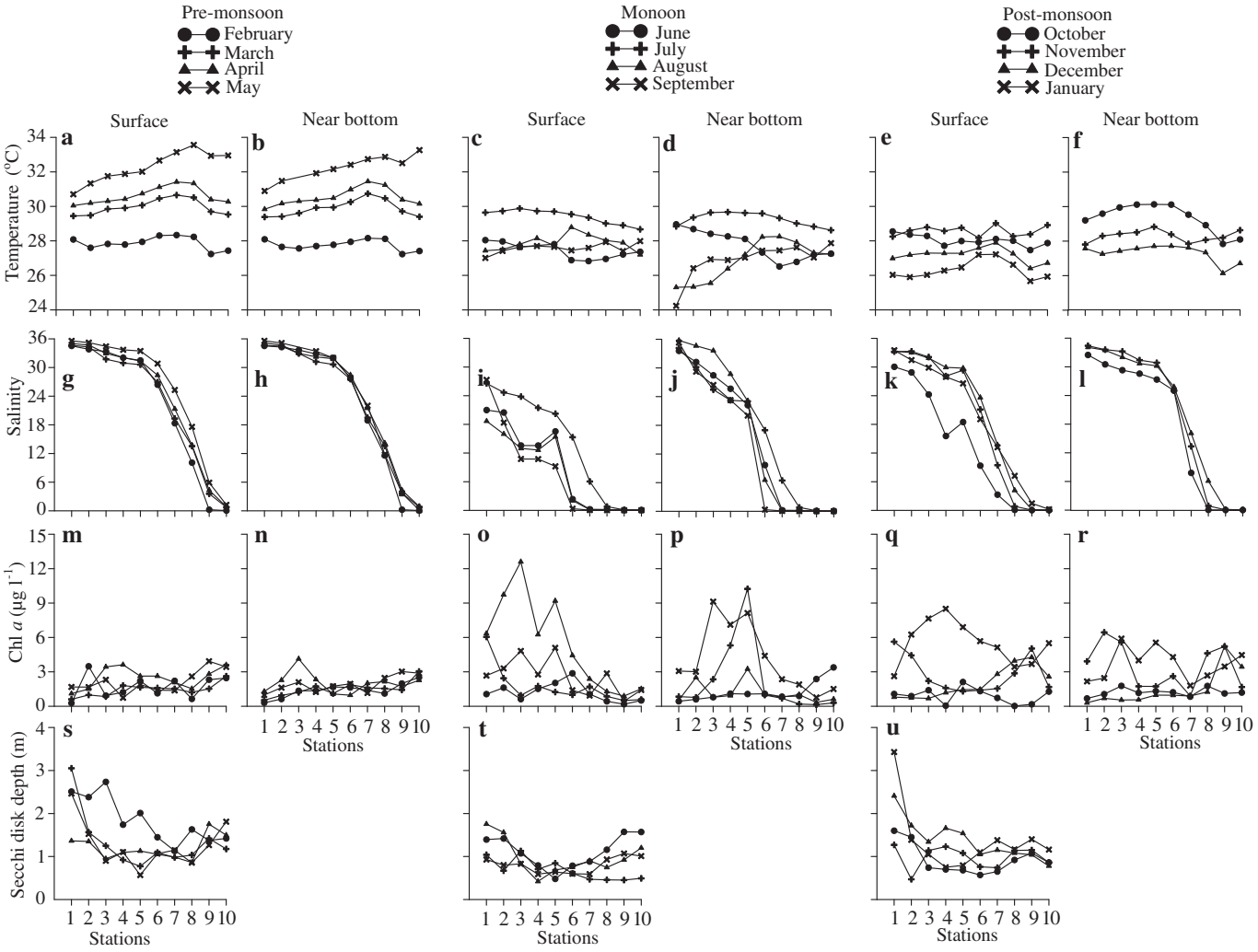

Fig. 3. Temporal and spatial variations in (a–f) temperature, (g–l) salinity, (m–r) chlorophyll *a* concentrations and (s–u) secchi disk depth in the Zuari estuary.

SYN-PEI abundance in the surface and NBW was highest in February at the mouth of the estuary (0.97×10^5 cells ml^{-1}) and reduced further upstream. Cell abundance reduced from March to May with a peak at S8 (Fig. 5a and b). It declined further by an order of magnitude after onset of MON (June) in surface and NBW and increased in July up to S5 (Fig. 5c and d). Subsequently, abundance decreased in August and increased in September (Fig. 5c and d). At the beginning of the PoM (October), abundance was high up to S5 with higher abundance in the NBW (Fig. 5e and f). From November to January, cell abundance was low ($<0.25 \times 10^5$ cells ml^{-1}). *SYN*-PEII showed a decreasing trend from mouth to middle of the estuary where salinity was >20. Monthly variation was very similar to *SYN*-PEI with lower abundance except during PoM (Fig. 5g–l). During PoM, cell abundance at the mouth of the estuary was $\sim 0.5 \times 10^5$ cells ml^{-1} (surface and NBW), which was higher than *SYN*-PEI abundance. During Mon, NBW cell abundance was higher than that at the surface. *SYN*-PEIII was observed at the upstream end (S9 and S10) during PrM (Fig. 5m and n). After the onset of MON, abundance declined in surface and NBW and it was observed from middle of the estuary where salinity was <0.5. Low (surface and NBW; $<0.07 \times 10^5$ cells ml^{-1}) abundance during MON, continued in the PoM season (October) (Fig. 5o and p). From November, abundance started increasing ($>0.13 \times 10^5$ cells ml^{-1}). *SYN*-PC showed an increasing trend from mouth to head of the estuary in surface and NBW. Abundance was high during PrM with highest abundance recorded in the NBW of S10 (1×10^5 cells ml^{-1}) in May. With the onset of MON, cell abundance declined (Fig. 5u and v) and later increased in July ($\sim 0.34 \times 10^5$ cells ml^{-1}) in the middle of the estuary in surface and NBW. In August, it increased (0.39×10^5 cells ml^{-1}) at the estuary mouth (surface) with a decreasing trend upstream whereas in the NBW abundance was low. During PoM, distribution trend was similar to PrM with comparatively lower abundance in surface and NBW (5w and x).

3.3. Influence of environmental factors on Synechococcus

The total *SYN* abundance showed a significant positive correlation with temperature (Fig. 6a). When plotted against salinity, *SYN*-PE and *SYN*-PC distribution showed a clear spatial pattern (Fig. 6b) wherein PC cells were abundant in the low saline waters whereas the PE cells were abundant in the high saline waters. The seasonal cycle of salinity also influenced *SYN* abundance in the Zuari estuary. During PrM, total *SYN* abundance showed a significant negative correlation ($r = -0.301$, $p < 0.001$) with salinity which was reversed during MON ($r = 0.568$, $p < 0.001$) and PoM ($r = 0.256$, $p < 0.05$). PCA displayed three factors in PrM and MON and four in PoM, which explained 68%, 64% and 87% of the variations of the environmental factors, respectively. During PrM, PC1 was highly loaded

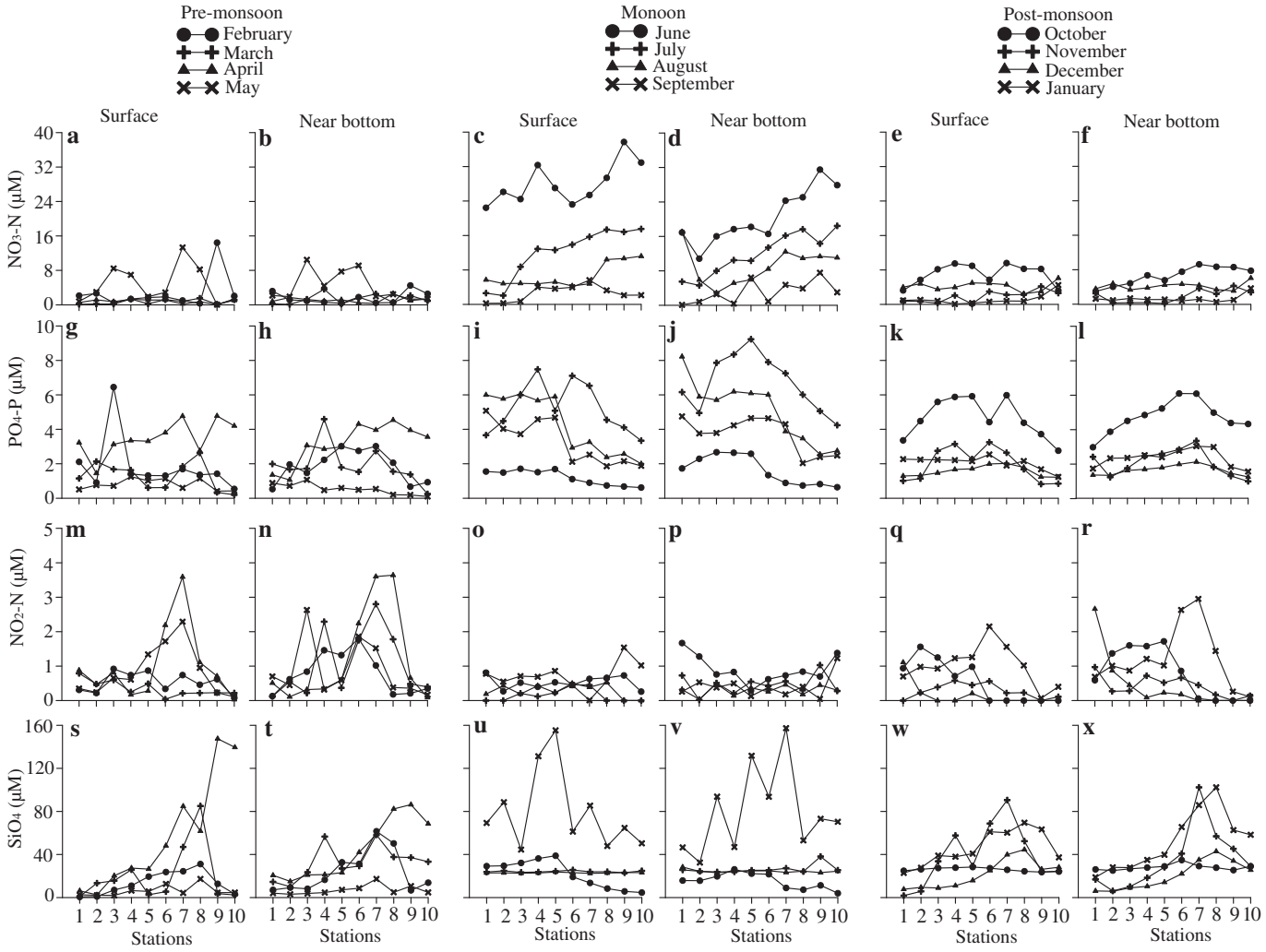

Fig. 4. Temporal and spatial variations in nutrient concentrations. (a–f) Nitrate, (g–l) phosphate, (m–r) nitrite and (s–x) silicate concentrations.

with phosphate, silicate and nitrite (Table 3). A strong load of salinity was detected in PC3. Stepwise multiple regression analysis showed that all *SYN* groups were significantly correlated with PC1 ($p < 0.05$) and PC3 ($p < 0.01$), which also included chl *a* whereas only *SYN*-PC correlated with PC2 (Table 4). During MON, *SYN* groups and chl *a* were strongly associated with PC1 where phosphate and salinity were highly loaded. *SYN*-PEIII and chl *a* were negatively related to PC2. PC3 was loaded with light (0.63) and nitrite (−0.74) where *SYN*-PC was positively correlated. Like PrM, all *SYN* groups were significantly correlated to salinity which was associated with PC2 along with nitrite during PoM (Tables 3 and 4). *SYN*-PC alone showed positive relation to PC1 where nitrate and phosphate were strongly loaded. None of the *SYN* groups showed correlation to PC3 which included temperature (0.75) and light (−0.90). Chl *a* indicated positive correlation to PC4 (Table 4).

3.4. Contribution of Synechococcus to total phytoplankton carbon biomass

Phytoplankton carbon biomass along the estuary varied from 50 to 127 µg C l^{-1} with higher carbon biomass (127 µg C l^{-1}) up to S5 at the surface (Fig. 7a and b). In the NBW, it was lower compared to that at the surface at the mouth of the estuary. *SYN* carbon contribution (%) to the total phytoplankton carbon biomass varied from 9 to 29% (surface and NBW; Fig. 7c and d). *SYN* contributed more to the total carbon at S8 and downstream end of the estuary. Compared to surface, NBW contribution was higher downstream. *SYN*-PEI (~13%) and *SYN*-PEII (~16%) groups contributed higher downstream. Their contribution was slightly higher in the NBW as compared to that in the surface. *SYN*-PC contributed higher (~17%) upstream (surface and NBW). *SYN*-PEIII contributed (~4%) only at the upstream (surface and NBW) end of the estuary. Significant negative correlation was observed between phytoplankton carbon biomass and total *SYN* carbon contribution in the estuary (Fig. 8a). Total *SYN* carbon contribution showed a significant positive correlation with salinity and phosphate (Fig. 8b and c).

4. Discussion

In the Zuari estuary, the annual variations in hydrodynamics were mainly controlled by the river runoff and tides during MON and tidal activity during non-MON periods (Qasim and Sen Gupta, 1981; Shetye and Murty, 1987). As a result, during dry season the estuary is vertically homogenous whereas during wet season it is stratified (Qasim and Sen Gupta, 1981; Shetye and Murty, 1987). Monsoonal influence can be such that the entire estuary is dominated by low saline waters as was observed in August (salinity 11). Similar observations have been reported from the

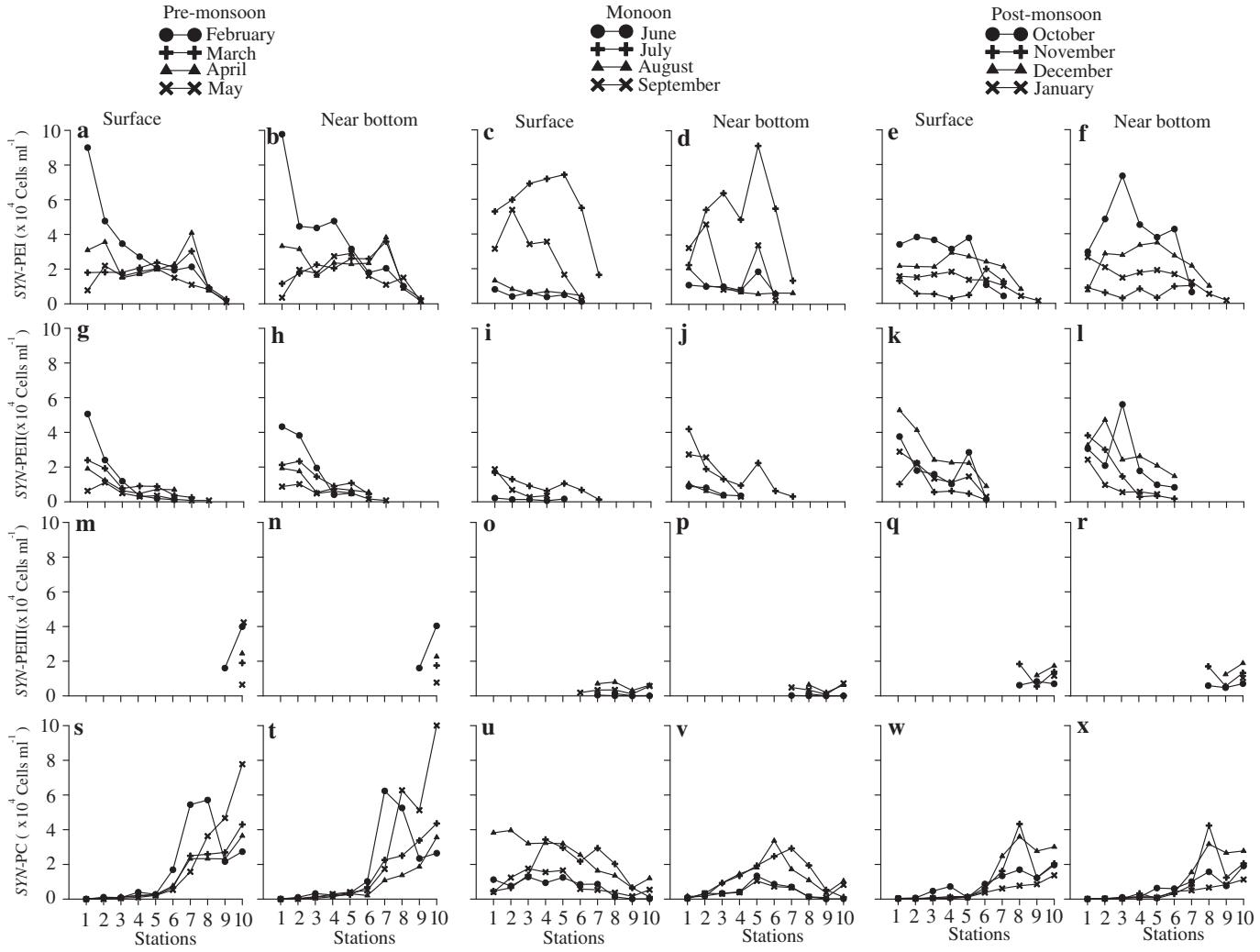

Fig. 5. Temporal and spatial variations in distribution of *Synechococcus* groups. (a–f) *SYN*-PEI, (g–l) *SYN*-PEII, (m–r) *SYN*-PEIII and (s–x) *SYN*-PC.

Mandovi estuary (salinity 0), which is adjacent to the Zuari estuary (Vijith et al., 2009). However, active and break phases in rainfall also brings weekly variations in water chemistry (Qasim and Sen Gupta, 1981).

4.1. Spatial variations of SYN distribution

Variations in salinity throughout the estuary were reflected in the distribution of *SYN* groups. Transition in dominance from PC-rich to PE-rich *SYN* at salinities of ~20–25 found in this study is consistent with the studies carried out in subtropical estuaries such as Pensacola Bay (Murrell and Lores, 2004), lower Chesapeake Bay (Ray et al., 1989) and Pearl river estuary (Zhang et al., 2013). This illustrates that salinity plays a key role in the spatial distribution of *SYN* along this monsoon influenced tropical estuary. To support this, in the present study PC's which strongly associated with salinity showed a significant correlation to all the *SYN* groups.

Vertical variation of *SYN* abundance was not significant in the present study as was observed for the Pearl River (Lin et al., 2010) where depth was comparatively higher (<60 m) than the Zuari estuary (Table 1). However, during MON at the estuary mouth high abundance of *SYN*-PEII in the NBW and *SYN*-PC in surface compared to that at surface and NBW respectively indicates that increased river runoff resulting in stratification of the water column influenced the distribution of these groups. Similarly, the higher abundance of *SYN*-PEI in NBW and *SYN*-PC in surface waters during early PoM (October) also shows the influence of rainfall and the resultant freshwater runoff. Presence of *SYN*-PC throughout the estuary even during dry season when there is no possibility of its influx from freshwater suggests that these groups are halotolerant and they can survive at high salinities. However, their comparatively lower abundance downstream implies that their growth rates are affected at higher salinities. Waterbury et al. (1986) reported that *SYN*-PE cells have an obligate requirement for elevated concentrations of ions while marine *SYN* isolates that lack PE are halotolerant and grows equally well in the seawater or freshwater. The presence of *SYN*-PE up to the upstream end could be facilitated by the tidal entry of seawater. *SYN*-PEI and *SYN*-PEII observed at higher salinities were also previously reported from North western Arabian coast, Mississippi river plume and the Pearl River estuary (Lin et al., 2010; Liu et al., 1998, 2004). The high PE intensity *SYN* strain is considered as characteristic of oceanic waters (*SYN*-PEII) and other strain (*SYN*-PEI) represents the coastal waters (Campbell et al., 1998). This suggests a possibility of the *SYN*-PEII influx from offshore waters into the estuary. Increased *SYN* PEIII abundance in freshwater suggests that this could be a freshwater adapted strain. Different *SYN* strains have been reported in a variety of freshwater systems based on their pigment characteristics (Callieri, 1996).

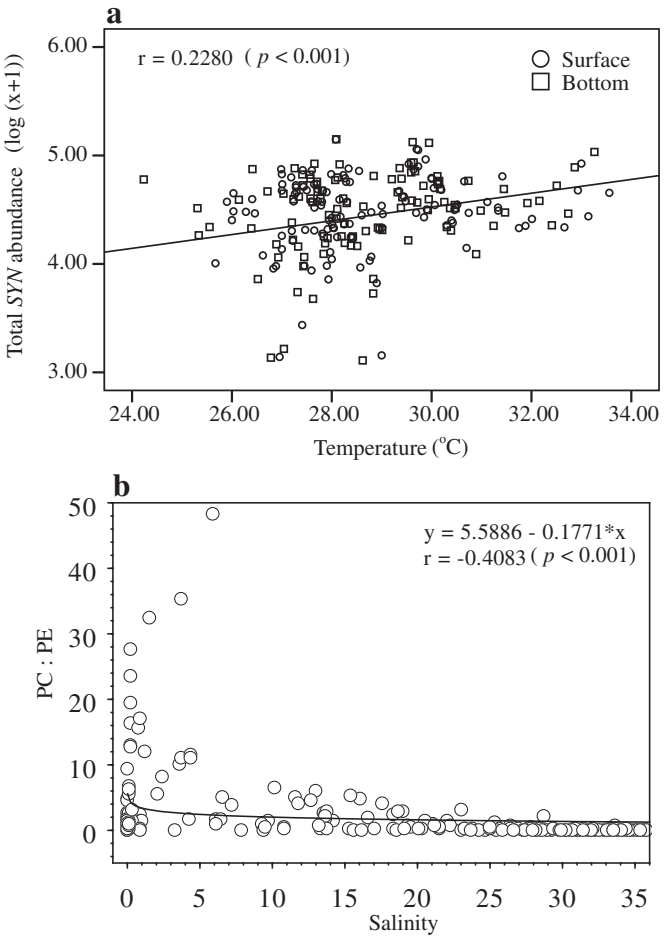

Fig. 6. Relationship between (a) total *SYN* abundance and temperature and (b) PC: PE rich *SYN* and salinity in the Zuari estuary. The curve was fitted under the logarithmic equation model.

4.2. Temporal variation of SYN groups

Total *SYN* abundance range in the present study was comparable to previous report for the same estuary (Mitbavkar et al., 2012) and higher than that reported for the other tropical coastal waters (Agawin et al., 2003). However, it was 1–2 magnitudes lower than that reported for subtropical estuaries like Florida Bay (Phlips et al., 1999), Chesapeake Bay (Wang et al., 2011) and Pensacola Bay (Marshall and Nesius, 1996; Murrell and Lores, 2004). While in Chesapeake Bay *SYN* cell abundance often exceeds 10^6 cells ml^{-1}, in a temperate estuary it ranged from 10^2 to 10^5 cells ml^{-1} (Agawin et al., 1998; Ning et al., 2000). The seasonal cycle of the *SYN* population differed from that in subtropical and temperate coastal and estuarine regions which can be attributed to the influence of South West monsoon that creates a seasonal cycle of hydrodynamics that varies from other latitudinal regions.

Several studies have established temperature as the key factor influencing the seasonal dynamics of *SYN* in tropics to temperate estuaries such as Chesapeake Bay (Ray et al., 1989; Wang et al., 2011), Pearl River (Qiu et al., 2010), Pensacola Bay (Murrell and Lores, 2004), Francisco Bay (Ning et al., 2000), Blanes Bay (Agawin et al., 1998), Western Pacific coast (Tsai et al., 2008) and Sagami Bay (Mitbavkar et al., 2009). These studies showed that warm period is favorable for *SYN* spp. Similarly, in the present study the total *SYN* abundance showed significant positive correlation with temperature (Fig. 6a), although a narrow temperature range exists (24–32 °C) throughout the year as compared to that in the subtropical (10–30 °C) and temperate estuaries (10–24 °C). The optimum temperature range of 27–30 °C was found to be favorable for *SYN* in the present study. Variations in the spatial distribution of salinity during the three seasons were reflected in the temporal distribution of *SYN*-PC which showed a negative relation with salinity as expected during the PrM and PoM but during MON it showed a positive relation because of the comparatively lower salinity downstream resulting in its higher abundance. *SYN*-PEI and

Table 4
Regression analysis of the factor scores (as independent factors) for the abundance of *SYN* groups in different seasons.

Dependent factor	R^2	*F*	β			
			PC1	PC2	PC3	PC4
Pre-monsoon						
SYN-PC	0.40	51.21**	0.184*	0.250**	−0.630**	–
SYN-PEI	0.55	94.27**	0.200*	0.004	0.740**	–
SYN-PEII	0.67	163.55**	−0.197*	−0.148	0.823**	–
SYN-PEIII	0.39	50.11**	−0.192*	−0.560	- 0.625**	–
Chlorophyll *a*	0.16	14.56**	0.060	0.139	−0.397**	–
Monsoon						
SYN-PC	0.41	13.81**	0.555**	−0.740	0.327**	–
SYN-PEI	0.29	30.69**	0.534**	0.038	0.058	–
SYN-PEII	0.10	8.95**	0.323**	0.206*	0.055	–
SYN-PEIII	0.16	15.47**	−0.410**	−0.226*	0.032	–
Chlorophyll *a*	0.05	4.21*	0.213*	−0.228*	0.054	–
Post-monsoon						
SYN-PC	0.43	51.12**	0.257*	−0.655**	- 0.004	0.516**
SYN-PEI	0.51	70.58**	−0.011	0.714**	0.000	−0.162*
SYN-PEII	0.84	84.22**	−0.079	0.736**	0.001	−0.538**
SYN-PEIII	0.50	16.01**	0.060	−0.691**	0.004	0.125
Chlorophyll *a*	0.30	4.16*	−0.508	0.030	−1.980	0.208*

R^2 – regression coefficient; *F*-value of the full model; β – standardized coefficient. $^*p < 0.05$, $^{**}p < 0.01$.

Table 3
Rotated component matrix (RCM) with varifactors (principal components, PCs) extracted in different seasons. Bold text denotes significant loading.

Parameter	Pre-monsoon (PrM)			Monsoon (MON)			Post-monsoon (PoM)			
	PC1	PC2	PC3	PC1	PC2	PC3	PC1	PC2	PC3	PC4
Salinity	−0.02	−0.08	**0.94**	**0.70**	0.02	−0.10	−0.24	**0.76**	0.04	−0.49
Temperature	−0.06	**0.72**	−0.05	0.33	**0.47**	0.36	0.33	0.24	**0.75**	−0.05
Secchi disk depth	−0.13	**−0.51**	0.15	−0.45	0.13	**0.63**	−0.02	0.15	**−0.90**	−0.02
Nitrate	−0.34	**0.63**	0.12	−0.47	**0.69**	−0.21	**0.90**	−0.30	0.08	−0.14
Phosphate	**0.92**	−0.16	0.11	**0.87**	−0.07	0.24	**0.89**	0.24	0.24	0.14
Nitrite	**0.60**	0.56	0.32	−0.20	0.09	**−0.74**	0.08	**0.89**	0.00	0.14
Silicate	**0.82**	0.01	−0.45	−0.02	**−0.87**	−0.02	−0.04	−0.01	−0.01	**0.98**
Eigenvalues	2.00	1.52	1.24	1.82	1.49	1.19	1.77	1.60	1.44	1.25
% of variance	28.61	21.76	17.68	26.05	21.27	16.96	25.21	22.91	20.56	17.89
Cumulative %	28.61	50.38	68.06	26.05	47.32	64.28	25.21	48.12	68.67	86.57

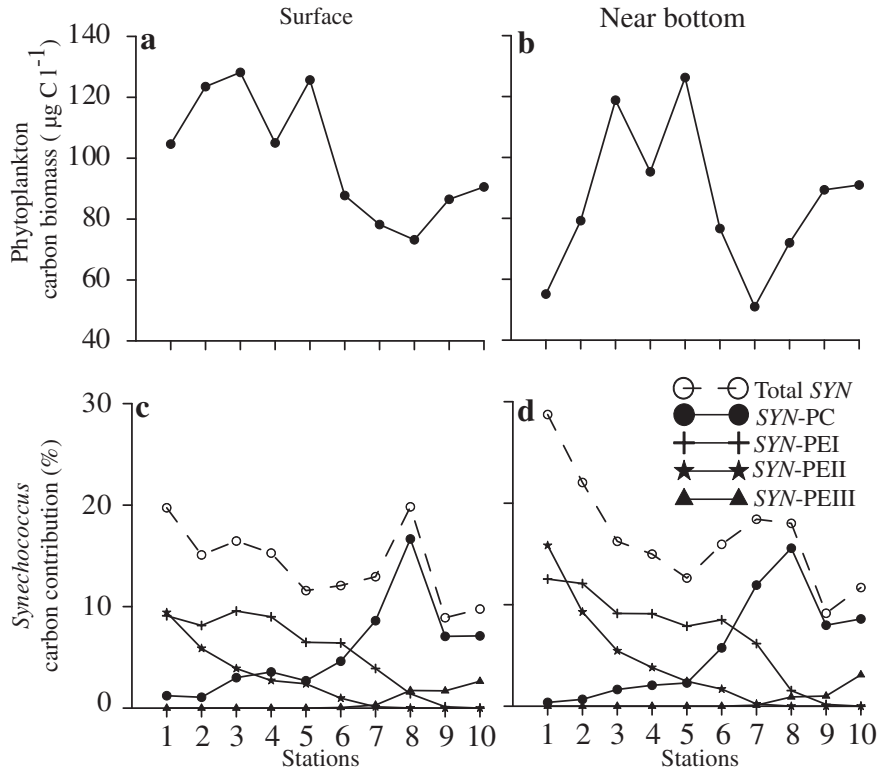

Fig. 7. (a, b) Total phytoplankton carbon biomass and (c, d) percentage contribution of *Synechococcus* to the total phytoplankton carbon biomass in the Zuari estuary.

SYN-PEII showed a positive and *SYN*-PEIII negative relation with salinity during the three seasons indicating that *SYN*-PEI and *SYN*-PEII preferred higher salinity and *SYN*-PEIII lower salinity.

Recent studies elucidate negative correlation between *SYN* abundance and nutrients (Qiu et al., 2010; Zhang et al., 2013). These studies suggest that *SYN* prefers reduced form of nitrate (ammonia) which was not measured in the present study. In this study, the positive correlation of *SYN*-PC to PC's which are strongly associated with nitrate and phosphate during the non-MON periods and with phosphate during the MON season suggests that both these nutrients could be important for this group. A laboratory experimental study proved that PC rich *SYN* grows well in high nitrate and phosphate concentration whereas PE rich *SYN* cannot tolerate high nitrate concentration (Ernst et al., 2005). Wyman et al. (1985) reported that *SYN* can use nitrate with lower concentration efficiently and dominates the conditions. These findings corroborate the non-significant relation of *SYN*-PE subgroups with nitrate and the positive relation with phosphate of *SYN*-PEI and *SYN*-PEII during the PrM and MON season in this study (Table 4). These observations indicate that nutrients could play a vital role in the temporal variation of *SYN* groups. Since silicate is not a requirement for this PP, the positive relationship in some cases may not be a causal one.

The low cell abundance observed during active MON could be a consequence of the prevailing environmental conditions such as increased turbidity due to influx of huge quantities of freshwater and restricted light availability due to increased cloud cover (Devassy and Goes, 1988). Biological processes like grazing (Wetz et al., 2011) and viral lysis (Pan et al., 2007) are also known to play a role in controlling *SYN* abundance, which we did not account for in the present study. During MON break increased salinity, temperature, nutrients (nitrate and phosphate), solar radiation and lower rainfall could have facilitated an increase in *SYN* abundance along with high phytoplankton biomass. Similar variations in phytoplankton biomass have been observed in this estuary with high and low biomass during MON break and during peak of MON, respectively (Patil and Anil, 2011; Pednekar et al., 2011). The increased freshwater runoff during this period was reflected in the dominance of *SYN*-PC from the mouth to head of the estuary and absence of *SYN*-PEII as well as lower cell abundance of *SYN*-PEIII. Towards the end of MON season, with the subsiding rainfall intensity and the corresponding lowered freshwater influx downstream along with the high nutrient concentrations and solar radiation, *SYN*-PEI, *SYN*-PEII and *SYN*-PEIII abundance increased in the estuary. Lowering of *SYN*-PC abundance could be a result of the gradual increase in salinity and low temperature. This period is considered to be conducive for the proliferation of phytoplankton (Patil and Anil, 2011; Pednekar et al., 2011) wherein phytoplankton biomass showed significant positive correlation with silicate. During PoM, all the *SYN* groups showed similar distribution as observed in PrM indicating return of favorable environmental conditions for their growth.

4.3. Contribution of Synechococcus to total phytoplankton carbon biomass

The contribution of *SYN* to the total phytoplankton carbon biomass in the Zuari estuary (9–29%) was lower than that reported for the Chesapeake Bay sub-estuary (34–52%; salinity 19.5–23.7) dominated by cyanobacteria (Ray et al., 1989) and higher than that reported in a tropical coastal region (<16%) at the river mouth (Agawin et al., 2003). However, contribution of picoplankton biomass to total phytoplankton biomass in the Cochin estuary, along the west coast of India, influenced by the SW monsoon ranged between 6.5% (salinity 3–9) and 11.2% (salinity >30; Madhu et al., 2009). In the present study *SYN* carbon contribution was inversely related to total phytoplankton biomass, which suggests that dominance of larger phytoplankton. Similarly a study conducted in North Carolina estuary showed inverse relation between

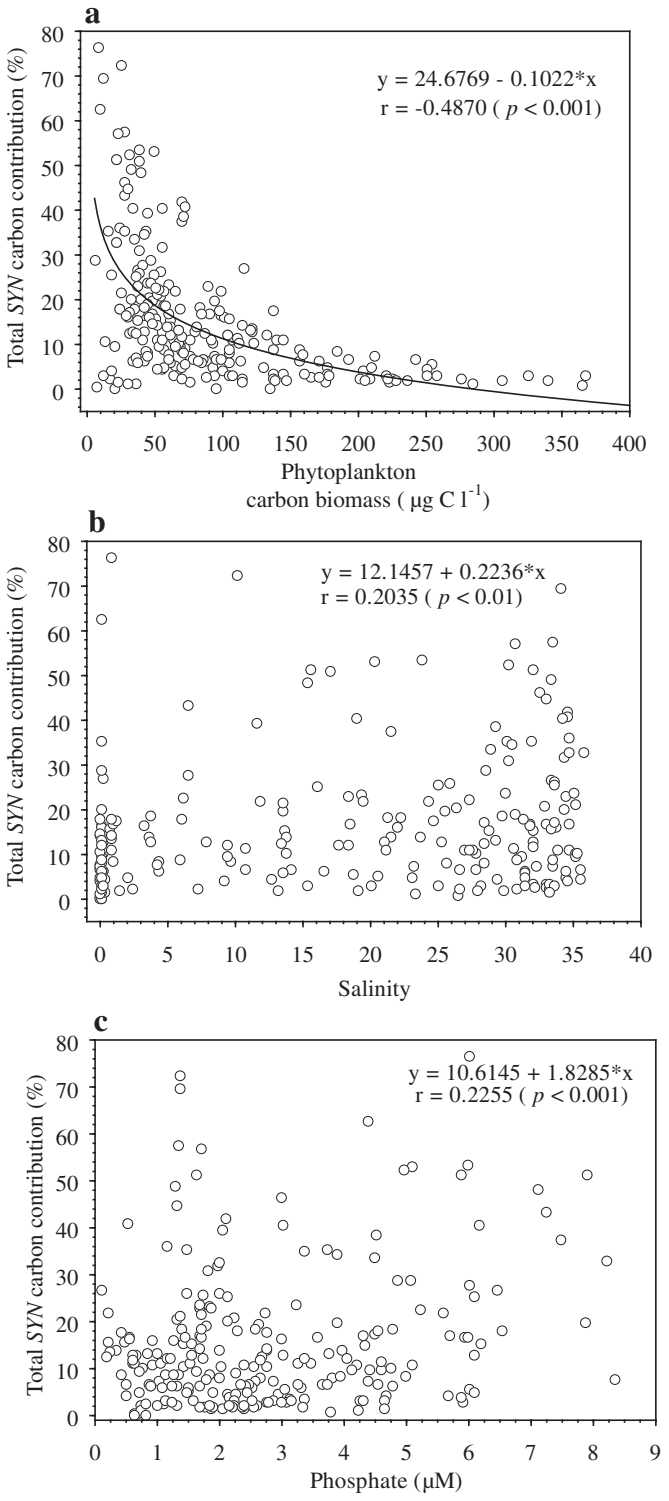

Fig. 8. Correlation analysis of total *SYN* carbon contribution (%) with (a) total phytoplankton carbon biomass, (b) salinity, (c) phosphate. The curve was fitted under the logarithmic equation model.

picoplankton contribution (~40%; salinity 0–26) and phytoplankton biomass (Gaulke et al., 2010) and concluded that variation in PP carbon contributions depends on various factors such as nutrients, light and stability of water column. These observations suggest that *SYN* contribution to total phytoplankton carbon biomass was within the range of other tropical estuaries and although lower than that reported for sub-tropical estuaries, could play a vital role in the microbial food web dynamics of estuarine regions.

In monsoonal estuaries where the freshwater runoff and tides regulate the hydrodynamics during the MON and non-MON periods respectively, the distribution pattern of these organisms both spatially (horizontal and vertical) and temporally, can serve as indicators of the source of water as well as the water stability (mixed or stratified) at a particular location in the estuary thereby providing information about the physical factors regulating the estuarine dynamics.

Acknowledgments

The authors wish to thank The Director, National Institute of Oceanography for his support. We are grateful to Dr. Sathish Shetye and Dr. A.C. Anil, Scientist, for their encouragement and support. We thank Mr. D. Sundar for providing CTD data. We also acknowledge anonymous reviewers for their valuable comments. This is NIO contribution #5459.

References

Agawin, N., Duarte, C., Agusti, S., McManus, L., 2003. Abundance, biomass and growth rates of *Synechococcus* sp. in a tropical coastal ecosystem (Philippines, South China Sea). Estuar. Coast. Shelf Sci. 56, 493–502.
Agawin, N.S., Duarte, C.M., Agusti, S., 1998. Growth and abundance of *Synechococcus* sp. in a Mediterranean Bay: seasonality and relationship with temperature. Mar. Ecol. Prog. Ser. 170, 45–53.
Azam, L., 1983. The ecological role of water-column microbes in the sea. Mar. Ecol. Prog. Ser. 10, 257–263.
Baudoux, A.C., Veldhuis, M.J., Witte, H.J., Brussaard, C.P., 2007. Viruses as mortality agents of picophytoplankton in the deep chlorophyll maximum layer during IRONAGES III. Limnol. Oceanogr. 52, 2519–2529.
Brown, S.L., Landry, M.R., Barber, R.T., Campbell, L., Garrison, D.L., Gowing, M.M., 1999. Picophytoplankton dynamics and production in the Arabian Sea during the 1995 Southwest Monsoon. Deep Sea Res. Part II Top. Stud. Oceanogr. 46, 1745–1768.
Callieri, C., 1996. Extinction coefficient of red, green and blue light and its influence on picocyanobacterial types in lakes at different trophic levels. Mem. Ist. Ital. Idrobiol. Dott Marco Marchi 54, 135–142.
Campbell, L., Landry, M., Constantinou, J., Nolla, H., Brown, S., Liu, H., Caron, D., 1998. Response of microbial community structure to environmental forcing in the Arabian Sea. Deep-Sea Res. Part II 45, 2301–2325.
Chiang, K.P., Tsai, A.Y., Tsai, P.J., Gong, G.C., Tsai, S.F., 2013. Coupling of the spatial dynamic of picoplankton and nanoflagellate grazing pressure and carbon flow of the microbial food web in the subtropical pelagic continental shelf ecosystem. Biogeosci. Dis. 10, 233–263.
Costa, L., Huszar, V., Ovalle, A., 2009. Phytoplankton functional groups in a tropical estuary: hydrological control and nutrient limitation. Estuar. Coasts 32, 508–521.
Devassy, V., Goes, J., 1988. Phytoplankton community structure and succession in a tropical estuarine complex (central west coast of India). Estuar. Coast. Shelf Sci. 27, 671–685.
Ernst, A., Deicher, M., Herman, P.M.J., Wollenzien, U.I.A., 2005. Nitrate and phosphate affect cultivability of cyanobacteria from environments with low nutrient levels. Appl. Environ. Microbiol. 71, 3379–3383.
Gallegos, C.L., 2001. Calculating optical water quality targets to restore and protect submersed aquatic vegetation: overcoming problems in partitioning the diffuse attenuation coefficient for photosynthetically active radiation. Estuaries 24, 381–397.
Gaulke, A.K., Wetz, M.S., Paerl, H.W., 2010. Picophytoplankton: a major contributor to planktonic biomass and primary production in a eutrophic, river-dominated estuary. Estuar. Coast. Shelf Sci. 90, 45–54.
Jochem, F., 1988. On the distribution and importance of picocyanobacteria in a boreal inshore area (Kiel Bight, Western Baltic). J. Plankton Res. 10, 1009–1022.
Lin, D., Zhu, A., Xu, Z., Huang, L., Fang, H., 2010. Dynamics of photosynthetic picoplankton in a subtropical estuary and adjacent shelf waters. J. Mar. Biol. Assoc. U. K. 90, 1319–1329.
Liu, H., Campbell, L., Landry, M., Nolla, H., Brown, S., Constantinou, J., 1998. *Prochlorococcus* and *Synechococcus* growth rates and contributions to production in the Arabian Sea during the 1995 Southwest and Northeast Monsoons. Deep-Sea Res. Part II 45, 2327–2352.
Liu, H., Dagg, M., Campbell, L., Urban-Rich, J., 2004. Picophytoplankton and bacterioplankton in the Mississippi River plume and its adjacent waters. Estuar. Coasts 27, 147–156.
Madhu, N.V., Jyothibabu, R., Balachandran, K.K., 2009. Monsoon-induced changes in the size-fractionated phytoplankton biomass and production rate in the

estuarine and coastal waters of southwest coast of India. Environ. Monitor. Assess. 166, 521–528.
Manoj, N., Unnikrishnan, A., 2009. Tidal circulation and salinity distribution in the Mandovi and Zuari estuaries: case study. J. Waterw. Port Coast. Ocean Eng. 135, 278–287.
Marshall, H.G., Lane, M.F., Nesius, K.K., Burchardt, L., 2009. Assessment and significance of phytoplankton species composition within Chesapeake Bay and Virginia tributaries through a long-term monitoring program. Environ. Monitor. Assess. 150, 143–155.
Marshall, H., Nesius, K., 1996. Phytoplankton composition in relation to primary production in Chesapeake Bay. Mar. Biol. 125, 611–617.
Mitbavkar, S., Rajaneesh, K., Anil, A., Sundar, D., 2012. Picophytoplankton community in a tropical estuary: detection of *Prochlorococcus*-like populations. Estuar. Coast. Shelf Sci. 107, 159–164.
Mitbavkar, S., Saino, T., Horimoto, N., Kanda, J., Ishimaru, T., 2009. Role of environment and hydrography in determining the picoplankton community structure of Sagami Bay, Japan. J. Oceanogr. 65, 195–208.
Murrell, M.C., Lores, E.M., 2004. Phytoplankton and zooplankton seasonal dynamics in a subtropical estuary: importance of cyanobacteria. J. Plankton Res. 26, 371–382.
Ning, X., Cloern, J.E., Cole, B.E., 2000. Spatial and temporal variability of picocyanobacteria *Synechococcus* sp. in San Francisco Bay. Limnol. Oceanogr., 695–702.
Paerl, H.W., 1977. Ultraphytoplankton biomass and production in some New Zealand lakes. N. Z. J. Mar. Freshw. Res. 11, 297–305.
Pan, L., Zhang, J., Zhang, L., 2007. Picophytoplankton, nanophytoplankton, heterotrohpic bacteria and viruses in the Changjiang Estuary and adjacent coastal waters. J. Plankton Res. 29, 187–197.
Parsons, T.R., Maita, Y., Lalli, C.M., 1984. Manual of Chemical and Biological Methods for Seawater Analysis. Pergamon, New York.
Partensky, F., Hess, W., Vaulot, D., 1999. *Prochlorococcus*, a marine photosynthetic prokaryote of global significance. Microbiol. Mol. Biol. Rev. 63, 106–127.
Patil, J.S., Anil, A.C., 2011. Variations in phytoplankton community in a monsoon-influenced tropical estuary. Environ. Monitor. Assess. 182, 291–300.
Pednekar, S.M., Matondkar, S.G.P., Gomes, H.D.R., Goes, J.I., Parab, S., Kerkar, V., 2011. Fine-scale responses of phytoplankton to freshwater influx in a tropical monsoonal estuary following the onset of southwest monsoon. J. Earth Syst. Sci. 120, 545–556.
Phlips, E.J., Badylak, S., Lynch, T.C., 1999. Blooms of the picoplanktonic cyanobacterium *Synechococcus* in Florida Bay, a subtropical inner-shelf lagoon. Limnol. Oceanogr. 44, 1166–1175.
Platt, T., Rao, D.S., Irwin, B., 1983. Photosynthesis of picoplankton in the oligotrophic ocean. Nature 301, 702–704.
Pomeroy, L.R., 1974. The ocean's food web, a changing paradigm. Bioscience 24, 499–504.
Qasim, S., Sen Gupta, R., 1981. Environmental characteristics of the Mandovi-Zuari estuarine system in Goa. Estuar. Coast. Shelf Sci. 13, 557–578.
Qiu, D., Huang, L., Zhang, J., Lin, S., 2010. Phytoplankton dynamics in and near the highly eutrophic Pearl River Estuary, South China Sea. Cont. Shelf Res. 30, 177–186.
Ray, R.T., Haas, L.W., Sieracki, M.E., 1989. Autotrophic picoplankton dynamics in a Chesapeake Bay sub-estuary. Mar. Ecol. Prog. Ser. MESEDT 52, 273–285.
Shetye, S., Murty, C., 1987. Seasonal variation of the salinity in the Zuari estuary, Goa, India. J. Earth Syst. Sci. 96, 249–257.
Shetye, S.R., 1999. Propagation of tides in the Mandovi and Zuari estuaries, Sadhana (Academy Proceedings in Engineering Sciences). Indian Acad. Sci. 24, 5–16.
Sin, Y., Wetzel, R.L., Anderson, I.C., 2000. Seasonal variation of size-fractionated phytoplankton along the salinity gradient in the York River estuary, Virginia (USA). J. Plankton Res. 22, 1945–1960.
Tsai, A.Y., Chiang, K.P., Chang, J., Gong, G.C., 2008. Seasonal variations in trophic dynamics of nanoflagellates and picoplankton in coastal waters of the western subtropical Pacific Ocean. Aquat. Microb. Ecol. 51, 263–274.
Vijith, V., Sundar, D., Shetye, S., 2009. Time-dependence of salinity in monsoonal estuaries. Estuar. Coast. Shelf Sci. 85, 601–608.
Wang, K., Wommack, K.E., Chen, F., 2011. Abundance and distribution of *Synechococcus* spp. and cyanophages in the Chesapeake Bay. Appl. Environ. Microbiol. 77, 7459–7468.
Waterbury, J.B., Watson, S.W., Valois, F.W., Franks, D.G., 1986. Biological and ecological characterization of the marine unicellular cyanobacterium *Synechococcus*. Can. Bull. Fish Aquat. Sci. 214, 71–120.
Wetz, M.S., Paerl, H.W., Taylor, J.C., Leonard, J.A., 2011. Environmental controls upon picophytoplankton growth and biomass in a eutrophic estuary. Aquat. Microb. Ecol. 63, 133.
Worden, A.Z., Nolan, J.K., Palenik, B., 2004. Assessing the dynamics and ecology of marine picophytoplankton: the importance of the eukaryotic component. Limnol. Oceanogr., 168–179.
Wyman, M., Gregory, R., Carr, N., 1985. Novel role for phycoerythrin in a marine cyanobacterium, *Synechococcus* strain DC2. Science 230, 818–820.
Zhang, X., Shi, Z., Ye, F., Zeng, Y., Huang, X., 2013. Picophytoplankton abundance and distribution in three contrasting periods in the Pearl River Estuary, South China. Mar. Freshw. Res. 64, 692–705.